UNIVERSITY OF CALIFORNIA, SAN DIEGO

SAN DIEGO STATE UNIVERSITY

Design, synthesis, and mechanistic studies of Sansalvamide A derivatives as anti-cancer agents

A dissertation submitted in partial satisfaction of the requirements for the degree of Doctor of Philosophy

in

Chemistry

by

Leslie Diane Alexander

Committee in charge:

University of California, San Diego

Professor William Gerwick
Professor Joseph Noel
Professor Jerry Yang

San Diego State University

Professor Shelli McAlpine, Chair
Professor Thomas Cole
Professor Constatine Tsoukas

2012

The Dissertation of Leslie Diane Alexander is approved, and it is acceptable in quality and form for publication on microfilm and electronically:

_____

_____

_____

_____

_____

_____
Chair

University of California, San Diego

San Diego State University

2012

DEDICATION

For my mom, William, and David

And in loving memory of my dad,
Drebelbis Andrew “Andy” Alexander

TABLE OF CONTENTS

LIST OF ABBREVIATIONS

17-AAG	17-allylamino-17-demethoxygeldanamycin
5-FU	5-fluorouracil
^{3}H	tritium
ACN	acetonitrile
ADP	adenosine diphosphate
AR	androgen receptor
ATP	adenosine triphosphate
BnBr	benzyl bromide
Boc	*tert*-butyloxycarbonyl
Cbz	Carbobenzyloxy
CCK-8	Cell Counting Kit 8
CTC	2-chlorotrityl
Cyp40	cyclophilin 40
DCM	dichloromethane
DDLD	double deprotected linear decapeptide
DDLP	double deprotected linear pentapeptide
DEPBT	3-(Diethoxyphosphoryloxy)-1,2,3-benzotriazin-4(3*H*)-one
DIC	diisopropylcarbodiimide
DIPEA	*N*-*N*-diisopropylethylamine
Di-SanA	Dimerized Sansalvamide A
DMF	dimethylformamide
DMSO	dimethyl sulfoxide

DVB	divinylbenzene
EA	ethyl acetate
ER	estrogen receptor
FKBP	FK506-binding protein
Fmoc	9-Fluorenylmethyloxycarbonyl
GDA	Geldanamycin
GR	glucocorticoid receptor
HATU	2-(1H-7-azabenzotriazol-1-yl)-1,1,3,3-tetramethyluronium hexafluorophosphate
HBr	hydrobromic acid
HBTU	2-(1H-benzotriazole-1-yl)-1,1,3,3-tetramethyluronium hexafluorophosphate
HCl	hydrochloric acid
Her2	human epidermal growth factor receptor 2
Hif-1α	hypoxia-inducible factor-1α
HOAT	hydroxy-7-azabenzotriazole
HOBT	1-hydroxybenzotriazole
HOP	Heat shock organizing protein
HPLC	High Performance Liquid Chromatography
Hsf-1	Heat shock factor 1
Hsp70	Heat shock protein 70
Hsp90	Heat shock protein 90
IC_{50}	half maximal inhibitory concentration
IP6K2	inositol hexakisphosphate kinase 2

IPA	isopropanol
LCMS	liquid chromatography mass spectrometry
Me	methyl
MeOH	methanol
MSI	microsatellite instability
MSS	microsatellite stability
NaH	sodium hydride
$NaHCO_3$	sodium bicarbonate
NaOH	sodium hydroxide
NCI	National Cancer Institute
NHS	*N*-hydroxysuccinimide
***N*-Me-aa**	*N*-methylated amino acid
NMR	^{1}H Nuclear Magnetic Resonance
PARP	poly(ADP-ribose) polymerase
PEG	polyethylene glycol
PG	protecting group
PLP	protected linear pentapeptide
PP5	protein phosphatase 5
PR	progesterone receptor
PyBOP	benzotriazol-1-yl-oxytripyrrolidinophosphonium hexafluorophosphate
RP-HPLC	reverse phase high performance liquid chromatography
SanA	Sansalvamide A
SAR	structure activity relationship
SDS-PAGE	sodium dodecyl sulfate-polyacrylamide gel electrophoresis

SHR	steroid hormone receptor
SPPS	solid phase peptide synthesis
TBTU	2-(1H-benzotriazole-1-yl)-1,1,3,3-tetramethyluronium tetrafluoroborate
TFA	trifluoroacetic acid
TFE	2,2,2-trifluoroethanol
THF	tetrahydrofuran
TLC	thin-layer chromatography
TPR	tetratricopeptide repeat

LIST OF SYMBOLS

α	alpha
β	beta
ºC	degree Celsius
K_d	dissociation constant
µl	microliter
µM	micromolar
mL	milliliter
mM	milimolar
nM	nanomolar
nm	nanometer

LIST OF FIGURES

ACKNOWLEDGMENTS

First and foremost, I would like to thank Professor Shelli McAlpine for her guidance, support, and friendship. Without her, this dissertation would not exist and I would not be the person I am today. Her mentorship went well beyond the lab and exceeded the duty of any advisor. Shelli taught me to have confidence in myself and my abilities, which not only applied to my research but also to other aspects of my life. I am truly grateful to have been a part of her lab.

Thank you to Erin for being such a great friend and lab mate, you were always there for me and your positive attitude made any difficult situation easier. To Stephanie and Melinda, I am so happy to have made friends like you. I truly enjoyed our times in the upstairs lab and always look forward to our get-togethers. To Vasko and Veronica, thank you for sparking my interest in biology, passing on your skills, and letting me bounce ideas off of you. To Eddie and Jay, thank you for always asking questions, I thoroughly enjoyed our discussions. To Debbie and Jeanette, it was a joy to work with you, and I am so excited that the future of the project lies with you. And to everyone who read my thesis chapters and listened to my practice talks, I want to say a huge thank you, I could not have done this without you!

To my family and friends, thank you for your encouragement, love, and patience. To my husband, David, thank you for your loving and believing in me, you mean so much to me and I could not have done this without you. To my mom, thank you for always being there for me. Whether in person or on the phone, you always had the most encouraging words for me that would help me through any situation.

I would like to acknowledge the co-authors of published papers of which I was primary or contributing author. Chapters 2 and 3, in part, contain material that has been published in Bioorganic and Medicinal Chemistry: Robert P. Sellers, Leslie D. Alexander, Victoria A. Johnson, Chun-Chieh Lin, Jeremiah Savage, Ricardo Corral, Jason Moss, Tim S. Slugocki, Erinprit K. Singh, Melinda R. Davis, Suchitra Ravula, Jamie E. Spicer, Jenna L Oelrich, Andrea Thornquist, Chung-Mao Pan, and Shelli R. McAlpine, **2010**, v15, p3287.

Chapter 3, in part, contains material that has been published in Bioorganic and Medicinal Chemistry Letters: Joseph Kunicki, Mark Petersen, Leslie D. Alexander, Veronica C. Ardi, Jeanette McConnell, and Shelli R. McAlpine, **2011**, v21, p4716. Leslie D. Alexander, James R. Partridge, David A. Agard, and Shelli R. Mcalpine, **2011**, v21, p7068. Deborah M. Ramsey, Jeanette R. McConnell, Leslie D. Alexander, Kaishin W. Tanaka, Chester M. Vera, and Shelli R. McAlpine, **2012**, v22, p3287.

Chapters 3 and 4, in part, contain material that has been published in ACS Chemical Biology: Veronica C. Ardi, Leslie D. Alexander, Victoria A. Johnson, and Shelli R. McAlpine, **2011**, v6, p1357.

Chapter 5, in part, contains material that has been published in Journal of Medicinal Chemistry: Leslie D. Alexander, Robert P. Sellers, Melinda R. Davis, Veronica C. Ardi, Victoria A. Johnson, Robert, C. Vasko, and Shelli R. McAlpine, **2009**, v52, p7927.

VITA

2006 Bachelor of Science, Biopsychology, University of California, Santa Barbara

2012 Doctor of Philosophy, Chemistry, University of California, San Diego and San Diego State University

PUBLICATIONS

** Denotes PI on papers, order of authors indicates relative intellectual contributions, where first author contributed the most after the PI contribution*

10. Deborah M. Ramsey, Jeanette R. McConnell, Leslie D. Alexander, Kaishin W. Tanaka, Chester M. Vera, Shelli R. McAlpine* An Hsp90 modulator that exhibits a unique mechanistic profile. *Bioorganic and Medicinal Chemistry Letters,* **2012**, v22, p3287-3290.

9. Melinda R. Davis, Erinprit K. Singh, Hendra Wahyudi, Leslie D. Alexander, Joseph Kunicki, Lidia A. Nazarova, Kelly Fairweather, Andrew Giltrap, Kate Jolliffe, and Shelli R. McAlpine* Peptidomimetic derivatives of Sansalvamide A. *Tetrahedron,* **2012**, v68, p1029-1051.

8. Leslie D. Alexander, James R. Partridge, David A. Agard, and Shelli R. Mcalpine*. A small molecule that preferentially binds the closed conformation of Hsp90. *Bioorganic and Medicinal Chemistry Letters,* **2011**, v21, p7068-7071.

7. Veronica C. Ardi, Leslie D. Alexander, Victoria A. Johnson, and Shelli R. McAlpine* Macrocycles that inhibit the binding between heat shock protein 90 and TPR-containing proteins. *ACS Chemical Biology,* **2011**, v6, p1357-1366.

6. Joseph Kunicki, Mark Petersen, Leslie D. Alexander, Veronica C. Ardi, Jeanette McConnell, and Shelli R. McAlpine* Synthesis and evaluation biotinylated Sansalvamide A analogs and their modulation of Hsp90. *Bioorganic and Medicinal Chemistry Letters,* **2011**, v21, 4716-4719.

5. Erinprit K. Singh, Lidia A. Nazarova, Stephanie A. Lapera, Leslie D. Alexander and Shelli R. McAlpine*. Histone deacetylase inhibitors: Synthesis of cyclic tetrapeptides and their triazole analogs. *Tetrahedron Letters,* **2010**, v51, p4357-4360.

4. Robert P. Sellers, Leslie D. Alexander, Victoria A. Johnson, Chun-Chieh Lin, Jeremiah Savage, Ricardo Corral, Jason Moss, Tim S. Slugocki, Erinprit K. Singh, Melinda R. Davis, Suchitra Ravula, Jamie E. Spicer, Jenna L Oelrich, Andrea Thornquist, Chung-Mao Pan, and Shelli R. McAlpine*. Design and synthesis of Hsp90 inhibitors: Exploring the SAR of Sansalvamide A derivatives. *Bioorganic and Medicinal Chemistry*, **2010**, v15, p6822-6856.

3. Victoria A. Johnson, Erinprit K. Singh, Lidia A. Nazarova, Leslie D. Alexander and Shelli R. McAlpine*. Macrocyclic Inhibitors of Hsp90. *Current Topics in Medicinal Chemistry*, **2010**, v10, p1380-1402.

2. Leslie D. Alexander, Robert P. Sellers, Melinda R. Davis, Veronica C. Ardi, Victoria A. Johnson, Robert, C. Vasko, and Shelli R. McAlpine*. Evaluation of Di-Sansalvamide A derivatives: Synthesis, SAR, and Mechanism of Action. *Journal of Medicinal Chemistry Letters*, **2009**, v52, p7927-7930.

1. Erinprit K. Singh, Robert P. Sellers, Leslie D. Alexander and Shelli R. McAlpine*. Conformational based design of macrocycles as antitumor agents. *Current Opinion in Drug Discovery*, **2008**, v11, p544-552.

FIELDS OF STUDY

Major Field: Chemistry (Bioorganic)

Studies in Organic Synthesis and Biochemistry
Professor Shelli R. McAlpine

ABSTRACT OF THE DISSERTATION

Design, synthesis, and mechanistic studies of Sansalvamide A derivatives as anti-cancer agents

by

Leslie Diane Alexander

Doctor of Philosophy in Chemistry

University of California, San Diego, 2012
San Diego State University, 2012

Professor Shelli McAlpine, Chair

Sansalvamide A (SanA) is a cyclic depsipeptide that was isolated from a marine fungus and demonstrates mid-micromolar anti-cancer activity in the NCI 60-cell line panel. Our laboratory has synthesized over 100 peptide derivatives of this molecule, 5 of which were contributed by the author of this dissertation. The design and solution-phase synthesis of these derivatives is described in Chapter 2. The author was also responsible

for attaching PEG-biotin and fluorescein tags to lead SanA derivatives to be used in mechanism of action studies.

Chapter 3 describes the mechanism of action studies that were completed with the lead derivatives, both untagged and tagged with PEG-biotin or fluorescein. The untagged compounds are tested in cell proliferation assays against the pancreatic cancer cell line PL-45 and the colon cancer cell line HCT-116. Two of the lead compounds are tested in caspase 3 apoptosis assays and PARP fragmentation analysis. The biotin-tagged compounds are used in pull down assays and it is determined that they bind to the N-middle domain of Hsp90, a well-established oncogenic protein. Hsp90 is responsible for regulating over 200 client proteins, many of which are oncogenic and involved in cancer cell growth. We show that SanA disrupts the binding between Hsp90 and four of these client proteins (Akt, Her2, Hif-1α, and IP6K2) in pure protein binding assays.

Chapter 4 investigates SanA's affect proteins that bind to Hsp90's C-domain via their tetratricopeptide repeats (TPRs). Using client protein binding assays, the author determines that the lead SanA derivative disrupts binding between Hsp90 and five TPR-containing proteins.

Finally, Chapter 5 describes the synthesis and preliminary mechanism of action studies of dimerized SanA derivatives (Di-SanA). These compounds are cyclic decapeptides with C-2 rotational symmetry. The author contributed 12 decapeptides, based on one lead derivative from the first generation, which investigated how the placement of D-amino acids around the ring would affect cytotoxicity. These derivatives were synthesized via solid-phase peptide chemistry. The author also investigated

mechanism of action of this class of compounds with cell proliferation assays, pull-down assays, and a client protein binding assay.

CHAPTER 1: INTRODUCTION

Cancer is currently the number one cause of death worldwide.[1] In the US alone, there are an estimated 1.6 million new cancer cases in 2012, and over 600,000 cancer-related deaths.[2] Thus, there is an urgent need for developing new and effective treatments, and it is crucial that we explore cancer cell growth mechanisms. The following dissertation will chronicle the chemical synthesis and mechanism of action of several structural analogs of the natural product depsipeptide Sansalvamide A (SanA).

PEPTIDES AS THERAPEUTICS

The development of peptides as drugs is prevalent in the pharmaceutical industry. From a biological perspective, peptide specificity to receptors and protein targets, as well as their potency and low toxicity, make them ideal drug candidates. From a synthetic perspective, their straightforward synthesis, and versatility in building blocks make them ideal therapeutics.

The disadvantages associated with peptides as therapeutics include their susceptibility to rapid enzymatic degradation and poor membrane permeability. Enzymatic degradation is an essential part of regulating cellular processes. Once a peptide or protein has performed its required function, it is broken down by proteases. Although this mechanism is required to maintain living systems, it leads to another obstacle in the development of pharmacological peptides. Scientists take many approaches to improve the stability of peptides. Placing features that are not present in native peptides in the body will stabilize peptide drugs because they are not easily recognized by proteases.[3] Most amino acids that make up proteins in mammals contain an L-amino acid configuration, also known as (*S)* stereochemistry. Including D-amino

acids (D-aas), *N*-methylated amino acids (*N*-Me-aas), and unnatural amino acids or modified natural amino acids within the backbone of peptide drug candidates are several features that have improved their biological stabilities (**Figure 1**).

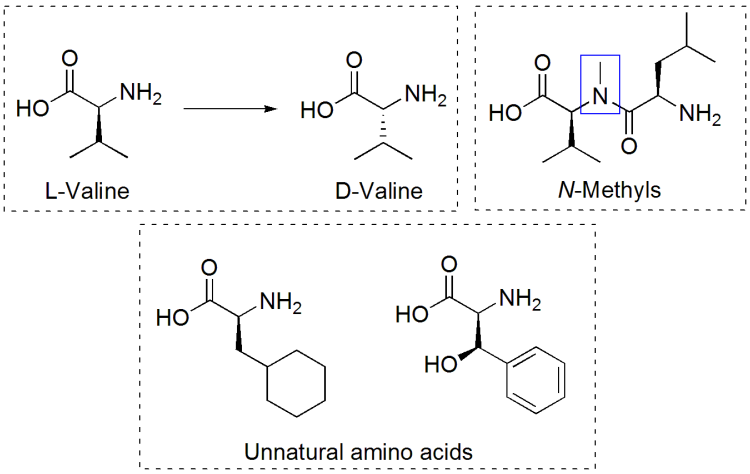

Figure 1: Examples of modifications to improve biological stability of peptides

Cyclization of peptides is another effective approach to increasing bioavailability of the peptide and maintaining bioactivity.[4] Linear peptides can adopt multiple conformations that may not be optimal for binding to their targets, thereby making them less effective drug candidates.[5] The structural rigidity associated with cyclic peptides allows them to bind more effectively to their targets and have greater resistance to proteolytic degradation than linear peptides.[4, 6] In addition, cyclized peptides generally have increased membrane permeability than linear peptides, which is due to intramolecular hydrogen bonding and the elimination of charged termini.[7, 8]

Macrocyclization of peptides can occur via many routes (**Figure 2**).[9] Head-to-tail cyclization is an intramolecular amide bond formation between the N- and C-termini of a linear peptide (**Figure 2a**). There are also many variations of cyclizations that involve the side-chains of amino acids in the linear precursor. Side-chain to C-terminus

cyclizations occur between the side-chain of an amino acid such as lysine and the C-terminus of a linear peptide (**Figure 2b**). In this type of cyclization, the N-terminus is protected by a protecting group that can be removed post-cyclization. An N-terminus to side-chain cyclization involves a linear peptide with free N-terminus and a protected C-terminus, and side-chains from amino acids such as aspartic acid or glutamic acid (**Figure 2c**). Side-chain to side-chain reactions require protecting both C- and N-termini of a linear peptide, or they can occur after head-to-tail cyclization to form multi-cyclic products. One type of side-chain to side-chain cyclization forms an amide bond between an amine-containing side-chain (lysine) and a carboxyl-containing side-chain (glutamic or aspartic acids) (**Figure 2d**). Another type is the formation of a disulfide bond between two cysteine residues via oxidation of their sulfhydryl-containing side-chains (**Figure 2e**). The variety of cyclizations available is important given that one or more of these types of cyclizations are present in most cyclic peptide-based drugs.

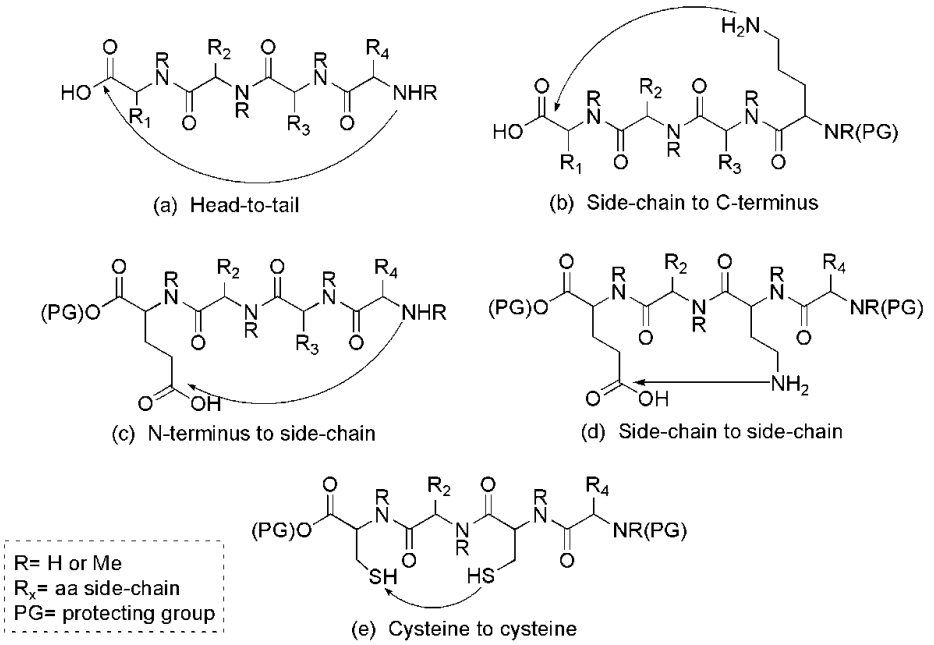

Figure 2: Different types of peptide cyclizations

There are currently about 60 peptide-based drugs on the market, 140 in clinical trials, and about 500-600 in preclinical development.[10, 11] Octreotide, aplidine, and cyclosporin A are examples of cyclic peptide drugs on the market (**Figure 3**). Octreotide is an octapeptide that mimics the peptide hormone somatostatin, and is used for the treatment of severe diarrhea.[12] Aplidine is a cyclic depsipeptide anti-cancer agent that received approval for treatment of acute lymphoblastic leukemia by the European Commission in 2003.[13] It is currently in Phase II clinical trials for treatment of malignant neoplasms and T cell lymphoma, and in Phase III trials for multiple myeloma.[13] Finally, cyclosporin A is a cyclic undecapeptide immunosuppressant drug. Although some peptide drugs have extracellular targets due to poor membrane permeability, cyclosporin A crosses T-cell membranes by passive diffusion.[8, 14] The ability of cyclosporin A to cross cell membranes is due, in part, to the hydrophobicity of its amino acids and seven *N*-methylated amino acids within the peptide ring. These characteristics allow cyclosporin A to interact favorably with lipophilic cell membranes.

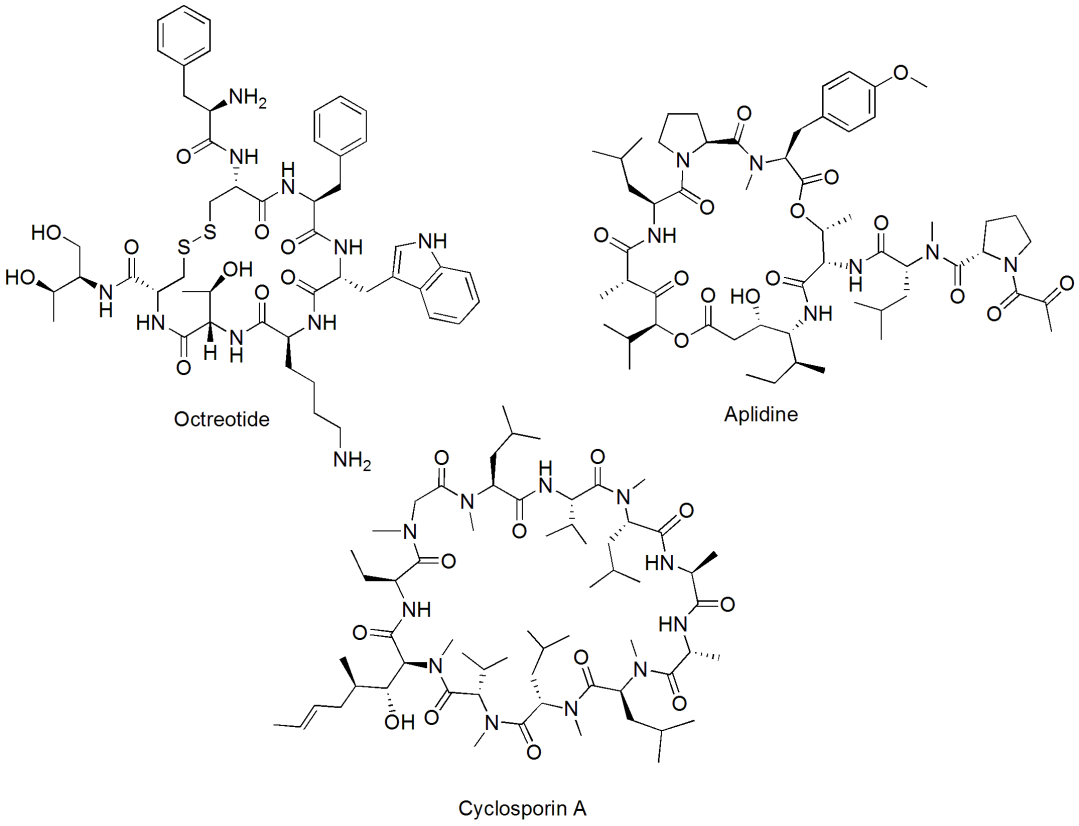

Figure 3: Structure of cyclic peptide drugs

BACKGROUND OF SANSALVAMIDE A

Sansalvamide A (SanA) is a cyclic depsipeptide that was isolated by the Fenical group in 1999 from a marine fungus of the genus *fusarium* off the coast of the Little Sansalvador Islands in the Bahamas.[15] Through extensive 1D and 2D NMR analysis, as well as with acid hydrolysis and gas chromatography (GC), they found that the peptide is composed of four amino acids (Leu, Phe, Leu, Val) and one leucic acid, all are L-amino acid configuration (**Figure 4**). As a depsipeptide, SanA contains one ester bond within the ring's backbone. In the National Cancer Institute's (NCI) 60-cell line panel, SanA exhibited a mean IC_{50} of 46.7μM. Fenical also showed that the hydrolyzed linear

pentapeptide had no cytotoxic activity in cell-based assays, which corroborates the superiority of cyclic peptides over linear peptides as potential drugs.

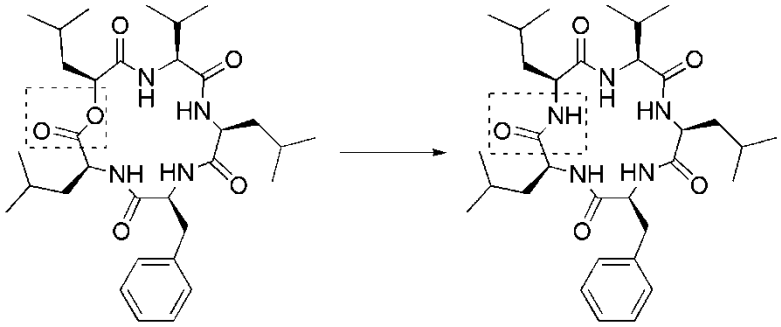

Figure 4: Structures of SanA depsipeptide and pentapeptide

In 2000, a year after SanA was discovered, the Silverman group used solid-phase synthesis to complete the first total synthesis of the SanA natural product. In addition, they verified its structure and cytotoxicity.[16] In 2002, Silverman's group synthesized the SanA pentapeptide to investigate whether the hydroxy acid (leucic acid), which was responsible for the ester bond, was essential for its bioactivity (**Figure 4**). Silverman found that the peptide exhibited 10-fold more potent activity compared to its depsipeptide counterpart.[17] Silverman's lead analogs incorporate *N*-Me amino acids and/or para-bromination on the phenylalanine residue (**Figure 5**).[18, 19] Using flow cytometry for cell cycle analysis, they found that their compounds caused G0/G1 cell cycle arrest. In addition, the compounds caused the depletion of cell cycle regulating proteins cdk4 and cdk6 in two pancreatic cancer cell lines.[19] Pancreatic cells treated with Silverman's derivative also tested positive when stained with Annexin V, meaning the compound induces apoptosis in cancer cells.[18]

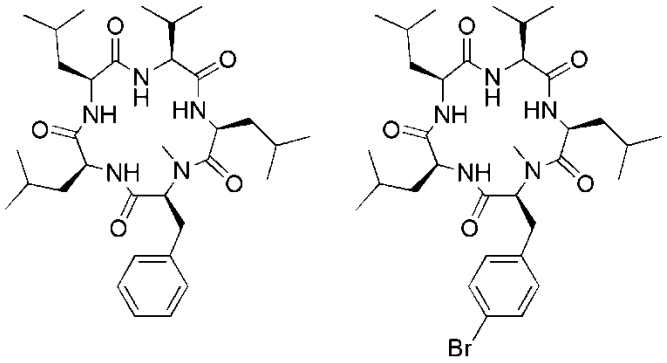

N-Methylated SanA derivative

para-brominated and *N*-Methylated SanA derivative

Figure 5: Sansalvamide A derivatives synthesized by the Silverman group

For the past seven years, our research group has focused on synthesizing potent derivatives of the SanA pentapeptide and investigating their mechanism of action. The SanA derivatives synthesized by our group incorporate D-amino acids, unnatural amino acids, and *N*-Me amino acids. The goal of these types of modifications is to improve stability and bioactivity. The SanA peptide, based on the natural product, contains all naturally-occurring L-configuration amino acids, which are easily recognized by proteases in the body and will result in rapid degradation of the compound. Incorporating D-aas and unnatural amino acids into the SanA scaffold will have several advantages: They will decrease protease recognition, increase biostability, and, ultimately, contribute to the development of SanA derivatives that are more potent as anti-cancer agents than the natural product. Including *N*-Me aas will provide proteolytic resistance, improve the pharmacological properties, and increase the structural rigidity of the cyclic peptides. Horst Kessler's group showed that incorporating single *N*-Me aas in cyclic pentapeptides locked them into single conformations. [20] A peptide locked into its bioactive conformation will bind to its target more effectively than a peptide adopting multiple

conformations. Further, Kessler's group reported that cyclic pentapeptides in single conformations have 5-fold increased membrane permeability over compounds adopting multiple conformations.[21] Finally, *N*-Me aas, like in cyclosporin A, add to the lipophilicity of macrocycles and increases their potential to cross the cell membrane.

Our group synthesized over one-hundred SanA peptide derivatives for our library that incorporate these types of modifications. As a result, we have produced four lead derivatives that all include a single *N*-Me-aa, at least one D-aa, and at least one unnatural amino acid. Mechanistic studies involving these SanA derivatives reveal that SanA acts via inhibition of heat shock protein 90 (Hsp90).

HEAT SHOCK PROTEIN 90

Hsp90 is a highly conserved chaperone protein that is associated with the folding, maturation, and stabilization of over 200 client proteins, many of which are oncogenic and involved in cancer cell growth.[22-26] In normal cells, Hsp90 consists of 1-2% of total cellular protein. In cancerous cells, this amount increases to 3-6% as the cells become more reliant on Hsp90 to protect mutated and over-expressed oncoproteins from degradation.[27, 28] Hsp90 is an adenosine triphosphate (ATP)-dependent protein that is expressed in the cytosol as two isoforms: Hsp90α and Hsp90β. The two isoforms share 85% sequence homology and they both appear to have the same function within the cytosol. [29] However, the recent discovery of extracellular Hsp90α has elicited a new role for this isoform in tumor cell motility and invasion.[30, 31] Cytosolic Hsp90α and Hsp90β both fold and stabilize oncogenic proteins in conjunction with co-chaperones. Co-chaperones are proteins that form complexes with Hsp90 and its clients, stabilize Hsp90's ATP-dependent conformations, and facilitate ATPase activity. Without these co-

chaperones, Hsp90 would not function, thus they are essential to the protein folding and stabilizing mechanism. Interestingly, the Hsp90 homologues located in the endoplasmic reticulum (glucose-related protein 94, GRP94) and mitochondria (tumour necrosis factor receptor-associated protein 1, TRAP1) appear to have ATP-dependent protein folding mechanisms, but no co-chaperones. [32-34] However, by lacking co-chaperones, GRP94 and TRAP1 do not regulate the same oncogenic proteins as cytosolic Hsp90.[35, 36] Instead, GRP94's main role is folding proteins that are involved in the immune response.[35] And TRAP1 is responsible for protecting the integrity of the mitochondria under stress.[37] Thus, Hsp90α and Hsp90β remain the main targets in developing Hsp90 inhibitors due to their association with oncogenic client proteins and pathways.

Hsp90 functions as a dimer, and each 90-kilodalton (kDa) monomer has three domains: an amino-terminal (N) domain, a middle (M) domain, and a carboxy-terminal (C) domain (**Figure 6**). The N-domain houses the ATP-binding pocket and is also responsible for binding to key co-chaperones including p23, activator of Hsp90 ATPase (Aha1), and cell division cycle 37 homolog (cdc37), which are involved in ATPase activity and kinase stability, respectively.[25, 38] The M-domain maintains interactions with most client proteins, many of which contribute to the six hallmarks of cancer: cell growth, angiogenesis, apoptosis, metastasis, immortality, and regulation of the cell cycle.[39] Examples of these oncogenic clients are shown in **Figure 6**. Interestingly, cdk4 and cdk6, which were shown by Silverman to be depleted in cells treated with their SanA derivatives, are associated with Hsp90.[19] The C-domain is responsible for dimerization of two 90-kDa monomers. In addition, the last five amino acids in the C-domain

(MEEVD) regulate binding to co-chaperones that contain tetratricopeptide repeats (TPRs). This interaction will be discussed in detail in Chapter 4.

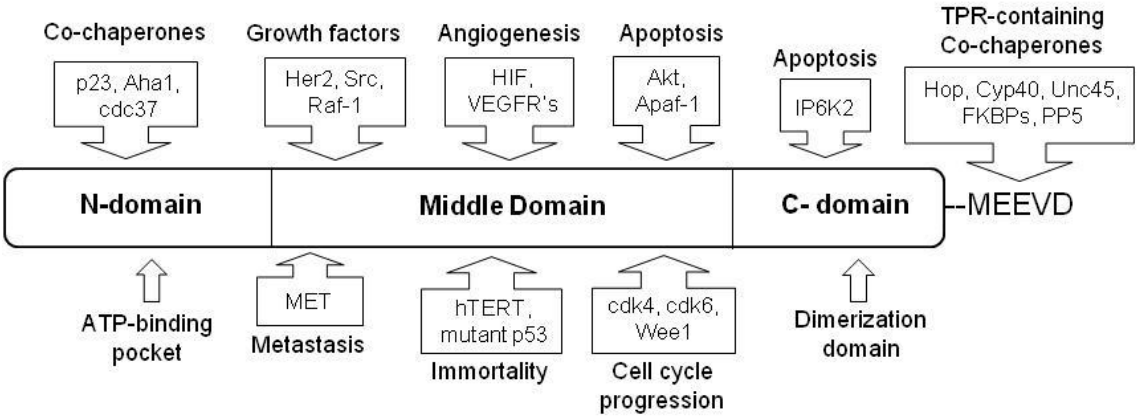

Figure 6: Schematic of Hsp90 domains and some of its client proteins and co-chaperones

In protein folding and maturation, Hsp90 functions with several co-chaperones, including heat shock protein 70 (Hsp70), heat shock organizing protein (Hop), p23, cdc37, Aha1, and the immunophilins. Hsp90 goes through a complex cycle involving a variety of ATP-dependent conformations (**Figure 7**).[25, 40] First, HOP facilitates the binding between Hsp70 and Hsp90, which allows the transfer of unfolded polypeptide from Hsp70 to Hsp90 (**1**). When C-domain co-chaperones bind, the Hsp70 complex is released (**2**). Next, ATP molecules bind to the pockets in both N-domains (**3**), which cause the dimer to move into a closed-twisted conformation (**4**). The co-chaperone p23 binds to Hsp90 and stabilizes the newly formed closed-twisted conformation (**5**). Aha1 facilitates the hydrolysis of ATP to ADP, which results in Hsp90 becoming a compact closed-twisted conformation (**6**). The last step of the cycle is the release of the mature, folded protein (**7**).

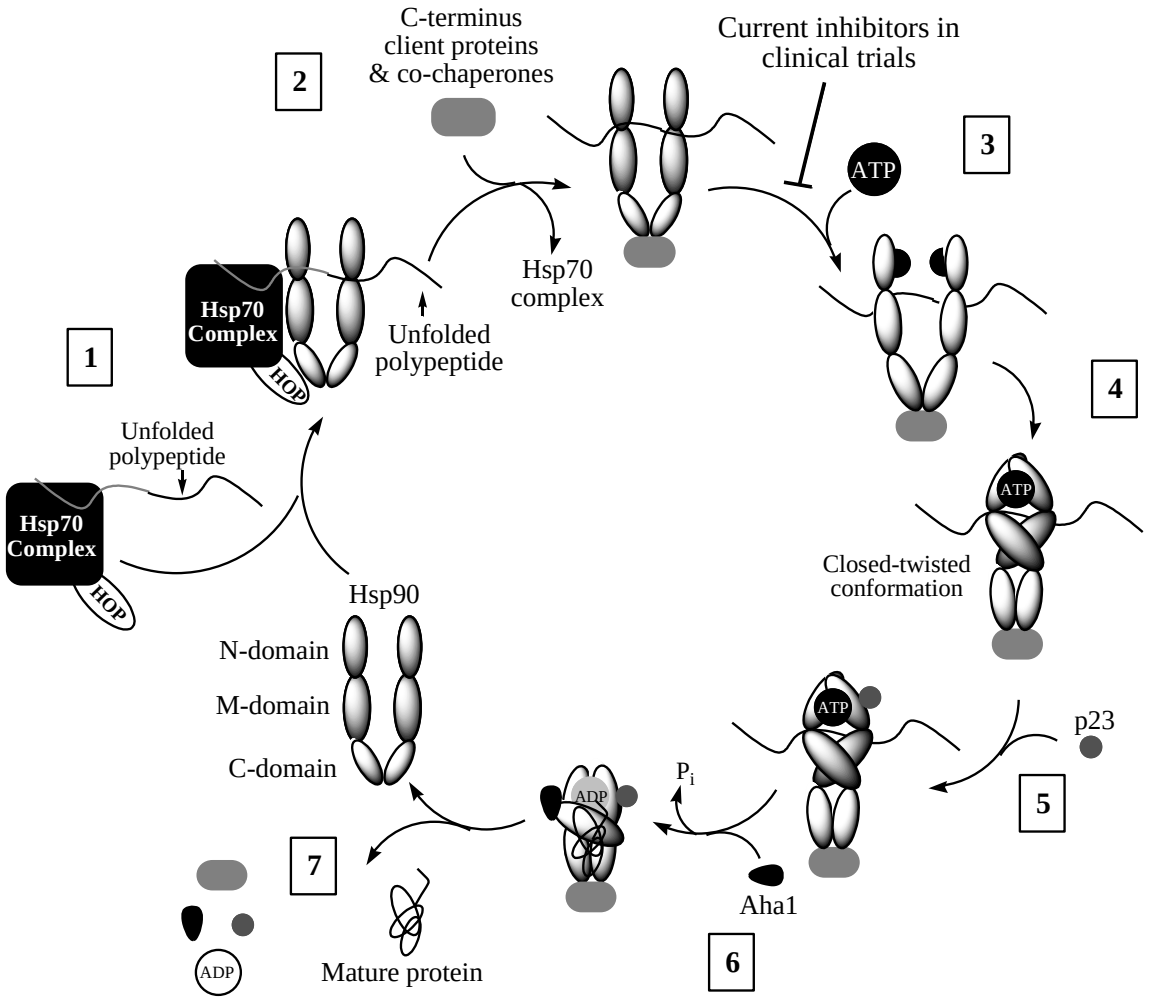

Figure 7: Diagram of Hsp90's protein folding mechanism

There are two main types of Hsp90 inhibitors. The first type competes with ATP for binding to the ATP pocket in the N-domain, thus disrupting Hsp90's ATP-dependent activity and, ultimately, its function (**Figure 7**).[41, 42] The second type of inhibitor binds to the C-domain and disrupts dimerization.[40] All 17 of the Hsp90 inhibitors in clinical trials bind to the N-domain.[43] The compound furthest along in trials is the ansamycin 17-*N*-Allylamino-17-demethoxygeldanamycin (17-AAG), which is in Phase II/III trials for the treatment of several types of cancer including breast, prostate, and thyroid cancers, as

well as leukemia and late-stage melanoma (**Figure 8**).[44] 17-AAG is a derivative of geldanamycin (GDA), a natural product that was discovered for its ability to compete with ATP for binding to Hsp90.[45] GDA's clinical development was ceased due to metabolic instability and unacceptable levels of hepatotoxicity. The presence of a reactive methoxy-substituted benzoquinone moiety in the ring contributed to GDA's poor pre-clinical activity.[46] When metabolized by liver enzymes, GDA can form reactive free radicals and induce hepatoxicity.[47] In 17-AAG, the electron-donating effects of the *N*-allyl group on the benzoquinone resulted in a decrease in radical formation compared to GDA when tested *in vitro*.[47] In addition, 17-AAG demonstrates increased potency over GDA in the NCI 60-cell line panel (123 nM versus 180 nM , respectively) and decreased toxicity in clinical trials.[48, 49]

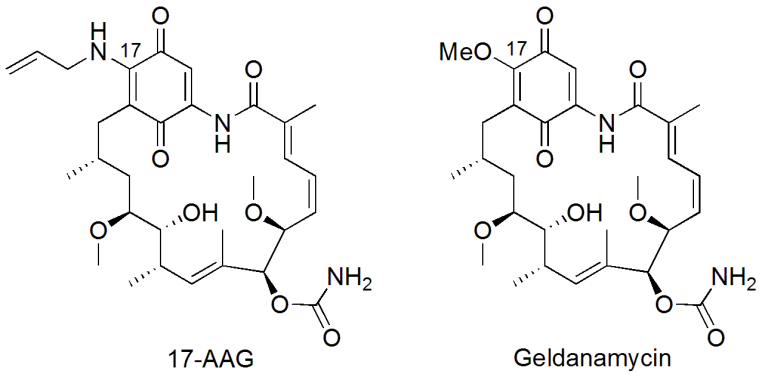

Figure 8: Structures of current Hsp90 inhibitors 17-AAG and Geldanamycin

Despite the number of drug candidates in clinical trials, none have obtained marketing approval yet, primarily due to formulation challenges and drug resistance seen in patients. Drug resistance is primarily caused by the activation of heat shock factor 1 (HSF-1) and subsequent over-expression of Hsp70.[50] HSF-1 is responsible for regulating the expression of the heat shock proteins when cells are under stress.[51] And Hsp70

compensates for Hsp90's protein folding and stabilizing function, and prevents cells from undergoing apoptosis. When Hsp90-inhibiting therapeutics are present in cells, they prevent Hsp90 from stabilizing and folding client proteins.[52, 53] This leads to stressed cells that respond by activating HSF-1, which causes the upregulation of Hsp70. Since Hsp70 can take over Hsp90's role, the cells are able to survive. The over-expression of HSF-1 and Hsp70 has decreased the efficacy of Hsp90 inhibitors in clinical trials, calling for a new approach to Hsp90 inhibition.[43]

CHAPTER 2: RATIONAL DESIGN AND SYNTHESIS OF SANSALVAMIDE A DERIVATIVES

The natural product-based Sansalvamide A peptide (SanA **1**) is composed of five L-amino acids. Our lab has developed a structure-activity relationship (SAR) for this class of molecules by making changes to the amino acid side chains while maintaining the pentapeptide backbone. We have designated each amino acid around the ring as position/residue I, II, III, IV, and V (**Figure 9**). Examples of amino acids incorporated into the derivatives for the SAR study are shown: D- configuration (D-aas), *N*-methylated (*N*-Me-aas), polar, non-polar, bulky, and small. Inclusion of D-aas protects the peptide against proteolytic breakdown.[6, 54, 55] *N*-Me-aas decrease the flexibility of peptides and lock them into single or minimal conformations, ultimately increasing their effectiveness in binding to their targets.[20] Including polar amino acids or those with hydrogen-bonding capabilities improves solubility of the peptide by solvating the compound.[56] In making decisions regarding amino acid substitutions, it was important to maintain an aromatic group at position I. Not only are aromatic moieties present in many peptide-based drugs, this amino acid appeared to play a key role in the symmetry of the peptide.[57] Via the synthesis of SanA analogs, our goal was to explore which amino acids most effectively improved growth inhibition activity when placed in positions I-V over that of SanA **1** activity.

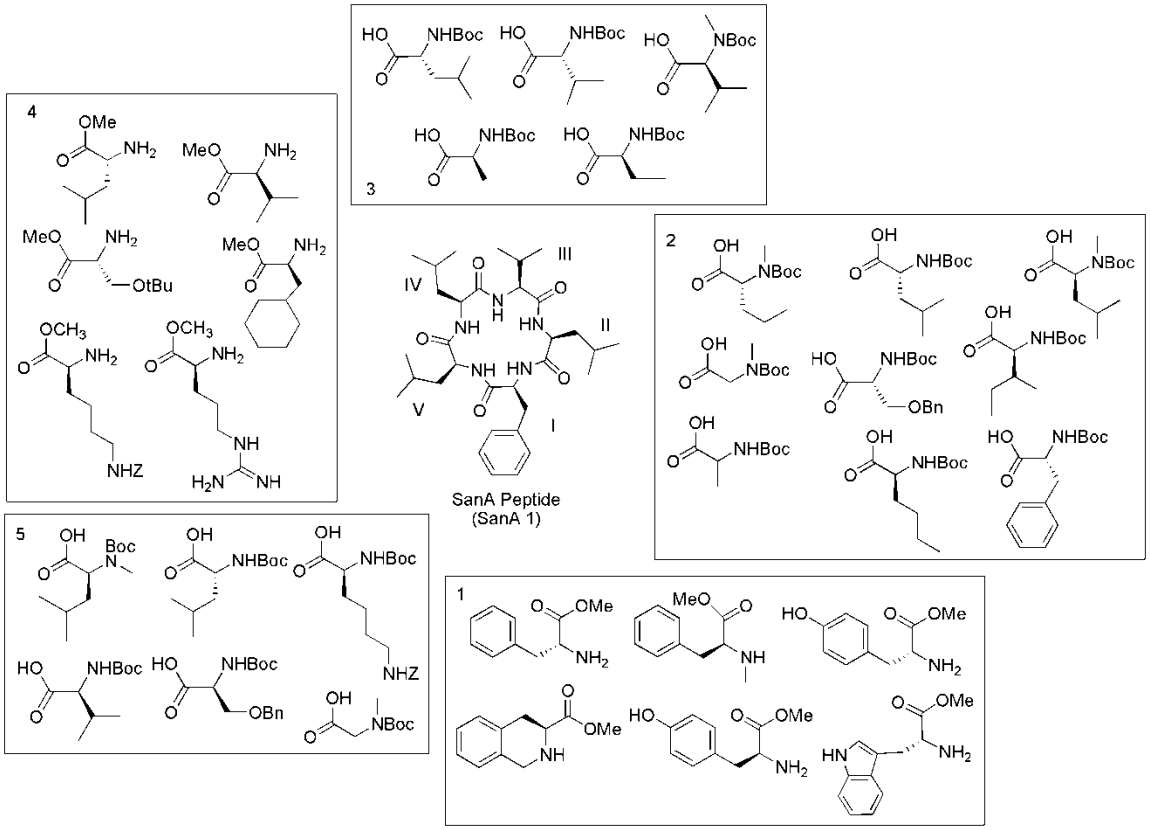

Figure 9: Sample of amino acids used in SanA SAR analysis

I contributed five compounds to the SanA peptide library. I made four starting from commercially-available amino acids, and one from a protected linear pentapeptide that was generated by colleague whereupon I deprotected, cyclized, and purified the SanA compound. The first three compounds were derived directly from SanA **1**, and all three had changes made at position I. In place of SanA **1**'s L-phenylalanine, SanA **2** incorporated a D-phenylalanine, SanA **3** had an *N*-methylated L-phenylalanine, and SanA **4** contained a D-tyrosine residue (**Figure 10**).

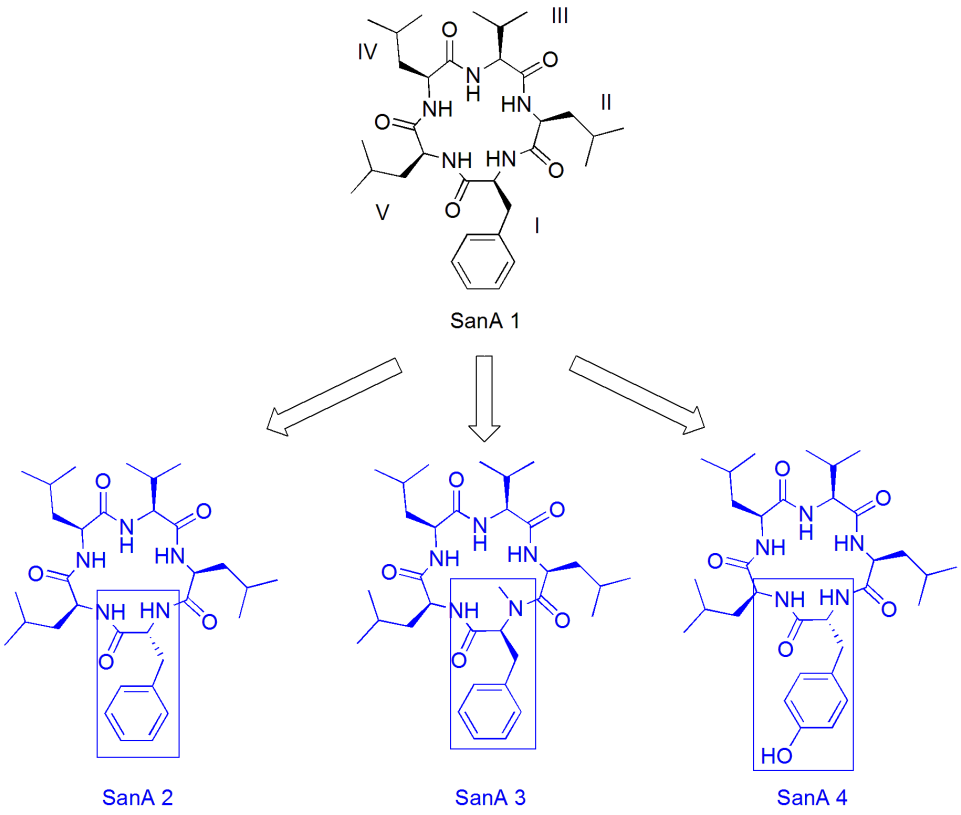

<u>Figure 10</u>: Rational design of SanA 2, 3, and 4. Note: Compounds colored blue were synthesized by the author.

The other two compounds that I contributed, SanA **8** and **9,** were designed at later stages in the project. They incorporated features from SanA derivatives that were more potent than SanA **1** in cytotoxicity assays against cancer cells. The goal of these two later-stage compounds was to investigate synergistic effects by combining the features of two potent compounds into one. The two D-aas in SanA **8** were derived from a combination of SanA **2**, mentioned earlier with the D-aa at position I, and SanA **5**, which contained a D-leucine at position II (**Figure 11**). SanA **9** was designed from SanA **6** and **7**. SanA **6** contains a D-phenylalanine at position II, whereas SanA **7** has a D-valine at position III (**Figure 11**).

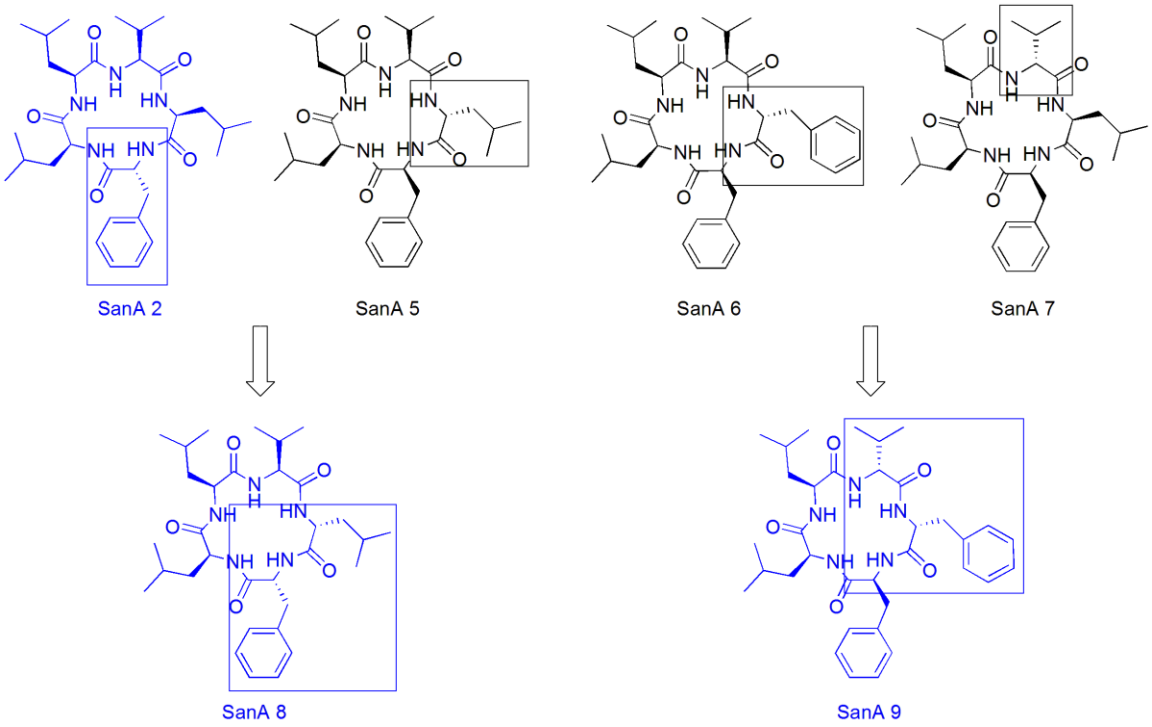

<u>Figure 11</u>: Rational design of SanA 8 and 9. Note: Compounds colored blue were synthesized by the author. Those colored black were synthesized by the author's colleagues.

RETROSYNTHETIC APPROACH FOR SANA SYNTHESIS

A convergent, two-fragment approach was taken for the synthesis of these SanA derivatives (**Figure 12**). **Fragment 1** is a tripeptide consisting of amino acids at positions I, II, and III, while **Fragment 2** is a dipeptide consisting of residues IV and V. Coupling residues III and IV, followed by deprotection of the amine- and acid-protecting groups, generates the linear peptide. Cyclization generates the final SanA analog. Using a convergent approach instead of a sequentially coupling each amino acid is beneficial in many ways. Purification and solubility of peptides becomes increasingly more difficult as the chain gets longer, synthesizing two fragments allows us to work with small, soluble peptide fragments for most of the synthesis, and avoids an additional step that

would require generation and purification of the tetrapeptide chain. Further, forming two fragments gives us the freedom to use a combinatorial strategy, where one batch of dipeptides can be split up and coupled to a variety of tripeptides, and vice versa. Utilizing a combinatorial strategy allows us to efficiently generate a diverse library of compounds.

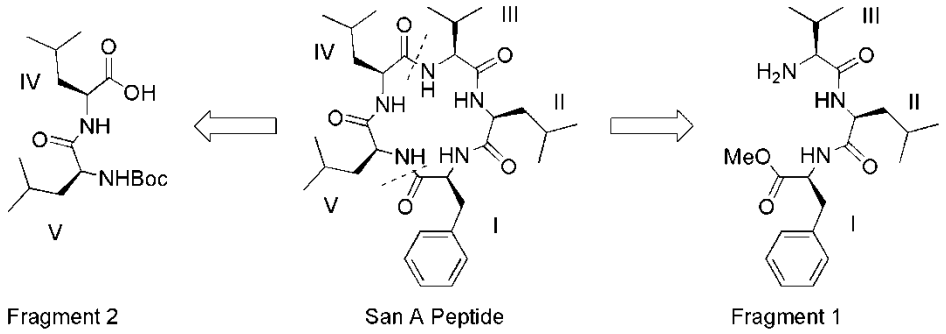

Figure 12: Retrosynthesis of SanA derivatives

SOLUTION-PHASE PEPTIDE SYNTHESIS AND MACROCYCLIZATION

The formation of peptide bonds is necessary for survival. Proteins are crucial for life, and since amino acids are building blocks for proteins the formation of an amide bond to generate proteins is essential in living species. While organisms form amide bonds via ribosomes or enzymes, chemists have created coupling reagents to aid in the reaction. In traditional chemical synthesis, the formation of a peptide bond begins by reacting the free carboxylic acid of an amino acid with a coupling reagent to form an activated ester (**Figure 13**). The carbonyl group of the acid is then susceptible when activated as an ester, versus as a free acid, to nucleophilic attack by the free amine of another amino acid.

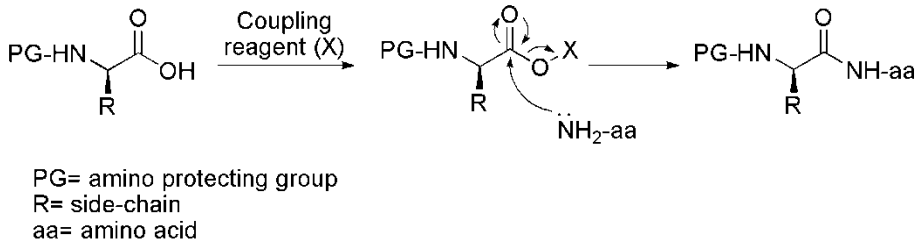

Figure 13: General mechanism of peptide coupling

Racemization can be a problem during peptide coupling. After the acid-activation, the carbonyl carbon can participate in an intramolecular oxazolone formation with the adjacent amide (**Figure 14**). Upon nucleophilic attack of the free amine on the oxazolone, there are two possible configurations that can be generated. In order to avoid this significant issue, coupling reagents have been optimized to increase the rate of the reaction, which decreases the chance of oxazolone formation and subsequent racemization. Thus, new reagents such as HBTU, HATU, DEPBT, and PyBOP are typically marketed as having less than 1-5% racemization occurring in certain reaction conditions thereby increasing overall yield and enantiomeric purity.

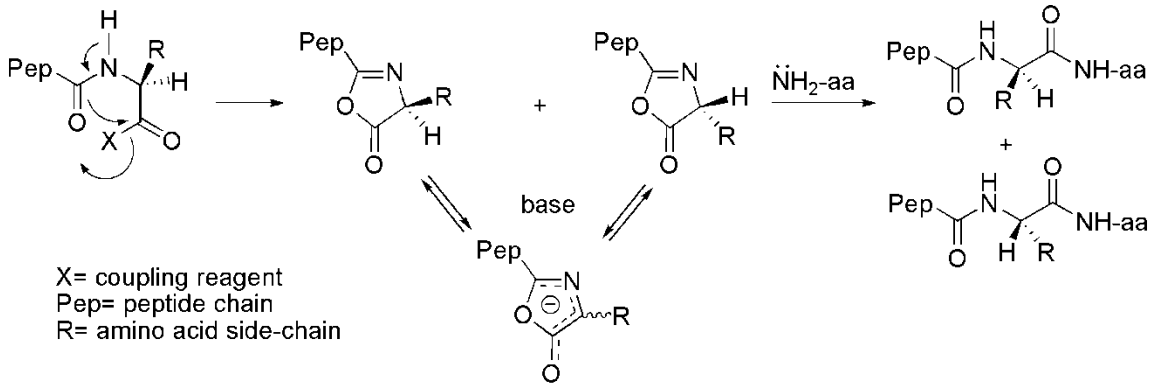

Figure 14: Mechanism of racemization that can occur during peptide coupling

There are approximately 100 coupling reagents available, each with unique reactivity, physical characteristics, and cost.[58] Unlike solid-support peptide synthesis,

which will be discussed later in this chapter, solution-phase chemistry does not use an excess of reagents, therefore it is preferable to utilize the least amount of the most effective coupling reagent in order to push the reaction to completion while limiting purification efforts. We use three main coupling reagents in our solution-phase synthesis 2-(1H-Benzotriazole-1-yl)-1,1,3,3-tetramethyluronium tetrafluoroborate (TBTU), O-(7-Azabenzotriazol-1-yl)-N,N,N',N'-tetramethyluronium hexafluorophosphate (HATU), and 3-(Diethylphosphoryloxy)-1,2,3-benzotriazin-4(3H)-one (DEPBT) (**Figure 15**). TBTU, one of the most popular and cost-effective coupling reagents, has been shown to significantly minimize racemization during peptide coupling.[59] HATU contains an azabenzotriazole ring that makes it one of the most efficient reagents due to its ability to act as an intramolecular base, which leads to racemization rates of less than 1%.[60] HATU is excellent for sterically hindered couplings, but is also very costly.[61] DEPBT has been shown to help prevent racemization and aid in the coupling of side-chains with free reactive groups.[62] Further, DEPBT is a neutral reagent, existing as hygroscopic salt, and has a longer shelf-life than TBTU or HATU. All of our couplings and cyclizations occur in the presence of a non-nucleophilic tertiary base, diisopropylethylamine (DIPEA), and utilize Boc-protected or MeO-protected amino acids.

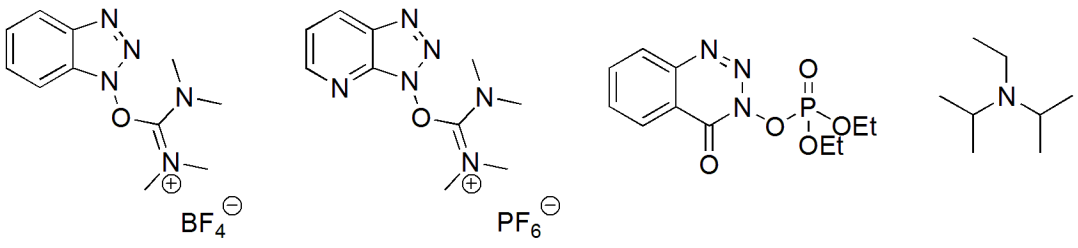

<u>Figure 15</u>: Coupling reagents used in solution-phase synthesis of SanA derivatives

SYNTHESIS OF FRAGMENT 1 FOR SANA 2, 8, AND 9

The synthesis of **Fragment 1** for SanA **2** (**Figure 16**) started with the formation of the dipeptide MeO-D-Phe-Leu-NHBoc using 1.1 equivalents of free amine MeO-D-Phe-NH_2, 1.0 equivalent of free acid HO-Leu-NHBoc and our standard peptide coupling conditions of 1.2 equivalents of coupling reagent TBTU and 4.0 equivalents of base DIPEA. The amino acids and coupling reagent were weighed out and added to a round-bottom flask, which was then purged with argon gas. Dry methylene chloride (DCM) was added to the flask for a final concentration of 0.1M, and the dry reagents were stirred until completely dissolved. After the addition of DIPEA, the reaction was allowed to run at room temperature for one hour and was monitored by thin-layer chromatography (TLC). Once complete, the reaction was diluted using DCM and a separatory funnel and the excess base and coupling reagents were extracted using two washes of 10% hydrochloric acid (HCl), ten washes of saturated sodium bicarbonate ($NaHCO_3$), and two washes of brine. The organic layer was then dried over sodium sulfate, filtered, and concentrated *in vacuo*. The pure dipeptide (MeO-D-Phe-Leu-NHBoc, 96.0% yield) was verified by ^{1}H NMR. The same conditions were used for the synthesis of **Fragment 1** dipeptides for SanA **8** (MeO-D-Phe-D-Leu-NHBoc, 98.7% yield) and **9** (MeO-Phe-D-Phe-NHBoc, 98.9% yield).

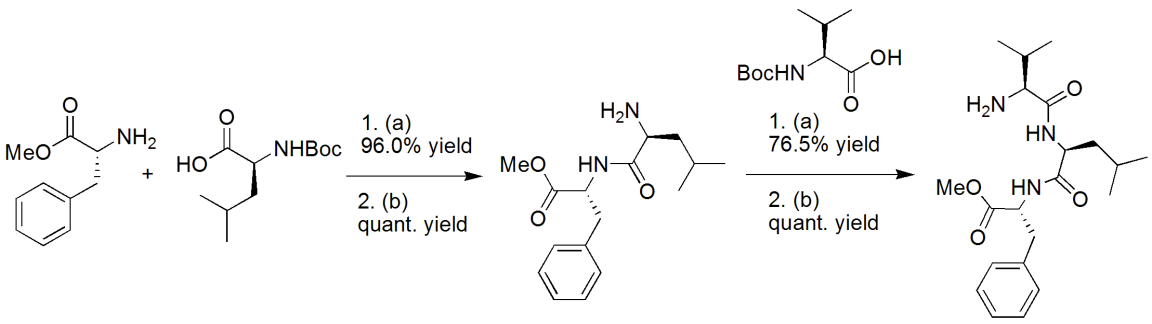

Conditions: (a) 1.0 eq free acid, 1.1 eq free amine, 1.2 eq TBTU, 4.0 eq DIPEA, 0.1M DCM (b) 1.0 eq peptide, 2.0 eq anisole, 0.1M DCM/TFA (3:1)

Figure 16: Synthesis of Fragment 1 for SanA 2

The removal of the Boc-protecting group from SanA **2** dipeptide MeO-D-Phe-Leu-NHBoc was performed using our standard Boc removal conditions. A solution of 25% trifluoroacetic acid (TFA) and 75% DCM was added to a round-bottom flask to generate a final concentration of 0.1M of the dipeptide. Scavenging reagent, anisole (2.0 equivalents), was subsequently added and the reaction was allowed to run at room temperature for 45 minutes. The reaction was monitored by TLC, where upon reaction completion, it was concentrated *in vacuo* to give the free amine dipeptide (MeO-D-Phe-Leu-NH_2) in a quantitative yield. The same steps were taken to generate free amine dipeptides for SanA **8** (MeO-D-Phe-D-Leu-NH_2) and **9** (MeO-Phe-D-Phe-NH_2).

The tripeptide for SanA **2** was synthesized utilizing 1.2 equivalents of the free amine dipeptide MeO-D-Phe-Leu-NH_2 generated above, 1.0 equivalent of free acid HO-Val-NHBoc, 1.2 equivalents of coupling reagent TBTU, and 4.0 equivalents of DIPEA. The dipeptide, amino acid, and coupling reagent were added to a round-bottom flask that was then capped and purged with argon gas. Dry DCM was added until a final concentration of 0.1M was reached, and the solid reagents were dissolved completely. After addition of DIPEA, the reaction ran for 1 hour at room temperature and was

monitored by TLC. Once complete, it was diluted in DCM and the excess reagents were extracted using two washes of 10% HCl, ten washes of saturated $NaHCO_3$, and two washes of brine. The organic layer was then dried over sodium sulfate, filtered, and concentrated *in vacuo*. The pure tripeptide (MeO-D-Phe-Leu-Val-NHBoc, 76.5% yield) was verified by ^1H NMR. The same procedure was used to form tripeptides for SanA **8** (MeO-D-Phe-D-Leu-Val-NHBoc, 97.2% yield) and **9** (MeO-Phe-D-Phe-D-Val-NHBoc, 98.9% yield).

The final step in the formation of **Fragment 1** for SanA **2** was the removal of the Boc protecting group from the protected tripeptide. Under open atmosphere, a solution of 25% TFA and 75% DCM was added to generate a final concentration of 0.1M of the tripeptide. Scavenging reagent, anisole (2.0 equivalents), was subsequently added and the reaction was allowed to run at room temperature for 45 minutes. The reaction was monitored by TLC. Upon reaction completion, it was concentrated *in vacuo* to give **Fragment 1** free amine tripeptide MeO-D-Phe-Leu-Val-NH_2 in a quantitative yield. The same procedure was used to form **Fragment 1** in quantitative yields for SanA **8** (MeO-D-Phe-D-Leu-NH_2) and **9** (MeO-Phe-D-Phe-D-Val-NH_2).

SYNTHESIS OF FRAGMENT 1 FOR SANA 4

For the synthesis of the dipeptide in SanA **4** (**Figure 17**), DEPBT was used as a coupling reagent since it is not necessary to protect the free hydroxyl group on the tyrosine amino acid.[62] Tyrosine's side-chain is slightly nucleophilic, and can compete with a free amine by reacting with an activated ester, resulting in side-reactions. However, it has been shown that free hydroxyl-containing side-chains do not react with DEPBT-containing activated esters, thus allowing for the free amines to react and form

an amide bond.[63] The synthesis of dipeptide MeO-D-Tyr-Leu-NHBoc for SanA **4** included 1.1 equivalents of free amine MeO-D-Tyr-NH_2, 1.0 equivalents of free acid HO-Leu-NHBoc, 1.2 equivalents of DEPBT, and 4.0 equivalents of DIPEA. The amino acids and coupling reagent were weighed into a round-bottom flask that was then capped and purged with argon gas. Dry DCM was added to the flask for a final concentration of 0.1M and the dry reagents were allowed to dissolve completely. After the addition of DIPEA, the reaction was allowed to run for 1.5 hours and was monitored by TLC. Once complete, the reaction was diluted in DCM, subjected to two aqueous washes of brine, dried over sodium sulfate and concentrated *in vacuo*. The crude material was purified via flash column chromatography using an ethyl acetate (EA) and hexanes (Hex) gradient solvent system. The product eluted at 50:50 EA:Hex and was concentrated *in vacuo*. Finally, the pure dipeptide (MeO-D-Tyr-Leu-NHBoc, 85% yield) was verified by ^{1}H NMR.

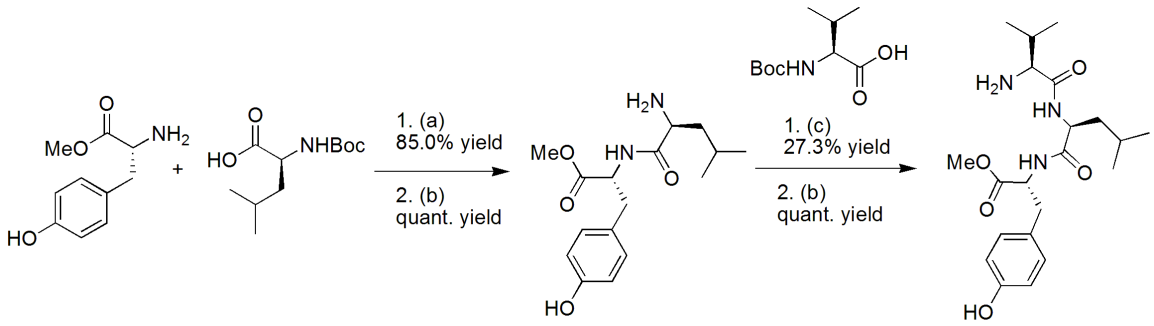

Conditions: (a) 1.0 eq free acid, 1.1 eq free amine, 1.2 eq DEPBT, 4.0 eq DIPEA, 0.1M DCM (b) 1.0 eq peptide, 2.0 eq anisole, 0.1M DCM/TFA (3:1) (c) 1.0 eq free acid, 1.1 eq free amine, 1.2 eq TBTU, 4.0 eq DIPEA, 0.1M DCM

Figure 17: Synthesis of Fragment 1 for SanA 4

The Boc protecting group was removed from dipeptide MeO-D-Tyr-Leu-NHBoc using our standard Boc removal conditions. Under open atmosphere, a solution of 25% TFA and 75% DCM was added to generate a final concentration of 0.1M of the

dipeptide. Scavenging reagent, anisole (2.0 equivalents), was subsequently added and the reaction was allowed to run at room temperature for 45 minutes. The reaction was monitored by TLC. Upon reaction completion, it was concentrated *in vacuo* to give the free amine dipeptide (MeO-D-Tyr-Leu-NH_2) in a quantitative yield.

The tripeptide for SanA **4** was synthesized utilizing 1.1 equivalents of the free amine dipeptide from above, 1.0 equivalent of HO-Val-NHBoc, and 1.2 equivalents of TBTU in a round-bottom flask. Due to solubility issues, dry acetonitrile (ACN) was added to the flask for a final concentration of 0.1M, instead of DCM. Once all the dry reagents dissolved completely, DIPEA was added and the reaction was allowed to run at room temperature for 1 hour while being monitored by TLC. Upon completion, the reaction was diluted in DCM, treated with two aqueous washes of brine, dried over sodium sulfate, and concentrated *in vacuo*. The crude product was purified via flash column chromatography using an EA/Hex gradient solvent system where the pure product eluted at 65:35 EA:Hex and was collected and concentrated *in vacuo*. The pure tripeptide (MeO-D-Tyr-Leu-Val-NHBoc, 27% yield) was verified by ^{1}H NMR and LCMS.

Finally, removal of the Boc from the above tripeptide was achieved in a 0.1M solution of 25% TFA and 75% DCM, with 2 equivalents of anisole. The reaction was allowed to run at room temperature for 45 minutes and was monitored by TLC. Once complete, the reaction was concentrated *in vacuo* to give **Fragment 1** for SanA **4** (MeO-D-Tyr-Leu-Val-NH_2) in a quantitative yield.

SYNTHESIS OF FRAGMENT 2 FOR 2, 4, 8, AND 9

Fragment 2 was identical for all four compounds (HO-Leu-Leu-NHBoc) and utilized identical synthetic conditions (**Figure 18**). First, the dipeptide for **Fragment 2** was formed using 1.1 equivalents of MeO-Leu-NH_2, 1.0 equivalent of HO-Leu-NHBoc, and 1.2 equivalents of TBTU. The dry reagents were added to a round-bottom flask, which was subsequently capped and purged with argon gas. Dry DCM was added to give a final concentration of 0.1M, followed by the addition of 4.0 equivalents of DIPEA. The reaction was allowed to run at room temperature for 1 hour and was monitored by TLC. Upon completion, the reaction was diluted with EA and was subjected to two washes of 10% HCl, ten washes of saturated sodium bicarbonate, and two washes of brine. The organic layer was then collected, dried over sodium sulfate, and concentrated *in vacuo* to give pure dipeptide MeO-Leu-Leu-NHBoc (96-99% yield for all reactions), which was verified by ^{1}H NMR.

The final step in the formation of **Fragment 2** is the hydrolysis of the methyl ester on dipeptide MeO-Leu-Leu-NHBoc. To a flask containing 1.0 equivalent of dipeptide and 8.0 equivalents of lithium hydroxide (LiOH) under open atmosphere, methanol (MeOH) was added until the final concentration was 0.1M. The reaction was was monitored by TLC. Once complete (~1hr), the reaction was transferred to a separatory funnel, diluted in DCM, and treated with pH 1 water to extract the excess base. After verifying that the aqueous layer was acidic (pH~1-3), the product was extracted with DCM, dried over sodium sulfate, and concentrated *in vacuo* to give the pure dipeptide **Fragment 2** HO-Leu-Leu-NHBoc (80-95% yield for all reactions).

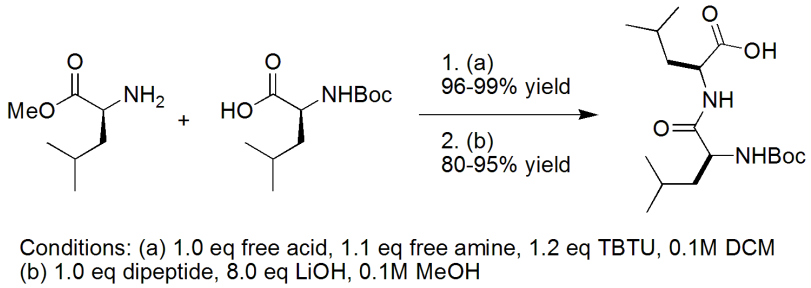

Conditions: (a) 1.0 eq free acid, 1.1 eq free amine, 1.2 eq TBTU, 0.1M DCM
(b) 1.0 eq dipeptide, 8.0 eq LiOH, 0.1M MeOH

Figure 18: Synthesis of Fragment 2 for all compounds

FORMATION OF PROTECTED LINEAR PENTAPEPTIDES

The protected linear pentapeptides (**PLP**s) for SanA **2**, **4**, **8**, and **9** were synthesized utilizing 1.1 equivalents of free amine tripeptide (**Fragment 1**) and 1.0 equivalent of free acid dipeptide (**Fragment 2**). A combination of 0.5-0.8 equivalents of HATU, 0.8 equivalents of TBTU, and 0-0.4 equivalents of DEPBT as coupling reagents were added to the two fragments, and these were dissolved in a 0.1M mixture of dry DCM and dry ACN (1:1, v/v) (**Figure 19**). Given the solubility challenges associated with the formation of linear pentapeptides, both DCM and ACN were used as solvents. **Fragment 2** and the coupling regents were weighed out into a round-bottom flask, which was subsequently purged with argon gas, and dissolved in half of the solvent volume. **Fragment 1** was placed in a separate round-bottom flask, which was purged with argon, and dissolved in the remaining volume of solvent. **Fragment 1** was then transferred via syringe to the flask containing **Fragment 2** and the coupling reagents. After 4.0-8.0 equivalents of DIPEA were added, the reactions were allowed to run for 1-2 hours at room temperature while being monitored by TLC and liquid chromatography/mass spectroscopy (LCMS). Upon completion, the crude material was diluted in DCM and the excess reagents were extracted with two washes of 10% HCl, four washes of saturated sodium bicarbonate, and two washes of saturated sodium chloride. The organic layers

were dried over sodium sulfate, concentrated *in vacuo*, and purities were checked by LCMS and TLC. The **PLP** for SanA **4** was found to be pure after the aqueous work-up and its structure was verified by ^{1}H NMR (**PLP 4**, MeO-D-Tyr-Leu-Val-Leu-Leu-NHBoc, 68.3% yield). SanA **2**, **8**, and **9** were further purified via flash column chromatography using an EA/Hex gradient solvent system where the pure products eluted at 75:25 EA:Hex and were concentrated *in vacuo*. The pure **PLP**s (**PLP 2**, MeO-D-Phe-Leu-Val-Leu-Leu-NHBoc, 10.2% yield; **PLP 8**, MeO-D-Phe-D-Leu-Val-Leu-Leu-NHBoc, 58.5% yield; **PLP 9**, MeO-Phe-D-Phe-D-Val-Leu-Leu-NHBoc, 80.8% yield) were verified by ^{1}H NMR and LCMS.

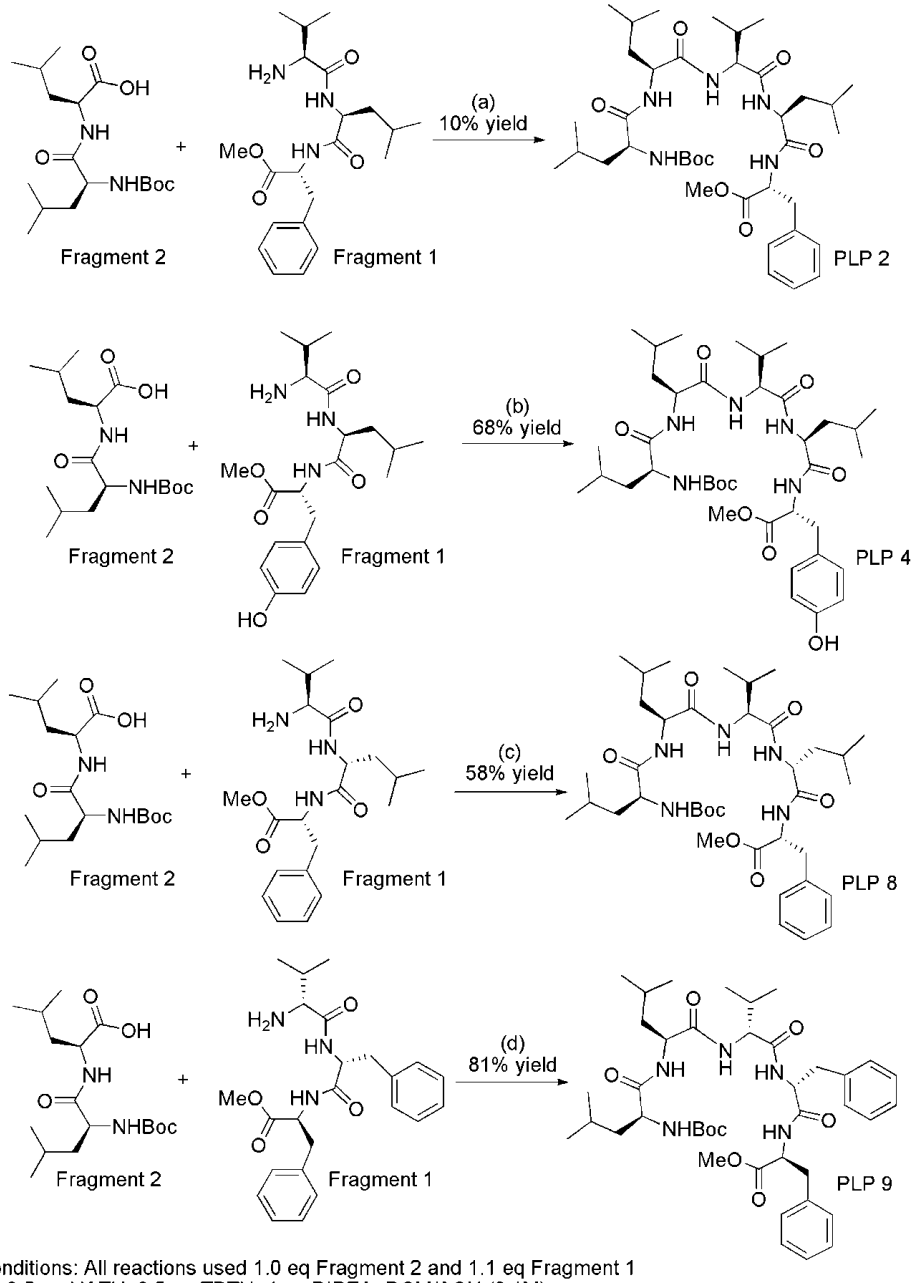

Figure 19: Formation of protected linear pentapeptides

DOUBLE-DEPROTECTION OF LINEAR PENTAPEPTIDES

The double-deprotections of **PLP**s for SanA **2**, **3**, **8**, and **9** were done in a two-step fashion where the methyl ester hydrolysis was performed first, followed by Boc removal

from the N-terminal residue. The acid deprotection followed our standard protocol where 1.0 equivalent of **PLP** was placed in a round-bottom flask, under open atmosphere, with 8.0 equivalents of LiOH. The dry reagents were dissolved in MeOH with a final concentration of 0.1M. The reaction was allowed to run overnight at room temperature. Upon completion of the reaction, verified by TLC, it was diluted in DCM and pH 1 aqueous solution was added until the aqueous layer was acidic (pH~1-3). The organic layer was collected, dried over sodium sulfate, and concentrated *in vacuo* to give the acid-deprotected pentapeptides: (HO-D-Phe-Leu-Val-Leu-Leu-NHBoc, 73% yield; HO-NMe-Phe-Leu-Val-Leu-Leu-NHBoc, 95% yield; HO-D-Phe-D-Leu-Val-Leu-Leu-NHBoc, 82% yield; HO-Phe-D-Phe-D-Val-Leu-Leu-NHBoc, 98% yield). Each pentapeptide was then dissolved in a solution of 25% TFA and 75% DCM, at 0.1M, with 2.0 equivalents of anisole. The reactions were allowed to run under open atmosphere at room temperature for 1 hour and were monitored by TLC. Once complete, the reactions were concentrated *in vacuo* to give double-deprotected linear pentapeptides (**DDLP**s) in quantative yields: HO-D-Phe-Leu-Val-Leu-Leu-NH_2 (**DDLP 2, Figure 20**); HO-NMe-Phe-Leu-Val-Leu-Leu-NH_2 (**DDLP 3, Figure 20**); HO-D-Phe-D-Leu-Val-Leu-Leu-NH_2, (**DDLP 8, Figure 21)**; HO-Phe-D-Phe-D-Val-Leu-Leu-NH_2 (**DDLP 9**, **Figure 22**).

The formation of double-deprotected linear pentapeptide for SanA **4** (**DDLP 4**) employed an *in situ* method due to the presence of the tyrosine residue. In this method, 1.0 equivalent of **PLP 4** and 2.0 equivalents of anisole were dissolved in THF to a final concentration of 0.1M. HCl was added drop-wise and the reaction ran for one week at room temperature while being monitored by LCMS. As needed, additional drops of HCl were added until the reaction reached completion. Finally, the reaction was concentrated

in vacuo to give **DDLP 4** (HO-D-Tyr-Leu-Val-Leu-Leu-NH_2, quantitative yield, **Figure 20**), which was verified by LCMS.

CYCLIZATION OF COMPOUNDS 2, 3, 4, 8, AND 9

As discussed in the introduction, macrocyclization of peptides can occur via many routes (Chapter 1, **Figure 2**). Head-to-tail cyclization, where the N-terminus of the peptide couples to the C-terminus, is one of the most common strategies. SanA analogs require maintaining the peptide backbone and thus the most appropriate cyclization method is head-to-tail. Macrocyclizations continue to be challenging reactions because of the flexibility and the formation of numerous aggregation states associated with the linear peptide precursors.[64, 65] In order to account for these factors and increase the efficiency of the reaction, cocktails of coupling reagents are often employed, and our group has found that a combination of TBTU, HATU, and DEPBT (at 1.2 total equivalents) leads to relatively high yields compared to using a single reagent at 1.2 equivalents.[66]

The macrocyclization for SanA **2** (**Figure 20**) was performed using 1.0 equivalent of **DDLP 2**, 0.4 equivalent of DEPBT, 0.5 equivalent of TBTU, and 0.6 equivalent of HATU. The dry reagents were placed in a round-bottom flask, purged with argon, and dissolved in a 0.007M solution of DCM/ACN (1:1, v/v). Cyclizations are typically performed in dilute conditions (10^{-3}-10^{-4} M) to prevent dimerization and oligomerization. After 6.0 equivalents of DIPEA were added, the reaction was allowed to run for 1.5 hours and was monitored by LCMS. Upon completion, the reaction was diluted in DCM and subjected to three aqueous washes of saturated ammonium chloride and concentrated *in vacuo*. The crude material was purified via flash column chromatography using an

EA/Hex gradient solvent system where the product eluted at 100% EA. The pure cyclized SanA **2** (D-Phe-Leu-Val-Leu-Leu, 79.8% yield) was verified by ^{1}H NMR and LCMS.

SanA **3** and **4** (**Figure 20**) followed the same procedure as SanA **2** but were further purified after flash column chromatography by reverse-phase high-performance liquid chromatography (RP-HPLC). The pure cyclized products (SanA **3**, NMe-Phe-Leu-Val-Leu-Leu, 51.2% yield) and (SanA **4**, D-Tyr-Leu-Val-Leu-Leu, 48.5% yield) were verified by ^{1}H NMR and LCMS.

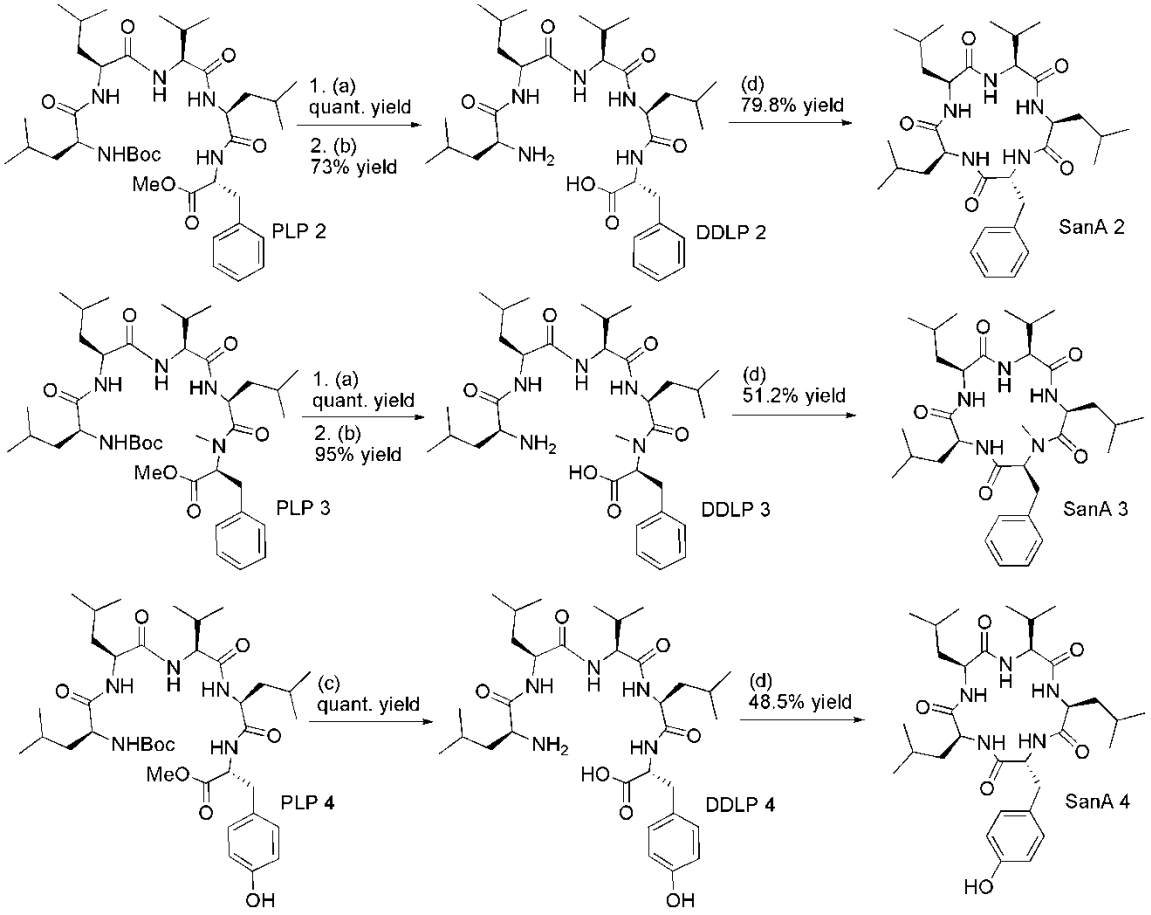

Figure 20: Deprotections and cyclizations of SanA 2, 3, 4

The conditions for SanA **8** and **9** were modified from those of described to cyclize **2, 3,** and **4.** High concentrations (0.1M-0.5M) of the **DDLP 8** and **9** were utilized in order to generate both the dimer (decapeptides) and monomer (pentapeptide/SanA **analog)** macrocycle. The dimer project will be discussed in detail in Chapter 5.

Cyclization of SanA **8** was done using 1.0 equivalent of **DDLP 8**, 0.7 equivalent of DEPBT, 0.5 equivalent of HATU, and 0.5 equivalent of TBTU (**Figure 21**). The reagents were weighed out in a round-bottom flask and purged with argon. Dry dimethylformamide (DMF) was added for a final concentration of 0.5M. After the addition of 8.0 equivalents of DIPEA, the reaction was allowed to run for 1.5 hours and was monitored by LCMS. Once the formation of monomer and dimer was complete, the reaction was diluted in DCM and subjected to two washes with brine. The organic layer was dried over sodium sulfate, concentrated *in vacuo*, and purified via flash column chromatography where a 1:1 mixture of monomer and dimer eluted at 75EA/25Hex and only monomer eluted at 100EA. The material was further purified by RP-HPLC. Unlike the other compounds' syntheses, racemization occurred with the linear precursor and during the cyclization of both the monomer and dimeric compounds. For the cyclic pentapeptide (monomer), it was not possible to separate the epimers by RP-HPLC, therefore a mixture of three products were isolated in a 4:1:1 ratio (as estimated by LCMS) and tested in cytotoxic assays. I was able to separate the decapeptide epimers by RP-HPLC.

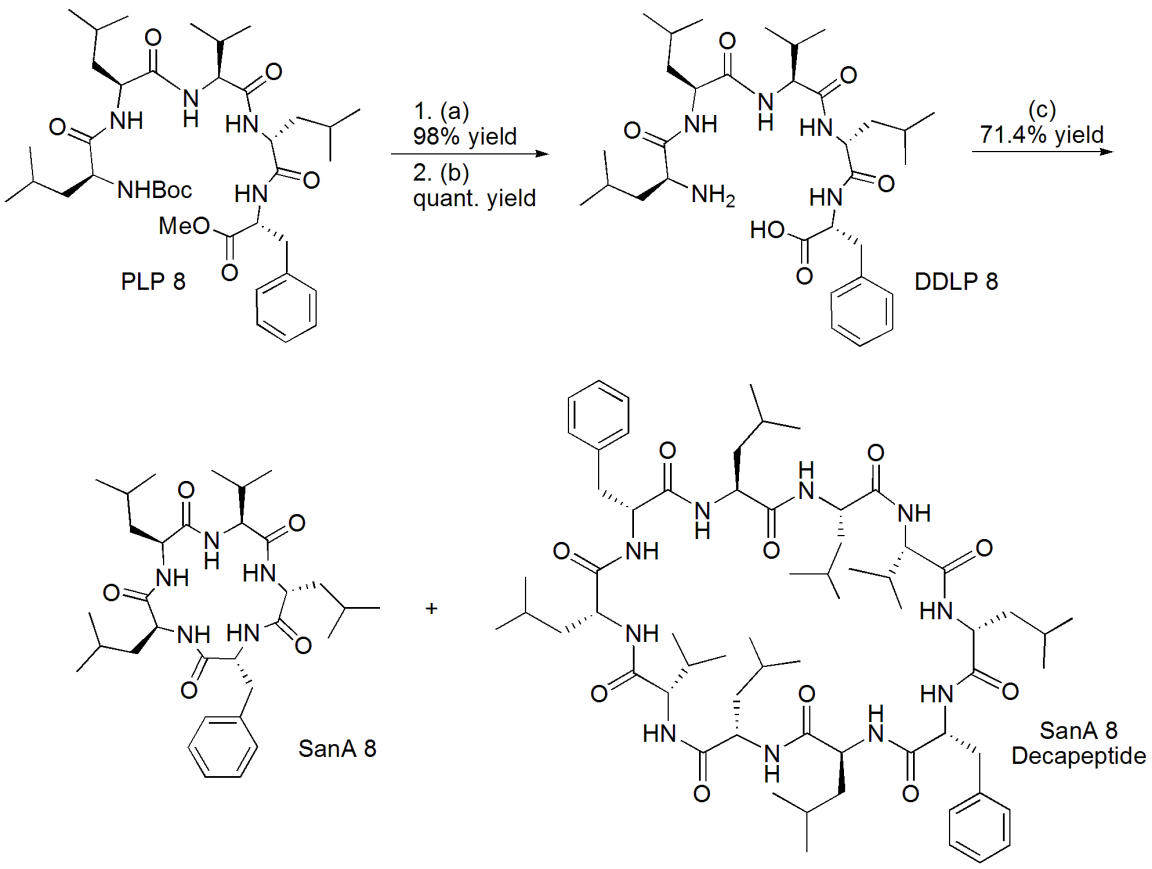

Conditions: (a) 1.0 eq PLP, 8.0 eq LiOH, MeOH (0.1M) (b) 2.0 eq anisole, 25% TFA, 75% DCM (0.1M) (c) 1.0 eq DDLP, 0.7 eq DEPBT, 0.5 eq HATU, 0.5 eq TBTU, 8.0 eq DIPEA, DMF (0.5M)

Figure 21: Double-deprotection and cyclization to form pentapeptide SanA 8 and its decapeptide derivative

SanA **9** was cyclized with 1.0 equivalent of **DDLP 9**, 0.5 equivalent of DEPBT, 0.7 equivalent of HATU, and 0.5 equivalent of TBTU (**Figure 22**). The reagents were placed in a round-bottom flask, purged with argon, and dissolved in 0.1M of dry ACN. After the addition of 8.0 equivalents of DIPEA, the reaction was allowed to run for 1 hour at room temperature and was monitored by LCMS. Upon completion, the reaction was diluted in DCM, subjected to two aqueous washes of saturated ammonium chloride, dried over sodium sulfate, and concentrated *in vacuo*. There was no presence of

epimerization in the products when analyzed by LCMS. The crude material was first purified by flash column chromatography where a 1:1 mixture of monomer and dimer eluted at 75EA/25Hex. The material was further purified by RP-HPLC to give the pure cyclic pentapeptide SanA **9** (Phe-D-Phe-D-Val-Leu-Leu) and decapeptide (Phe-D-Phe-D-Val-Leu-Leu-Phe-D-Phe-D-Val-Leu-Leu) (67.1% combined yield).

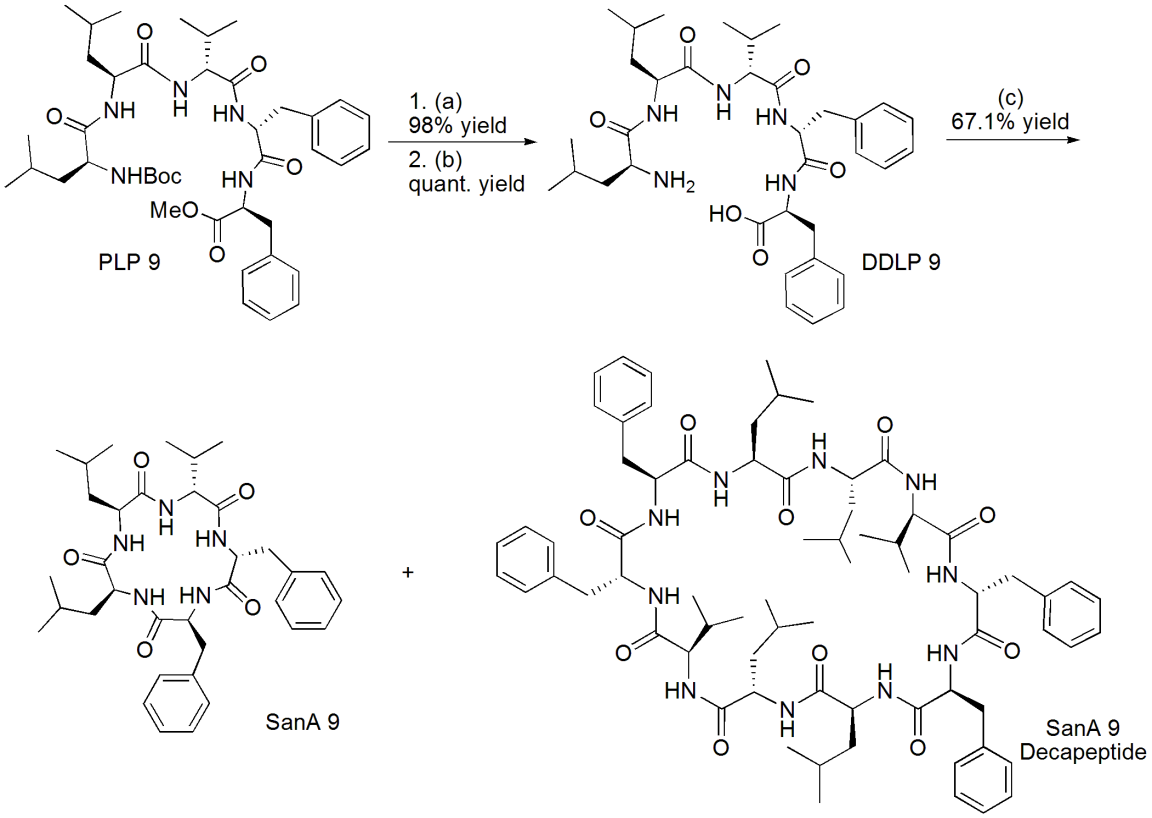

Conditions: (a) 1.0 eq PLP, 8.0 eq LiOH, MeOH (0.1M) (b) 2.0 eq anisole, 25% TFA, 75% DCM (0.1M)
(c) 1.0 eq DDLP, 0.5 eq DEPBT, 0.7 eq HATU, 0.5 eq TBTU, 8.0 eq DIPEA, ACN (0.1M)

Figure 22: Double-deprotection and cyclization to form pentapeptide SanA 9 and its decapeptide derivative

PEG-BIOTIN AND FLUORESCEIN-TAGGED DERIVATIVES

Attaching functional tags is one method that can be used to investigate a compound's mechanism of action. Several types of tags can be attached depending on

the mechanistic assay. These include radioactive tags, biotinylated poly-ethylene glycol chains (PEG-biotin), and fluorescent-based tags. Our mechanism of action studies required a PEG_4-biotin tag, which would be used in conjunction with streptavidin resin in pull down assays. In addition, we also conjugated a fluorescein tag for imaging studies and fluorescence polarization anisotropy experiments. Biotin, which is also known as vitamin B7, and the avidin-relative, streptavidin, have an extremely high affinity for each other ($K_d = 4 \times 10^{-14}$ M)[67], making it one of the strongest non-covalent interactions in nature and an ideal tool in pull-down assays.[68, 69] Fluorescein, often used for imaging, is excited at 494 nm and emits a signal at 521 nm, which can be measured and read on a fluorometer. These tags will facilitate determining SanA's mechanism of action in cancer cells, and the results of these studies will be discussed in Chapter 3.

From our library of SanA derivatives, we tagged our lead compounds: SanA **1**, **12**, and **13** (**Figure 23).** To evaluate the impact of PEG_4-biotin and fluorescein on binding to SanA's target, we designed analogs that incorporate a tag at four positions around the peptide ring, whereby we sequentially exchanged residues I-IV for a lysine. Lysine was then coupled to the fluorescein or biotin. This approach allows us to determine the optimal tag position for maximum binding to the protein target.

Both the PEG_4-biotin and fluorescein starting materials were purchased as N-hydroxysuccinimide (NHS) esters, which rapidly react with free lysines, and were coupled to the compounds under slightly basic conditions. I contributed **13-T-III (Figure 23)**, which I made using a combination of solid-phase and solution-phase chemistry. This analog was then tagged with both PEG_4-biotin and fluorescein. In addition, I was given five compounds with free lysines (**1-T-III**, **12-T-I**, **12-T-III**, **13-T-**

I, and **13-T-II)**, which had been synthesized by my colleagues, to which I attached PEG_4-biotin. In addition, my colleagues provided the free lysine analogs of **1-T-II**, **1-T-III**, **1-T-IV**, **12-T-I**, **12-T-III**, **12-T-IV**, and **13-T-II**, to which I attached a fluorescein tag.

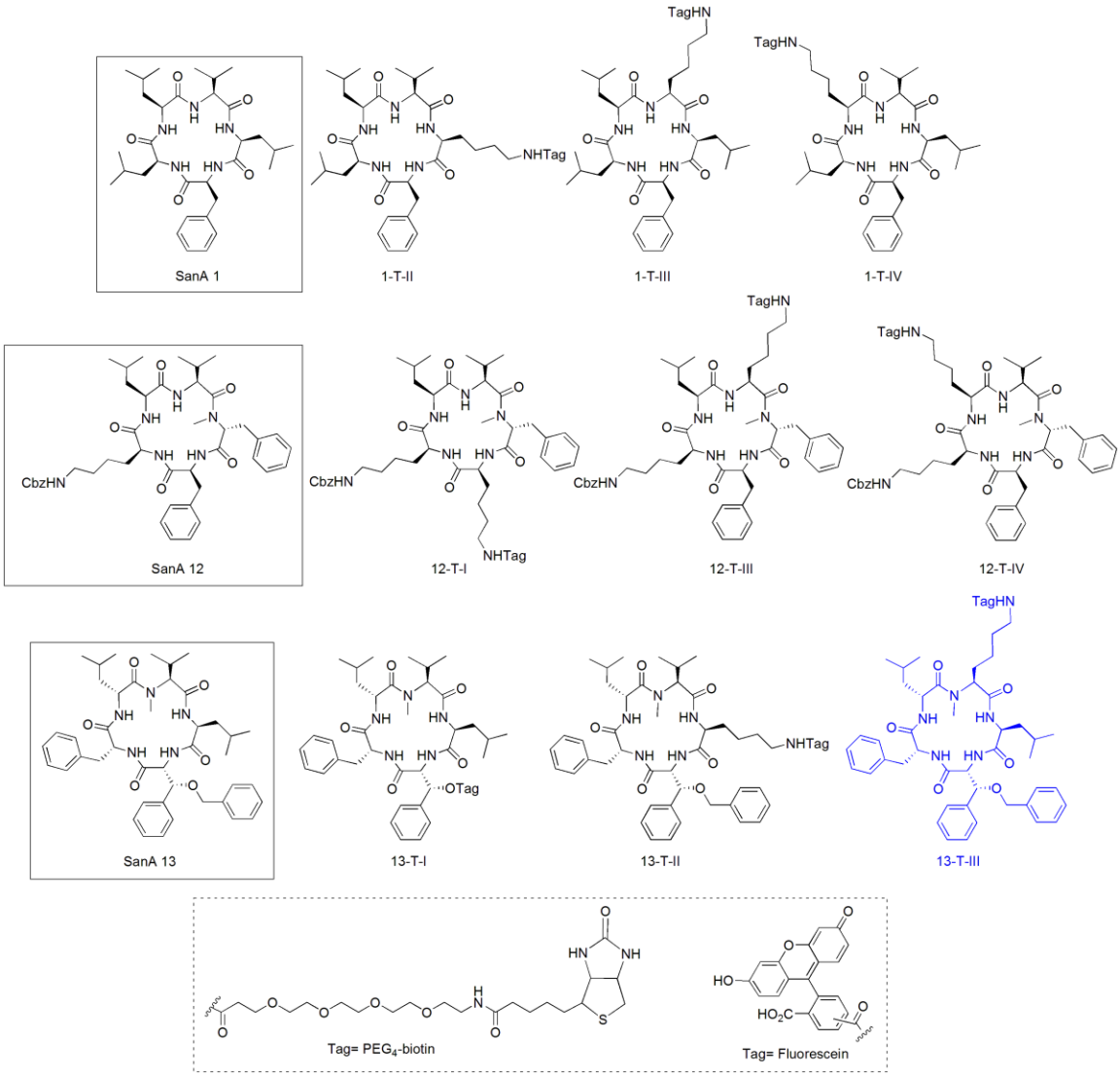

Figure 23: Tagged derivatives of SanA 1, 12, and 13

SOLID-PHASE PEPTIDE SYNTHESIS

Solid-phase peptide synthesis (SPPS) was first introduced by R.B. Merrifield in 1963 as a solution to solubility and purification challenges that are associated with

synthesizing long-chain polypeptides in solution.[70] He reported a method that involves covalently attaching the first amino acid to a polymer support and sequentially coupling and deprotecting the desired amino acids until the target peptide was reached. Utilizing a polymer for the support meant that filtration was essentially the only purification required. The linear peptide can then be cleaved from the polymer support and taken on to its next step. There are many advantages to this method: reactions are pushed to completion using excess reagents and purification by filtration leads to rapid generation of compounds. These advantages mean that insolubility problems associated with long polypeptide chains are avoided until the final product is generated.

When Merrifield first introduced this Nobel Prize-winning chemistry, he used carboxybenzyl (Cbz)-protected amino acids that were deprotected under harsh acidic conditions with 30% hydrobromic acid (HBr). The peptides were cleaved from the resin using sodium hydroxide (NaOH). Since then, SPPS has been improved with the introduction of mild base-labile Fmoc-protected amino acids, and the utilization of linkers between the resin and terminal amino acid that allows peptide cleaving to occur of under gentle conditions. Further, in the past few decades, the development of resins, linkers, protecting groups, and cleaving conditions has allowed solid-phase chemistry to be applied to a wide range of chemistry. Reactions other than linear peptide coupling have been developed using a polymer-supported approaches including on-resin peptide cyclizations, heterocycle formations, and alkylations.[71, 72]

The solid-phase protocol used in our lab utilizes 1% divinylbenzene (DVB) polystyrene resin that is pre-loaded with the desired amino acid residue. The amino acid is connected to the resin by a 2-chlorotrityl (CTC) linker that allows peptide cleavage to

occur with trifluoroethanol (TFE) and DCM (1:1, v/v). Fmoc-protected amino acids were used and the coupling reaction was aided by coupling reagents 1-hydroxy-benzotriazole (HOBt) and diisopropylcarbodiimide (DIC) (**Figure 24**). When coupling to an *N*-Me amino acid, which is more hindered than a NH-amino acid, 1-hydroxy-7-aza-benzotriazole (HOAt) is substituted for HOBt. Like HATU, HOAt is a very effective but costly reagent.

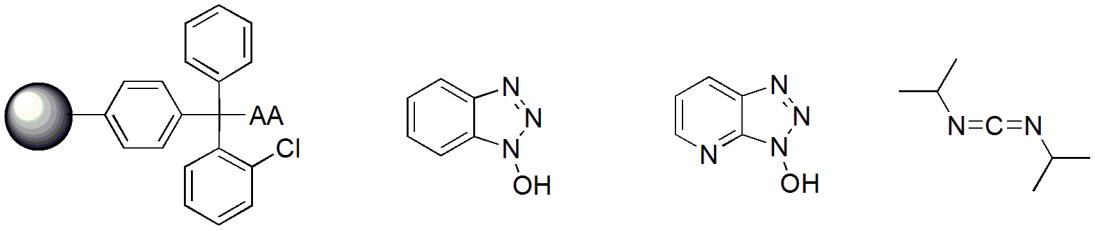

2-CTC resin HOBt HOAt DIC

Figure 24: SPPS materials and reagents

One of the disadvantages of solid-phase chemistry is the difficulty in monitoring reactions. Given that we are only synthesizing pentapeptides, we utilize literature precedent and assume most couplings are complete after two hours.[73] However, to verify completion, we initially tested each reaction using the ninhydrin test, also known as the Kaiser test. A small amount of resin is treated with a 1:1:1 solution of ninhydrin (5%, w/v) in ethanol, phenol (4:1, w/v) in ethanol, and potassium cyanide (2%, w/v) in pyridine. The vial containing the beads are heated and in the presence of a free-amine, the resin turns blue; if the resin is capped with Fmoc-protected amines, the resin will remain yellow/orange, which confirms that the coupling is complete. We found that coupling N-Me amino acids required the reaction to run overnight, while coupling to an NH-amino acid was complete after two hours.

SOLID-PHASE SYNTHESIS OF 13-TAG-III

I synthesized **13-T-III** by incorporating a *N*-Me-Lys(Boc) into position III in place of the *N*-Me-Val. The parent compound, SanA **13**, incorporated a racemic amino acid (Fmoc-(2R,3R)/(2S,3S)-β-OH-Phe-OH) at position I, and the phenyl serine was subsequently benzylated. For SanA **13**, separation and characterization of the diastereomers was only possible by RP-HPLC after benzylation and not at any step prior.[74] It was expected that the derivatives containing the lysine tag would exhibit similar properties with regard to the separation of diastereomers.

SOLID-PHASE SYNTHESIS OF 13-T-III

Synthesis of **13-T-III** followed our standard solid-phase synthesis protocol and began with 1.0 equivalent of pre-loaded CTC-D-leucine-NH_2 resin (1g scale, 0.81 mmol/g resin loading), 3.0 equivalents of Fmoc-D-Phe-OH, 3.0 equivalents of HOBt, and 6.0 equivalents of DIC (**Figure 25**). The resin was placed in a polypropylene cartridge fitted with a frit and swelled in DMF for 30 minutes. Meanwhile, the amino acid and coupling reagent were dissolved in a 0.2M final concentration of DMF. The cartridge was then drained and the amino acid/coupling reagent mixture was added, followed by the addition of DIC. The reaction was allowed to run overnight under open atmosphere and at room temperature. After a ninhydrin test verified completion, the reaction was filtered and washed three times with DMF to give the Fmoc-protected resin-bound dipeptide (Resin-CTC-Leu-Lys(Boc)-*N*-MeFmoc).

.

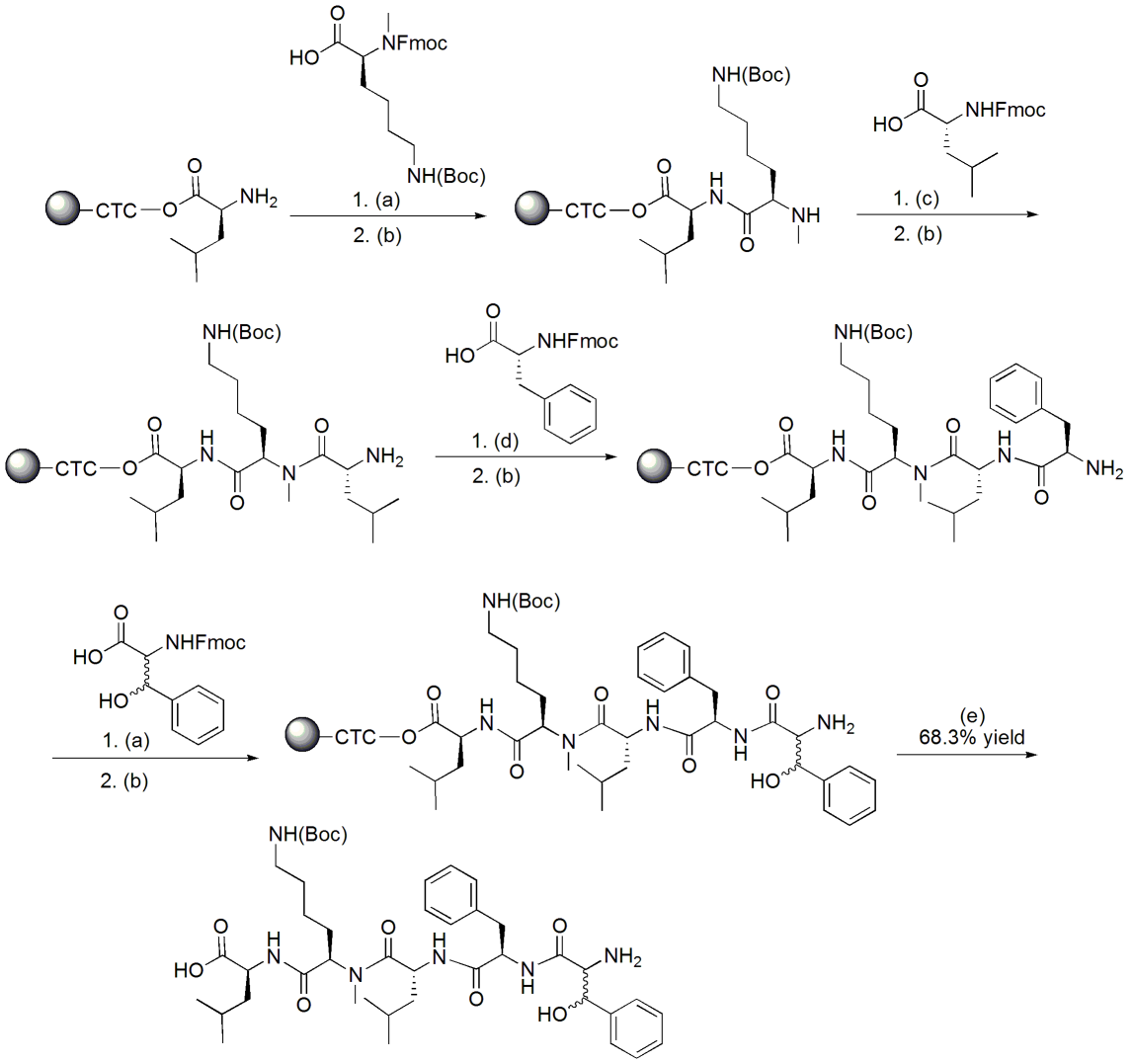

Conditions: (a) 1.2 eq amino acid, 3.0 eq HOBt, 6.0 eq DIC, DMF (0.2M) (b) 20% piperidine/DMF
(c) 3.0 eq amino acid, 3.0 eq HOAt, 6.0 eq DIC, DMF (0.2M) (d) 3.0 eq amino acid, 3.0 eq HOBt, 6.0 eq DIC, DMF (0.2M)
(e) 50% TFE/DCM (10mL/g resin)

Figure 25: SPPS of DDLP 13-T-III

The dipeptide was subjected to our standard Fmoc-removal conditions where it was washed for 5 minutes in a 20% piperidine in DMF solution, 10 minutes in a fresh 20% piperidine in DMF solution, two DMF rinses, one IPA wash, one DMF wash, one IPA wash, and three DMF washes. The free-amine resin-bound dipeptide (Resin-CTC-Leu-Lys(Boc)-*N*-MeH) was then ready for the next amino acid coupling.

The same coupling and deprotection procedure described above was followed for the coupling of Fmoc-D-Leu-OH, except HOAt (3.0 equivalents) was substituted for HOBt since the coupling occurred at a hindered, *N*-methylated amino terminus. The final couplings of Fmoc-D-Phe-OH (3.0 equivalents) and racemic Fmoc-(2R,3R)/(2S,3S)-β-OH-Phe-OH (1.2 equivalents) utilized HOBt (3.0 equivalents). After the final deprotection in 20% piperidine in DMF solution, the resin-bound pentapeptide (Resin-CTC-Leu-*N*-Me-Lys(Boc)-D-Leu-D-Phe-[(2R,3R)/(2S,3S)-β-OH-Phe]-NH_2) was subjected to three DMF washes, three IPA washes, and three MeOH washes, then was drained thoroughly and dried *in vacuo* overnight.

The pentapeptide was cleaved from the resin in a TFE/DCM (1:1) solution at a concentration of 10 mL per gram of dry resin. The mixture was shaken for 24 hours at room temperature. Finally, the solution was filtered from the resin and concentrated *in vacuo* to give the **DDLP** (HO- Leu-NMe-Lys(Boc)-D-Leu-D-Phe-[(2R,3R)/(2S,3S)-β-OH-Phe]-NH_2, 68.3% yield), which was verified for mass and purity by LCMS.

Cyclization was performed using a syringe pump and dilute conditions to avoid dimerization (**Figure 26**). The cyclization used 1.0 equivalent of **DDLP 13-T-III**, 0.7 equivalent of HATU, 0.7 equivalent of TBTU, 0.7 equivalent of DEPBT, 8.0 equivalents of DIPEA, and dry DCM at a final concentration of 0.005M. The coupling reagents were added to a round-bottom flask that was subsequently purged with argon. The reagents dissolved in half of the DCM, and half of the DIPEA (4.0 equivalents) was added to the flask. **DDLP 13-T-III** was dissolved in the remaining amount of dry DCM, placed into a syringe, and added to the coupling reagent-containing flask over the course of two hours using a syringe pump (8 mL/hour). After the first hour, the remaining DIPEA (4.0

equivalents) was added. After all of the **DDLP** was added, the reaction was allowed to run overnight at room temperature. Upon completion, as determined by LCMS, the reaction was quenched with three washes of saturated ammonium chloride. The organic solution was then dried over sodium sulfate and concentrated *in vacuo*. The cyclized product ([(2R,3R)/(2S,3S)-β-OH-Phe-Leu-*N*-Me-Lys(Boc)-D-Leu-D-Phe, 87.9% yield) was verified by LCMS and ^{1}H NMR.

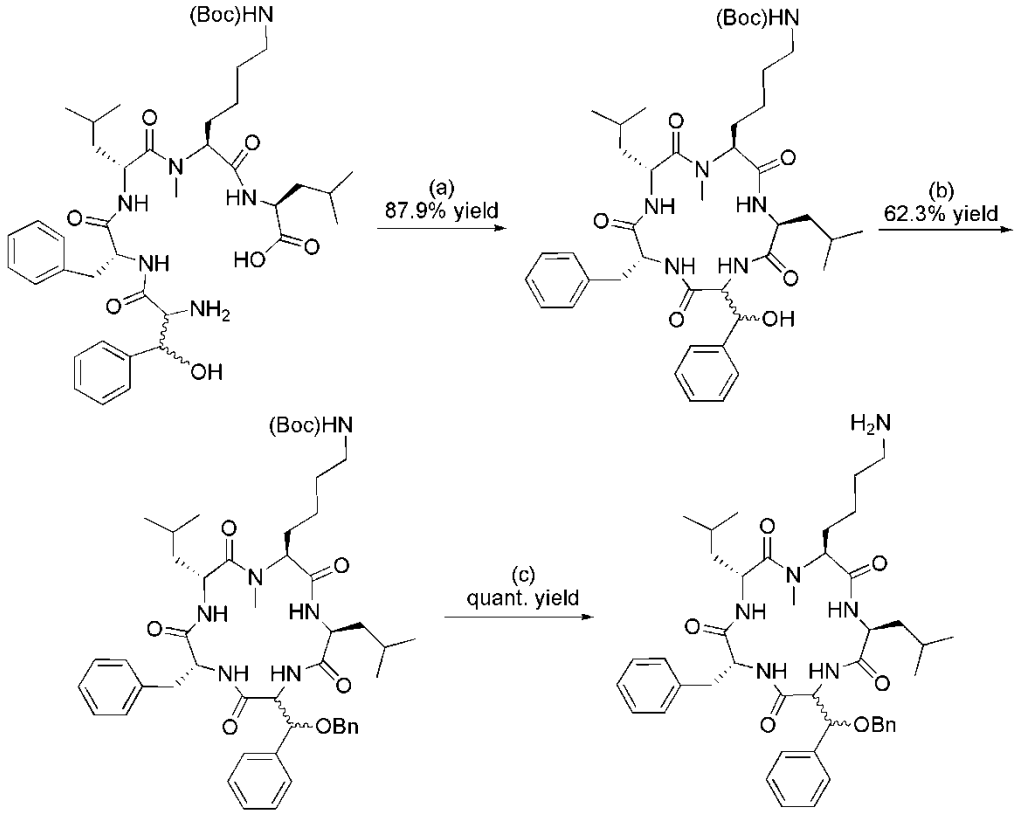

Conditions: (a) 1.0 eq DDLP, 0.7 eq DEPBT, 0.7 eq HATU, 0.7 eq TBTU, 8.0 eq DIPEA, DCM (0.005M)
(b) 4.0 eq NaH, 4.0 eq BnBr, THF (0.1M) (c) 25% TFA, 75% DCM (0.1M), 2.0 eq anisole

Figure 26: Cyclization and subsequent reactions for 13-T-III synthesis

Benzylation of the free phenyl serine was performed using 1.0 equivalent of the cyclized pentapeptide, 4.0 equivalents of NaH, and 4.0 equivalents of BnBr in dry tetrahydrofuran (THF) at a final concentration of 0.1M. The compound was dissolved in

THF in a round-bottom flask purged with argon, and then NaH and BnBr (2.0 equivalents each) were added. The reaction was allowed to run for two hours and was checked by LCMS. With only starting material present, an additional 2.0 equivalents of both NaH and BnBr were added, and the reaction was allowed to proceed overnight. Upon completion, the reaction was diluted in DCM and quenched with two washes of DI water. The organic solution was dried over sodium sulfate and concentrated *in vacuo* to give the benzylated product ([(2R,3R)/(2S,3S)-β-OBn-Phe]-Leu-*N*-Me-Lys(Boc)-D-Leu-D-Phe, 62.3% yield).

Finally, the lysine was deprotected using our standard solution-phase amine deprotection procedure where 1.0 equivalent of the benzylated peptide was dissolved in a solution of 25% TFA in DCM, followed by the addition of scavenging reagent, anisole (2.0 equivalents). The reaction was allowed to run at room temperature for 45 minutes. Upon verification of completion by LCMS, the reaction was concentrated *in vacuo* to give the free lysine-containing pentapeptide ([(2R,3R)/(2S,3S)-β-OBn-Phe]-Leu-*N*-Me-Lys-D-Leu-D-Phe, quantitative yield), which was ready to be tagged by PEG_4-biotin and fluorescein.

As noted earlier, the parent compound SanA **13** was synthesized using a racemic amino acid (Fmoc-(2R,3R)/(2S,3S)-β-OH-Phe-OH) and its diastereomer (SanA **14**) was separated via RP-HPLC after the benzylation step. The same strategy did not work for the synthesis of **13-T-II** or **13-T-III**. Beginning from the cyclization step and on to the final tagging with PEG_4-biotin or fluorescein, there was only one peak consisting of both diastereomers. Since it was impossible to separate the two via RP-HPLC, we elected to use the mixture in the subsequent bioassays. The IC_{50}s of SanA **13** and its diastereomer

(SanA **14**) were comparable (3.27μM vs 5.75μM, respectively), therefore it was likely that they were acting via the same mechanism of action and would give us comparable results.

COUPLING OF PEG-BIOTIN AND FLUORESCEIN

Attaching the PEG_4-biotin tag to **1-T-III**, **12-T-I**, **12-T-III**, **13-T-II**, and **13-T-III** required 1.0 equivalent of the deprotected lysine-containing compound and 1.2 equivalents of NHS-PEG_4-biotin. Both the peg-biotin and the SanA compound were placed in a 4 mL vial and dissolved to a 0.1M final concentration in DCM (**Figure 27**). After addition of DIPEA (8.0 equivalents) the reaction was stirred overnight at room temperature under open atmosphere. Upon verification of completion by LCMS, the reaction was concentrated *in vacuo*, re-dissolved in 70% MeOH and 30% DMSO, and purified via RP-HPLC to give the biotinylated cyclic peptides: **1-T-III-biot**, Phe-Leu-Lys(Peg-biotin)-Leu-Leu, 87% yield; **12-T-I-biot**, Lys(Peg-biotin)-*N*-Me-D-Phe-Val-Leu-Lys(Cbz), 75% yield; **12-T-III-biot**, Phe-*N*-Me-D-Phe-Lys(Peg-biotin)-Leu-Lys(Cbz), 91% yield; **13-T-II-biot**, (2R,3R)/(2S,3S)β-OBn-Phe-Lys(Peg-biotin)-*N*-Me-Val-D-Leu-D-Phe, 86% yield; and **13-T-III-biot**, (2R,3R)/(2S,3S)β-OBn-Phe-Leu-*N*-Me-Lys(Peg-biotin)-D-Leu-D-Phe, 30% yield.

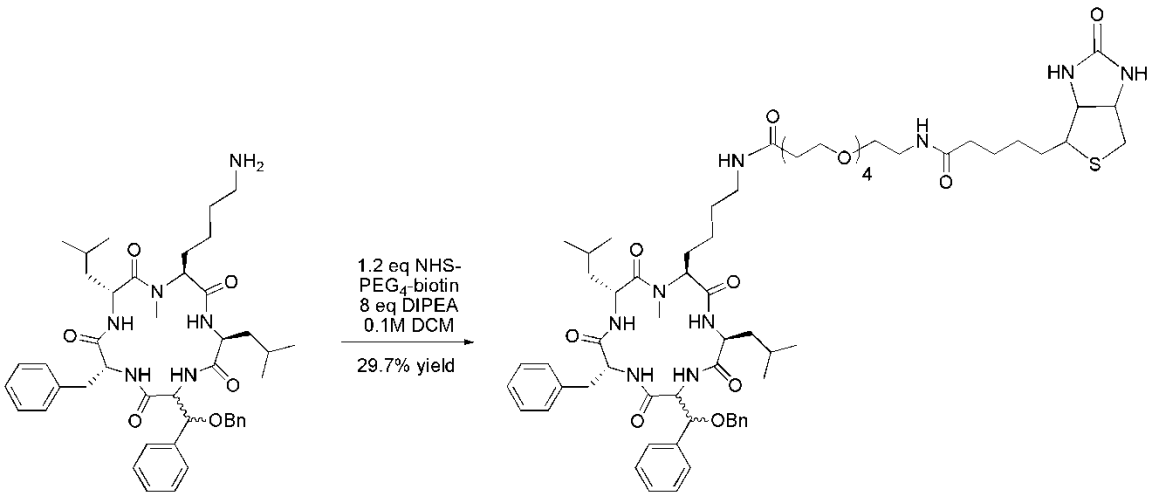

Figure 27: Coupling of PEG_4-biotin to 13-T-III

Coupling of PEG_4-biotin to the free phenyl serine on SanA **13-T-I** proved to be was significantly more challenging than coupling to all of the other SanA molecules (**Figure 28**). Under the same reaction conditions there was only starting material present after 24 hours and no product. Subsequent addition of a total of 4.0 equivalents of DIPEA and 2.2 equivalents of NHS-PEG_4-biotin over the course of two weeks resulted in a small amount (<5%) of product and starting material (~95%). The reaction was concentrated *in vacuo* and purified by RP-HPLC, where the minor amount of product was isolated ([(2R,3R)β-O-(Peg-biotin)-Phe]-Leu-*N*-Me-Val-D-Leu-D-Phe, 4% yield) and the starting material recovered. Note: 13-T-I free serine was synthesized and separated from its diastereomer by a colleague prior to my tagging it, therefore the final biotinylated product only contains one configuration.

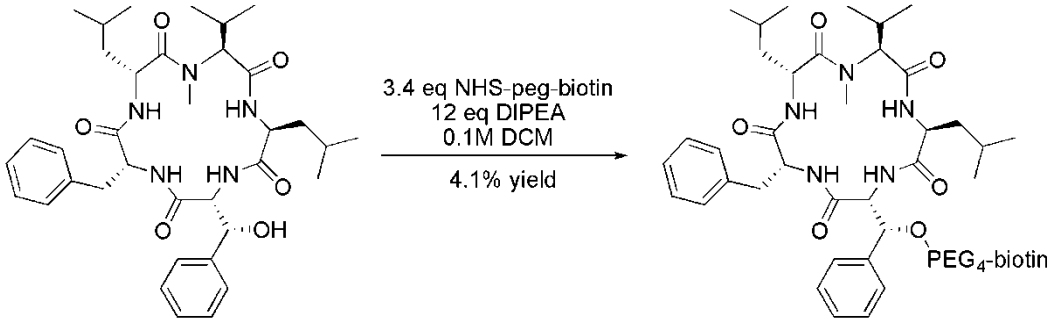

Figure 28: Coupling of PEG_4-biotin to 13-T-I

The fluorescein tags were added using 1.0 equivalent of free-lysine-containing compound, 1.5 equivalent of NHS-fluorescein, and 8.0 equivalents of DIPEA in 0.1M solution of DCM (**Figure 29**). The reactions were run in vials overnight under atmospheric conditions and at room temperature. Upon verification that the reaction was completed, it was concentrated *in vacuo* and purified by RP-HPLC. This method generated fluorescein-tagged compounds: **1-T-II-fluor**, Phe-Lys(Fluorescein)-Val-Leu-Leu, 46% yield; **1-T-III-fluor**, Phe-Leu-Lys(Fluorescein)-Leu-Leu, 49% yield; **1-T-IV-fluor**, Phe-Leu-Val-Lys(Fluorescein)-Leu, 82% yield; **12-T-I-fluor**, Lys(Fluorescein)-*N*-Me-D-Phe-Val-Leu-Lys(Cbz), 75% yield; **12-T-III-fluor**, Phe-*N*-Me-D-Phe-Lys(Fluorescein)-Leu-Lys(Cbz), 71% yield; **12-T-IV-fluor**, Phe-*N*Me-D-Phe-Val-Lys(Fluorescein)-Lys(Cbz), 59% yield; **13-T-II-fluor**, (2R,3R)/(2S,3S)β-OBn-Phe-Lys(Fluorescein)-*N*-Me-Val-D-Leu-D-Phe, 47% yield; and **13-T-III-fluor**, (2R,3R)/(2S,3S)β-OBn-Phe-Leu-*N*-Me-Lys(Fluorescein)-D-Leu-D-Phe, 45% yield.

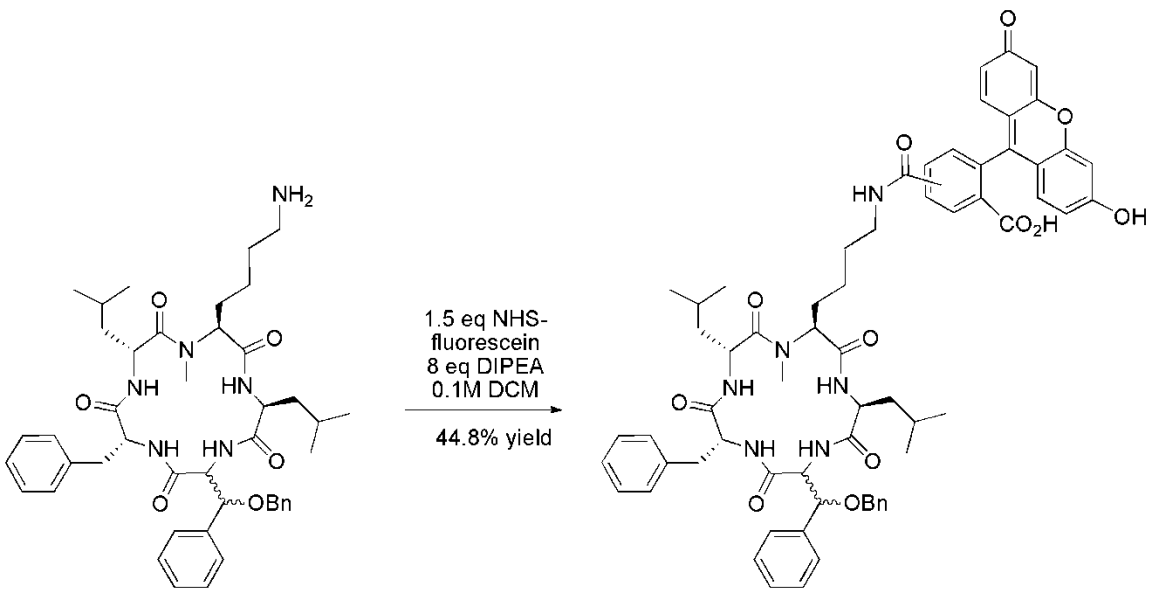

Figure 29: Coupling of fluorescein to 13-T-III

SUMMARY

Described was the successful solution and solid-phase synthesis of compounds that contributed to the SAR study of SanA-amide and determining SanA's mechanism of action. Five derivatives included D-aas and *N*-Me-aas on the SanA scaffold. All final purified compounds were tested against pancreatic and colon cancer cell lines, where they were analyzed for their growth inhibition activity (Chapter 3).

The other derivatives incorporated tags on three of the SanA library's lead compounds. Compounds tagged with PEG_4-biotin are used in conjunction with streptavidin resin in pull-down assays. Compounds tagged with fluorescein are used to determine binding constants via fluorescence polarization anisotropy and in imaging studies. Methods, data, and conclusions from these assays are discussed in Chapter 3.

ACKNOWLEDGEMENTS

This chapter contains material that has been published in Bioorganic and Medicinal Chemistry: Robert P. Sellers, Leslie D. Alexander, Victoria A. Johnson, Chun-Chieh Lin, Jeremiah Savage, Ricardo Corral, Jason Moss, Tim S. Slugocki, Erinprit K. Singh, Melinda R. Davis, Suchitra Ravula, Jamie E. Spicer, Jenna L Oelrich, Andrea Thornquist, Chung-Mao Pan, and Shelli R. McAlpine, **2010**, v15, p3287.

CHAPTER 3: DETERMINING THE MECHANISM OF ACTION OF SANA DERIVATIVES

CYTOTOXICITY ASSAYS

Sansalvamide A (SanA) exhibited a mean IC_{50} of 46.7μM in the National Cancer Institute's 60-cell line panel.[15] Our goal was to synthesize analogs that would be significantly more potent than the natural product. As such, we evaluated our derivatives for their anti-cancer activity. After the synthesis and purification of the cyclic peptides, the compounds were dissolved in DMSO to a 5mM stock concentration, and tested against numerous cancer cell lines including pancreatic (BxPc3 and PL-45), colon (HCT-116 and HCT-15), prostate (DU-145), and cervical (HeLa). The methods and data reported in this chapter focus on the cytotoxicity of SanA in PL-45 and HCT-116 cells, which were the main focus of my project.

Pancreatic cancer is the fourth most deadly cancer in the US and has a 95% mortality rate within a five year period.[75] Patient response to chemotherapeutics is minimal and current drugs only serve to extend the life of the patient between a few months to a few years.[76] Given the immediate need for a new class of pancreatic cancer drug candidates, we are interested in seeing SanA's effect against pancreatic cancer cells. PL-45 cells were derived from a patient with pancreatic cancer in 1992 and contain mutated oncogenes p53, which is involved in apoptosis, and K-ras, which regulates growth factors.[77-79] Testing our compounds on this commonly used cell line will provide an indicator of how our molecules will perform against pancreatic cancer tumor models.

Colon carcinogenesis can occur through two different pathways, one having microsatellite stability (MSS) and the other having microsatellite instability (MSI).[80]

Microsatellites are repeating sequences of DNA, and while these are present in normal tissue, MSI occurs when there is damage to the DNA repair process, also known as mismatch repair (MMR).[81] As a result of a defect in MMR, the DNA sequence repeats can either shorten or lengthen during DNA replication, which leads to MSI. Diagnosing MSI colon cancer in patients can serve as a predictor of a negative response to chemotherapeutics, specifically 5-fluorouracil (5-FU), which is a current drug on the market for colon cancer. In clinical studies, patients with MSS colon cancers had better survival rates than those with MSI when both were treated with 5-FU.[82] Given the lack of MSI-effective colon cancer drugs, the development of novel drug candidates that target MSI positive cancers will help solve the challenge of drug resistance. Therefore we examined the cytotoxicity of SanA derivatives against HCT-116 cells. HCT-116s are widely used in cancer research and are known as being microsatellite instable.[83] Generating a small molecule inhibitor of HCT-116 cancer cells that successfully blocks their growth would be a valuable lead.

To measure the effect of SanA derivatives on cell proliferation, I used both thymidine uptake and colorimetric methods. Radiolabeled-thymidine uptake is frequently used to determine cell growth by approximating the number of living cells that are actively synthesizing DNA and subsequently dividing.[84-86] There are many options when choosing radio-labeled thymidine for cell proliferation studies: tritium-labeled (^{3}H) and carbon-14-labeled (^{14}C)-thymidine are two of the most common derivatives. Tritium-labeled (^{3}H) thymidine incorporates into DNA with higher specificity and efficiency than ^{14}C-thymidine,[87] making it the method of choice for analyzing the effect of SanA on cancer cell proliferation.

Thymdine uptake assays involve the addition of ^{3}H-methyl-thymidine to cells that have been treated with a compound or control, and the radio-labeled thymidine is then incorporated into the DNA of cells that are actively dividing (**Figure 30**). After incorporation, the cells are harvested onto special filter paper and the amount of thymidine present is analyzed by a scintillation counter.

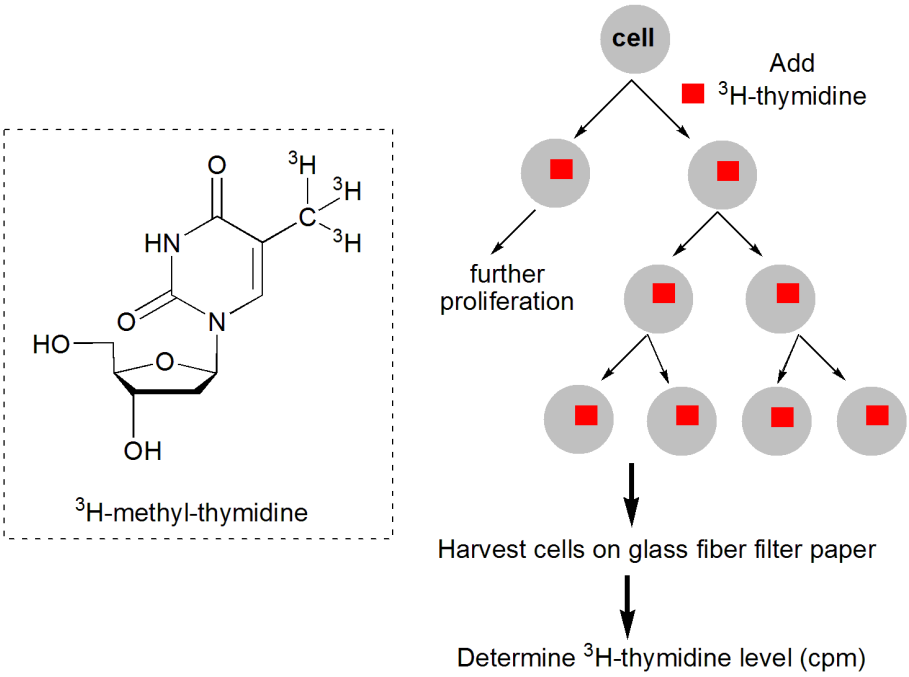

Figure 30: Basic schematic of thymidine uptake assay

I performed thymidine uptake assays in which the cells were treated with single concentrations of SanA derivatives for 72 hours. PL-45 or HCT-116 cells were plated in 96-well plates using 2000 cells per well; the number of cells was determined based on the growth rate of the cell line. The cells were allowed to incubate for 6-16 hours at 37 ºC. SanA derivatives dissolved in DMSO were subsequently added directly to the wells with final concentrations of 5 or 10 µM compound and 1% DMSO. Compound-free 1% DMSO was used as the control for normal cell proliferation and compounds with known

anti-proliferative activity were used as positive controls to validate each assay. The treated cells were allowed to incubate for 55 hours at 37 ºC. Next, 1 microcurie (µCi) of tritiated thymidine was added to each well, and the cells were allowed to incubate at 37 ºC for an additional 17 hours. Finally, the cells were trypsinized and harvested via vacuum filtration onto glass fiber filter paper, and analyzed for the presence of thymidine using scintillation fluid and a scintillation counter. The amount of thymidine present was reported in counts per minute (cpm), and values for the compound-treated cells were compared to that of the DMSO-only cells (control) to give percent growth inhibition. Between six to eight wells were used per compound or control, and all errors were less than ±5% standard error of the mean.

Although thymidine uptake assays provide valuable data, and are often the assay of choice,[74, 88-90] the cost and safety factor (radioactivity) prompted us to explore environmentally-friendly options for screening compound cyototoxicity. Cheap, fast, and radioactivity-free methods involve colorimetric assays that are easily analyzed using a plate reader. The colorimetric assays are based on tetrazolium salts that are cleaved into formazans by mitochondrial enzymes, inducing a colorimetric change that can be read at wavelengths around 440-460 nm.[91] Only live cells have mitochondrial activity, therefore the absorbance detected is proportional to the number of living cells. The absorbance of each well containing compound-treated cells is compared to control wells in order to calculate percent growth inhibition.

We used the colorimetric assay Cell Counting Kit-8 (CCK-8, manufactured by Dojindo) whereby the presence of live cells is detected by the color change of the water-soluble tetrazolium salt (WST-8, **Figure 31**). Initially a yellow color, the molecule

undergoes reduction in the presence of mitochondrial dehydrogenases to give WST-8 Formazan, which is an orange color. The absorbance of each well is measured at 450nm using a plate reader.

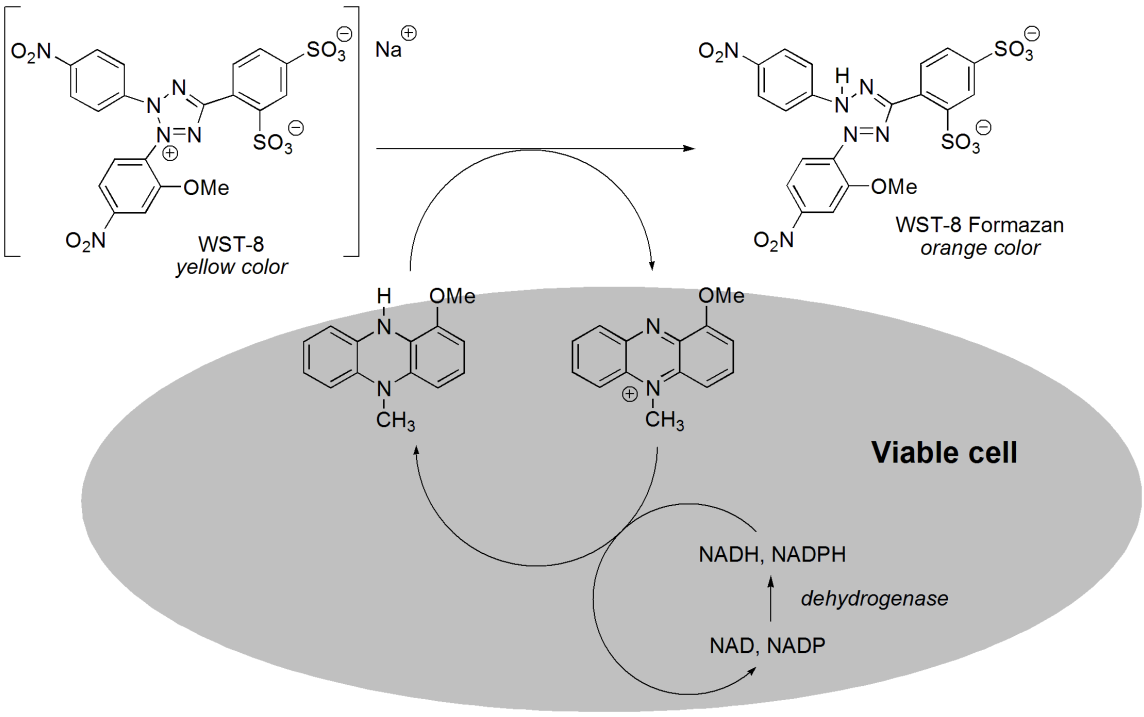

<u>Figure 31</u>: Mechanism of CCK-8 assay

There have been reports comparing data obtained by colorimetric assays and thymidine uptake assays, and the results indicate that the output is similar.[92] In order to verify the efficacy of the CCK-8 assay as an alternative measurement for cell proliferation, my colleagues and I compared the results of thymidine uptake and CCK-8 assays using PL-45s and HCT-116s. We determined that the IC_{50}s of lead compounds remained comparable (within 2 fold), although the screening concentration had to be increased from ~10 µM to between 25-50 µM. Thus, the CCK-8 assay successfully replaced the tritiated thymidine uptake assay as our main method for evaluating compounds' effects on cell proliferation.

Prior to CCK-8, the SanA derivatives I synthesized in Chapter 2 were tested for their effects on cell proliferation using only thymidine uptake. My colleagues and I screened these compounds in PL-45 cells, since the cytotoxicity of the parent compounds had also been tested in this cell line.

We found that making single modifications at position I, including the addition of an *N*-Me-aa, D-aa, and D-tyrosine residue, all produced increased cytotoxic activity (**Figure 32**, black bars). There was also a small positive synergistic effect when combining the D-aas of SanA **2** and **5** into SanA **8**. However, there was a negative effect combining the two phenyl alanines and D-aa of SanA **6** and **7** into SanA **9**.

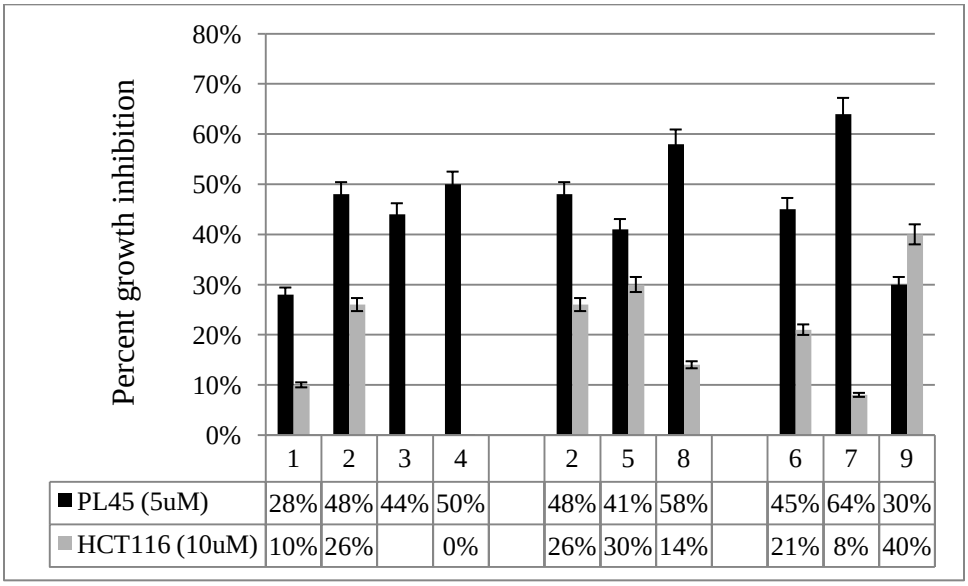

	1	2	3	4		2	5	8		6	7	9
PL45 (5uM)	28%	48%	44%	50%		48%	41%	58%		45%	64%	30%
HCT116 (10uM)	10%	26%		0%		26%	30%	14%		21%	8%	40%

<u>Figure 32</u>: Thymidine uptake assay data and structures for SanA derivatives. The compounds in blue were synthesized by the author and the compounds in black were synthesized by the author's colleagues. All of the HCT-116 cytotoxicity data was generated by the author. The PL-45 data was generated by the author and colleagues. (Figure continued on next page).

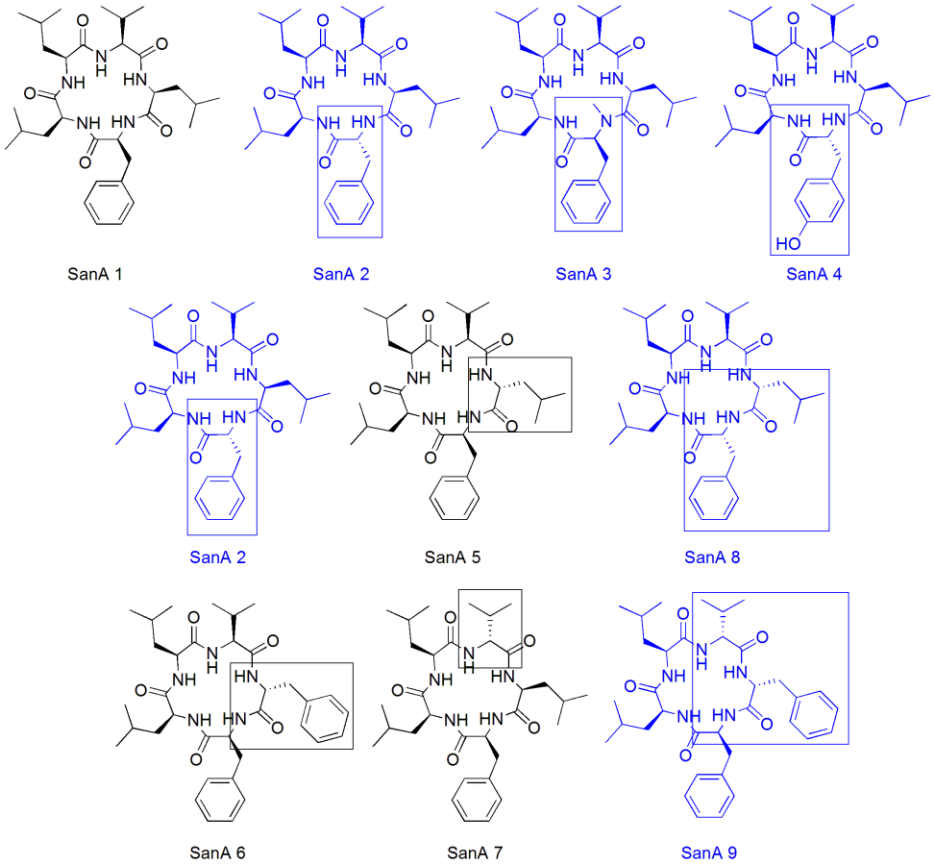

<u>Figure 32 (continued)</u>: Thymidine uptake assay data and structures for SanA derivatives. The compounds in blue were synthesized by the author and the compounds in black were synthesized by the author's colleagues. All of the HCT-116 cytotoxicity data was generated by the author. The PL-45 data was generated by the author and colleagues.

To further assess potential differences in cytotoxicity between various cell lines, I performed assays in which both the parent compounds and their derivatives were tested in HCT-116 cells. It was not surprising given the drug resistance of HCT-116 that all of the compounds demonstrated reduced cytotoxic activity in HCT-116s compared to PL-45 despite increasing the screening concentration to 10 μM (**Figure 32**, gray bars).[83] However, most of the derivatives showed increased potency over SanA **1**. The most notable compound from this series was SanA **9**, with its two consecutive D-aas and two

phenyl alanine moieties. The derivatives I synthesized contributed to a series of over one-hundred derivatives, which led to the design and synthesis of our lead compounds SanA **11**, **12**, **13**, and **15** (**Figure 33**).

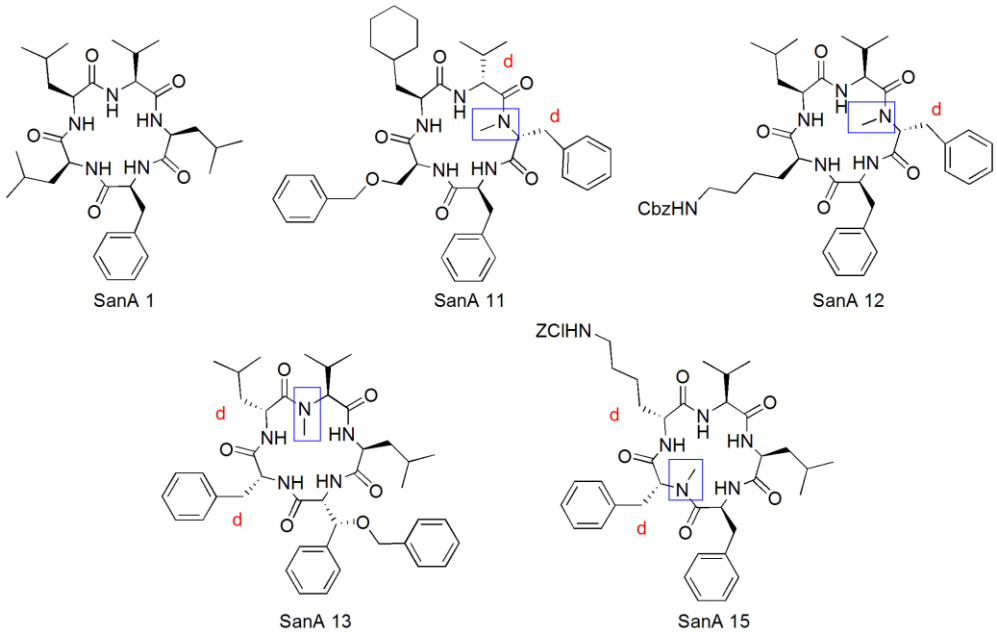

Figure 33: Structures of SanA 1 and lead derivatives 11, 12, 13, and 15

Inclusion of a single *N*-Me-aa, at least one D-aa, and the presence of three aromatic groups (including the carbobenzyloxy-based lysine protecting groups in SanA **12** and **15**) are common characteristics of all the lead compounds. Horst Kessler's group showed through NMR studies that the inclusion of an *N*-methylated D-aa in cyclic pentapeptides led to structures that preferred a single conformation.[20, 93] Further, the group demonstrated that structures with conformational homogeneity had better permeability across the membrane than those adopting multiple conformations. Thus, the *N*-Me-aa and D-aas in our lead structures most likely contribute to conformational rigidity and perhaps increased diffusion through the membrane.[21] Further, our SAR indicates that the multiple phenylalanines play an important role in potency since our leads all contain

at least 2 phenyl moieties. Presumably these aromatic residues have favorable hydrophobic interactions with protein targets.[57]

In HCT-116 cells, our lead compounds demonstrated greater than 90% growth inhibition at 10 μM in thymidine uptake assays. In order to further elucidate their bioactivity, we determined the IC_{50} for the lead compounds. IC_{50}s are generally used to evaluate the effectiveness of drug candidates, and is defined as the concentration at which 50% of growth is inhibited. The IC_{50}s for our lead compounds were determined following the standard thymidine uptake protocol. Multiple concentrations were tested (from 0 to 10 μM) in order to generate a curve from which the concentration at 50% growth inhibition could be extrapolated. My colleagues and I used this method to determine IC_{50}s in HCT-116 and PL-45 cells for our lead compounds (**Figure 34**). We found that all of the lead compounds exhibit an average of 10-fold increased potency over the natural product peptide SanA **1,** with low-micromolar IC_{50}s. These values are also comparable to the IC_{50} of 5-FU (~5 μM), the current drug on the market for the treatment of both pancreatic and colon cancers.[94]

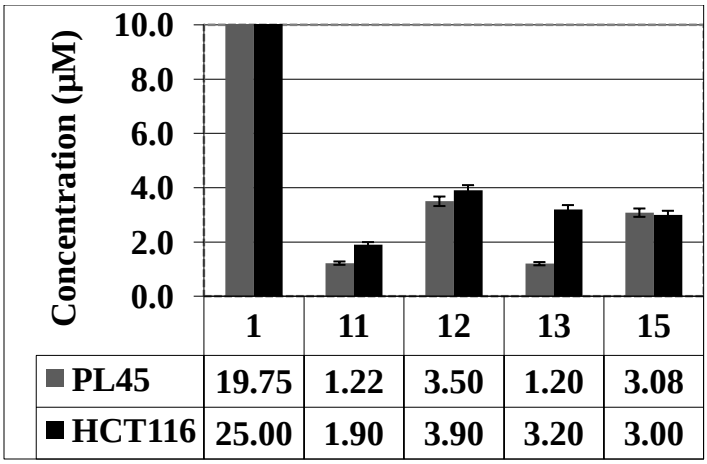

	1	11	12	13	15
PL45	19.75	1.22	3.50	1.20	3.08
HCT116	25.00	1.90	3.90	3.20	3.00

Figure 34: IC_{50} values and structures of lead compounds. The author generated data for 11, 12, 13, and 15 in HCT-116 cells. The data for SanA 1 and PL-45 cells was generated by the author's colleagues.

These lead compounds demonstrate a significant improvement in potency over SanA **1** and will be used in the remainder of mechanism of action studies contained in the rest of this chapter, as well as in Chapter 4.

APOPTOSIS STUDIES

Based on the cytotoxicity assay data, we know that our SanA derivatives are inhibiting cell proliferation. However, we are interested in knowing if and how they are inducing cell death. There are two major ways a cell can die: they can either go through necrosis or a process called apoptosis. Necrosis is a passive, uncontrolled process that involves cell and organelle swelling.[95, 96] In necrosis, the cell looses its membrane integrity, which releases the cell's cytoplasmic contents into the extracellular environment. This non-ideal process is toxic to neighboring cells and results in an inflammatory response.[97]

Apoptosis (also known as programmed cell death, or PCD) is a controlled process in which either extracellular or intracellular factors trigger a cascade of signaling proteins. These signals lead to apoptosis. Unlike necrosis, apoptosis causes cell shrinkage, DNA fragmentation, and other biochemical characteristics that render the cell ready to be digested by neighboring cells or macrophages.[97, 98] Apoptosis is necessary to maintain a healthy living system, and does not typically initiate harmful immune responses. Apoptosis is involved in the regeneration of skin, gut, and bone marrow cells, and is responsible for recognizing and disposing of abnormal cells. However, cancerous cells often contain mutations or an over-expression of anti-apoptotic proteins. Thus, evading apoptosis is known as one of the hallmarks of cancer and is a characteristic found in most cancer types.[39]

In general, a cell can enter apoptosis through two pathways: the extrinsic death receptor pathway and the intrinsic mitochondrial pathway. Factors that contribute to the choice of pathway taken by the cell include: cell type, the origination of the initial death signal, genetics, and the presence or absence of pro- and anti-apoptotic proteins. Cysteine aspartate-specific proteases (caspases) are proteins that are very prevalent in apoptotic processes and, while caspase-independent apoptosis exists, much is known about caspase-dependent cell death and the mechanisms cancer cells take to develop resistance to these pathways.[39] Caspase-dependent apoptosis is depicted in **Figure 35**. In the mitochondrial intrinsic caspase-dependent pathway, an apoptotic signal activates pro-apoptotic proteins Bax/Bak, which then signal to the mitochondrion to release cytochrome C. Cytochrome C activates Apaf-1, which then goes on to activate caspase 9, which activates caspase 3. Caspase 3 is responsible for the cleavage of nuclear and

cytosolic proteins, which ultimately leads to apoptosis. The extrinsic pathway, which relies on the activation of the death receptor, leads to the activation of caspase 8 followed by caspase 3 and, finally, apoptosis.[99, 100]

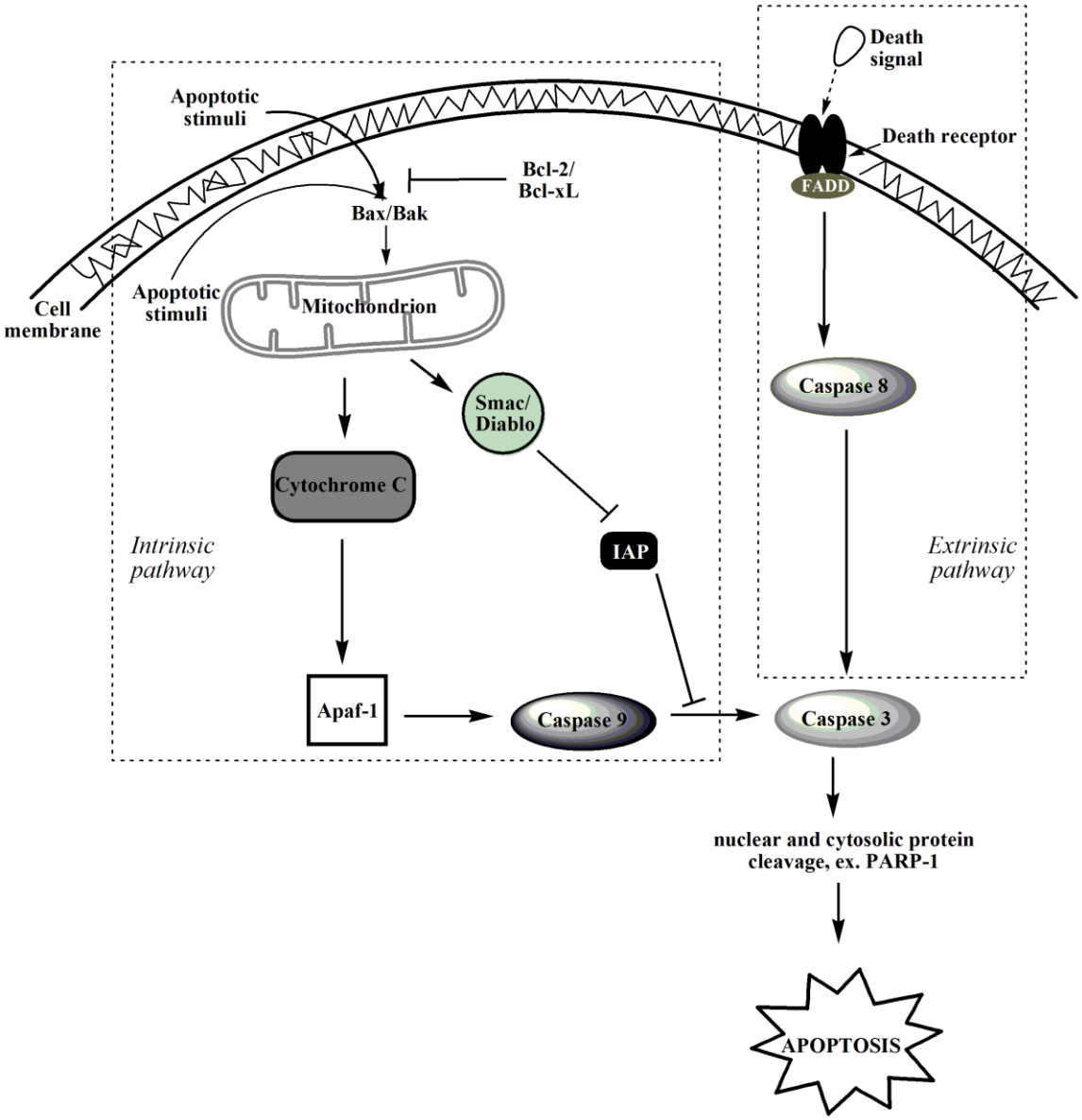

Figure 35: Intrinsic and extrinsic caspase-dependent apoptotic pathways

One of the proteins cleaved by caspase 3 is poly(ADP-ribose) polymerase (PARP), which is located in the nucleus and is associated with DNA repair.[101] PARP is a 113-kilodalton (kDa) protein that is cleaved into fragments when the cell undergoes apoptosis. It is widely known that caspase 3 is responsible for clipping PARP into 89-kDa and 24-kDa fragments (**Figure 36**).[102] However, studies have also shown that PARP exhibits different fragmentation patterns depending on the enzyme by which it is cleaved. Investigating the fragmentation patterns associated with PARP can help shed light on the characteristics of caspase-associated apoptosis and is a common method used to determine if cell death is occurring via caspase-3-dependent apoptosis.[103]

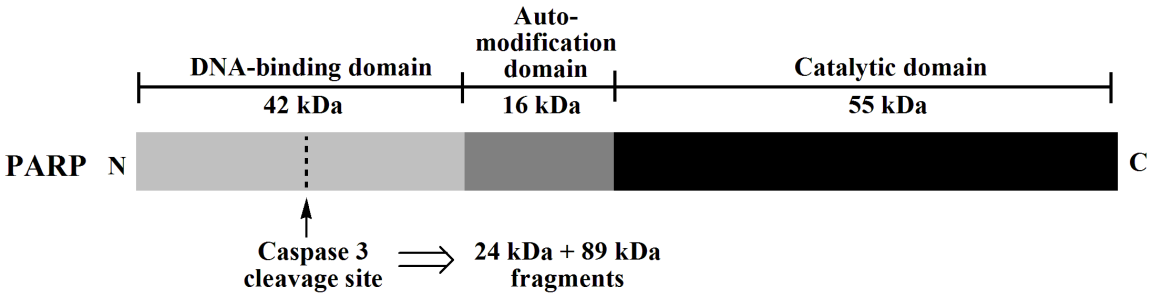

Figure 36: Representation of PARP functional domains and enzyme cleavage sites

There are many ways of detecting apoptosis in cells and tissues. Caspase-3 activity, mitochondrial activity, cytochrome C release, and Annexin V assays are all methods for detecting apoptosis. Sensitivities of the different assays vary greatly, and limitations include the impermeability of detection reagent and the inability to distinguish between events occurring in dying cells versus those events that indicate live cell activity. Our lab has previously shown that one SanA derivative induced apoptosis via Annexin V, which is a reagent that stains for phosphatidylserine residues that are presented on the cell

surface when the cell begins dying. While it is an excellent way to detect early apoptosis, it is limited in that it does not define the mechanism by which apoptosis is occurring.

To deduce the events occurring inside the cells treated with SanA, I chose to investigate the lead compounds SanA **13** and **15** for their induction of caspase-3 dependent apoptosis in HCT-116 cells via caspase 3 activity assays and PARP fragmentation analysis of the lysate. Because caspase 3 activity and PARP fragmentation are some of the last events occurring during caspase-dependent apoptosis, these assays will indicate if SanA is inducing cell death involving caspases versus caspase-independent apoptosis or even necrosis.

In the caspase assay for SanA **13**, 7.5×10^5 HCT-116 cells were seeded in tissue-culture grade petri dishes and allowed to incubate overnight. The media from each plate was aspirated and replaced with media containing 1-50 µM SanA **13**. DMSO (1%) was used as the control. The cells were incubated with compound for 24 hours and then were collected from the plate via trypsinization. They were lysed using a freeze-thaw method in dry ice and acetone. The cellular debris was pelleted, and the remaining lysate was analyzed for caspase 3 activity, with 30 µg of total lysate per well and 3-4 wells per compound or control. SanA **13** induces caspase 3 activity in a concentration-dependent fashion (**Figure 37**). At 1 and 5µM, there were slight increases in activity. But significant increases were seen at 25µM and 50µM, where the lysate showed 2-fold and 3-fold greater activity over the control (DMSO) lysate, respectively. There was no difference in caspase 3 activity between untreated cells and DMSO-treated cells (data not shown). While the concentrations of SanA **13** at which caspase activity is detected are several fold higher than its IC_{50}, this trend is consistent with data published for other anti-

cancer compounds that demonstrate apoptotic activity and is the result of the assay reagent requiring a large amount of caspase 3 activity to display visible detection.[104-106]

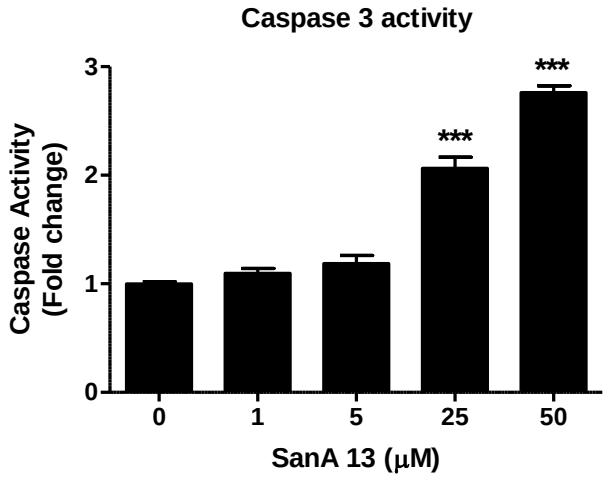

Figure 37: Caspase 3 activity for SanA 13-treated HCT-116 cell lysates. Statistical analysis was performed by an unpaired t test. ***p < 0.001.

The cell lysate from the caspase assay was also analyzed via western blot for PARP fragmentation where 10 µg of total protein was denatured in sample buffer and resolved on a sodium dodecyl sulfate polyacrylamide gel electrophoresis (SDS-PAGE) gel. The proteins were visualized via Western blot using an antibody for PARP and its corresponding enzyme-cleaved fragments. Reaffirming the caspase 3 data, I observed a decrease in the amount of full-length PARP with increasing concentrations of SanA **13** (**Figure 38**). In addition, the presence of 89 kDa PARP fragments at 25 µM and 50 µM concentrations also indicate that the cell is undergoing apoptosis, at least in part, through the cleavage of PARP. GAPDH, a constitutively expressed protein, was used as the loading control. Interestingly, the presence of a ~55 kDa band was also present at the two higher concentrations. There have been many reports of such 50—70 kDa PARP

fragments occurring in other cells induced by apoptosis.[102, 103] In addition, traditional proteases can cleave at the functional domains of PARP.[103] Given that PARP fragmentation for SanA **13** is associated with increased caspase 3 activity, these patterns are likely apoptosis-related.

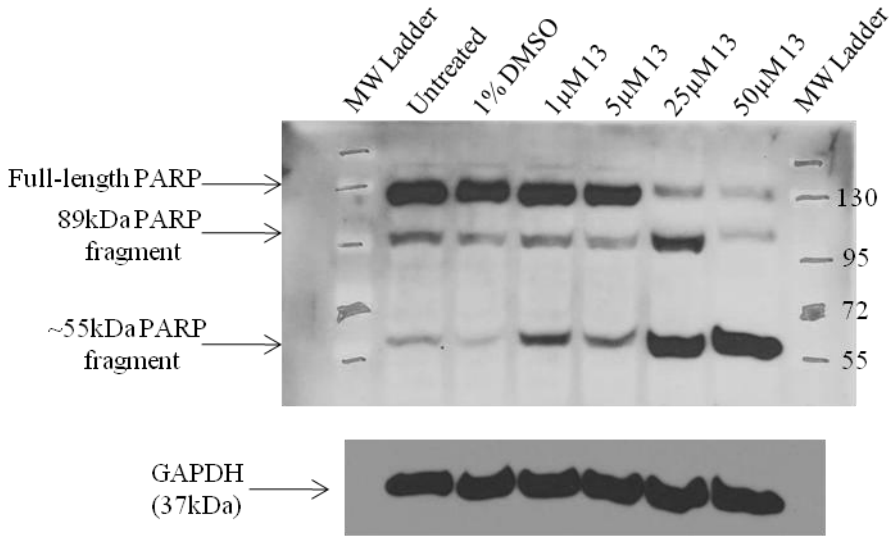

<u>Figure 38</u>: Western blot analysis of PARP in SanA 13-treated HCT-116 cell lysate, with GAPDH as loading control

Surprisingly, despite SanA 15's relatively low IC_{50}, the same caspase assay indicated that there was no caspase 3 activity (data not shown). Further, a decrease in full-length PARP and the presence of a ~55-kDa fragment is only noticeable at the 50 μM concentration point (**Figure 39**). Thus, while SanA **15** is obviously inhibiting cell proliferation with a low micromolar IC_{50}, we cannot conclude whether it is killing cells through a caspase 3-dependent apoptotic mechanism.

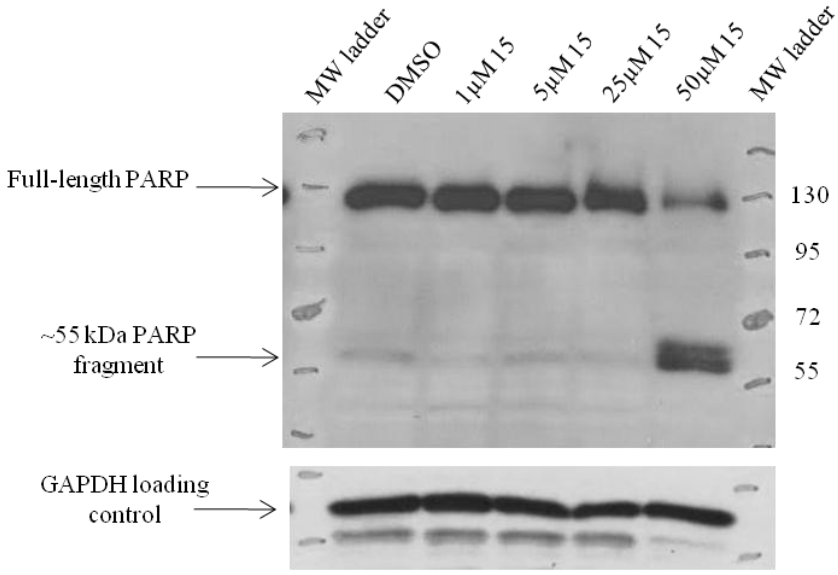

Figure 39: Western blot analysis of PARP in SanA 15-treated HCT-116 cell lysate

Using a caspase 3 activity assay along with PARP fragmentation analysis, SanA **13** appears to be acting through a caspase 3-dependent apoptotic mechanism. SanA **15**, however, does not show indications of caspase 3 activity and could be going through a different pathway of cell death. It is still possible that SanA **15** could be inducing apoptosis through a pathway that is caspase 3-independent. Both compounds were taken on in further mechanism of action studies and their activities were compared to see if they were acting through a similar mechanism, despite their difference in caspase activity.

CELL LYSATE PULL DOWN ASSAYS

A common approach utilized in determining the mechanism of action for a compound are affinity-based assays involving cellular lysate.[107, 108] The assay (illustrated in **Figure 40)** involves synthesizing a molecule to include a linker. This linker-molecule is incubated with cell lysate. Binding the linker-molecule-protein to a solid-support

produces the protein target. The complex then undergoes a series of washes to remove any non-specific binding. The proteins that remain bound to the molecule are resolved on an SDS-PAGE gel. Sequencing the gel provides molecular weights of possible protein targets. While there are several drawbacks associated with affinity-based assays, including non-specific binding that may provide false positives, this approach is extremely successful in determining the protein targets for numerous small molecules including the natural product Didemnin B and the immunosuppressant FK506.[109]

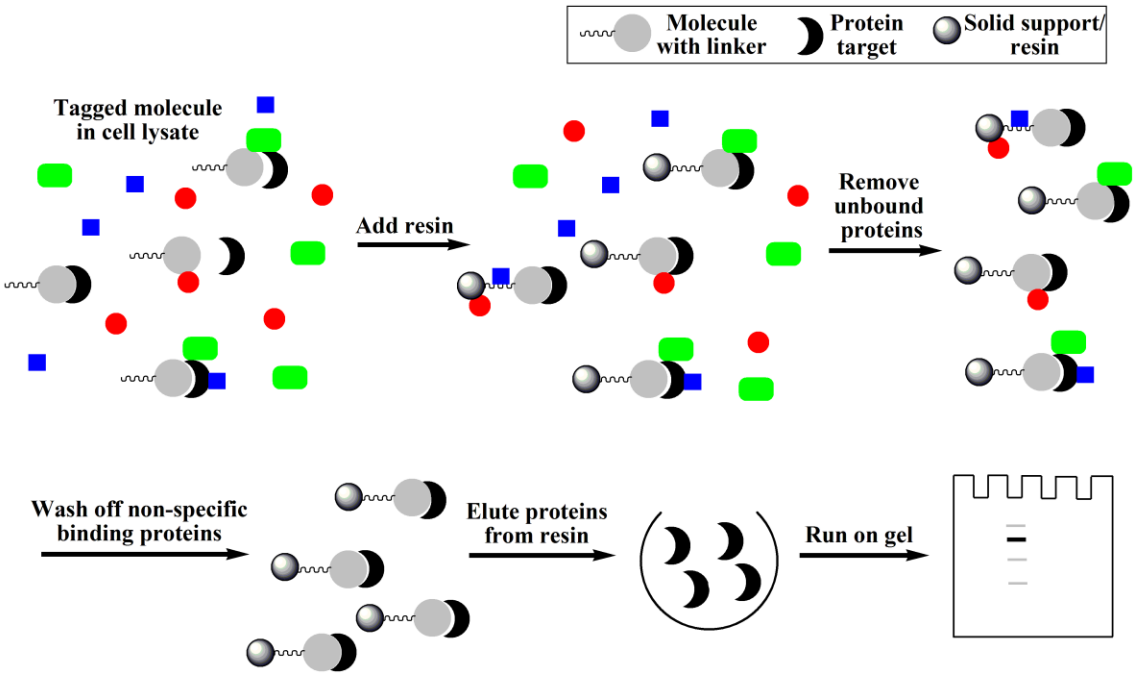

Figure 40: Affinity-based assay to determine protein target of a small molecule

Previous group members developed a protocol for a lysate pull down using SanA **1-T-IV-biotin** and determined, through sequencing analysis, that the compound bound to Hsp90.[110] However, this method utilized a large amount of compound (0.5 mg) per assay. I worked out conditions that improved the assay efficiency, whereby only a small amount of compound was required for successful experiments.

My method involved growing HCT-116 cells to confluency over three days, then harvesting and lysing them in NP-40 lysis buffer containing protease inhibitors. After quantitating the amount of lysate, 0.1 mg **1-T-IV-biotin**, dissolved in DMSO, was incubated with either 2 mg or 4 mg of total lysate for 24 hours; both NHS-PEG_4-biotin and DMSO were used as negative controls. NeutrAvidin resin was added to the experiments and incubated for 2 hours at 4 ºC. The experiments containing 2 mg of lysate were then washed with wash buffer for 30 minutes at 4 ºC followed by three washes for 10-15 minutes at room temperature. The experiments with 4 mg of lysate were washed seven times for 10-15 minutes each, three of the washes were at 4 ºC and four at room temperature. After the washes, the proteins were eluted with sample buffer and resolved on an SDS-PAGE gel. The gel was stained with coomassie blue and analyzed for Hsp90 via western blot (**Figure 41**). The experiments utilizing 2 mg of lysate and four washes, versus 4 mg of lysate and seven washes, gave the best results, with Hsp90 only being pulled down by **1-T-IV-biotin** and not the PEG-biotin and DMSO controls. Thus using these conditions for pull-down assays will allow us to use 75% less protein and 80% less compound than our original published protocol and it gives identical results to the previous assay.

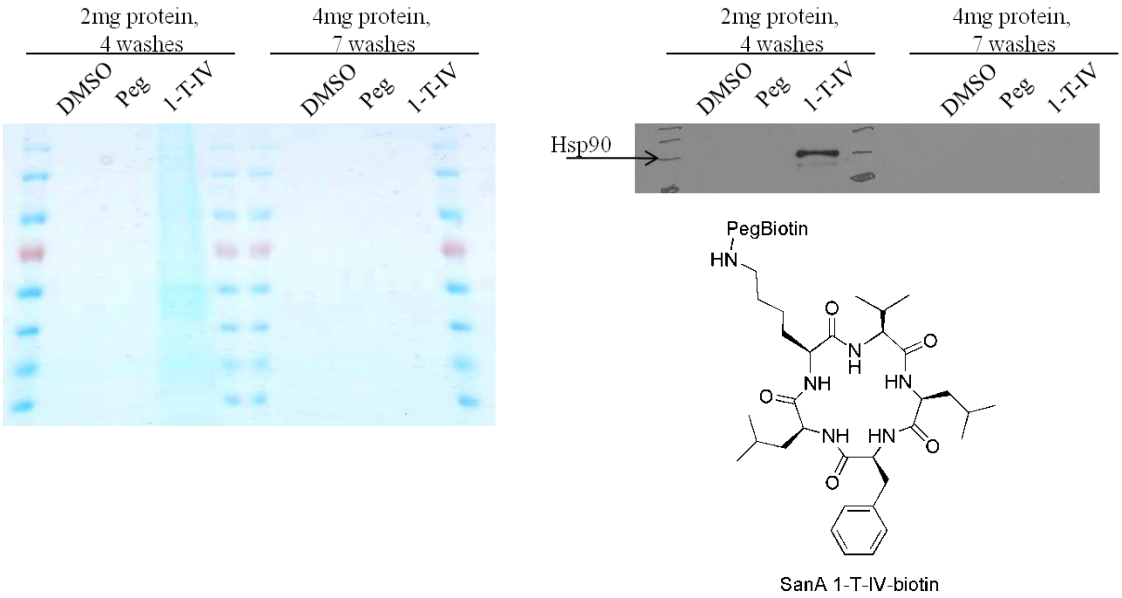

Figure 41: Lysate pull-down test experiment- Coomassie blue gel and Western blot for Hsp90

The optimized conditions were used for lysate pull-down assays using SanA **1-T-III-biotin** and **12-T-IV-biotin** as well as two of the biotin-tagged derivatives of SanA **13** (**13-T-II-biotin** and **13-T-III-biotin**) and SanA **15** (**15-T-II-biotin**, **15-T-III-biotin**) (**Figure 42**). After the proteins were eluted with sample buffer, run on an SDS-PAGE gel, and transferred to a PVDF, the presence of Hsp90 in the pulled down protein was detected by western blot. Interestingly, SanA **1-T-III-biotin**, **12-T-IV-biotin**, as well as two of the SanA 13-tagged derivatives pulled down Hsp90, but neither of the SanA 15-tagged compounds pulled down the protein.

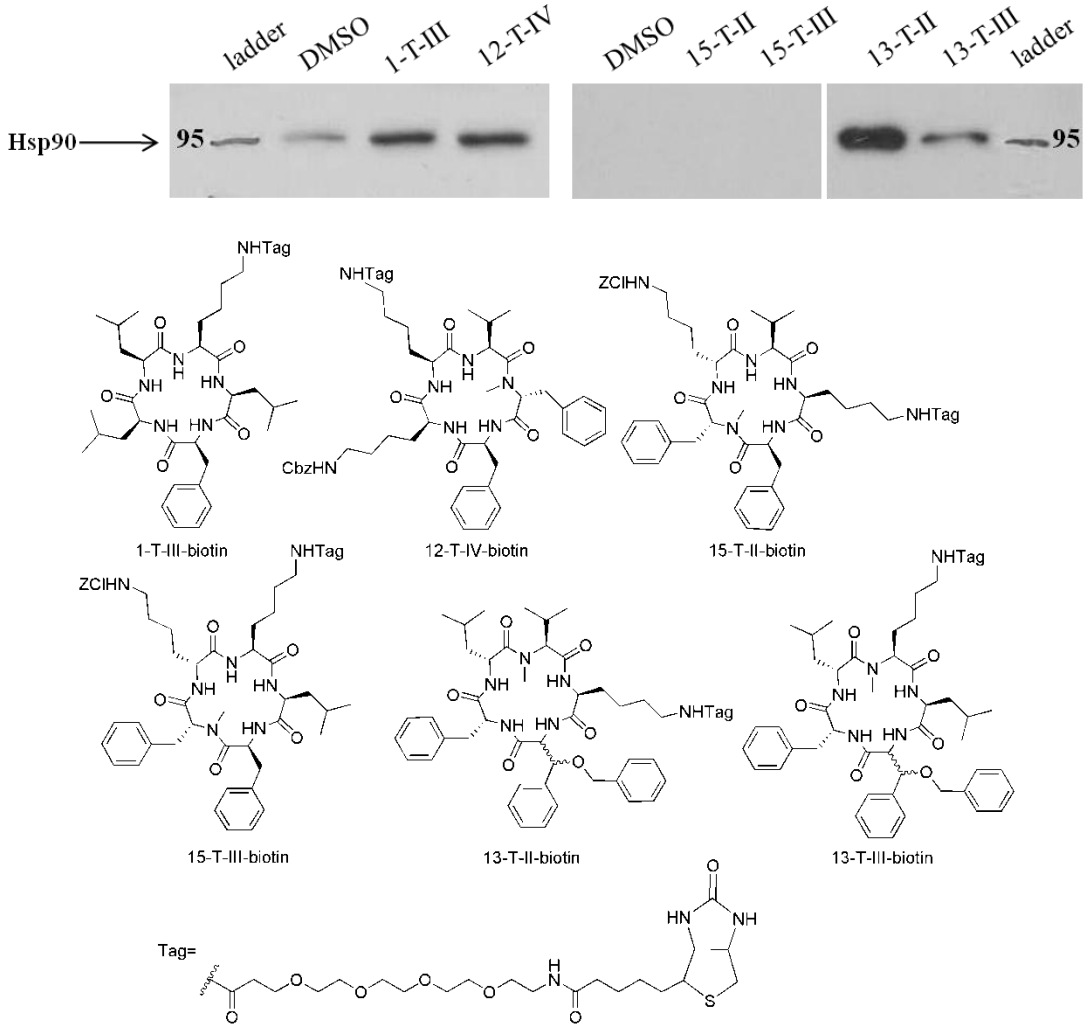

Figure 42: Cell lysate pull-down assay analysis by western blot, using an antibody for Hsp90, and structures of tagged compounds used in assay

In summary, a pull down assay in cell lysate was used to determine the protein target for four SanA derivatives. I confirmed that SanA **1** bound to Hsp90 in cell lysate. Further, I showed that SanA derivatives **12** and **13** also bound to Hsp90 in cell lysate while SanA **15** did not.

DOMAINS PULL DOWN ASSAYS

As discussed in Chapter 1, Hsp90 contains three functional domains: the N-terminal domain (N), which houses the ATP-binding pocket, the middle domain (M),

which is mainly involved in client protein associations, and the C-terminal domain (C), which is responsible for dimerization of two Hsp90 monomers. In order to narrow down the specific region of Hsp90 where SanA molecules bind, my colleagues performed pull-down assays using purified glutathione S-transferase (GST)-tagged Hsp90 domains including the N, NM, MC, and C, and our biotinylated compounds. They found that SanA **1** and **12** biotinylated derivatives bind exclusively to the NM domain.[110, 111] In addition, my colleagues and I performed a domain pull down assay for SanA **13** derivatives using **13-T-I-biotin**, **13-T-II-biotin**, and **13-T-III-biotin**.

In the assay, purified GST-tagged Hsp90 domains and biotin-tagged SanA derivatives were incubated together for 2 hours at room temperature, with gentle agitation. NeutrAvidin resin was added to each experiment, and the slurry was incubated for 45 minutes at room temperature. The resin was then washed four times with wash buffer and three times with binding buffer (20mM Tris, 150mM NaCl, 1% Triton-X-100, pH= 7.4). Finally, the proteins were eluted off the resin with sample buffer and resolved on a 4-20% SDS-PAGE gel. Proteins were visualized using silver stain according to the manufacturer's protocol. Similar to SanA **12**, we found that SanA **13**, too, bound almost exclusively to the NM middle domain (**Figure 43**).

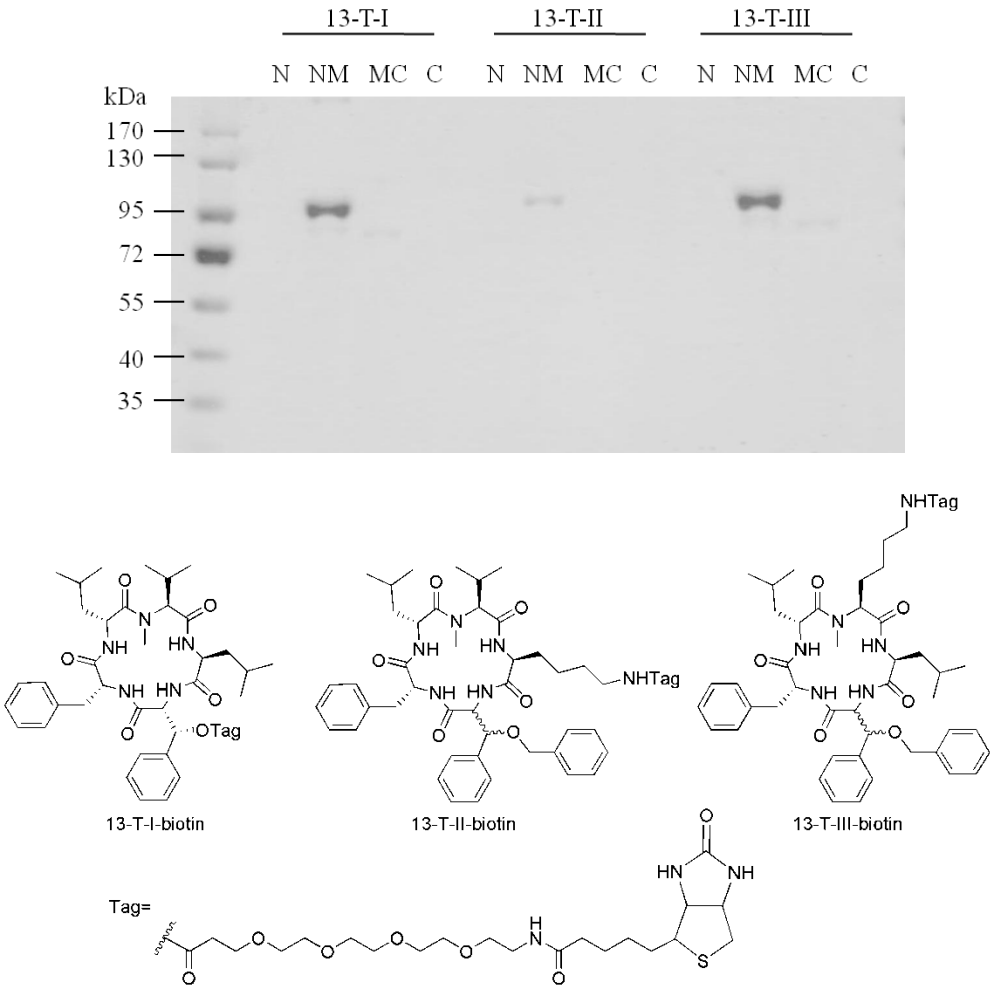

<u>Figure 43</u>: Results of domain pull down with SanA 13-tagged derivatives, silver-stained gel

All Hsp90 inhibitors currently in clinical trials bind to the ATP-binding pocket in the N-domain. However, all three SanA compounds (SanA **1**, **12**, and **13**) bind exclusively to the NM domain of Hsp90, making them a unique class of molecules. Since the biotin-tagged compounds provided such valuable information, we used the fluorescein-tagged compounds to determine SanA's binding affinity for Hsp90.

SUMMARY OF FLUORESCEIN-TAGGED SANA DATA

The fluorescein-tagged SanA derivatives I synthesized in Chapter 2 were used by a collaborator in fluorescence polarization anisotropy to determine the dissociation constants (K_ds) of SanA to Hsp90. Fluorescence polarization anisotropy uses pure protein and measures the tumbling rate of the attached fluorophore (i.e. fluorescein) on the small molecule. As the tagged-compound is exposed and binds to an increasing amount of target protein, its tumbling rate will continually slow down until it reaches saturation. Similar to IC_{50}s, a curve is generated to determine the K_d. Our collaborator determined that the K_ds to Hsp90 for SanA **1**, **12**, and **13** are in the mid-micromolar range (~50 μM). This is a 40-fold higher affinity than the Hsp90 inhibitor novobiocin (K_d~ 2 mM).[112]

Hsp90 also undergoes a series of ATP-driven conformational changes. Thus, our collaborators investigated SanA's preference for two of Hsp90 conformations by inducing the closure of the Hsp90 dimer into its closed-twisted ATP-bound form (**Figure 44**). They found that the compounds exhibit a 2-fold higher affinity for Hsp90's 'closed' conformation over its 'open' conformation (**Figure 44**). This is the first report of a small molecule preferring Hsp90's closed state. Additionally, the NM interface changes dramatically during the course of Hsp90's ATPase cycle, thus this data is also consistent with our compounds binding to the NM domain.[25, 113]

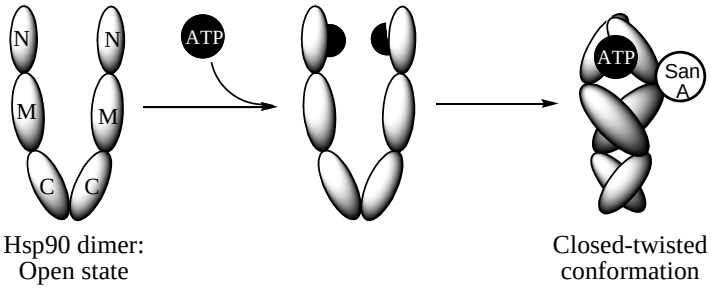

Figure 44: Hsp90's ATP-driven conformational changes

Utilizing two different types of tagged SanA derivatives (PEG_4-biotin and fluorescein), we have shown that the compounds bind to Hsp90. The next goal was to determine the whether the untagged derivatives also bind the target protein.

COMPETITIVE BINDING ASSAYS

One disadvantage of using affinity methods to determine protein targets of small molecules is that the linker may disrupt binding to the protein. While the position of the linker is often determined based on SAR analysis, it is not always guaranteed that incorporating the linker will not affect bioactivity or binding to the target.[107] Biotinylated derivatives of SanA **1** and SanA **13** bind to Hsp90, thus we wanted to verify the specificity of binding of untagged SanA using a competition assay.

A competitive binding assay between **1-T-III-biotin** and SanA **13** using native Hsp90 would give an indication if the two compounds bound to the same site within Hsp90. **1-T-III-biotin,** dissolved in DMSO, was incubated with 150 nM of native Hsp90 in assay buffer with a final concentration of 10 µM compound and 2% DMSO overall. Reactions were incubated at room temperature, with gentle agitation, for one hour allowing the protein to bind to the compound. SanA **13** was added to each reaction, with final concentrations of 0-25 µM, and incubated for 1 hour at room temperature. Controls

included DMSO in the presence of **1-T-III-biotin** (positive control) and absence of **1-T-III-biotin** (negative control). NeutrAvidin resin was added to all of the reactions and incubated for 30 minutes at room temperature. The resin was isolated and washed four times with wash buffer. Finally, the protein complexes were eluted in sample buffer and resolved on an SDS-PAGE gel, followed by Western blot analysis for the presence of Hsp90. The amount of Hsp90 detected for each concentration of SanA **13** was compared to that of DMSO, which was set at 100% Hsp90 binding to **1-T-III-biotin**. The negative control experiment indicated that Hsp90 binding was specific to the biotinylated compound.

The results show that increasing concentrations of untagged SanA **13** successfully compete with **1-T-III-biotin** for binding to Hsp90 with an IC_{50} of 0.92 µM (**Figure 45**). This type of competition assay has been observed in literature with compounds that bind to the N-terminal ATP-binding pocket of Hsp90 and indicates that the two compounds share the same binding site in Hsp90.[114]

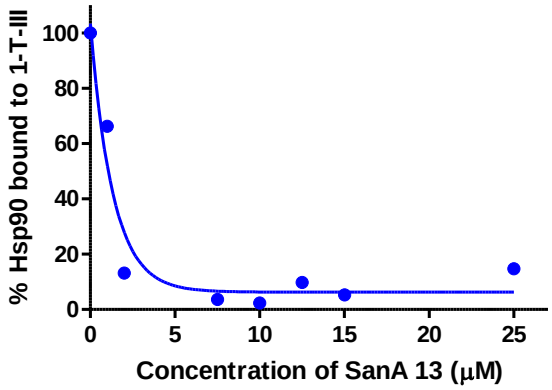

Figure 45: Results from competitive binding assay with SanA 1-T-III-biot and SanA 13

A similar assay was performed to see if SanA **13** would compete with its tagged derivative, **13-T-III-biot**, for binding to Hsp90. The affinity of Hsp90 for both the tagged and untagged derivatives of SanA **13** is verified by the results from our affinity purification assay, which is considered to be a valid approach for measuring specificity in protein-ligand interactions.[107-109] We had previously shown that SanA **1** could compete with its tagged derivative with an IC_{50} of 19.7 µM, which is comparable to its IC_{50} in cell culture.[74] The results of the experiment that I performed with SanA **13** shows that it can compete with its tagged derivative with an IC_{50} of 3.6 µM (**Figure 46**), which is also comparable to its IC_{50} in cell culture.

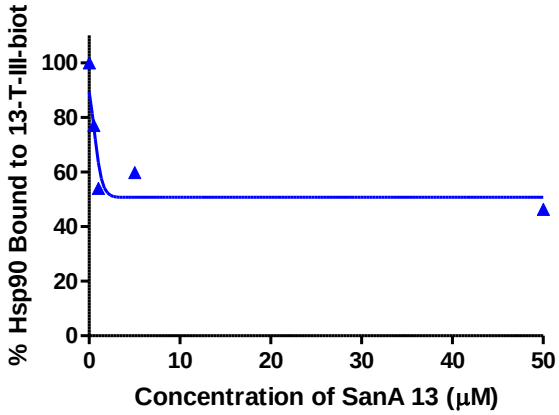

Figure 46: Competitive binding assay between SanA 13-T-III-biot and SanA 13

The competitive binding assays show that the binding of biotinylated-SanA to Hsp90 is due to a highly selective binding event between the N-middle domain. Further, since the untagged molecules successfully competed with the tagged compounds, these compounds are all binding to the same binding pocket of the N-middle domain within Hsp90.

Determining that our untagged, parent compounds bind to Hsp90 at a specific site allows us to use these compounds to address questions regarding Hsp90 modulation. Measuring direct binding interactions (protein-compound NMR studies), effects on Hsp90 localization and metastasis (microscopy), effects on Hsp90 depletion or over-expression (rescue experiments), as well as effects on Hsp90-client protein interactions (biochemical binding assays) will provide valuable data on this new class of Hsp90 inhibitors. As such, my main focus and contribution to this project was the development of client protein binding assays.

HSP90-CLIENT PROTEIN BINDING ASSAYS

Hsp90 helps regulate over 200 client proteins and co-chaperones. Several SanA derivatives bind to Hsp90, thus we were interested in determining if the compounds affected the interaction of client proteins with Hsp90.

The client proteins we initially chose to investigate include Akt, human epidermal growth factor receptor 2 (Her2), hypoxia-inducible factor-1 (Hif-1a), and inositol hexakisphosphate kinase 2 (IP6K2). Akt is a serine/threonine kinase that helps regulate pathways involved in proliferation and apoptosis. Many studies have determined that Akt has anti-apoptotic effects within those pathways.[115] Her2, also known as ErbB2, is over-expressed in many breast cancers and is highly dependent on Hsp90.[116, 117] In tumor cells, Her2 has been shown to activate Akt.[118] Her2 is very sensitive to Hsp90 inhibitors in clinical trials and its degradation can serve as a hallmark of Hsp90 inhibition.[43] Hif-1 is a protein that is involved in gene transcription under hypoxic conditions; it is responsible for regulating genes that code for proteins that help deliver oxygen to tissues.[119] Finally, IP6K2 was recently discovered as an Hsp90 client protein and has

been reported to be pro-apoptotic when not bound to Hsp90.[120] Unlike Hif-1, Akt, and Her2, which bind Hsp90's middle domain, IP6K2 binds to the C-terminal domain. The C-domain is responsible for dimerization and is mainly known for binding to co-chaperones that contain tetratricopeptide repeats (TPRs).

The binding assays utilized native Hsp90 protein with GST or His-tagged client proteins, where all proteins used were purchased. Native Hsp90 (100 or 150 nM) incubated with various concentrations of compound (0-10 μM) for one hour at room temperature with gentle agitation (**Figure 47**). Tagged client protein (50 or 75 nM) was then added and allowed to incubate for an additional hour at room temperature. Assays containing GST-tagged proteins were incubated with immobilized glutathione resin. Assays with His-tagged clients used metal talon affinity resin. The resin was incubated for 30 minutes at room temperature and then was washed three times with wash buffer. Finally, the proteins were eluted in sample buffer and resolved on an SDS-PAGE gel. Proteins were analyzed by Western blot or by staining with Coomassie Brilliant blue. The amount of Hsp90 present for each concentration of compound was compared to the amount present in the DMSO control. The values were normalized to the amount of client protein detected on the gel or western blot, and the graphs were generated using GraphPad Prism software.

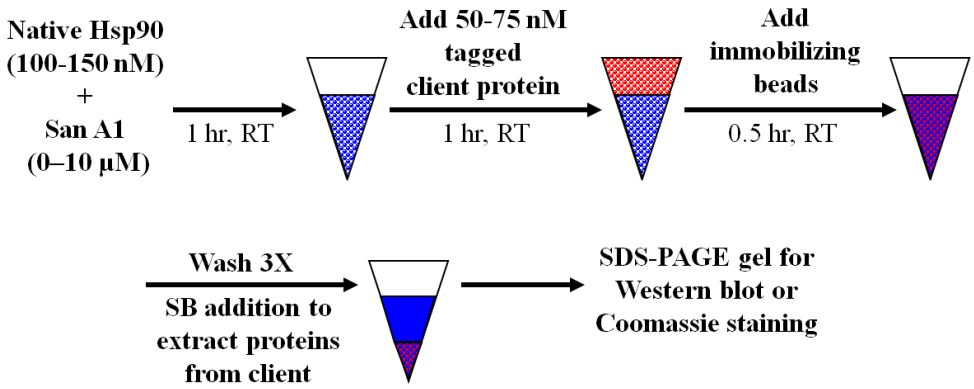

Figure 47: Hsp90-client protein binding assay method

Based on our previous results, we chose to investigate the impact of SanA **1**, **11**, **12**, **13**, and **15** in these Hsp90-client protein binding assays. **17-AAG** was used as a positive control since it has already been reported to affect the binding of Akt, Her2, and Hif-1a to Hsp90.[43] I used the procedure described to generate all of the data in the Hif-1a and Akt graphs, as well as for SanA **15** in the Her2 graph (**Figure 48**). Data for the other compounds on the Her2 graphs, as well as the entire IP6K2 graph, were generated by my colleagues.

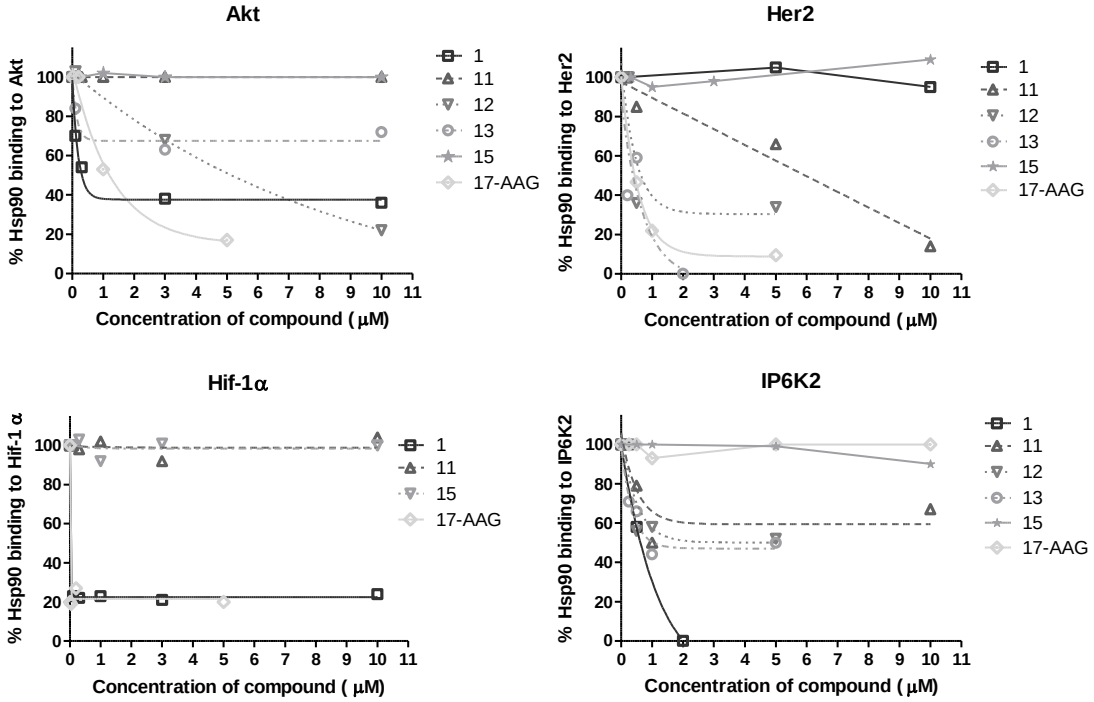

<u>Figure 48</u>: Hsp90-client protein binding assay data with Akt, Her2, Hif-1α, and IP6K2

In the Akt-Hsp90 binding assay, SanA **1**, **12**, **13**, and **17-AAG** disrupt the interaction in a concentration-dependent manner, while SanA **11** and **15** do not. With Her2-Hsp90, all of the compounds, except SanA **1** and **15**, disrupt binding. These are valuable findings given the important role both client proteins play in cell proliferation and survival. Disrupting the Akt-Hsp90 interaction has been reported to lead to the desphorylation and inactivation of Akt, which increases cell sensitivity to apoptosis.[115] In addition, Her2 activates Akt in cancer cells. Therefore, disrupting the Her2-Hsp90 complex leads to the degradation of Her2 and decreased Akt activity.[118]

The Hif-1-Hsp90 binding assays were only completed with four compounds. However, I found that SanA **1** and **17-AAG** disrupt the interaction, while SanA **11** and **15**

do not. Hif-1α is expressed in the majority of late-stage tumors, and treatment with current Hsp90 inhibitors, including 17-AAG, leads to its decreased expression and degradation.[43]

Finally, all of the SanA derivatives disrupt the IP6K2-Hsp90 interaction except for SanA **15** and **17-AAG**. Given that IP6K2 elicits pro-apoptotic activity when it is not bound to Hsp90, these results are favorable and further indicate that SanA induces apoptotic events in cells. Furthermore, this binding assay confirms previously published studies for **17-AAG,** where it elicits an effect on client proteins that bind to the M-domain (Akt, Her2, Hif-1α) but not on most proteins that bind to the C-domain, specifically IP6K2.[120]

SanA **15** is the sole SanA derivative does not disrupt the binding between any of the selected client proteins and Hsp90. While the IC_{50} for SanA **15** is similar to that of **12** and **13**, it exhibits unique behavior in our mechanism of action studies. Because these studies are preliminary, we will not rule out that SanA **15** is still acting via a different mechanism of Hsp90 inhibition.

These binding assays were performed where SanA or 17-AAG was allowed to bind to Hsp90 first. The client protein was added second and competes with the compound for binding to Hsp90. To investigate the reverse effect, I also performed binding assays where the client protein-Hsp90 complex was allowed to form first, and SanA was added second to see if it could compete with the client. This type of reverse experiment was conducted by another research group using novobiocin, the C-domain-binding molecule. The authors found that novobiocin would only have an effect on the binding of the client protein when it was allowed to bind to Hsp90 first.[121]

I did reverse binding assay using SanA **1** and **13** with the client proteins Akt and IP6K2. The protocol was the same as previously described except that Akt or IP6K2 was allowed to incubate with Hsp90 for the first hour at room temperature, followed by the addition of increasing concentrations of SanA **1** and **13**. The reverse binding assay results show that SanA **1** disrupts the binding of Akt-Hsp90 and IP6K2-Hsp90 with similar IC_{50}s as in the initial protocol (**Figure 49**). SanA **13** had a similar effect with the IP6K2-Hsp90 interaction and was actually more effective at disrupting Akt and Hsp90 than in the first assay. These results suggest that SanA's binding site is available in the presence or absence of these client proteins, and that SanA binding to Hsp90 likely induces conformational changes that results in a loss of client protein binding as opposed to inhibiting the client from binding directly.

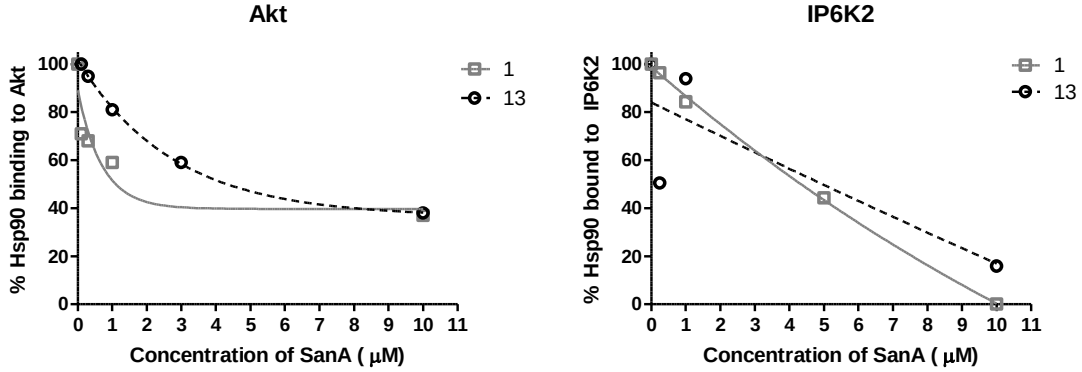

Figure 49: Reverse binding assay where the client-protein Hsp90 complex is allowed to form before the addition of SanA 1 and 13.

SUMMARY AND CONCLUSIONS

This chapter outlines our preliminary studies on the SanA mechanism of action. I was able to show that these derivatives demonstrate anti-proliferative activity in both PL-

45 and HCT-116 cells. Further, lead derivative, SanA **13**, successfully induced apoptosis that was detected via caspase 3 activity and PARP fragmentation methods. Using the biotinylated derivatives of SanA **1**, **12**, and **13**, whose syntheses were discussed in Chapter 2, my colleagues and I demonstrated that the compounds pull down Hsp90 in cell lysates, as well as Hsp90's NM domain in purified domain pull down assays. The fluorescein-tagged derivatives that I synthesized were used by our collaborator to determine that SanA exhibited mid-micromolar K_ds to Hsp90. And, finally, using pure protein binding assays, we were able to show that SanA disrupts the interaction between Hsp90 and its client proteins Akt, Her2, Hif-1α, and IP6K2, all of which have been identified as key proteins in cancer proliferation and survival.

Interestingly, all of the SanA compounds, except SanA **15**, disrupt the binding between Hsp90 and IP6K2, a client protein that binds to Hsp90's C-domain. SanA derivatives bind to the NM domain. Current inhibitors that bind to Hsp90's N-domain do not affect this interaction. Thus, SanA molecules have a novel mechanism of Hsp90 inhibition. SanA's effect on additional C-terminal binding client proteins and co-chaperones will be discussed further in Chapter 4.

ACKNOWLEDGEMENTS

This chapter contains material that has been published in Bioorganic and Medicinal Chemistry: Robert P. Sellers, Leslie D. Alexander, Victoria A. Johnson, Chun-Chieh Lin, Jeremiah Savage, Ricardo Corral, Jason Moss, Tim S. Slugocki, Erinprit K. Singh, Melinda R. Davis, Suchitra Ravula, Jamie E. Spicer, Jenna L Oelrich, Andrea Thornquist, Chung-Mao Pan, and Shelli R. McAlpine, **2010**, v15, p3287. Material that has been published in Bioorganic and Medicinal Chemistry Letters: Joseph Kunicki,

Mark Petersen, Leslie D. Alexander, Veronica C. Ardi, Jeanette McConnell, and Shelli R. McAlpine, **2011**, v21, p4716. Leslie D. Alexander, James R. Partridge, David A. Agard, and Shelli R. Mcalpine, **2011**, v21, p7068. Deborah M. Ramsey, Jeanette R. McConnell, Leslie D. Alexander, Kaishin W. Tanaka, Chester M. Vera, and Shelli R. McAlpine, **2012**, v22, p3287. And material that has been published in ACS Chemical Biology: Veronica C. Ardi, Leslie D. Alexander, Victoria A. Johnson, and Shelli R. McAlpine, **2011**, v6, p1357.

CHAPTER 4: SANSALVAMIDE A AND TETRATRICOPEPTIDE REPEAT-CONTAINING PROTEINS

BACKGROUND OF HSP90 CO-CHAPERONES WITH TPRS

The experiments discussed in Chapter 3 demonstrate that SanA derivatives bind to Hsp90's NM domain and inhibit the interaction of several client proteins including Hif-1α, Her2, Akt, and IP6K2. Unlike most client proteins that bind to Hsp90's M-domain, IP6K2 binds to the C-domain.[120] There are currently no reports of molecules that bind to the N or NM region and allosterically inhibit C-domain binding proteins. All 17 Hsp90 inhibitors in clinical trials target the same ATP-binding pocket in the Hsp90's N-domain.[43] However, none of the inhibitors have been approved for marketing, and drug resistance, via the activation of heat shock factor 1 (Hsf-1) and subsequent upregulation of Hsp70, presents a major hurdle. In the presence of current Hsp90 inhibitors, Hsp70's ability to save cells from apoptosis and to compensate for Hsp90's protein folding and stabilizing function has decreased the efficacy of the molecules in clinical trials. Given the need for the development of novel Hsp90 inhibitors, we explored SanA's unique ability to bind to Hsp90's NM domain and affect proteins that bind to Hsp90's C-domain.

Hsp90's C-domain serves two essential purposes: dimerization of two Hsp90 monomers, and regulating binding of tetratricopeptide (TPR)-containing co-chaperones via MEEVD (M= methionine, E= glutamic acid, E= glutamic acid, V= valine, D= aspartic acid), the last five amino acids on Hsp90's C-terminus. TPRs mediate protein-protein interactions and are often present in multi-protein complexes.[122] A TPR domain

is a degenerate 34 amino acid sequence found in many proteins within a variety of organisms. The amino acids that make up the 34 residue sequence are rarely conserved across individual TPRs.[123] Rather, the defining feature of a TPR is the helix-turn-helix secondary structure, where the residues involved in binding to proteins are presented on the outer faces of the helices.[122]

Only when TPRs form domains are they able to modulate protein-protein interactions. TPR domains are made up of 3-16 tandem TPRs, with 3 being the most common amongst human, yeast, bacterial, and plant genomes.[122] The first crystal structure of a TPR domain was solved for protein phosphatase 5 (PP5), a co-chaperone of Hsp90. It revealed that the three TPRs form a groove that interacts with MEEVD.[124] This type of motif is present in other TPR-containing proteins that bind to Hsp90. **Figure 50**, below, illustrates the MEEVD sequence (in white) interacting with the electrostatically positive (denoted by blue color) groove of a TPR domain in Heat shock organizing protein (HOP).

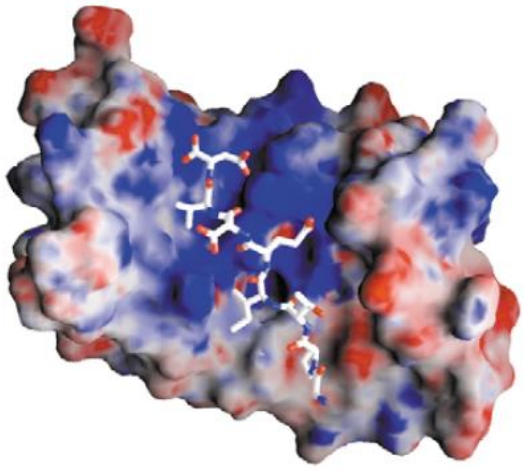

<u>Figure 50</u>: MEEVD bound to one of HOP's TPR domains. Positive electrostatic potential is blue, and negative is red. Original figure is from Kajander et al. *J. Biol. Chem.* 2009, v284, p25364- 25374.

TPR domains are found in numerous client proteins and co-chaperones regulated by both Hsp90 and Hsp70. Specifically, Hsp90 has sixteen co-chaperones that bind via their TPR domains to the MEEVD sequence in Hsp90.[40] Chaperone specificity for Hsp90 is attributed to specific hydrophobic interactions that occur between the TPR region of the chaperones and residues upstream of the MEEVD sequence in the C-domain.[123] In addition to the hydrophobic interaction, which dictates specificity, the strong electrostatic MEEVD-TPR interaction is derived from tight hydrogen bonding between acidic residues in MEEVD and basic residues presented by the TPR helix. The side-chain and terminal carboxylic group of the final residue, aspartic acid, form a hydrogen bond clamp to the TPR domains.[125] In addition, three positively-charged residues (two lysines and one arginine) have been identified within the TPR domains of PP5, FKBP52, and HOP, as being critical for forming an interaction with Hsp90's MEEVD region. [126, 127] **Figure 51** illustrates the interaction of MEEVD and the three

residues (K229, K301, and R305) in HOP's TPR domain. Two asparagines and a tyrosine residue within HOP's domain also form hydrogen bonding interactions with MEEVD.

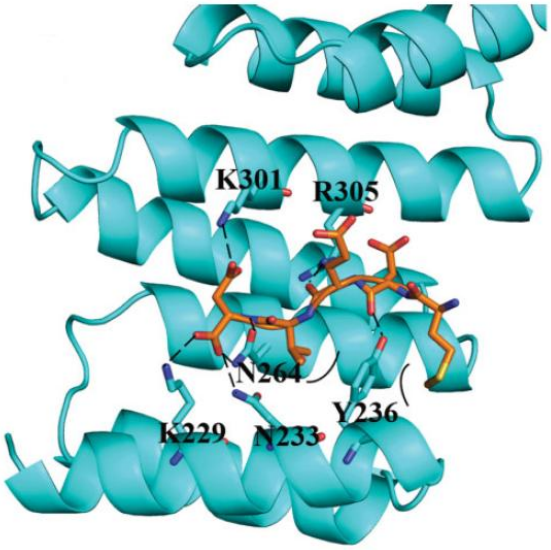

Figure 51: MEEVD interaction with specific residues in the TPR domain of HOP. Figure from Alag, et al. *Protein Science*. 2009, v18, p2115- 2124.

For our investigation of SanA's affect on TPR-containing proteins, we focused on five of Hsp90's TPR-containing co-chaperones. Via binding assays with native Hsp90 we investigated how SanA impacted the binding event between Hsp90 and the following co-chaperones: Fk506 binding protein 38 and 52 (FKBP38 and FKBP52), cyclophilin 40 (Cyp40), the UCS domain-containing protein Unc-45, and HOP.

FKBP52 and Cyp40 are immunophilins, which are proteins named for their ability to bind to the immunosuppressant drugs FK506 and Cyclosporin A, respectively. Both proteins are structurally similar and have been shown to compete with each other for binding to Hsp90.[128] In complexes with Hsp90 and p23, FKBP52 and Cyp40 are among the immunophilins that are essential in the assembly of steroid hormone receptors (SHRs)

(**Figure 52**). SHRs are critical to cellular development, primarily at the gene transcription level, and over-expression of these receptors plays a role in the development and progression of many cancers.[129] Specifically, the androgen receptor (AR), glucocorticoid receptor (GR), estrogen receptor (ER), and progesterone receptor (PR) are associated with the development of cancer cells.[130] Since SHRs rely heavily on the Hsp90-immunophilin complex for their maturation, a molecule that inhibits these complexes would be applicable to a wide range of cancers.

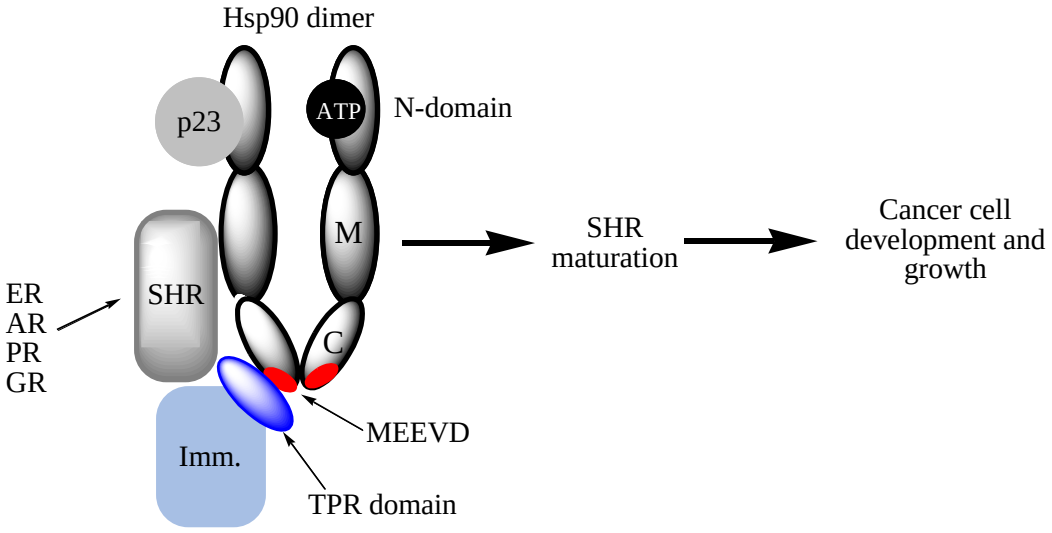

Figure 52: Hsp90-immunophilin complex leads to the maturation of SHRs in cancer

FKBP38, while a member of the immunophilin family, is not involved in SHR assembly.[131] It obtained its name from its homology to the immunophilins. Although FKBP38 is known for its ability to bind Hsp90 via its TPR domain, its primary mechanism involves inhibiting Bcl-2, an anti-apoptotic protein.[132] FKBP38 does not promote apoptosis when bound to Hsp90 (**Figure 53, Box A**). Thus, preventing FKBP38 from accessing Hsp90 promotes apoptosis by inhibiting Bcl-2's anti-apoptotic function (**Figure 53, Box B**).

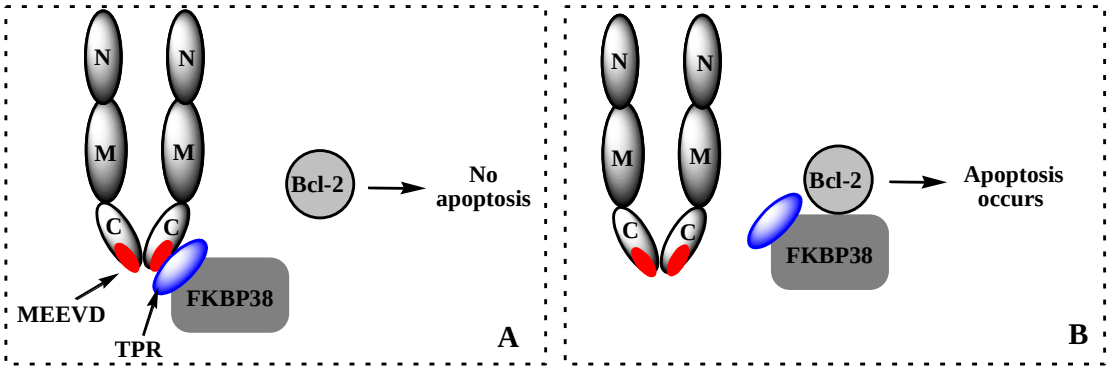

Figure 53: FKBP38-Hsp90 affect on Bcl-2 mediated apoptosis

HOP is a co-chaperone that facilitates the transfer of unfolded polypeptides from Hsp70 to Hsp90, and it contains three TPR domains.[133] One domain is responsible for binding to Hsp70's EEVD sequence, one binds to Hsp90's MEEVD sequence, and little is known about the purpose of the third domain (**Figure 54**).[134] Without HOP, the Hsp70 and Hsp90 interaction is minimal, thus this protein is crucial for Hsp90's protein folding function. [135]

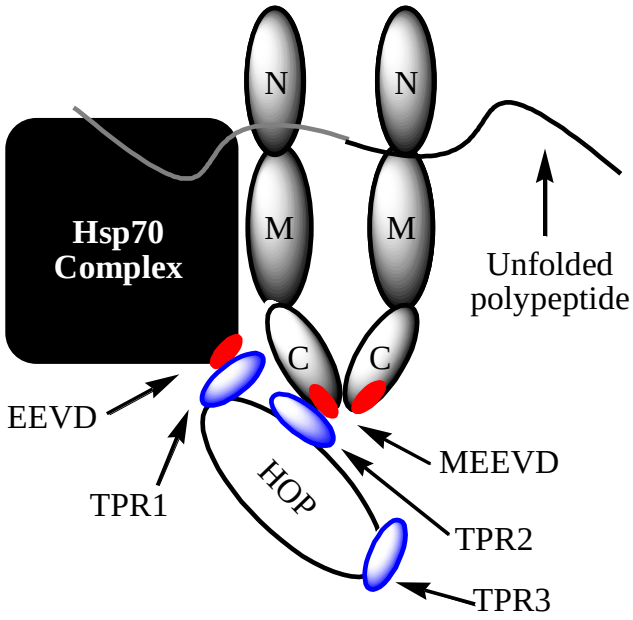

Figure 54: Diagram of Hsp70-HOP-Hsp90 complex

Finally, Unc45 is a co-chaperone that is involved in the assembly and folding of myosin, it is also important to myosin's function.[136] Myosin is an essential motor protein, required for cell division and motility.[137] Unc45 binds to Hsp90 via a single TPR domain located in its N-terminal region, while it binds myosin via its C-terminal domain.[136] The Hsp90-Unc45 interaction is required for the folding and maturation of myosin's motor domain, and the depletion of Unc45 *in vitro* inhibits cell proliferation and fusion.[138] Therefore, a molecule that inhibits this interaction will directly affect cancer cell proliferation.

Hsp90 inhibitors that modulate the N-terminus, including GDA and 17-AAG, do not inhibit the binding of these TPR-containing co-chaperones to Hsp90. Thus, our SanA derivatives, which bind to the N-middle domain, are novel Hsp90 inhibitors with a unique mechanism. Although degradation of the SHRs is observed with both GDA and 17-AAG, it is via a mechanism independent of immunophilin modulation. N-terminal Hsp90 inhibitors block the binding of p23, a co-chaperone that is important, but not essential, in the Hsp90-immunophilin-SHR complex (**Figure 52**).[139] p23 is responsible for promoting the release of mature SHRs from Hsp90. However, Hsp90 can still fold immature SHRs and facilitate their maturation in p23's absence.[140] The depletion of p23 in a cell sensitizes it to Hsp90 inhibitors, making N-terminal Hsp90 inhibitors more effective at inducing apoptosis in p23's absence. Therefore, in addition to current challenges with Hsf-1 and Hsp70-related drug resistance, p23 is a factor in cells' resistance mechanism against N-terminal Hsp90 inhibitors.[141] Disrupting the Hsp90-immunophilin interaction via our SanA molecule is likely to be more effective because p23-associated drug resistance is exclusive to N-terminal inhibitors. Further, unlike p23,

the immunophilins are required for SHR development.[130] Thus, this novel mechanism has two important advantages over the current mechanisms of current Hsp90 inhibitors.

Exploring the inhibition mechanism of molecules that bind to the C-domain [novobiocin and coumermycin A1 (**Figure 55**)] often focuses on their ability interrupt Hsp90 dimerization. However, they have been shown to affect GR production *in vivo*, potentially by inhibiting the Hsp90-immunophilin interaction.[121] Novobiocin is a coumarin antibiotic that binds to a nucleotide-binding site located in Hsp90's C-domain.[142] Allan et al. reported that novobiocin depletes GR protein in HeLa cells treated with 1 mM of the compound. Further, in the low millimolar range, novobiocin disrupts the binding of TPR-containing immunophilins FKBP52, Cyp40, and PP5 to a C-domain protein fragment of Hsp90 in *in vitro* binding assays.[121] The authors suggest that novobiocin's binding site in the C-domain overlaps with the region of Hsp90 upstream of MEEVD, which is involved in hydrophobic interactions with TPR-proteins. Thus, novobiocin directly interferes with these interactions.

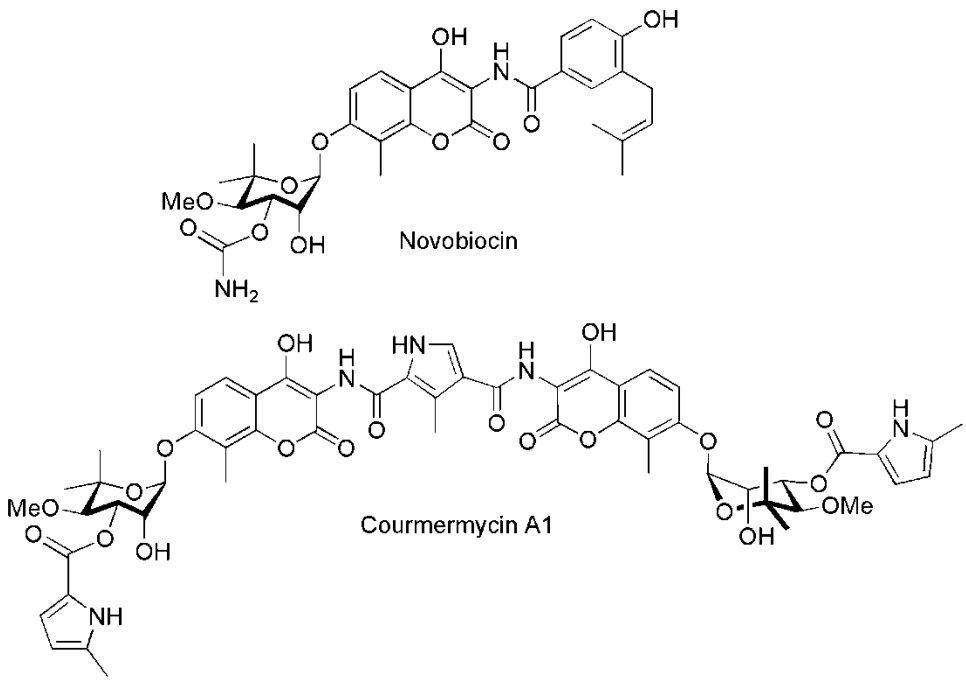

Figure 55: Novobiocin and Coumermycin A1 bind to Hsp90's C-terminal domain

Coumermycin A1 is structurally related to novobiocin, but has improved cytotoxic activity over novobiocin (IC_{50}~ 9 µM versus ~ 470 µM in SKBr3 cells, respectively). [143] In addition to their study of novobiocin, Allan et al. also found that coumermycin depletes GR protein in HeLa cells at 50 µM, which is a 20-fold lower concentration than novobiocin. Experiments examining coumermycin's affect on the Hsp90-immunophilin interaction were not conducted in the study. However, its structural similarity to novobiocin means that they likely share the same binding pocket in Hsp90.[142] Thus, coumermycin's ability to deplete GR protein is likely the result of the same Hsp90-immunophilin inhibition mechanism as novobiocin, where it interferes with the hydrophobic interactions that occur upstream from MEEVD.

Given the high concentrations of novobiocin required for detectable immunophilin inhibition, it is unlikely to make an effective tool in our binding assays for

studying the interaction between the TPR-containing proteins and Hsp90. Coumermycin A1 was used as a positive control in our studies on the Hsp90-TPR interaction because it causes the depletion of GR at a concentration 20-fold lower than novobiocin. Further, these binding assays will confirm that, like novobiocin, coumermycin affects GR via inhibition of immunophilin binding to Hsp90.

PURE PROTEIN BINDING ASSAYS

In addition to coumermycin, SanA **13** was used in binding assays to determine its effect on the interaction between Hsp90 and the TPR-containing proteins. As shown in Chapter 3, SanA **13** induces caspase 3-dependent apoptosis and selectively pulls down Hsp90's NM domain. In addition, SanA **13** inhibits the binding between Hsp90 and client proteins that bind to the M-domain, as well as IP6K2. Given that IP6K2 binds to the C-domain, like TPR-containing proteins, we wanted to develop SanA **13**'s mechanistic profile as an allosteric Hsp90 inhibitor. SanA **15** and **17-AAG** were the SanA and Hsp90 inhibitor negative controls, respectively, because we did not expect to observe an effect with these two compounds. SanA **15** did not disrupt the binding between Hsp90 and any client proteins in Chapter 3, including IP6K2. And **17-AAG** has not been shown to affect the binding of TPR-containing co-chaperones to Hsp90.

Following the binding assay method described in Chapter 3, I performed the experiments using native Hsp90 and GST- or His-tagged FKBP38, FKBP52, HOP, Unc-45, and Cyp40. The assay involved incubating native Hsp90 with several concentrations (0 up to 25 μM) of SanA **13**, **15**, coumermycin, or 17-AAG for one hour, followed by the addition of the tagged client protein for one hour. Immobilizing beads were added for 30 minutes and then were washed thoroughly three times with wash buffer. The proteins

were eluted with sample buffer and resolved on an SDS-PAGE gel. The proteins were visualized by Western blot to determine the amount of Hsp90 and client protein.

SanA **13** inhibits the binding of Hsp90 to the immunophilins FKBP52 and Cyp40, both of which are involved in the folding and maturation of SHRs, at IC_{50}s of 1.07 µM and 0.70 µM, respectively (**Figure 56**). FKBP52 and Cyp40 are structurally similar and can compete with each other for binding to Hsp90, which means their interactions with Hsp90 are similar. Thus, it is reasonable that SanA **13** would affect the binding of both FKBP52 and Cyp40 with comparable IC_{50}s. Given the essential roles they protein play in SHR production by forming complexes with Hsp90, SanA's ability to disrupt this interaction means that it will directly affect SHRs.

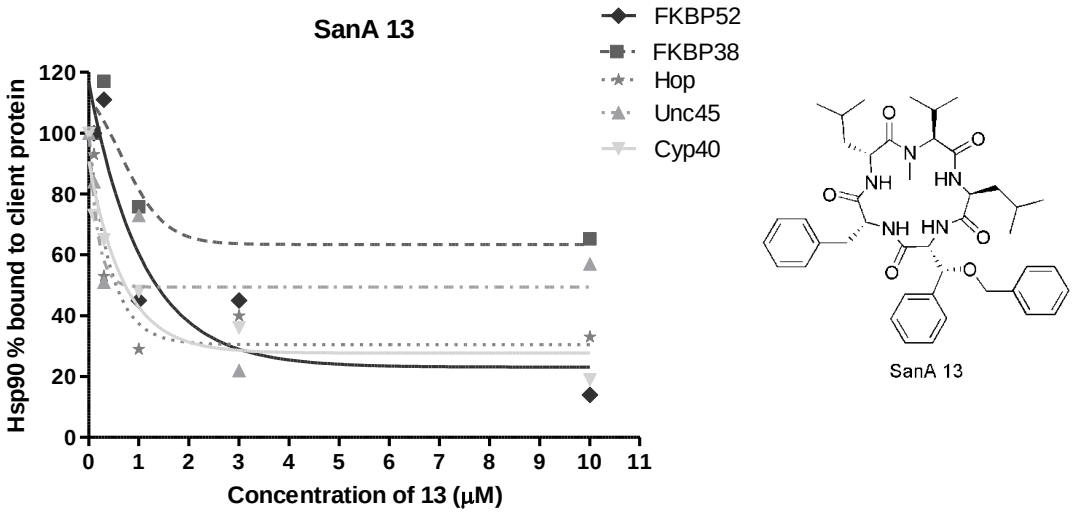

Figure 56: SanA 13 inhibits binding between Hsp90 and TPR-containing proteins

SanA **13** also inhibited the Hsp90-HOP interaction with an IC_{50} of 0.55 µM. HOP is crucial for binding to both Hsp70 and Hsp90, and facilitating the transfer of unfolded polypeptides from 70 to 90. Without HOP, the chaperones would not interact, the polypeptide would not be transferred, and the protein folding cycle would cease to

progress. Therefore, SanA has the ability to prevent initial processes in folding of oncogenic client proteins.

Adding to SanA **13**'s versatility, I also found that it inhibits Unc45 from binding to Hsp90 with an IC_{50} of 0.75 µM. Both Hsp90 and Unc45 are required for the folding of myosin's motor domain and the depletion of Unc45 in a cell causes an arrest in cell proliferation. Thus, SanA **13** has the ability to affect myosin-related cell proliferation by binding to Hsp90 and inhibiting its interaction with Unc45.

Finally, only 63% of Hsp90 was bound to FKBP38 (versus 100% binding in the 0 µM control) in the presence of 2-10 µM SanA **13**, i.e. SanA demonstrated 37% inhibition of the Hsp90-FKBP38 interaction. The concentration required for SanA **13** to inhibit the FKBP38-Hsp90 interaction is not consistent with the mid-nanomolar and low micromolar IC_{50}s found with the FKBP52, Cyp40, HOP, and Unc45 assays. However, FKBP38 has a direct role in promoting apoptosis when it is free from Hsp90 by binding to the anti-apoptotic protein Bcl-2. Thus, any inhibition of the Hsp90-FKBP38 interaction caused by SanA will increase potential apoptotic events within cancer cells.

Despite SanA **15**'s nearly identical IC_{50} to SanA **13**, it demonstrated unique behavior in Chapter 3. Unlike SanA **13**, **15** did not demonstrate evidence of inducing caspase 3-related apoptosis and its biotin-tagged derivatives did not pull down Hsp90 in cell lysate. Further, it did not have any effect in the Hsp90 client protein assays on the interaction between Hsp90 and Hif-1, Akt, Her or IP6K2. Accordingly, it did not disrupt the binding between Hsp90 and the TPR-containing proteins FKBP52, FKBP38, HOP, and Unc45 (**Figure 57**). These results validate that SanA **15** exhibits anti-proliferative effects via a mechanism unlike that of SanA **13**. However, given that there are still many

other aspects to investigate in Hsp90's function, we cannot rule out that SanA **15**'s mechanism of action is unrelated to Hsp90. Using imaging and NMR methods, additional studies on this molecule's unique mechanistic profile are currently being performed by my colleagues.

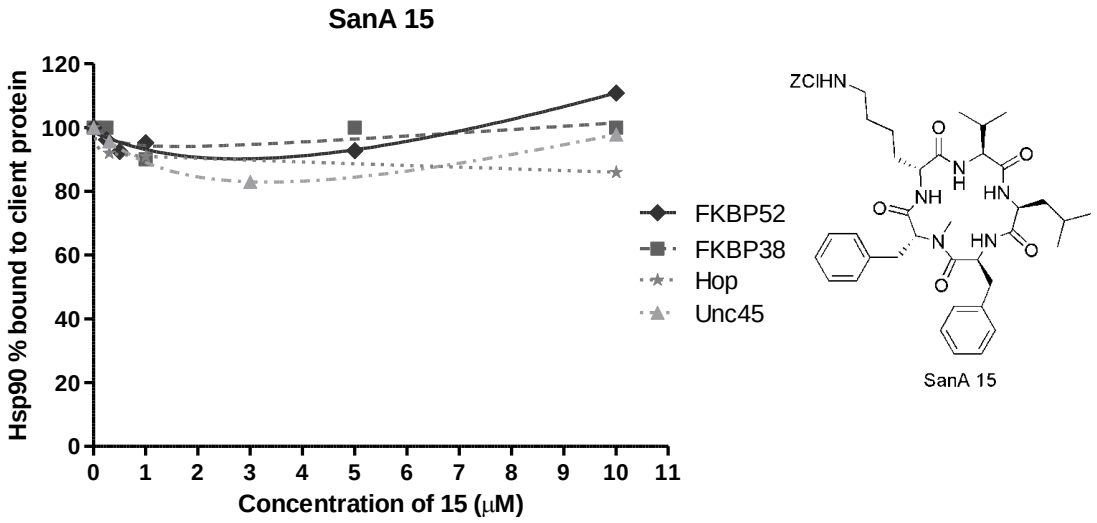

Figure 57: SanA 15 as a negative control in Hsp90-TPR protein binding assays

We demonstrated in Chapter 3 that 17-AAG disrupts the binding between Hsp90 and Akt, Her2, and Hif-1a, clients that bind to Hsp90's middle domain. However, 17-AAG did not disrupt the IP6K2-Hsp90 interaction, confirming the literature precedence that the N-terminal inhibitors do not affect binding of C-domain client proteins and co-chaperones.[40, 120] As predicted for the TPR-protein binding assays, 17-AAG did not disrupt the binding of the TPR-containing proteins to Hsp90, even at concentrations up to 5 μM (**Figure 58**). These results illustrate the limitations associated with 17-AAG's Hsp90 inhibition mechanism, where it is specific to inhibiting Hsp90's ATPase activity and only affects a select group of client proteins that bind to the middle domain. Further,

17-AAG's results highlight SanA's versatility in modulating proteins that bind to both the middle and C-domain.

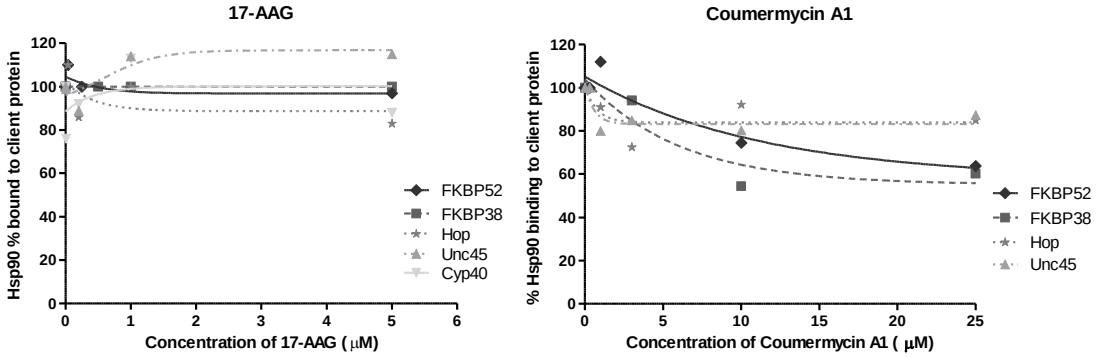

Figure 58: Hsp90 inhibitors 17-AAG and Coumermycin A1 binding assay data

Coumermycin demonstrated slight inhibition of Hsp90 binding to TPR-proteins, but not with mid-nanomolar and low-micromolar IC_{50}s exhibited by SanA **13**. Only 60% of Hsp90 bound to both FKBP38 and FKBP52 in the presence of 25 μM coumermycin, or 40% of Hsp90 was inhibited by the compound. For HOP and Unc45, approximately 80% of Hsp90 bound to the proteins, thus coumermycin only inhibited 20% of Hsp90. The decreased effect observed with coumermycin can be attributed its higher IC_{50} values, 9-70 μM, in various cell lines),[142, 143] compared to SanA, whose IC_{50} is less than 5 μM in PL-45 and HCT-116 cell lines. Further, coumermycin is likely binding to the same site in Hsp90's C-domain as novobiocin and subsequently disrupting the hydrophobic interactions that occur between the immunophilins and Hsp90 upstream from MEEVD. TPR-containing proteins do not bind to Hsp90 with identical hydrophobic interactions, which contributes to binding specificity.[126] Therefore, the location and degree of hydrophobic interaction occurring upstream of MEEVD varies by protein. Thus, if HOP and Unc45's hydrophobic interactions with Hsp90 do not overlap with coumermycin's

binding site as much as FKBP38 or FKBP52's interacting regions, a decreased effect would be observed.

Coumermycin's activity in these binding assays highlights the advantage of SanA's allosteric effect versus coumermycin or novobiocin's direct effect. With SanA, modulating the entire C-domain means inhibiting all TPR proteins with similar activity, whereas coumermycin is limited to disrupting protein interactions that overlap its binding pocket.

REVERSE BINDING ASSAYS

The data illustrating SanA **13**'s affect on the binding between Hsp90 and TPR-containing proteins (**Figure 56**) was generated using a protocol that allowed the compound to bind to Hsp90 first before the addition of the TPR-protein. Because SanA binds to the NM domain and disrupts the binding of C-domain co-chaperones, it is inducing an allosteric affect, causing Hsp90 to undergo a conformational change. The inhibition of TPR-proteins and Hsp90 that we observed with SanA is potentially the result of client proteins having a lower binding affinity for Hsp90's altered conformation than for its native (drug-free) form. However, under biological conditions, some Hsp90 proteins will be bound to TPR-containing proteins when SanA is added. To account for these potential limitations, I conducted reverse binding assays where the Hsp90-client complex was formed first, followed by the addition of compound. This method addresses two issues: 1) Is SanA's binding site in the N-middle domain still available upon binding of TPR proteins to Hsp90? It is possible that TPR proteins induce a change on Hsp90 that renders SanA's site altered or blocked. 2) Is SanA able to produce the same effect on a pre-formed Hsp90-TPR protein complex as it does when it binds to Hsp90 first?

Utilizing SanA **13** and three TPR containing proteins, FKBP38, FKBP52, and HOP, I conducted reverse binding assays in which Hsp90 and the TPR proteins were allowed to incubate for 1 hour, followed by the addition of compound for one hour. The client proteins were immobilized and the resin was washed three times with wash buffer. The proteins were eluted with sample buffer, resolved in an SDS-PAGE gel, and visualized via Western blot. As seen when Hsp90 was allowed to bind first with Akt and IP6K2 before adding the compound (Chapter 3, **Figure 49**), SanA **13** also inhibited the binding of all three TPR-containing proteins to Hsp90 (**Figure 59**). However, the degree of inhibition was not as strong as when the SanA-Hsp90 complex formed first. In the reverse binding assays, ~80% of Hsp90 bound to HOP in the presence of SanA **13** (i.e. ~20% was inhibited), whereas the IC_{50} in the original assay was 0.55 μM. For FKBP52, ~30% of Hsp90 was inhibited from binding to the co-chaperone by SanA **13**, compared to an IC_{50} of 1.07 μM in the first assay. Finally, ~20% of Hsp90 was inhibited from binding to FKBP38 by SanA **13**, compared to 37% in the first assay.

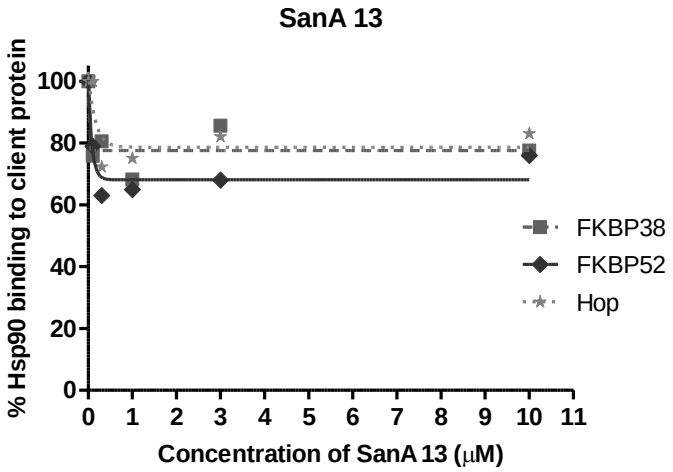

Figure 59: Results of the SanA 13 reverse binding assay with Hsp90 and FKBP38, FKBP52, and HOP

The decreased effect of SanA can be attributed to the two issues discussed: Either SanA's binding site is altered when TPR proteins are bound, thus decreasing the affinity of the compound to Hsp90, or the TPR-Hsp90 complex is more stable when the two proteins are allowed to interact in the absence of an inhibitor than when they are attempting to interact in the presence of an inhibitor. However, these assays show that SanA **13** does inhibit binding between TPR-containing proteins and Hsp90 when it is added after the formation of the protein complex. Furthermore, this characteristic was not seen when novobiocin was tested in binding assays with FKBP52, Cyp40, and PP5. In these assays, novobiocin only affected co-chaperone binding to Hsp90 when it was allowed to bind to Hsp90 first.[121] That means, in a cell, novobiocin is only effective as an inhibitor if Hsp90's C-domain is free from TPR-containing proteins. Thus, SanA **13** demonstrates a novel mechanism by which it modulates Hsp90 both in the presence or absence of TPR-containing proteins.

HOP AND MC-DOMAIN BINDING ASSAYS

It has been established that SanA **13** binds to the NM domain of Hsp90, and the binding assay results in this chapter indicate SanA **13**'s strong effectiveness at blocking binding between Hsp90 and TPR-containing proteins. Modulating the immunophilins via a unique mechanism provides an effective new lead that targets Hsp90 as well as the opportunity to use SanA **13** as a tool to explore this mechanism. Confirming the binding assay results and SanA **13'**s binding site at the N-middle domain would strengthen SanA's mechanistic profile as an allosteric Hsp90 inhibitor. Performing binding assays using only Hsp90's MC domain would validate that SanA is binding to the NM domain and allosterically inhibiting the binding of TPR-containing proteins. Eliminating SanA

13's binding site in the NM domain would result in SanA **13** having no effect on the binding event between Hsp90 and the TPR-containing proteins.

Following the same protocol described in Chapter 3 and for the binding assays in this chapter, several concentrations (0 to 10 μM) of SanA **13**, **15**, **17-AAG**, and coumermycin were incubated with purified GST-tagged MC domain for one hour, followed by the addition of His-tagged HOP protein for one hour. HOP was immobilized with metal talon affinity resin, and the proteins were eluted with sample buffer, resolved on an SDS-PAGE gel, and analyzed via Western blot. In addition to SanA **13**, both SanA **15** and **17-AAG** were used as negative controls to validate our results. SanA **15** does not affect Hsp90 in binding assays, and **17-AAG** only binds to the N-domain and has no effect on binding between TPR-proteins and Hsp90. Coumermycin was used as a positive control because it binds in the C-domain and directly inhibits binding of TPR-proteins.

As expected, none of the three compounds (SanA **13**, **15**, and **17-AAG**) inhibited the binding between HOP and the MC domain (**Figure 60**). Since the binding sites for SanA **13** and **17-AAG** are no longer on the protein, these compounds are not expected to have any effect on the binding event between Hsp90 and HOP. And SanA **15** has not demonstrated any affect in previous binding assays in chapters 3 or 4. Appropriately, coumermycin had comparable inhibitory activity to when the binding assay is run using full-length protein, where ~80% of Hsp90 was bound to the client protein (20% inhibition of the binding interaction) in both assays. Given that the binding site for coumermycin is at the C-terminus, unlike the other three compounds, it would have the ability to directly inhibit the HOP-Hsp90 interaction (**Figure 60**). In summary, eliminating the NM

interface supports our previous evidence that SanA binds to the NM domain and induces an allosteric affect on Hsp90, thereby modulating TPR-containing co-chaperones.

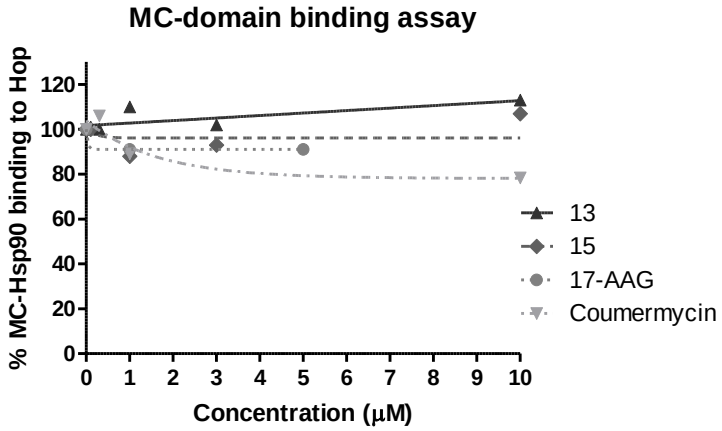

Figure 60: Results of MC-domain binding assay with SanA, 17-AAG, and Coumermycin

SUMMARY AND CONCLUSIONS FROM SANSALVAMIDE A MECHANISM OF ACTION STUDIES

This mechanism demonstrated by SanA **13** is unique to any compound reported, where SanA binds to the NM region of Hsp90 and affects the binding of TPR-containing co-chaperones. Using pure protein binding assays, I showed that increasing concentrations of SanA **13** successfully disrupts the binding between Hsp90 and TPR-containing proteins FKBP38, FKBP52, HOP, Unc-45, and Cyp40. SanA's disruption of the Hsp90 and client protein interaction was observed when SanA bound to Hsp90 prior to the addition of client protein, as well as when the client-Hsp90 complex was allowed to form before the addition of compound. The co-chaperones used in the binding assays are involved in SHR production, apoptosis, and myosin function, thus SanA **13** affects a multitude of processes that are essential to cancer cell development, proliferation, and

survival. In addition, using only Hsp90's MC domain, I found that SanA did not disrupt the binding of the clients and Hsp90, which validates that SanA binds to the NM region and causes an allosteric effect on the client proteins and co-chaperones.

There are still a number factors and pathways to investigate in SanA's inhibitory mechanism on Hsp90. However, SanA's ability to bind to Hsp90 and modulate the binding of client proteins and co-chaperones demonstrates its potential role in elucidating the function that client proteins and co-chaperones involved in cancer cell progression. Using pull-down assays, *in vitro* binding assays, fluorescence anisotropy, and apoptosis studies, we have begun to expose the unique mechanism of this cyclic pentapeptide. Based on the data collected, our compounds act at a distinct and earlier point in Hsp90's protein folding cycle than either GDA or 17-AAG (**Figure 61**). As seen in **Figure 61, Box 1**, SanA inhibits the binding of C-terminal client proteins and co-chaperones. Further, shown in **Box 2**, SanA successfully inhibits the binding of HOP, which is responsible for docking Hsp90 to Hsp70, and facilitating the transfer of unfolded polypeptides between Hsp70 to Hsp90. Given the drug resistance associated with 17-AAG in clinical trials, SanA's ability to affect multiple parts of Hsp90's cycle, including Hsp70's mechanism will make SanA more effective against resistance mechanism than all N-terminal Hsp90 inhibitors.

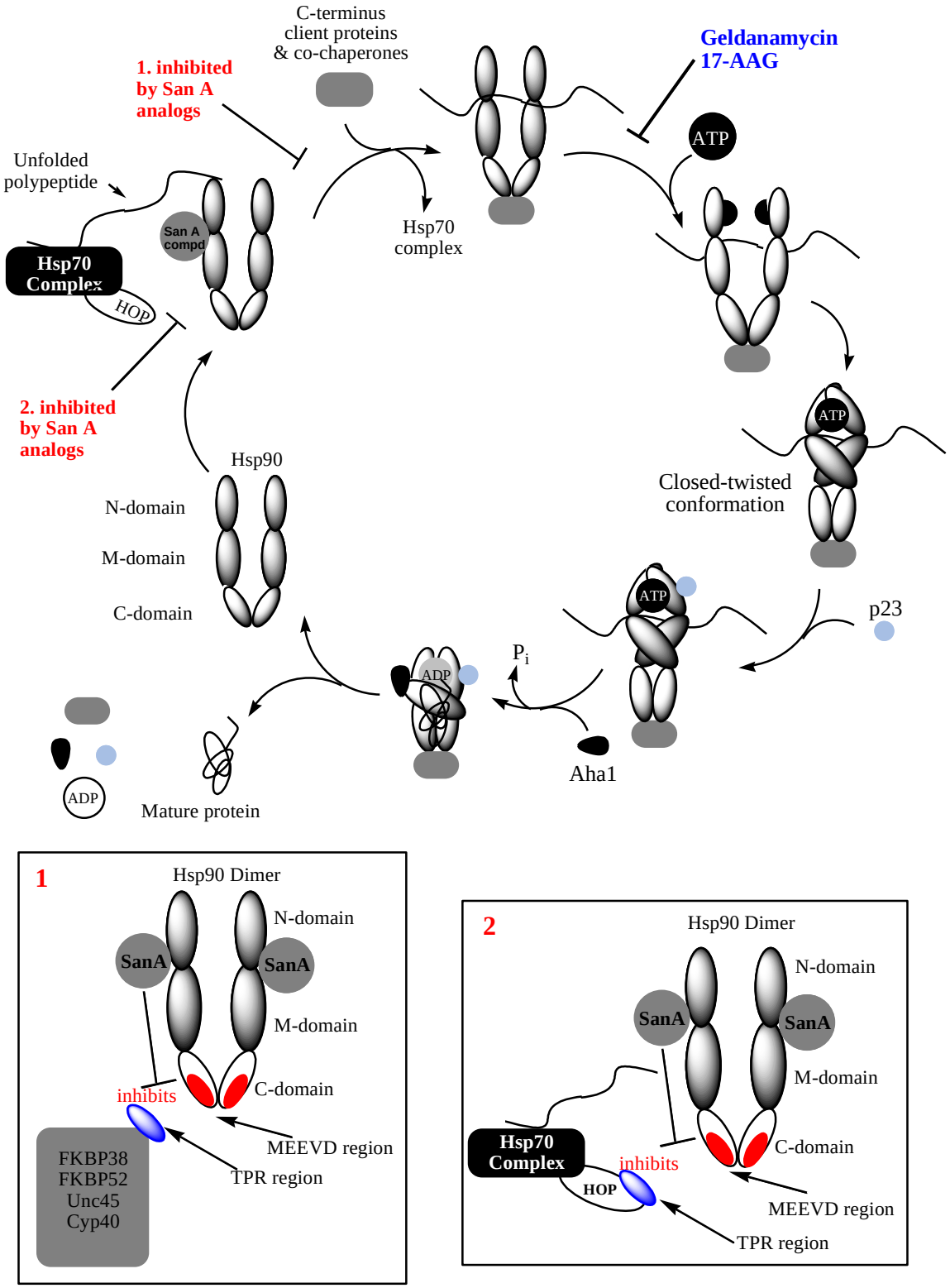

Figure 61: Diagram of Hsp90's folding cycle and SanA's effect

Hsp90's involvement in folding, protecting, and modulating oncogenic proteins associated with all of the hallmarks of cancer makes it an ideal target in cancer therapeutics. Further, Hsp90 exists in 2-3 fold higher amounts in cancer cells than normal cells, which means that drugs will be more selective, resulting in fewer side-effects during treatment than non-selective drugs that affect both normal and cancerous cells. However, the drug resistance mechanisms associated with current inhibitors in clinical trials, including Hsf-1 activation and Hsp70 up-regulation, has delayed their advancement from clinical to market. Thus, there is an urgent need for the development of Hsp90 inhibitors with new mechanisms of action. The experiments described in both chapter 3 and this chapter, describe a novel Hsp90 inhibitor. The unique mechanism demonstrated by SanA will contribute to the development of more effective cancer therapeutics.

ACKNOWLEDGEMENTS

This chapter contains material that has been published in ACS Chemical Biology: Veronica C. Ardi, Leslie D. Alexander, Victoria A. Johnson, and Shelli R. McAlpine, **2011**, v6, p1357.

CHAPTER 5: SYNTHESIS, SAR, AND MECHANISM OF ACTION OF DIMERIZED SANSALVAMIDE A DERIVATIVES

Dimerization and oligomerization are motifs commonly found in nature. Dimerized natural products include potential anti-cancer agents torreyanic acid and curcumin, as well as the marketed antibiotic Gramicidin S (**Figure 62**). Many proteins also function as dimers including the therapeutic targets Hsp90, tubulin, and topoisomerase II enzymes.[144, 145] One advantage of dimeric compounds is that they can simultaneously bind two monomeric targets at once, thereby halving the therapeutic dose. Alternatively, dimeric compounds can bind to both monomers of a dimeric target protein. In the case of Gramicidin S, its symmetrical, dimeric structure allows it to adopt an amphipathic conformation that is favorable for bacterial cell permeation.[146, 147] Monomeric compounds are only capable of binding to a single protein or adopting unfavorable conformations. Thus, investigating dimeric molecules can lead to the discovery of effective drugs.

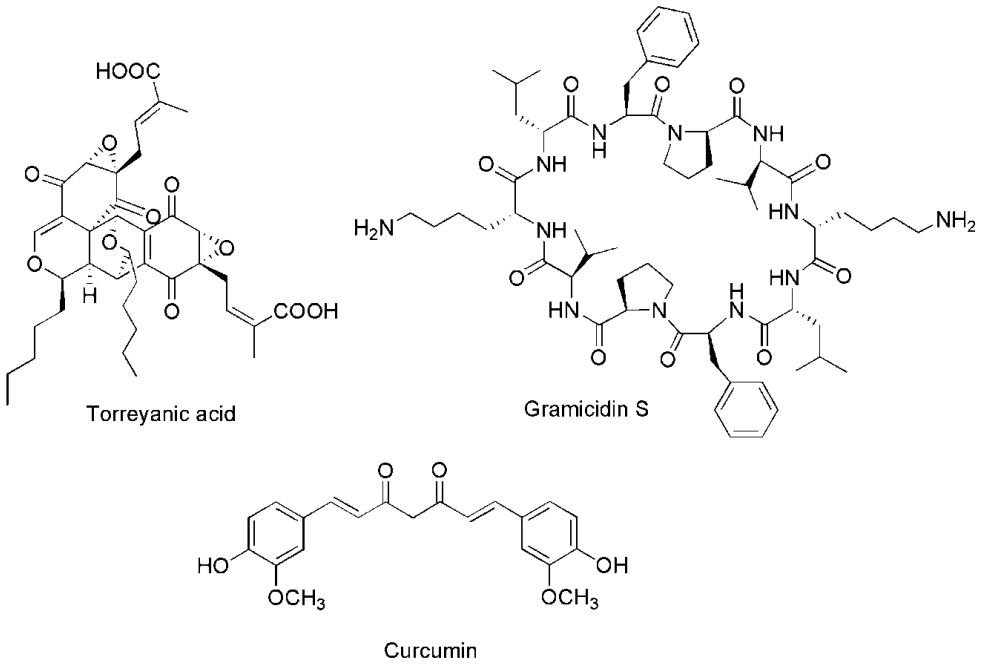

Figure 62: Examples of dimeric natural products

Chapters 3 and 4 discuss the unique mechanism of action of cyclic pentapeptide SanA, which binds to the N-middle domain of Hsp90. I described how SanA allosterically inhibits the binding of Hsp90's client proteins and co-chaperones, specifically those that bind to Hsp90's C-domain. SanA's unique mechanism combined with the advantages of dimerized natural products prompted us to design dimerized SanA derivatives (Di-SanA). These derivatives were evaluated for their potential anti-cancer activity in cancer cell lines.

Large molecules are not ideal drug candidates due to their high molecular weights and perceived low bioavailability. However, there several large macrocyclic drugs currently on the market: the undecapeptide immunosuppressant Cyclosporin A (MW=1185), the antifungal compound Caspofungin (MW=1093), the last-resort antibiotic Vancomycin (MW= 1431), an eight amino acid peptide-based anticancer agent

Aplidine (MW=1096), and decapeptide Gramicidin S (MW= 1140).[148, 149] The success of these large macrocyclic drugs in treating diseases sets a precedent in exploring the therapeutic potential of Di-SanA derivatives (MW=1170).

RATIONAL DESIGN OF DI-SANA DERIVATIVES

The first five derivatives of the Di-SanA series were synthesized via solution-phase chemistry by previous group members.[150] These decapeptides, like Gramicidin S, contain rotational C-2 symmetry where they are identical when rotated 180º around the center of the macrocycle. To obtain this symmetry, they are synthesized from two identical pentapeptide fragments that are cyclized head-to-tail (**Figure 63**). The redundancy of amino acid residues around the Di-SanA macrocycle means that there are two positions called I, II, III, IV, and V in our naming system for designating amino acid positions around the ring.

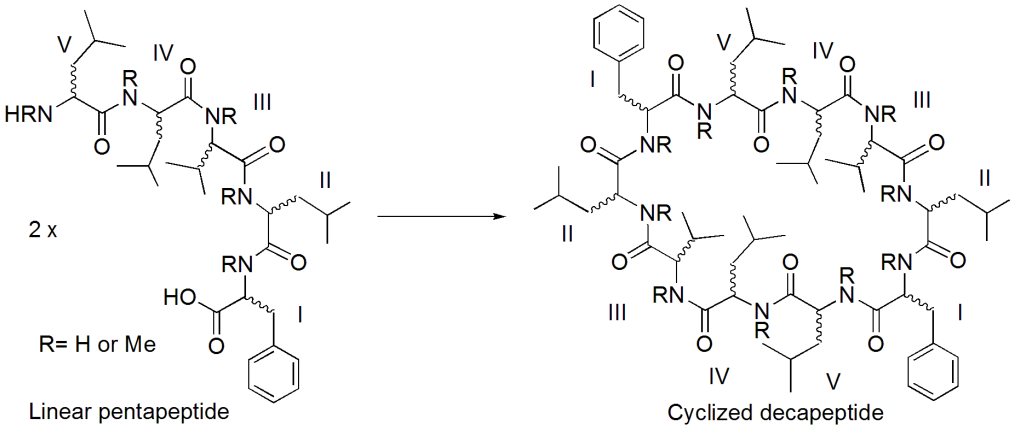

Figure 63: Formation of C-2 symmetrical Di-SanA derivatives

The first five Di-SanA derivatives included Phe, Leu, and Val and focused on changes in stereochemistry (L→D) and *N*-methylation (**Figure 64**). We maintained the hydrophobicity of the amino acids because we anticipated it would mimic the successful undecapeptide drug, cyclosporin A (Chapter 1, **Figure 3**), which enters cells via passive

membrane diffusion. Cyclosporin A is made up of hydrophobic amino acids (leucines, valines, and alanines) and contains one D-aa and seven *N*-methylated residues. Thus, we incorporated these types of key features into Di-SanA derivatives **1-5** in an attempt to generate a lead compound.

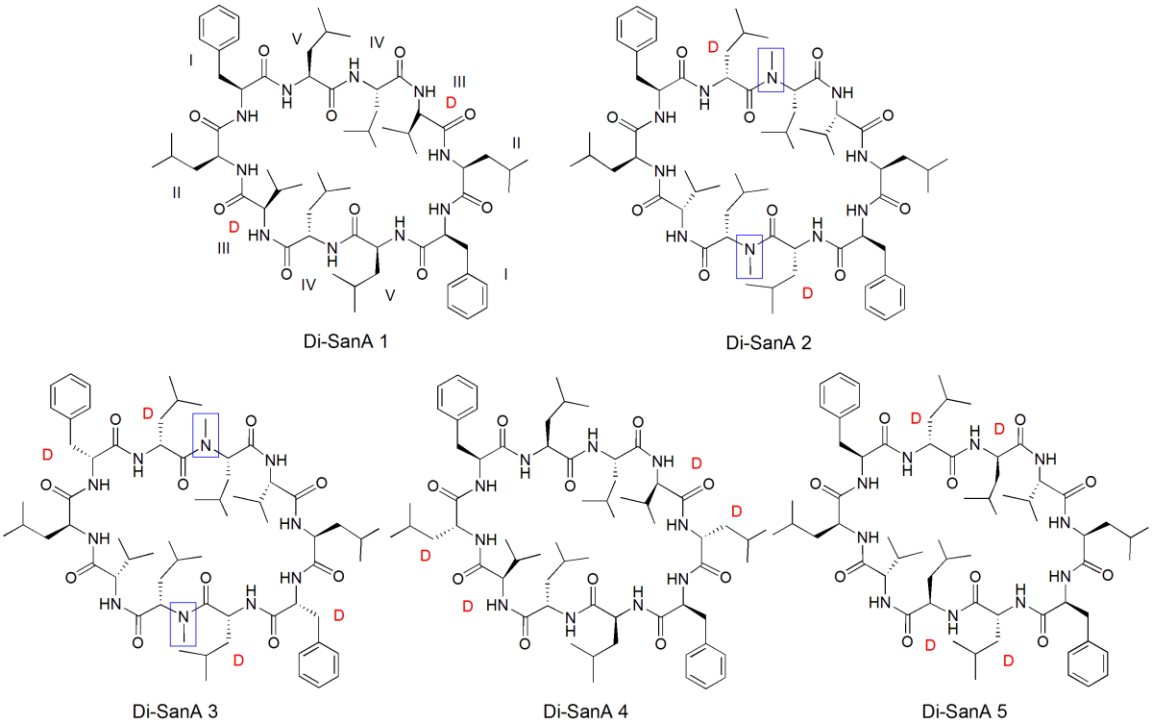

<u>Figure 64</u>: First generation Di-SanA derivatives 1-5

Di-SanA derivatives **1-5** were evaluated at 5 μM in cytotoxicity assays against pancreatic cancer cell lines PL-45 and BxPc3, as well as in HCT-116 colon cancer cells. One of the compounds, Di-SanA **4**, exhibited low nanomolar IC_{50} activity (1.5-19.9 nM) in all three cell lines (**Figure 65**). Di-SanA **4** contains two consecutive D-aas at positions II and III, for a total of 4 D-aas. The biological and conformational stability associated with D-aas contributes to more potent and effective compounds than those containing all L-aas.[6, 55]

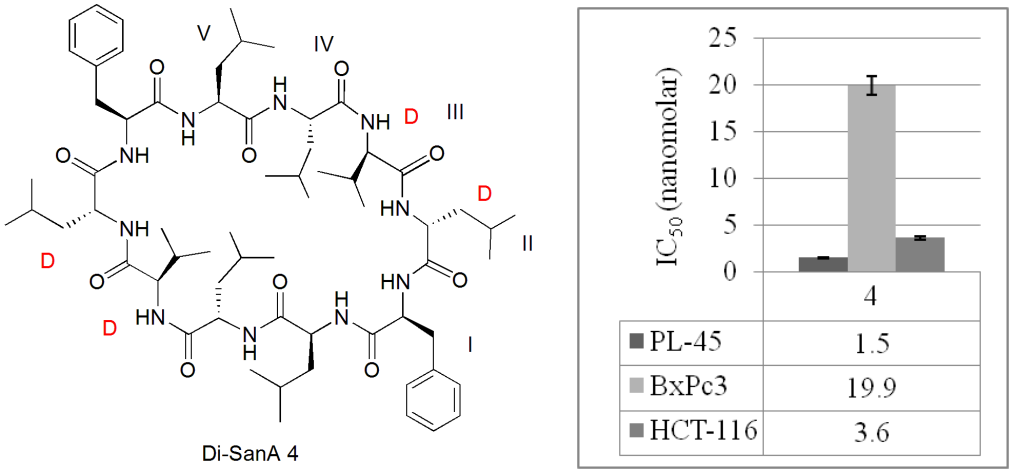

Figure 65: Structure of Di-SanA 4 and its corresponding IC_{50} values in several cell lines

Structure-activity relationship (SAR) analysis for this class of compounds was accomplished by synthesizing 12 second-generation Di-SanA derivatives. These D-aas were included at several C-2 symmetrical positions around the decapeptide ring in order to explore how their placement would affect cytotoxicity. In addition, synthesizing asymmetrical decapeptides in the second generation would determine if symmetry was essential for bioactivity.

We investigated the importance of 2 consecutive D-aas that were seen in lead compound Di-SanA **4** by designing compounds that contained no consecutive D-aas. Di-SanA **4** had 2 D-aas at positions II and III, for a total of 4 D-aas within the macrocycle. With no consecutive D-aas, Di-SanA **6** contains a D-aa at both positions I (**Figure 66**). Compounds **7** and **8** contain D-aas at positions II and IV, respectively. Synthesizing these derivatives would allow us to determine if the 2 consecutive D-aas present in Di-SanA **4** were necessary for its activity.

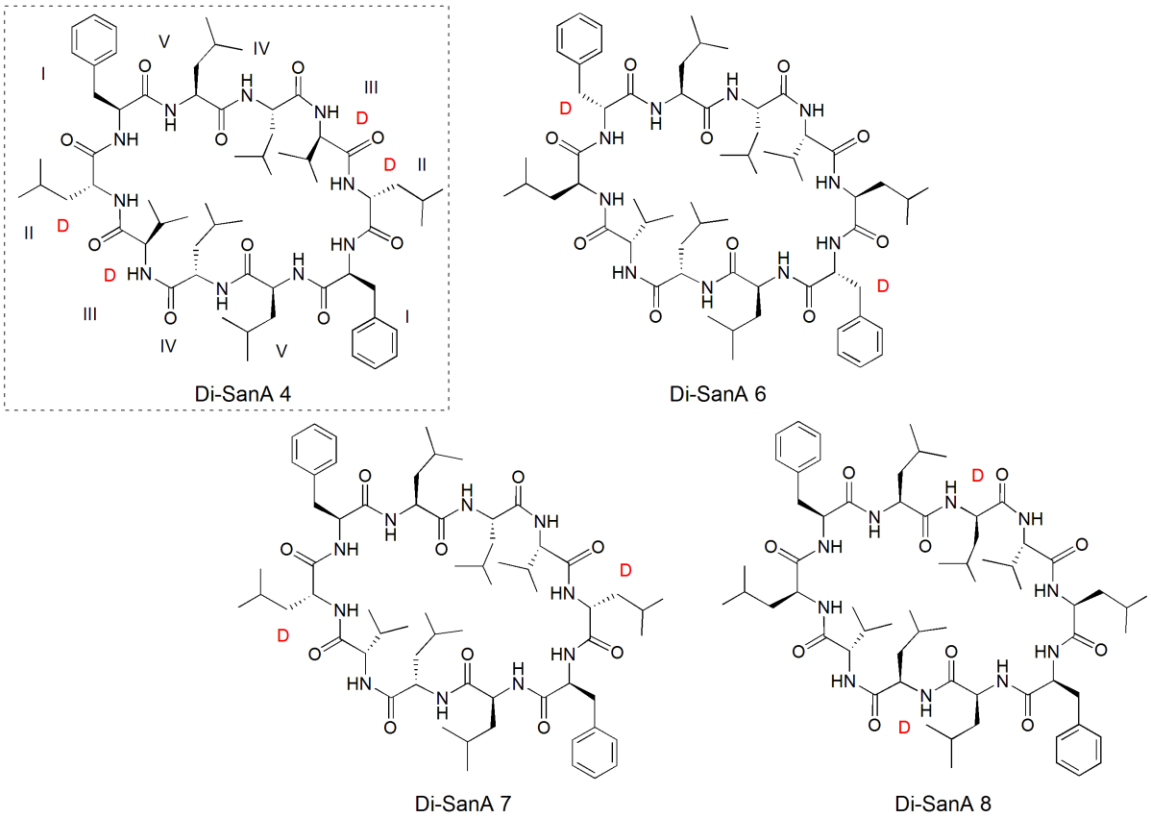

Figure 66: C-2 symmetrical Di-SanA derivatives with no consecutive D-aas

Designing symmetrical compounds with 2 consecutive D-aas were aimed at evaluating the importance of this motif. **Di-SanA 9** contains 2 consecutive D-aas at position I and II. **Di-SanA 10** has 2 consecutive D-aas also at positions II and III, but with a phenylalanine at position II instead of a leucine (**Figure 67**). Both compounds were synthesized via solution-phase dimerization of linear pentapeptides, as discussed in Chapter 2.

Including 3 or more consecutive D-aas would determine if the number of D-aas played a role in the anti-cancer activity of this class of compounds. Thus, symmetrical decapeptides **11**, **12**, and **13** were designed (**Figure 67**). Di-SanA **11** contains 3 D-aas at

positions I through III. Di-SanA **12** has 3 consecutive D-aas at positions II through IV. Di-SanA **13** contains 4 consecutive D-aas at positions I through IV.

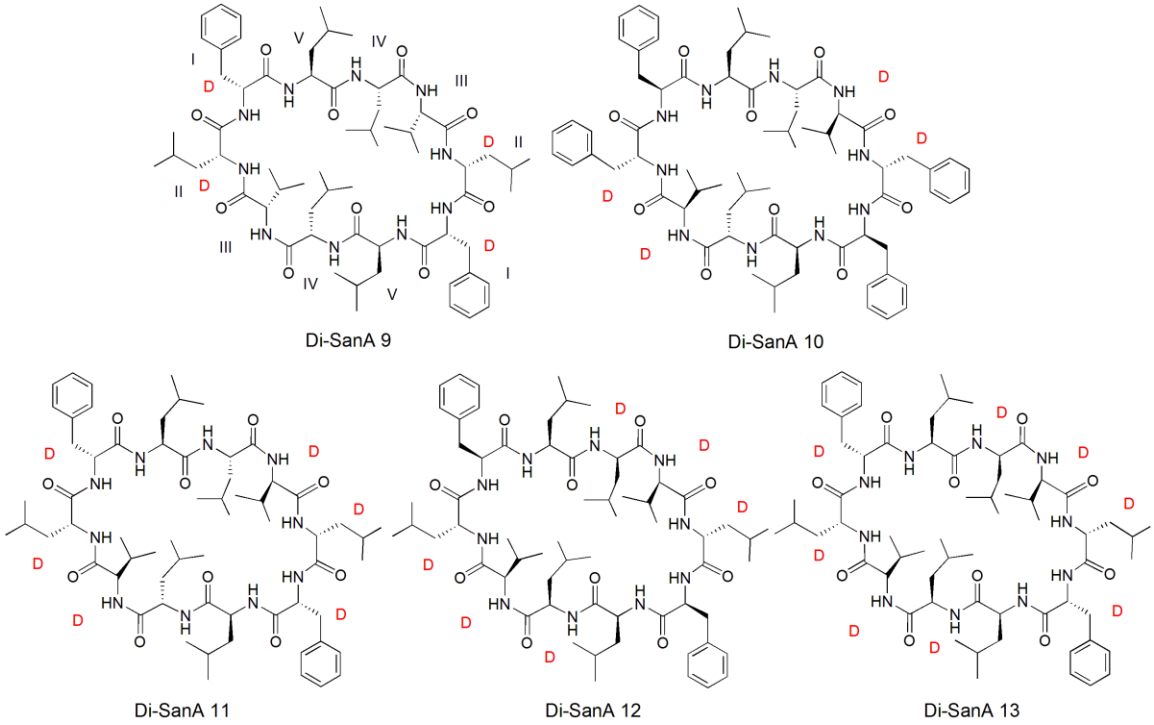

Figure 67: C-2 symmetrical Di-SanA derivatives with two or more consecutive D-aas

Finally, asymmetrical decapeptides include Di-SanA **14**, **15**, **16**, and **17** (**Figure 68**). Given the asymmetry, the residues are designated as positions I through X. All of the derivatives contained between 2 to 4 consecutive D-aas within the macrocycle. Di-SanA **14** has D-aas at positions I through III and at positions VII and VIII; **15** has 3 D-aas at positions II-IV and 4 at positions VI through IX; **16** contains 3 D-aas at positions I-III and 3 at positions VII-IX; and **17** has 3 D-aas at positions I-III and 4 at positions VI-IX.

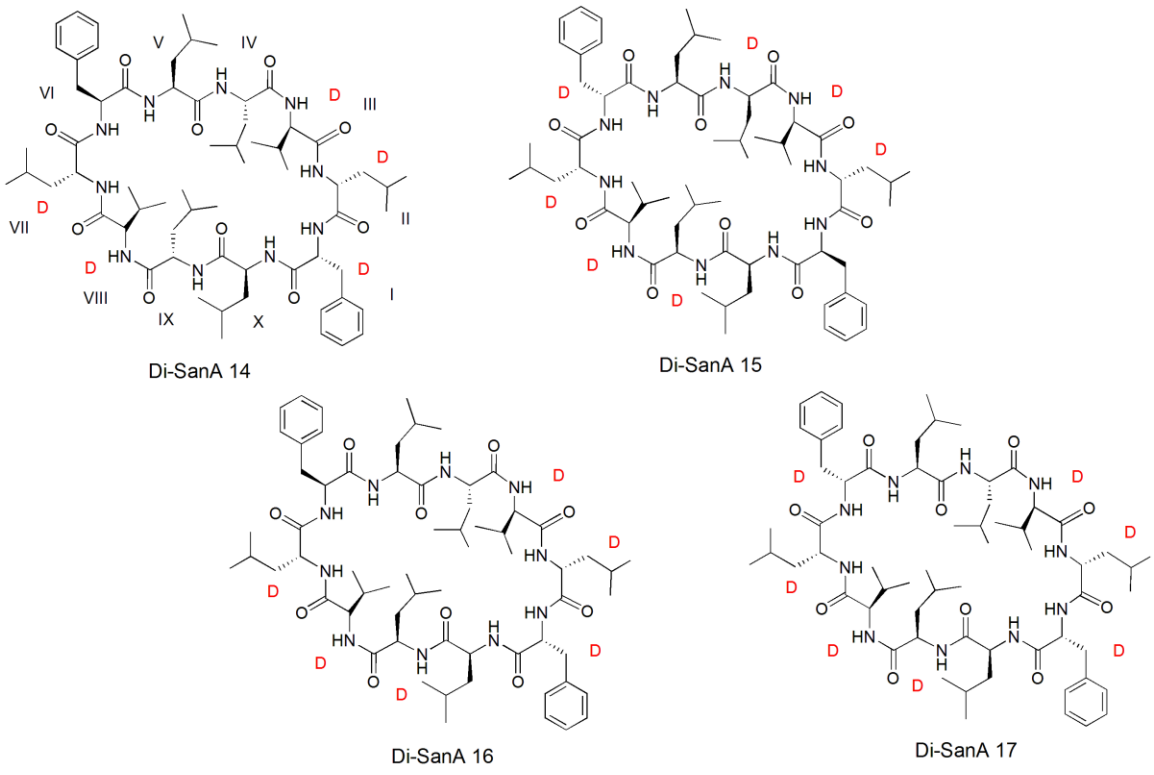

Figure 68: Asymmetrical Di-SanA decapeptide derivatives

SOLID-PHASE SYNTHESIS OF C-2 SYMMETRICAL DECAPEPTIDES

Di-SanA **9** and **10** were synthesized using solution-phase chemistry as previously discussed in Chapter 2. Our solid-phase peptide synthesis (SPPS) protocol, also described in Chapter 2, was used to synthesize the linear precursors of the second generation Di-SanA derivatives. SPPS is more efficient and less time-consuming than solution-phase synthesis, ultimately allowing for the rapid generation of Di-SanA molecules. Elimination of the cyclic pentapeptide occurred by contructing linear decapeptides precursors on solid-support, followed by solution-phase cyclization of the decapeptide.

Using the SPPS protocol described in Chapter 2, linear decapeptides for Di-SanA **11**, **12**, and **13** were synthesized utilizing pre-loaded D-Phe CTC resin (for **11** and **13**,

0.50 mmol/gram resin loading; 0.5 g scale) and Phe CTC resin (**12**, 0.50 mmol/gram resin loading; 0.5 g scale). Fmoc-protected amino acids (3.0 equivalents) were coupled using HOBt (3.0 equivalents) and DIC (6.0 equivalents) as coupling reagents (**Figure 69**). Peptide couplings were performed in 0.2 M DMF solutions. The linear peptides were cleaved from the resin using a TFE/DCM (1:1, v/v) solution and analyzed by LCMS for the presence and purity of double-deprotected linear decapeptides (**DDLD**). Unfortunately, only linear nonapeptide formed for **11**, and **DDLDs** for **12** and **13** made up only 20% of the cleaved material, the other 80% contained a mixture of nonapeptides, octapeptides, and other impurities. Cyclizations of **DDLD 12** and **13** were attempted using a cocktail of coupling reagents (0.5 equivalents DEPBT, 0.7 equivalents HATU, 0.5 equivalents TBTU) in DMF/ACN (3:1) to a final concentration of 0.01M. The linear peptides were very insoluble, thus the need for DMF. Unfortunately, neither reaction formed cyclized decapeptide product.

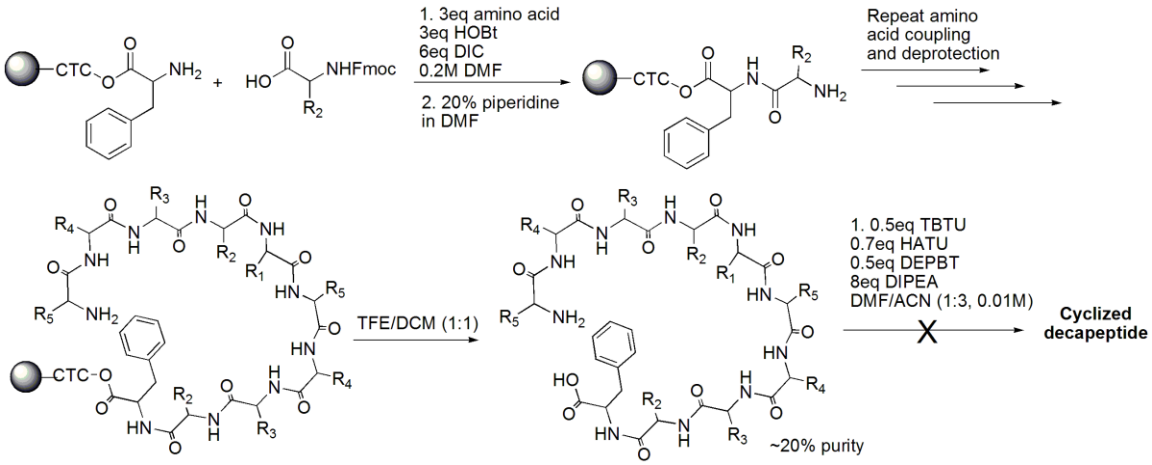

Figure 69: Initial synthetic route for Di-SanA 11, 12, and 13

The success of cyclizing large macrocycles depends on the conformation of the linear precursor.[151] Intramolecular hydrogen bonding associated with long, linear

peptides is unpredictable and cyclizations often result in low yields. Because of the low synthesis yields of Di-SanA **11**, **12**, and **13** using the decapaptide synthesis approach, and the failed cyclizations, synthesis via dimerization of pentapeptides might be the most viable option. Pre-loaded CTC-Phe or CTC-D-Phe resin was used for the construction of the linear pentapeptides for **11**, **12**, and **13** (**Figure 70**). The resin was subjected to the TFE/DCM cleaving solution resulting in the cleaved pentapeptide. Although all three cleaved pentapeptides were isolated in low yields (10-30%), LCMS analysis found all three to be greater than 90% pure. Cyclizations were performed using a cocktail of coupling reagents (0.5 equivalents DEPBT, 0.7 equivalents HATU, 0.5 equivalents TBTU) in DMF to a final concentration of 0.1M. For Di-SanA **11**, both cyclic pentapeptide and decapeptide formed in a 4:1 ratio based on LCMS analysis of the crude product. Only decapeptide formed for Di-SanA **12**. And both cyclized products formed for Di-SanA **13** in a 2:1 pentapeptide to decapeptide ratio. The decapeptide was purified and separated from the pentapeptide by RP-HPLC.

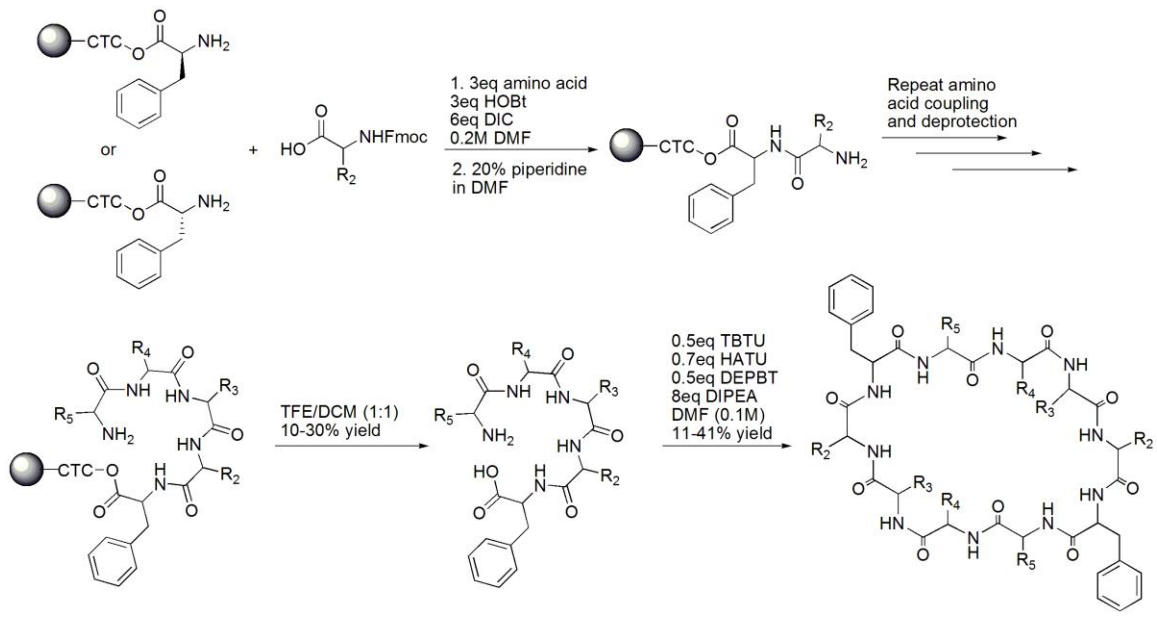

Compound	Resin	R_2	R_3	R_4	R_5
11	CTC-D-Phe-NH_2	D-Leu	D-Val	Leu	Leu
12	CTC-Phe-NH_2	D-Leu	D-Val	D-Leu	Leu
13	CTC-D-Phe-NH_2	D-Leu	D-Val	D-Leu	Leu

Figure 70: Synthesis of Di-SanA 11, 12, and 13

Following the same SPPS protocol described in Chapter 2, the double-deprotected linear pentapeptides for Di-SanA **6**, **7**, and **8** were synthesized and cleaved from CTC-Leu resin (**Figure 71**). Using CTC-Leu resin, I achieved significantly better yields (39% for Di-SanA **6**, 42% for Di-SanA **7**, and 89% for Di-SanA **8**) than had been obtained by the CTC-Phe or CTC-D-Phe resins when synthesizing compounds **11**-**13** (10-30%). Cyclizations were performed using the same cocktail of coupling reagents (0.5 equivalents DEPBT, 0.7 equivalents HATU, 0.5 equivalents TBTU) and concentrated conditions (0.1M DMF) successfully gave the cyclic decapeptides, along with their pentapeptide counterparts. Based on LCMS analysis, the cyclization of Di-SanA **17** resulted in a 3:1 ratio of cyclic pentapeptide to decapeptide, Di-SanA **18** had a 4:1 ratio,

and Di-SanA **20** resulted in a 1:2 ratio. The decapeptides were purified and separated from the pentapeptides using a combination of flash column chromatography and RP-HPLC.

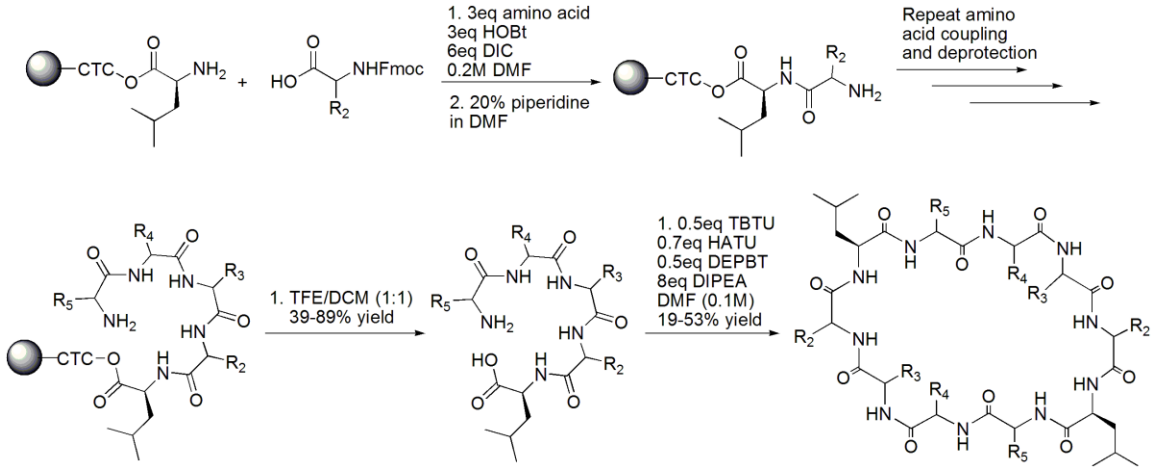

Compound	Resin	R_2	R_3	R_4	R_5
6	CTC-Leu-NH_2	Val	Leu	Leu	D-Phe
7	CTC-Leu-NH_2	Leu	Phe	D-Leu	Val
8	CTC-Leu-NH_2	Val	D-Leu	Leu	Phe

Figure 71: General synthesis of C-2 symmetrical Di-SanA derivatives

SOLID-PHASE SYNTHESIS OF ASYMMETRICAL DI-SANA DERIVATIVES

Because of the asymmetry associated with Di-SanA **14**, **15**, **16**, and **17**, forming the linear decapeptide on solid-phase was the only synthesis option. CTC-Leu resin was used because the yields obtained in the cleaving step are higher than when using CTC-Phe or D-Phe resins. The linear decapeptides for Di-SanA **14**, **15**, **16**, and **17**, were synthesized following the standard SPPS protocol (**Figure 72**). The ninth amino acids for these compounds were allowed to couple overnight, and two individual couplings of the tenth amino acids were performed to ensure only decapeptide products formed. Cleaving from the resin gave the linear precursors. The decapeptides were cyclized using

a cocktail of coupling reagents and DMF to a final concentration of 0.1M. The resulting decapeptides were purified by RP-HPLC.

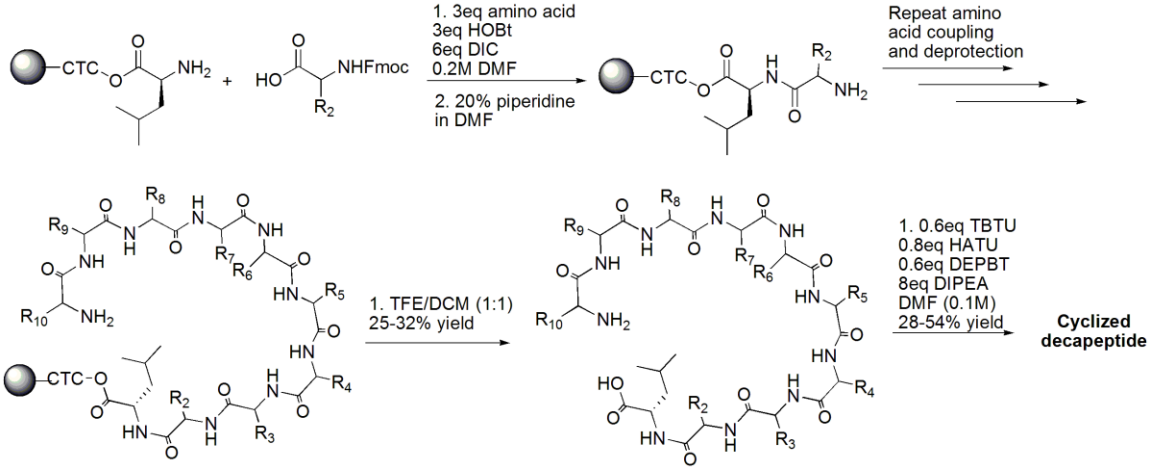

Cmpd	Resin	R_2	R_3	R_4	R_5	R_6	R_7	R_8	R_9	R_{10}
14	Leu	Phe	D-Leu	D-Val	Leu	Leu	D-Phe	D-Leu	D-Val	Leu
15	Leu	D-Phe	D-Leu	D-Val	D-Leu	Leu	Phe	D-Leu	D-Val	D-Leu
16	Leu	D-Phe	D-Leu	D-Val	Leu	Leu	Phe	D-Leu	D-Val	D-Leu
17	Leu	D-Phe	D-Leu	D-Val	Leu	Leu	D-Phe	D-Leu	D-Val	D-Leu

Figure 72: General synthesis of non-C-2 symmetrical Di-SanA derivatives

CYTOTOXICITY DATA

Di-SanA derivatives were tested at 5 µM against both HCT-116 and PL-45 cancer cell lines using the thymidine uptake protocol described in Chapter 3. None of the newly synthesized derivatives demonstrated improved potency over lead compound Di-SanA **4** (99% growth inhibition, **Figure 73**). Di-SanA **13**, which is C-2 symmetrical with a total of 8 D-aas and 2 L-aas, was the most potent of the new derivatives with 40% growth inhibition in HCT-116s and 79% growth inhibition in PL-45s. The asymmetrical derivatives (**14**, **15**, **16**, and **17**) and the compounds that did not contain consecutive D-aas (**6**, **7**, and **8**) did not demonstrate significant anti-proliferative activity. Thus, the

presence of C-2 symmetry and two consecutive D-aas is important for the potency of Di-SanA **4**.

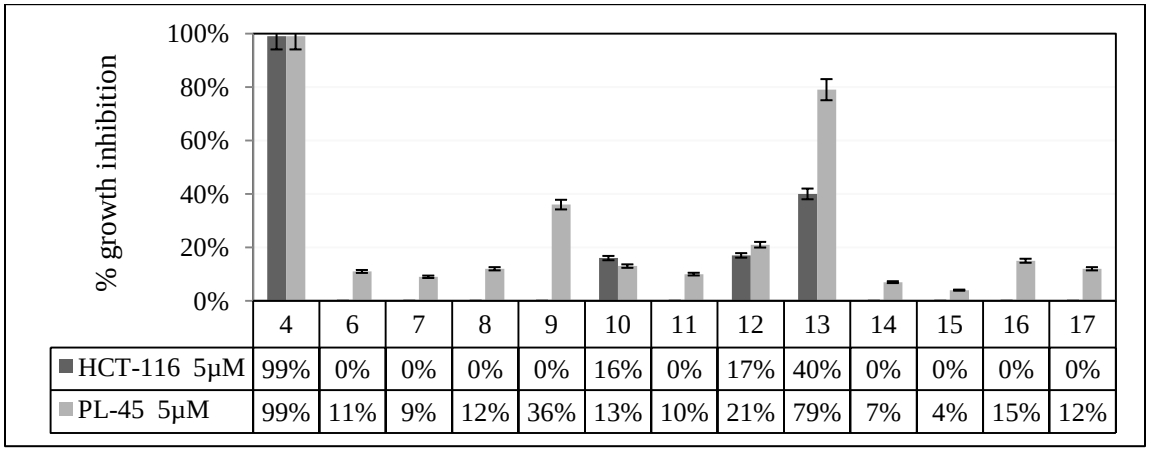

	4	6	7	8	9	10	11	12	13	14	15	16	17
HCT-116 5µM	99%	0%	0%	0%	0%	16%	0%	17%	40%	0%	0%	0%	0%
PL-45 5µM	99%	11%	9%	12%	36%	13%	10%	21%	79%	7%	4%	15%	12%

Figure 73: Cytotoxicity data of Di-SanA derivatives in HCT-116 and PL-45 cell lines using thymidine uptake. HCT-116 data was produced by the author and PL-45 data was generated by the author's colleague.

CELL LYSATE PULL-DOWN ASSAY

From the cytotoxicity assays, it is evident that Di-SanA **4** remains the lead decapeptide derivative and that its nanomolar potency is unique. We investigated its mechanism of action by following the same approach that was taken for the initial mechanism of action studies for SanA: cell lysate pull down assay. My colleague synthesized a biotinylated derivative of Di-SanA **4** (**Figure 74**), and I subsequently ran a pull down assay in HCT-116 cell lysate in order to determine its potential protein target.

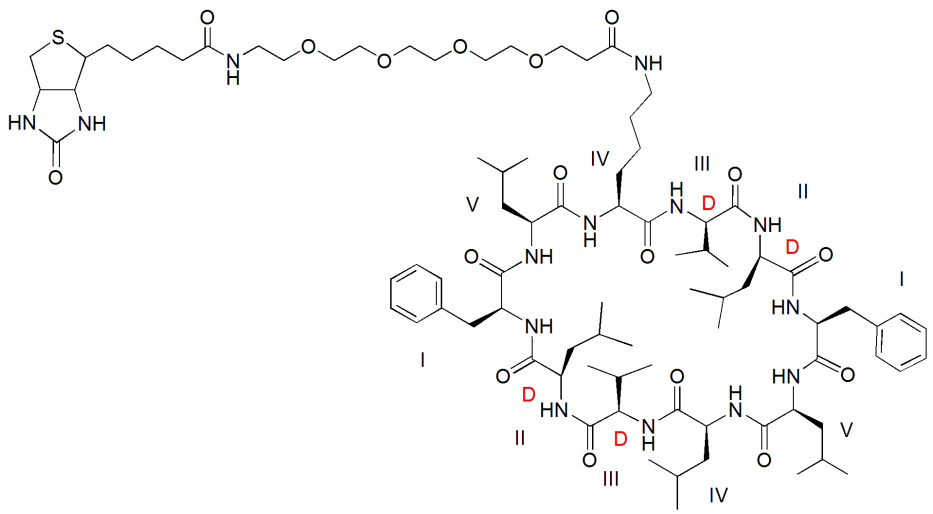

<u>Figure 74</u>: Structure of Di-SanA 4 tagged with PEG_4-biotin (4-T-IV-biotin) to be used in pull-down assays

In the assay, Di-SanA **4-T-IV-biotin** was incubated with HCT-116 cell lysate for 42 hours at 4 ºC followed by the addition of NeutrAvidin resin for 2 hours at 4 ºC and 2 hours at room temperature. The resin was washed ten times with wash buffer and the proteins were eluted from the resin with sample buffer. Proteins were resolved on an SDS-PAGE gel and visualized with silver stain using following the manufacturer's protocol. The band containing the proteins pulled down by **4-T-IV-biotin** was sequenced by LC/MS/MS and screened against a protein database. Cytosolic Hsp90 was identified as one of the proteins pulled down (**Figure 75**), and I verified it by Western blot. Other proteins found in the sequencing include myosin, tubulin, and actin, which are all known to be associated with Hsp90.[136, 152-154] Since Di-SanA **4** is a dimerized derivative of the cyclic pentapeptide SanA, which also pulls down Hsp90, it is not surprising that they share the same protein target. In addition, Di-SanA **4**'s potential capability to bind to both monomers of an Hsp90 dimer is an explanation for its low nanomolar potency compared to the low micromolar potency of the lead monomeric SanA derivatives.

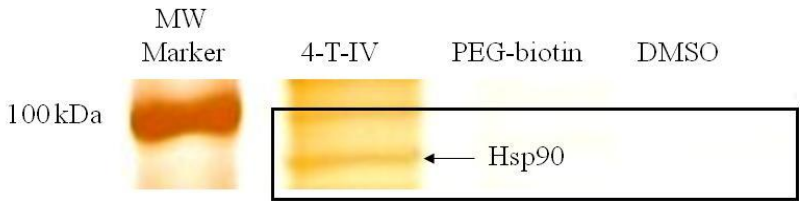

Figure 75: Cropped silver-stained gel from Di-SanA 4-T-IV-biotin cell lysate pull-down assay

IP6K2-HSP90 BINDING ASSAY

Hsp90 is associated with hundreds of oncogenic client proteins that are involved in apoptotic pathways, and its inhibition leads to cell death via apoptosis rather than necrosis. Like SanA, we anticipated that Di-SanA **4**'s binding to Hsp90 would cause a disruption in client protein-Hsp90 binding interactions. We investigated compound **4**'s affect on the binding between Hsp90 and its C-domain client protein, IP6K2. Since IP6K2 is pro-apoptotic when it is not bound to Hsp90, disrupting this interaction would lead to pro-apoptotic events and, ultimately, cell death. In addition, investigating Di-SanA's affect on the binding of IP6K2 to Hsp90 would indicate if the compound modulated C-domain binding compounds, similar to SanA.

I performed a binding assay following the same procedure described in Chapters 3 and 4 where Di-SanA was incubated with native Hsp90 first, followed by the addition of GST-tagged IP6K2. After protein elution and analysis, it was found that Di-SanA **4** successfully inhibits the binding between IP6K2 and Hsp90 in low nanomolar concentrations (IC_{50}~ 1.7 nM) that correspond to its IC_{50}s in cytotoxicity assays (1.5- 20 nM) (**Figure 76**). The pro-apoptotic role IP6K2 takes when its binding to Hsp90 is disrupted suggests that Di-SanA **4**'s potency comes, in part, from apoptotic effect it induces in cancer cells via Hsp90 inhibition.

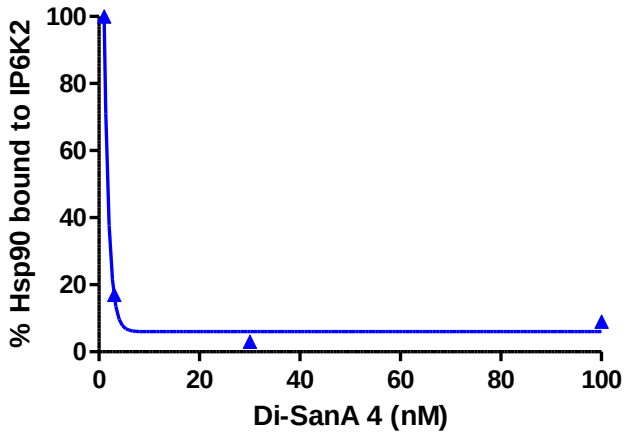

Figure 76: Client protein binding assay with Di-SanA 4 and Hsp90-IP6K2

SUMMARY AND CONCLUSIONS

The SAR analysis of Di-SanA compounds established that the placement of D-aas around the decapeptide ring played a significant role in potency. We found that the low nanomolar potency exhibited by Di-SanA **4** is unique to that compound as no other derivatives demonstrated comparable potency in pancreatic and colon cancer cell lines. Preliminary mechanism of action studies were completed using a biotinylated derivative of Di-SanA **4** in HCT-116 cell lysate. We determined that this compound, like its cyclic pentapeptide relative, bound to Hsp90. Further, pure protein binding assays show that Di-SanA **4** disrupts the binding between Hsp90 and the pro-apoptotic C-terminal-binding client protein IP6K2.

Upon re-synthesizing Di-SanA **4** via both solution-phase and solid-phase chemistry methods, we found that we could not replicate the nanomolar potency exhibited by the original compound in cytotoxicity assays against PL-45, BxPc3, and HCT-116s. Thus, although we obtained promising initial data using the original

compound, we were not able to continue exploring this class of molecules as potential Hsp90 inhibitors.

ACKNOWLEDGEMENTS

This chapter contains material that has been published in Journal of Medicinal Chemistry: Leslie D. Alexander, Robert P. Sellers, Melinda R. Davis, Veronica C. Ardi, Victoria A. Johnson, Robert, C. Vasko, and Shelli R. McAlpine, **2009**, v52, p7927.

CHAPTER 6: EXPERIMENTAL

GENERAL SYNTHETIC PROCEDURES

GENERAL SOLUTION-PHASE SYNTHESIS REMARKS

All peptide coupling reactions were performed in glass round-bottom flasks capped with rubber septa and run at room temperature under argon gas, unless otherwise stated. Coupling of PEG-biotin or fluorescein tags were performed in 24 mL or 40 mL glass vials at room temperature under open atmosphere. Reactions were stirred with magnetic stir bars. Anhydrous DCM, anhydrous ACN, and anhydrous DMF were purchased from Sigma-Aldrich and packaged under nitrogen gas with an AcroSeal® extra wide septum. Anhydrous DIPEA was purchased from Sigma-Aldrich and packaged under nitrogen gas in a Sure/Seal™ amber glass bottle. All amino acids and coupling reagents were purchased from Novabiochem, Peptides International, Chem Impex, Sigma Aldrich, ChemPep, or Fisher Scientific. Amino acids were either protected at the amino terminus with the Boc-protecting group or protected at the carboxy-terminus as a methyl ester. Purification via flash chromatography was performed using 230-400 mesh 32-63 micron 60Å silica gel from Silicycle, and the solvents were purchased from Fisher Scientific in 20L aluminum drums. Peptide purity was verified using ^{1}H NMR, LC/MS, and/or RP-HPLC. ^{1}H NMR spectra were performed on Varian spectrometers at 200, 400 or 600 MHz. Chloroform-*d* (7.27 ppm), methanol-d_4 (3.34 ppm), or acetone-d_6 (2.05 ppm) was used as a reference point. LC/MS data was performed on Agilent Technologies 1200 series quaternary pump and acquired on the Agilent LC/MSN Trap XCT Plus

System. HPLC data was acquired with a Waters Flex Inject System and acquired on 2487 dual wavelength absorbance detector (215λ and 222λ).

GENERAL SOLUTION-PHASE PEPTIDE COUPLING

All peptide couplings utilized 1.1 equivalents of free amine and 1.0 equivalents of free acid. For the formation of dipeptides and tripeptides, 1.2 equivalents of TBTU was used as a coupling reagent unless otherwise stated. The flask was purged with argon gas, and the contents inside were dissolved in anhydrous DCM (0.1M). If necessary, anhydrous ACN was used to increase solubility of the materials. Once dissolved, anhydrous DIPEA (4-8 equivalents) was added to the reaction flask. The solution was stirred at room temperature for 1-2 hours and monitored *via* TLC every 20-30 minutes. Upon completion, the peptides were subjected to an **Acid-base work-up/purification:** two aqueous washes of 10% HCl (100 mL each), ten washes of sodium bicarbonate solution (100 mL, sat. aq.), and two washes of brine (100 mL). If necessary, the dipeptides and tripeptides were further purified via flash column chromatography using an ethyl acetate:hexanes gradient solvent system.

Linear pentapeptide synthesis utilized tripeptide free amine (1.1 equivalents), dipeptide free acid (1.0 equivalents) and TBTU, HATU and/or DEPBT (up to a total of 1.2-1.5 equivalents). The flask was purged with argon gas, and the contents inside were dissolved in anhydrous DCM, and/or anhydrous ACN (0.1 M). If necessary, anhydrous DMF was used to increase solubility of the materials. Once dissolved, anhydrous DIPEA (8 equivalents) was added to the reaction flask. The solution was stirred at room temperature for 1-3 hours and monitored *via* TLC and LC/MS every 20-30 minutes. Upon completion, the excess base was removed by dissolving the crude solution in 100

mL of EA and extracting it twice with 100 mL of aqueous 10% HCl*. The organic layer was then washed 4-10 times with DI water saturated with sodium bicarbonate. The organic layer was collected, dried over anhydrous sodium sulfate, filtered, and concentrated *in vacuo*. Pentapeptides were purified *via* flash column chromatography using an ethyl acetate:hexane gradient system to purify the desired product.

SOLUTION-PHASE AMINE DEPROTECTION

Deprotection of the Boc-protected peptide was performed under open atmosphere in a round-bottom flask. The reaction was run in a 0.1M solution of 25% TFA and 75% DCM. The peptide was first dissolved in DCM followed by the addition of TFA and 2.0 equivalents of anisole. The solution was stirred at room temperature for 45 minutes and was monitored every 15 minutes by TLC. Upon completion, the reaction was concentrated *in vacuo* and to give the free-amine peptide in a quantitative yield.

SOLUTION-PHASE ACID DEPROTECTION

Methyl ester hydrolysis was done under open atmosphere in a round-bottom flask. The peptide (1.0 equivalent) and 8.0 equivalents of lithium hydroxide were dissolved in methanol to a final concentration of 0.1M. The reaction was allowed to run for 1 hour up to overnight and was monitored by TLC. Once complete, the reaction was diluted in DCM and treated with pH 1 water. The aqueous layer was tested for acidity and, if needed, drops of HCl were added until pH= 3. Finally, the product was extracted several times with DCM, dried over sodium sulfate, and concentrated *in vacuo* to give the free-acid peptide.

IN SITU DOUBLE DEPROTECTION

The double deprotection of both the amine and acid protecting groups on the linear peptide was performed under open atmosphere. The protected linear peptide was dissolved in THF to a final concentration of 0.1M, followed by the addition of 2.0 equivalents of anisole. HCl was added dropwise over the course of one week and the reaction was monitored by LCMS. Upon completion, the reaction was concentrated *in vacuo* to give the double-deprotected linear peptide.

MACROCYCLIZATION PROCEDURE

All pentapeptides were acid and amine deprotected using the general deprotection methods described above. Three coupling agents (DEPBT, HATU, and TBTU) were used at ~0.5 to 0.75 equivalents each. The dry double deprotected peptide and coupling agents were dissolved in acetonitrile and/or methylene chloride (various ratios based on solubility of materials) at a concentration of 0.1M to 0.007M. 6-10 equivalents of DIPEA were then added to the reaction. TLC (macrocycle R_f similar to protected linear pentapeptide) and LCMS were used to monitor the reaction which was usually finished in 1-3 hours. If reaction was not complete in 2 hours, additional coupling agents (~0.5-1 equivalent total) were added. If reaction was complete, then work-up was done by extracting with 10% aqueous hydrochloric acid and saturated sodium bicarbonate. After back extraction of aqueous layers with large quantities of methylene chloride, the organic layers were combined, dried over sodium sulfate, filtered and concentrated *in vacuo*. All macrocycles were first purified by flash column chromatography using an ethyl acetate/hexane gradient on silica gel. Finally, when necessary, reversed-phase HPLC was

used for additional purification using a gradient of acetonitrile and deionized water with 0.1% TFA.

MACROCYCLIZATION PROCEDURE (SYRINGE PUMP)

Three coupling agents (DEPBT, HATU, and TBTU) were used at 0.5 to 0.75 equiv each. These coupling agents were dissolved in 1/2 of a calculated volume of dry methylene chloride and/or acetonitrile that would give a 0.005–0.007 M overall concentration when included in the volume used for the deprotected peptide. The crude, dry, double deprotected peptide (free acid and free amine) was dissolved in the other 1/2 solvent volume of methylene chloride. DIPEA (8 equiv) was then added to the solution containing coupling reagents dissolved in methylene chloride. The double deprotected peptide was then added to the bulk solution dropwise using a syringe pump at a rate of 8 mL/h. The reaction was monitored via LCMS and generally complete in 2-4 h after the addition of all of the double deprotected peptide. Upon completion, the reaction was worked up by washing with aqueous HCl (pH 1) and saturated sodium bicarbonate. After back extraction of aqueous layers with large quantities of DCM, the organic layers were combined, dried, filtered and concentrated. All macrocycles were first purified by flash column chromatography using an ethyl acetate/hexane gradient on silica gel. Finally, when necessary, reversed-phase HPLC was used for additional purification using a gradient of acetonitrile and deionized water with 0.1% TFA.

BENZYLATION

The cyclized peptide was dissolved in THF to make a 0.1 M solution. Sodium hydride (60% NaH in mineral oil, w/w) was used at 4.0 equivalents and dissolved in the 0.1M solution. Benzyl bromide (4 equivalents) was then added to the reaction, which was

allowed to run and monitored by LCMS. More sodium hydride and benzyl bromide were added, as needed, in increments of 2 equivalents each. Upon completion, the reaction was diluted in DCM and subject to two aqueous washes of DI water. The organic layer was collected and dried *in vacuo*.

COUPLING OF PEG_4-BIOTIN

The coupling of PEG_4-biotin was performed in a 4 mL glass vial with a screw top. The free lysine-containing peptide was placed in the vial, with a magnetic stir-bar, along with 1.2 equivalents of NHS-PEG-biotin. Both were dissolved in DCM to a final concentration of 0.1M followed by the addition of 8.0 equivalents of DIPEA. The reaction was allowed to run for 2 hours up until overnight and was monitored by LCMS. Upon completion, the reaction was concentrated *in vacuo*, re-dissolved in a solution of 80% MeOH and 20% DMSO, and purified via RP-HPLC.

COUPLING OF FLUORESCEIN

The coupling of fluorescein was performed in a 4 mL glass vial with a screw top. The free lysine-containing peptide was placed in the vial, with a magnetic stir-bar, along with 1.2-1.8 equivalents of NHS-fluorescein. The reagents were dissolved in DCM to a final concentration of 0.1M, followed by the addition of 8.0 equivalents of DIPEA. The reactions were allowed to run for at least 3 hours up until overnight and were monitored by LCMS. Upon completion, the solution was concentrated *in vacuo*, re-dissolved in a solution of ACN and DMSO (ratios vary), and purified via RP-HPLC.

GENERAL SOLID-PHASE SYNTHESIS REMARKS

Solid-phase peptide synthesis was performed in a polypropylene solid-phase extraction cartridge fitted with a 20 µm polyethylene frit purchased from Applied

Separations (Allentown, PA). 2-chlorotrityl resins were purchased in pre-loaded form with L-Leucine, L-Phenylalanine, and D-Phenylalanine attached at its carboxyl. Resins were swelled in DMF for 30 minutes prior to assembly of the linear peptide sequence. Incoming amino acids were protected at the amino terminus with the Fmoc protecting group, unless otherwise stated. Solid-phase syntheses were performed on a 1 g resin scale (typical resin loading= 0.5-0.8 mmol/g) unless otherwise stated. All reactions were performed at room temperature under open atmosphere.

GENERAL SOLID-PHASE PEPTIDE COUPLING

Fmoc-protected amino acids were coupled using 1.2-3.0 equivalents of amino acid, 3.0 equivalents of HOBt, and 6.0 equivalents of DIC. Couplings were performed in DMF at 0.2 M, with respect to the resin loading as 1.0 equivalent. Couplings were allowed to proceed for a minimum of 2 hours, and were assayed via ninhydrin test (aka Kaiser test) to verify completion. Once complete, the coupling reaction solution was drained. The resin was washed 3 x 1 min in DMF and subjected to the solid-phase amine deprotection procedure. **Note**: Fmoc and N-methyl amino acids are coupled according to the cycle above, however for subsequent coupling onto the secondary amino terminus, HOBt was substituted with HOAt, and the coupling was allowed to proceed overnight.

SOLID-PHASE AMINE DEPROTECTION

The Fmoc-protected resin-bound peptide was subjected to the following series of washes to remove the Fmoc group: 20% piperidine in DMF (1 x 5min, 1 x 10min), DMF (2 x 1min), IPA (1 x 1min), DMF (1 x 1min), IPA (1 x 1min), and DMF (3 x 1min).

SOLID-PHASE N-TERMINAL AMINE DEPROTECTION

The Fmoc protecting group on the peptide's final amino acid was removed with a modified series of washes: 20% piperidine in DMF (1 x 5min, 1 x 10min), DMF (3 x 1min), IPA (3 x 1min), and MeOH (3 x 1min). After the washes, the resin was drained well and dried *in vacuo* overnight.

SOLID-PHASE CLEAVING FROM RESIN

Linear peptides were cleaved from the resin in a solution of 50% TFE and 50% DCM. The dried peptide-bound resin was stirred in the solution in either in a round-bottom flask with a magnetic stir-bar or in a 40 mL vial with a septa cap. All reactions were performed under open atmosphere at room temperature and allowed to run for 24 hours. Upon completion, the solution was filtered and concentrated *in vacuo* to give the free linear peptide.

METHODS OF CHROMATOGRAPHIC PURITY

Method A

Instrument: Agilent 1200 Series HPLC

Agilent 62440A LC/MSD Trap

Column: Zorbax SB-C18

2.1x30mm 3.5-Micron

Mobile Phase A: 0.1% (v/v) formic acid, 100% (v/v) water

Mobile Phase B: 0.1% (v/v) formic acid, 100% (v/v) acetonitrile

Gradient:	Time (min)	Profile %A	Profile %B
	0	80	20
	4.5	10	90
	4.6	10	90

7.0	85	15

Flow Rate: 1.0 ml/min

Injection: 4µL

Solvent: 100% Methanol

Method B

Instrument: Waters Flex Inject

Waters 2487 Dual λ Absorbance Detector

Column: Symmetry C_{18} 3.5µm

4.6x75mm Column

Mobile Phase A: 0.1% (v/v) Trifluoroacetic acid, 100% (v/v) water

Mobile Phase B: 0.1% (v/v) Trifluoroacetic acid, 100% (v/v) acetonitrile

λ_1: 215nm

λ_2: 222nm

Gradient:	Time (min)	Profile %A	Profile %B
	0	70	30
	4.00	0	100
	13.00	0	100
	15.00	70	30
	16.00	70	30

Flow rate: 0.50 ml/min

Injection: 20 µL

Solvent: 100% Methanol

GENERAL BIOCHEMICAL ASSAY PROCEDURES

All cancer cells lines used in our SanA studies were grown in tissue-culture grade plates in Dulbecco's Modified Eagle Medium (DMEM) supplemented with 10% heat-inactivated fetal bovine serum (FBS) and 1% penicillin/streptomycin, unless otherwise specified. They were housed in a water-jacketed incubator at 37 ºC, under a 5% CO_2 atmosphere. The cells were passaged every 2-4 days. All cell lines were obtained from either ATCC or from collaborators in the San Diego area.

All proteins separated and analyzed by gel electrophoresis were denatured in 4x laemmli sample buffer and were loaded onto 4-20% gradient SDS-PAGE gel, unless otherwise specified. All coomassie staining and silver staining were done according to manufacturers' protocols. For gels analyzed by western blot, the proteins were transferred to PVDF membranes that were subsequently blocked with a solution of 5% dry milk in TBST.

SanA derivatives used in the biochemical assays were dissolved in a 5mM solution of cell-grade DMSO and stored at 4 ºC. Back-up compounds (not dissolved in solvent) were stored at -20 ºC. The compounds were tested for decomposition 2-3 times a year via LCMS and most derivatives remained stable for more than 2 years when dissolved in solution, and indefinitely when kept dry.

THYMIDINE UPTAKE ASSAYS

Proliferation of the PL-45 pancreatic cancer cells and HCT-116 colon cancer cells was tested in the presence and absence of the compounds using ^{3}H-thymidine uptake assays. Cells treated with the compounds were compared to dimethyl sulfoxide (DMSO) controls for their ability to proliferate as indicated by the incorporation of ^{3}H-thymidine

into their DNA. Cells were cultured in 96 well plates at a concentration of 2000-4000 cells/well in DMEM (Gibco) supplemented with L-glutamine, 10% fetal bovine serum and 1% penicillin-streptomycin antibiotic. After overnight incubation, the compounds were added. The compounds were dissolved in DMSO (at a final concentration of 1.0%) and tested at the concentrations indicated in the manuscript. The DMSO control was also at 1.0%. After the cells had been incubated with the compounds for 56 h, 1µCi ^{3}H-thymidine per well was added and the cells were cultured for an additional 16-18 h (for the cells to have a total of 72 h treatment), at which time the cells were harvested using a PHD cell harvester (Cambridge Technology Inc.). The samples were then counted (CPM) in a scintillation counter for 1.5 m. Decreases in ^{3}H-thymidine incorporation, as compared to DMSO controls, are an indication that the cells are no longer progressing through the cell cycle or synthesizing DNA, as is shown in the studies presented. Mean growth inhibition (n=8-12) is the 1 minus CPM of compound-treated cells over DMSO-treated cells. IC_{50} were determined using 0, 0.1, 0.5, 5, 10, and 50 µM of compound (in 1% DMSO final concentration). All calculations including mean, SEM, and IC_{50} were performed on Excel or Prism.

CCK-8

Proliferation of the PL-45 pancreatic cancer cells and HCT-116 colon cancer cells was tested in the presence and absence of the compounds using Cell Counting Kit-8 (Dojindo, catalog number CK04-11). Cells treated with the compounds were compared to dimethyl sulfoxide (DMSO) controls for their ability to proliferate as indicated the absorbance measured at 450nm on a microplate reader. Cells were cultured in 96 well

plates at a concentration of 2000-4000 cells/well in DMEM (Gibco) supplemented with L-glutamine, 10% fetal bovine serum and 1% penicillin-streptomycin antibiotic. After overnight incubation, the compounds were added. The compounds were dissolved in DMSO (at a final concentration of 1.0%) and tested at the concentrations indicated in the manuscript. The DMSO control was also at 1.0%. After the cells had been incubated with the compounds for 72 h, 10µl CCK-8 solution per well was added and the cells were incubated for an additional 2-4 h. Absorbances at λ= 450nm were measured twice throughout the 2-4 h period using a Tecan Infinite 200 Platereader. Decreases in absorbances, as compared to DMSO controls, are an indication that the cells are no longer living and producing mitochondrial activity, as is shown in the studies presented. Data was analyzed for mean and SEM by Excel and/or Prism.

CELL LYSATE PULL DOWN ASSAYS

Protein pull down was carried out following a standard batch purification method in 1.5 mL micro centrifuge tubes. Biotinylated compounds were pre-dissolved in DMSO to which crude cellular protein from the lysates of HCT-116 cells was added along with lysis cocktail (500 mM Tris, 150 mM NaCl, 500 mM EDTA, 1% NP-40) to give a final 1-5% DMSO concentration. Samples were incubated for 24 hours at 4 ^{o}C. The biotin-conjugated compounds were immobilized by the addition of NeutrAvidin^{TM} resin slurry and incubated for 2 hours at 4 ^{o}C. The unbound proteins were removed by washing 4 times with 500 µl of wash buffer (20 mM Tris pH 7.4, 150 mM NaCl, 1% Triton X-100), one wash was 30 minutes at 4 ^{o}C and three washes were 10-15 minutes each at room temperature. After wash buffer removal, the biotinylated molecule along with bound protein complex was eluted from the NeutrAvidin^{TM} resin by boiling in SDS-PAGE

sample buffer for 15 min. Elution was ran on a 4-20% SDS-PAGE gel and visualized with Pierce Silver Stain kit, coomassie blue stain, and or Western blot. For **Di-SanA 16-T-IV-biotin** pull down analysis, the prominent protein gel band(s) were analyzed by Nano-LC/MS/MS analysis (Scripps Mass Spec facility), and comparison of peptide fragmentation results were screened against the NCBInr Eukaryotic database, identifying Hsp90 with an excellent expectancy value. NHS-PEGylated Biotin linker and DMSO were used as the negative controls. Relative protein concentrations were determined with densometric software, Image J.

DOMAINS PULL DOWN ASSAY

Gst-tagged Hsp90 proteins containing N-, NM-, MC-, or C-domain were expressed and purified from BL21 (DE3) *Escherichia coli*. A batch purification was completed according to manufacturer's protocol (Thermo Scientific, Immobilized Glutathione cat#15160). To verify that San A-amide derivatives are binding to a specific domain of Hsp90, we performed a domain pull down using 5 µM of purified Hsp90 proteins (i.e. N-, NM-, MC-, or C-domain). All reactions were performed in MilliQ Ultrapure water. Biotinylated SanA (10 µM) or DMSO (control, 2% final concentration) was added to each reaction and incubated for 2 hours at room temperature. Then, 25 µl of NeutrAvidin^{TM} agarose resin was prepared according to manufacturer's protocol (Thermo Scientific, cat#209200), added to each reaction, and incubated for an additional 45 minutes at room temperature. After 4 washes with wash buffer (20 mM Tris-HCl, 300 mM NaCl, 1% (v/v) triton X-100, pH 7.4) and 3 washes with binding buffer (20 mM Tris-HCl, 150 mM NaCl, 1% (v/v) triton X-100, pH 7.4), proteins were eluted from NeutrAvidin resin with 20 µl sample buffer and boiling. Samples were ran on a SDS-

PAGE gel, and visualized by silver staining using standard manufacturer's protocol (Pierce, cat#24621).

CLIENT PROTEIN BINDING ASSAYS

The binding affinity between Hsp90 and its co-chaperone (i.e. FKBPs and Hop) or client proteins (i.e. IP6K2) were completed using 100-150 nM (final concentration) of human native protein Hsp90 (Enzo Life Sciences) and 75-50 nM (final concentration) of recombinant co-chaperone or client proteins (GST-FKBP38: Abnova cat# H00023770-P01. His-FKBP38: Abcam cat# ab91801. GST-FKBP52: Abnova H00002288-P01. His-FKBP52: Abcam ab91801. GST-IP6K2: Abnova H00051447-P01. His-Her2: R&D Systems 1129-ER-050. His-Akt: Millipore 14-276. His-Hop: Stressmarq SPR-302. His-Cyp40: Abcam ab78815. His-PP5: Abcam ab91714. GST-Hif-1α: Abnova H00055662-P01. His-Unc45: kindly provided by the Huxford lab at SDSU). Experiments were conducted using five different concentrations of San A (0-10 µM), 17-AAG (0-5 µM) or coumermycin A1 (0-25 µM). Protein pull down was completed using Immobilized Glutathione agarose (Pierce, cat#20211) or Talon-Metal Affinity Resin (Clontech, cat#635501), followed by three washes of the bead (20 mM Tris-HCl, 300 mM NaCl, 1% (v/v) triton X-100, pH 7.4), and finally boiling the beads with 4x Laemmli sample buffer. Samples were analyzed using 4-20% SDS-PAGE gel, followed by either coomassie blue stain and/or standard Western blot protocol to detect Hsp90 (Stressgen rabbit polyclonal anti-Hsp90 antibody, cat#SPA-836) and its co-chaperone or client proteins (R&D Systems rat monoclonal anti-FKBP38 antibody, cat#MAB3580; Abcam rabbit

polyclonal anti-FKBP52 antibody, cat# ab2926; Santa Cruz Biotechnology goat polyclonal anti-Hop antibody, cat# sc-27962; Santa Cruz Biotechnology goat anti-IP6K2 antibody, cat#SC-10425, anti-His tag). The respective ratio of Hsp90 to its co-chaperone or client proteins were analyzed via Image J and transformed to a percent of Hsp90 bound to co-chaperone or client proteins.

CASPASE 3 ASSAY

Caspase-3 analyses were completed according to manufacturer's protocol (Promega, cat# G7351). Briefly, 1 x 10^6 HCT-116 cells was treated with compound (0-50 µM) for 24 hours. Cells were harvested and lysed according to manufacturer's protocol. A total of 30 µg of protein lysate was used per well in the assay and the lysate incubated with the caspase detection reagent for 4 hours. Absorbances were read on a Tecan Infinite 200 Platereader at λ= 405nm and analyzed via Prism.

PARP FRAGMENTATION ANALYSIS

Lysate prepared from the Caspase-3 analyses above was loaded onto a 4-20% SDS-PAGE gradient gel, using 10 µg of total protein per lane. The proteins were resolved and transferred to a PVDF for Western blot analysis using a PARP-1 antibody (Enzo Life Sciences, rabbit polyclonal, cat# ALX-210-302-R100) and GAPDH (Santa Cruz Biotech, rabbit polyclonal, cat# sc-25778) for the loading control. Densiometric analyses were performed using ImageJ software and statistical analyses were performed using Prism software.

SYNTHESIS OF CHAPTER 2 DERIVATIVES

SYNTHESIS OF SANA 2

Dipeptide MeO-D-Phe-Leu-NHBoc

Following the "**General solution-phase peptide synthesis**" procedure, a mixture of H-D-Phe-OMe•HCl (0.48 g, 2.21 mmol), Boc-Leu-OH•H_2O (0.50 g, 2.01 mmol), TBTU (0.77 g, 2.41 mmol), and DIPEA (1.40 mL, 8.02 mmol) were dissolved in 20.1 mL of anhydrous DCM (0.1M), 1.0 mL of anhydrous ACN was also added to improve solubility. The reaction was stirred for 1 h. The reaction mixture was diluted in ethyl acetate (100 mL) and subjected to the "**General acid-base work-up**". The organic layer was collected, dried over sodium sulfate, and concentrated *in vacuo* to give the pure dipeptide MeO-D-Phe-Leu-NHBoc (96.0% yield) as a white powder.

Rf: 0.74 (35% EA/Hex)

^{1}H NMR (200 MHz, $CDCl_3$): δ 0.89 (d, 6H), 1.45 (s, 9H), 1.51-1.64 (m, 3H), 3.08-3.13 (m, 2H), 3.72 (s, 3H), 4.05-4.15 (m, αH), 4.76 (d, NH), 4.80-4.92 (m, αH), 6.55 (d, NH), 7.08-7.18 (m, 2H), 7.22-7.36 (m, 3H).

Dipeptide MeO-D-Phe-Leu-NH_2

Following the "**General solution-phase amine deprotection**" procedure, MeO-D-Phe-Leu-NHBoc (756 mg, 1.93 mmol) was dissolved in a 19.3 mL solution of DCM/TFA (3:1, v/v, 0.1M) along with anisole (0.42 mL, 3.85 mmol). The reaction mixture was allowed to stir for 45 minutes, and then was concentrated in vacuo to give MeO-D-Phe-Leu-NH_2 in a quantitative yield. This dipeptide was taken on to the next coupling step without any further purification or characterization.

Tripeptide MeO-D-Phe-Leu-Val-NHBoc

Following the "**General solution-phase peptide synthesis**" procedure, a mixture of MeO-D-Phe-Leu-NH_2 (565 mg, 1.93 mmol), Boc-Val-OH (381 mg, 1.75 mmol), TBTU (676 mg, 2.41 mmol), and DIPEA (1.20 mL, 7.02 mmol) were dissolved in 17.5 mL of anhydrous DCM (0.1M), 1.0 mL of anhydrous ACN was also added to improve the solubility of the mixture. The solution was stirred for 2 h. The reaction mixture was then diluted in ethyl acetate (100 mL) and subjected the "**General acid-base work-up**". The organic layer was collected, dried over sodium sulfate, and concentrated *in vacuo* to give the pure tripeptide MeO-D-Phe-Leu-Val-NHBoc (98.9% yield) as a white powder.

Rf: 0.68 (50% EA/Hex)

^{1}H NMR (200 MHz, $CDCl_3$): δ 0.84-0.96 (m, 12H), 1.15-1.32 (m, 3H), 1.46 (s, 9H), 2.04-2.18 (m, 1H), 2.98-3.14 (m, 2H), 3.71 (s, 3H), 4.36-4.44 (m, αH), 4.78-4.87 (m, αH), 4.95 (m, αH), 6.27 (d, NH), 6.61 (d, NH), 7.09-7.17 (m, 5H).

Tripeptide MeO-D-Phe-Leu-Val-NH_2

Following the "**General solution-phase amine deprotection**" procedure, MeO-D-Phe-Leu-Val-NHBoc (659 mg, 1.34 mmol) was dissolved in a 10.1 mL solution of DCM/TFA (3:1, v/v, 0.1M) along with anisole (0.29 mL, 2.68 mmol). The reaction mixture was allowed to stir for 1.5 hours, and then was concentrated *in vacuo* to give MeO-D-Phe-Leu-Val-NH_2 in a quantitative yield. This tripeptide was taken on to the next coupling step without any further purification or characterization.

Dipeptide MeO-Leu-Leu-NHBoc

Following the "**General solution-phase peptide synthesis**" procedure, a mixture of H-Leu-OMe•HCl (0.40 g, 2.21 mmol), Boc-Leu-OH•H_2O (0.50 g, 2.01 mmol), TBTU (0.77 g, 2.41 mmol), and DIPEA (1.40 mL, 8.02 mmol) were dissolved in 20.1 mL of

anhydrous DCM (0.1M). The reaction was stirred for 1 h. The reaction mixture was diluted in ethyl acetate (100 mL) and subjected to the "**General acid-base work-up**" procedure. The organic layer was collected, dried over sodium sulfate, and concentrated *in vacuo* to give the pure dipeptide MeO-Leu-Leu-NHBoc (97.2% yield) as a white powder.

Rf: 0.57 (30% EA/Hex)

^{1}H NMR (200 MHz, $CDCl_3$): δ 0.90-1.00 (m, 12H), 1.46 (s, 9H), 1.50-1.75 (m, 6H + H_20), 3.73 (s, 3H), 4.02-4.17 (m, αH), 4.58-4.65 (m, αH), 4.85 (d, NH), 6.41 (d, NH).

Dipeptide HO-Leu-Leu-NHBoc

Following the "**General solution-phase acid deprotection**" procedure, MeO-Leu-Leu-NHBoc (698 mg, 1.94 mmol) and lithium hydroxide (653 mg, 15.6 mmol) was dissolved in 19.4 mL of methanol (0.1M). The reaction mixture was allowed to stir for 1 hour. The reaction was diluted in DCM (100 mL) and treated with pH 1 water (100 mL). After verifying that the aqueous layer remained acidic (pH ~3), the product was extracted with five washes of DCM (100 mL each). The organic layers were combined, dried over sodium sulfate, and concentrated in vacuo to give the pure dipeptide HO-Leu-Leu-NHBoc (99% yield). This dipeptide was taken on to the next coupling step without any further purification or characterization.

Linear pentapeptide MeO-D-Phe-Leu-Val-Leu-Leu-NHBoc

Following the "**General solution-phase peptide synthesis**" procedure, a mixture of Boc-Leu-Leu-OH (669 mg, 1.94 mmol), TBTU (311 mg, 0.970 mmol), HATU (369 mg, 0.970 mmol) and DIPEA (1.20 mL, 7.02 mmol) were dissolved in a 9.7 mL solution of anhydrous DCM and ACN (1:1, v/v). MeO-D-Phe-Leu-Val-NH_2 (837 mg, 2.13 mmol)

was dissolved in another 9.7 mL anhydrous DCM/ACN solution and was added, by long-needle syringe, to the mixture containing the coupling reagents (0.1M final concentration). The solution was stirred for 1.5 h. The reaction was then diluted in DCM (100 mL) and subjected to two aqueous washes of 10% HCl (100 mL each) and four washes of sodium bicarbonate solution (100 mL, sat. aq.). The organic layers were combined, dried over sodium sulfate, and concentrated *in vacuo* to give the crude peptide. The peptide was purified by flash column chromatography using an ethyl acetate/hexanes gradient solvent system where the pure linear pentapeptide eluted at 65EA/35Hex. The pure linear pentapeptide (10.1% yield) was verified by NMR.

Rf: 0.61 (50% EA/Hex)

^{1}H NMR (500 MHz, $CDCl_3$): δ 0.85-1.00 (m, 24H), 1.28 (s, 9H), 1.47 (m, 6H), 1.66-1.80 (m, 3H), 2.33 (m, 1H), 3.06-3.20 (m, 2H), 3.67 (s, 3H), 3.99 (m, αH), 4.22 (m, αH), 4.28 (m, αH), 4.44 (m, αH), 4.73 (m, αH), 4.91 (br, NH), 5.36 (NH), 6.60 (m, NH), 6.88 (br, NH), 7.02 (br, NH), 7.19-7.34 (m, 5H).

Linear pentapeptide HO-D-Phe-Leu-Val-Leu-Leu-NHBoc

Following the "**General solution-phase acid deprotection**" procedure, MeO-D-Phe-Leu-Val-Leu-Leu-NHBoc (141 mg, 0.196 mmol) and lithium hydroxide (66 mg, 1.57 mmol) was dissolved in 1.96 mL of methanol (0.1M). An additional 0.20 mL of methanol was added to the reaction to increase solubility. The reaction mixture was allowed to stir overnight. The reaction was diluted in DCM (100 mL) and treated with pH 1 water (100 mL). After verifying that the aqueous layer remained acidic (pH ~3), the product was extracted with five washes of DCM (100 mL each). The organic layers were combined, dried over sodium sulfate, and concentrated in vacuo to give the linear

pentapeptide HO-D-Phe-Leu-Val-Leu-Leu-NHBoc (73.2% yield). This pentapeptide was taken on to the next deprotection step without any further purification or characterization.

Linear pentapeptide HO-D-Phe-Leu-Val-Leu-Leu-NH_2

Following the "**General solution-phase amine deprotection**" procedure, HO-D-Phe-Leu-Val-Leu-Leu-NHBoc (101 mg, 0.143 mmol) was dissolved in a 1.43 mL solution of DCM/TFA (3:1, v/v, 0.1M) along with anisole (0.031 mL, 0.286 mmol). The reaction mixture was allowed to stir for 1 hour, and then was concentrated *in vacuo* to give the double-deprotected linear pentapeptide HO-D-Phe-Leu-Val-Leu-Leu-NH_2 (73.1% yield), which was verified by LCMS.

LCMS: m/z called for $C_{32}H_{53}N_5O_6$ (M+1) = 604.4, found 604.3.

Cyclic pentapeptide D-Phe-Leu-Val-Leu-Leu

Following the "**General macrocyclization procedure**", HO-D-Phe-Leu-Val-Leu-Leu-NH_2 (63.2 mg, 0.104 mmol), DEPBT (12.4 mg, 0.0416 mmol), HATU (23.7 mg, 0.0624 mmol), TBTU (16.8 mg, 0.0522 mmol), and DIPEA (0.109 mL, 0.624 mmol) were dissolved in 14.9 mL of anhydrous DCM and ACN (1:1, v/v, 0.007M). The reaction was allowed to stir for 1.5 h and was monitored by LCMS. Upon completion, the reaction was worked up with 2 washes of saturated ammonium chloride (aqueous) and back-extracted with DCM. The organic layers were collected, dried over sodium sulfate, and concentrated *in vacuo*. The pentapeptide was purified by flash column chromatography using an EA/Hex gradient solvent system where the pure product eluted at 100EA. The pure cyclic pentapeptide D-Phe-Leu-Val-Leu-Leu (79.8% yield) was verified by NMR and LCMS.

Rf: 0.57 (75% EA/Hex)

^{1}H NMR (500 MHz, CD_3OD): δ 0.64 (d, 3H), 0.76 (d, 3H), 0.83-1.00 (m, 18H), 1.21-1.38 (m, 6H), 1.38-1.70 (m, 3H), 2.52-2.61 (m, 1H), 2.92-3.03 (m, 2H), 4.05-4.13 (m, 2αH), 4.40-4.52 (m, 3αH), 7.19-7.30 (m, 5H).

LCMS: m/z called for $C_{32}H_{51}N_5O_5$ (M+1) = 586.39, found 586.3.

SYNTHESIS OF SANA 3

Note: The protected linear pentapeptide for **SanA 3** was synthesized and purified by the author's colleague.

Linear pentapeptide HO-*N*-Me-Phe-Leu-Val-Leu-Leu-NHBoc

Following the "**General solution-phase acid deprotection**" procedure, MeO-*N*-Me-Phe-Leu-Val-Leu-Leu-NHBoc (185.1 mg, 0.253 mmol) and lithium hydroxide (84.7 mg, 2.02 mmol) was dissolved in 2.53 mL of methanol (0.1M). The reaction mixture was allowed to stir overnight. Completion was verified by TLC. The reaction was diluted in DCM (100 mL) and treated with pH 1 water (100 mL). After verifying that the aqueous layer remained acidic (pH ~3), the product was extracted with five washes of DCM (100 mL each). The organic layers were combined, dried over sodium sulfate, and concentrated in vacuo to give the linear pentapeptide HO-*N*-Me-Phe-Leu-Val-Leu-Leu-NHBoc (181.9 mg, 100% yield). This pentapeptide was taken on to the next deprotection step without any further purification or characterization.

Double-deprotected linear pentapeptide HO-*N*-Me-Phe-Leu-Val-Leu-Leu-NH_2

Following the "**General solution-phase amine deprotection**" procedure, HO-*N*-Me-Phe-Leu-Val-Leu-Leu-NHBoc (181.9 mg, 0.253 mmol) was dissolved in a 2.53 mL solution of DCM/TFA (3:1, v/v, 0.1M), along with anisole (0.055 mL, 0.506 mmol). The reaction mixture was allowed to stir for 1 hour, and then was concentrated *in vacuo* to

give the double-deprotected linear pentapeptide HO-*N*-Me-Phe-Leu-Val-Leu-Leu-NH_2 (156 mg, 99.6% yield), which was verified by LCMS.

LCMS: m/z called for $C_{33}H_{55}N_5O_5$ (M+1) = 618.42, found 618.4.

Cyclic pentapeptide *N*-Me-Phe-Leu-Val-Leu-Leu

Following the "**General macrocyclization procedure**", HO-*N*-Me-Phe-Leu-Val-Leu-Leu-NH_2 (156 mg, 0.252 mmol), DEPBT (30.1 mg, 0.101 mmol), HATU (57.0 mg, 0.151 mmol), TBTU (40.0 mg, 0.126 mmol), and DIPEA (0.264 mL, 1.51 mmol) were dissolved in 36.0 mL of anhydrous DCM and ACN (1:1, v/v, 0.007M). The reaction was allowed to stir for 2.5 h and was monitored by TLC. Upon completion, the reaction was worked up with 2 washes of saturated ammonium chloride (aqueous) and back-extracted with DCM. The organic layers were collected, dried over sodium sulfate, and concentrated *in vacuo*. The pentapeptide was purified by flash column chromatography using an EA/Hex gradient solvent system where the semi-pure product eluted at 100EA. Further purification as performed using RP-HPLC to give the cyclic pentapeptide *N*-Me-Phe-Leu-Val-Leu-Leu (51.2% yield) was verified by NMR and LCMS.

Rf: 0.32 (75% EA/Hex)

^{1}H NMR (500 MHz, CD_3OD): δ 0.73 (d, 3H), 0.77 (d, 3H), 0.83-1.05 (m, 18H), 1.28-1.40 (m, 3H), 1.41-1.68 (m, 9H), 2.51-2.63 (m, 1H), 3.02-3.10 (m, 1H), 3.12-3.19 (m, 1H), 3.15 (s, 3H), 4.20-4.28 (m, 1αH), 4.30-4.35 (m, 1αH), 4.81-4.89 (m, 1αH), 5.03-5.10 (m, 1αH), 7.19-7.33 (m, 5H), 7.55 (d, N<u>H</u>), 8.05 (d, N<u>H</u>), 8.33 (d, N<u>H</u>).

LCMS: m/z called for $C_{33}H_{53}N_5O_5$ (M+1) = 600.4, found 600.4.

SYNTHESIS OF SANA 4

Dipeptide MeO-D-Tyr-Leu-NHBoc

Following the "**General solution-phase peptide synthesis**" procedure, a mixture of H-D-Tyr-OMe•HCl (0.512 g, 2.21 mmol), Boc-Leu-OH•H_2O (0.500 g, 2.01 mmol), DEPBT (0.721 g, 2.41 mmol), and DIPEA (1.40 mL, 8.02 mmol) were dissolved in 20.1 mL of anhydrous DCM (0.1M). The reaction was stirred for 1.5 h. The reaction mixture was diluted in DCM (100 mL) and quenched with two saturated sodium chloride washes (100 mL, sat. aq.). The organic layers were collected, dried over sodium sulfate, and concentrated *in vacuo* to give the crude dipeptide. The dipeptide was purified via flash column chromatography using an EA/Hex gradient solvent system where the pure product eluted at 50% EA/Hex. The pure dipeptide MeO-D-Tyr-Leu-NHBoc (85.3% yield) was verified by NMR.

Rf: 0.39 (50% EA/Hex)

^{1}H NMR (200 MHz, $CDCl_3$): δ 0.91 (d, 6H), 1.45 (s, 9H), 3.02-3.07 (m, 1H), 3.72 (s, 3H), 4.04-4.17 (m, αH), 4.73-4.85 (m, αH), 4.98 (br, O<u>H</u>) 6.75 (d, 2H), 6.94-7.02 (m, 2H).

Dipeptide MeO-D-Tyr-Leu-NH_2

Following the "**General solution-phase amine deprotection**" procedure, MeO-D-Tyr-Leu-NHBoc (701 mg, 1.71 mmol) was dissolved in a 17.1 mL solution of DCM/TFA (3:1, v/v, 0.1M) along with anisole (0.37 mL, 3.42 mmol). The reaction mixture was allowed to stir for 1 h, and then was concentrated *in vacuo* to give MeO-D-Tyr-Leu-NH_2 in a quantitative yield. This dipeptide was taken on to the next coupling step without any further purification or characterization.

Tripeptide MeO-D-Tyr-Leu-Val-NHBoc

Following the "**General solution-phase peptide synthesis**" procedure, a mixture of MeO-D-Tyr-Leu-NH_2 (695 mg, 2.24 mmol), Boc-Val-OH (444 mg, 2.04 mmol), TBTU (786 mg, 2.45 mmol), and DIPEA (1.42 mL, 8.16 mmol) were dissolved in 20.4 mL of anhydrous ACN (0.1M). The solution was stirred for 1 h. The reaction mixture was then diluted in DCM (60 mL) and quenched with two saturated sodium chloride washes (100 mL, sat. aq.). The organic layers were collected, dried over sodium sulfate, and concentrated *in vacuo* to give the crude dipeptide. The dipeptide was purified via flash column chromatography using an ethyl acetate and hexanes gradient solvent system where the pure product eluted at 65% EA/Hex. The pure tripeptide MeO-D-Tyr-Leu-Val-NHBoc (27.2% yield) was verified by NMR.

Rf: 0.52 (50% EA/Hex)

^{1}H NMR (600 MHz, CD_3OD): δ 0.82-0.93 (m, 12H), 1.27-1.44 (m, 2H), 1.45 (s, 9H), 1.96-2.05 (m, 1H), 2.18 (m, 1H), 2.82-2.87 (m, 1H), 3.11 (m, 1H), 3.70 (s, 3H), 3.82 (m, αH), 4.43 (m, αH), 4.61 (m, αH), 5.34 (O<u>H</u>), 6.70 (d, 2H), 7.01 (d, 2H).

<u>Note</u>: Dipeptide HO-Leu-Leu-NHBoc for the following linear pentapeptide was synthesized by the author's colleague.

Linear pentapeptide MeO-D-Tyr-Leu-Val-Leu-Leu-NHBoc

Following the "**General solution-phase peptide synthesis**" procedure, a mixture of Boc-Leu-Leu-OH (370 mg, 0.505 mmol), DEPBT (60 mg, 0.202 mmol), HATU (96 mg, 0.252 mmol), TBTU (48 mg, 0.151 mmol), and DIPEA (0.71 mL, 4.04 mmol) were dissolved in a 6.0 mL solution of anhydrous DCM. MeO-D-Tyr-Leu-Val-NH_2 (227 mg, 0.556 mmol) was dissolved in another 6.0 mL anhydrous DCM and was added, by long-needle syringe, to the mixture containing the coupling reagents (0.05M final

concentration). The solution was stirred for 2 h. The reaction was then diluted in DCM (100 mL) and subjected to two aqueous washes of 10% HCl (100 mL each), four washes of sodium bicarbonate solution (100 mL, sat. aq.), and one wash of saturated sodium chloride (100 mL, sat. aq.). The organic layers were combined, dried over sodium sulfate, and concentrated *in vacuo*. Upon analysis by TLC, LCMS, and NMR, the product (MeO-D-Tyr-Leu-Val-Leu-Leu-NHBoc, 68.2% yield) was found mostly pure and was not taken on for further purification.

Rf: 0.46 (65% EA/Hex)

^{1}H NMR (400 MHz, CD_3OD): δ 0.72-0.88 (m, 24H), 1.15-1.47 (m, 6H), 1.35 (s, 9H), 1.48-1.65 (m, 3H), 1.90-1.99 (m, 1H), 2.71-2.81 (m, 1H), 2.95-3.07 (m, 1H), 3.59 (s, 3H), 3.96-4.08 (m, 2αH), 4.27-4.39 (m, 2αH), 4.48-4.53 (m, 1αH), 6.60 (d, 2H), 6.92 (d, 2H).

LCMS: m/z called for $C_{38}H_{63}N_5O_9$ (M+1) = 734.46, found 734.4.

Double-deprotected linear pentapeptide HO-D-Tyr-Leu-Val-Leu-Leu-NH_2

Following the general "***In situ* double deprotection**" procedure, MeO-D-Tyr-Leu-Val-Leu-Leu-NHBoc (253 mg, 0.344 mmol) and anisole (0.074 mL, 0.688 mmol) were dissolved in 3.44 mL of THF. HCl was added dropwise (7 drops) and the reaction was allowed to run overnight. By LCMS, no product had formed and there was no change in the amount of starting material, so additional HCl was added (7 drops) and allowed to run for four days. When reaction did not indicate completion, an additional 5 drops of HCl was added over three days. Finally, the reaction was concentrated *in vacuo* and analyzed by LCMS.

LCMS: m/z called for $C_{32}H_{53}N_5O_7$ (M+1) = 620.39, found 620.4.

Cyclic pentapeptide D-Tyr-Leu-Val-Leu-Leu

Following the "**General macrocyclization procedure**", HO-D-Tyr-Leu-Val-Leu-Leu-NH_2 (214 mg, 0.344 mmol), DEPBT (41.0 mg, 0.137 mmol), HATU (78.0 mg, 0.206 mmol), TBTU (55.0 mg, 0.172 mmol), and DIPEA (0.360 mL, 2.06 mmol) were dissolved in 49.1 mL of anhydrous DCM and ACN (1:1, v/v, 0.007M). Anhyrdous DMF (10 mL) was added to improve solubility. The reaction was allowed to stir for 1.5 h and was monitored by LCMS. Upon completion, the reaction was worked up with 2 washes of saturated sodium chloride (150 mL each, sat. aq.) and back-extracted with DCM. The organic layers were collected, dried over sodium sulfate, and concentrated *in vacuo*. The pentapeptide was purified by flash column chromatography using an EA/Hex gradient solvent system where the semi-pure product eluted at 100EA. Further purification was performed using RP-HPLC to give the cyclic pentapeptide D-Tyr-Leu-Val-Leu-Leu (48.5% yield) was verified by NMR, LCMS, and analytical HPLC.

Rf: 0.27 (100% EA)

^{1}H NMR (600 MHz, CD_3OD): δ 0.66 (d, 3H), 0.79 (d, 3H), 0.89-1.00 (m, 18H), 1.26-1.42 (m, 2H), 1.44-1.72 (m, 7H), 2.58-2.67 (m, 1H), 2.84-2.93 (m, 2H), 4.05-4.11 (m, 1αH), 4.32-4.38 (m, 1αH), 4.43-4.50 (m, 1αH), 4.50-4.57 (m, 1αH), 6.70 (d, 2H), 7.02 (d, 2H), 7.49 (d, N<u>H</u>), 8.12 (d, N<u>H</u>), 8.29 (d, N<u>H</u>), 8.76 (d, N<u>H</u>)

LCMS: m/z called for $C_{32}H_{51}N_5O_6$ (M+1) = 602.38, found 602.4.

SYNTHESIS OF SANA 8 AND DI-SANA 8

Dipeptide MeO-D-Phe-D-Leu-NHBoc

Following the "**General solution-phase peptide synthesis**" procedure, a mixture of H-D-Phe-OMe•HCl (0.951 g, 4.40 mmol), Boc-D-Leu-OH (1.0 g, 4.00 mmol), TBTU (1.54

g, 4.80 mmol), and DIPEA (2.80 mL, 16.00 mmol) were dissolved in 44.1 mL of anhydrous DCM (0.1M). The reaction was stirred for 1 h. The reaction mixture was diluted in ethyl acetate (100 mL) and subjected to the "**General acid-base work-up**" procedure. The organic layer was collected, dried over sodium sulfate, and concentrated *in vacuo* to give the pure dipeptide MeO-D-Phe-D-Leu-NHBoc as a white powder (98.7% yield).

Rf: 0.56 (30% EA/Hex)

^{1}H NMR (200 MHz, $CDCl_3$): δ 0.86 (d, 6H), 1.43 (s, 9H), 1.60-1.71 (m, 2H+ H_20), 3.08-3.18 (m, 2H), 3.71 (s, 3H), 4.02-4.14 (m, αH), 4.73-4.85 (m, αH), 6.47 (d, 1 N<u>H</u>), 7.07-7.15 (m, 2H), 7.23-7.33 (m, 3H).

Dipeptide MeO-D-Phe-D-Leu-NH_2

Following the "**General solution-phase amine deprotection**" procedure, MeO-D-Phe-D-Leu-NHBoc (1.55 g, 3.95 mmol) was dissolved in a 39.5 mL solution of DCM/TFA (3:1, v/v, 0.1M) along with anisole (0.86 mL, 7.90 mmol). The reaction mixture was allowed to stir for 1 hour, and then was concentrated in vacuo to give MeO-D-Phe-D-Leu-NH_2 in a quantitative yield. This dipeptide was taken on to the next coupling step without any further purification or characterization.

Tripeptide MeO-D-Phe-D-Leu-Val-NHBoc

Following the "**General solution-phase peptide synthesis**" procedure, a mixture of MeO-D-Phe-D-Leu-NH_2 (1.15 g, 3.95 mmol), Boc-Val-OH (0.780 g, 3.59 mmol), TBTU (1.38 g, 4.30 mmol), and DIPEA (2.5 mL, 14.4 mmol) were dissolved in 35.9 mL of anhydrous DCM (0.1M). The solution was stirred for 2 h. The reaction mixture was then diluted in ethyl acetate (100 mL) and subjected to the "**General acid-base work-up**"

procedure. The organic layer was collected, dried over sodium sulfate, and concentrated *in vacuo* to give the pure tripeptide MeO-D-Phe-D-Leu-Val-NHBoc as a white powder (97.0% yield).

Rf: 0.54 (50% EA/Hex)

^{1}H NMR (200 MHz, $CDCl_3$): δ 0.8-1.1 (m, 12H), 1.4 (s, 9H), 1.6-1.8 (m, 3H), 2.1-2.2 (m, 1H), 3.0-3.2 (m, 2H), 3.7 (s, 3H), 3.8-4.0 (m, αH), 4.4-4.5 (m, αH), 4.7-4.9 (m, αH), 4.9 (br, 1H), 6.1-6.3 (d, 1H), 6.5-6.6 (br, 1H), 7.1-7.4 (m, 5H).

Tripeptide MeO-D-Phe-D-Leu-Val-NH_2

Following the "**General solution-phase amine deprotection**" procedure, MeO-D-Phe-D-Leu-Val-NHBoc (1.72 g, 3.49 mmol) was dissolved in a 34.9 mL solution of DCM/TFA (3:1, v/v, 0.1M) along with anisole (0.76 mL, 6.99 mmol). The reaction mixture was allowed to stir for 1.5 hours, and then was concentrated *in vacuo* to give MeO-D-Phe-Leu-Val-NH_2 in a quantitative yield. This tripeptide was taken on to the next coupling step without any further purification or characterization.

Dipeptide MeO-Leu-Leu-NHBoc

Following the "**General solution-phase peptide synthesis**" procedure, a mixture of H-Leu-OMe•HCl (0.80 g, 4.41 mmol), Boc-Leu-OH•H_2O (1.00 g, 4.01 mmol), TBTU (1.54 g, 4.81 mmol), and DIPEA (2.79 mL, 16.00 mmol) were dissolved in 40.1 mL of anhydrous DCM (0.1M). The reaction was stirred for 1 h. The reaction mixture was diluted in ethyl acetate (100 mL) and subjected to the "**General acid-base work-up**" procedure. The organic layer was collected, dried over sodium sulfate, and concentrated *in vacuo* to give the pure dipeptide MeO-Leu-Leu-NHBoc as a white powder (98% yield).

Rf: 0.57 (30% EA/Hex)

^{1}H NMR (200 MHz, $CDCl_3$): δ 0.80-1.00 (m, 12H), 1.21-1.32 (m, 4H), 1.45 (s, 9H), 1.53-1.77 (m, 2H+ H_20), 3.73 (s, 3H), 4.04-4.19 (m, αH), 4.52-4.71 (m, αH), 4.83 (br, 1 NH), 6.43 (br, 1 NH).

Dipeptide HO-Leu-Leu-NHBoc

Following the "**General solution-phase acid deprotection**" procedure, MeO-Leu-Leu-NHBoc (698 mg, 1.94 mmol) and lithium hydroxide (653 mg, 15.6 mmol) was dissolved in 19.4 mL of methanol (0.1M). The reaction mixture was allowed to stir for 1 h. The reaction was diluted in DCM (100 mL) and treated with pH 1 water (100 mL). After verifying that the aqueous layer remained acidic (pH ~3), the product was extracted with five washes of DCM (100 mL each). The organic layers were combined, dried over sodium sulfate, and concentrated *in vacuo* to give the pure dipeptide HO-Leu-Leu-NHBoc. This dipeptide was taken on to the next coupling step without any further purification or characterization.

Linear pentapeptide MeO-D-Phe-D-Leu-Val-Leu-Leu-NHBoc

Following the "**General solution-phase peptide synthesis**" procedure, a mixture of Boc-Leu-Leu-OH (1.09 mg, 3.17 mmol), DEPBT (284 mg, 0.950 mmol), HATU (361 mg, 0.950 mmol), TBTU (611 mg, 1.90 mmol), and DIPEA (4.43 mL, 25.4 mmol) were dissolved in a 6.0 mL solution of anhydrous DCM (0.025M). MeO-D-Phe-Leu-Val-NH_2 (1.37 g, 3.49 mmol) was dissolved in another 15.8 mL anhydrous DCM and ACN (1:1, v/v) and was added, by long-needle syringe, to the mixture containing the coupling reagents (0.1M final concentration). Anhydrous THF (1 mL) and DMF (3 drops) were added to improve solubility. The solution was stirred for 1.5 h and was monitored by

TLC. The reaction was then diluted in DCM (100 mL) and subjected to two aqueous washes of 10% HCl (100 mL each), four washes of sodium bicarbonate solution (100 mL, sat. aq.), and two washes of saturated sodium chloride (100 mL, sat. aq.). The organic layers were combined, dried over sodium sulfate, and concentrated *in vacuo*. Crude material was purified by flash column chromatography using an EA/Hex gradient solvent system where the product eluted at 75EA/25Hex and was verified by NMR. (MeO-D-Phe-D-Leu-Val-Leu-Leu-NHBoc, 58.0% yield).

Rf: 0.52 (50% EA/Hex)

^{1}H NMR (400 MHz, CD_3OD): δ 0.8-1.0 (m, 24H), 1.4 (s, 9H), 3.1-3.2 (m, 2H), 3.7 (s, 3H), 4.2 (m, 2αH), 4.4-4.5 (m, 2αH), 4.6-4.7 (m, αH), 7.2-7.3 (m, 5H).

Linear pentapeptide HO-D-Phe-D-Leu-Val-Leu-Leu-NHBoc

Following the "**General solution-phase acid deprotection**" procedure, MeO-D-Phe-D-Leu-Val-Leu-Leu-NHBoc (475 mg, 0.661 mmol) and lithium hydroxide (222 mg, 5.28 mmol) was dissolved in 6.61 mL of methanol (0.1M). The reaction mixture was allowed to stir overnight. Completion was verified by TLC. The reaction was diluted in DCM (100 mL) and treated with pH 1 water (100 mL). After verifying that the aqueous layer remained acidic (pH ~3), the product was extracted with five washes of DCM (100 mL each). The organic layers were combined, dried over sodium sulfate, and concentrated *in vacuo* to give the linear pentapeptide HO-D-Phe-D-Leu-Val-Leu-Leu-NHBoc (81.5% yield). This pentapeptide was taken on to the next deprotection step without any further purification or characterization.

Double-deprotected linear pentapeptide HO-D-Phe-D-Leu-Val-Leu-Leu-NH_2

Following the "**General solution-phase amine deprotection**" procedure, HO-D-Phe-D-Leu-Val-Leu-Leu-NHBoc (381 mg, 0.539 mmol) was dissolved in a 4.04 mL solution of DCM/TFA (3:1, v/v, 0.1M), along with anisole (0.12 mL, 1.08 mmol). The reaction mixture was allowed to stir for 2 h, and then was concentrated *in vacuo* to give the double-deprotected linear pentapeptide HO-D-Phe-D-Leu-Val-Leu-Leu-NH_2 (quantitative yield), which was verified by LCMS.

LCMS: m/z called for $C_{32}H_{53}N_5O_6$ (M+1) = 604.4, found 604.3.

Macrocycle D-Phe-D-Leu-Val-Leu-Leu

Following the "**General macrocyclization procedure**", HO-D-Phe-D-Leu-Val-Leu-Leu-NH_2 (163 mg, 0.269 mmol), DEPBT (56.3 mg, 0.188 mmol), HATU (51.1 mg, 0.135 mmol), TBTU (43.1 mg, 0.135 mmol), and DIPEA (0.38 mL, 2.15 mmol) were dissolved in 0.54 mL of anhydrous DMF (0.5M). The reaction was allowed to stir for 1.5 h and was monitored by LCMS for the formation of cyclic pentapeptide and decapeptide. Upon completion, the ratio of cyclic pentapeptide to cyclic decapeptide products was approximately 1:1. The reaction was diluted in DCM (100 mL) and worked up with 2 washes of saturated sodium chloride (100 mL each, sat. aq.) and back-extracted with DCM. The organic layers were collected, dried over sodium sulfate, and concentrated *in vacuo*. The products were initially purified by flash column chromatography using an EA/Hex gradient solvent system where the semi-pure mixture (1:1) of pentapeptide and decapeptide products eluted at 75EA. Further purification and separation was performed using RP-HPLC. Both the cyclic pentapeptide and decapeptide (71.4% combined yield) were analyzed by NMR, LCMS, and analytical HPLC.

Rf: 0.50 (80% EA/Hex)

Cylized pentapeptide

^{1}H NMR (600 MHz, CD_3OD): δ 0.8-1.0 (m, 24H), 1.2-1.4 (m, 3H), 1.5-1.7 (m, 6H), 2.9-3.1 (m, 1H), 3.2-3.4 (m, 1H), 3.6-3.8 (m, 1H), 4.0-4.1 (m, 1αH), 4.1-4.2 (m, 2αH), 4.2-4.4 (m, 1αH), 4.6-4.8 (m, 1αH), 7.2-7.4 (m, 5H).

LCMS: m/z calcd for $C_{32}H_{51}N_5O_5$ (M+23) = 608.39, found 608.6.

Cyclized decapeptide

^{1}H NMR (600 MHz, CD_3OD): δ 0.74-1.00 (m, 48H), 1.42-1.85 (m, 20H), 1.98-2.10 (m, 2H), 2.64-2.71 (m, 2H), 2.91-2.97 (m, 2H), 3.61-3.68 (m, 2H), 4.02-4.12 (m, 3αH), 4.42-4.52 (m, 2αH), 4.59-4.70 (m, 2αH), 7.18-7.32 (m, 10H), 7.50 (d, N<u>H</u>), 7.58 (d, N<u>H</u>), 7.67 (d, N<u>H</u>), 8.16 (d, N<u>H</u>), 8.24 (m, 2N<u>H</u>), 8.35 (m, 2N<u>H</u>), 8.52 (d, 2N<u>H</u>).

LCMS: m/z called for $C_{64}H_{102}N_{10}O_{10}$ (M+1) = 1171.78, found 1175.1.

SYNTHESIS OF SANA 9 AND DI-SANA 9

Dipeptide MeO-Phe-D-Phe-NHBoc

Following the "**General solution-phase peptide synthesis**" procedure, a mixture of H-Phe-OMe (0.450 g, 2.00 mmol), Boc-D-Phe-OH (0.500 g, 1.90 mmol), TBTU (0.724 g, 2.30 mmol), and DIPEA (1.30 mL, 7.60 mmol) were dissolved in 18.8 mL of anhydrous DCM (0.1M). The reaction was stirred for 1 h. The reaction mixture was diluted in ethyl acetate (100 mL) and subjected to the "**General acid-base work-up**" procedure. The organic layer was collected, dried over sodium sulfate, and concentrated *in vacuo* to give the pure dipeptide MeO-Phe-D-Phe-NHBoc as a white powder (99.6% yield).

Rf: 0.61 (35% EA/Hex)

^{1}H NMR (200 MHz, $CDCl_3$): δ 1.40 (s, 9H), 2.88-3.15 (m, 4H), 3.68 (s, 3H), 4.30-4.40 (m, αH), 4.79-4.94 (m, αH), 6.30-6.39 (m, 1H), 6.91-6.98 (m, 1H), 7.15-7.33 (m, 10H).

Dipeptide MeO-Phe-D-Phe-NH_2

Following the "**General solution-phase amine deprotection**" procedure, MeO-Phe-D-Phe-NHBoc (0.798 g, 1.87 mmol) was dissolved in an 18.7 mL solution of DCM/TFA (3:1, v/v, 0.1M) along with anisole (0.41 mL, 3.74 mmol). The reaction mixture was allowed to stir for 1 h, and then was concentrated in vacuo to give MeO-Phe-D-Phe -NH_2 in a quantitative yield. This dipeptide was taken on to the next coupling step without any further purification or characterization.

Tripeptide MeO-Phe-D-Phe-D-Val-NHBoc

Following the "**General solution-phase peptide synthesis**" procedure, a mixture of MeO-Phe-D-Phe -NH_2 (0.610 g, 1.87 mmol), Boc-D-Val-OH (0.369 g, 1.70 mmol), TBTU (0.655 g, 2.04 mmol), and DIPEA (1.5 mL, 8.50 mmol) were dissolved in 17.0 mL of anhydrous DCM (0.1M). The solution was stirred for 1 h. The reaction mixture was then diluted in ethyl acetate (100 mL) and subjected to the "**General acid-base work-up**" procedure. The organic layer was collected, dried over sodium sulfate, and concentrated *in vacuo* to give the pure tripeptide MeO-Phe-D-Phe-D-Val-NHBoc as a white powder (99.6% yield).

Rf: 0.50 (50% EA/Hex)

^{1}H NMR (200 MHz, $CDCl_3$): δ 0.72-0.94 (m, 6H), 1.44 (s, 9H), 2.05-2.10 (m, 1H), 2.95-3.08 (m, 4H), 3.65 (s, 3H), 3.82-3.90 (m, αH), 4.60-4.79 (m, 2αH), 4.80-4.88 (m, 1H), 6.39-6.52 (m, 2H), 6.90-7.00 (m, 2H), 7.15-7.36 (m, 10H).

Tripeptide MeO-Phe-D-Phe-D-Val-NH_2

Following the "**General solution-phase amine deprotection**" procedure, MeO-Phe-D-Phe-D-Val-NHBoc (0.890 g, 1.70 mmol) was dissolved in a 17.0 mL solution of

DCM/TFA (3:1, v/v, 0.1M) along with anisole (0.37 mL, 3.40 mmol). The reaction mixture was allowed to stir for 1 h, and then was concentrated *in vacuo* to give MeO-Phe-D-Phe-D-Val-NH_2 in a quantitative yield. This tripeptide was taken on to the next coupling step without any further purification or characterization.

Dipeptide MeO-Leu-Leu-NHBoc

Following the "**General solution-phase peptide synthesis**" procedure, a mixture of H-Leu-OMe•HCl (0.402 g, 2.21 mmol), Boc-Leu-OH•H_2O (0.500 g, 2.01 mmol), TBTU (0.774 g, 2.41 mmol), and DIPEA (1.40 mL, 8.02 mmol) were dissolved in 20.1 mL of anhydrous DCM (0.1M). The reaction was stirred for 1.5 h. The reaction mixture was diluted in ethyl acetate (100 mL) and subjected to the "**General acid-base work-up**" procedure. The organic layer was collected, dried over sodium sulfate, and concentrated *in vacuo* to give the pure dipeptide MeO-Leu-Leu-NHBoc as a white powder (89.4% yield). This dipeptide was taken on to the next coupling step without any further purification or characterization.

Rf: 0.57 (30% EA/Hex)

Dipeptide HO-Leu-Leu-NHBoc

Following the "**General solution-phase acid deprotection**" procedure, MeO-Leu-Leu-NHBoc (0.664 g, 1.85 mmol) and lithium hydroxide (0.621 g, 14.8 mmol) was dissolved in 18.5 mL of methanol (0.1M). The reaction mixture was allowed to stir for 3 h. The reaction was diluted in DCM (100 mL) and treated with pH 1 water (100 mL). After verifying that the aqueous layer remained acidic (pH ~3), the product was extracted with five washes of DCM (100 mL each). The organic layers were combined, dried over sodium sulfate, and concentrated in vacuo to give the pure dipeptide HO-Leu-Leu-

NHBoc (0.573 g, 89.7% yield). This dipeptide was taken on to the next coupling step without any further purification or characterization.

Pentapeptide MeO-Phe-D-Phe-D-Val-Leu-Leu-NHBoc

Following the "**General solution-phase peptide synthesis**" procedure, a mixture of Boc-Leu-Leu-OH (532 mg, 1.54 mmol), HATU (505 mg, 1.33 mmol), TBTU (346 mg, 1.08 mmol), and DIPEA (2.2 mL, 12.3 mmol) were dissolved in a 7.7 mL solution of anhydrous DCM. MeO-Phe-D-Phe-D-Val-NH_2 (1.37 g, 3.49 mmol) was dissolved in another 7.7 mL anhydrous DCM, and was added, by long-needle syringe, to the mixture containing the coupling reagents (0.1M final concentration). The reaction was stirred for 1 hour and was monitored by TLC. Upon completion, the reaction was then diluted in DCM (100 mL) and subjected to two aqueous washes of 10% HCl (100 mL each), two washes of sodium bicarbonate solution (100 mL, sat. aq.), and two washes of saturated sodium chloride (100 mL, sat. aq.). The organic layers were combined, dried over sodium sulfate, and concentrated *in vacuo*. Crude material was purified by flash column chromatography using an EA/Hex gradient solvent system where the product eluted at 75EA/25Hex. The pure pentapeptide (MeO-Phe-D-Phe-D-Val-Leu-Leu-NHBoc, 80.2% yield) was verified by NMR.

Rf: 0.55 (75% EA/Hex)

^{1}H NMR (400 MHz, CD_3OD): δ 0.67-0.86 (m, 6H), 0.90-1.00 (m, 12H), 1.42 (s, 9H), 1.49-1.75 (m, 4H), 1.90-2.02 (m, 1H), 2.03-2.14 (m, 1H), 2.74-2.80 (m, 1H), 2.90-3.00 (m, 2H), 3.01-3.14 (m, 2H), 3.67 (s, 3H), 3.96-4.18 (m, 2αH), 4.35-4.40 (m, αH), 4.54-4.67 (m, 2αH), 7.08-7.29 (m, 10H).

Linear pentapeptide HO-Phe-D-Phe-D-Val-Leu-Leu-NHBoc

Following the "**General solution-phase acid deprotection**" procedure, MeO-Phe-D-Phe-D-Val-Leu-Leu-NHBoc (931 mg, 1.24 mmol) and lithium hydroxide (415 mg, 9.89 mmol) was dissolved in 12.4 mL of methanol (0.1M). The reaction mixture was allowed to stir overnight. Completion was verified by TLC. The reaction was diluted in DCM (100 mL) and treated with pH 1 water (100 mL). After verifying that the aqueous layer remained acidic (pH ~1-3), the product was extracted with five washes of DCM (100 mL each). The organic layers were combined, dried over sodium sulfate, and concentrated *in vacuo* to give the linear pentapeptide HO-Phe-D-Phe-D-Val-Leu-Leu-NHBoc (98.0% yield). This pentapeptide was taken on to the next deprotection step without any further purification or characterization.

Double-deprotected linear pentapeptide HO-Phe-D-Phe-D-Val-Leu-Leu-NH_2

Following the "**General solution-phase amine deprotection**" procedure, HO-Phe-D-Phe-D-Val-Leu-Leu-NHBoc (904 mg, 1.22 mmol) was dissolved in a 12.2 mL solution of DCM/TFA (3:1, v/v, 0.1M), along with anisole (0.27 mL, 2.44 mmol). The reaction mixture was allowed to stir for 45 min, and then was concentrated *in vacuo* to give the double-deprotected linear pentapeptide HO-Phe-D-Phe-D-Val-Leu-Leu-NH_2 (quantitative yield), which was verified by LCMS.

LCMS: m/z called for $C_{35}H_{51}N_5O_6$ (M+1) = 638.38, found 638.4.

Macrocycle Phe-D-Phe-D-Val-Leu-Leu

Following the "**General macrocyclization procedure**", HO-Phe-D-Phe-D-Val-Leu-Leu-NH_2 (259 mg, 0.405 mmol), DEPBT (60.2 mg, 0.202 mmol), HATU (107.1 mg, 0.283 mmol), TBTU (64.9 mg, 0.202 mmol), and DIPEA (0.56 mL, 3.24 mmol) were dissolved in 4.05 mL of anhydrous ACN (0.1M). The reaction was allowed to stir for 1 h, and was

monitored by LCMS for the formation of cyclic pentapeptide and decapeptide. Upon completion, the ratio of cyclic pentapeptide to cyclic decapeptide products was approximately 1:1. The reaction was diluted in DCM (100 mL) and worked up with 2 washes of saturated ammonium chloride (100 mL each, sat. aq.) and back-extracted with DCM. The organic layers were collected, dried over sodium sulfate, and concentrated *in vacuo*. The products were initially purified by flash column chromatography using an EA/Hex gradient solvent system where the semi-pure mixture (1:1) of pentapeptide and decapeptide products eluted at 75EA. Further purification and separation was performed using RP-HPLC. Both the cyclic pentapeptide and decapeptide (67.1% combined yield) were analyzed by NMR, LCMS, and analytical HPLC.

Cyclized pentapeptide Rf: 0.34 (75% EA/Hex)

^{1}H NMR (400 MHz, CD_3OD): δ 0.8-1.0 (m, 24H), 1.2-1.4 (m, 3H), 1.5-1.7 (m, 6H), 2.9-3.1 (m, 1H), 3.2-3.4 (m, 1H), 3.6-3.8 (m, 1H), 4.0-4.1 (m, 1αH), 4.1-4.2 (m, 2αH), 4.2-4.4 (m, 1αH), 4.6-4.8 (m, 1αH), 7.2-7.4 (m, 5H).

LCMS: m/z calcd for $C_{35}H_{49}N_5O_5$ (M+1) = 620.37, found 621.0.

Cyclized decapeptide Rf: 0.56 (75% EA/Hex)

^{1}H NMR (600 MHz, CD_3OD): δ 0.68-1.00 (m, 36H), 1.52-1.84 (m, 12H), 2.02-2.13 (m, 2H), 2.85-2.98 (m, 4H), 3.01-3.11 (m, 2H), 3.12-3.16 (m, 2H), 3.97 (m, αH), 4.30-4.45 (m, 2αH), 4.52 (m, 2αH), 4.65 (m, 2αH), 7.02 (d, NH), 7.09-7.34 (m, 20H), 7.57 (d, NH), 7.72 (d, NH), 7.99 (d, NH), 8.25 (d, NH), 8.44 (d, NH).

LCMS: m/z calcd for $C_{70}H_{98}N_{10}O_{10}$ (M+1) = 1239.75, found 1240.8.

SYNTHESIS OF 13-T-III

Dipeptide Resin-Leu-*N*-Me-Lys(Boc)-NH_2

CTC-Leu-NH_2 resin (1.08 g, 0.874 mmol) was swelled in DMF for 30 min and drained. Then, following the "**General solid-phase peptide coupling**" procedure, the resin, Fmoc-*N*-Me-Lys-OH (0.50 g, 1.05 mmol), HOBt (0.40 g, 2.62 mmol), and DIC (0.81 mL, 5.24 mmol) were combined in 4.37 mL of DMF (0.2M, to the resin loading). The reaction was shaken overnight. Completion of the reaction was verified by ninhydrin test. The resin was washed three times with DMF and subjected to the "**General solid-phase amine deprotection**" procedure to give the resin-bound free-amine dipeptide in a quantitative yield.

Tripeptide Resin-Leu-*N*-Me-Lys(Boc)-D-Leu-NH_2

Following the "**General solid-phase peptide coupling**" procedure, Resin-Leu-*N*-Me-Lys(Boc)-NH_2 (0.874 mmol), Fmoc-D-Leu-OH (0.93 g, 2.62 mmol), HOAt (0.36 g, 2.62 mmol), and DIC (0.81 mL, 5.24 mmol) were combined in 4.37 mL of DMF (0.2M, to the resin loading). The reaction was shaken overnight. Completion of the reaction was verified by ninhydrin test. The resin was washed three times with DMF and subjected to the "**General solid-phase amine deprotection**" procedure to give the resin-bound free-amine tripeptide in a quantitative yield.

Tetrapeptide Resin-Leu-*N*-Me-Lys(Boc)-D-Leu-D-Phe-NH_2

Following the "**General solid-phase peptide coupling**" procedure, Resin-Leu-*N*-Me-Lys(Boc)-D-Leu-NH_2 (0.874 mmol), Fmoc-D-Phe-OH (1.01 g, 2.62 mmol), HOBt (0.40 g, 2.62 mmol), and DIC (0.81 mL, 5.24 mmol) were combined in 4.37 mL of DMF (0.2M, to the resin loading). The reaction was shaken overnight. Completion of the reaction was verified by ninhydrin test. The resin was washed three times with DMF and

subjected to the "**General solid-phase amine deprotection**" procedure to give the resin-bound free-amine tetrapeptide in a quantitative yield.

Pentapeptide Resin-Leu-*N*-Me-Lys(Boc)-D-Leu-D-Phe-[(2R,3R)/(2S,3S)-β-OH-Phe]-NH_2

Following the "**General solid-phase peptide coupling**" procedure, Resin-Leu-*N*-Me-Lys(Boc)-D-Leu-D-Phe-NH_2 (0.874 mmol), Fmoc-[(2R,3R)/(2S,3S)-β-OH-Phe]-OH (0.43 g, 1.06 mmol), HOBt (0.33 g, 2.16 mmol), and DIC (0.81 mL, 5.24 mmol) were combined in 3.50 mL of DMF (0.25M, to the resin loading). The reaction was shaken overnight. Completion of the reaction was verified by ninhydrin test. The resin was washed three times with DMF and subjected to the "**General solid-phase N-terminal amine deprotection**" procedure to give the resin-bound free-amine pentapeptide in a quantitative yield.

Double-deprotected pentapeptide HO-Leu-*N*-Me-Lys(Boc)-D-Leu-D-Phe-[(2R,3R)/(2S,3S)-β-OH-Phe]-NH_2

The linear peptide was cleaved from the resin following the "**Solid-phase cleaving from resin**" procedure. Resin-Leu-*N*-Me-Lys(Boc)-D-Leu-D-Phe-[(2R,3R)/(2S,3S)-β-OH-Phe]-NH_2 (1.45 g) was stirred in a 15 mL solution of TFE/DCM (1:1, v/v, 10 mL/g resin) for 24 h. The solution was filtered from the resin and concentrated *in vacuo* to give the DDLP (475.5 mg, 68.3% yield).

Macrocyclic pentapeptide [(2R,3R)/ (2S/3S)-β-OH-Phe]-Leu-*N*-Me-Lys(Boc)-D-Leu-D-Phe

Following the "**General macrocyclization (syringe pump) procedure**", HO-[(2R,3R)/(2S/3S)-β-OH-Phe]-Leu-*N*-Me-Lys(Boc)-D-Leu-D-Phe-NH_2 (190 mg, 0.238 mmol) was

dissolved in 17.0 mL of dry DCM and loaded into a syringe. In a round-bottom flask, DEPBT (50.0 mg, 0.167 mmol), HATU (63.0 mg, 0.167 mmol), TBTU (54.0 mg, 0.167 mmol), and DIPEA (0.165 mL, 0.950 mmol) were dissolved in 17 mL of anhydrous DCM. The peptide in the syringe was injected into the flask at a rate of 8mL/hour. After the first hour, additional DIPEA (0.165 mL, 0.950 mmol) was added. The final concentration of the reaction was 0.007M. The reaction was allowed to stir for 1 h after the addition of all of the peptide and was monitored by LCMS. Upon completion, the reaction was worked up with 2 washes of saturated ammonium chloride (150 mL each, sat. aq.) and back-extracted with DCM. The organic layers were collected, dried over sodium sulfate, and concentrated *in vacuo*. The pentapeptide was purified by flash column chromatography using an EA/Hex gradient solvent system where the pure product eluted at 100EA. The cyclized pentapeptide ([(2R,3R)/ (2S/3S)-β-OH-Phe]-Leu-*N*-Me-Lys(Boc)-D-Leu-D-Phe, 87.9% yield) was verified by NMR and LCMS.

LCMS: m/z calcd for $C_{42}H_{62}N_6O_8$ (M+1) = 779.46, found 779.0.

Benzylated macrocycle[(2R,3R)/(2S/3S)-β-OBn-Phe]-Leu-*N*-Me-Lys(Boc)-D-Leu-D-Phe

Following the general "**Benzylation**" procedure, cyclized [(2R,3R)/(2S/3S)-β-OH-Phe]-Leu-*N*-Me-Lys(Boc)-D-Leu-D-Phe (185 mg, 0.238 mmol) was dissolved in 2.38 mL of anhydrous THF (0.1M). NaH (23.0 mg, 0.952 mmol, 60% in mineral oil, w/w) was added and the reaction was subsequently re-purged with argon gas. After the addition of BnBr (0.11 mL, 0.952 mmol), the reaction was allowed to run for three hours and was checked by LCMS. Additional NaH (11.5 mg, 0.476 mmol) was added at three hours and the reaction proceeded to run overnight. Upon checking the reaction by LCMS,

additional BnBr (0.06 mL, 0.476 mmol) was added and the reaction ran overnight again. Upon completion, the reaction was diluted in DCM (50 mL), quenched with two DI water washes (50 mL each), dried over sodium sulfate, and concentrated *in vacuo*. The product (62.3% yield) was analyzed by LCMS and not subjected to further purification.

LCMS: m/z calcd for $C_{49}H_{68}N_6O_8$ (M+1) = 869.51, found 873.9.

Deprotected lysine macrocycle [(2R,3R)/(2S/3S)-β-OBn-Phe]-Leu-*N*-Me-Lys-D-Leu-D-Phe

Following the "**General solution-phase amine deprotection**" procedure, [(2R,3R)/(2S/3S)-β-OBn-Phe]-Leu-*N*-Me-Lys(Boc)-D-Leu-D-Phe (126.8 mg, 0.148 mmol) was dissolved in a 1.5 mL solution of DCM/TFA (3:1, v/v, 0.1M), along with anisole (0.03 mL, 0.296 mmol). The reaction was allowed to run for 45 minutes. Completion was verified by LCMS and the reaction was concentrated *in vacuo* to give the free lysine-containing macrocycle in a quantitative yield. This product was taken on to the tagging step without any further purification or characterization.

SYNTHESIS OF 13-T-III-PEG-BIOTIN

[(2R,3R)/ (2S/3S)-β-OBn-Phe]-Leu-N-Me-Lys(Peg-biotin)-D-Leu-D-Phe

Following the "**General coupling of PEG$_4$-biotin**" procedure, cyclized [(2R,3R)/(2S/3S)-β-OBn-Phe]-Leu-*N*-Me-Lys-D-Leu-D-Phe (9.0 mg, 0.012 mmol), NHS-PEG$_4$-biotin (8.2 mg, 0.014 mmol), and DIPEA (0.016 mL, 0.094 mmol) were dissolved in 0.12 mL of DCM (0.1M). The reaction was allowed to run overnight. Upon completion, the reaction was concentrated *in vacuo*, and purified via RP-HPLC to give the biotinylated compound (29.7% yield).

LCMS: m/z calcd for $C_{65}H_{95}N_9O_{13}S$ (M+1) = 1242.68, found 1244.1.

SYNTHESIS OF 13-T-III-FLUORESCEIN

[(2R,3R)/ (2S/3S)-β-OBn-Phe]-Leu-*N*-Me-Lys(Fluorescein)-D-Leu-D-Phe

Following the "**General coupling of fluorescein**" procedure, cyclized [(2R,3R)/(2S/3S)-β-OBn-Phe]-Leu-*N*-Me-Lys-D-Leu-D-Phe (9.9 mg, 0.0123 mmol), NHS-fluorescein (10.5 mg, 0.0221 mmol), and DIPEA (0.017 mL, 0.0984 mmol) were dissolved in 0.12 mL of DCM (0.1M). The reaction was allowed to run for 3 h. The crude reaction was concentrated *in vacuo* and purified via RP-HPLC to give the tagged peptide (44.8% yield).

LCMS: m/z calcd for $C_{65}H_{70}N_6O_{12}$ (M+1) = 1127.51, found 1127.5 .

SYNTHESIS OF 1-T-III-PEG-BIOTIN

Following the "**General coupling of PEG_4-biotin**" procedure, cyclized Phe-Leu-Lys-Leu-Leu (9.9 mg, 0.0161 mmol), NHS-PEG_4-biotin (9.0 mg, 0.0153 mmol), and DIPEA (0.07 mL, 0.0405 mmol) were dissolved in 0.15 mL of DCM (0.1M). The reaction was allowed to run overnight. Upon completion, the reaction was concentrated *in vacuo*, and purified via RP-HPLC to give the biotinylated compound (87.3% yield).

LCMS: m/z calcd for $C_{54}H_{89}N_9O_{12}S$ (M+1) = 1088.6, found 1088.6.

SYNTHESIS OF 12-T-I-PEG-BIOTIN

Following the "**General coupling of PEG_4-biotin**" procedure, cyclized Lys-*N*-Me-D-Phe-Val-Leu-Lys(Cbz) (9.5 mg, 0.0124 mmol), NHS-PEG_4-biotin (8.8 mg, 0.0149 mmol), and DIPEA (0.02 mL, 0.0995 mmol) were dissolved in 0.12 mL of DCM (0.1M). The reaction was allowed to run overnight. Upon completion, the reaction was concentrated *in vacuo*, and purified via RP-HPLC to give the biotinylated compound (74.8% yield).

^{1}H NMR (400 MHz, CD_3OD): δ 0.8-1.0 (m, 12H), 1.0-1.2 (m, 2H), 1.3-1.8 (m, 21H), 2.0-2.1 (m, 2H), 2.2 (t, 2H), 2.4 (t, 2H), 2.7 (t, 1H), 2.9 (m, 1H), 3.1 (s, 3H), 3.1-3.2 (m, 7H), 3.5-3.8 (m, 12H), 3.9 (m, 1H), 4.1-4.2 (m, 2H), 4.3 (m, αH), 4.5 (m, 2αH), 5.1 (s, 2H), 5.2 (t, 1H), 7.2-7.4 (m, 10H), 7.8 (d, 1H), 7.9 (d, 1H), 8.0 (d, 1H), 8.3 (d, 1H).

LCMS: m/z calcd for $C_{62}H_{96}N_{10}O_{14}S$ (M+1) = 1237.68, found 1238.2.

SYNTHESIS OF 12-T-III-PEG-BIOTIN

Following the "**General coupling of PEG_4-biotin**" procedure, cyclized Phe-*N*-Me-D-Phe-Lys-Leu-Lys(Cbz) (10.5 mg, 0.0129 mmol), NHS-PEG_4-biotin (9.1 mg, 0.0155 mmol), and DIPEA (0.02 mL, 0.103 mmol) were dissolved in 0.13 mL of DCM (0.1M). Additional NHS-PEG-biotin (4.0 mg, 0.00679 mmol) was added after 4 h and the reaction was allowed to continue overnight. Upon completion, the reaction was concentrated *in vacuo*, and purified via RP-HPLC to give the pure biotinylated compound Phe-*N*-Me-D-Phe-Lys(Peg-biotin)-Leu-Lys(Cbz) (90.6% yield).

^{1}H NMR (400 MHz, CD_3OD): δ 0.8-1.0 (m, 6H), 1.3-1.8 (m, 21H), 2.2 (t, 2H), 2.4 (t, 2H), 2.7 (t, 1H), 2.8 (s, 3H), 2.9-3.0 (m, 2H), 3.1-3.2 (m, 2H), 3.2 (m, 1H), 3.4 (m, 2H), 3.5 (m, 2H), 3.6 (s, 12H), 3.7 (m, 2H), 4.2 (m, αH), 4.3 (m, αH), 4.5 (m, αH), 4.6-4.7 (m, 2H), 5.1 (s, 2H), 5.2 (t, 1H), 7.2-7.4 (m, 15H), 7.4 (d, 1H), 7.9 (d, 1H), 8.1 (d, 1H), 8.4 (d, 1H).

LCMS: m/z calcd for $C_{66}H_{96}N_{10}O_{14}S$ (M+1) = 1284.68, found 1285.8.

SYNTHESIS OF 13-T-I-PEG-BIOTIN

Following the "**General coupling of PEG_4-biotin**" procedure, cyclized [(2R,3R)-β-OH-Phe]-Leu-*N*-Me-Val-D-Leu-D-Phe (7.0 mg, 0.0108 mmol), NHS-PEG_4-biotin (7.6 mg, 0.0129 mmol), and DIPEA (0.015 mL, 0.0864 mmol) were dissolved in 0.11 mL of DCM

(0.1M). Additional NHS-PEG-biotin (7.6 mg, 0.0108 mmol) and DIPEA (4 equivalents) was added over the course of two weeks. The reaction could not be pushed to completion, less than 5% product formed and 95% starting material remained. The reaction was concentrated *in vacuo*, and the product and starting material were separated via RP-HPLC. The pure biotinylated compound [(2R,3R)-β-OPeg-biotin-Phe]-Leu-*N*-Me-Val-D-Leu-D-Phe (4.1% yield).

LCMS: m/z calcd for $C_{57}H_{86}N_8O_{13}S$ (M+1) = 1123.6, found 1124.6.

SYNTHESIS OF 13-T-II-PEG-BIOTIN

Following the "**General coupling of PEG_4-biotin**" procedure, cyclized [(2R,3R)/ (2S,3S)-β-OBn-Phe]-Lys-*N*-Me-Val-D-Leu-D-Phe (6.3 mg, 8.34 μmol), NHS-PEG_4-biotin (5.9 mg, 0.0100 mmol), and DIPEA (0.011 mL, 0.0667 mmol) were dissolved in 0.083 mL of DCM (0.1M). The reaction was allowed to run overnight. Upon completion, the reaction was concentrated *in vacuo* and purified by RP-HPLC. The pure biotinylated compound [(2R,3R)/ (2S/3S)-β-OBn-Phe]-Lys(Peg-biotin)-*N*-Me-Val-D-Leu-D-Phe (85.5% yield).

^{1}H NMR (400 MHz, CD_3OD): δ 0.8-1.0 (m, 12H), 1.3-1.4 (m, 4H), 1.4-1.8 (m, 11H), 2.2 (t, 2H), 2.4 (t, 2H), 2.8 (s, 3H), 2.9 (m, 2H), 3.2 (m, 5H), 3.4 (m, 2H), 3.5 (m, 2H), 3.6 (s, 12H), 3.7 (m, 2H), 4.2-4.5 (m, 4αH), 4.7 (m, 4H), 6.8 (m, 2H), 7.2-7.4 (m, 15H), 7.8 (d, 1H), 8.0 (d, 1H), 8.2 (d, 1H), 8.3 (d, 1H).

LCMS: m/z calcd for $C_{64}H_{93}N_9O_{13}S$ (M+1) = 1228.7, found 1228.7+23.

SYNTHESIS OF 1-T-II-FLUORESCEIN

Following the "**General coupling of fluorescein**" procedure, cyclized Phe-Lys-Val-Leu-Leu (8.0 mg, 0.0133 mmol), NHS-fluorescein (11.0 mg, 0.0239 mmol), and DIPEA

(0.018 mL, 0.106 mmol) were dissolved in 0.13 mL of DCM (0.1M). To improve solubility, and addition 0.2 mL was added. The reaction was allowed to run for 3 h. The crude reaction was concentrated *in vacuo*, re-dissolved in 33% DMSO/67% ACN and purified via RP-HPLC to give the tagged peptide Phe-Lys(Fluor)-Val-Leu-Leu (46.1% yield).

^{1}H NMR (400 MHz, $(CD_3)_2CO$): δ 0.8-1.0 (m, 18H), 1.2-1.4 (m, 4H), 1.5 (m, 2H), 1.6 (m, 6H), 2.0 (solvent peak), 3.0 (5H, under residual H_2O peak), 4.2 (m, 2αH), 4.5 (m, 2αH), 4.6 (1αH), 6.6-6.8 (m, 6H), 7.2-7.4 (m, 5H), 7.7 (s, 1H), 7.8 (1H), 7.9 (1H), 8.0 (d, 1H), 8.2 (d, 1H).

LCMS: m/z called for $C_{53}H_{62}N_6O_{11}$ (M+1) = 959.4, found 959.0.

SYNTHESIS OF 1-T-III-FLUORESCEIN

Following the "**General coupling of fluorescein**" procedure, cyclized Phe-Leu-Lys-Leu-Leu (10.4 mg, 0.0169 mmol), NHS-fluorescein (12.0 mg, 0.0254 mmol), and DIPEA (0.042 mL, 0.135 mmol) were dissolved in 0.17 mL of DCM (0.1M). The reaction was allowed to run overnight. The crude reaction was concentrated *in vacuo*, re-dissolved in 1.2 mL 50% DMSO/50% ACN, and purified via RP-HPLC to give the tagged peptide Phe-Leu-Lys(Fluor)-Leu-Leu (44.8% yield).

^{1}H NMR (400 MHz, $(CD_3)_2CO$): δ 0.8-1.0 (m, 18H), 1.2-1.4 (m, 4H), 1.5 (m, 2H), 1.6 (m, 6H), 2.0 (solvent peak), 3.3 (m, 2H), 3.5 (m, 2H), 4.3 (m, 2αH), 4.5 (m, 2αH), 4.7 (1αH), 6.6-6.8 (m, 6H), 7.2-7.4 (m, 5H), 7.8-7.9 (m, 4H), 8.0 (1H), 8.2 (1H), 8.3 (d, 1H), 8.4 (d, 1H), 8.5 (s, 1H).

LCMS: m/z called for $C_{54}H_{64}N_6O_{11}$ (M+1) = 973.5, found 973.4.

SYNTHESIS OF 1-T-IV-FLUORESCEIN

Following the "**General coupling of fluorescein**" procedure, cyclized Phe-Leu-Val-Lys-Leu (12.0 mg, 0.0200 mmol), NHS-fluorescein (14.0 mg, 0.0300 mmol), and DIPEA (0.03 mL, 0.16 mmol) were dissolved in 0.20 mL of DCM (0.1M). The reaction was allowed to run overnight. The crude reaction was concentrated *in vacuo*, re-dissolved in 1.2 mL 50% DMSO/50% ACN, and purified via RP-HPLC to give the tagged peptide Phe-Leu-Val-Lys(Fluor)-Leu (82.4% yield).

^{1}H NMR (400 MHz, $(CD_3)_2CO$): δ 0.8-1.0 (m, 18H), 1.1-1.2 (m, 4H), 1.5-1.8 (m, 8H), 2.0 (solvent peak), 2.5 (m, 2H), 3.1 (dd, 1H), 3.2 (m, 2H), 4.2 (αH), 4.5 (2αH), 4.7 (αH), 5.1 (αH), 6.6-6.8 (m, 5H), 7.2-7.4 (m, 5H), 7.7 (d, 2H), 7.9 (2H), 8.1 (1H), 8.2 (1H), 8.4 (d, 1H), 8.5 (1H).

LCMS: m/z called for $C_{53}H_{62}N_6O_{11}$ (M+1) = 959.4, found 959.7.

SYNTHESIS OF 12-T-I-FLUORESCEIN

Following the "**General coupling of fluorescein**" procedure, cyclized Lys-*N*-Me-D-Phe-Val-Leu-Lys(Cbz) (16.0 mg, 0.0209 mmol), NHS-fluorescein (20.0 mg, 0.0419 mmol), and DIPEA (0.03 mL, 0.167 mmol) were dissolved in 0.21 mL of DCM (0.1M). The reaction was allowed to run for 5 h. The crude reaction was concentrated *in vacuo*, re-dissolved in 1.2 mL 50% DMSO/50% ACN and purified via RP-HPLC to give the tagged peptide Lys(Fluor)-*N*-Me-D-Phe-Val-Leu-Lys(Cbz) (75.4% yield).

^{1}H NMR (400 MHz, $(CD_3)_2CO$): δ 0.6-0.7 (m, 3H), 0.8-1.0 (m, 9H), 1.2 (s, 1H), 1.3-1.6 (m, 8H), 1.6-1.9 (m, 7H), 2.1 (solvent peak), 2.6 (m, 1H), 2.8 (s, 3H), 2.9 (m, 2H), 3.1 (m, 5H), 3.5 (m, 2H), 4.1 (αH), 4.2 (αH), 4.4 (2αH), 5.0 (s, 2H), 5.2 (m, 1H), 6.4 (br, 1H),

6.6-6.7 (dd, 4H), 6.8 (d, 2H), 7.1-7.4 (m, 10H), 7.5 (d, 1NH), 7.8 (d, 1H), 7.9 (dd, 2H), 8.1 (d, 1H), 8.2 (1H), 8.3 (d, 1H), 8.5 (s, 1H).

LCMS: m/z called for $C_{62}H_{71}N_7O_{13}$ (M+1) = 1122.5, found 1121.9.

SYNTHESIS OF 12-T-III-FLUORESCEIN

Following the "**General coupling of fluorescein**" procedure, cyclized Phe-*N*-Me-D-Phe-Lys-Leu-Lys(Cbz) (7.0 mg, 0.00862 mmol), NHS-fluorescein (8.2 mg, 0.0172 mmol), and DIPEA (0.012 mL, 0.0690 mmol) were dissolved in 0.086 mL of DCM (0.1M). The reaction was allowed to run overnight. Upon completion, the reaction was diluted to a total of 1.5 mL DCM, and subjected to 1.2 mL pH 1 aqueous wash. The organic layer was concentrated *in vacuo* to give the pure tagged peptide Phe-*N*-Me-D-Phe-Lys(Fluor)-Leu-Lys(Cbz) (71.3% yield).

LCMS: m/z called for $C_{66}H_{71}N_7O_{13}$ (M+1) = 1170.5, found 1171.5.

SYNTHESIS OF 12-T-IV-FLUORESCEIN

Following the "**General coupling of fluorescein**" procedure, cyclized Phe-*N*-Me-D-Phe-Val-Lys-Lys(Cbz) (8.3 mg, 0.0104 mmol), NHS-fluorescein (5.9 mg, 0.0125 mmol), and DIPEA (0.014 mL, 0.0832 mmol) were dissolved in 0.02 mL of DCM (0.05M). The reaction was allowed to run overnight. Upon completion, the crude reaction was concentrated *in vacuo* and purified by RP-HPLC to give the pure tagged peptide Phe-*N*-Me-D-Phe-Val-Lys(Fluor)-Lys(Cbz) (58.7% yield).

^{1}H NMR (400 MHz, $(CD_3)_2CO$): δ 0.6 (m, 2H), 0.8-0.9 (m, 4H), 1.2-1.4 (m, 4H), 1.4-1.6 (m, 4H), 1.6-1.8 (m, 4H), 2.0 (solvent peak), 2.6 (s, 3H), 2.8 (m, 3H), 3.0-3.1 (m, 2H), 3.4 (m, 2H), 4.3 (2αH), 4.7 (2αH), 5.0 (s, 2H), 5.3 (m, 1H), 6.6-6.8 (m, 6H), 7.1-7.4 (m, 15H), 7.7 (1H), 8.0 (d, 2H), 8.2 (m, 1H), 8.4 (d, 1H), 8.5 (s, 1H).

LCMS: m/z called for $C_{65}H_{59}N_7O_{13}$ (M+1) = 1156.5, found 1155.9.

SYNTHESIS OF 13-T-II-FLUORESCEIN

Following the "**General coupling of fluorescein**" procedure, cyclized [(2R,3R)/ (2S/3S)-β-OBn-Phe]-Lys-*N*-Me-Val-D-Leu-D-Phe (6.3 mg, 8.34 μmol), NHS-fluorescein (5.9 mg, 0.0125 mmol), and DIPEA (0.011 mL, 0.0667 mmol) were dissolved in 0.083 mL of DCM (0.1M). The reaction was allowed to run overnight. Upon completion, the reaction was concentrated *in vacuo* and purified by RP-HPLC. The pure fluorescein-tagged compound [(2R,3R)/ (2S/3S)-β-OBn-Phe]-Lys(Fluor)-*N*-Me-Val-D-Leu-D-Phe was verified by LCMS (47.2% yield).

SYNTHESIS OF CHAPTER 5 DERIVATIVES

SYNTHESIS OF DI-SANA 17

Dipeptide Resin-Leu-Val-NH_2

CTC-Leu-NH_2 resin (2.10 g, 1.70 mmol) was swelled in DMF for 30 min and drained. Then, following the "**General solid-phase peptide coupling**" procedure, the resin, Fmoc-Val-OH (1.73 g, 5.10 mmol), HOBt (0.78 g, 5.10 mmol), and DIC (1.6 mL, 10.2 mmol) were combined in 8.50 mL of DMF (0.2M, to the resin loading). The reaction was shaken for 2 h. Completion of the reaction was verified by ninhydrin test. The resin was washed three times with DMF and subjected to the "**General solid-phase amine deprotection**" procedure to give the resin-bound free-amine dipeptide in a quantitative yield. This dipeptide was synthesized for both 17 and 20; it was split in half after this step.

Tripeptide Resin-Leu-Val-Leu-NH_2

Following the "**General solid-phase peptide coupling**" procedure, the Resin-Leu-Val-NH_2 (0.850 mmol), Fmoc-Leu-OH (0.90 g, 2.55 mmol), HOBt (0.39 g, 2.55 mmol), and DIC (0.79 mL, 5.10 mmol) were combined in 4.25 mL of DMF (0.2M, to the resin loading). The reaction was shaken for 2 h. Completion of the reaction was verified by ninhydrin test. The resin was washed three times with DMF and subjected to the "**General solid-phase amine deprotection**" procedure to give the resin-bound free-amine tripeptide in a quantitative yield.

Tetrapeptide Resin-Leu-Val-Leu-Leu-NH_2

Following the "**General solid-phase peptide coupling**" procedure, the Resin-Leu-Val-Leu-NH_2 (0.850 mmol), Fmoc-Leu-OH (0.90 g, 2.55 mmol), HOBt (0.39 g, 2.55 mmol), and DIC (0.79 mL, 5.10 mmol) were combined in 4.25 mL of DMF (0.2M, to the resin loading). The reaction was shaken overnight. Upon completion, the resin was washed three times with DMF and subjected to the "**General solid-phase amine deprotection**" procedure to give the resin-bound free-amine tetrapeptide in a quantitative yield.

Pentapeptide Resin-Leu-Val-Leu-Leu-D-Phe-NH_2

Following the "**General solid-phase peptide coupling**" procedure, the Resin-Leu-Val-Leu-Leu-NH_2 (0.850 mmol), Fmoc-D-Phe-OH (0.99 g, 2.55 mmol), HOBt (0.39 g, 2.55 mmol), and DIC (0.79 mL, 5.10 mmol) were combined in 4.25 mL of DMF (0.2M, to the resin loading). The reaction was shaken for 4 h. Completion was verified by ninhydrin test. The resin was washed three times with DMF and subjected to the "**General solid-phase N-terminal amine deprotection**" procedure to give the resin-bound free-amine tetrapeptide in a quantitative yield. The resin dried *in vacuo* overnight.

Double-deprotected pentapeptide HO-Leu-Val-Leu-Leu-D-Phe-NH_2

The linear peptide was cleaved from the resin following the "**Solid-phase cleaving from resin**" procedure. Resin-Leu-Val-Leu-Leu-D-Phe-NH_2 (1.30 g) was stirred in a 13 mL solution of TFE/DCM (1:1, v/v, 10 mL/g resin) for 24 h. The solution was filtered from the resin and concentrated *in vacuo* to give the DDLP (0.201 g, 39.2% yield).

Cyclized decapeptide D-Phe-Leu-Val-Leu-Leu-D-Phe-Leu-Val-Leu-Leu

Following the "**Macrocyclization**" procedure, DDLP HO-Leu-Val-Leu-Leu-D-Phe-NH_2 (180 mg, 0.298 mmol), DEPBT (44 mg, 0.149 mmol), HATU (79 mg, 0.209 mmol), TBTU (47 mg, 0.149 mmol), and DIPEA (0.42 mL, 2.38 mmol) were dissolved in 2.98 mL of anhydrous DMF (0.1M). The reaction was stirred for 1.5 h and was monitored by LCMS and TLC. Upon completion, the reaction was diluted in 50 mL of EA and quenched with a pH 1 aqueous wash (50 mL) and two washes of brine (50 mL each). The organic layers were combined, dried over sodium sulfate, and concentrated *in vacuo*. The crude material was initially purified by flash column chromatography using an EA/Hex gradient solvent system. Semi-pure decapeptide eluted at 75EA/25Hex and was further purified by RP-HPLC to give the cyclized decapeptide (18.3% yield).

Rf: 0.42 (65% EA/Hex)

^{1}H NMR (600 MHz, CD_3OD): δ 0.62 (d, 6H), 0.70 (d, 6H), 0.88-0.96 (m, 36H), 1.24-1.35 (m, 3H), 1.48-1.73 (m, 13H), 1.78-1.85 (m, 2H), 1.92-2.00 (m, 2H), 2.96-3.00 (m, 4H), 4.14-4.22 (m, 2αH), 4.37-4.48 (m, 4αH), 4.56-4.67 (m, 4αH), 7.09-7.19 (m, 10H), 8.05-8.14 (m, 4 N<u>H</u>), 8.35 (d, 2 N<u>H</u>), 8.58 (d, 2 N<u>H</u>), 8.84 (d, 2 N<u>H</u>).

LCMS: m/z called for $C_{64}H_{102}N_{10}O_{10}$ (M+1) = 1171.78, found 1194.8 (+23).

SYNTHESIS OF DI-SANA 18

Dipeptide Resin-Leu-Leu-NH_2

CTC-Leu-NH_2 resin (1.05 g, 0.850 mmol) was swelled in DMF for 30 min and drained. Then, following the "**General solid-phase peptide coupling**" procedure, the resin, Fmoc-Leu-OH (0.90 g, 2.55 mmol), HOBt (0.39 g, 2.55 mmol), and DIC (0.79 mL, 5.10 mmol) were combined in 4.25 mL of DMF (0.2M, to the resin loading). The reaction was shaken for 2 h. Completion of the reaction was verified by ninhydrin test. The resin was washed three times with DMF and subjected to the "**General solid-phase amine deprotection**" procedure to give the resin-bound free-amine dipeptide in a quantitative yield.

Tripeptide Resin-Leu-Leu-Phe-NH_2

Following the "**General solid-phase peptide coupling**" procedure, Resin-Leu-Leu-NH_2 (0.850 mmol), Fmoc-Phe-OH (0.99 g, 2.55 mmol), HOBt (0.39 g, 2.55 mmol), and DIC (0.79 mL, 5.10 mmol) were combined in 4.25 mL of DMF (0.2M, to the resin loading). The reaction was shaken for 2 h. Completion of the reaction was verified by ninhydrin test. The resin was washed three times with DMF and subjected to the "**General solid-phase amine deprotection**" procedure to give the resin-bound free-amine tripeptide in a quantitative yield.

Tetrapeptide Resin-Leu-Leu-Phe-D-Leu-NH_2

Following the "**General solid-phase peptide coupling**" procedure, Resin-Leu-Leu-Phe-NH_2 (0.850 mmol), Fmoc-D-Leu-OH (0.90 g, 2.55 mmol), HOBt (0.39 g, 2.55 mmol), and DIC (0.79 mL, 5.10 mmol) were combined in 4.25 mL of DMF (0.2M, to the resin loading). The reaction was shaken overnight. Upon completion, the resin was washed three times with DMF and subjected to the "**General solid-phase amine deprotection**" procedure to give the resin-bound free-amine tetrapeptide in a quantitative yield.

Pentapeptide Resin-Leu-Leu-Phe-D-Leu-Val-NH_2

Following the "**General solid-phase peptide coupling**" procedure, Resin-Leu-Leu-Phe-D-Leu-NH_2 (0.850 mmol), Fmoc-D-Leu-OH (0.90 g, 2.55 mmol), HOBt (0.39 g, 2.55 mmol), and DIC (0.79 mL, 5.10 mmol) were combined in 4.25 mL of DMF (0.2M, to the resin loading). The reaction was shaken for 4 h. Completion was verified by ninhydrin test. The resin was washed three times with DMF and subjected to the "**General solid-phase N-terminal amine deprotection**" procedure to give the resin-bound free-amine pentapeptide in a quantitative yield. The resin was dried *in vacuo* overnight.

Double-deprotected pentapeptide HO-Leu-Leu-Phe-D-Leu-Val-NH_2

The linear peptide was cleaved from the resin following the "**Solid-phase cleaving from resin**" procedure. Resin-Leu-Leu-Phe-D-Leu-Val-NH_2 (1.30 g) was stirred in a 13 mL solution of TFE/DCM (1:1, v/v, 10 mL/g resin) for 24 h. The solution was filtered from the resin and concentrated *in vacuo* to give the DDLP (0.455 g, 88.6% yield).

Cyclized decapeptide Phe-D-Leu-Val-Leu-Leu-Phe-D-Leu-Val-Leu-Leu

Following the "**Macrocyclization**" procedure, DDLP HO-Leu-Leu-Phe-D-Leu-Val-NH_2 (202 mg, 0.334 mmol), DEPBT (49 mg, 0.167 mmol), HATU (89 mg, 0.233 mmol), TBTU (54 mg, 0.167 mmol), and DIPEA (0.46 mL, 2.67 mmol) were dissolved in 3.34 mL of anhydrous DMF (0.1M). The reaction was stirred for 1 h and was monitored by LCMS. Upon completion, the reaction was diluted in 50 mL of DCM and quenched with a pH 1 aqueous wash (50 mL), a saturated sodium bicarbonate wash (50 mL), and one wash of brine (50 mL). The organic layers were combined, dried over sodium sulfate, and concentrated *in vacuo*. The crude material was initially purified by flash column chromatography using an EA/Hex gradient solvent system. A 1:1 mixture of

pentapeptide and decapeptide eluted at 75% EA/Hex and the two were separated by RP-HPLC to give the pure cyclized decapeptide (53.3% yield).

Rf: 0.50 (70% EA/Hex)

^{1}H NMR (600 MHz, CD_3OD): δ 0.72 (d, 6H), 0.79-0.98 (m, 42H), 1.20-1.27 (m, 2H), 1.29-1.39 (m, 4H), 1.33-1.41 (m, 6H), 1.65-1.71 (m, 2H), 1.72-1.83 (m, 4H), 2.04-2.10 (m, 2H), 2.64-2.70 (m, 2H), 3.46-3.52 (m, 2H), 4.00-4.04 (m, 2αH), 4.05-4.11 (m, 2αH), 4.60-4.66 (m, 2αH), 4.73-4.79 (m, 2αH), 4.80-4.88 (m, 2αH), 7.18-7.21 (m, 2H), 7.22-7.28 (m, 2H), 8.14 (d, 2 NH), 8.20 (d, 2 NH), 8.26 (d, 2 NH), 8.55 (d, 2 NH).

LCMS: m/z called for $C_{64}H_{102}N_{10}O_{10}$ (M+1) = 1171.78, found 1174.2.

SYNTHESIS OF DI-SANA 20

Dipeptide Resin-Leu-Val-NH_2

The synthesis of this dipeptide can be found under "Synthesis of Di-SanA 17."

Tripeptide Resin-Leu-Val-D-Leu-NH_2

Following the "**General solid-phase peptide coupling**" procedure, the Resin-Leu-Val-NH_2 (0.850 mmol), Fmoc-D-Leu-OH (0.90 g, 2.55 mmol), HOBt (0.39 g, 2.55 mmol), and DIC (0.79 mL, 5.10 mmol) were combined in 4.25 mL of DMF (0.2M, to the resin loading). The reaction was shaken for 2 h. Completion of the reaction was verified by ninhydrin test. The resin was washed three times with DMF and subjected to the "**General solid-phase amine deprotection**" procedure to give the resin-bound free-amine tripeptide in a quantitative yield.

Tetrapeptide Resin-Leu-Val-D-Leu-Leu-NH_2

Following the "**General solid-phase peptide coupling**" procedure, the Resin-Leu-Val-Leu-NH_2 (0.850 mmol), Fmoc-Leu-OH (0.90 g, 2.55 mmol), HOBt (0.39 g, 2.55 mmol),

and DIC (0.79 mL, 5.10 mmol) were combined in 4.25 mL of DMF (0.2M, to the resin loading). The reaction was shaken overnight. Upon completion, the resin was washed three times with DMF and subjected to the "**General solid-phase amine deprotection**" procedure to give the resin-bound free-amine tetrapeptide in a quantitative yield.

Pentapeptide Resin-Leu-Val-D-Leu-Leu-Phe-NH_2

Following the "**General solid-phase peptide coupling**" procedure, the Resin-Leu-Val-D-Leu-Leu-NH_2 (0.850 mmol), Fmoc-Phe-OH (0.99 g, 2.55 mmol), HOBt (0.39 g, 2.55 mmol), and DIC (0.79 mL, 5.10 mmol) were combined in 4.25 mL of DMF (0.2M, to the resin loading). The reaction was shaken for 4 h. Completion was verified by ninhydrin test. The resin was washed three times with DMF and subjected to the "**General solid-phase N-terminal amine deprotection**" procedure to give the resin-bound free-amine tetrapeptide in a quantitative yield. The resin dried *in vacuo* overnight.

Double-deprotected pentapeptide HO-Leu-Val-D-Leu-Leu-Phe-NH_2

The linear peptide was cleaved from the resin following the "**Solid-phase cleaving from resin**" procedure. Resin-Leu-Val-D-Leu-Leu-Phe-NH_2 (1.23 g) was stirred in a 12 mL solution of TFE/DCM (1:1, v/v, 10 mL/g resin) for 24 h. The solution was filtered from the resin and concentrated *in vacuo* to give the DDLP (0.382 g, 74.5% yield).

Cyclized decapeptide Phe-Leu-Val-D-Leu-Leu-Phe-Leu-Val-D-Leu-Leu

Following the "**Macrocyclization**" procedure, DDLP HO-Leu-Val-D-Leu-Leu-Phe-NH_2 (207 mg, 0.343 mmol), DEPBT (51 mg, 0.171 mmol), HATU (91 mg, 0.240 mmol), TBTU (55 mg, 0.171 mmol), and DIPEA (0.48 mL, 2.74 mmol) were dissolved in 3.43 mL of anhydrous DMF (0.1M). The reaction was stirred for 1 h and was monitored by TLC. Upon completion, the reaction was diluted in 50 mL of DCM and quenched with a

pH 1 aqueous wash (50 mL), a saturated sodium bicarbonate wash (50 mL), and one wash of brine (50 mL). The organic layers were combined, dried over sodium sulfate, and concentrated *in vacuo*. The crude material was initially purified by flash column chromatography using an EA/Hex gradient solvent system. Semi-pure decapeptide eluted at 75% EA/Hex and was further purified by RP-HPLC to give the pure cyclized decapeptide (42.8% yield).

Rf: 0.53 (75% EA/Hex)

^{1}H NMR (400 MHz, CD_3OD): δ 0.85-1.01 (m, 48H), 1.40-1.64 (m, 14H), 1.65-1.80 (m, 2H), 1.80-1.93 (m, 2H), 2.43-2.58 (m, 2H), 2.70-2.78 (m, 2H), 2.91-2.97 (m, 2H), 4.32-4.43 (m, 6αH), 4.57-4.63 (m, 2αH), 6.95-7.12 (m, 10H), 7.90 (d, 2 N<u>H</u>), 8.20 (m, 5 N<u>H</u>), 8.56 (d, 2 N<u>H</u>).

LCMS: m/z called for $C_{64}H_{102}N_{10}O_{10}$ (M+1) = 1171.78, found 1174.4.

SYNTHESIS OF DI-SANA 21

Dipeptide Resin-D-Phe-D-Leu-NH_2

CTC-D-Phe-NH_2 resin (1.35 g, 0.972 mmol) was swelled in DMF for 30 min and drained. Then, following the "**General solid-phase peptide coupling**" procedure, the resin, Fmoc-D-Leu-OH (1.03 g, 2.92 mmol), HOBt (0.45 g, 2.92 mmol), and DIC (0.90 mL, 5.83 mmol) were combined in 4.86 mL of DMF (0.2M, to the resin loading). The reaction was shaken for 2 h. Completion of the reaction was verified by ninhydrin test. The resin was washed three times with DMF and subjected to the "**General solid-phase amine deprotection**" procedure to give the resin-bound free-amine dipeptide in a quantitative yield.

Tripeptide Resin-D-Phe-D-Leu-D-Val-NH_2

Following the "**General solid-phase peptide coupling**" procedure, Resin-D-Phe-D-Leu-NH_2 (0.972 mmol), Fmoc-D-Val-OH (0.99 g, 2.92 mmol), HOBt (0.45 g, 2.92 mmol), and DIC (0.90 mL, 5.83 mmol) were combined in 4.86 mL of DMF (0.2M, to the resin loading). The reaction was shaken for 2 h. Completion of the reaction was verified by ninhydrin test. The resin was washed three times with DMF and subjected to the "**General solid-phase amine deprotection**" procedure to give the resin-bound free-amine tripeptide in a quantitative yield.

Tetrapeptide Resin-D-Phe-D-Leu-D-Val-Leu-NH_2

Following the "**General solid-phase peptide coupling**" procedure, Resin-D-Phe-D-Leu-D-Val-NH_2 (0.972 mmol), Fmoc-Leu-OH (1.03 g, 2.92 mmol), HOBt (0.45 g, 2.92 mmol), and DIC (0.90 mL, 5.83 mmol) were combined in 4.86 mL of DMF (0.2M, to the resin loading). The reaction was shaken for 2 h. Completion of the reaction was verified by ninhydrin test. The resin was washed three times with DMF and subjected to the "**General solid-phase amine deprotection**" procedure to give the resin-bound free-amine tetrapeptide in a quantitative yield.

Pentapeptide Resin-D-Phe-D-Leu-D-Val-Leu-Leu-NH_2

Following the "**General solid-phase peptide coupling**" procedure, Resin-D-Phe-D-Leu-D-Val-Leu-NH_2 (0.972 mmol), Fmoc-Leu-OH (1.03 g, 2.92 mmol), HOBt (0.45 g, 2.92 mmol), and DIC (0.90 mL, 5.83 mmol) were combined in 4.86 mL of DMF (0.2M, to the resin loading). The reaction was shaken for 2 h. Completion of the reaction was verified by ninhydrin test. The resin was washed three times with DMF and subjected to the "**General solid-phase N-terminal amine deprotection**" procedure to give the resin-

bound free-amine pentapeptide in a quantitative yield. The resin was dried *in vacuo* overnight.

Double-deprotected pentapeptide HO-D-Phe-D-Leu-D-Val-Leu-Leu-NH_2

The linear peptide was cleaved from the resin following the "**Solid-phase cleaving from resin**" procedure. Resin-D-Phe-D-Leu-D-Val-Leu-Leu-NH_2 (1.59 g) was stirred in a 16 mL solution of TFE/DCM (1:1, v/v, 10 mL/g resin) for 24 h. The solution was filtered from the resin and concentrated *in vacuo* to give the DDLP (0.064 g, 12.0% yield).

Cyclized decapeptide D-Phe-D-Leu-D-Val-Leu-Leu-D-Phe-D-Leu-D-Val-Leu-Leu

Following the "**Macrocyclization**" procedure, DDLP HO-D-Phe-D-Leu-D-Val-Leu-Leu-NH_2 (64 mg, 0.106 mmol), DEPBT (16 mg, 0.0530 mmol), HATU (28 mg, 0.0742 mmol), TBTU (17 mg, 0.0530 mmol), and DIPEA (0.15 mL, 0.874 mmol) were dissolved in 1.06 mL of anhydrous DMF (0.1M). The reaction was stirred for 1 h and was monitored by LCMS. Upon completion, the reaction was diluted in 50 mL of DCM and quenched with a pH 1 aqueous wash (50 mL) and two washes of brine (50 mL each). The organic layers were combined, dried over sodium sulfate, and concentrated *in vacuo* to give the crude product. The material was purified via RP-HPLC to give the cyclic decapeptide (40.1% yield).

Rf: 0.59 (75% EA/Hex)

^{1}H NMR (600 MHz, CD_3OD): δ 0.67 (d, 6H), 0.74 (d, 6H), 0.81-1.10 (m, 36H), 1.27-1.48 (m, 7H), 1.50-1.64 (m, 4H), 1.68-1.76 (m, 5H), 1.78-1.87 (m, 2H), 2.15 (br, 2H), 2.88-2.94 (m, 2H), 3.02-3.10 (m, 2H), 3.91 (br, 1αH), 4.04 (br, 1αH), 4.26 (br, 2αH), 4.35-4.42 (m, 2αH), 7.20-7.32 (m, 10H), 7.68 (br, N<u>H</u>), 8.25 (br, 2 N<u>H</u>), 8.43 (br, N<u>H</u>).

LCMS: m/z called for $C_{64}H_{102}N_{10}O_{10}$ (M+1) = 1171.78, found 1172.5.

SYNTHESIS OF DI-SANA 22

Dipeptide Resin-Phe-D-Leu-NH_2*

CTC-Phe-NH_2 resin (2.50 g, 1.60 mmol) was swelled in DMF for 30 min and drained. Then, following the "**General solid-phase peptide coupling**" procedure, the resin, Fmoc-D-Leu-OH (1.69 g, 4.80 mmol), HOBt (0.73 g, 4.80 mmol), and DIC (1.48 mL, 9.60 mmol) were combined in 8.0 mL of DMF (0.2M, to the resin loading). The reaction was shaken overnight. Completion of the reaction was verified by ninhydrin test. The resin was washed three times with DMF and subjected to the "**General solid-phase amine deprotection**" procedure to give the resin-bound free-amine dipeptide in a quantitative yield.

* This dipeptide was to be used for two compounds, thus the amounts utilized were doubled.

Tripeptide Resin-Phe-D-Leu-D-Val-NH_2

Following the "**General solid-phase peptide coupling**" procedure, Resin-Phe-D-Leu-NH_2 (1.60 mmol), Fmoc-D-Val-OH (1.62 g, 4.80 mmol), HOBt (0.73 g, 4.80 mmol), and DIC (1.48 mL, 9.60 mmol) were combined in 8.0 mL of DMF (0.2M, to the resin loading). The reaction was shaken for 2 h. Completion of the reaction was verified by ninhydrin test. The resin was washed three times with DMF and subjected to the "**General solid-phase amine deprotection**" procedure to give the resin-bound free-amine tripeptide in a quantitative yield. The resin was split into two equal batches, one to be used for Di-SanA 1767 synthesis and one for the synthesis of a different compound.

Tetrapeptide Resin-Phe-D-Leu-D-Val-D-Leu-NH_2

Following the "**General solid-phase peptide coupling**" procedure, Resin-Phe-D-Leu-D-Val-NH_2 (0.800 mmol), Fmoc-D-Leu-OH (0.850 g, 2.40 mmol), HOBt (0.360 g, 2.40 mmol), and DIC (0.75 mL, 4.80 mmol) were combined in 4.0 mL of DMF (0.2M, to the resin loading). The reaction was shaken for 2 h. Completion of the reaction was verified by ninhydrin test. The resin was washed three times with DMF and subjected to the "**General solid-phase amine deprotection**" procedure to give the resin-bound free-amine tetrapeptide in a quantitative yield.

Pentapeptide Resin-Phe-D-Leu-D-Val-D-Leu-Leu-NH_2

Following the "**General solid-phase peptide coupling**" procedure, Resin-Phe-D-Leu-D-Val-D-Leu-NH_2 (0.800 mmol), Fmoc-Leu-OH (0.850 g, 2.40 mmol), HOBt (0.360 g, 2.40 mmol), and DIC (0.75 mL, 4.80 mmol) were combined in 4.0 mL of DMF (0.2M, to the resin loading). The reaction was shaken for 2 h. Completion of the reaction was verified by ninhydrin test. The resin was washed three times with DMF and subjected to the "**General solid-phase N-terminal amine deprotection**" procedure to give the resin-bound free-amine pentapeptide in a quantitative yield. The resin was dried *in vacuo* overnight.

Double-deprotected pentapeptide HO-Phe-D-Leu-D-Val-D-Leu-Leu-NH_2

The linear peptide was cleaved from the resin following the "**Solid-phase cleaving from resin**" procedure. Resin-Phe-D-Leu-D-Val-D-Leu-Leu-NH_2 (1.67 g) was stirred in a 16.7 mL solution of TFE/DCM (1:1, v/v, 10 mL/g resin) for 24 h. The solution was filtered from the resin and concentrated *in vacuo* to give the DDLP (0.150 g, 30.0% yield).

Cyclized decapeptide Phe-D-Leu-D-Val-D-Leu-Leu-Phe-D-Leu-D-Val-D-Leu-Leu

Following the "**Macrocyclization**" procedure, DDLP HO-Phe-D-Leu-D-Val-D-Leu-Leu-NH_2 (145 mg, 0.240 mmol), DEPBT (36 mg, 0.120 mmol), HATU (64 mg, 0.168 mmol), TBTU (39 mg, 0.120 mmol), and DIPEA (0.33 mL, 1.92 mmol) were dissolved in 2.4 mL of anhydrous DMF (0.1M). The reaction was stirred for 1 h and was monitored by LCMS. Upon completion, the reaction was diluted in 100 mL of DCM and quenched with a saturated ammonium chloride wash (100 mL) and two washes of brine (75 mL each). The organic layers were combined, dried over sodium sulfate, and concentrated *in vacuo* to give the crude product. The material was initially purified using flash column chromatography with an EA/Hex gradient solvent system. Semi-pure product eluted at 75EA/25Hex and was further purified via RP-HPLC to give the cyclic decapeptide (38.2% yield).

Rf: 0.50 (75% EA/Hex)

^{1}H NMR (600 MHz, CD_3OD): δ 0.74 (d, 12H), 0.82-0.98 (m, 36H), 1.16-1.26 (m, 2H), 1.33-1.40 (m, 2H), 1.40-1.54 (m, 4H), 1.55-1.74 (m, 10H), 2.12-2.20 (m, 2H), 2.81-2.88 (m, 2H), 4.20-4.25 (m, 2αH), 4.33-4.38 (m, 2αH), 4.43-4.49 (m, 2αH), 4.52-4.57 (m, 2αH), 4.57-4.62 (m, 2αH), 7.21-7.32 (m, 10H), 7.63 (d, 2 N<u>H</u>), 7.73 (d, 2 N<u>H</u>), 8.15 (d, 2 N<u>H</u>), 8.32 (d, 2 N<u>H</u>), 8.46 (d, 2 N<u>H</u>).

LCMS: m/z called for $C_{64}H_{102}N_{10}O_{10}$ (M+1) = 1171.78, found 1194.4 (+23).

SYNTHESIS OF DI-SANA 23

Dipeptide Resin-D-Phe-D-Leu-NH_2

CTC-D-Phe-NH_2 resin (1.26 g, 0.907 mmol) was swelled in DMF for 30 min and drained. Then, following the "**General solid-phase peptide coupling**" procedure, the resin, Fmoc-D-Leu-OH (0.96 g, 2.72 mmol), HOBt (0.42 g, 2.72 mmol), and DIC (0.84

mL, 5.44 mmol) were combined in 4.5 mL of DMF (0.2M, to the resin loading). The reaction was shaken overnight. Completion of the reaction was verified by ninhydrin test. The resin was washed three times with DMF and subjected to the "**General solid-phase amine deprotection**" procedure to give the resin-bound free-amine dipeptide in a quantitative yield.

Tripeptide Resin-D-Phe-D-Leu-D-Val-NH_2

Following the "**General solid-phase peptide coupling**" procedure, Resin-D-Phe-D-Leu-NH_2 (0.907 mmol), Fmoc-D-Val-OH (0.92 g, 2.72 mmol), HOBt (0.42 g, 2.72 mmol), and DIC (0.84 mL, 5.44 mmol) were combined in 4.5 mL of DMF (0.2M, to the resin loading). The reaction was shaken for 2 h. Completion of the reaction was verified by ninhydrin test. The resin was washed three times with DMF and subjected to the "**General solid-phase amine deprotection**" procedure to give the resin-bound free-amine tripeptide in a quantitative yield.

Tetrapeptide Resin-D-Phe-D-Leu-D-Val-D-Leu-NH_2

Following the "**General solid-phase peptide coupling**" procedure, Resin-D-Phe-D-Leu-D-Val-NH_2 (0.907 mmol), Fmoc-D-Leu-OH (0.96 g, 2.72 mmol), HOBt (0.42 g, 2.72 mmol), and DIC (0.84 mL, 5.44 mmol) were combined in 4.5 mL of DMF (0.2M, to the resin loading). The reaction was shaken for 2 h. Completion of the reaction was verified by ninhydrin test. The resin was washed three times with DMF and subjected to the "**General solid-phase amine deprotection**" procedure to give the resin-bound free-amine tetrapeptide in a quantitative yield.

Pentapeptide Resin-D-Phe-D-Leu-D-Val-D-Leu-Leu-NH_2

Following the "**General solid-phase peptide coupling**" procedure, Resin-D-Phe-D-Leu-D-Val-D-Leu-NH_2 (0.907 mmol), Fmoc-Leu-OH (0.96 g, 2.72 mmol), HOBt (0.42 g, 2.72 mmol), and DIC (0.84 mL, 5.44 mmol) were combined in 4.5 mL of DMF (0.2M, to the resin loading). The reaction was shaken for 2 h. Completion of the reaction was verified by ninhydrin test. The resin was washed three times with DMF and subjected to the "**General solid-phase N-terminal amine deprotection**" procedure to give the resin-bound free-amine pentapeptide in a quantitative yield. The resin was dried *in vacuo* overnight.

Double-drotected pentapeptide HO-D-Phe-D-Leu-D-Val-D-Leu-Leu-NH_2

The linear peptide was cleaved from the resin following the "**Solid-phase cleaving from resin**" procedure. Resin-D-Phe-D-Leu-D-Val-D-Leu-Leu-NH_2 (1.55 g) was stirred in a 15.5 mL solution of TFE/DCM (1:1, v/v, 10 mL/g resin) for 24 h. The solution was filtered from the resin and concentrated *in vacuo* to give the DDLP (0.057 g, 10.4% yield).

Cyclized decapeptide D-Phe-D-Leu-D-Val-D-Leu-Leu-D-Phe-D-Leu-D-Val-D-Leu-Leu

Following the "**Macrocyclization**" procedure, DDLP HO-D-Phe-D-Leu-D-Val-D-Leu-Leu-NH_2 (57 mg, 0.0945 mmol), DEPBT (14 mg, 0.0472 mmol), HATU (25 mg, 0.0661 mmol), TBTU (15 mg, 0.0472 mmol), and DIPEA (0.13 mL, 0.756 mmol) were dissolved in 0.945 mL of anhydrous DMF (0.1M). The reaction was stirred for 1 h and was monitored by LCMS. Upon completion, the reaction was diluted in 50 mL of DCM and quenched with two pH=1 aqueous washes (50 mL each) and two washes of brine (50 mL each). The organic layers were combined, dried over sodium sulfate, and

concentrated *in vacuo* to give the crude product. The material was dissolved in 2.5 mL of 80% ACN/20% DMSO and purified via RP-HPLC to give the cyclic decapeptide (11.1% yield).

^{1}H NMR (600 MHz, CD_3OD): δ 0.75-1.03 (m, 48H), 1.28-1.48 (m, 4H), 1.29-1.71 (m, 14H), 2.27-2.37 (m, 2H), 2.84-2.90 (m, 2H), 3.08-3.16 (m, 2H), 4.08-4.15 (m, 2αH), 4.20-4.27 (m, 2αH), 4.46-4.52 (m, 2αH), 4.61-4.68 (m, 2αH), 7.12-7.32 (m, 10H), 8.06 (d, 2 NH), 8.14 (d, 2 NH), 8.18 (d, 2 NH), 8.54 (br, NH).

LCMS: m/z called for $C_{64}H_{102}N_{10}O_{10}$ (M+1) = 1171.78, found 1198.5 (+23+4).

SYNTHESIS OF DI-SANA 24

Dipeptide Resin-Leu-Phe-NH_2

CTC-Leu-NH_2 resin (1.34 g, 1.08 mmol) was swelled in DMF for 30 min and drained. Then, following the "**General solid-phase peptide coupling**" procedure, the resin, Fmoc-Phe-OH (1.26 g, 3.25 mmol), HOBt (0.50 g, 3.25 mmol), and DIC (1.00 mL, 6.48 mmol) were combined in 5.4 mL of DMF (0.2M, to the resin loading). The reaction was shaken overnight. Completion of the reaction was verified by ninhydrin test. The resin was washed three times with DMF and subjected to the "**General solid-phase amine deprotection**" procedure to give the resin-bound free-amine dipeptide in a quantitative yield.

Tripeptide Resin-Leu-Phe-D-Leu-NH_2

Following the "**General solid-phase peptide coupling**" procedure, Resin-Leu-Phe-NH_2 (1.08 mmol), Fmoc-D-Leu-OH (1.15 g, 3.25 mmol), HOBt (0.50 g, 3.25 mmol), and DIC (1.00 mL, 6.48 mmol) were combined in 5.4 mL of DMF (0.2M, to the resin loading). The reaction was shaken for 2 h. Completion of the reaction was verified by ninhydrin

test. The resin was washed three times with DMF and subjected to the "**General solid-phase amine deprotection**" procedure to give the resin-bound free-amine tripeptide in a quantitative yield.

Tetrapeptide Resin-Leu-Phe-D-Leu-D-Val-NH_2

Following the "**General solid-phase peptide coupling**" procedure, Resin-Leu-Phe-D-Leu-NH_2 (1.08 mmol), Fmoc-D-Val-OH (1.10 g, 3.25 mmol), HOBt (0.50 g, 3.25 mmol), and DIC (1.00 mL, 6.48 mmol) were combined in 5.4 mL of DMF (0.2M, to the resin loading). The reaction was shaken for 2 h. Completion of the reaction was verified by ninhydrin test. The resin was washed three times with DMF and subjected to the "**General solid-phase amine deprotection**" procedure to give the resin-bound free-amine tetrapeptide in a quantitative yield.

Pentapeptide Resin-Leu-Phe-D-Leu-D-Val-Leu-NH_2

Following the "**General solid-phase peptide coupling**" procedure, Resin-Leu-Phe-D-Leu-D-Val-NH_2 (1.08 mmol), Fmoc-Leu-OH (1.15 g, 3.25 mmol), HOBt (0.50 g, 3.25 mmol), and DIC (1.00 mL, 6.48 mmol) were combined in 5.4 mL of DMF (0.2M, to the resin loading). The reaction was shaken for 2 h. Completion of the reaction was verified by ninhydrin test. The resin was washed three times with DMF and subjected to the "**General solid-phase amine deprotection**" procedure to give the resin-bound free-amine pentapeptide in a quantitative yield.

Hexapeptide Resin-Leu-Phe-D-Leu-D-Val-Leu-Leu-NH_2

Following the "**General solid-phase peptide coupling**" procedure, Resin-Leu-Phe-D-Leu-D-Val-Leu-NH_2 (1.08 mmol), Fmoc-Leu-OH (1.15 g, 3.25 mmol), HOBt (0.50 g, 3.25 mmol), and DIC (1.00 mL, 6.48 mmol) were combined in 5.4 mL of DMF (0.2M, to

the resin loading). The reaction was shaken overnight. Completion of the reaction was verified by ninhydrin test. The resin was washed three times with DMF and subjected to the "**General solid-phase amine deprotection**" procedure to give the resin-bound free-amine hexapeptide in a quantitative yield.

Heptapeptide Resin-Leu-Phe-D-Leu-D-Val-Leu-Leu-D-Phe-NH_2

Following the "**General solid-phase peptide coupling**" procedure, Resin-Leu-Phe-D-Leu-D-Val-Leu-Leu-NH_2 (1.08 mmol), Fmoc-D-Phe-OH (1.26 g, 3.25 mmol), HOBt (0.50 g, 3.25 mmol), and DIC (1.00 mL, 6.48 mmol) were combined in 5.4 mL of DMF (0.2M, to the resin loading). The reaction was shaken overnight. Completion of the reaction was verified by ninhydrin test. The resin was washed three times with DMF and subjected to the "**General solid-phase amine deprotection**" procedure to give the resin-bound free-amine heptapeptide in a quantitative yield.

Octapeptide Resin-Leu-Phe-D-Leu-D-Val-Leu-Leu-D-Phe-D-Leu-NH_2

Following the "**General solid-phase peptide coupling**" procedure, Resin-Leu-Phe-D-Leu-D-Val-Leu-Leu-D-Phe-NH_2 (1.08 mmol), Fmoc-D-Leu-OH (1.15 g, 3.25 mmol), HOBt (0.50 g, 3.25 mmol), and DIC (1.00 mL, 6.48 mmol) were combined in 5.4 mL of DMF (0.2M, to the resin loading). The reaction was shaken overnight. Completion of the reaction was verified by ninhydrin test. The resin was washed three times with DMF and subjected to the "**General solid-phase amine deprotection**" procedure to give the resin-bound free-amine octapeptide in a quantitative yield. The presence of the octapeptide was verified by LCMS analysis of 2 mg resin-cleaved peptide.

Nonapeptide Resin-Leu-Phe-D-Leu-D-Val-Leu-Leu-D-Phe-D-Leu-D-Val-NH_2

Following the "**General solid-phase peptide coupling**" procedure, Resin-Leu-Phe-D-Leu-D-Val-Leu-Leu-D-Phe-D-Leu-NH_2 (1.08 mmol), Fmoc-D-Val-OH (1.10 g, 3.25 mmol), HOBt (0.50 g, 3.25 mmol), and DIC (1.00 mL, 6.48 mmol) were combined in 5.4 mL of DMF (0.2M, to the resin loading). The reaction was shaken overnight. Completion of the reaction was verified by ninhydrin test. The resin was washed three times with DMF and subjected to the "**General solid-phase amine deprotection**" procedure to give the resin-bound free-amine nonapeptide in a quantitative yield.

Decapeptide Resin-Leu-Phe-D-Leu-D-Val-Leu-Leu-D-Phe-D-Leu-D-Val-Leu-NH_2

Following the "**General solid-phase peptide coupling**" procedure, Resin-Leu-Phe-D-Leu-D-Val-Leu-Leu-D-Phe-D-Leu-D-Val-NH_2 (1.08 mmol), Fmoc-Leu-OH (1.15 g, 3.25 mmol), HOBt (0.50 g, 3.25 mmol), and DIC (1.00 mL, 6.48 mmol) were combined in 5.4 mL of DMF (0.2M, to the resin loading). The reaction was shaken for 3 h and drained. To ensure complete coupling of the final amino acid, the resin was subjected to a new batch of Fmoc-Leu-OH (1.15 g, 3.25 mmol), HOBt (0.50 g, 3.25 mmol), and DIC (1.00 mL, 6.48 mmol) combined in 5.4 mL of DMF (0.2M). The reaction was shaken overnight. Completion of the reaction was verified by ninhydrin test. The resin was washed three times with DMF and subjected to the "**General solid-phase N-terminal amine deprotection**" procedure to give the resin-bound free-amine decapeptide in a quantitative yield. The resin was dried *in vacuo* overnight.

Double-deprotected decapeptide HO-Leu-Phe-D-Leu-D-Val-Leu-Leu-D-Phe-D-Leu-D-Val-Leu-NH_2

The linear peptide was cleaved from the resin following the "**Solid-phase cleaving from resin**" procedure. Resin-Leu-Phe-D-Leu-D-Val-Leu-Leu-D-Phe-D-Leu-D-Val-Leu-NH_2

(2.0 g) was stirred in a 20 mL solution of TFE/DCM (1:1, v/v, 10 mL/g resin) for 24 h. The solution was filtered from the resin and concentrated *in vacuo* to give the DDLD (0.296 g, 23.1% yield).

Cyclized decapeptide Phe-D-Leu-D-Val-Leu-Leu-D-Phe-D-Leu-D-Val-Leu-Leu

Following the "**Macrocyclization**" procedure, DDLD HO-Leu-Phe-D-Leu-D-Val-Leu-Leu-D-Phe-D-Leu-D-Val-Leu-NH_2 (172 mg, 0.144 mmol), DEPBT (26 mg, 0.0867 mmol), HATU (44 mg, 0.115 mmol), TBTU (28 mg, 0.0867 mmol), and DIPEA (0.20 mL, 1.15 mmol) were dissolved in 1.44 mL of anhydrous DMF (0.1M). The reaction was stirred for 1 h and was monitored by LCMS. Upon completion, the reaction was diluted in 50 mL of DCM and quenched with two pH=1 aqueous wash (50 mL each), one wash of saturated sodium bicarbonate (50 mL, sat. aq.) and two washes of brine (50 mL each). The organic layers were combined, dried over sodium sulfate, and concentrated *in vacuo* to give the crude product. The material was purified via semi-prep RP-HPLC to give the pure cyclic decapeptide (52.0% yield).

Rf: 0.32 (75% EA/Hex)

^{1}H NMR (600 MHz, CD_3OD): δ 0.7-1.02 (m, 48H), 1.28-1.60 (m, 12H), 1.62-1.80 (m, 6H), 2.10-2.20 (m, 2H), 2.96-3.08 (m, 2H), 3.15-3.22 (m, 2H), 4.03-4.08 (m, αH), 4.12-4.24 (m, 2αH), 4.30-4.40 (m, 3αH), 4.40-4.47 (m, αH), 4.50-4.57 (m, αH), 7.17-7.30 (m, 10H), 7.81 (d, 2 N<u>H</u>), 7.91 (d, 2 N<u>H</u>), 8.05 (br, 2 N<u>H</u>), 8.29 (br, 2 N<u>H</u>).

LCMS: m/z called for $C_{64}H_{102}N_{10}O_{10}$ (M+1) = 1171.78, found 1173.0.

SYNTHESIS OF DI-SANA 25

Dipeptide Resin-Leu-D-Phe-NH_2*

CTC-Leu-NH_2 resin (3.06 g, 2.48 mmol) was swelled in DMF for 30 min and drained. Then, following the "**General solid-phase peptide coupling**" procedure, the resin, Fmoc-D-Phe-OH (2.88 g, 7.44 mmol), HOBt (1.14 g, 7.44 mmol), and DIC (2.3 mL, 14.9 mmol) were combined in 12.4 mL of DMF (0.2M, to the resin loading). The reaction was shaken overnight. Completion of the reaction was verified by ninhydrin test. The resin was washed three times with DMF and subjected to the "**General solid-phase amine deprotection**" procedure to give the resin-bound free-amine dipeptide in a quantitative yield.

* This dipeptide was meant for the synthesis of Di-SanA 25, 26, and 27, thus a greater amount of reagents were used.

Tripeptide Resin-Leu-D-Phe-D-Leu-NH_2*

Following the "**General solid-phase peptide coupling**" procedure Resin-Leu-D-Phe-NH_2, Fmoc-D-Leu-OH (2.62 g, 7.44 mmol), HOBt (1.14 g, 7.44 mmol), and DIC (2.3 mL, 14.9 mmol) were combined in 12.4 mL of DMF (0.2M, to the resin loading). The reaction was shaken overnight. Completion of the reaction was verified by ninhydrin test. The resin was washed three times with DMF and subjected to the "**General solid-phase amine deprotection**" procedure to give the resin-bound free-amine tripeptide in a quantitative yield.

* This tripeptide was meant for the synthesis of Di-SanA 25, 26, and 27, thus a greater amount of reagents were used.

Tetrapeptide Resin-Leu-D-Phe-D-Leu-D-Val-NH_2*

Following the "**General solid-phase peptide coupling**" procedure Resin-Leu-D-Phe-D-Leu-NH_2, Fmoc-D-Val-OH (2.52 g, 7.44 mmol), HOBt (1.14 g, 7.44 mmol), and DIC

(2.3 mL, 14.9 mmol) were combined in 12.4 mL of DMF (0.2M, to the resin loading). The reaction was shaken overnight. Completion of the reaction was verified by ninhydrin test. The resin was washed three times with DMF and subjected to the "**General solid-phase amine deprotection**" procedure to give the resin-bound free-amine tetrapeptide in a quantitative yield. The resin was divided into thirds, based on total weight, one-third was used for the continued synthesis of Di-SanA 25. The continued synthesis of the other two-thirds will be described in "**Synthesis of Di-SanA 26**."

* This tetrapeptide was meant for the synthesis of Di-SanA 25, 26, and 27, thus a greater amount of reagents were used.

Pentapeptide Resin-Leu-D-Phe-D-Leu-D-Val-D-Leu-NH_2

Following the "**General solid-phase peptide coupling**" procedure Resin-Leu-D-Phe-D-Leu-D-Val-NH_2, Fmoc-D-Leu-OH (0.87 g, 2.48 mmol), HOBt (0.37 g, 2.48 mmol), and DIC (0.76 mL, 4.96 mmol) were combined in 4.1 mL of DMF (0.2M, to the resin loading). The reaction was shaken overnight. Completion of the reaction was verified by ninhydrin test. The resin was washed three times with DMF and subjected to the "**General solid-phase amine deprotection**" procedure to give the resin-bound free-amine pentapeptide in a quantitative yield.

Hexapeptide Resin-Leu-D-Phe-D-Leu-D-Val-D-Leu-Leu-NH_2

Following the "**General solid-phase peptide coupling**" procedure Resin-Leu-D-Phe-D-Leu-D-Val-D-Leu-NH_2, Fmoc-Leu-OH (0.87 g, 2.48 mmol), HOBt (0.37 g, 2.48 mmol), and DIC (0.76 mL, 4.96 mmol) were combined in 4.1 mL of DMF (0.2M, to the resin loading). The reaction was shaken for 3 h. Completion of the reaction was verified by ninhydrin test. The resin was washed three times with DMF and subjected to the

"**General solid-phase amine deprotection**" procedure to give the resin-bound free-amine hexapeptide in a quantitative yield.

Heptapeptide Resin-Leu-D-Phe-D-Leu-D-Val-D-Leu-Leu-Phe-NH_2

Following the "**General solid-phase peptide coupling**" procedure Resin-Leu-D-Phe-D-Leu-D-Val-D-Leu-Leu-NH_2, Fmoc-Phe-OH (0.95 g, 2.48 mmol), HOBt (0.37 g, 2.48 mmol), and DIC (0.76 mL, 4.96 mmol) were combined in 4.1 mL of DMF (0.2M, to the resin loading). The reaction was shaken overnight. Completion of the reaction was verified by ninhydrin test. The resin was washed three times with DMF and subjected to the "**General solid-phase amine deprotection**" procedure to give the resin-bound free-amine heptapeptide in a quantitative yield.

Octapeptide Resin-Leu-D-Phe-D-Leu-D-Val-D-Leu-Leu-Phe-D-Leu-NH_2

Following the "**General solid-phase peptide coupling**" procedure Resin-Leu-D-Phe-D-Leu-D-Val-D-Leu-Leu-Phe-NH_2, Fmoc-D-Leu-OH (0.87 g, 2.48 mmol), HOBt (0.37 g, 2.48 mmol), and DIC (0.76 mL, 4.96 mmol) were combined in 4.1 mL of DMF (0.2M, to the resin loading). The reaction was shaken overnight. Completion of the reaction was verified by ninhydrin test. The resin was washed three times with DMF and subjected to the "**General solid-phase amine deprotection**" procedure to give the resin-bound free-amine octapeptide in a quantitative yield.

Nonapeptide Resin-Leu-D-Phe-D-Leu-D-Val-D-Leu-Leu-Phe-D-Leu-D-Val-NH_2

Following the "**General solid-phase peptide coupling**" procedure Resin-Leu-D-Phe-D-Leu-D-Val-D-Leu-Leu-Phe-D-Leu-NH_2, Fmoc-D-Val-OH (0.84 g, 2.48 mmol), HOBt (0.37 g, 2.48 mmol), and DIC (0.76 mL, 4.96 mmol) were combined in 4.1 mL of DMF (0.2M, to the resin loading). The reaction was shaken overnight. Completion of the

reaction was verified by ninhydrin test. The resin was washed three times with DMF and subjected to the "**General solid-phase amine deprotection**" procedure to give the resin-bound free-amine nonapeptide in a quantitative yield.

Decapeptide Resin-Leu-D-Phe-D-Leu-D-Val-D-Leu-Leu-Phe-D-Leu-D-Val-D-Leu-NH_2

Following the "**General solid-phase peptide coupling**" procedure Resin-Leu-D-Phe-D-Leu-D-Val-D-Leu-Leu-Phe-D-Leu-D-Val-NH_2, Fmoc-D-Leu-OH (0.87 g, 2.48 mmol), HOBt (0.37 g, 2.48 mmol), and DIC (0.76 mL, 4.96 mmol) were combined in 4.1 mL of DMF (0.2M, to the resin loading). The reaction was shaken overnight. Completion of the reaction was verified by ninhydrin test. The resin was washed three times with DMF and subjected to the "**General solid-phase N-terminal amine deprotection**" procedure to give the resin-bound free-amine decaapeptide in a quantitative yield. The resin was dried *in vacuo* overnight.

Double-deprotected decapeptide HO-Leu-D-Phe-D-Leu-D-Val-D-Leu-Leu-Phe-D-Leu-D-Val-D-Leu-NH_2

The linear peptide was cleaved from the resin following the "**Solid-phase cleaving from resin**" procedure. Resin-Leu-D-Phe-D-Leu-D-Val-D-Leu-Leu-Phe-D-Leu-D-Val-D-Leu-NH_2 (1.7 g) was stirred in a 17 mL solution of TFE/DCM (1:1, v/v, 10 mL/g resin) for 24 h. The solution was filtered from the resin and concentrated *in vacuo* to give the DDLD (0.280 g, 28.5% yield).

Cyclized decapeptide D-Phe-D-Leu-D-Val-D-Leu-Leu-Phe-D-Leu-D-Val-D-Leu-Leu

Following the "**Macrocyclization**" procedure, DDLD HO-Leu-D-Phe-D-Leu-D-Val-D-Leu-Leu-Phe-D-Leu-D-Val-D-Leu-NH_2 (138 mg, 0.118 mmol), DEPBT (21 mg, 0.0706

mmol), HATU (36 mg, 0.0942 mmol), TBTU (23 mg, 0.0706 mmol), and DIPEA (0.16 mL, 0.942 mmol) were dissolved in 1.18 mL of anhydrous DMF (0.1M). The reaction was stirred for 1.5 h and was monitored by LCMS. Upon completion, the reaction was diluted in 50 mL of EA and quenched with two pH=1 aqueous wash (50 mL each), one wash of saturated sodium bicarbonate (50 mL, sat. aq.) and two washes of brine (50 mL each). The organic layers were combined, dried over sodium sulfate, and concentrated *in vacuo* to give the crude product. The material was initially purified via semi-prep RP-HPLC, and again with analytical RP-HPLC to give the pure cyclic decapeptide (54.0% yield).

Rf: 0.62 (75% EA/Hex)

^{1}H NMR (600 MHz, CD_3OD): δ 0.76-1.10 (m, 48H), 1.27-1.88 (m, 18H), 1.92-2.04 (m, 2H), 2.82-2.88 (m, 1H), 2.91-3.01 (m, 1H), 3.24-3.30 (m, 1H), 3.41-3.51 (m, 1H), 3.90 (br, αH), 3.99 (br, αH), 4.08 (br, αH), 4.18 (m, 2αH), 4.42 (m, αH), 4.63 (m, 2αH), 4.77 (m, αH), 7.14-7.38 (m, 10H), 7.44 (br, NH), 7.55 (br, NH), 7.60 (br, NH), 7.83 (m, NH), 7.88 (br, NH), 7.96 (br, NH), 8.14 (br, NH), 8.25 (br, NH), 8.57 (d, NH).

LCMS: m/z called for $C_{64}H_{102}N_{10}O_{10}$ (M+1) = 1171.78, found 1196.1 (+23+1).

SYNTHESIS OF DI-SANA 26

Note: The synthesis of the linear tetrapeptide and precursors is described in "**Synthesis of Di-SanA 25**."

Pentapeptide Resin-Leu-D-Phe-D-Leu-D-Val-Leu-NH_2*

Following the "**General solid-phase peptide coupling**" procedure Resin-Leu-D-Phe-D-Leu-D-Val-NH_2 (0.825 mmol), Fmoc-Leu-OH (1.75 g, 4.96 mmol), HOBt (0.75 g, 4.96 mmol), and DIC (1.53 mL, 9.92 mmol) were combined in 8.25 mL of DMF (0.2M, to the

resin loading). The reaction was shaken overnight. Completion of the reaction was verified by ninhydrin test. The resin was washed three times with DMF and subjected to the "**General solid-phase amine deprotection**" procedure to give the resin-bound free-amine pentapeptide in a quantitative yield.

* This pentapeptide was meant for the synthesis of both Di-SanA 26 and 27.

Hexapeptide Resin-Leu-D-Phe-D-Leu-D-Val-Leu-Leu-NH_2*

Following the "**General solid-phase peptide coupling**" procedure Resin-Leu-D-Phe-D-Leu-D-Val-Leu-NH_2 (0.825 mmol), Fmoc-Leu-OH (1.75 g, 4.96 mmol), HOBt (0.75 g, 4.96 mmol), and DIC (1.53 mL, 9.92 mmol) were combined in 8.25 mL of DMF (0.2M, to the resin loading). The reaction was shaken for 4 h. Completion of the reaction was verified by ninhydrin test. The resin was washed three times with DMF and subjected to the "**General solid-phase amine deprotection**" procedure to give the resin-bound free-amine hexaapeptide in a quantitative yield. The resin was divided in half, based on total weight. One half was used for the continued synthesis of Di-SanA 26 and the other half for the synthesis of Di-SanA 27.

* This hexapeptide was meant for the synthesis of both Di-SanA 26 and 27.

Heptapeptide Resin-Leu-D-Phe-D-Leu-D-Val-Leu-Leu-Phe-NH_2

Following the "**General solid-phase peptide coupling**" procedure Resin-Leu-D-Phe-D-Leu-D-Val-Leu-Leu-NH_2 (0.825 mmol), Fmoc-Phe-OH (0.95 g, 2.48 mmol), HOBt (0.37 g, 2.48 mmol), and DIC (0.76 mL, 4.96 mmol) were combined in 4.1 mL of DMF (0.2M, to the resin loading). The reaction was shaken overnight. Completion of the reaction was verified by ninhydrin test. The resin was washed three times with DMF and

subjected to the "**General solid-phase amine deprotection**" procedure to give the resin-bound free-amine heptapeptide in a quantitative yield.

Octapeptide Resin-Leu-D-Phe-D-Leu-D-Val-Leu-Leu-Phe-D-Leu-NH_2

Following the "**General solid-phase peptide coupling**" procedure Resin-Leu-D-Phe-D-Leu-D-Val-Leu-Leu-Phe-NH_2 (0.825 mmol), Fmoc-D-Leu-OH (0.87 g, 2.48 mmol), HOBt (0.37 g, 2.48 mmol), and DIC (0.76 mL, 4.96 mmol) were combined in 4.1 mL of DMF (0.2M, to the resin loading). The reaction was shaken overnight. Completion of the reaction was verified by ninhydrin test. The resin was washed three times with DMF and subjected to the "**General solid-phase amine deprotection**" procedure to give the resin-bound free-amine octapeptide in a quantitative yield.

Nonapeptide Resin-Leu-D-Phe-D-Leu-D-Val-Leu-Leu-Phe-D-Leu-D-Val-NH_2

Following the "**General solid-phase peptide coupling**" procedure Resin-Leu-D-Phe-D-Leu-D-Val-Leu-Leu-Phe-D-Leu-NH_2 (0.825 mmol), Fmoc-D-Val-OH (0.84 g, 2.48 mmol), HOBt (0.37 g, 2.48 mmol), and DIC (0.76 mL, 4.96 mmol) were combined in 4.1 mL of DMF (0.2M, to the resin loading). The reaction was shaken overnight. Completion of the reaction was verified by ninhydrin test. The resin was washed three times with DMF and subjected to the "**General solid-phase amine deprotection**" procedure to give the resin-bound free-amine nonapeptide in a quantitative yield.

Decapeptide Resin-Leu-D-Phe-D-Leu-D-Val-Leu-Leu-Phe-D-Leu-D-Val-D-Leu-NH_2

Following the "**General solid-phase peptide coupling**" procedure Resin-Leu-D-Phe-D-Leu-D-Val-Leu-Leu-Phe-D-Leu-D-Val-NH_2 (0.825 mmol), Fmoc-D-Leu-OH (0.87 g, 2.48 mmol), HOBt (0.37 g, 2.48 mmol), and DIC (0.76 mL, 4.96 mmol) were combined in 4.1 mL of DMF (0.2M, to the resin loading). The reaction was shaken overnight.

Completion of the reaction was verified by ninhydrin test. The resin was washed three times with DMF and subjected to the "**General solid-phase N-terminal amine deprotection**" procedure to give the resin-bound free-amine decapeptide in a quantitative yield.

Decapeptide HO-Leu-D-Phe-D-Leu-D-Val-Leu-Leu-Phe-D-Leu-D-Val-D-Leu-NH_2

The linear peptide was cleaved from the resin following the "**Solid-phase cleaving from resin**" procedure. Resin-Leu-D-Phe-D-Leu-D-Val-Leu-Leu-Phe-D-Leu-D-Val-D-Leu-NH_2 (2.0 g) was stirred in a 20 mL solution of TFE/DCM (1:1, v/v, 10 mL/g resin) for 24 h. The solution was filtered from the resin and concentrated *in vacuo* to give the DDLD (0.311 g, 31.6% yield).

Cyclized decapeptide D-Phe-D-Leu-D-Val-Leu-Leu-Phe-D-Leu-D-Val-D-Leu-Leu

Following the "**Macrocyclization**" procedure, DDLD HO-Leu-D-Phe-D-Leu-D-Val-Leu-Leu-Phe-D-Leu-D-Val-D-Leu-NH_2 (176 mg, 0.148 mmol), DEPBT (27.0 mg, 0.0887 mmol), HATU (45.5 mg, 0.118 mmol), TBTU (27.8 mg, 0.0887 mmol), and DIPEA (0.21 mL, 1.18 mmol) were dissolved in 1.48 mL of anhydrous DMF (0.1M). The reaction was stirred overnight and was monitored by LCMS. Additional TBTU (50.0 mg) and DIPEA (0.10 mL) was added after three hours. Upon completion, the reaction was diluted in 75 mL of EA and quenched with two washes of saturated sodium bicarbonate (75 mL, sat. aq.) and two washes of brine (50 mL each). The organic layers were combined, dried over sodium sulfate, and concentrated *in vacuo* to give the crude product. The material was initially purified via semi-prep RP-HPLC, and again with analytical RP-HPLC to give the cyclic decapeptide (28.8% yield).

LCMS: m/z called for $C_{64}H_{102}N_{10}O_{10}$ (M+1) = 1171.78, found 1195.1 (+23).

SYNTHESIS OF DI-SANA 27

Note: The synthesis for the hexapeptide and precursors was discussed in "Synthesis of Di-SanA 26."

Heptapeptide Resin-Leu-D-Phe-D-Leu-D-Val-Leu-Leu-D-Phe-NH_2

Following the "**General solid-phase peptide coupling**" procedure Resin-Leu-D-Phe-D-Leu-D-Val-Leu-Leu-NH_2 (0.825 mmol), Fmoc-D-Phe-OH (0.95 g, 2.48 mmol), HOBt (0.37 g, 2.48 mmol), and DIC (0.76 mL, 4.96 mmol) were combined in 4.1 mL of DMF (0.2M, to the resin loading). The reaction was shaken overnight. Completion of the reaction was verified by ninhydrin test. The resin was washed three times with DMF and subjected to the "**General solid-phase amine deprotection**" procedure to give the resin-bound free-amine heptapeptide in a quantitative yield.

Octapeptide Resin-Leu-D-Phe-D-Leu-D-Val-Leu-Leu-D-Phe-D-Leu-NH_2

Following the "**General solid-phase peptide coupling**" procedure Resin-Leu-D-Phe-D-Leu-D-Val-Leu-Leu-D-Phe-NH_2 (0.825 mmol), Fmoc-D-Leu-OH (0.87 g, 2.48 mmol), HOBt (0.37 g, 2.48 mmol), and DIC (0.76 mL, 4.96 mmol) were combined in 4.1 mL of DMF (0.2M, to the resin loading). The reaction was shaken overnight. Completion of the reaction was verified by ninhydrin test. The resin was washed three times with DMF and subjected to the "**General solid-phase amine deprotection**" procedure to give the resin-bound free-amine octapeptide in a quantitative yield.

Nonapeptide Resin-Leu-D-Phe-D-Leu-D-Val-Leu-Leu-D-Phe-D-Leu-D-Val-NH_2

Following the "**General solid-phase peptide coupling**" procedure Resin-Leu-D-Phe-D-Leu-D-Val-Leu-Leu-D-Phe-D-Leu-NH_2 (0.825 mmol), Fmoc-D-Val-OH (0.85 g, 2.48 mmol), HOBt (0.37 g, 2.48 mmol), and DIC (0.76 mL, 4.96 mmol) were combined in 4.1

mL of DMF (0.2M, to the resin loading). The reaction was shaken overnight. Completion of the reaction was verified by ninhydrin test. The resin was washed three times with DMF and subjected to the "**General solid-phase amine deprotection**" procedure to give the resin-bound free-amine nonapeptide in a quantitative yield.

Decapeptide Resin-Leu-D-Phe-D-Leu-D-Val-Leu-Leu-D-Phe-D-Leu-D-Val-D-Leu-NH_2

Following the "**General solid-phase peptide coupling**" procedure Resin-Leu-D-Phe-D-Leu-D-Val-Leu-Leu-D-Phe-D-Leu-D-Val-NH_2 (0.825 mmol), Fmoc-D-Leu-OH (0.87 g, 2.48 mmol), HOBt (0.37 g, 2.48 mmol), and DIC (0.76 mL, 4.96 mmol) were combined in 4.1 mL of DMF (0.2M, to the resin loading). The reaction was shaken overnight and drained. To ensure complete coupling of the final amino acid, the resin was subjected to a new batch of Fmoc-D-Leu-OH (0.87 g, 2.48 mmol), HOBt (0.37 g, 2.48 mmol), and DIC (0.76 mL, 4.96 mmol) combined in 4.1 mL of DMF (0.2M). Completion of the reaction was verified by ninhydrin test. The resin was washed three times with DMF and subjected to the "**General solid-phase N-terminal amine deprotection**" procedure to give the resin-bound free-amine decapeptide in a quantitative yield. The resin was dried *in vacuo* overnight.

Decapeptide HO-Leu-D-Phe-D-Leu-D-Val-Leu-Leu-D-Phe-D-Leu-D-Val-D-Leu-NH_2

The linear peptide was cleaved from the resin following the "**Solid-phase cleaving from resin**" procedure. Resin-Leu-D-Phe-D-Leu-D-Val-Leu-Leu-D-Phe-D-Leu-D-Val-D-Leu-NH_2 (1.3 g) was stirred in a 13 mL solution of TFE/DCM (1:1, v/v, 10 mL/g resin)

for 24 h. The solution was filtered from the resin and concentrated *in vacuo* to give the DDLD (0.134 g, 13.6% yield).

Cyclized decapeptide D-Phe-D-Leu-D-Val-Leu-Leu-D-Phe-D-Leu-D-Val-D-Leu-Leu

Following the "**Macrocyclization**" procedure, DDLD HO-Leu-D-Phe-D-Leu-D-Val-Leu-Leu-D-Phe-D-Leu-D-Val-D-Leu-NH_2 (94 mg, 0.0789 mmol), DEPBT (13.7 mg, 0.0473 mmol), HATU (24.5 mg, 0.0631 mmol), TBTU (14.6 mg, 0.0473 mmol), and DIPEA (0.11 mL, 0.631 mmol) were dissolved in 0.80 mL of anhydrous DMF (0.1M). The reaction was stirred for 1.5 h and was monitored by LCMS. Upon completion, the reaction was diluted in 75 mL of EA and quenched with two washes of saturated sodium bicarbonate (75 mL, sat. aq.) and two washes of brine (50 mL each). The organic layers were combined, dried over sodium sulfate, and concentrated *in vacuo* to give the crude product. The material was purified via RP-HPLC to give the cyclic decapeptide (51.0% yield).

LCMS: m/z called for $C_{64}H_{102}N_{10}O_{10}$ (M+1) = 1171.78, found 1194.7 (+23).

REFERENCES

1. Cancer Fact Sheet. http://www.who.int/mediacentre/factsheets/fs297/en/ (accessed 02/2012).

2. Howlader, N.; Noone, A. M.; Krapcho, M.; Neyman, N.; Aminou, R.; Waldron, W.; Altekruse, S. F.; Kosary, C. L.; Ruhl, J.; Tatalovich, Z.; Cho, H.; Mariotto, A.; Eisner, M. P.; Lewis, D. R.; Chen, H. S.; Feuer, E. J.; Cronin, K. A.; (eds) SEER Cancer Statistics Review, 1975-2009 (Vintage 2009 Populations). http://seer.cancer.gov/csr/1975_2009_pops09/sections.html.

3. Adessi, C.; Soto, C., Converting a peptide into a drug: Strategies to improve stability and bioavailability. *Curr. Med. Chem.* **2002,** *9* (9), 963-978.

4. Davies, J. S., The cyclization of peptides and depsipeptides. *Journal of Peptide Science* **2003,** *9*, 471-501.

5. Katsara, M.; Tselios, T.; Deraos, S.; Deraos, G.; Matsoukas, M.-T.; Lazoura, E.; Matsoukas, J.; Apostolopoulos, V., Round and round we go: cyclic peptides in disease. *Curr. Med. Chem.* **2006,** *13*, 2221-2232.

6. Rink, R.; Arkema-Meter, A.; Baudoin, I.; Post, E.; Kuipers, A.; Nelemans, S. A.; Haas Jimoh Akanbi, M.; Moll, G. N., To protect peptide pharmaceuticals against peptidases. *J. Pharmacol. and Toxicol. Methods* **2010,** *61*, 210-218.

7. Rezai, T.; Bock, J. E.; Zhou, M. V.; Kalyanaraman, C.; Lokey, R. S.; Jacobson, M. P., Conformational flexibility, internal hydrogen bonding, and passive membrane permeability: Successful in silico prediction of the relative permeabilities of cyclic peptides. *J. Am. Chem. Soc.* **2006,** *128*, 14073-14080.

8. Rezai, T.; Yu, B.; Millhauser, G. L.; Jacobson, M. P.; Lokey, R. S., Testing the conformational hypothesis of passive membrane permeability using synthetic cyclic peptide diastereomers. *J. Am. Chem. Soc.* **2006,** *128*, 2510-2511.

9. White, C. J.; Yudin, A. K., Contemporary strategies for peptide macrocyclization. *Nature Chem.* **2011,** *3*, 509-524.

10. Thayer, A. M., Making peptides at large scale. *C&EN* **2011,** *89* (22), 21-25.

11. Lax, R., The future of peptide development in the pharmaceutical industry. *PharManufacturing: The International Peptide Rev.* **2010**, 10-15.

12. Ezzat, S.; Ren, S. G.; Braunstein, G. D.; Melmed, S., Octreotide stimulates insulin-like growth factor-binding protein-1: a potential pituitary-independent mechanism for drug action. *JCEM* **1992,** *75* (6), 1459-1463.

13. Lee, J.; Currano, J. N.; Carroll, P. J.; Joullie, M. M., Didemnins, tamandarins and related natural products. *Nat. Prod. Rep.* **2012,** *29*, 404-424.

14. Belshaw, P. J.; Schreiber, S. L., Cell-specific calcineurin inhibition by a modified cyclosporin. *J. Am. Chem. Soc.* **1997,** *119*, 1805-1806.

15. Belofsky, G. N.; Jensen, P. R.; Fenical, W., Sansalvamide: A new cytotoxic cyclic depsipeptide produced by a marine fungus of the genus *Fusarium*. *Tetrahedron Lett.* **1999,** *40*, 2913-2916.

16. Lee, Y.; Silverman, R. B., Rapid, high-yield, solid-phase synthesis of the antitumor antibiotic Sansalvamide A using a side-chain-tethered phenylalanine building block. *Org. Lett.* **2000,** *2*, 3743-3746.

17. Gu, W.; Liu, S.; Silverman, R. B., Solid-phase, Pd-Catalyzed silicon-aryl carbon bond formation. Synthesis of Sansalvamide A peptide. *Org. Lett.* **2002,** *4*, 4171-4174.

18. Ujiki, M.; Milam, B.; Ding, X.-Z.; Roginsky, A. B.; Salabat, M. R.; Talamonti, M. S.; Bell, R. H.; Gu, W.; Silverman, R. B.; Adrian, T. E., A novel peptide sansalvamide A analogue inhibits pancreatic cancer cell growth through G0/G1 cell-cycle arrest. *Biochemical and Biophysical Research Communications* **2006,** *340*, 1224-1228.

19. Heiferman, M. J.; Salabat, M. R.; Ujiki, M. B.; Strouch, M. J.; Cheon, E. C.; Silverman, R. B.; Bentrem, D. J., Sansalvamide induces pancreatic cancer growth arrest through changes in the cell cycle. *Anticancer Res.* **2010,** *30*, 73-78.

20. Chatterjee, J.; Mierke, D. F.; Kessler, H., N-methylated cyclic pentaalanine peptides as template structures. *J. Am. Chem. Soc.* **2006,** *128*, 15164-15172.

21. Chatterjee, J.; Ovadia, O.; Gilon, C.; Hoffman, A.; Mierke, D.; Kessler, H., *N*-methylated cyclic pentapeptides as template structures. In *Peptides for youth: The proceedings of the 20th American Peptide Symposium*, 2009; Vol. 109.

22. Chaudhury, S., Welch, T.R. & Blagg, B. S. J., Hsp90 as a Target for Drug Development. *Chem. Med. Chem.* **2006,** *1* (12), 1331-1340.

23. McDonald, E.; Workman, P.; Jones, K., Inhibitors of the Hsp90 molecular chaperone: attacking the master regulator in cancer. *Curr. Top. Med. Chem.* **2006,** *6*, 1091-1107.

24. Neckers, L., Hsp90 inhbitors as novel cancer chemotherapeutic agents. *Trends Mol. Med.* **2002,** *8*, S55-S61.

25. Pearl, L. H.; Prodromou, C., Structure and mechanism of the Hsp90 molecular chaperone machinery. *Annu. Rev. Biochem.* **2006,** *75*, 271-294.

26. Trepel, J., Mollapour, M., Giaccone, G., Neckers, L., Targeting the dynamic Hsp90 complex in cancer. *Nature Reviews: Cancer* **2010,** *10*, 537-549.

27. Kamal, A.; Thao, L.; Sensintaffar, J.; Zhang, L.; Boehm, M. F.; Fritz, L. C.; Burrows, F. J., A high-affinity conformation of Hsp90 confers tumour selectivity on Hsp90 inhibitors. *Nature* **2003,** *425*, 407-410.

28. Goetz, M. P.; Toft, D. O.; Ames, M. M.; Erlichman, C., The Hsp90 chaperone complex as a novel target for cancer therapy. *Annals of Oncology* **2003,** *14*, 1169-1176.

29. Hickey, E.; Brandon, S. E.; Sadis, S.; Smale, G.; WEber, L. A., Molecular cloning of sequences encoding the human heat-shock proteins and their expression during hyperthermia. *Gene* **1986,** *43* (1-2), 147-154.

30. Sidera, K.; Patsavoudi, E., Extracellular Hsp90: Conquering the cell surface. *Cell Cycle* **2008,** *7* (11), 1564-1568.

31. McCready, J.; Sims, J. D.; Chan, D.; Jay, D. G., Secretion of extracellular hsp90a via exosomes increases cancer cell motility: a role for plasminogen activation. *BMC Cancer* **2012,** *10*, 294.

32. Dollins, D. E.; Warren, J. J.; Immormino, R. M.; Gewirth, D. T., Structures of GRP94-nucleotide complexes reveal mechanistic differences between the hsp90 chaperones. *Mol. Cell.* **2007,** *28*, 41-56.

33. Frey, S.; Leskovar, A.; Reinstein, J.; Buchner, J., The ATPase cycle of the endoplasmic chaperone Grp94. *J. Biol. Chem.* **2007,** *282*, 35612-35620.

34. Leskovar, A.; Wegele, H.; Werbeck, N. D.; Buchner, J.; Reinstein, J., The ATPase cycle of the mitochondrial Hsp90 analog Trap1. *J. Biol. Chem.* **2008,** *283*, 11677-11688.

35. Eletto, D.; Dersh, D.; Argot, Y., GRP94 in ER quality control and stress responses. *Seminars in Cell & Develop. Biol.* **2010,** *21*, 479-485.

36. Felts, S. J.; Owen, B. A.; Nguyen, P.; Trepel, J.; Donner, D. B.; Toft, D. O., The hsp90-related protein TRAP1 is a mitochondrial protein with distinct functional properties. *J. Biol. Chem.* **2000,** *275* (5), 3305-12.

37. Altieri, D. C.; Stein, G. S.; Lian, J. B.; Languino, L. R., TRAP-1, the mitochondrial Hsp90. *Biochim. Biophys.* **2012,** *1823*, 767-773.

38. Siligardi, G.; Panaretou, B.; Meyer, P.; Singh, S.; Woolfson, D. N.; Piper, P. W.; Pearl, L. H.; Prodromou, C., Regulation of Hsp90 ATPase activity by the co-chaperone Cdc37p/p50cdc37. *J. Biol. Chem.* **2002,** *277* (23), 20151-9.

39. Hanahan, D.; Weinberg, R. A., The hallmarks of cancer. *Cell* **2000,** *100* (1), 57-70.

40. Donnelly, A.; Blagg, B. S. J., Novobiocin and additional inhibitors of the Hsp90 C-terminal nucleotide-binding pocket. *Curr. Med. Chem* **2008,** *15*, 2702-2717.

41. Hadden, M. K.; Lubbers, D. J.; Blagg, B. S. J., Geldanamycin, radicicol, and chimeric inhibitors of the Hsp90 N-terminal ATP binding site. *Curr. Top. Med. Chem.* **2006,** *6* (11), 1173-1182.

42. Grenert, J. P.; Sullivan, W. P.; Fadden, P.; Haystead, T. A.; Clark, J.; Mimnaugh, E.; Krutzsch, H.; Ochel, H. J.; Schulte, T. W.; Sausville, E.; Neckers, L. M.; Toft, D. O., The amino-terminal domain of heat shock protein 90 (hsp90) that binds geldanamycin is an ATP/ADP switch domain that regulates hsp90 conformation. *J. Biol. Chem.* **1997,** *272* (38), 23843-50.

43. Neckers, L.; Workman, P., Hsp90 molecular chaperone inhibitors: Are we there yet? *Clin. Cancer. Res.* **2012,** *18*, 64-76.

44. http://clinicaltrials.gov/ct2/results?term=17-AAG&pg=2.

45. Whitesell, L.; Shifrin, S. D.; Schwab, G.; Neckers, L. M., Benzoquinonoid ansamycins possess selective tumoricidal activity unrelated to src kinase inhibition. *Cancer Res.* **1992,** *52* (7), 1721-8.

46. Supko, J. G.; Hickman, R. L.; Grever, M. R.; Malspeis, L., Preclinical pharmacologic evaluation of geldanamycin as an antitumor agent. *Cancer Chemother. Pharmacol.* **1995,** *36* (4), 305-15.

47. Samuni, Y.; Ishii, H.; Hyoda, F.; Samuni, U.; Krishna, M. C.; Goldstein, S.; Mitchell, J. B., Reactive oxygen species mediate hepatotoxicity induced by the Hsp90 inhibitor geldanamycin and its analogs. *Free Radic. Biol. Med.* **2010,** *48*, 1559-1563.

48. Smith, V.; Sausville, E. A.; Camalier, R. F.; Fiebig, H.-H.; Burger, A. M., Comparison of 17-dimethylaminoethylamino-17-demethoxy-geldanamycin (17DMAG) and 17-allylamino-17-demethoxygeldanamycin (17AAG) in vitro: effects on Hsp90 and client proteins in melanoma models. *Cancer Chemother. Pharmacol.* **2005,** *56* (2), 126-137.

49. Goetz, M. P.; Toft, D.; Reid, J.; Ames, M.; Stensgard, B.; Safgren, S.; Adjei, A. A.; Sloan, J.; Atherton, P.; Vasile, V.; Salazaar, S.; Adjei, A.; Croghan, G.; Erlichman, C., Phase I trial of 17-allylamino-17-demethoxygeldanamycin in patients with advanced cancer. *J. Clin. Oncol.* **2005,** *23* (6), 1078-87.

50. Winklhofer, K. F.; Reintjes, A.; Hoener, M. C.; Voellmy, R.; Tatzelt, J., Geldanamycin restores a defective heat shock response in vivo. *J. Biol. Chem.* **2001,** *276* (48), 45160-45167.

51. Sarge, K. D.; Murphy, S. P.; Morimoto, R. I., Activation of heat shock gene transcription factor 1 involves oligomerization, acquisition of DNA-binding activity, and nuclear localization and can occur in the absence of stress. *Mol. Cell. Biol.* **1993,** *13* (3), 1392-1407.

52. Powers, M. V.; Jones, K.; Barillari, C.; Westwood, I.; van Montfort, R. L. M.; Workman, P., Targeting HSP70. *Cell Cycle* **2010,** *9* (8), 1542-1550.

53. Patury, S.; Miyata, Y.; Gestwicki, J. E., Pharmacological targeting of the Hsp70 chaperone. *Curr. Top. Med. Chem.* **2009,** *9* (15), 1337-1351.

54. Bessalle, R.; Kapitkovsky, A.; Gorea, A.; Shalit, I.; Fridkin, M., All-D-magainin: chirality, antimicrobial activity and proteolytic resistance. *FEBS* **1990,** *274*, 151-155.

55. Hong, S. Y.; Oh, J. E.; Lee, K.-H., Effect of D-amino acid substitution on the stability, the secondary structure, and the activity of membrane-active peptide. *Biochemical Pharmacology* **1999,** *58*, 1775-1780.

56. Golovanov, A. P.; Hautbergue, G. M.; Wilson, S. A.; Lian, L.-Y., A simple method for improving protein solubility and long-term stability. *J. Am. Chem. Soc.* **2004,** *126*, 8933-8939.

57. Lee, Y.; Silverman, R. B., Efficient solid-phase synthesis of compounds containing phenylalanine and its derivatives via side-chain attachment to the polymer support. *J. Am. Chem. Soc.* **1999,** *121*, 8407-8408.

58. Montalbetti, C. A. G. N.; Falque, V., Amide bond formation and peptide coupling. *Tetrahedron* **2005,** *61*, 10827-10852.

59. Knorr, R.; Trzeuak, A.; Bannwarth, W.; Gillessen, D., New coupling reagents in peptide chemistry. *Tetrahedron Lett.* **1999,** *30*, 1927.

60. Carpino, L. A., 1-hydroxy-7-azabenzotriazole. *J. Am. Chem. Soc.* **1993,** *115*, 4397-4398.

61. Angell, Y. M.; Garcia-Echeverria, C.; Rich, D. H., Comparative studies of the coupling of N-methylated, sterically hindered amino acids during solid-phase peptide synthesis. *Tetrahedron Lett.* **1994,** *35*, 5981-5984.

62. Ye, Y. H.; Li, H.; Jiang, X., DEPBT as an efficient coupling reagent for amide bond formation with remarkable resistance to racemization. *Biopolymers* **2004,** *80* (2-3), 172-178.

63. Liu, P.; Sun, B.-y.; Chen, X.-h.; Tian, G.-l.; Ye, Y.-h., Application of DEPBT for synthesis of N-protected peptide alcohols and its derivatives. *Synth. Comm.* **2002,** *32* (3), 473-480.

64. Lambert, J. N.; Mitchell, J. P.; Roberts, K. D., The synthesis of cyclic peptides. *J. Chem. Soc. Perkin Trans. 1* **2001**, 471-484.

65. Li, P.; Roller, P. P., Cyclization strategies in peptide derived drug design. *Curr. Top. Med. Chem.* **2002,** *2*, 325-341.

66. Styers, T. J.; Rodriguez, R. A.; Pan, P.-S.; McAlpine, S. R., High-yielding macrocyclization conditions used in the synthesis of novel Sansalvamide A derivatives. *Tetrahedron Lett.* **2006,** *47*, 515-517.

67. Laitinen, O. H.; Hytonen, V. P.; Nordlund, H. R.; Kulomaa, M. S., Genetically engineered avidins and streptavidins. *Cell. Mol. Life Sci.* **2006,** *63*, 2992-3017.

68. Wilchek, M.; Bayer, E. A., The avidin-biotin complex in bioanalytical applications. *Anal. Biochem.* **1988,** *171*, 1-32.

69. Wilchek, M.; Bayer, E. A., Introduction to avidin-biotin technology. *Methods Enzymol.* **1990,** *184*, 5-13.

70. Merrifield, R. B., Solid Phase Peptide Synthesis. I. The synthesis of a tetrapeptide. *J. Am. Chem. Soc.* **1963,** *85* (14), 2149-2154.

71. Hall, D. G.; Manku, S.; Wang, F., Solution- and solid-phase strategies for the design, synthesis, and screening of libraries based on natural product templates: A comprehensive study. *J. Combi. Chem.* **2001,** *3*, 125-150.

72. Thompson, L. A.; Ellman, J. A., Synthesis and applications of small molecule libraries. *Chem. Rev.* **1996,** *96*, 555-600.

73. Fields, G. B., Solid-phase peptide synthesis. In *Molecular Biomethods Handbook*, Rapley, R.; Walker, J. M., Eds. Humana Press Inc: Totowa, NJ, 1998; pp 527-545.

74. Sellers, R. P.; Alexander, L. D.; Johnson, V. A.; Lin, C.-C.; Savage, J.; Corral, R.; Moss, J.; Slugocki, T. S.; Singh, E. K.; Davis, M. R.; Ravula, S.; Spicer, J. E.; Oelrich, J. L.; Thornquist, A.; Pan, C.-M.; McAlpine, S. R., Design and synthesis of Hsp90 inhibitors: Exploring the SAR of Sansalvamide A derivatives. *Bio. Med. Chem.* **2010,** *18*, 6822- 6856.

75. Siegel, R.; Naishadham, D.; Jemal, A., Cancer statistics, 2012. *CA Cancer J. Clin.* **2012,** *62* (1), 10-29.

76. Hidalgo, M., Pancreatic Cancer. *N Engl J Med* **2010,** *362* (17), 1605-1617.

77.http://www.atcc.org/ATCCAdvancedCatalogSearch/ProductDetails/tabid/452/Default.aspx?ATCCNum=CRL-2558&Template=cellBiology.

78. Caldas, C.; Hahn, S. A.; da Costa, L. T.; Redston, M. S.; Schutte, M.; Seymour, A. B.; Weinstein, C. L.; Hruban, R. H.; Yeo, C. J.; Kern, S. E., Frequent somatic mutations and homozygous deletions of the p16 (MTS1) gene in pancreatic adenocarcinoma. *Nat. Genet.* **1994,** *8* (1), 27-32.

79. Jaffee, E. M.; Schutte, M.; Gossett, J.; Adler, A. J.; Thomas, M.; Greten, T. F.; Hruban, R. H.; Yeo, C. J.; Griffin, C. A., Development and characterization of a cytokine-secreting pancreatic adenocarcinoma vaccine from primary tumors for use in clinical trials. *Cancer J. Sci. Am.* **1998,** *4* (3), 194-203.

80. Boland, C. R.; Goel, A., Microsatellite instability in colorectal cancer. *Gastroenterology* **2010,** *138*, 2073-2087.

81. Ionov, Y.; Peinado, M. A.; Malkhosyan, S.; Shibata, D.; Perucho, M., Ubiquitous somatic mutations in simple repeated sequences reveal a new mechanism for colonic carcinogenesis. *Nature* **1993,** *363*, 558-561.

82. Sinicrope, F. A.; Sargent, D. J., Molecular pathways: Microsatellite instability in colorectal cancer: Prognostic, predictive, and therapeutic implications. *Clin Cancer Res* **2012,** *18*, 1506-1512.

83. Camps, J.; Armengol, G.; del Rey, J.; Lozano, J. J.; Vauhkonen, H.; Prat, E.; Egozcue, J.; Sumoy, L.; Knuutila, S.; Miro, R., Genome-wide differences between microsatellite stable and unstable colorectal tumors. *Carcinogenesis* **2005,** *27* (3), 419-428.

84. Ahern, T.; Taylor, G. A.; Sanderson, C. J., An evaluation of an assay for DNA synthesis in lymphocytes with [3H]thymidine and harvesting on to glass fibre filter discs. *J. Immunol. Methods* **1976,** *10*, 329-336.

85. Fink, R. M.; Fink, K., Relative retention of H3 and C14 labels of nucleosides incorporated into nucleic acids of neurospora. *J. Biol. Chem.* **1962,** *237* (9), 2889-2891.

86. Knudsen, R. C.; Ahmed, A. A.; Sell, K. W., An in vitro microassay for lymphotoxin using microculture plates and the multiple automated sample harvester. *J. Immunol. Methods* **1974,** *5*, 55-63.

87. Painter, R. B.; Drew, R. M.; Rasmussen, R. E., Limitations in the use of carbon-labeled and tritium-labeled thymidine in cell culture studies. *Radiation Research* **1964,** *21* (3), 355-366.

88. Otrubova, K.; Lushington, G. H.; Vander Velde, D.; McGuire, K. L.; McAlpine, S. R., A comprehensive study of Sansalvamide A derivatives and their structure-activity relationships against drug-resistant colon cancer cell lines. *J. Med. Chem.* **2008,** *51*, 530-544.

89. Pan, P. S.; Vasko, R. C.; Lapera, S. A.; Johnson, V. A.; Sellers, R. P.; Lin, C.-C.; Pan, C.-M.; Davis, M. R.; Ardi, V. C.; McAlpine, S. R., A comprehensive study of Sansalvamide A derivatives: their structure-activity relationships and their binding mode to Hsp90. *Bio. Org. Med. Chem* **2009,** *17*, 5806-5825.

90. Rodriguez, R. A.; Pan, P.-S.; Pan, C.-M.; Ravula, S.; Lapera, S. A.; Singh, E. K.; Styers, T. J.; Brown, J. D.; Cajica, J.; Parry, E.; Otrubova, K.; McAlpine, S. R., Synthesis of Second Generation Sansalvamide A derivatives: Novel Templates as Potent Anti-tumor Agents. *J. Org. Chem.* **2007,** *72*, 1980-2002.

91. Berridge, M. V.; Tan, A. S.; McCoy, K. D.; Wang, R., The biochemical and cellular basis of cell proliferation assays that use tetrazolium salts. *Biochemica* **1996,** (4), 14-19.

92. Bounous, D. I.; Campagnoli, R. P.; Brown, J., Comparison of MTT colorimetric assay and tritiated thymidine uptake for lymphocyte proliferation assays using chicken splenocytes. *Avian Dieseases* **1992,** *36* (4), 1022-1027.

93. Heller, M.; Sukopp, M.; Tsomaia, N.; John, M.; Mierke, D. F.; Reif, B.; Kessler, H., The conformation of cyclo(-Dpro-ala-) as a model for cyclic pentapeptides of the DL type. *J. Am. Chem. Soc.* **2006,** *128*, 13806-13814.

94. Boyer, J.; McLean, E. G.; Aroori, S.; al., E., Characterization of P53 wild-type and null isogenic colorectal cancer cell lines resistant to 5-fluorouracil, oxaliplatin, and irinotecan. *Clin. Cancer. Res.* **2004,** *10*, 2158-2167.

95. Power, C.; Fanning, N.; Redmond, H. P., Cellular apoptosis and organ injury in sepsis: a review. *Shock* **2002,** *18* (3), 197-211.

96. Ziegler, U.; Groscurth, P., Morphological features of cell death. *News Physiol. Sci.* **2004,** *19*, 124-128.

97. O'Brien, M. A.; Kirby, R., Apoptosis: A review of pro-apoptotic and anti-apoptotic pathways and dysregulation in disease. *J. Vet. Emergency and Critical Care* **2008,** *18* (6), 572-585.

98. Kanduc, D.; Mittelman, A.; Serpico, R.; Sinigaglia, E.; Sinha, A. A.; Natale, C.; Santacroce, R.; Di Corcia, M. G.; Lucchese, A.; Dini, L.; Pani, P.; Santacroce, S.; Simone, S.; Bucci, R.; Farber, E., Cell death: apoptosis versus necrosis (review). *Int. J. Oncol.* **2002,** *21* (1), 165-170.

99. Elmore, S., Apoptosis: A review of programmed cell death. *Toxicol. Pathol.* **2007,** *35* (4), 495-516.

100. Saraste, A.; Pulkki, K., Morphologic and biochemical hallmarks of apoptosis. *Cardio. Res.* **2000,** *45*, 528-537.

101. Soldani, C.; Scovassi, A. I., Poly(ADP-ribose) polymerase-1 cleavage during apoptosis: An update. *Apoptosis* **2002,** *7*, 321-328.

102. Wesierska-Gadek, J.; Gueorguieva, M.; Wojciechowski, J.; Tudzarova-Trajkovska, S., In vivo activated caspase-3 cleaves PARP-1 in rat liver after administration of the hepatocarcinogen *N*-Nitrosomorpholine (NNM) generating the 85 kDa fragment. *J. Cell. Biochem.* **2004,** *93*, 774-787.

103. Duriez, P. J.; Shah, G. M., Cleavage of poly(ADP-ribose) polymerase: a sensitive parameter to study cell death. *Biochem. Cell. Biol.* **1997,** *75*, 337-349.

104. Nakahara, T.; Takeuchi, M.; Kinoyama, I.; Minematsu, T.; Shirasuna, K.; Matsuhisa, A.; Kita, A.; Tominaga, F.; Yamanaka, K.; Kudoh, M.; Sasamata, M., YM155, a novel small-molecule survivin suppressant, induces regression of established human hormone-refractory prostate tumor xenografts. *Cancer Res.* **2007,** *67*, 8014-8021.

105. Watanabe, M.; Hitomi, M.; van der Wee, K.; Rothenberg, F.; Fisher, S. A.; Zucker, R.; Svoboda, K. K. H.; Goldsmith, E. C.; Heiskanen, K. M.; Nieminen, A.-L.,

The pros and cons of apoptosis assays for use in the study of cells, tissues, and organs. *Microsc. Microanal.* **2002,** *8*, 375-391.

106. Zobel, K.; Wang, L.; Varfolomeev, E.; Franklin, M. C.; Elliott, L. O.; Wallweber, H. J. A.; Okawa, D. C.; Flygare, J. A.; Vucic, D.; Fairbrother, W. J.; Deshayes, K., Design, synthesis, and biological activity of a potent smac mimetic that sensitizes cancer cells to apoptosis by antagonizing IAPs. *ACS Chem. Biol.* **2006,** *1* (8), 525-533.

107. Sato, S.-i.; Murata, A.; Shirakawa, T.; Uesugi, M., Biochemical target isolation for novices: Affinity-based strategies. *Chem. & Biol.* **2010,** *17*, 616-622.

108. Terstappen, G. C.; Schlupen, C.; Raggiaschi, R.; Gaviraghi, G., Target deconvolution strategies in drug discovery. *Nat. Rev. Drug Discov.* **2007,** *6*, 891-903.

109. Lomenick, B.; Olsen, R. W.; Huang, J., Identification of direct protein targets of small molecules. *ACS Chem. Biol.* **2011,** *6* (1), 34-46.

110. Vasko, R. C.; Rodriguez, R.; Ardi, V.; Cunningham, C.; Agard, D. A.; McAlpine, S. R., Mechanistic studies of Sansalvamide A peptide: an allosteric modulator of Hsp90. *ACS Med. Chem. Lett.* **2010,** *1* (1), 4-8.

111. Kunicki, J. B.; Petersen, M. N.; Alexander, L. D.; Ardi, V. C.; McConnell, J. R.; McAlpine, S. R., Synthesis and evaluation of biotinylated sansalvamide A analogs and their modulation of Hsp90. *Bioorg. Med. Chem. Lett.* **2011,** *21* (16), 4716-4719.

112. Shelton, S. N.; Shawgo, M. E.; Matthews, S. B.; Lu, Y.; Donnelly, A. C.; Szabla, K.; Tanol, M.; Vielhauer, G. A.; Rajewski, R. A.; Matts, R. L.; Blagg, B. S. J.; Robertson, J. D., KU135, a novel novobiocin-derived c-terminal inhibitor of the 90-kDa heat shock protein, exerts potent antiproliferative effects in human leukemic cells. *Molecular Pharmacology* **2009,** *76*, 1314- 1322.

113. Southworth, D. R.; Agard, D. A., Species-dependent ensembles of conserved conformational states define the Hsp90 chaperone ATPase cycle. *Mol. Cell.* **2008,** *32*, 631-640.

114. Le Brazidec, J. Y.; Kamal, A.; Busch, D.; Thao, L.; Zhang, L.; Timony, G.; Grecko, R.; Trent, K.; Lough, R.; Salazar, T.; Khan, S.; Burrows, F.; Boehm, M. F., Synthesis and biological evaluation of a new class of geldanamycin derivatives as potent inhibitors of Hsp90. *J. Med. Chem.* **2004,** *47* (15), 3865-73.

115. Sato, S.; Fujita, N.; Tsuruon, T., Modulation of Akt kinase activity by binding to Hsp90. *Proc. Nat. Acad. Sci.* **2000,** *97* (20), 10832-10837.

116. Miller, P.; DiOrio, C.; Moyer, M.; Schnur, R.; Bruskin, A.; Cullen, W.; Moyer, J., Depletion of the *erb*B-2 gene product p185 by benzoquinoid ansamycins. *Cancer Res.* **1994,** *54*, 2724-2730.

117. Slamon, D.; Clark, G.; Wong, S.; Levin, W.; Ullrich, A.; McGuire, W., Human breast cancer: correlation of relapse and survival with amplification of the HER-2/neu oncogene. *Science* **1987,** *235* (4785), 177-182.

118. Basso, A. D.; Solit, D. B.; Munster, P. N.; Rosen, N., Ansamycin antibiotics inhibit Akt activation and cyclin D expression in breast cancer cells that over-express HER2. *Oncogene* **2002,** *21,* 1159-1166.

119. Zhong, H.; De Marzo, A.; Laughner, E.; Lim, M.; Hilton, D.; Zagzag, D.; Buechler, P.; Isaacs, W.; Semenza, G.; Simons, J., Overexpression of hypoxia-inducible factor 1a in common human cancers and their metastases. *Cancer Res.* **1999,** *59,* 5830-5835.

120. Chakraborty, A.; Koldobskiy, M. A.; Sixt, K. M.; Juluri, K.; Mustafa, A. K.; Snowman, A. M.; van Rossum, D. B.; Patterson, R. L.; Snyder, S. H., Hsp90 regulates cell survival via inositol hexakisphosphate kinase-2. *PNAS* **2008,** *105,* 1134-1139.

121. Allan, R.; Mok, D.; Ward, B.; Ratajczak, T., Modulation of chaperone function and cochaperone interaction by novobiocin in the c-terminal domain of Hsp90. *J. Biol. Chem.* **2006,** *281* (11), 7161-7171.

122. Blatch, G. L.; Lassle, M., The tetratricopeptide repeat: a structural motif mediating protein-protein interactions. *BioEssays* **1999,** *21,* 932-939.

123. D'Andrea, L. D.; Regan, L., TPR proteins: the versatile helix. *Trends in Biochem. Sci.* **2003,** *28* (12), 655-662.

124. Das, A. K.; Cohen, P. T. W.; Barford, D., The structure of the tetratricopeptide repeats of protein phosphatase 5: implications for TPR-mediated protein-protein interactions. *EMBO J* **1998,** *17* (5), 1192-1199.

125. Ramsey, A. J.; Russell, L. C.; Chinkers, M., C-terminal sequences of hsp70 and hsp90 as non-specific anchors for tetratricopeptide repeat (TPR) proteins. *Biochem. J.* **2009,** *423,* 411-419.

126. Ramsey, A. J.; Russell, L. C.; Whitt, S. R.; Chinkers, M., Overlapping sites of tetratricopeptide repeat protein binding and chaperone activity in heat shock protein 90. *J. Biol. Chem.* **2000,** *275* (23), 17857-17862.

127. Russell, L. C.; Whitt, S. R.; Chen, M.-S.; Chinkers, M., Identification of conserved residues required for the binding of a tetratricopeptide repeat domain to heat shock protein 90. *J. Biol. Chem.* **1999,** *274* (29), 20060-20063.

128. Ratajczak, T.; Ward, B.; Cluning, C.; Allan, R., Cyclophilin 40: An Hsp90-cochaperone associated with apo-steroid receptors. *Int. J. Biochem. & Cell. Bio.* **2009,** *41,* 1652-1655.

129. Ahmad, N.; Kuman, R., Steroid hormone receptors in cancer development: A target for cancer therapeutics. *Cancer Lett.* **2011,** *300*, 1-9.

130. Pratt, W.; Galigniana, M.; Harrell, J.; DeFranco, D., Role of hsp90 and the hsp90-binding immunophilins in signalling protein movement. *Cell Sig.* **2004,** *16*, 857-872.

131. Edlich, F.; Weiwad, M.; Erdmann, F.; Fanghanel, J.; Jarczowski, F.; Rahfeld, J.-U.; Fischer, G., Bcl-2 regulator FKBP38 is activated by Ca^{2+}/ calmodulin. *EMBO J* **2005,** *24*, 2688-2699.

132. Edlich, F.; Erdmann, F.; Jarczowski, F.; Moutty, M.-C.; Weiwad, M.; Fischer, G., The Bcl-2 regulator FKBP38-Calmodulin-Ca^{2+} is inhibited by Hsp90. *J. Biol. Chem.* **2007,** *282* (21), 15341-15348.

133. Wegele, H.; Wandinger, S.; Schmid, A.; Reinstein, J.; Buchner, J., Substrate transfer from the chaperone Hsp70 to Hsp90. *J. Mol. Biol.* **2006,** *356*, 802-811.

134. Odunuga, O.; Longshaw, V.; Blatch, G., Hop: more than an Hsp70/Hsp90 adaptor protein. *BioEssays* **2004,** *26*, 1058-1068.

135. Wegele, H.; Muller, L.; Buchner, J., Hsp70 and Hsp90--a relay team for protein folding. *Rev. Physiol. Biochem. Pharmacol.* **2004,** *15*, 1-44.

136. Barral, J.; Hutagalung, A.; Brinker, A.; Hartl, F.; Epstein, H., Role of the myosin assembly protein UNC-45 as a molecular chaperone for myosin. *Science* **2002,** *295*, 669-671.

137. Yu, Q.; Bernstein, S. I., UCS proteins: Managing the myosin motor. *Curr. Biol.* **2003,** *13*, R525-R527.

138. Liu, L.; Srikakulam, R.; Winkelmann, D. A., Unc45 activates Hsp90-dependent folding of the myosin motor domain. *J. Biol. Chem.* **2008,** *283* (19), 13185-13193.

139. Pratt, W. B.; Toft, D. O., Regulation of signaling protein function and trafficking by the hsp90/hsp70-based chaperone machinery. *Experimental Biology and Medicine* **2003,** *228*, 111-133.

140. Chadli, A.; Felts, S. J.; Wang, Q.; Sullivan, W. P.; Botuyan, M. V.; Fauq, A.; Ramirez-Alvarado, M.; Mer, G., Celastrol inhibits Hsp90 chaperoning of steroid receptors by inducing fibrillization of the co-chaperone p23. *J. Biol. Chem.* **2010,** *285* (6), 4224-4231.

141. Forafonov, F.; Toogun, O.; Grad, I.; Suslova, E.; Freeman, B.; Picard, D., p23/Sba1p protects against Hsp90 inhibitors independently of its intrinsic chaperone activity. *Mol. Cell. Biol.* **2008,** *28* (10), 3446-3456.

142. Marcu, M. G.; Schulte, T. W.; Neckers, L., Novobiocin and related coumarins and depletion of heat shock protein 90-dependent signaling proteins. *J.. Natl. Cancer Inst.* **2000,** *92*, 242-248.

143. Burlison, J.; Blagg, B., Synthesis and evaluation of coumermycin A1 analogues that inhibit the Hsp90 protein folding machinery. *Org Lett* **2006,** *8* (21), 4855-4858.

144. Hadden, M. K.; Blagg, B. S. J., Dimeric approaches to anti-cancer chemotherapeutics. *Anti-Cancer Agents in Medicinal Chemistry* **2008,** *8*, 807-816.

145. Wayne, N.; Bolon, D. N., Dimerization of Hsp90 is required for in vivo function. Design and analysis of monomers and dimers. *J Biol Chem* **2007,** *282* (48), 35386-95.

146. Rackovsky, S.; Scheraga, H. A., Intermolecular anti-parallel B sheet: Comparison of predicted and observed conformations of gramicidin S. *Proc. Natl. Acad. Sci. USA* **1980,** *77* (12), 6965-6967.

147. Katsu, T.; Kobayashi, H.; Fujita, Y., Mode of action of gramicidin S on *Escherichia coli* membrane. *Biochim. Biophys. Acta* **1986,** *860*, 608-619.

148. Le Tourneau, C.; Raymond, E.; Faivre, S., Reports of Clinical Benefit of Plitidepsin (Aplidine), a New Marine-Derived Anticancer Agent, in Patients With Advanced Medullary Thyroid Carcinoma

Curr. Pharm. Des. **2007,** *13*, 3427-3429.

149. Starzl, T. E.; Klintmalm, G. B.; Porter, K. A.; Iwatsuki, S.; Schroter, G. P., Liver transplantation with use of cyclosporin a and prednisone

New England Journal of Medicine **1981,** *305*, 266-269.

150. Davis, M. R.; Styers, T. J.; Rodriguez, R. A.; Pan, P.-S.; Vasko, R. C.; McAlpine, S. R., Synthesis and cytotoxicity of a new class of potent decapeptide macrocycles. *Org. Lett.* **2008,** *10*, 177-180.

151. Brady, S. F.; Varga, S. L.; Freidinger, R. M.; Schwenk, D. A.; Mendlowski, M.; Holly, F. W.; Veber, D. F., Practical synthesis of cyclic peptides, with an example of dependence of cyclization yield upon linear sequence. *J. Org. Chem.* **1979,** *44* (18), 3101-3105.

152. Sanchez, E. R., Redmond, T., Scherrer, L.C., Bresnick, E.H., Welsh, M.J., Pratt, W.B., Evidence that the 90 kDa heat shock protein is associated with tubulin-containing complexes in L cell cytosol and in intack PtK cells. *Mol. Endocrinol.* **1988**, 756-760.

153. Koyasu, S. N., E.; Kadowaki, T.; Matsuzaki, F.; Lidia, K.; Harada, F.; Kasuga, M.; Sakai, H.; Yahara, I., Two mammalian heat shock proteins, Hsp90 and Hsp100, are actin-binding proteins. *Proc. Natl. Acad. Sci.* **1986,** *83*, 8054-8058.

154. Fostinis, Y.; Theodoropoylos, P. A.; Gravanis, A.; Stournaras, C., Heat shock protein Hsp90 and its association with the cytoskeleton: A morphological study. *Biochem. Cell. Biol.* **1992,** *70*, 779-786.

APPENDIX A

1H NMR, LCMS, HPLC DATA FOR SANSALVAMIDE A AND DI-SANSALVAMIDE A DERIVATIVES

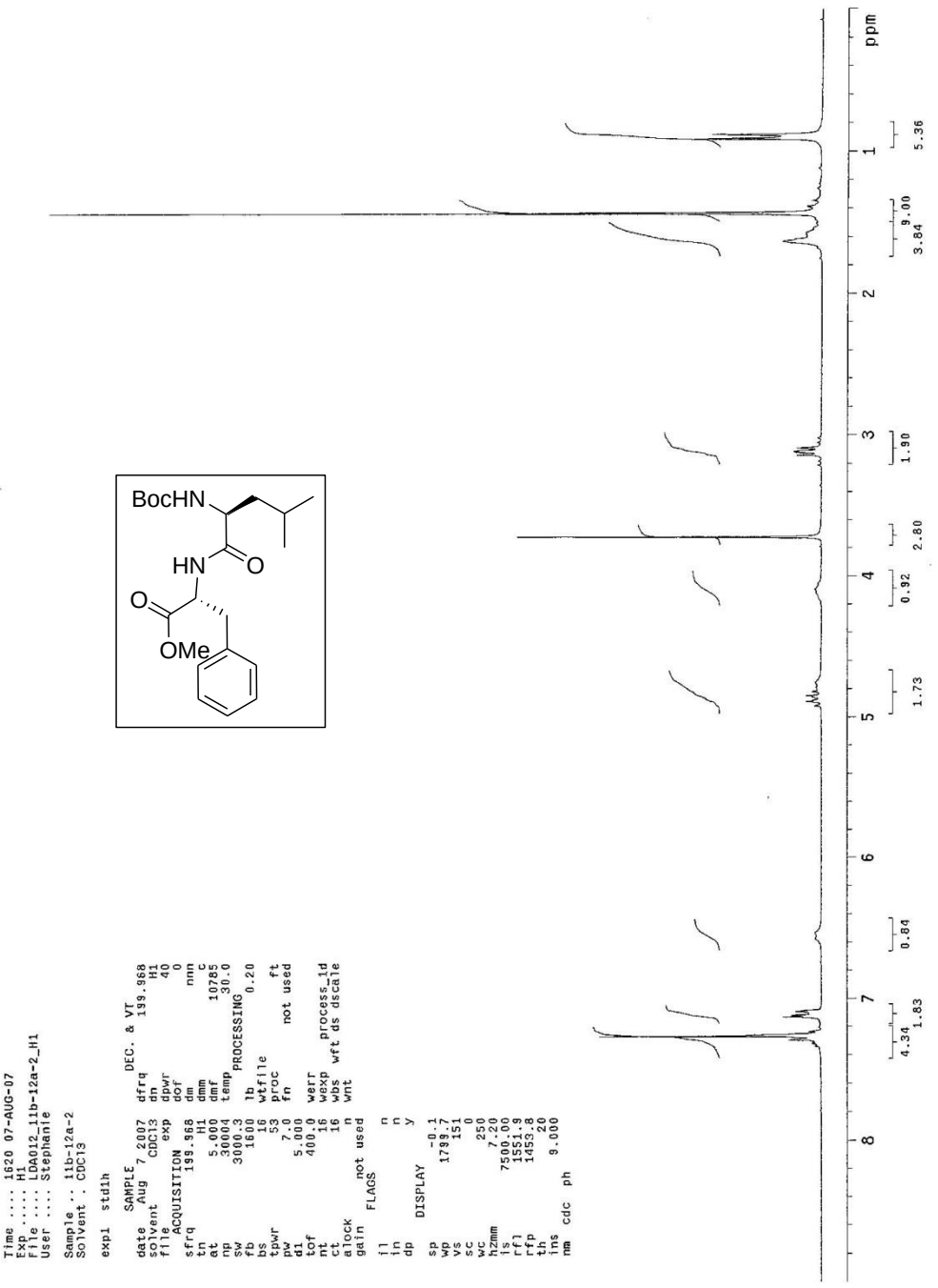

SanA 2 ^{1}H NMR: MeO-D-Phe-Leu-NHBoc

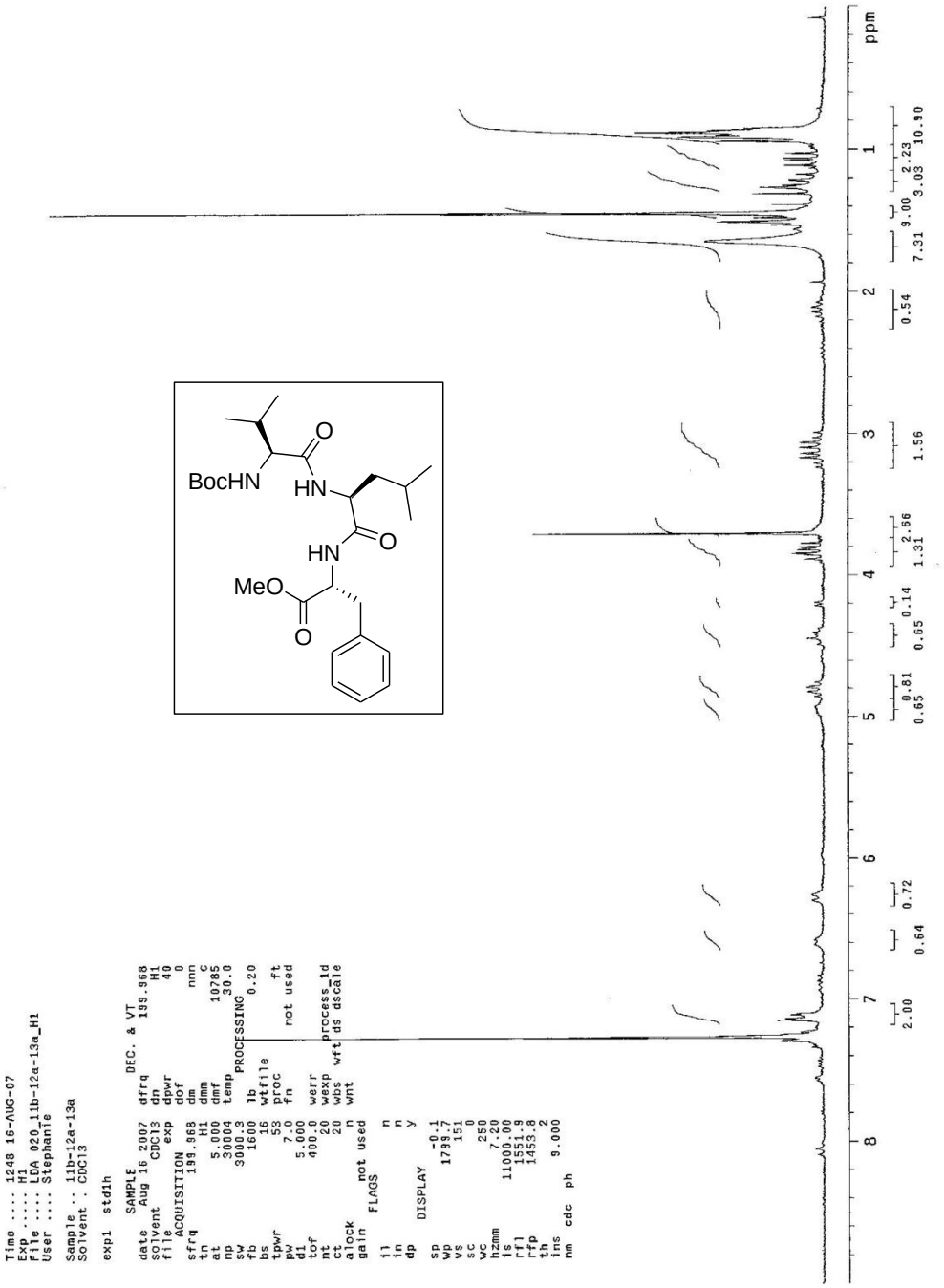

SanA 2 ^{1}H NMR Tripeptide: MeO-D-Phe-Leu-Val-NHBoc

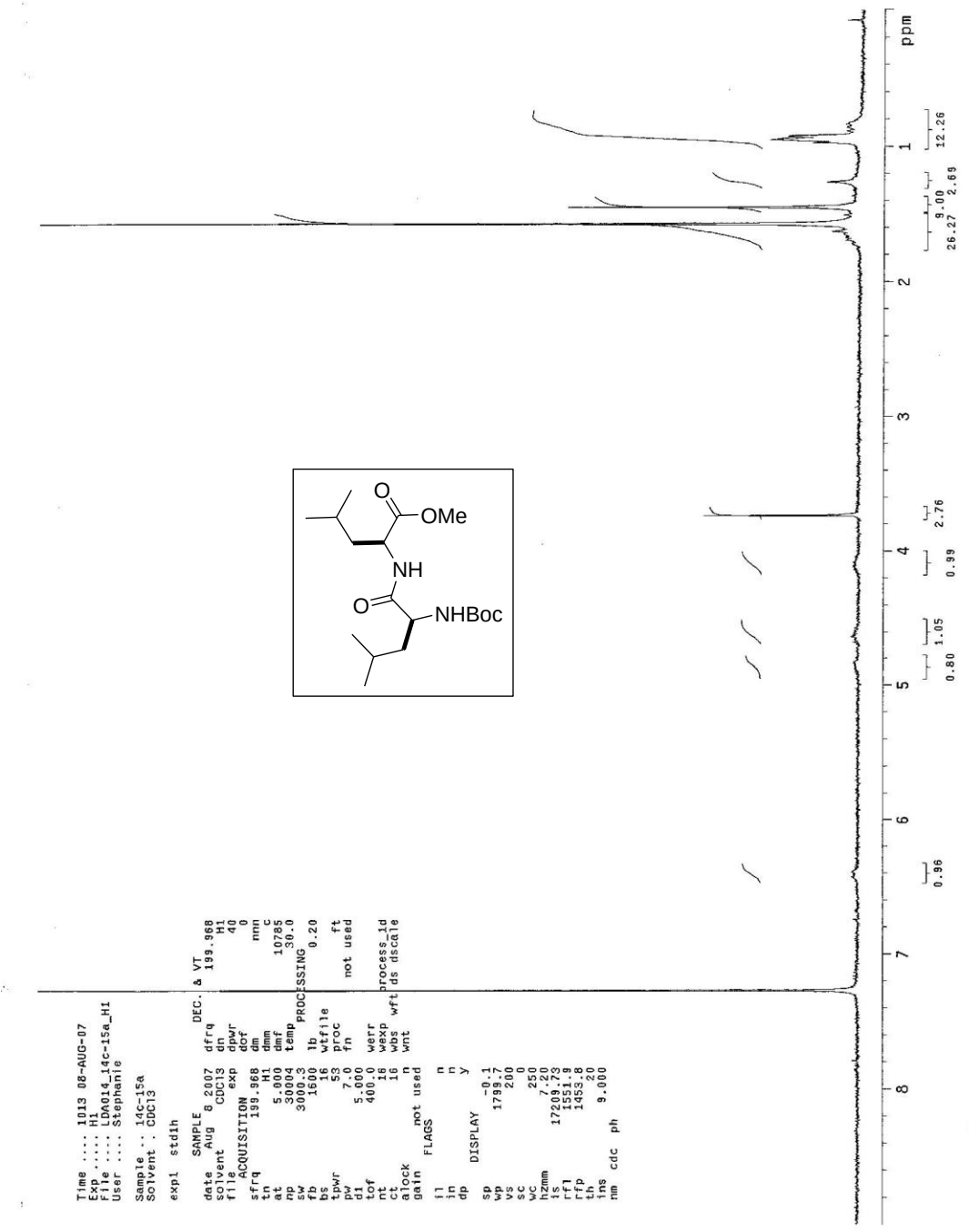

SanA 2 ^{1}H NMR Dipeptide: MeO-Leu-Leu-NHBoc

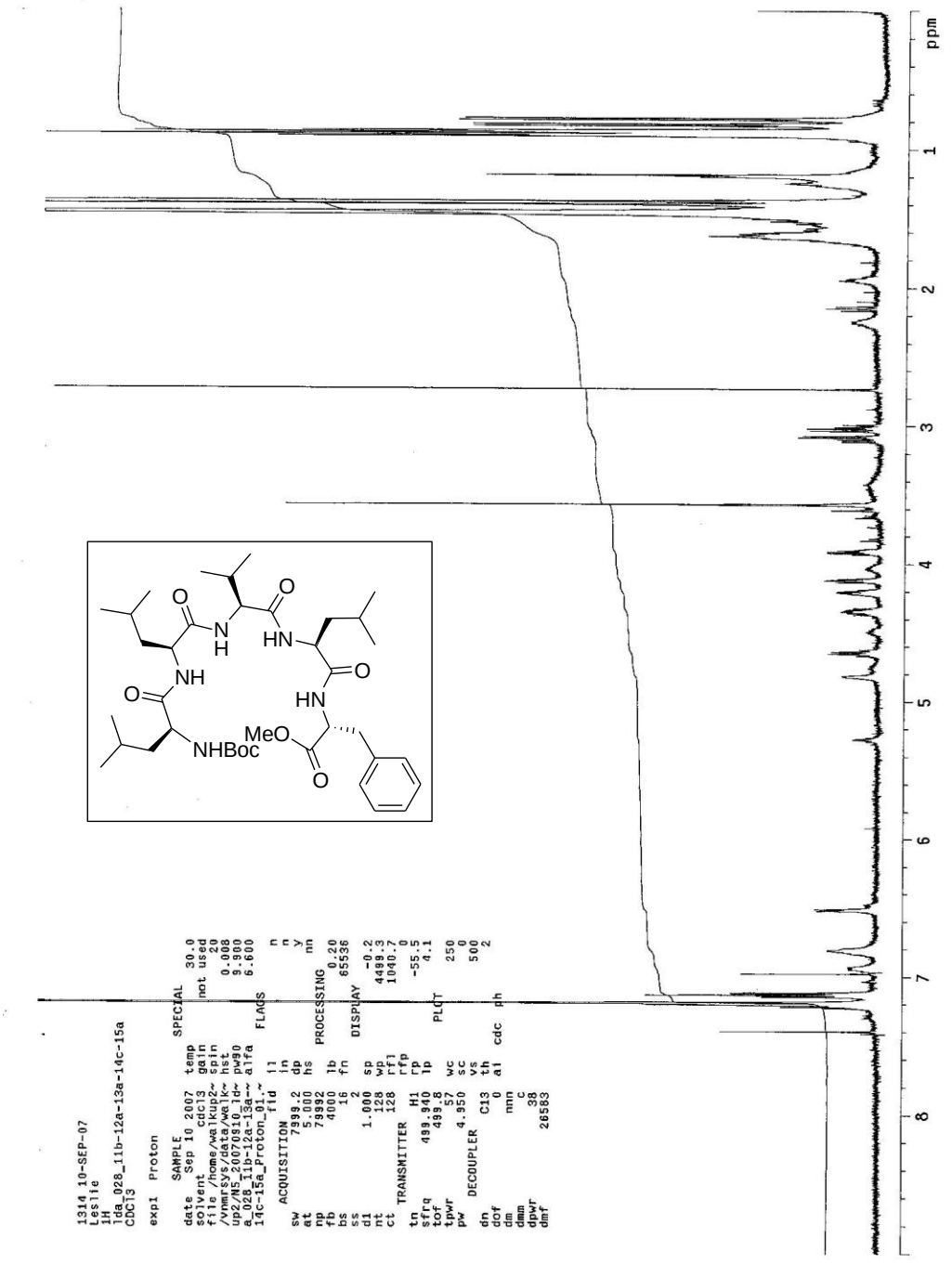

SanA 2 ^{1}H NMR Linear Pentapeptide: MeO-D-Phe-Leu-Val-Leu-Leu-NHBoc

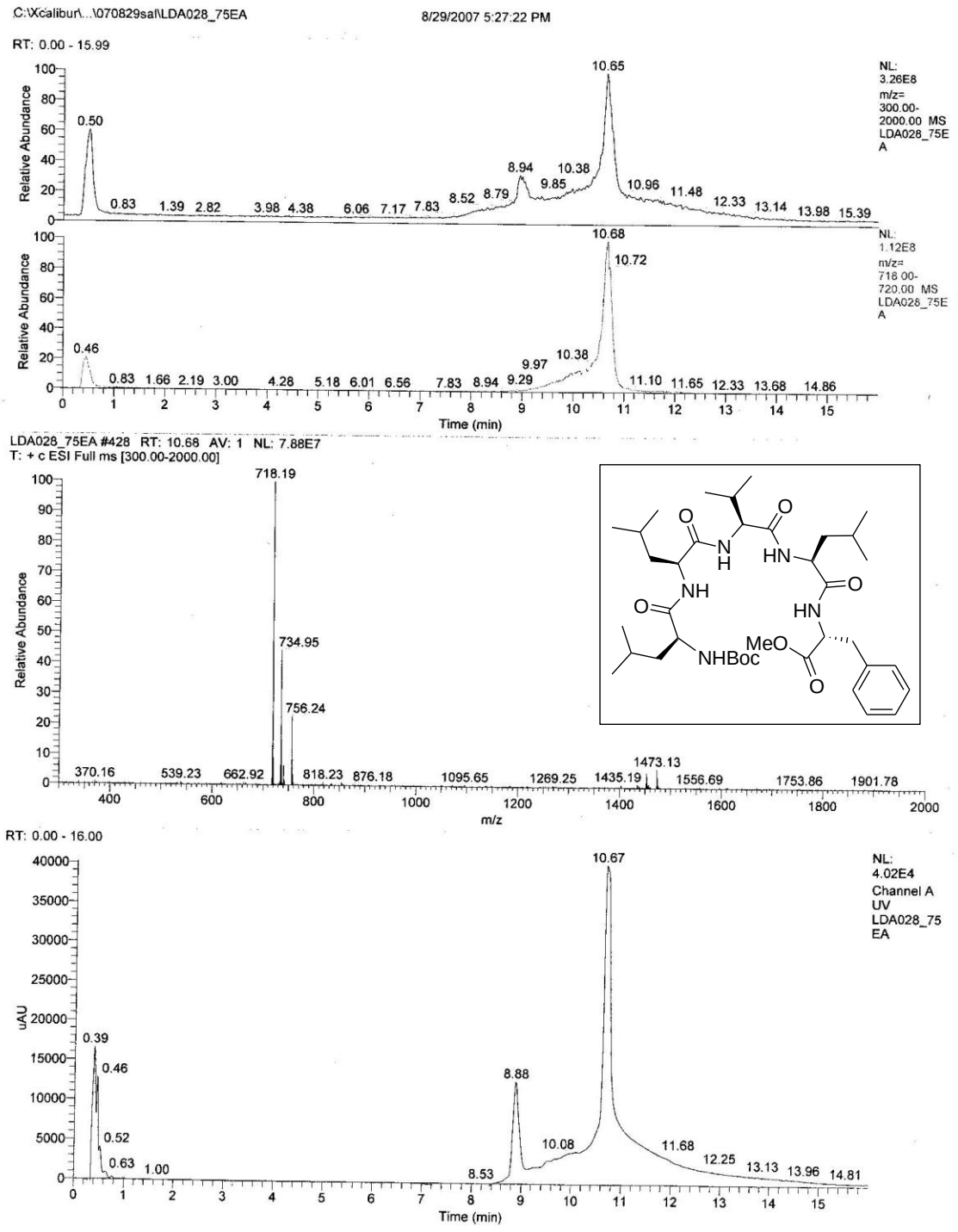

SanA 2 LCMS Linear Pentapeptide: MeO-D-Phe-Leu-Val-Leu-Leu-NHBoc (MW= 718)

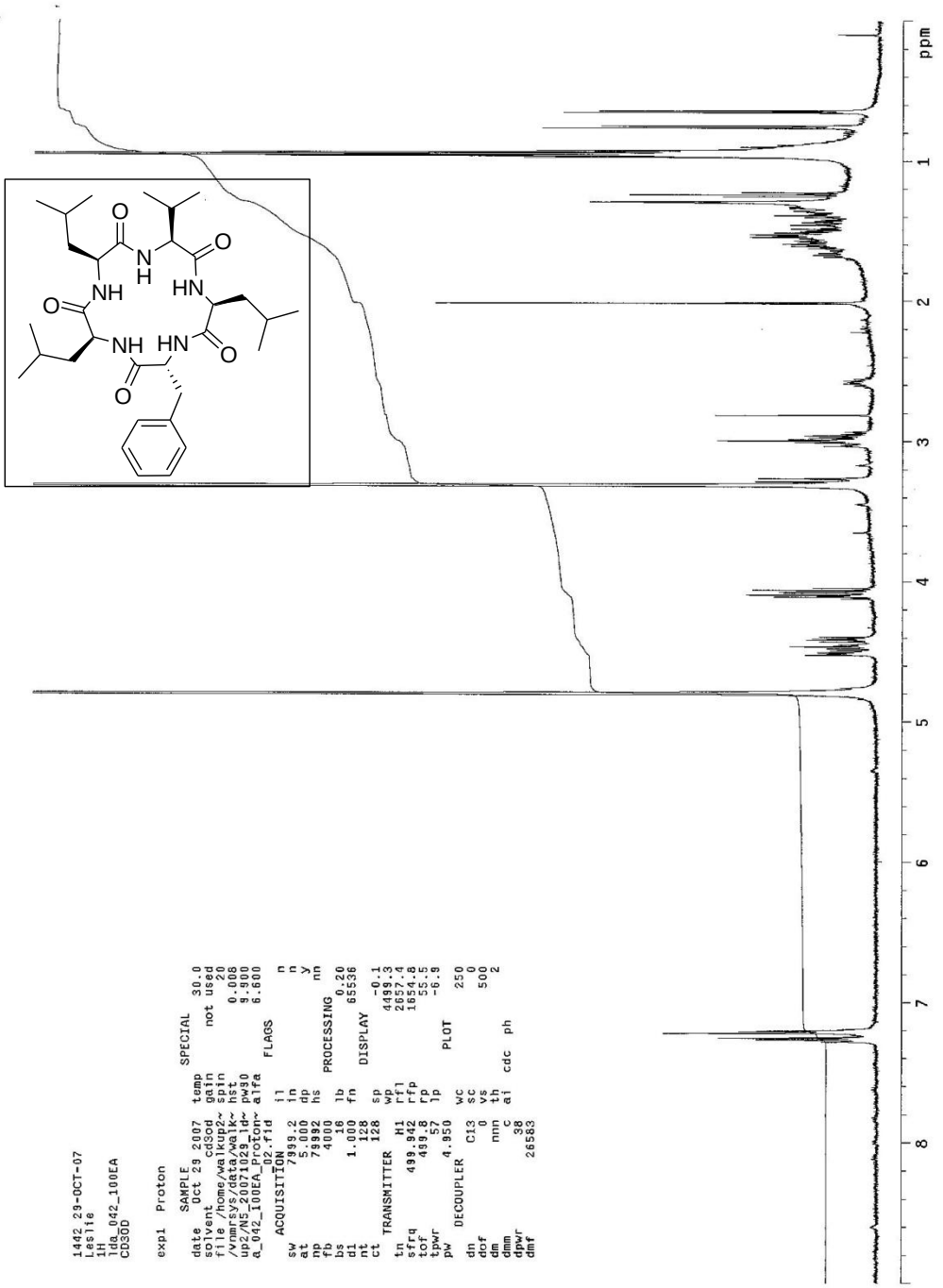

SanA 2 ^{1}H NMR Cyclized Pentapeptide: D-Phe-Leu-Val-Leu-Leu

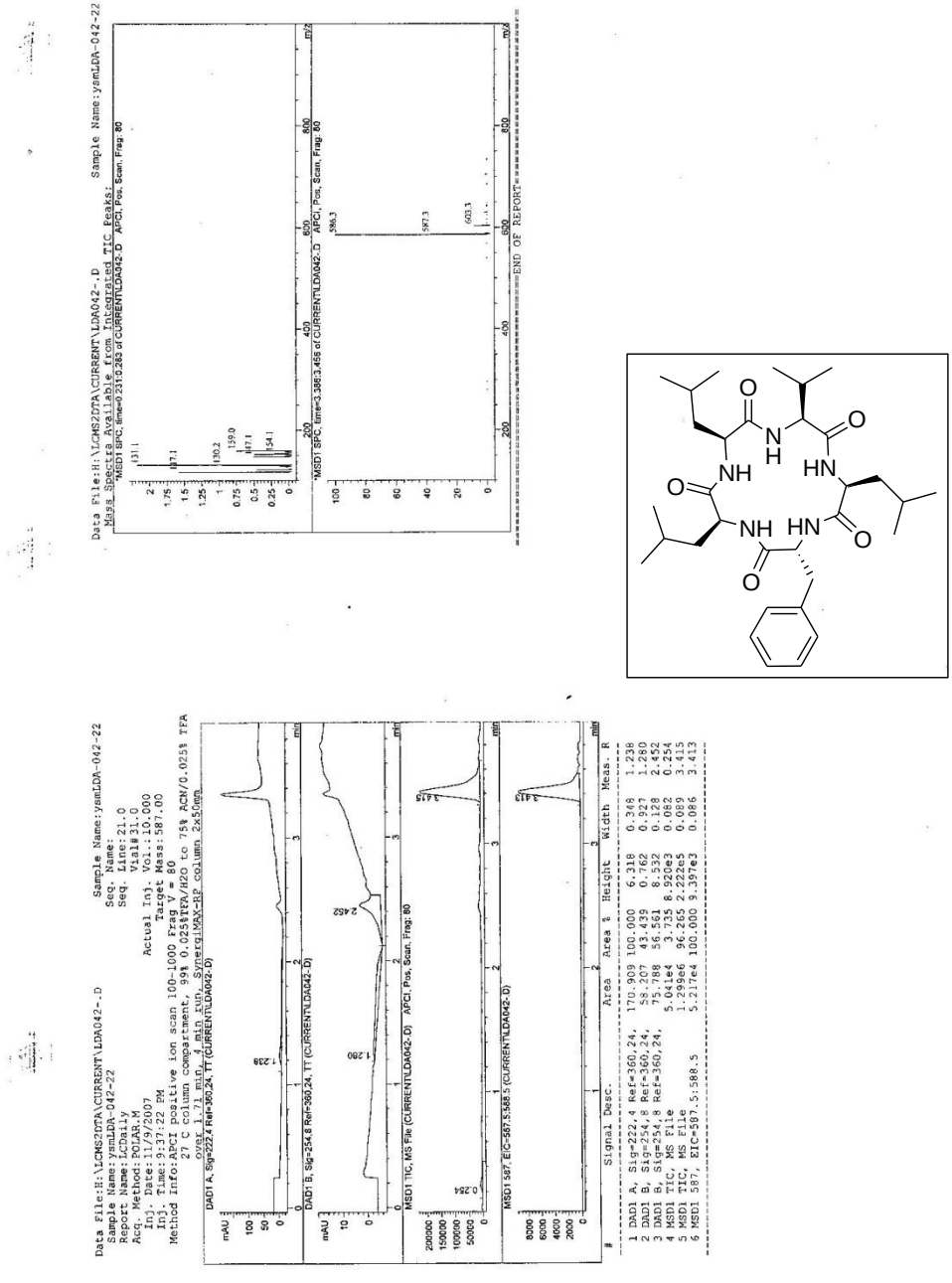

SanA 2 LCMS Cyclized Pentapeptide: D-Phe-Leu-Val-Leu-Leu (MW= 586)

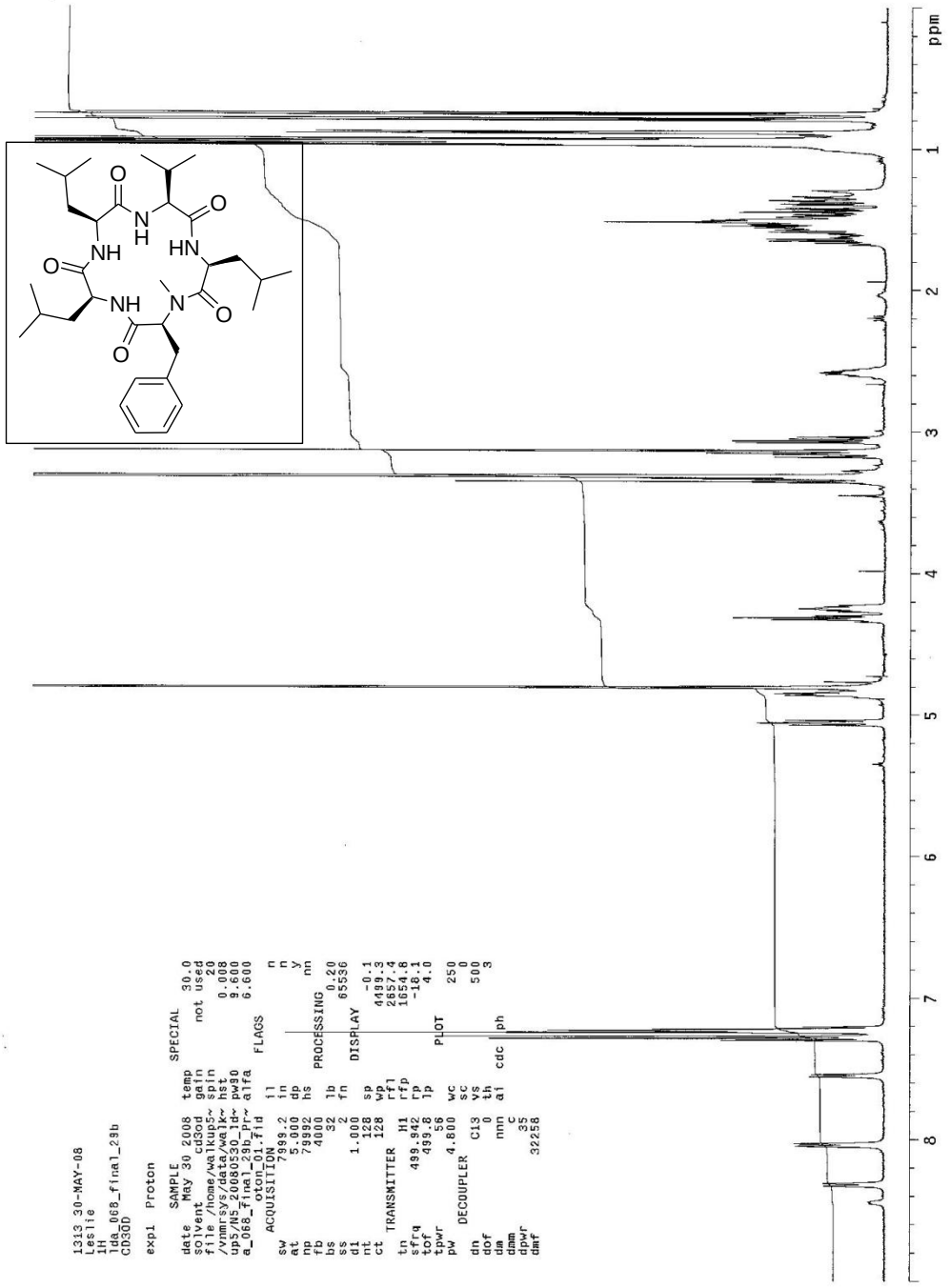

SanA 3 ^{1}H NMR Cyclized Pentapeptide: *N*-Me-Phe-Leu-Val-Leu-Leu

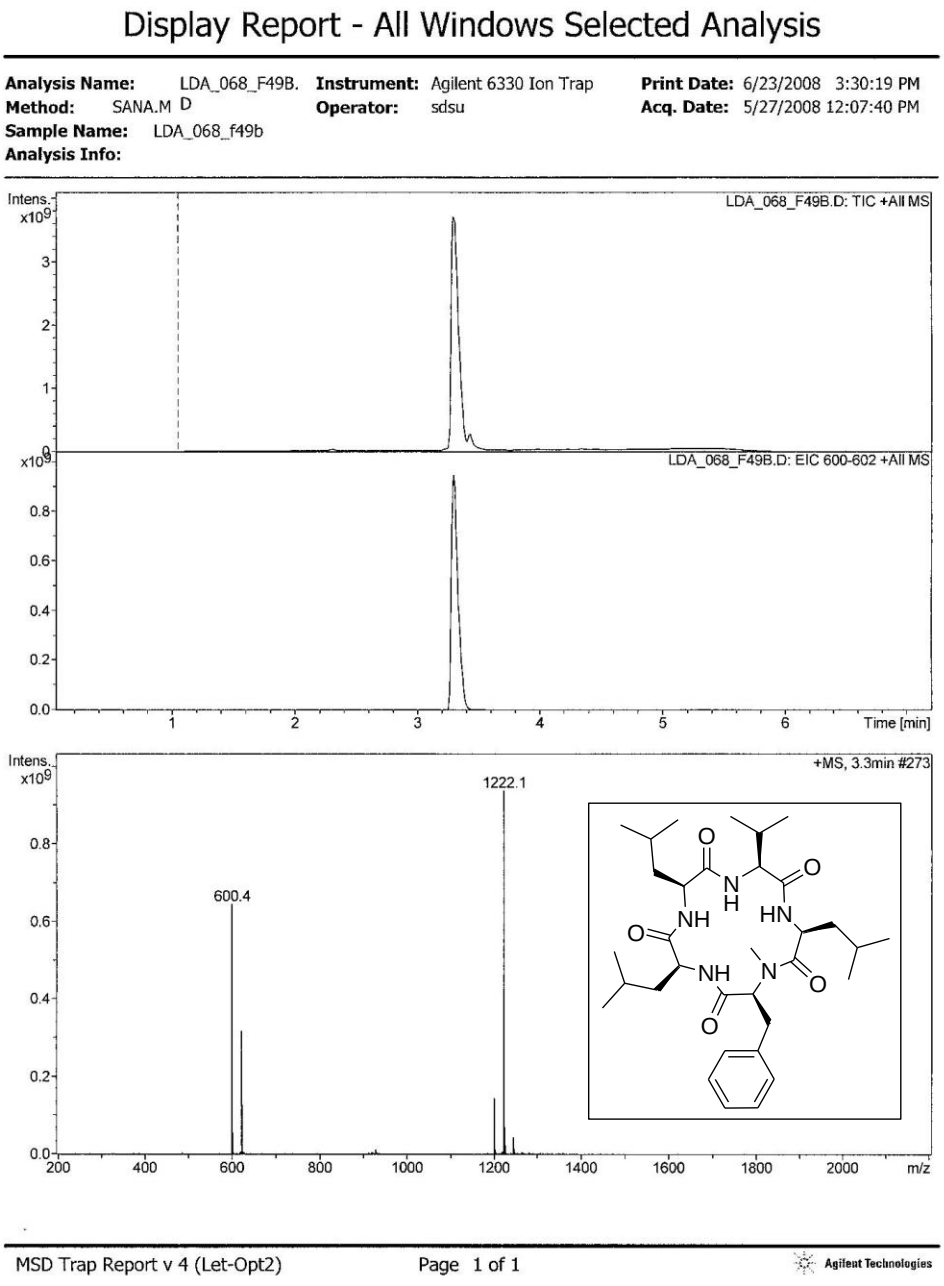

SanA 3 LCMS Cyclized Pentapeptide: *N*-Me-Phe-Leu-Val-Leu-Leu (MW= 600)

San Diego State University; Department of Chemis

Project Name: Defaults
Reported by User: shelli

Breeze

SAMPLE INFORMATION

Sample Name:	LDA_068_29-backup3	Acquired By:	shelli
Sample Type:	Unknown	Sample Set Name:	
Vial:	1	Acq. Method:	PrimarySanA_SS
Injection #:	197	Date Acquired:	6/10/2008 11:17:05 AM
Run Time:	16.00 Minutes	Injection Volume:	25.00 ul

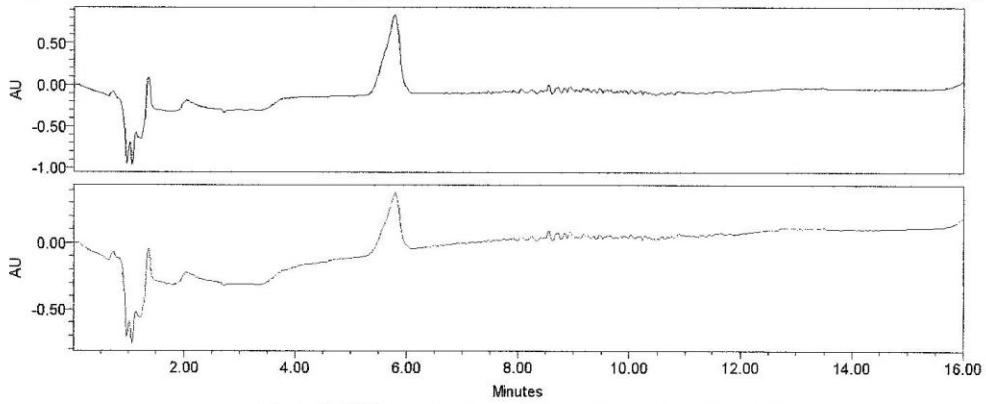

Channel: 2487Channel 1 Channel Desc.: Processing Method: ****
Channel: 2487Channel 2 Channel Desc.: Processing Method: ****

	Peak Name	RT (min)	Area (µV*sec)	% Area	Height (µV)	Amount	Units
1	****	****	****	****	****	****	****
2	****	****	****	****	****	****	****

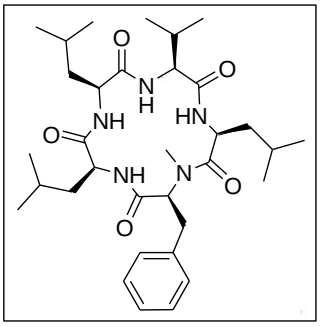

Report Method: Injection Summary Report Printed 11:33:19 AM6/10/2008 Page: 1 of 1

SanA 3 HPLC trace Cyclized Pentapeptide: *N*-Me-Phe-Leu-Val-Leu-Leu

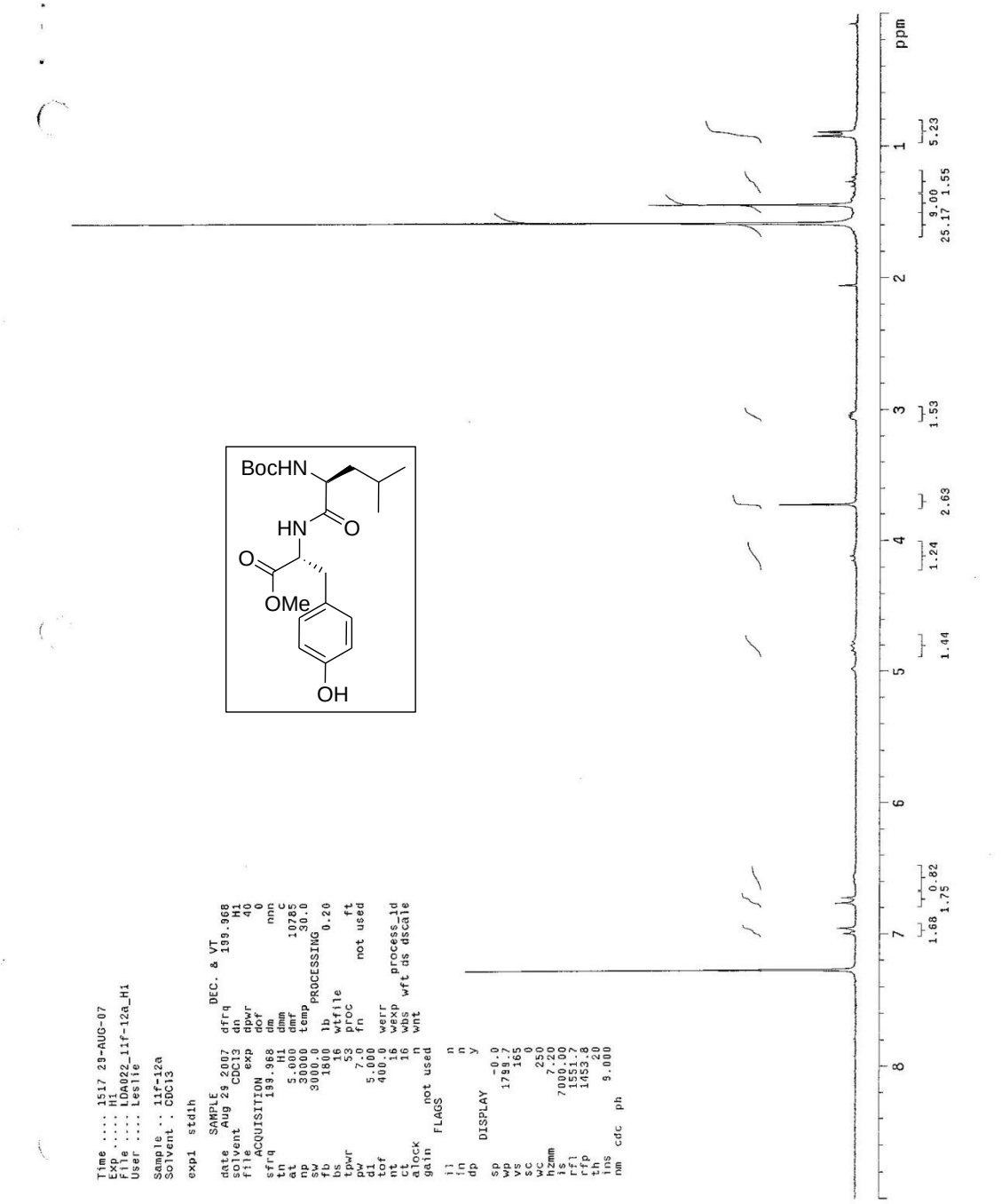

SanA 4 ^{1}H NMR Dipeptide: MeO-D-Tyr-Leu-NHBoc

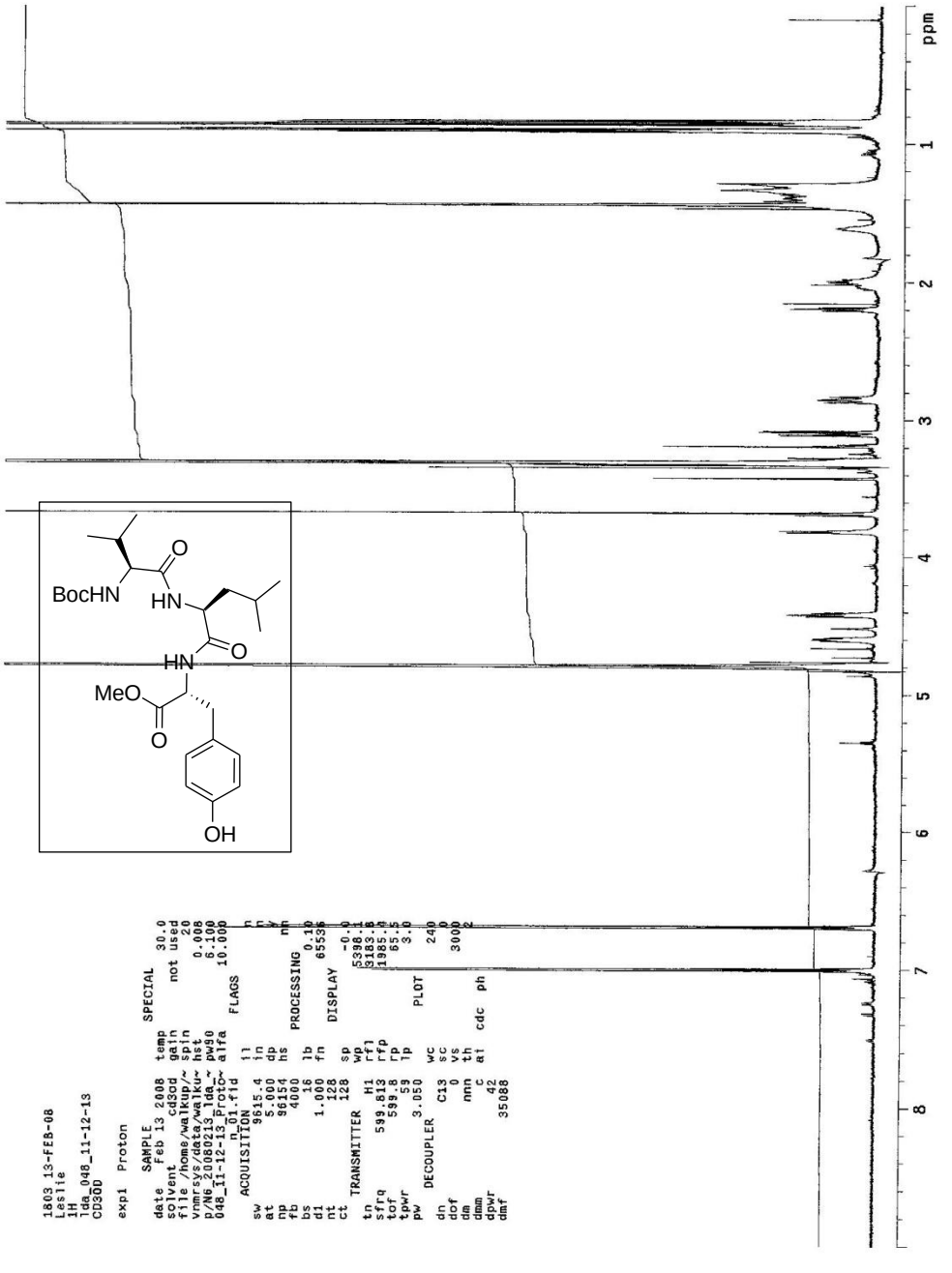

SanA 4 ^{1}H NMR Tripeptide: MeO-D-Tyr-Leu-Val-NHBoc

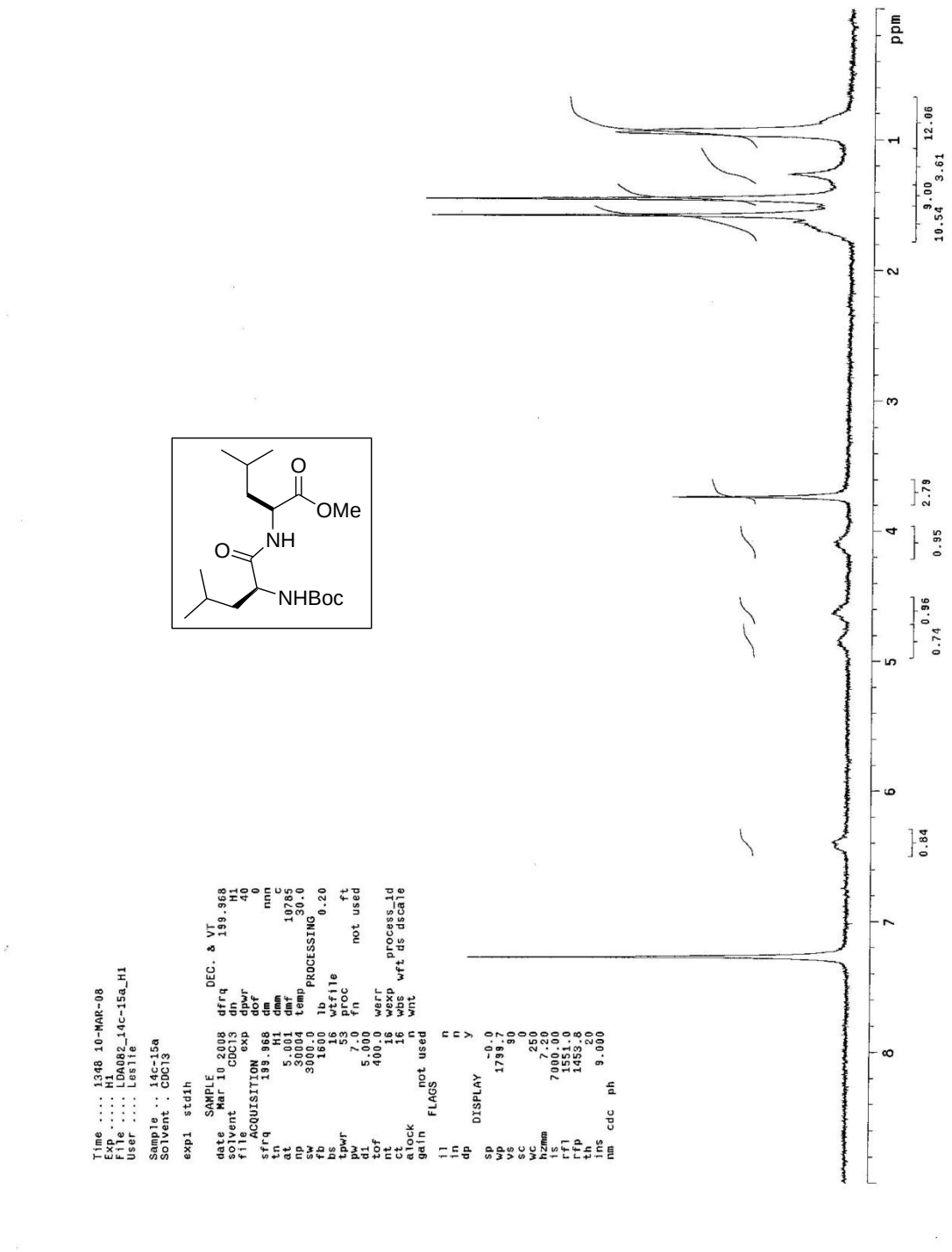

SanA 4 ^{1}H NMR Dipeptide: MeO-Leu-Leu-NHBoc

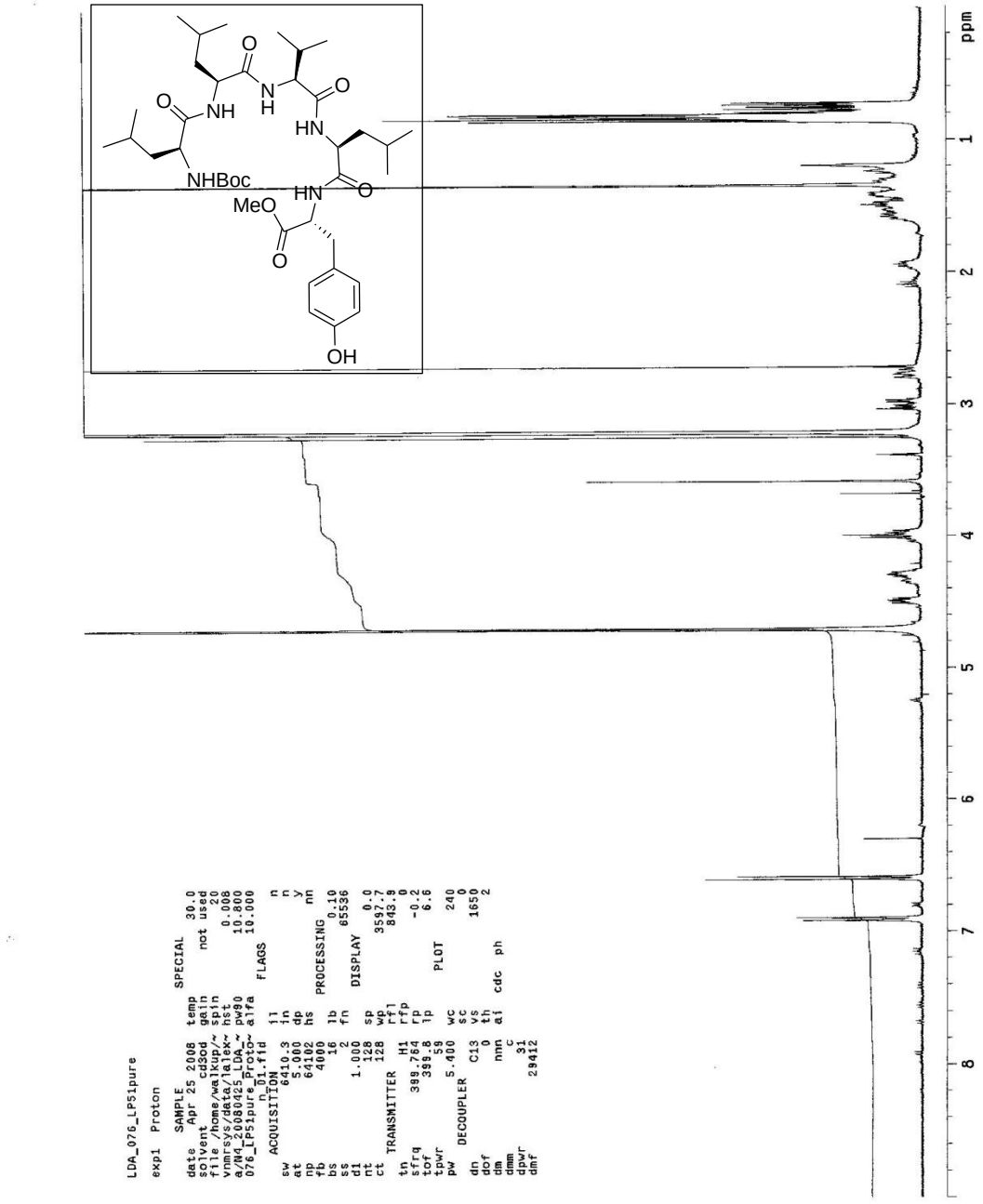

SanA 4 ^{1}H NMR Linear Pentapeptide: MeO-D-Tyr-Leu-Val-Leu-Leu-NHBoc

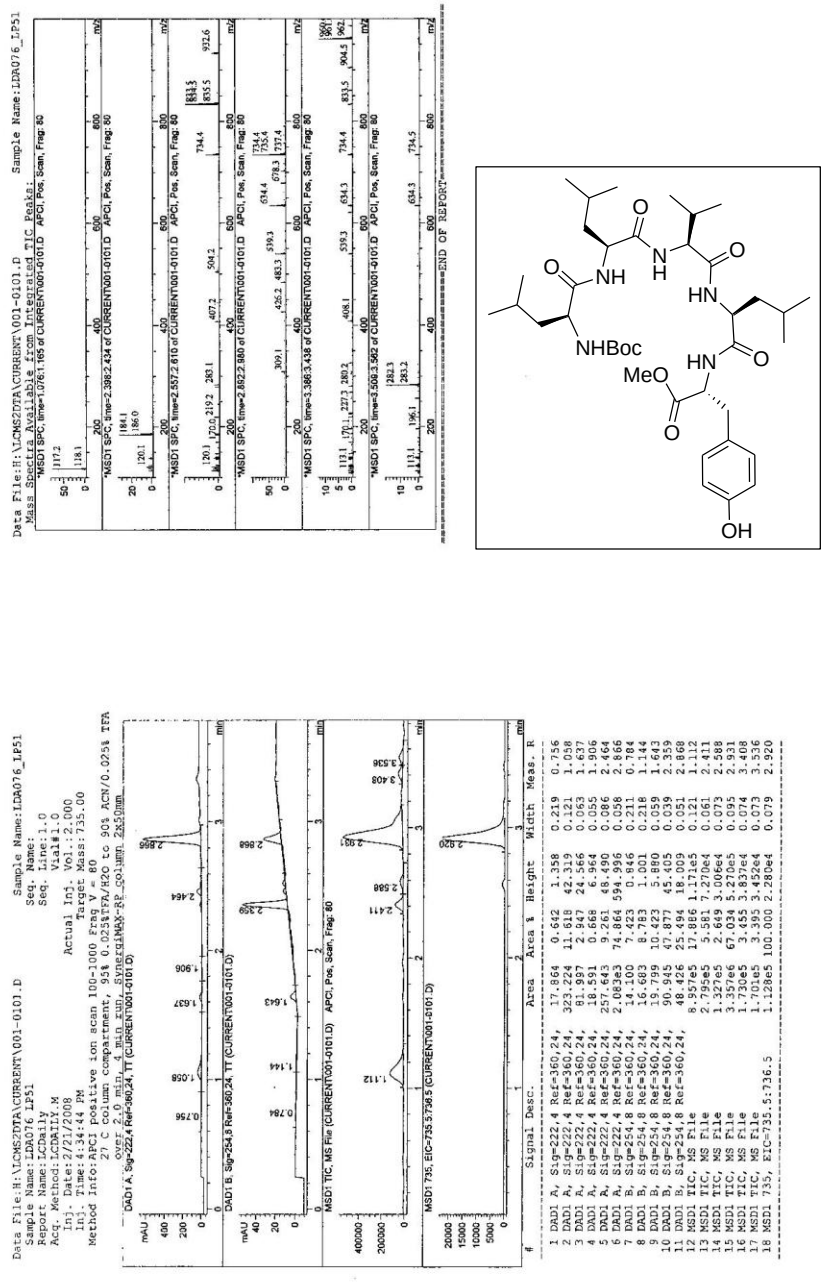

SanA 4 LCMS Linear Pentapeptide: MeO-D-Tyr-Leu-Val-Leu-Leu-NHBoc (MW= 735)

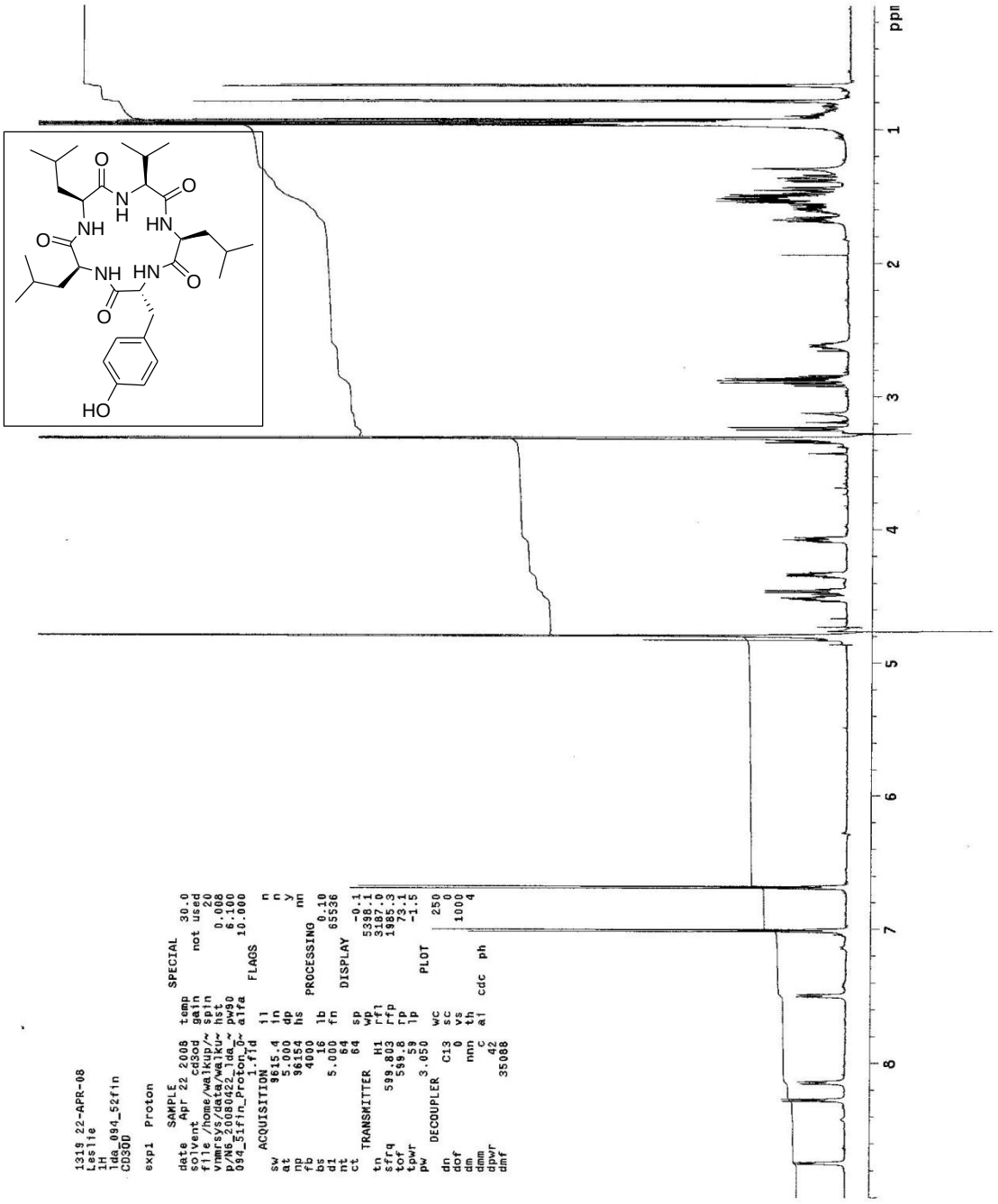

SanA 4 ^{1}H-NMR Cyclized Pentapeptide: D-Tyr-Leu-Val-Leu-Leu

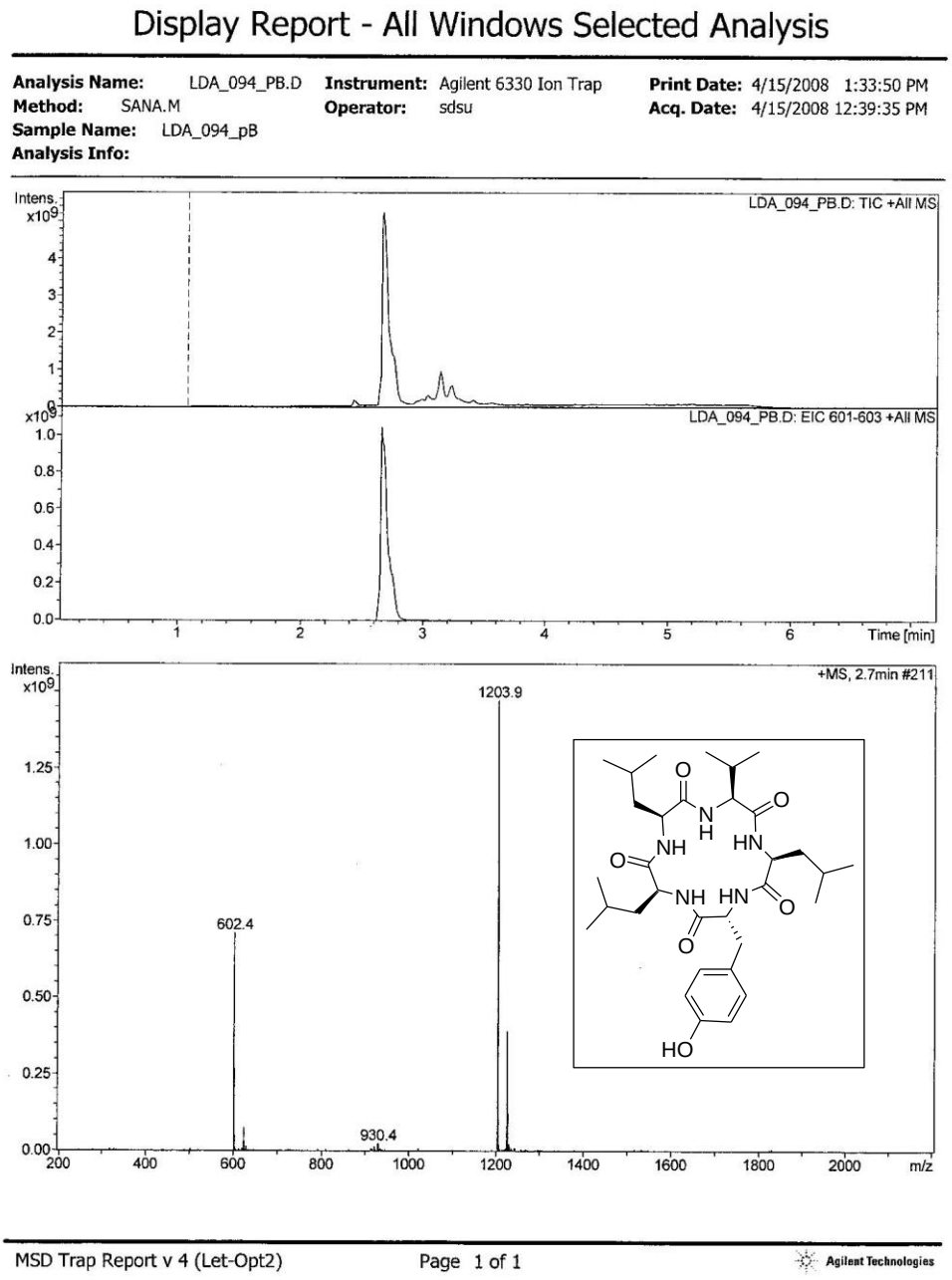

SanA 4 LCMS Cyclized Pentapeptide: D-Tyr-Leu-Val-Leu-Leu (MW= 602)

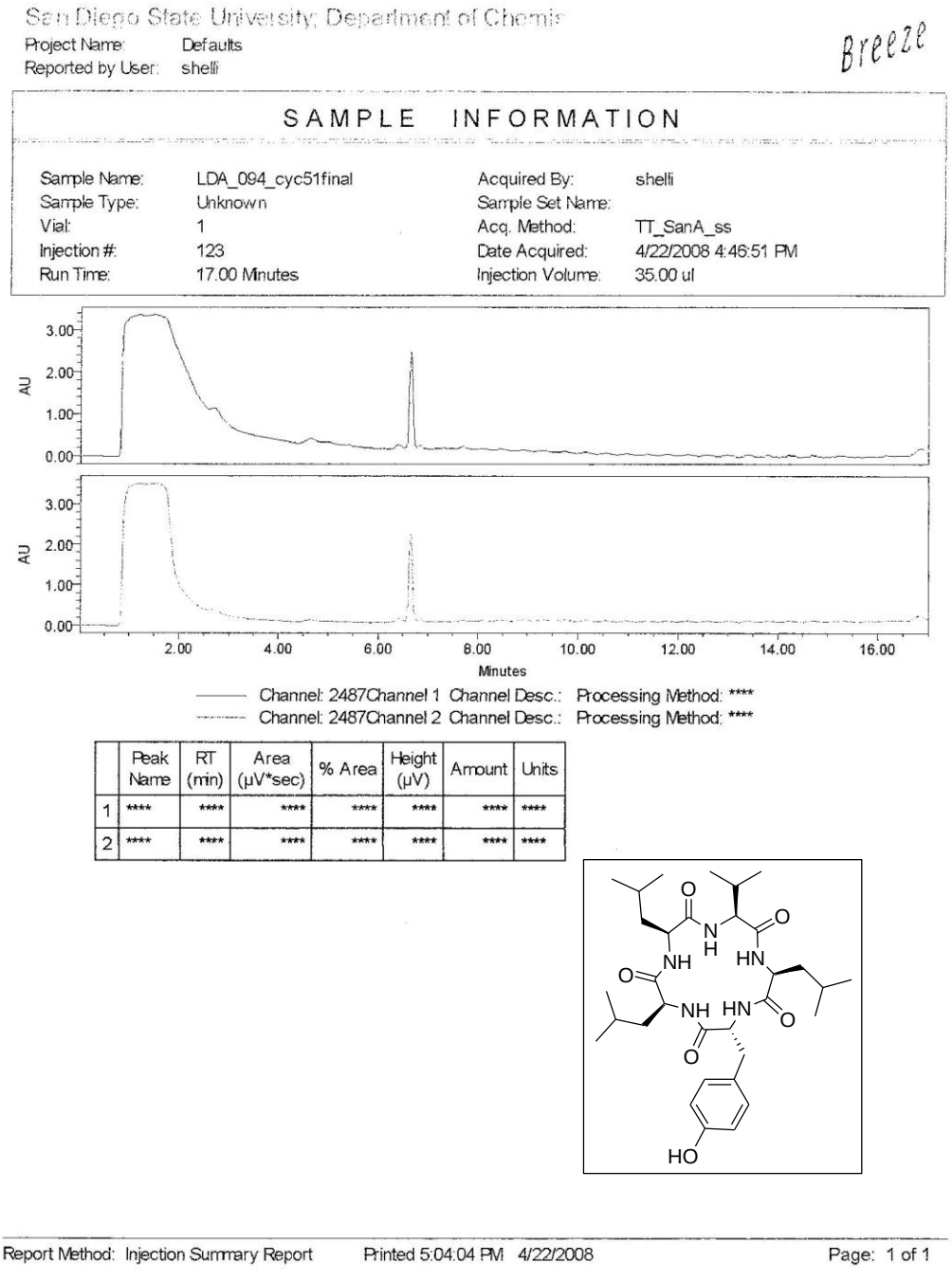

SanA 4 HPLC trace Cyclized Pentapeptide: D-Tyr-Leu-Val-Leu-Leu

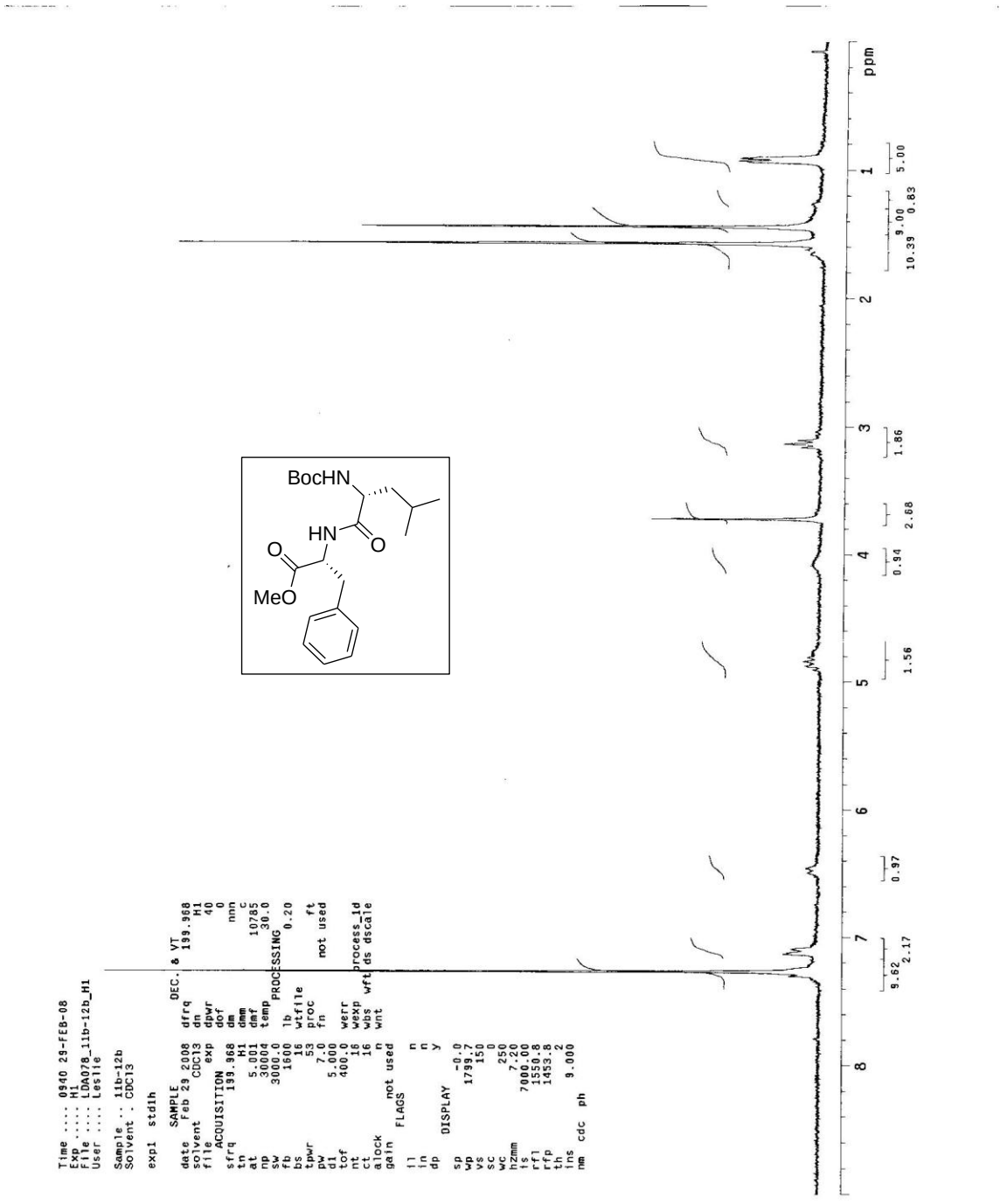

SanA 8 ^{1}H-NMR Dipeptide: MeO-D-Phe-D-Leu-NHBoc

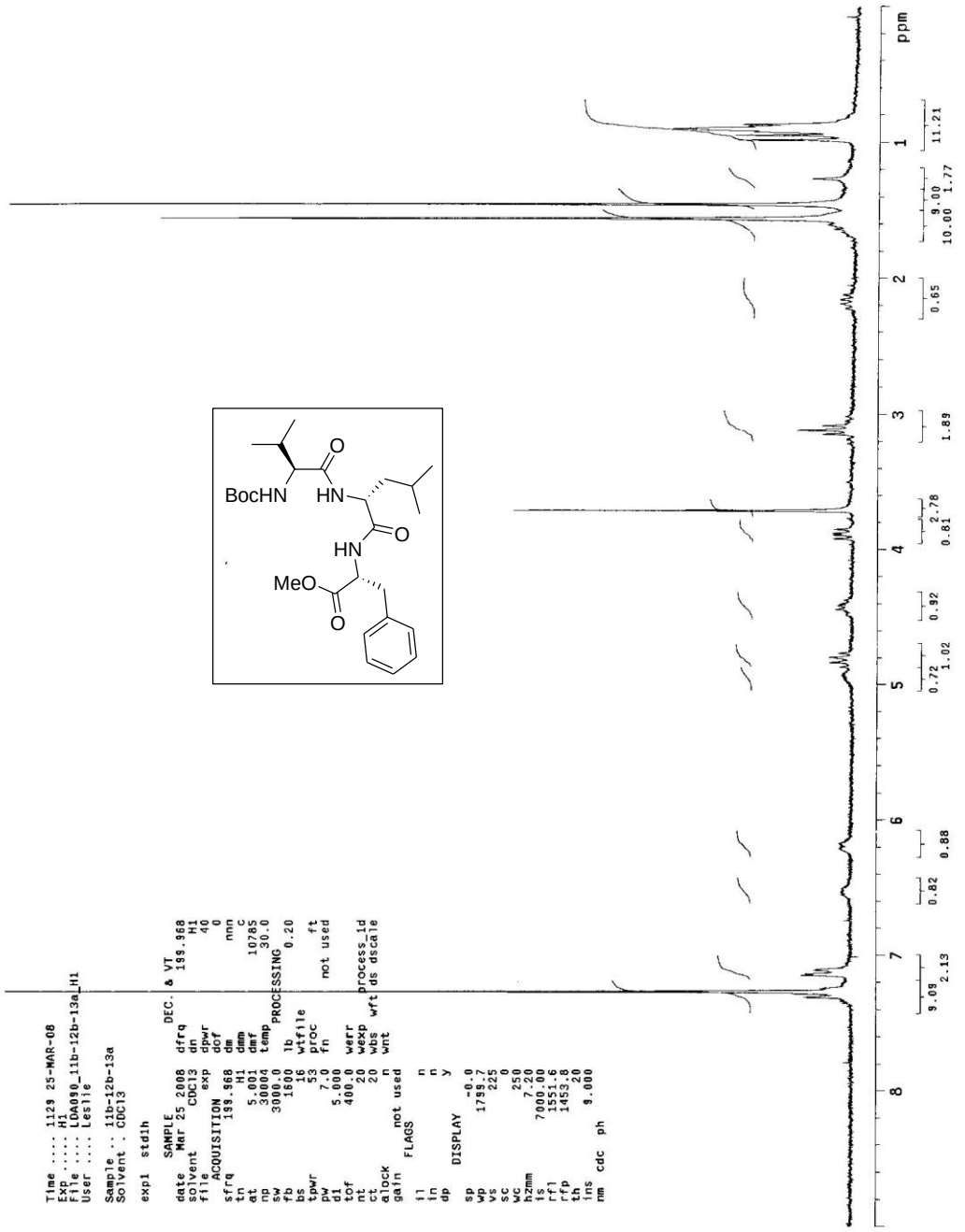

SanA 8 ^{1}H-NMR Tripeptide: MeO-D-Phe-D-Leu-Val-NHBoc

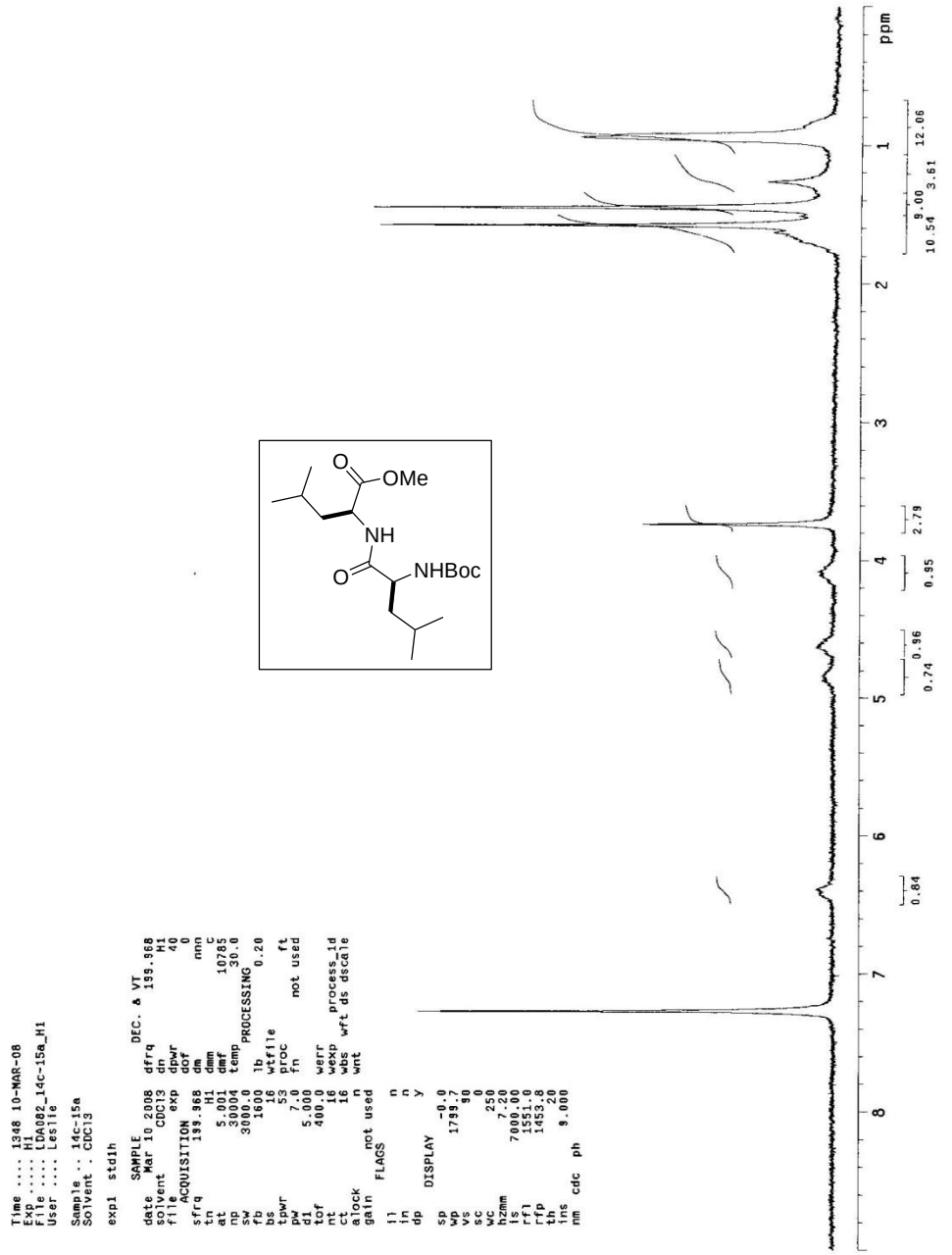

SanA 8 ^{1}H-NMR Dipeptide: MeO-Leu-Leu-NHBoc

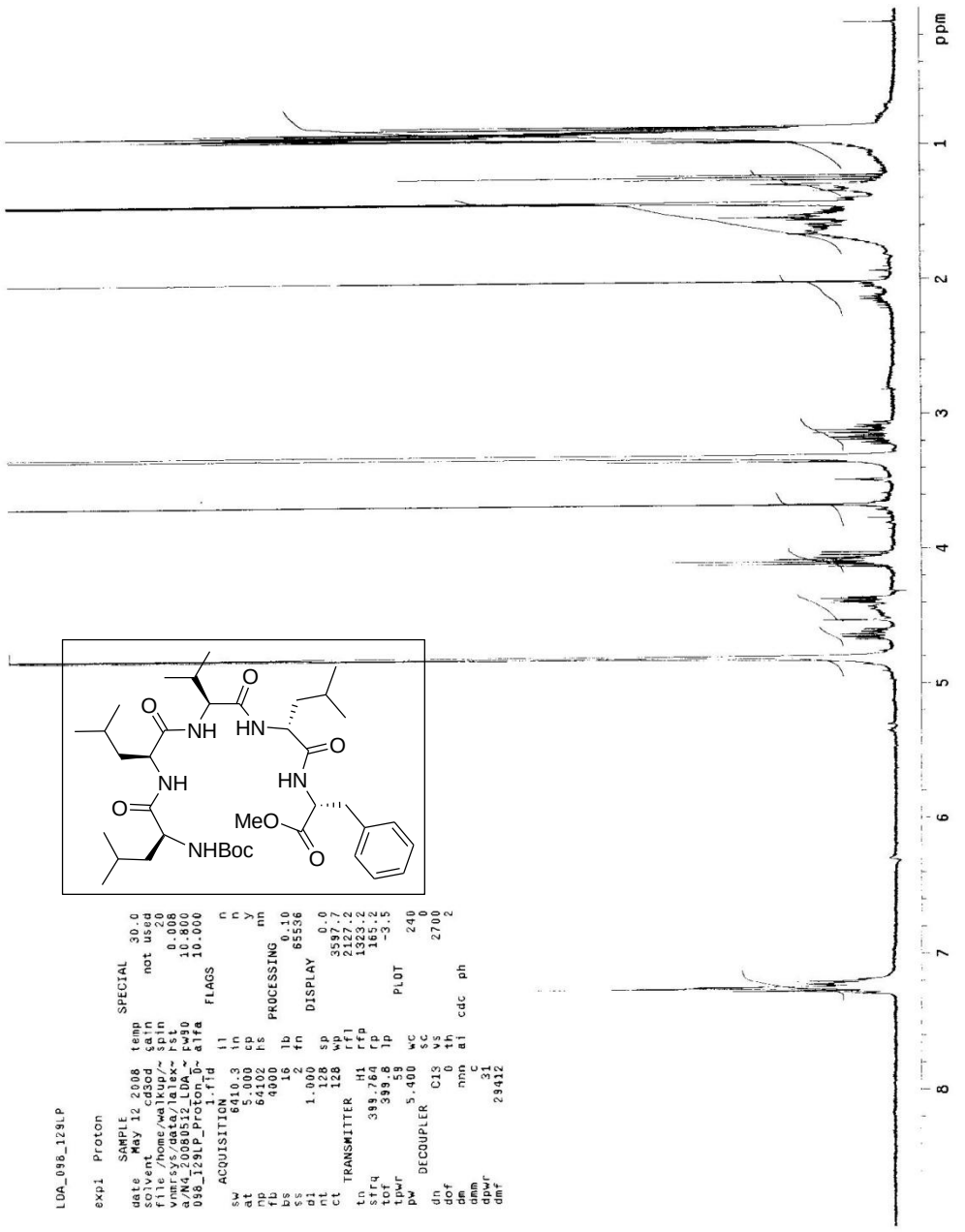

SanA 8 ^{1}H-NMR Linear Pentapeptide: MeO-D-Phe-D-Leu-Val-Leu-Leu-NHBoc

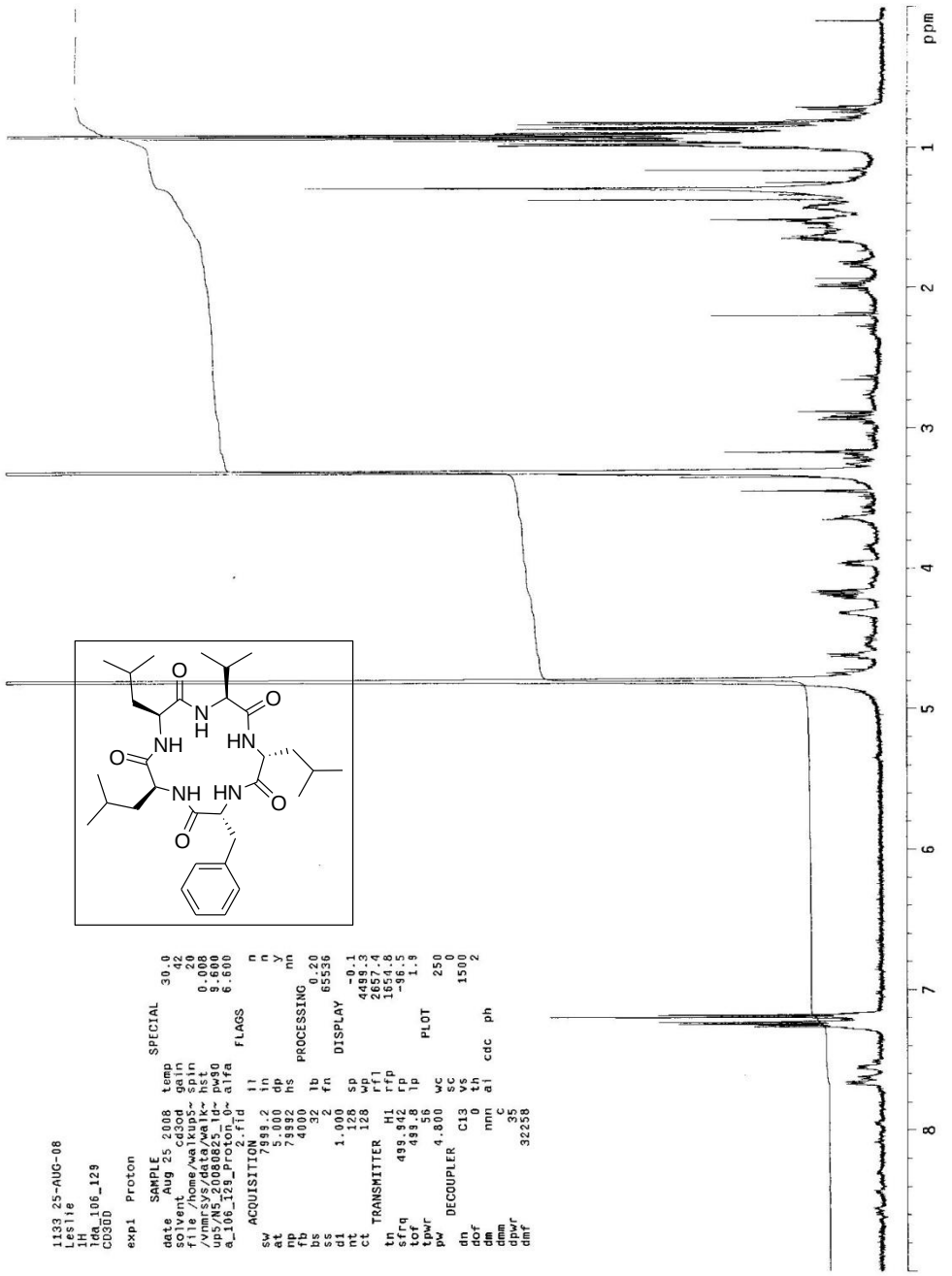

SanA 8 ^{1}H-NMR Cyclized Pentapeptide: D-Phe-D-Leu-Val-Leu-Leu

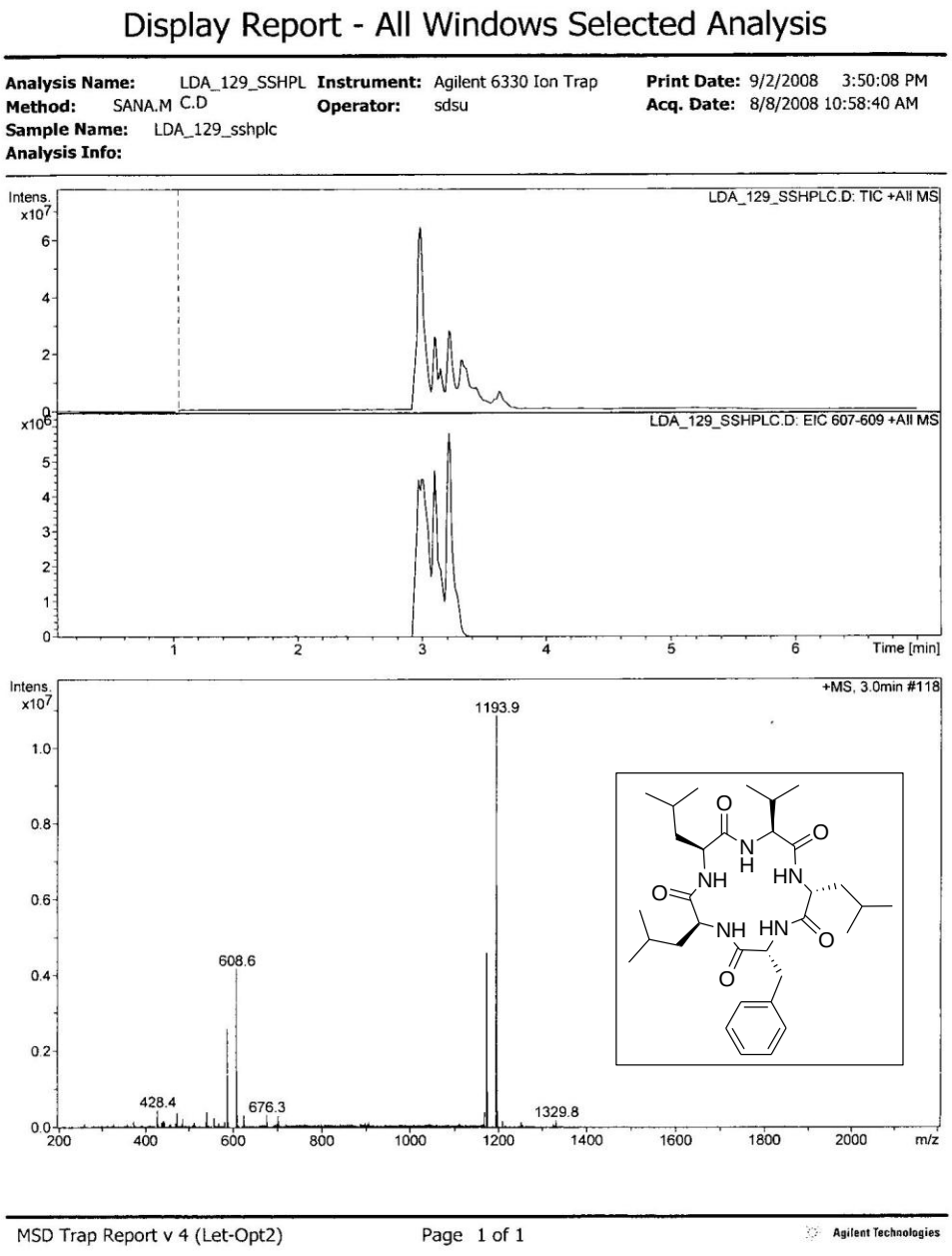

SanA 8 LCMS Cyclized Pentapeptide: D-Phe-D-Leu-Val-Leu-Leu (MW=586)

San Diego State University; Department of Chemis

Project Name: Defaults
Reported by User: shelli

Breeze

SAMPLE INFORMATION

Sample Name:	LDA_129_inj1	Acquired By:	shelli
Sample Type:	Unknown	Sample Set Name:	
Vial:	1	Acq. Method:	PrimarySanA_SS_new
Injection #:	5	Date Acquired:	8/6/2008 2:27:33 PM
Run Time:	16.00 Minutes	Injection Volume:	100.00 ul

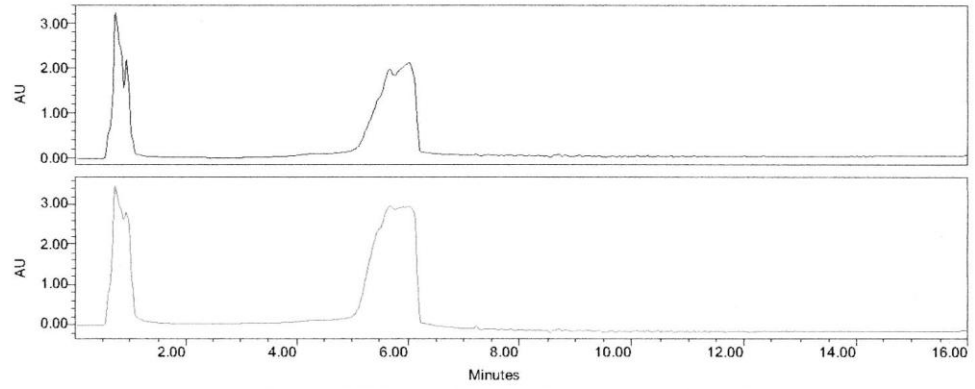

Channel: 2487Channel 1 Channel Desc.: Processing Method: *
Channel: 2487Channel 2 Channel Desc.: Processing Method: *

	Peak Name	RT (min)	Area (V*sec)	% Area	Height (V)	Amount	Units
1	****	****	****	****	****	****	****
2	****	****	****	****	****	****	****

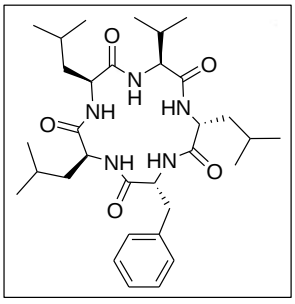

Report Method: Injection Summary Report Printed 2:43:48 PM 8/6/2008 Page: 1 of 1

SanA 8 HPLC Cyclized Pentapeptide: D-Phe-D-Leu-Val-Leu-Leu

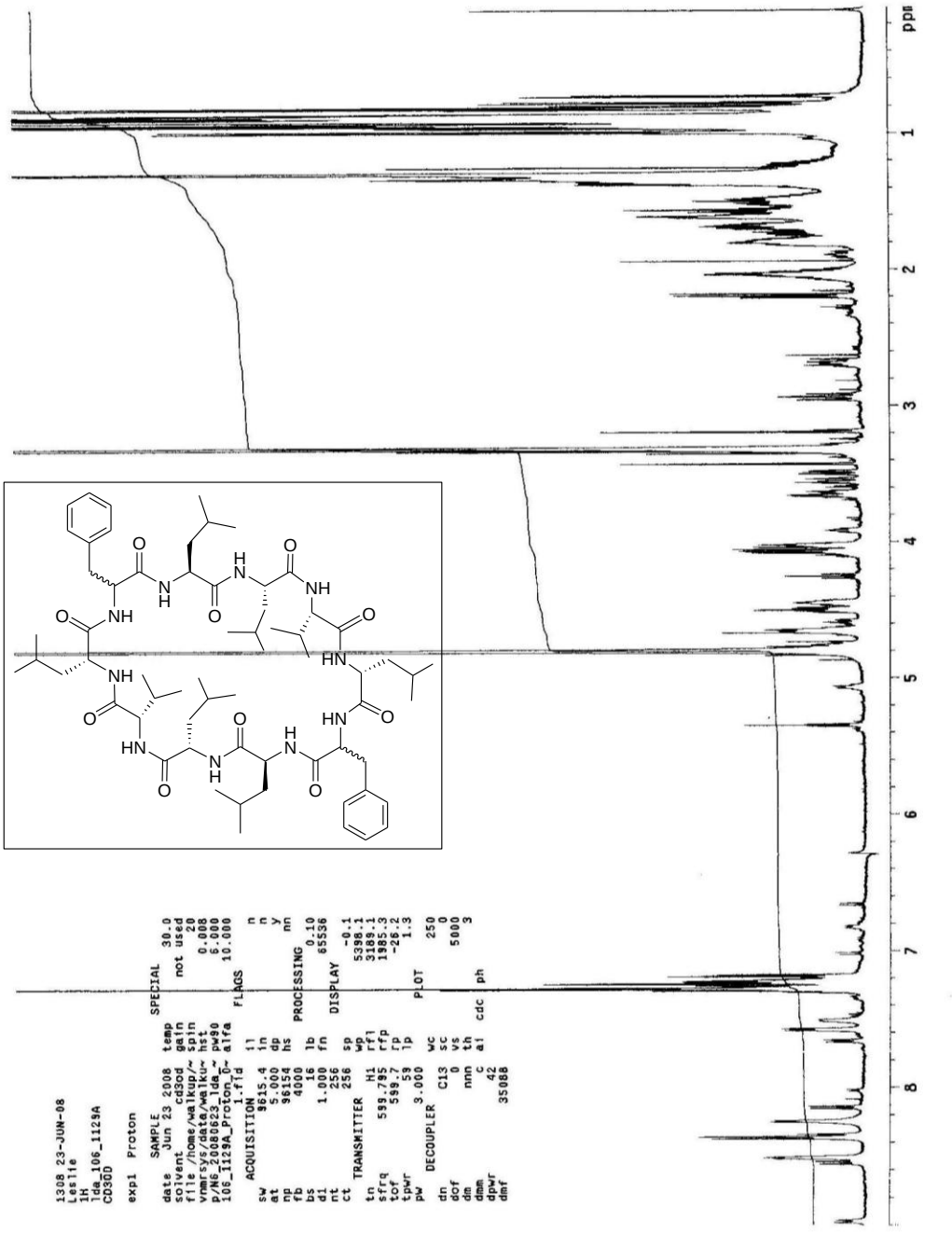

Di-SanA 8 ^{1}H-NMR Cyclized Decapeptide: D-Phe-D-Leu-Val-Leu-Leu-D-Phe-D-Leu-Val-Leu-Leu

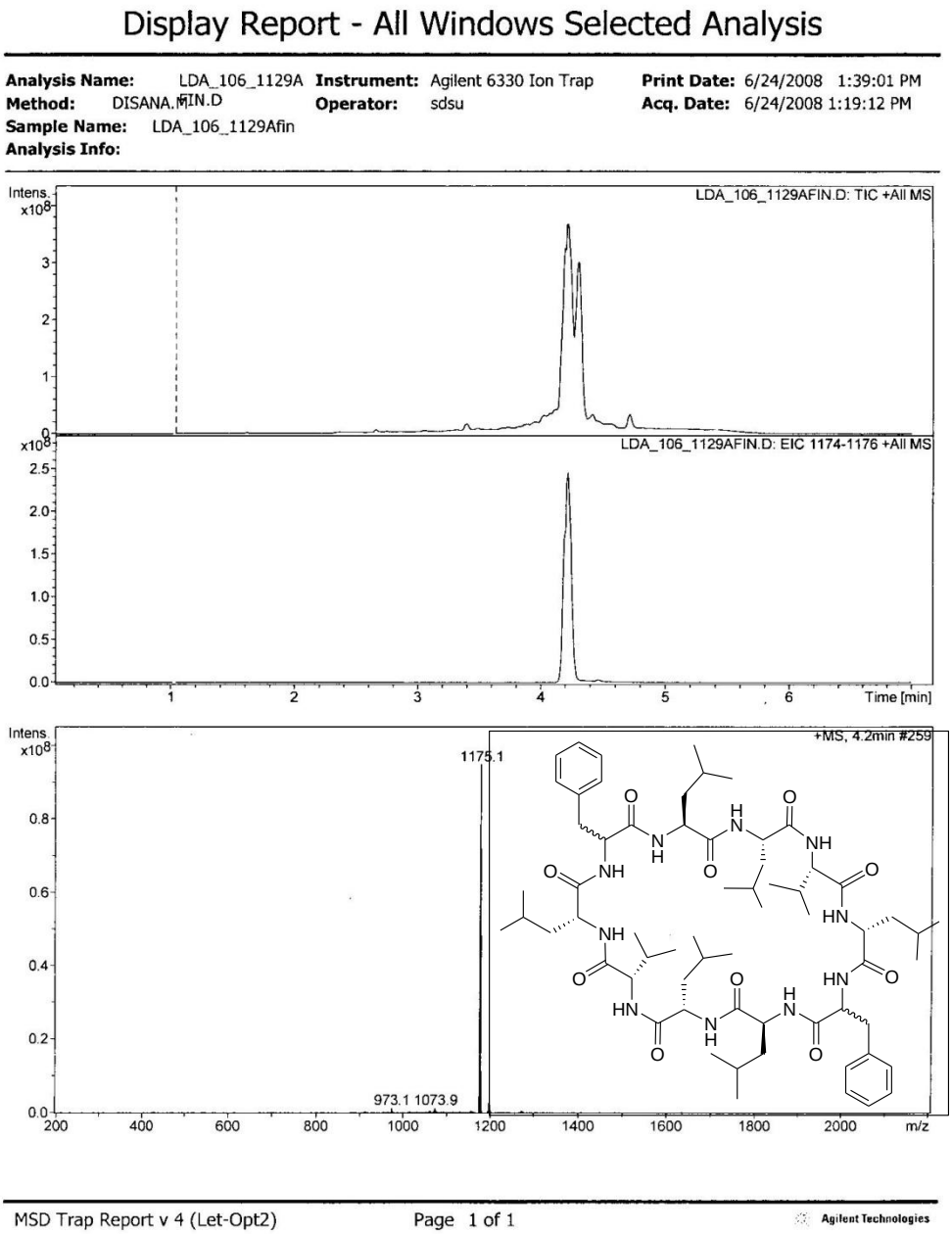

Di-SanA 8 LCMS Cyclized Decapeptide: D-Phe-D-Leu-Val-Leu-Leu-D-Phe-D-Leu-Val-Leu-Leu (MW=1172)

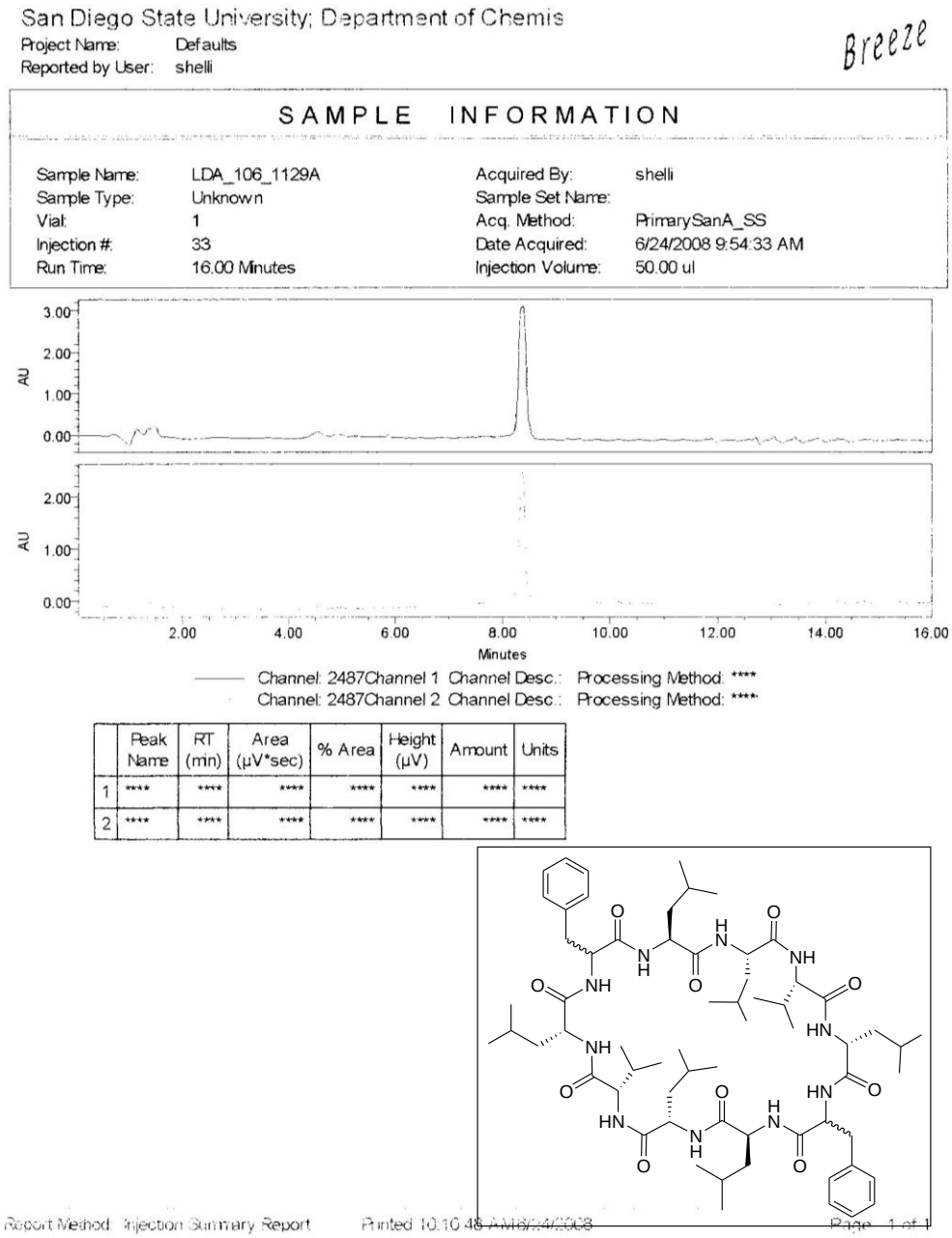

Di-SanA 8 HPLC trace Cyclized Decapeptide: D-Phe-D-Leu-Val-Leu-Leu-D-Phe-D-Leu-Val-Leu-Leu

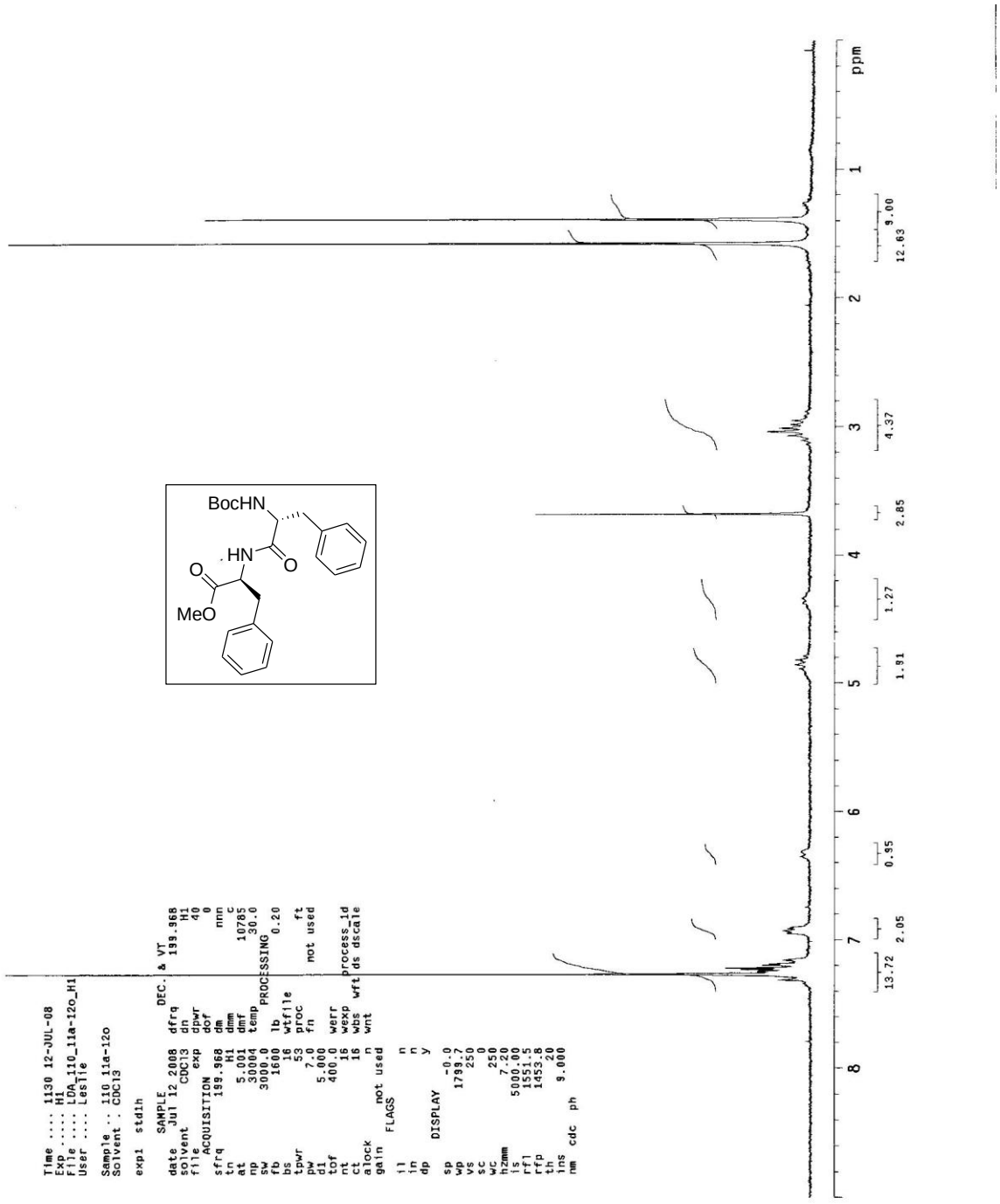

SanA 9 ^{1}H-NMR Dipeptide: MeO-Phe-D-Phe-NHBoc

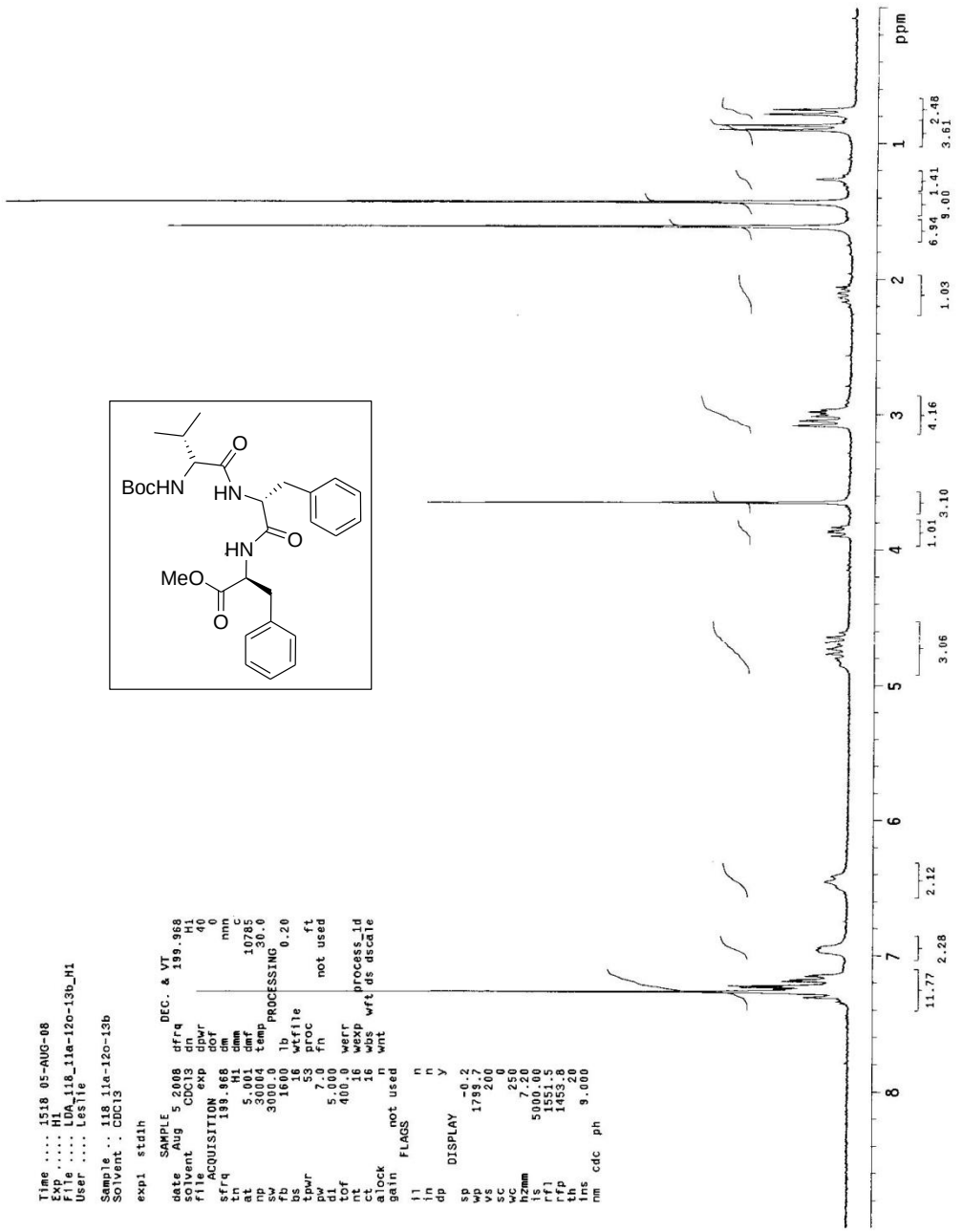

SanA 9 ^{1}H-NMR Tripeptide: MeO-Phe-D-Phe-D-Val-NHBoc

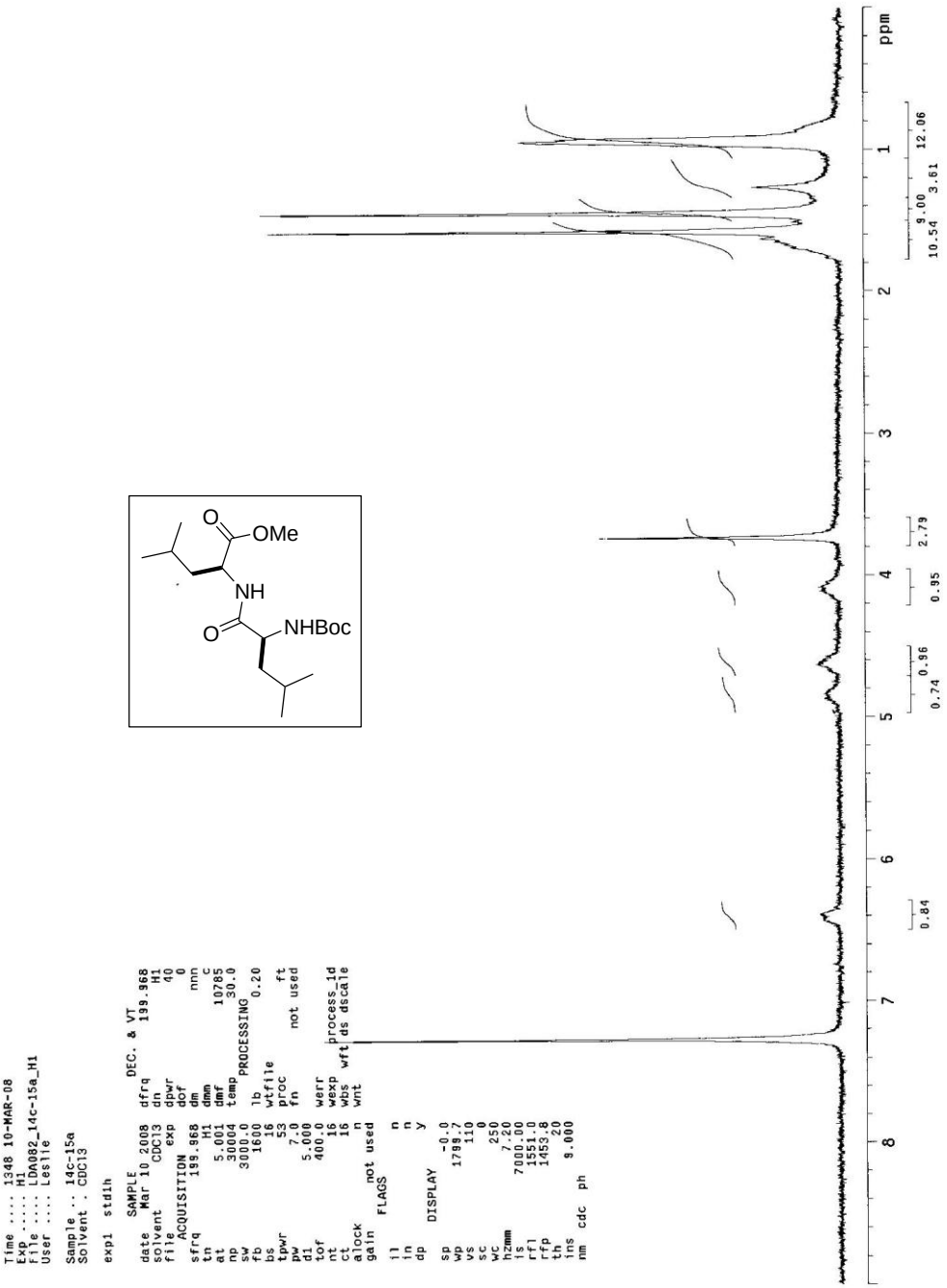

SanA 9 ^{1}H-NMR Dipeptide: MeO-Leu-Leu-NHBoc

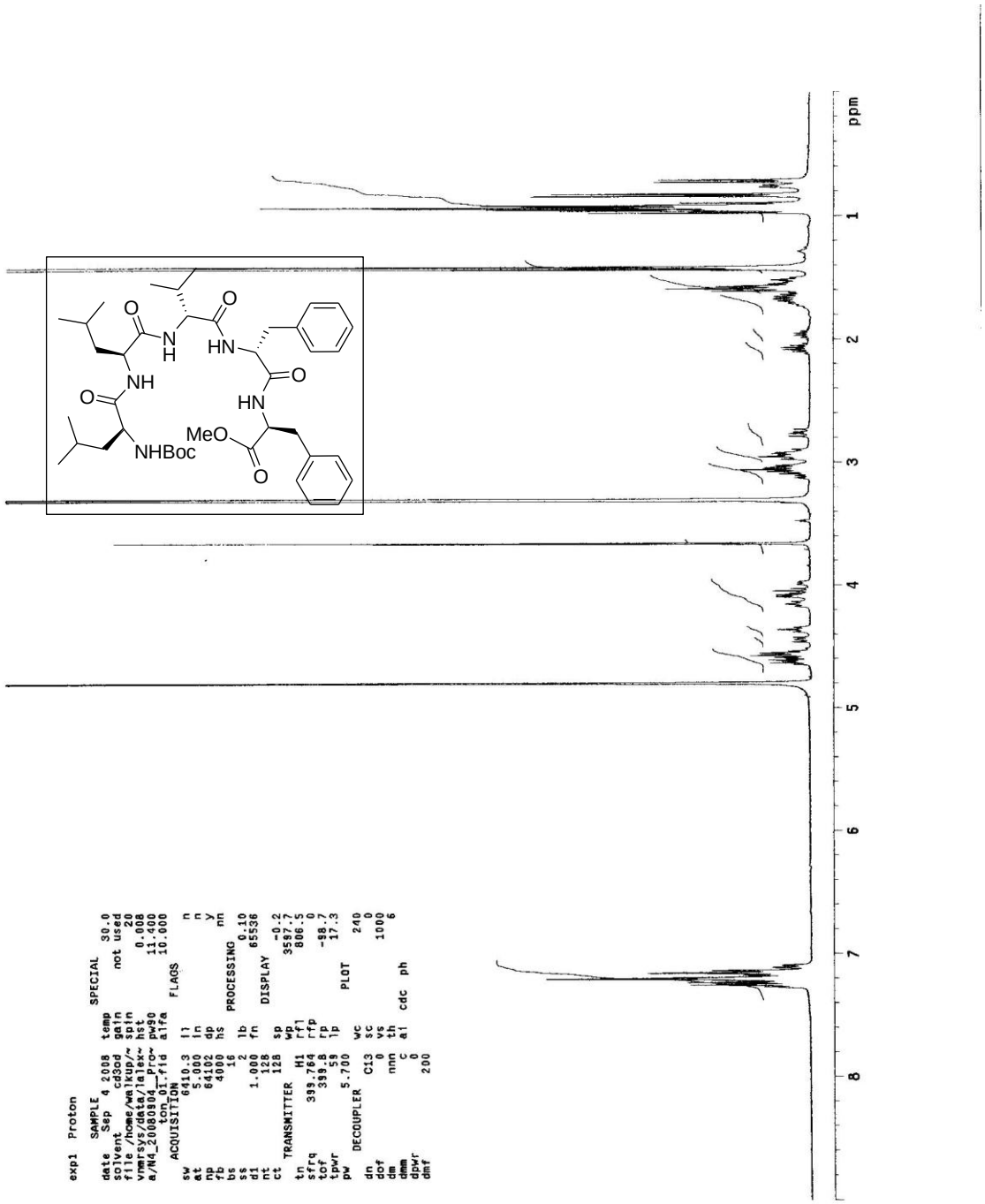

SanA 9 ^{1}H-NMR Linear Pentapeptide: MeO-Phe-D-Phe-D-Val-Leu-Leu-NHBoc

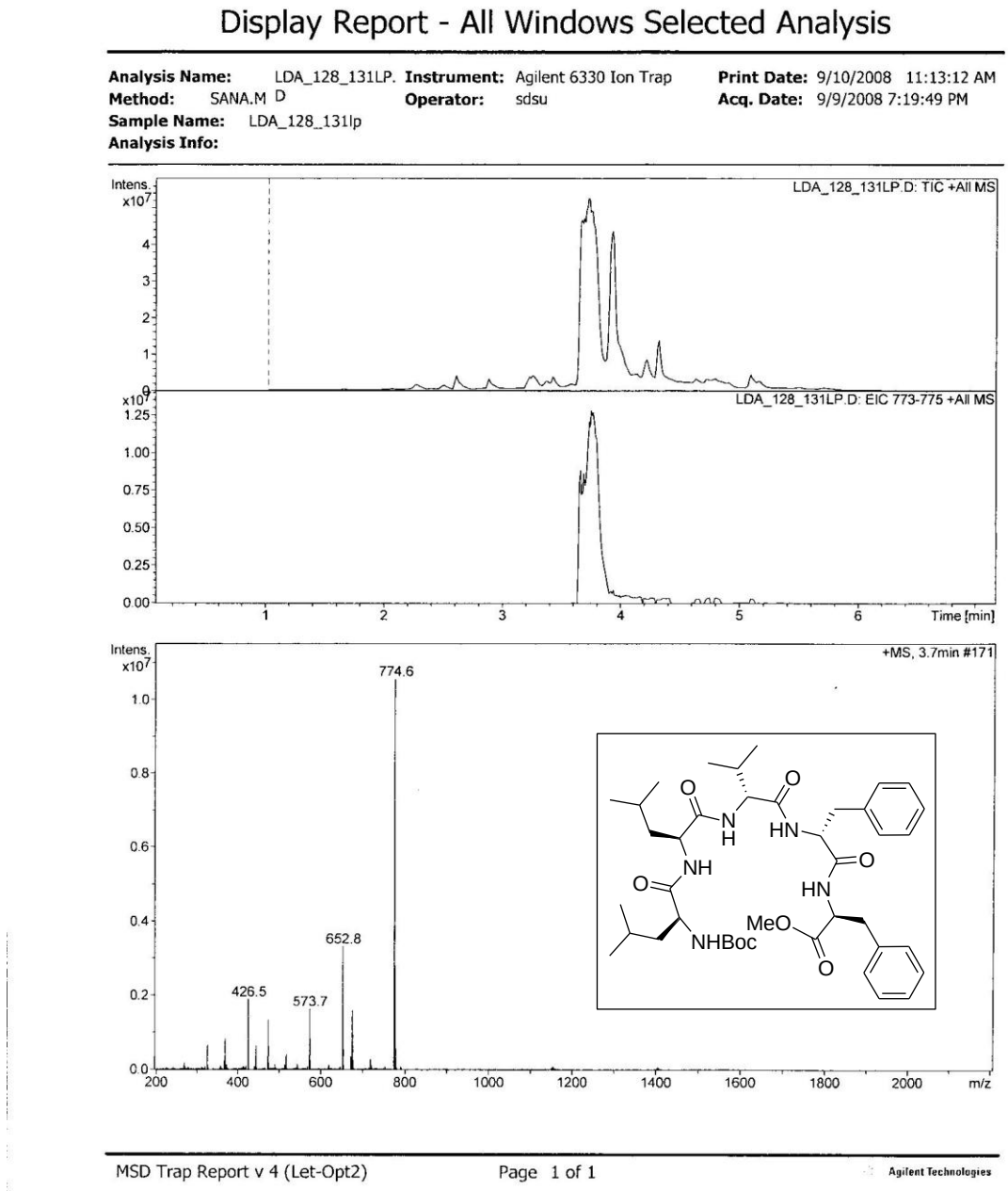

SanA 9 LCMS Linear Pentapeptide: MeO-Phe-D-Phe-D-Val-Leu-Leu-NHBoc (MW=752)

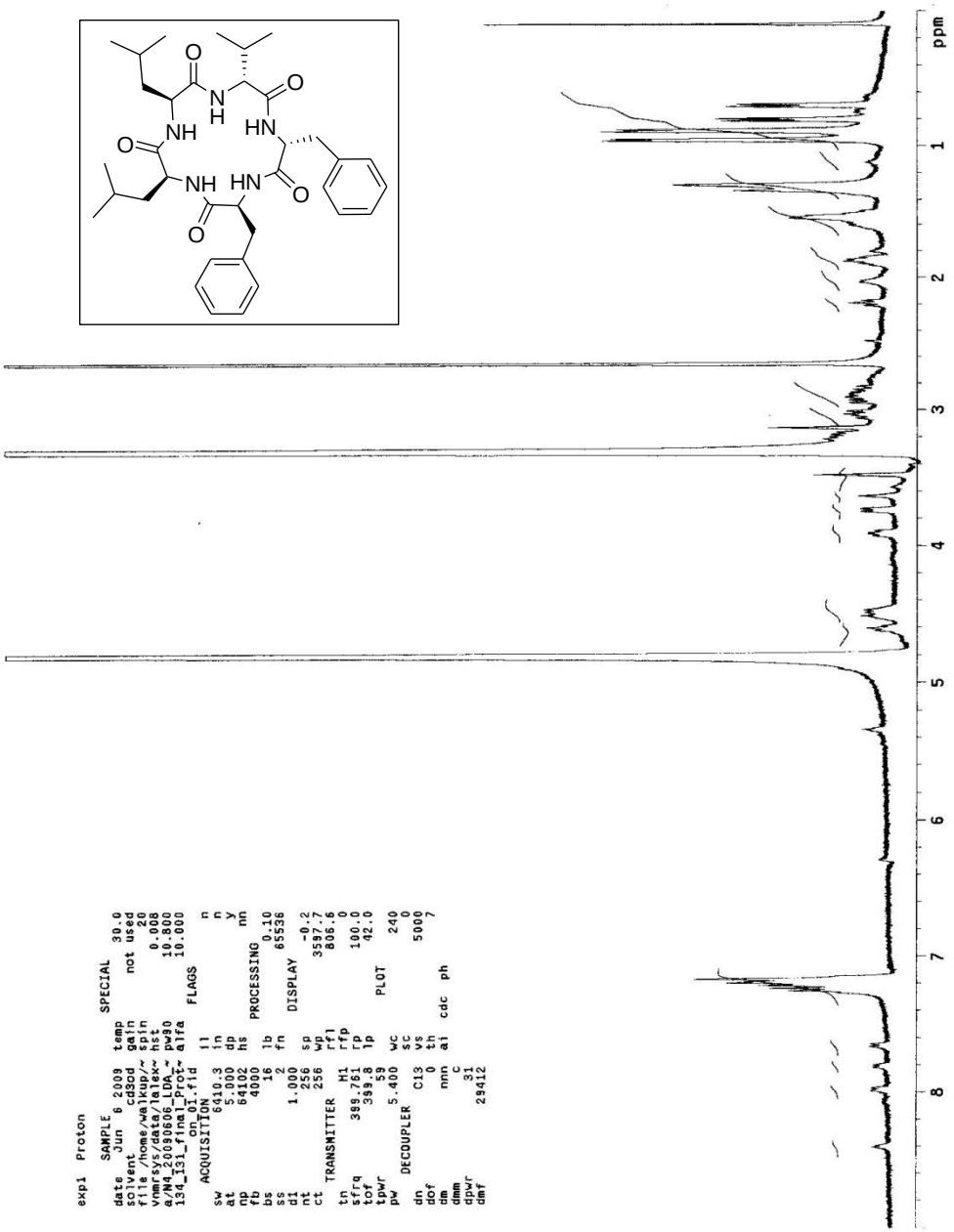

SanA 9 ^{1}H-NMR Cyclized Pentapeptide: Phe-D-Phe-D-Val-Leu-Leu

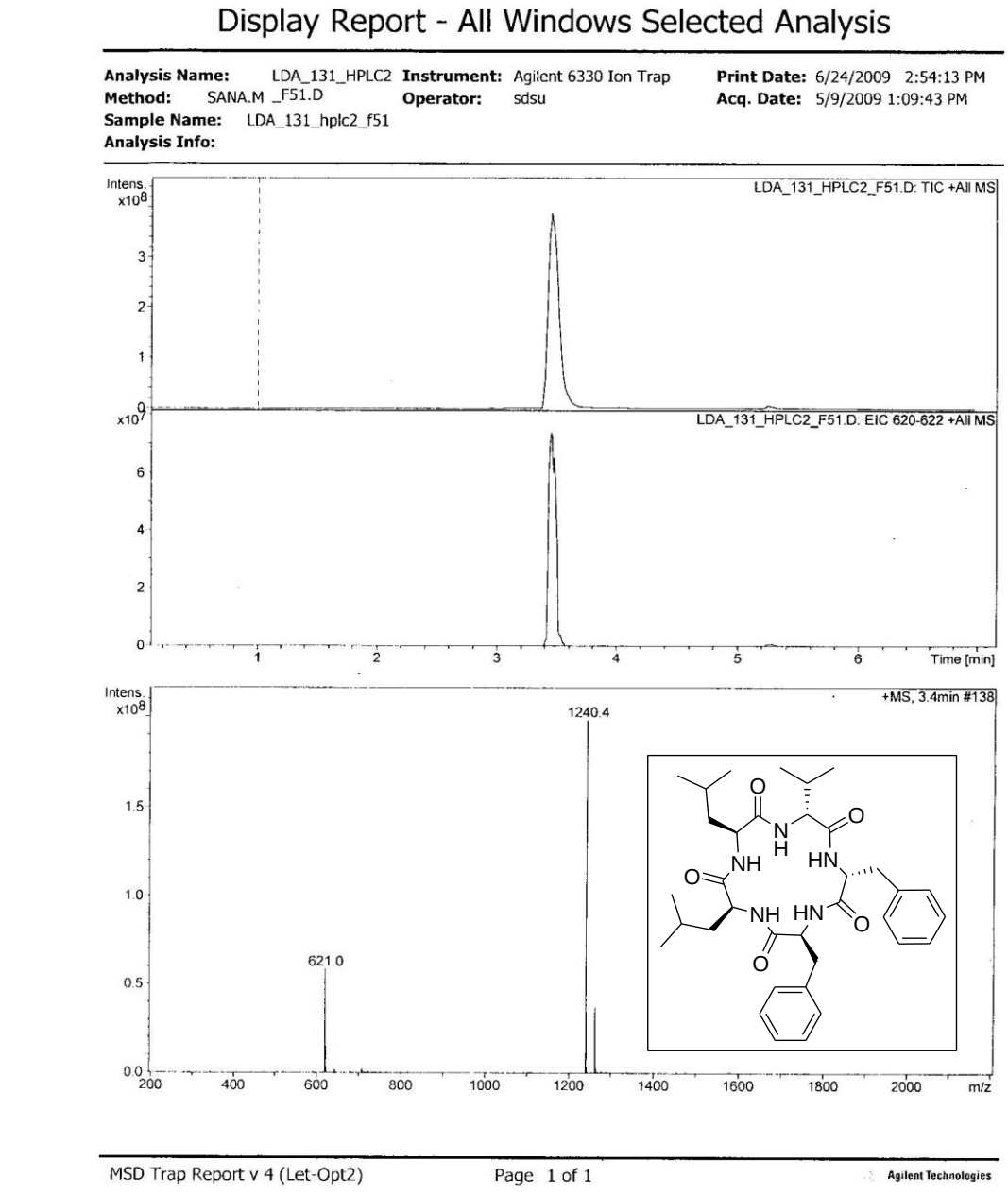

SanA 9 LCMS Cyclized Pentapeptide: Phe-D-Phe-D-Val-Leu-Leu (MW=620)

SDSU

Project Name: Defaults
Reported by User: System

Breeze

SAMPLE INFORMATION

Sample Name:	LDA_131_final	Acquired By:	System
Sample Type:	Unknown	Sample Set Name:	
Vial:	1	Acq. Method:	primary_sanA_ss_ACN
Injection #:	333	Date Acquired:	6/1/2009 11:08:15 AM
Run Time:	16.00 Minutes	Injection Volume:	30.00 ul

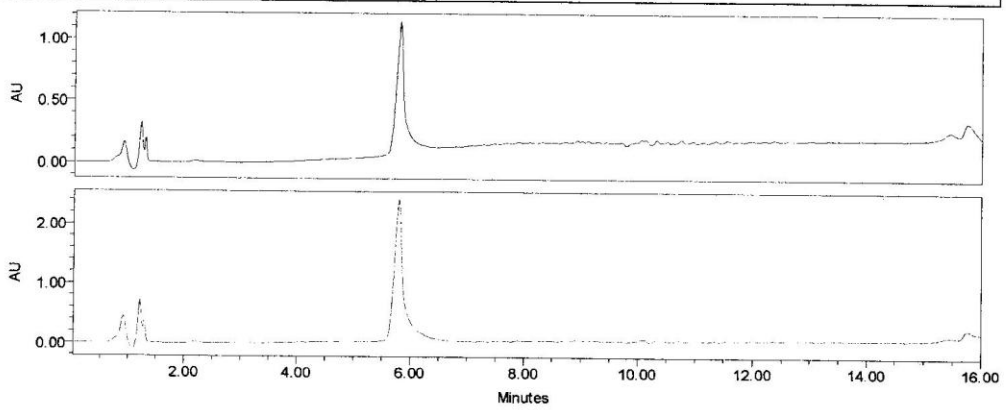

Channel: 2487Channel 1 Channel Desc.: Processing Method: ****
Channel: 2487Channel 2 Channel Desc.: Processing Method: ****

	Peak Name	RT (min)	Area (µV*sec)	% Area	Height (µV)	Amount	Units
1	****	****	****	****	****	****	****
2	****	****	****	****	****	****	****

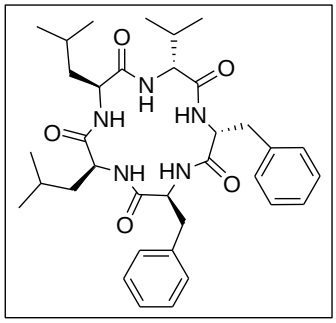

Report Method: Injection Summary Report Printed 11:24:29 AM 6/1/2009 Page: 1 of 1

SanA 9 HPLC trace Cyclized Pentapeptide: Phe-D-Phe-D-Val-Leu-Leu

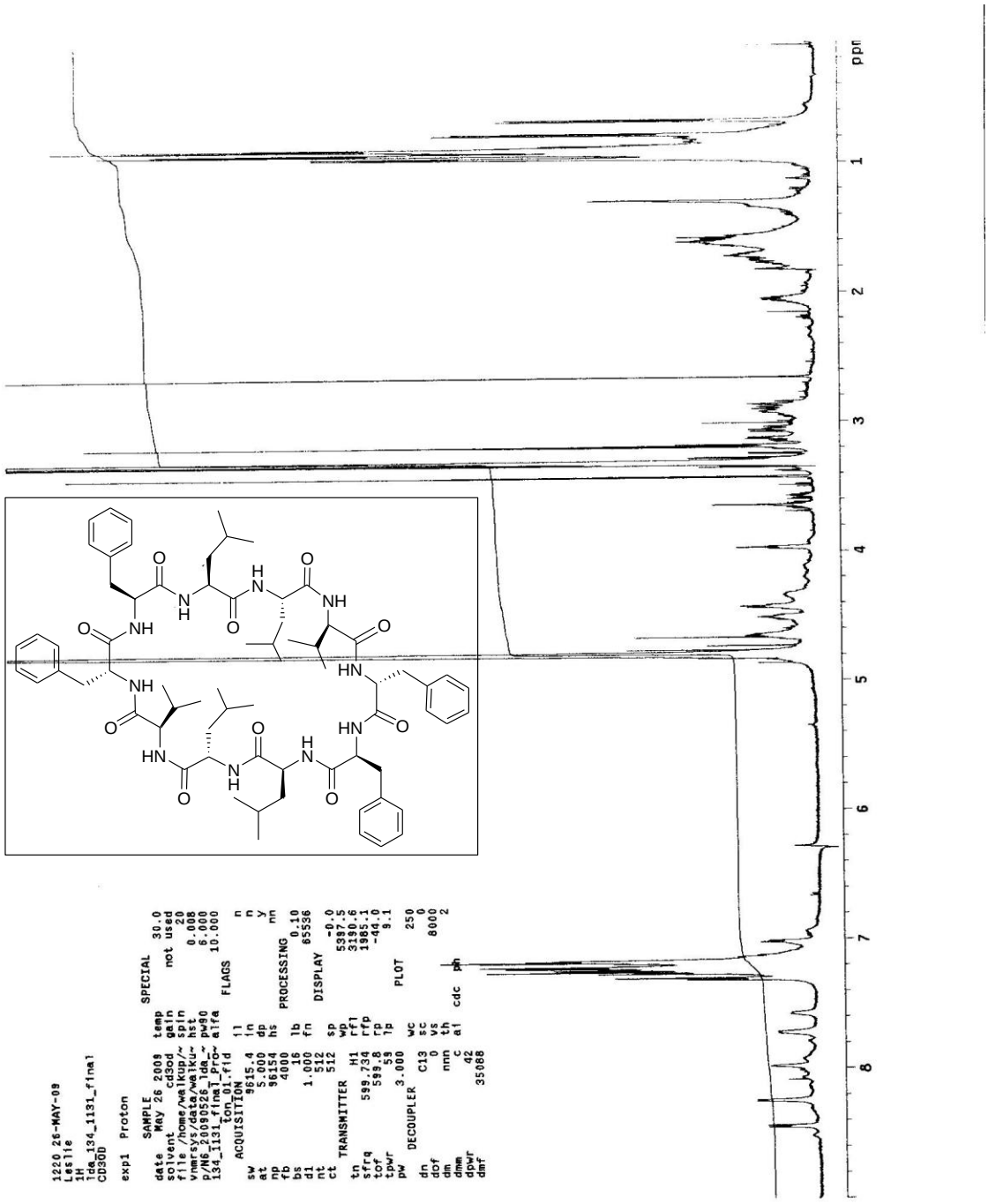

Di-SanA 9 ^{1}H-NMR Cyclized Decapeptide: Phe-D-Phe-D-Val-Leu-Leu-Phe-D-Phe-D-Val-Leu-Leu

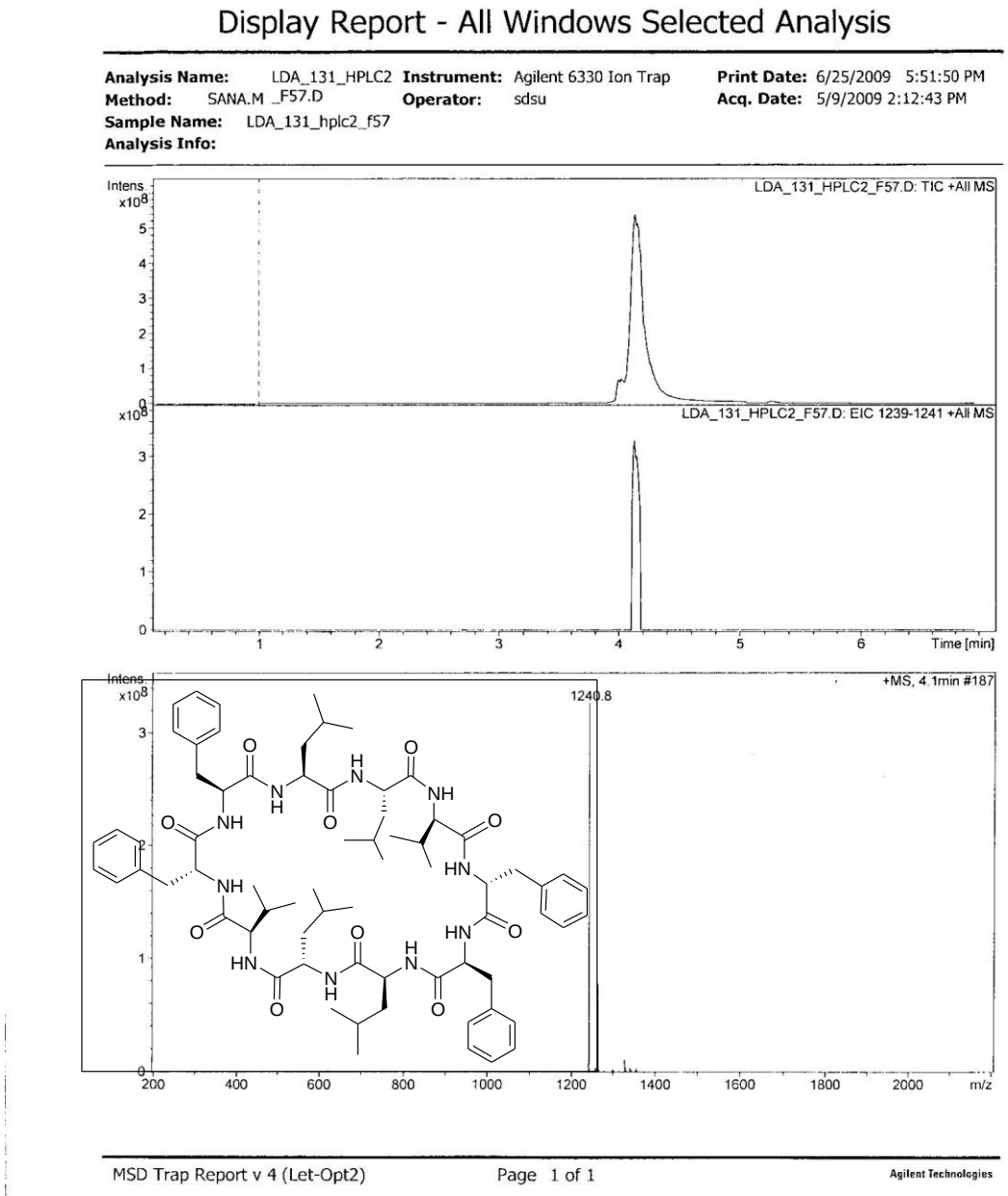

Di-SanA 9 LCMS Cyclized Decapeptide: Phe-D-Phe-D-Val-Leu-Leu-Phe-D-Phe-D-Val-Leu-Leu (MW = 1240)

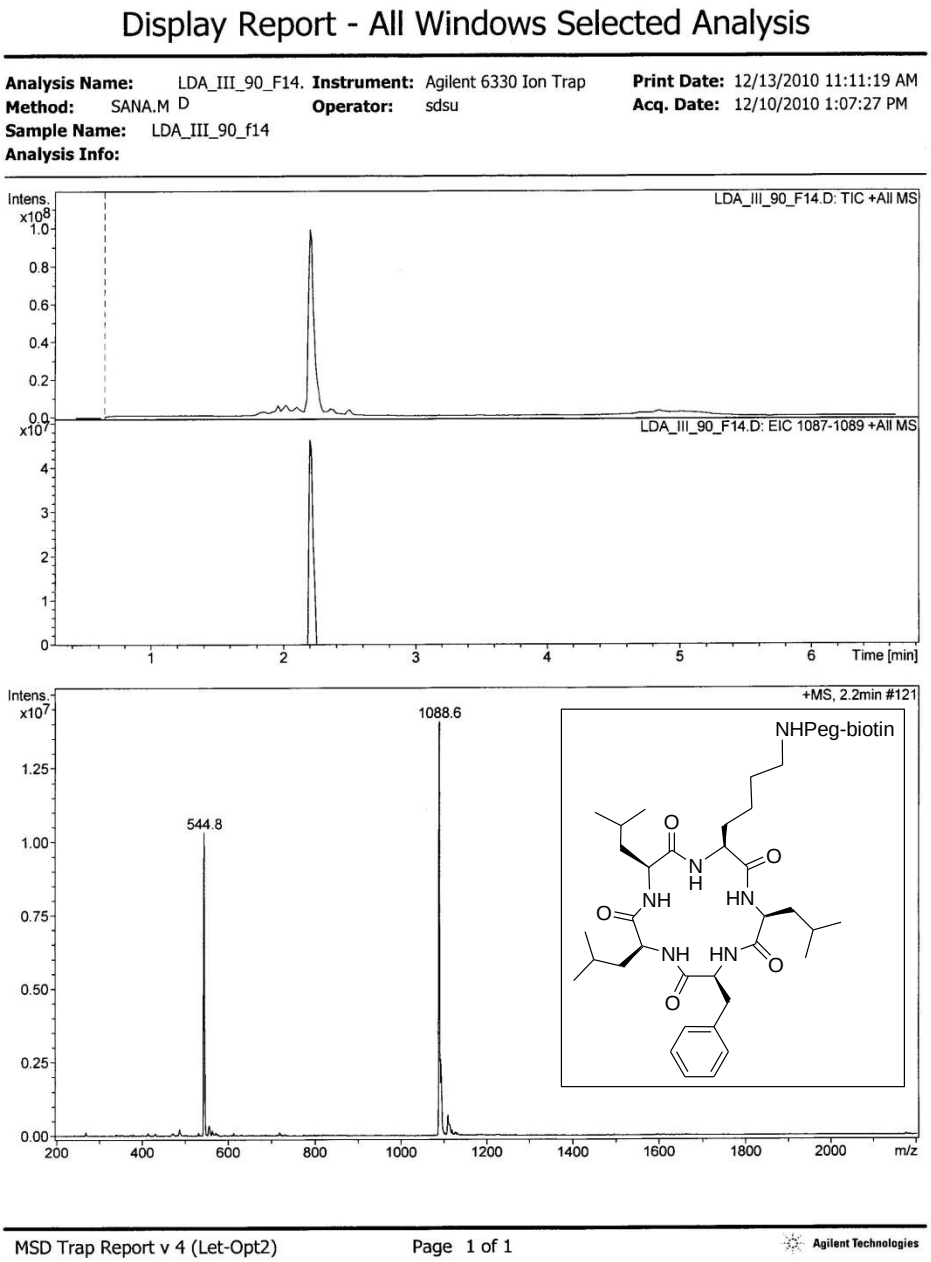

SanA 1-T-III-Biotin LCMS: Phe-Leu-Lys(Peg-biotin)-Leu-Leu (MW= 1088)

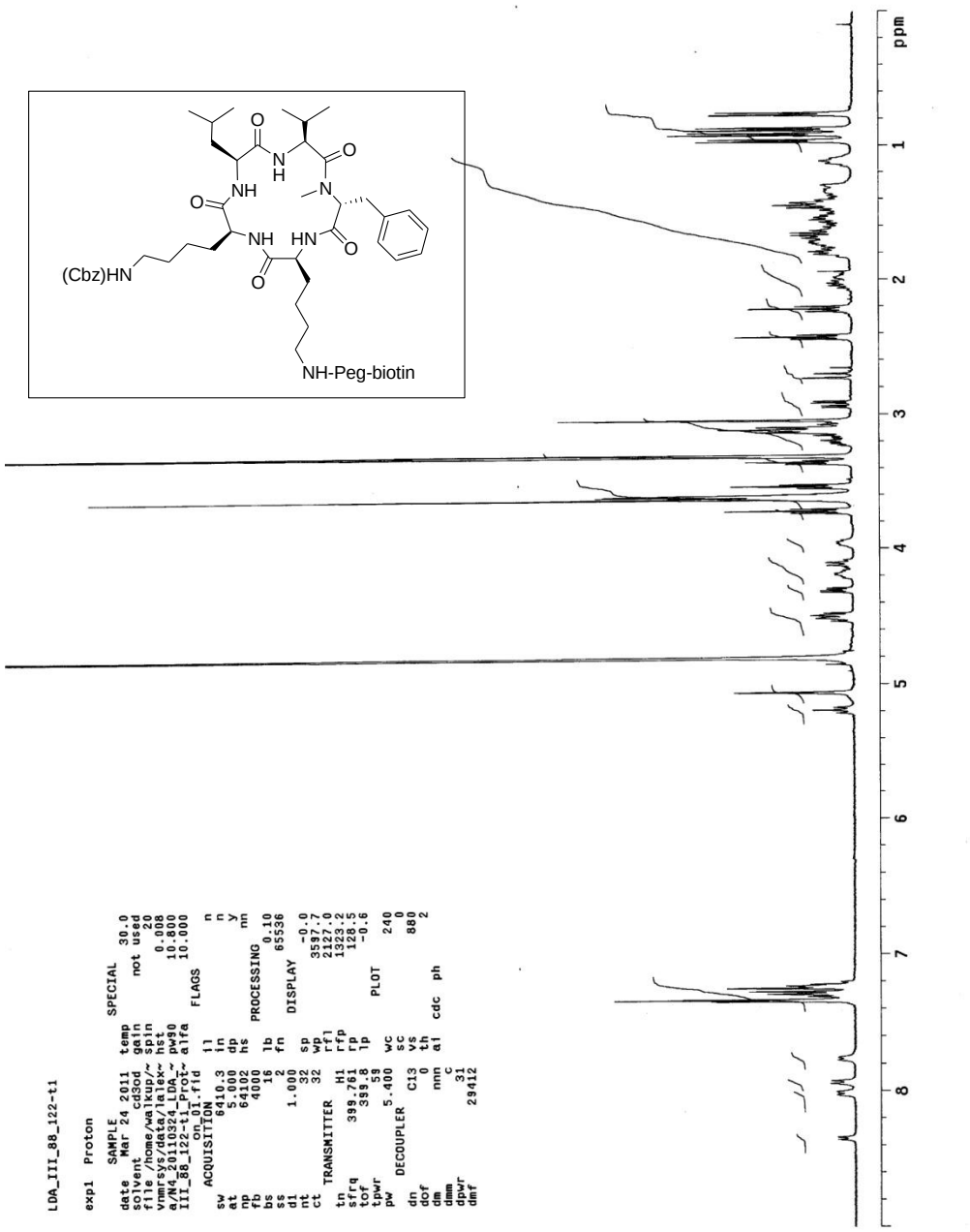

SanA 12-T-I-Biotin ^{1}H-NMR: Lys(Peg-biotin)-*N*-Me-D-Phe-Val-Leu-Lys(Cbz)

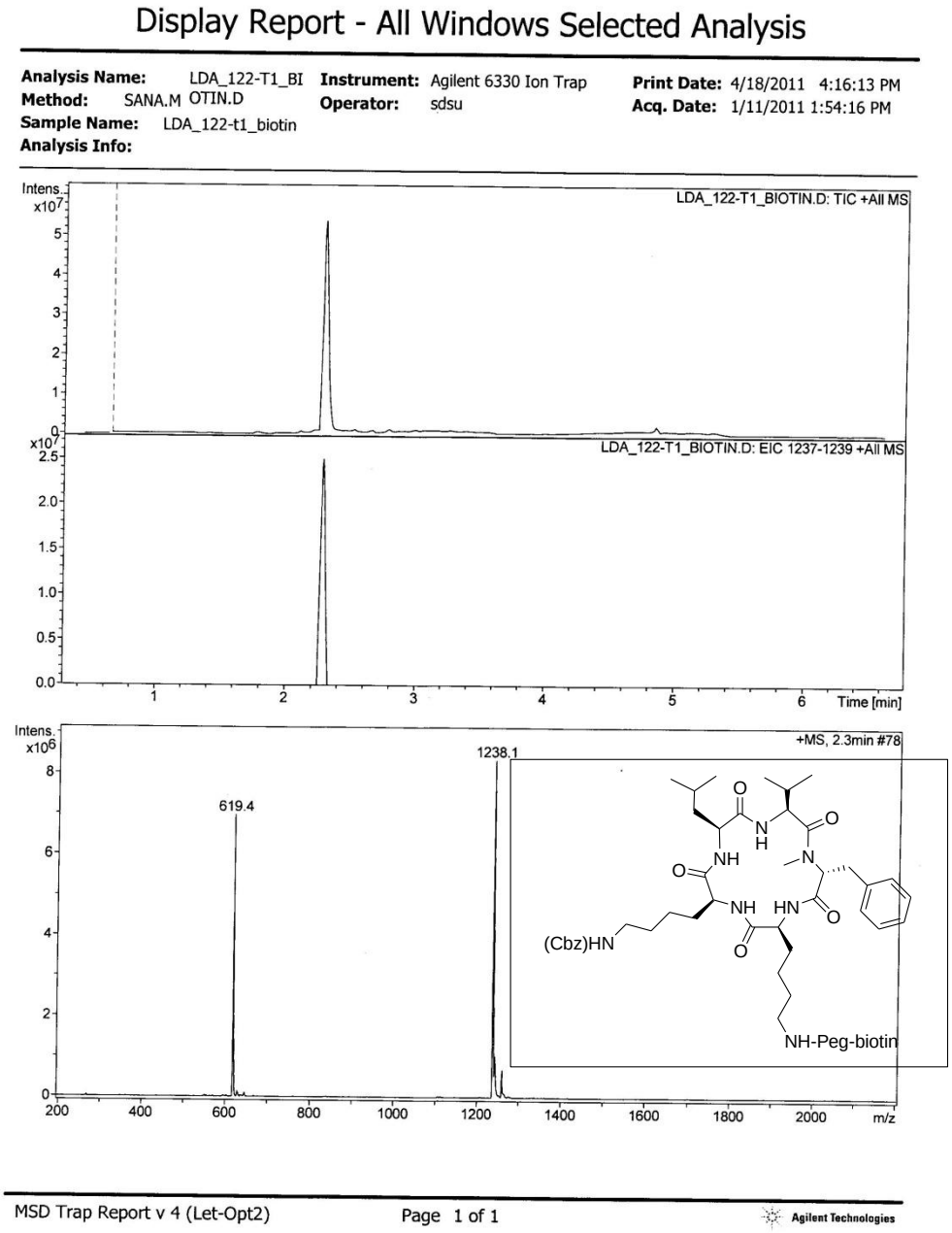

SanA 12-T-I-Biotin LCMS: Lys(Peg-biotin)-*N*-Me-D-Phe-Val-Leu-Lys(Cbz) (MW= 1237)

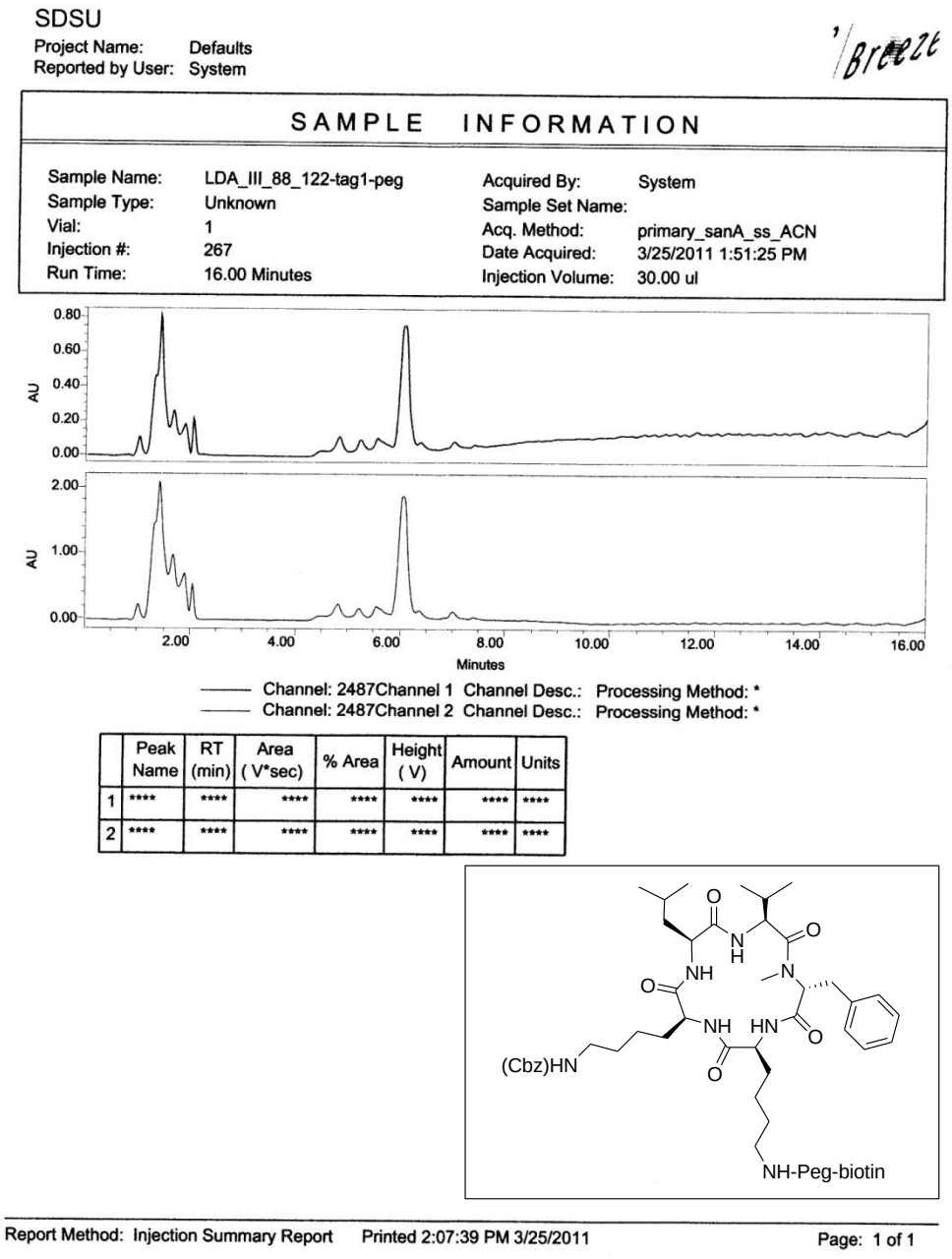

SanA 12-T-I-Biotin HPLC trace: Lys(Peg-biotin)-*N*-Me-D-Phe-Val-Leu-Lys(Cbz)

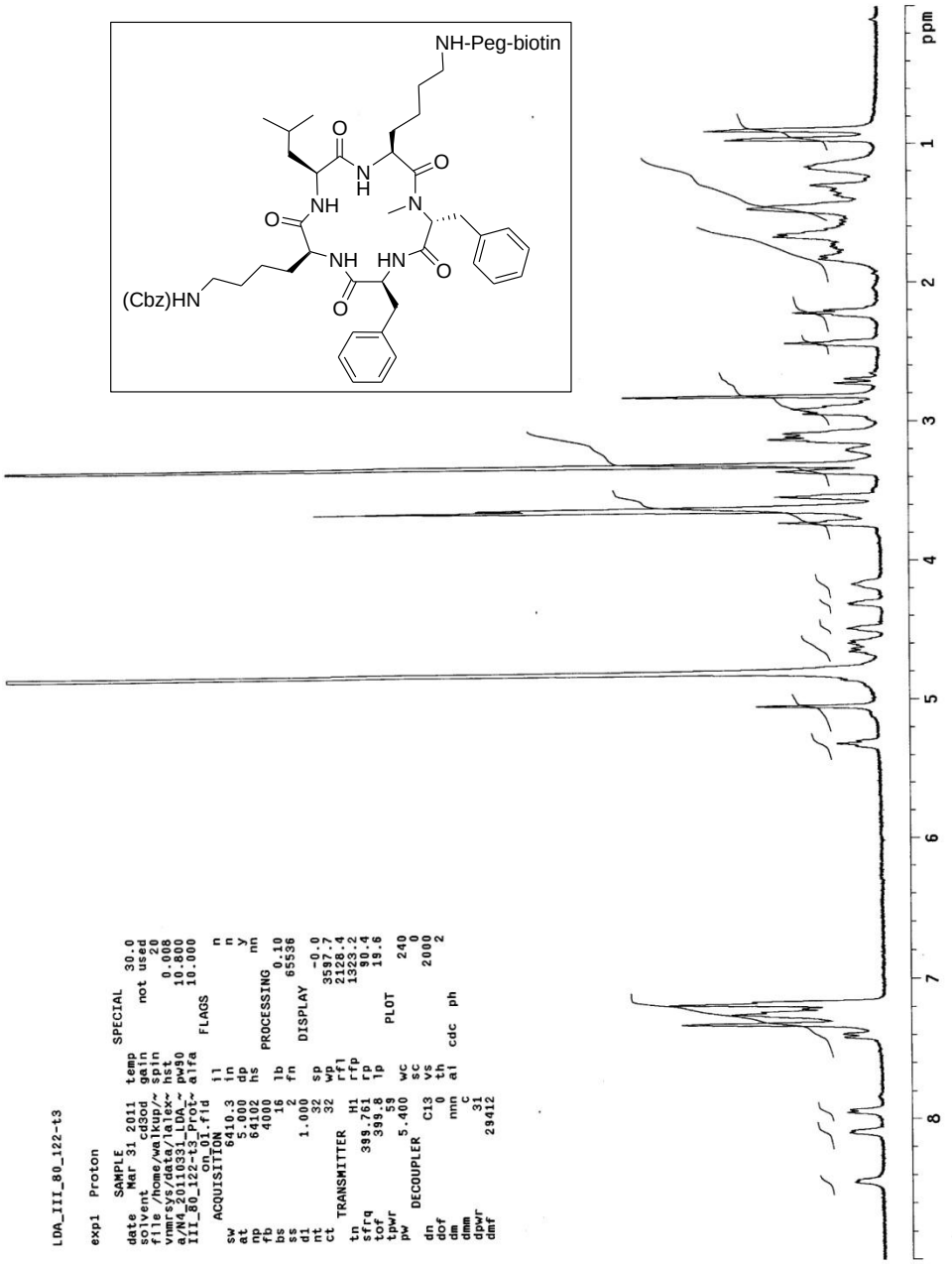

SanA 12-T-III-Biotin 1H-NMR: Phe-N-Me-D-Phe-Lys(Peg-biotin)-Leu-Lys(Cbz)

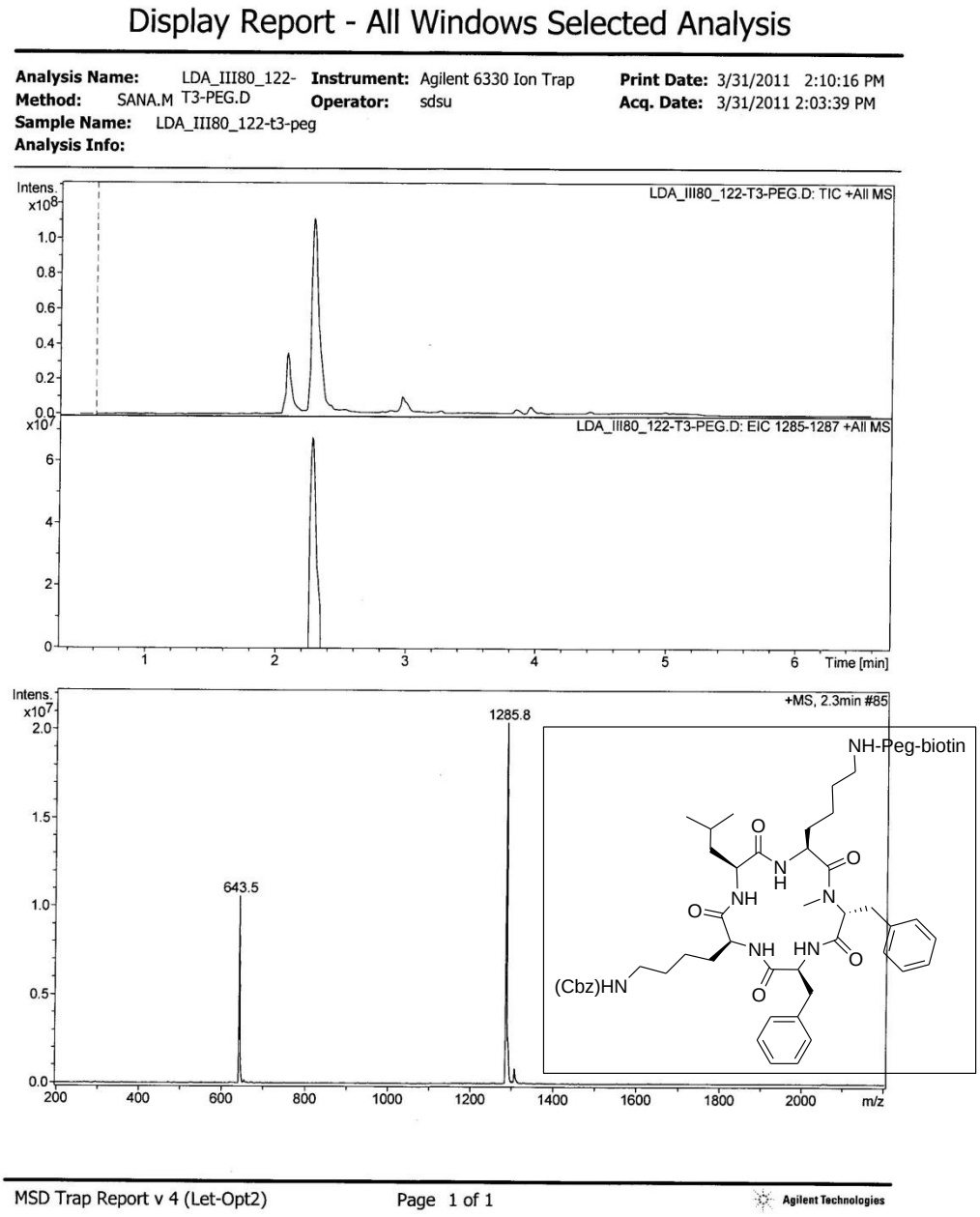

SanA 12-T-III-Biotin LCMS: Phe-*N*-Me-D-Phe-Lys(Peg-biotin)-Leu-Lys(Cbz) (MW= 1284)

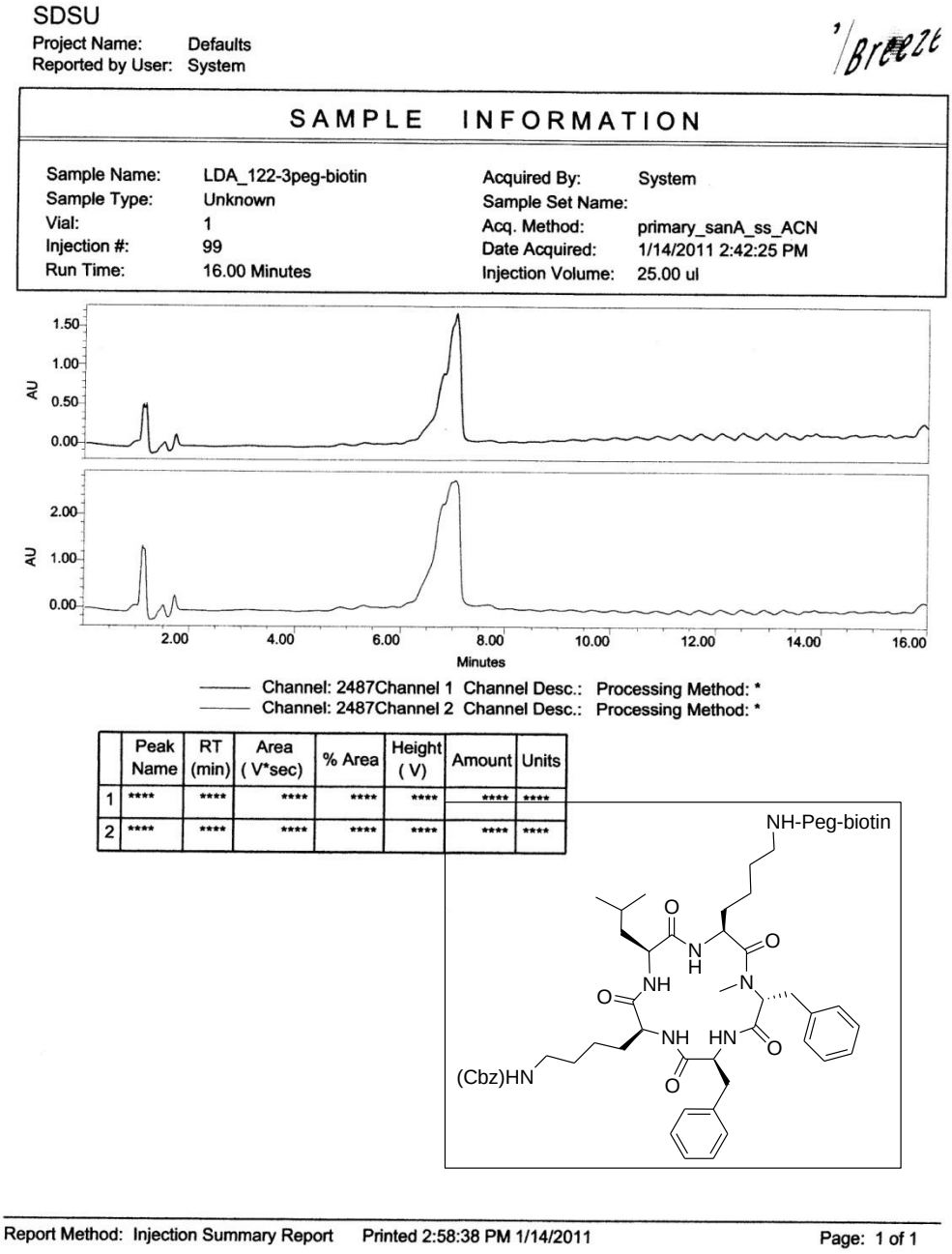

SanA 12-T-III-Biotin HPLC trace: Phe-*N*-Me-D-Phe-Lys(Peg-biotin)-Leu-Lys(Cbz)

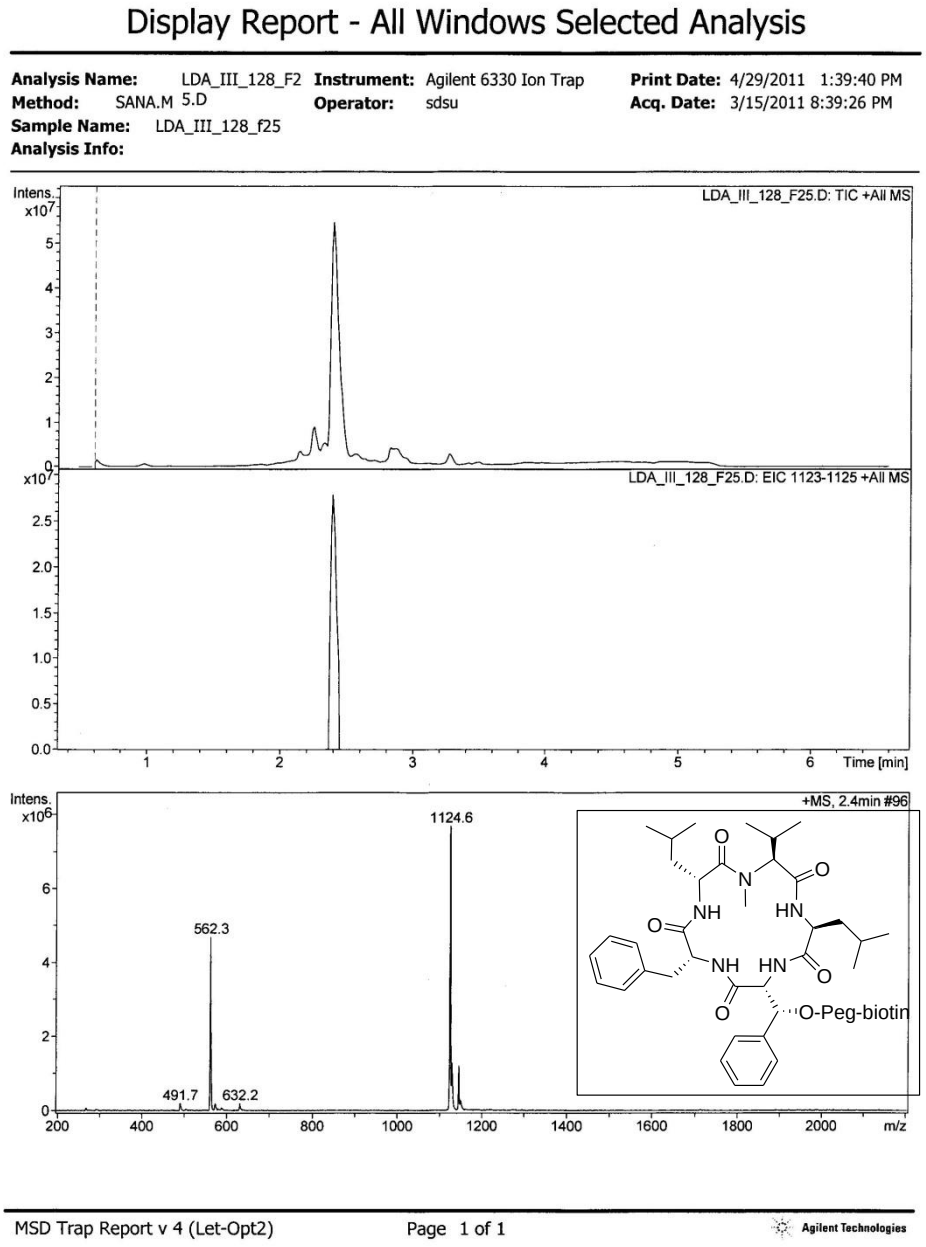

SanA 13-T-I-Biotin LCMS: (2R, 3R)-β-O(Peg-biotin)-Phe-Leu-*N*-Me-Val-D-Leu-D-Phe (MW= 1123)

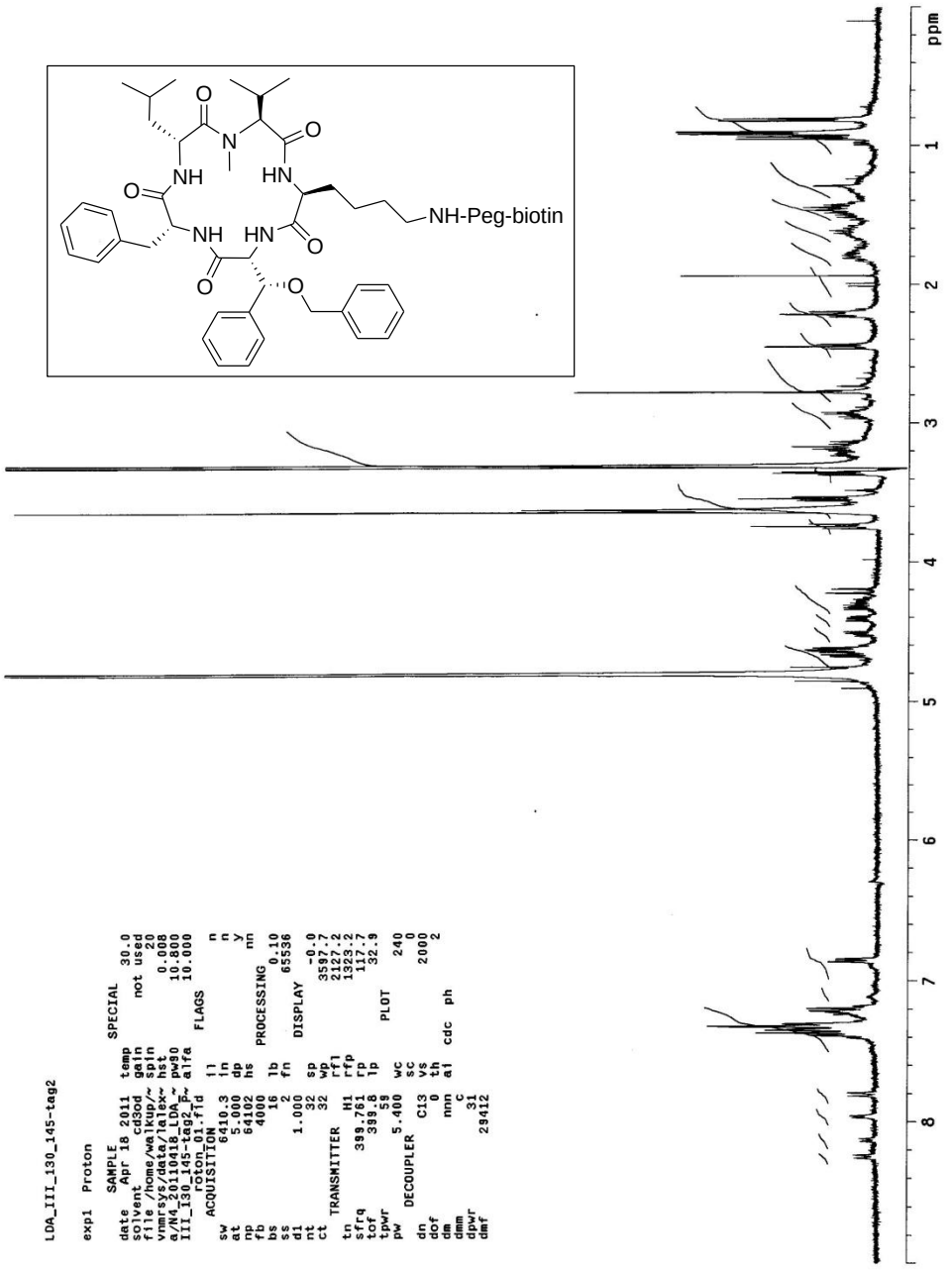

SanA 13-T-II-Biotin ^{1}H-NMR: (2R,3R)/ (2S,3S)-β-OBn-Phe-Lys(Peg-biotin)-*N*-Me-Val-D-Leu-D-Phe

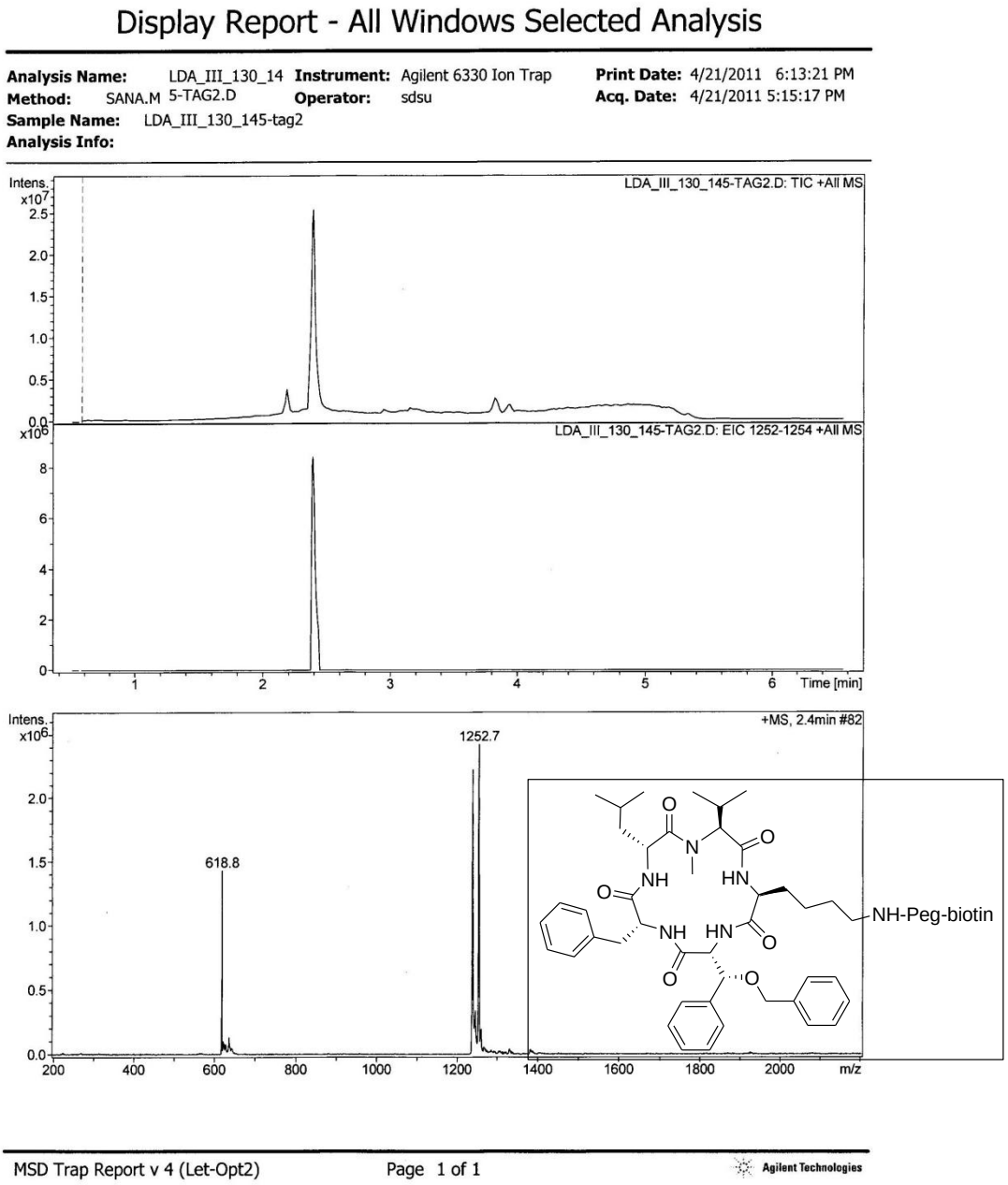

SanA 13-T-II-Biotin LCMS: (2R,3R)/ (2S,3S)-β-OBn-Phe-Lys(Peg-biotin)-*N*-Me-Val-D-Leu-D-Phe MW= (1230+23)

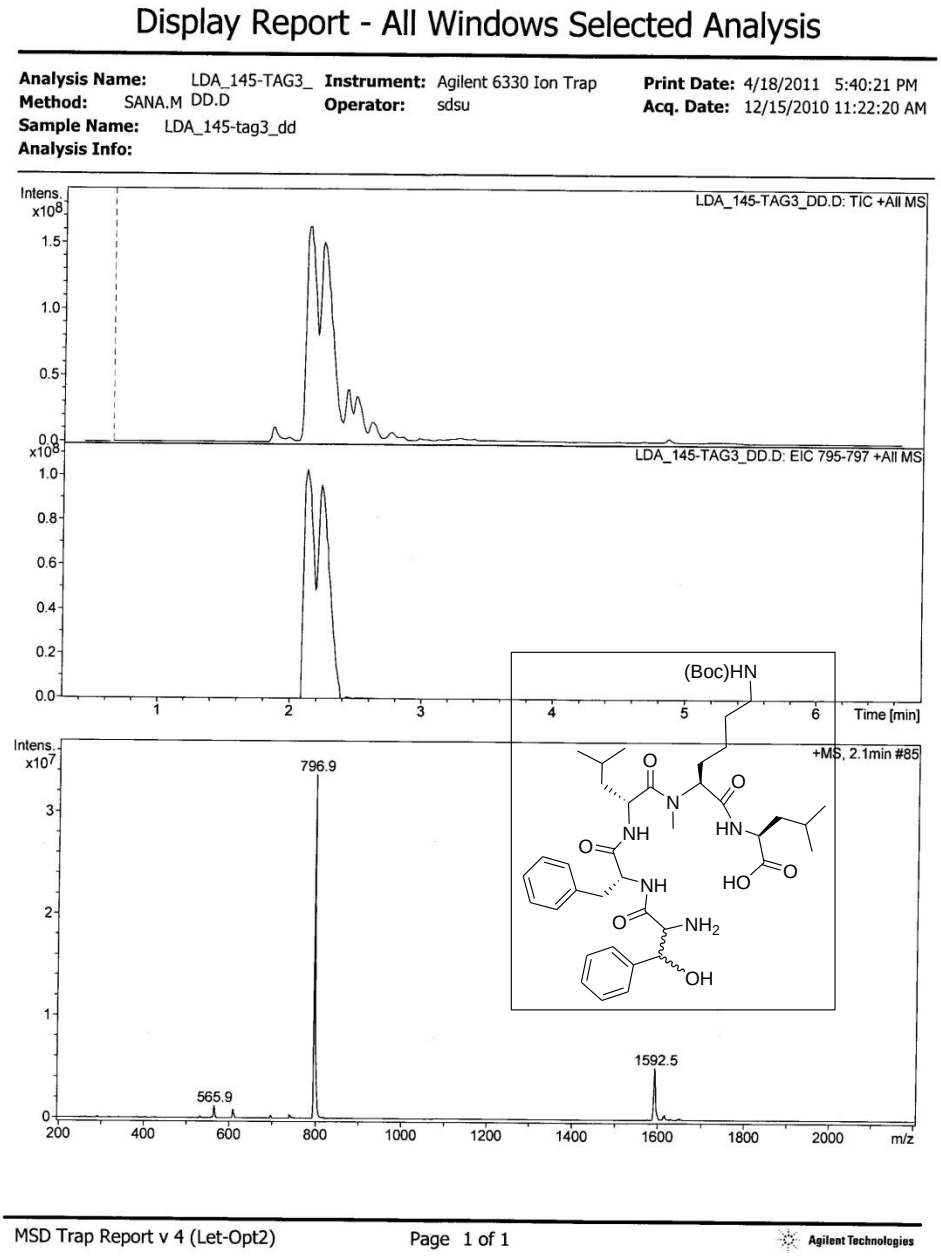

SanA 13-T-III LCMS DDLP: NH_2-(2R,3R)/ (2S,3S)-β-OH-Phe-Leu-*N*-Me-Lys(Boc)-D-Leu-D-Phe-OH (MW=797)

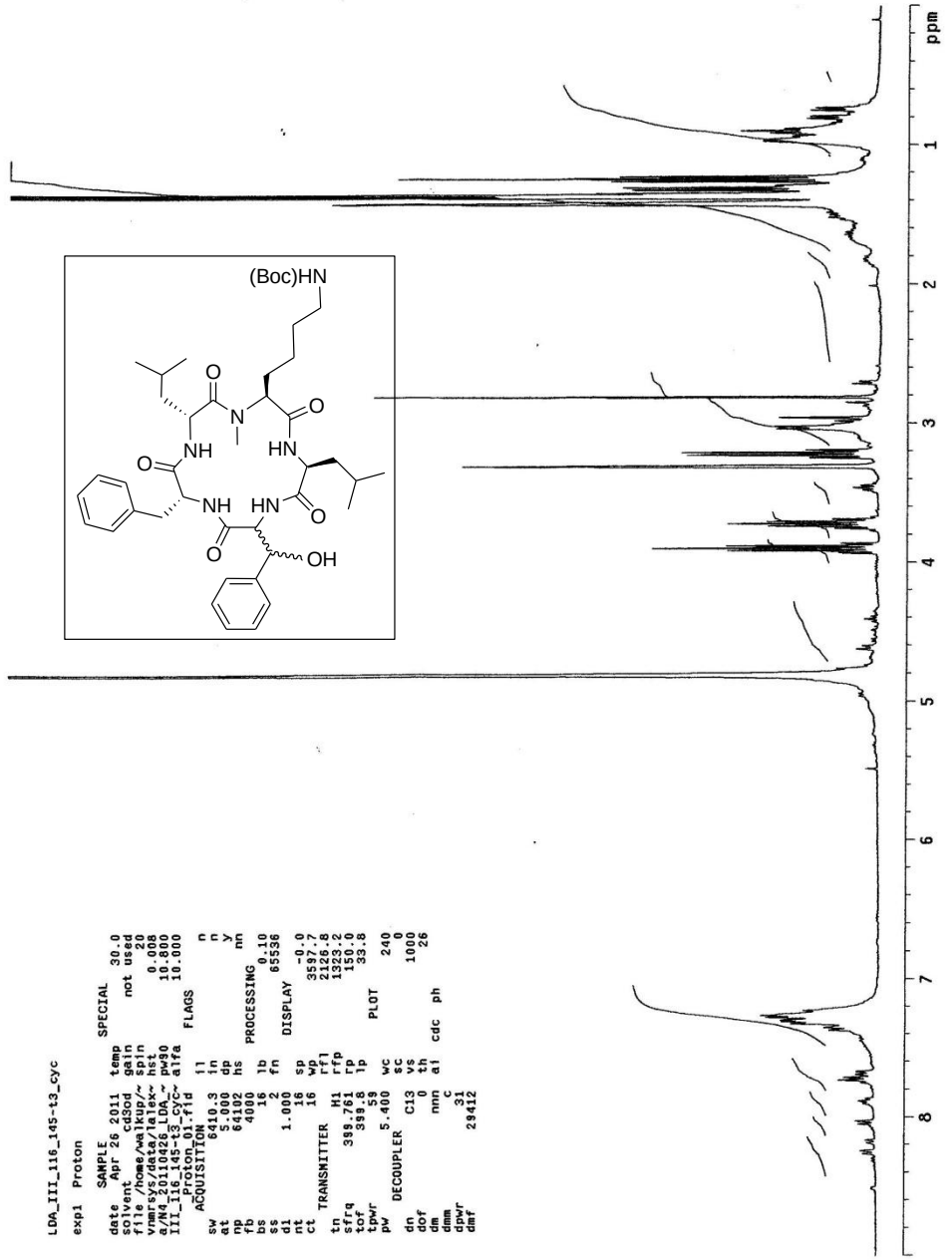

SanA 13-T-III ^{1}H-NMR Cyclized Pentapeptide: (2R,3R)/ (2S,3S)-β-OH-Phe-Leu-*N*-Me-Lys(Boc)-D-Leu-D-Phe

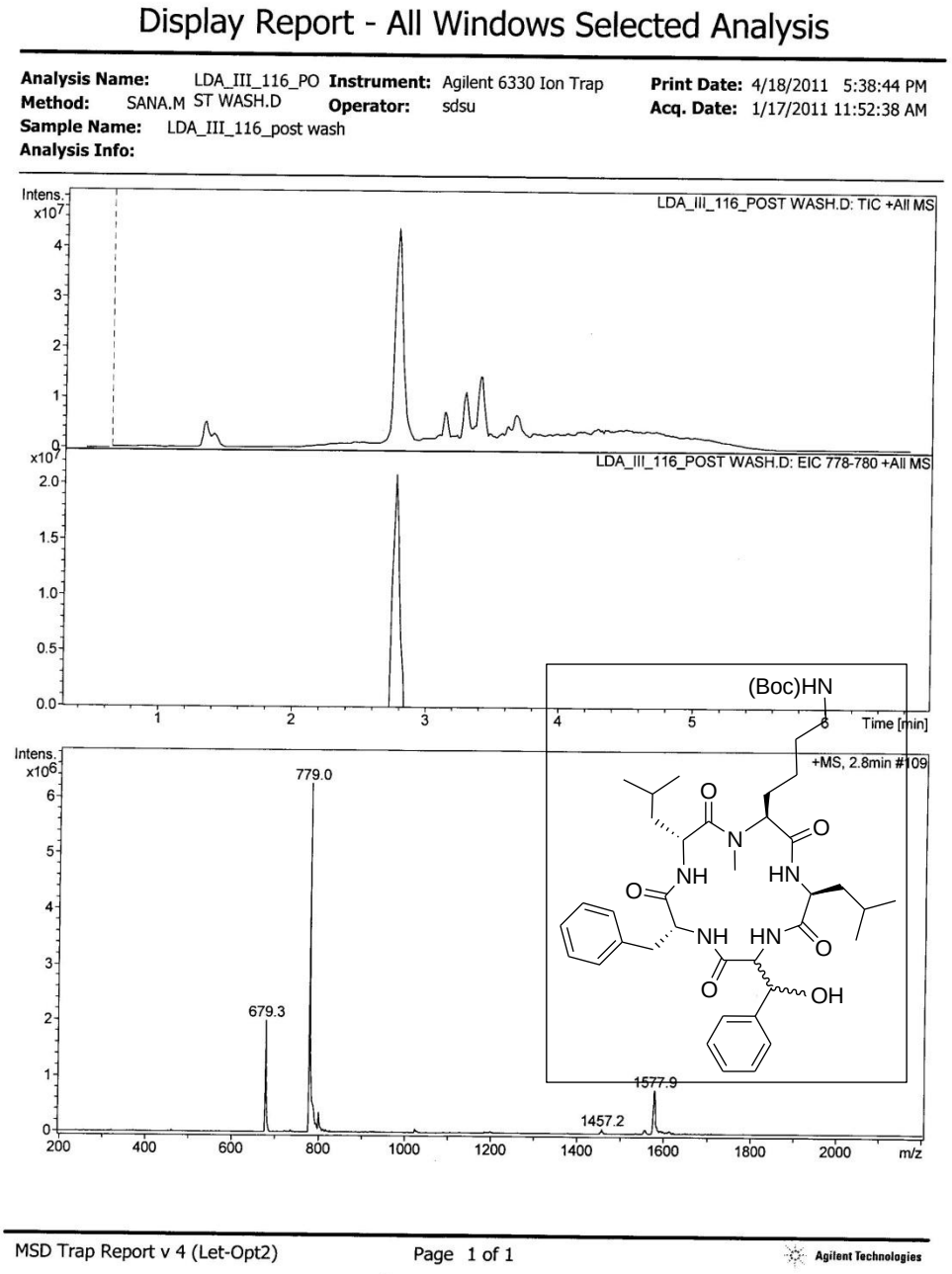

SanA 13-T-III LCMS Cyclized Pentapeptide: (2R,3R)/ (2S,3S)-β-OH-Phe-Leu-*N*-Me-Lys(Boc)-D-Leu-D-Phe (MW= 779)

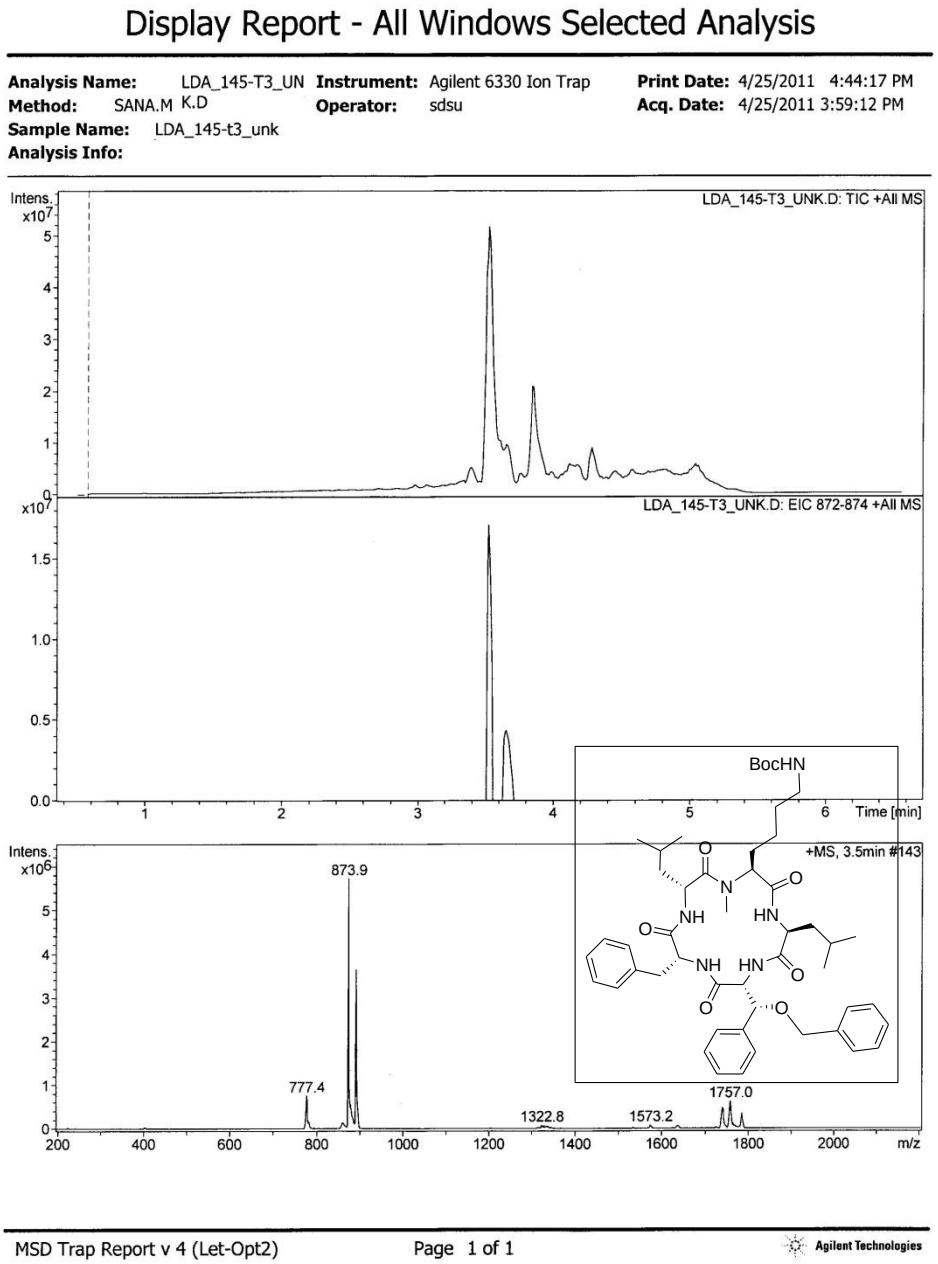

SanA 13-T-III LCMS Cyclized Pentapeptide: (2R,3R)/ (2S,3S)-β-OBn-Phe-Leu-*N*-Me-Lys(Boc)-D-Leu-D-Phe (MW= 869)

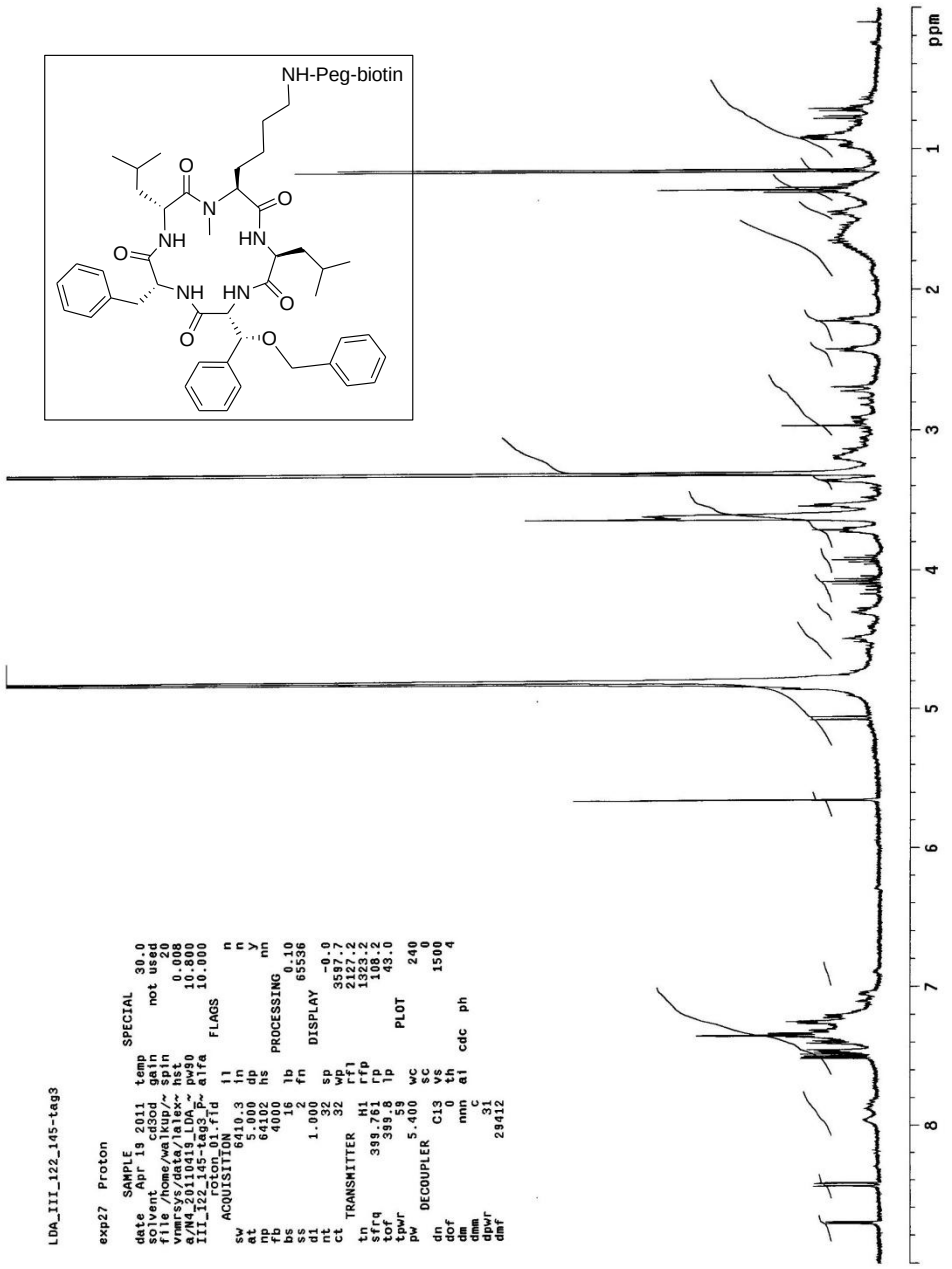

SanA 13-T-III-Biotin ^{1}H-NMR Cyclized Pentapeptide: (2R,3R)/ (2S,3S)-β-OBn-Phe-Leu-*N*-Me-Lys(Peg-biotin)-D-Leu-D-Phe

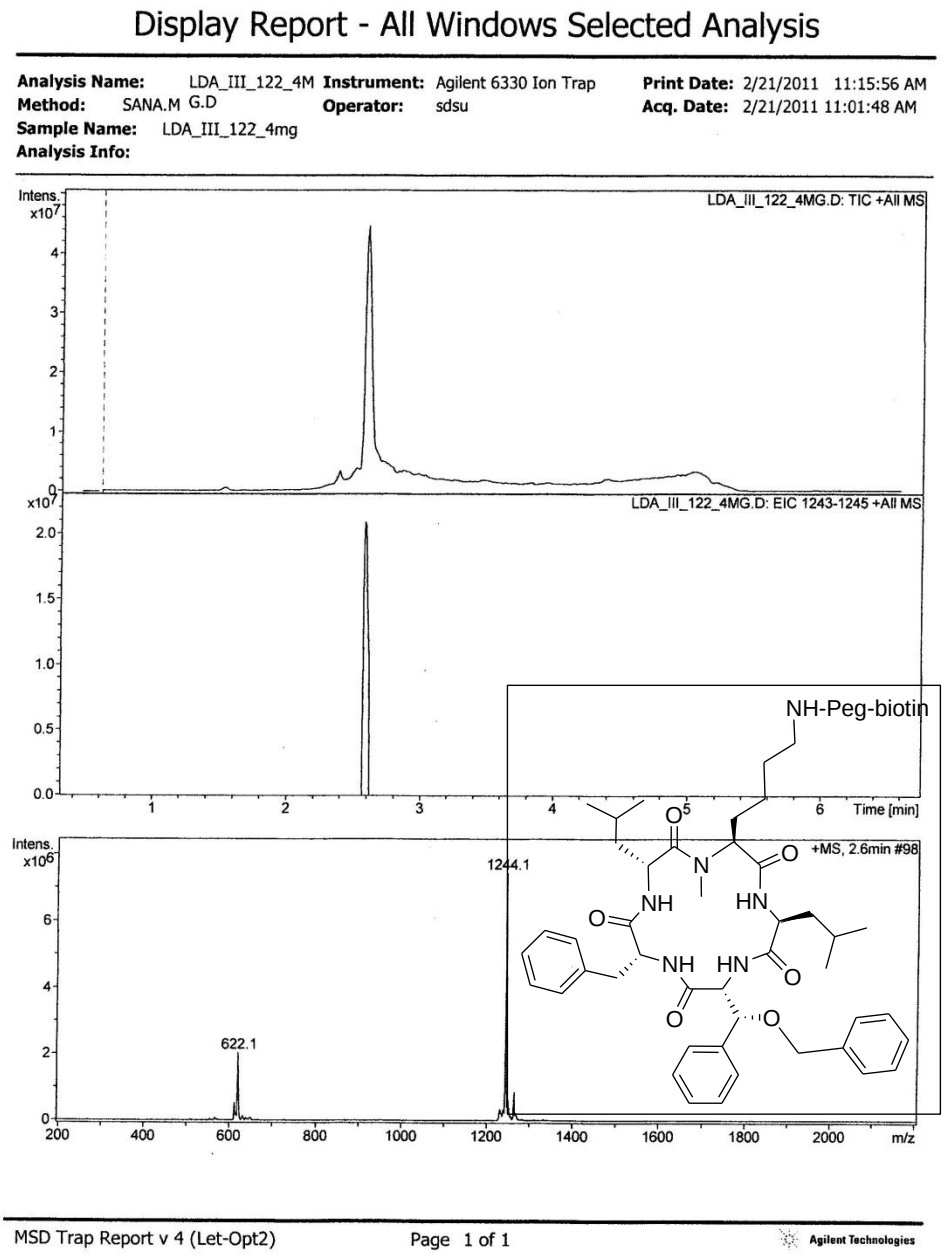

SanA 13-T-III-Biotin LCMS Cyclized Pentapeptide: (2R,3R)/ (2S,3S)-β-OBn-Phe-Leu-*N*-Me-Lys(Peg-biotin)-D-Leu-D-Phe (MW= 1243)

SDSU
Project Name: Defaults
Reported by User: System

'Breeze

SAMPLE INFORMATION

Sample Name:	LDA_145-t3_peg-biotin	Acquired By:	System
Sample Type:	Unknown	Sample Set Name:	
Vial:	1	Acq. Method:	primary_sanA_ss_ACN
Injection #:	177	Date Acquired:	3/2/2011 2:47:17 PM
Run Time:	16.00 Minutes	Injection Volume:	25.00 ul

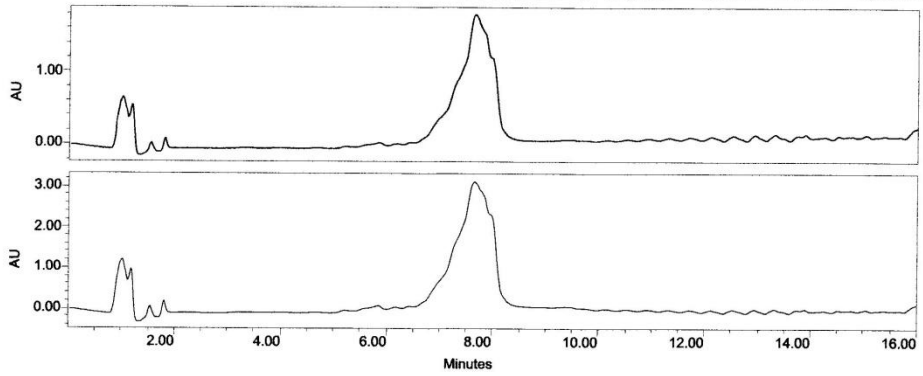

Channel: 2487Channel 1 Channel Desc.: Processing Method: *
Channel: 2487Channel 2 Channel Desc.: Processing Method: *

	Peak Name	RT (min)	Area (V*sec)	% Area	Height (V)	Amount	Units
1	****	****	****	****	****	****	****
2	****	****	****	****	****	****	****

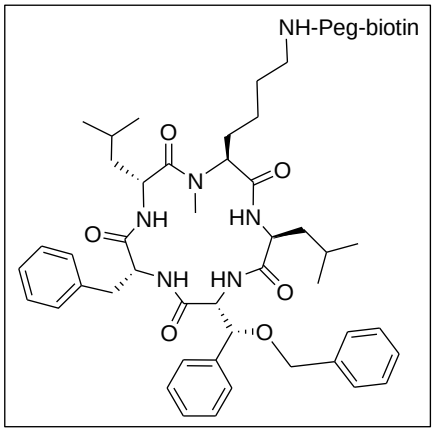

Report Method: Injection Summary Report Printed 3:03:29 PM 3/2/2011 Page: 1 of 1

SanA 13-T-III-Biotin HPLC trace Cyclized Pentapeptide: (2R,3R)/ (2S,3S)-β-OBn-Phe-Leu-*N*-Me-Lys(Peg-biotin)-D-Leu-D-Phe

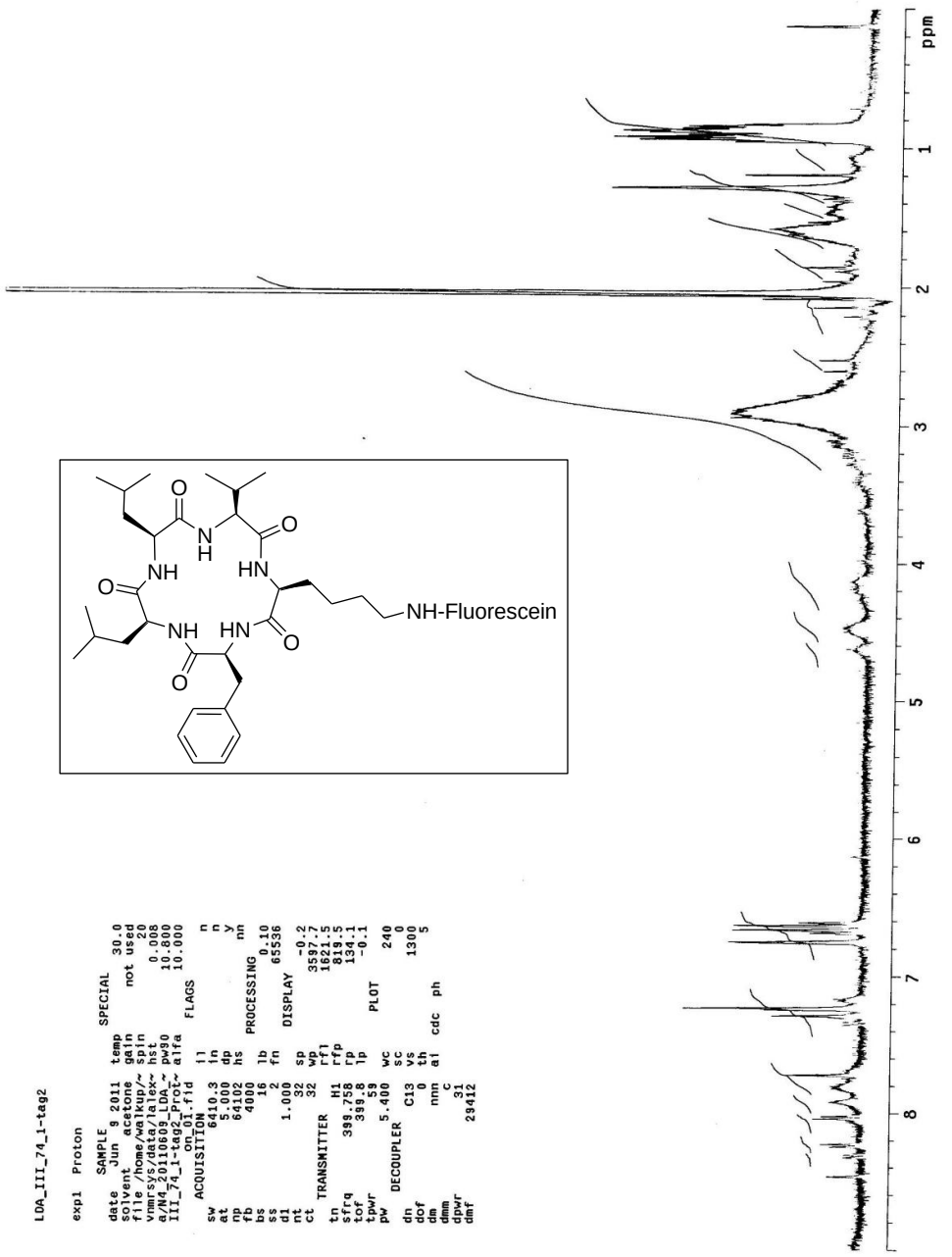

SanA 1-T-II-Fluorescein ^{1}H-NMR: Phe-Lys(Fluor)-Val-Leu-Leu

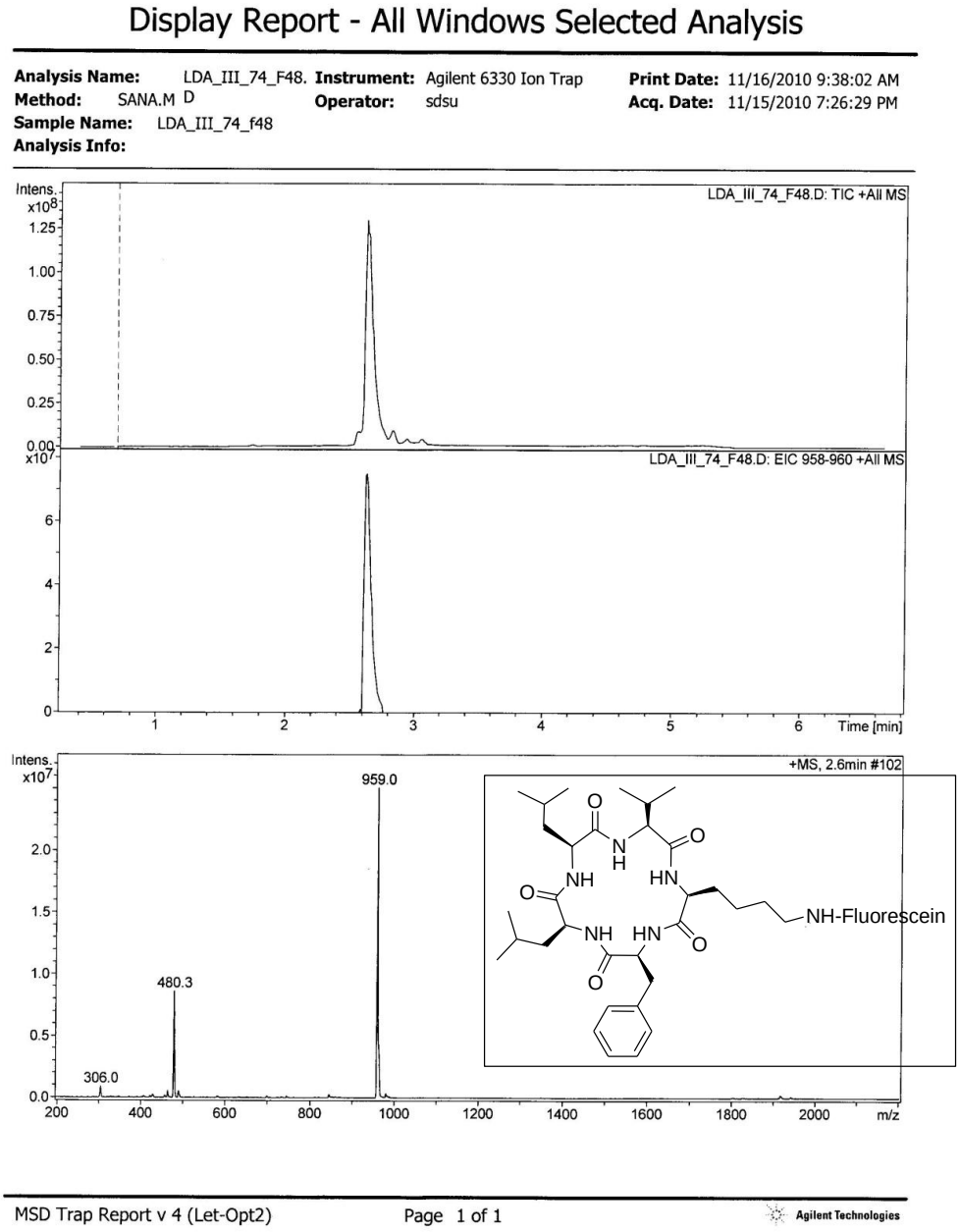

SanA 1-T-II-Fluorescein LCMS: Phe-Lys(Fluor)-Val-Leu-Leu (MW= 959)

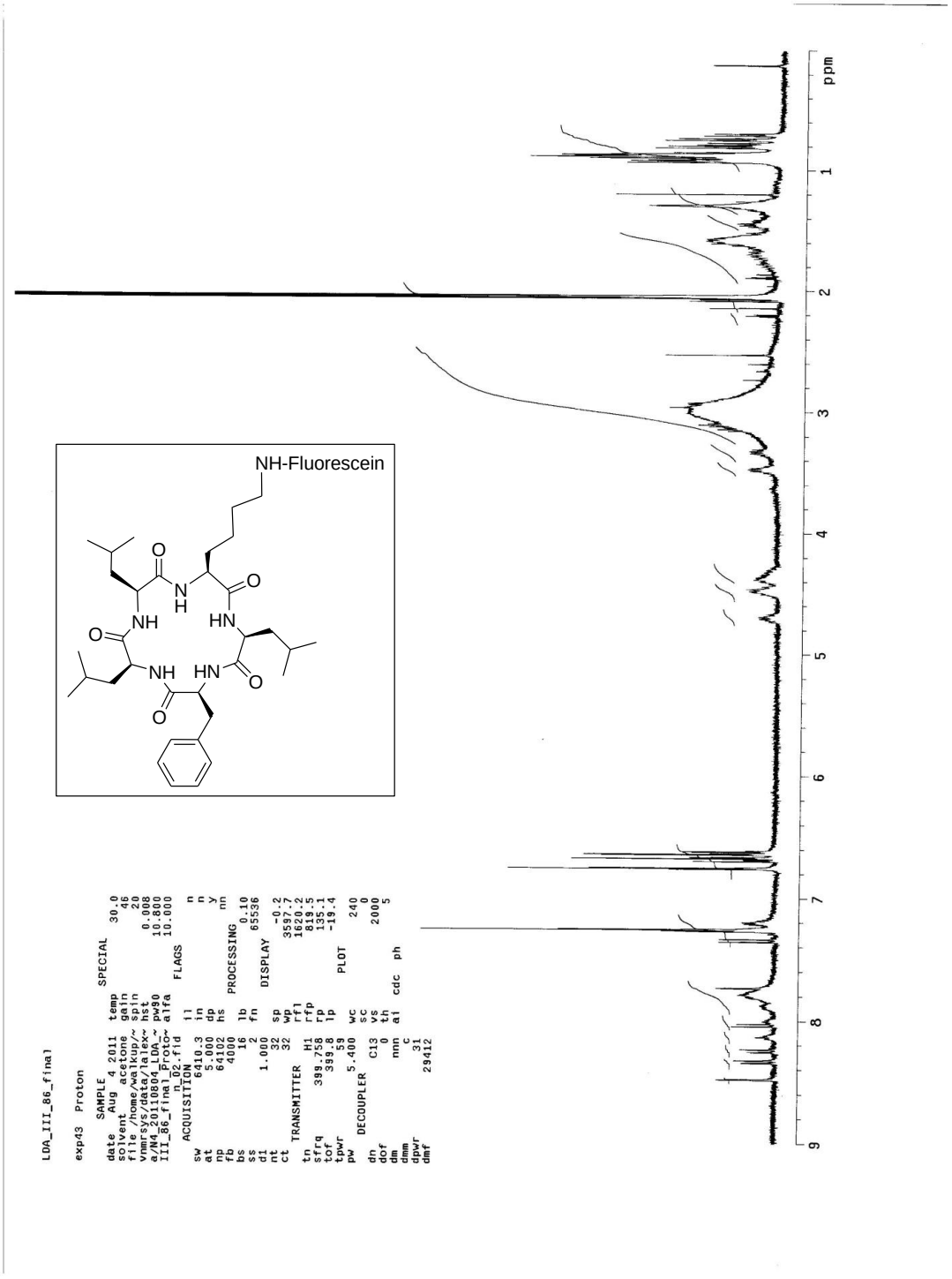

SanA 1-T-III-Fluorescein ^{1}H NMR: Phe-Leu-Lys(Fluor)-Leu-Leu

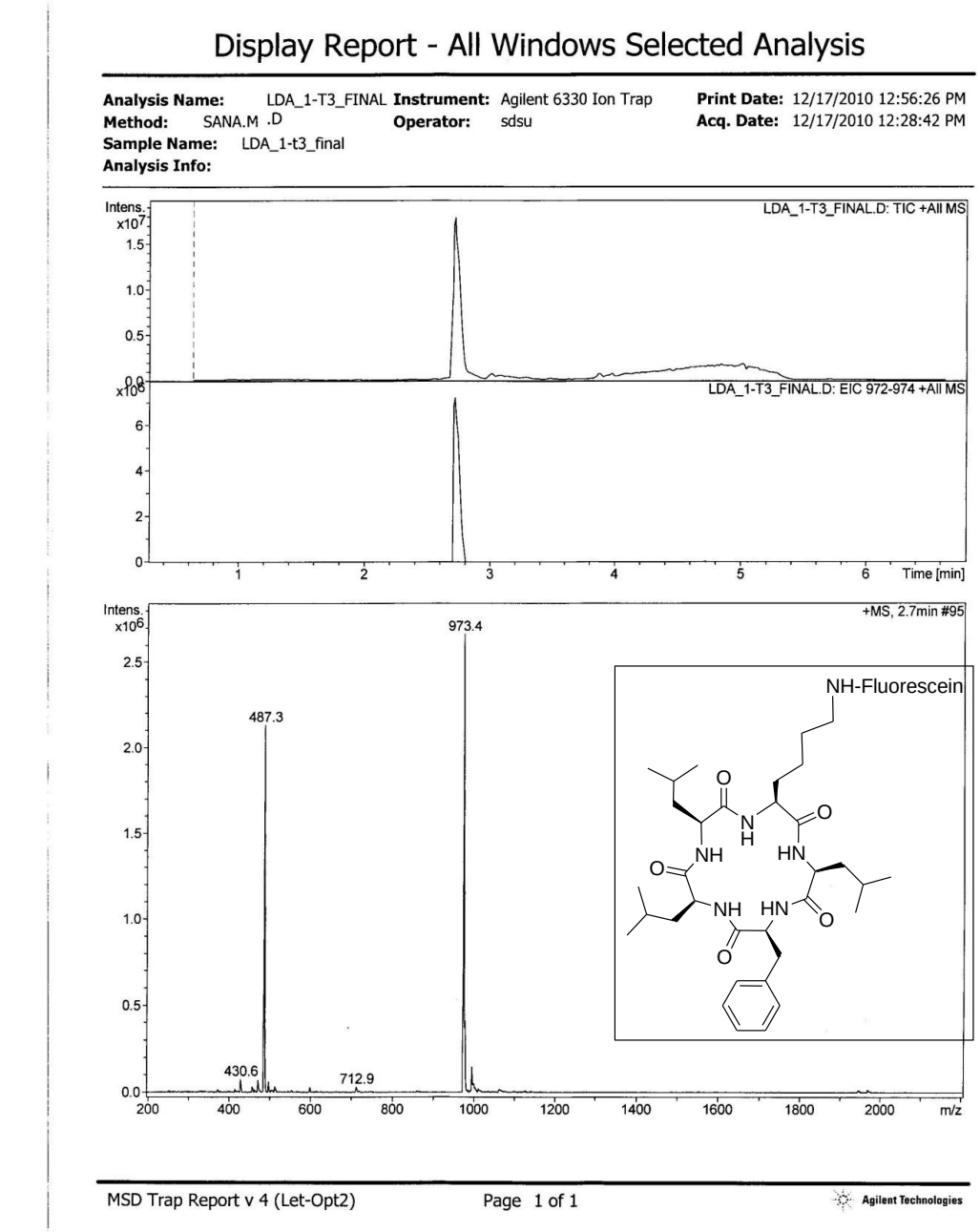

SanA 1-T-III-Fluorescein LCMS: Phe-Leu-Lys(Fluor)-Leu-Leu (MW= 973)

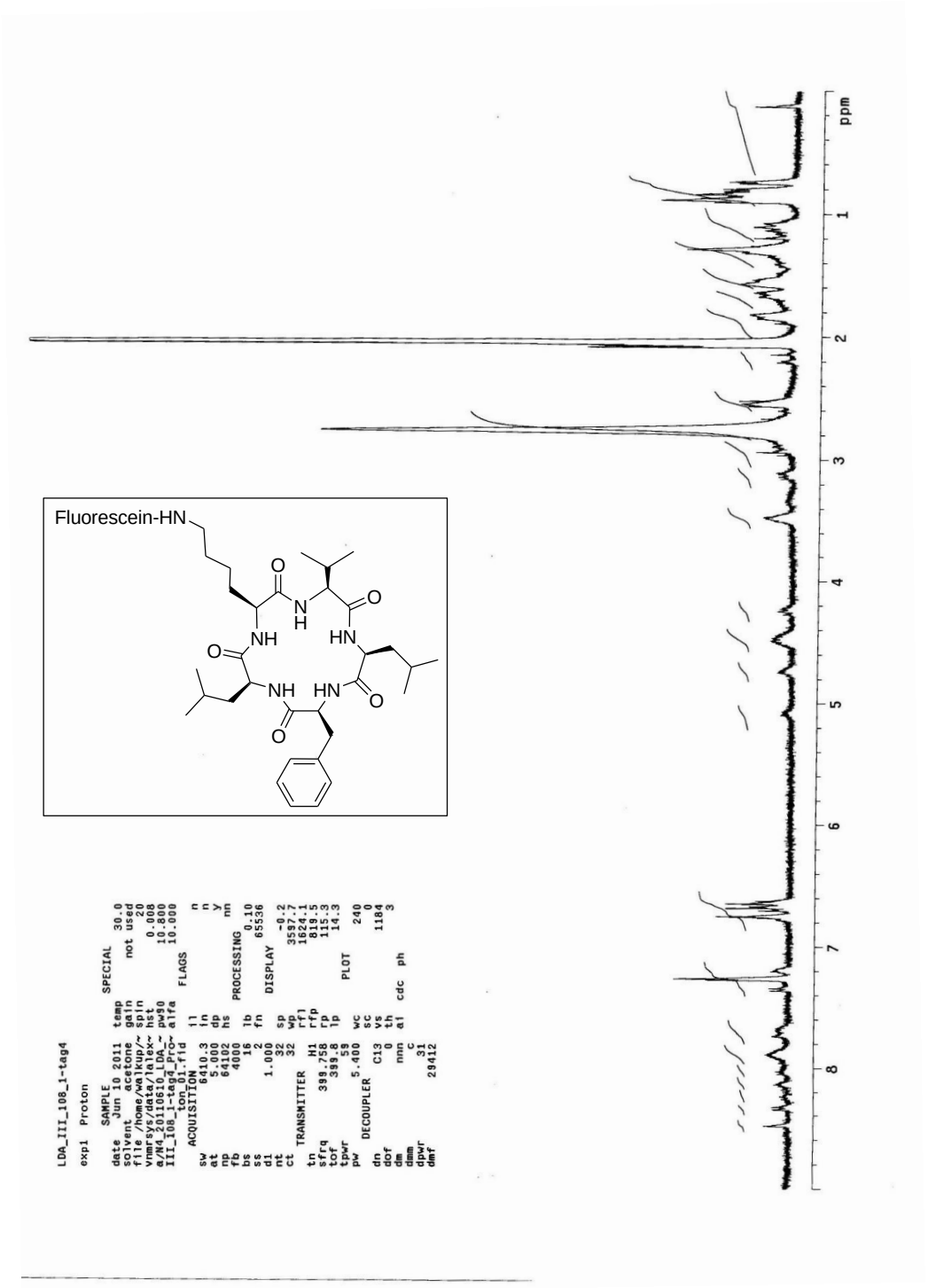

SanA 1-T-IV-Fluorescein ^{1}H NMR: Phe-Leu-Val-Lys(Fluor)-Leu

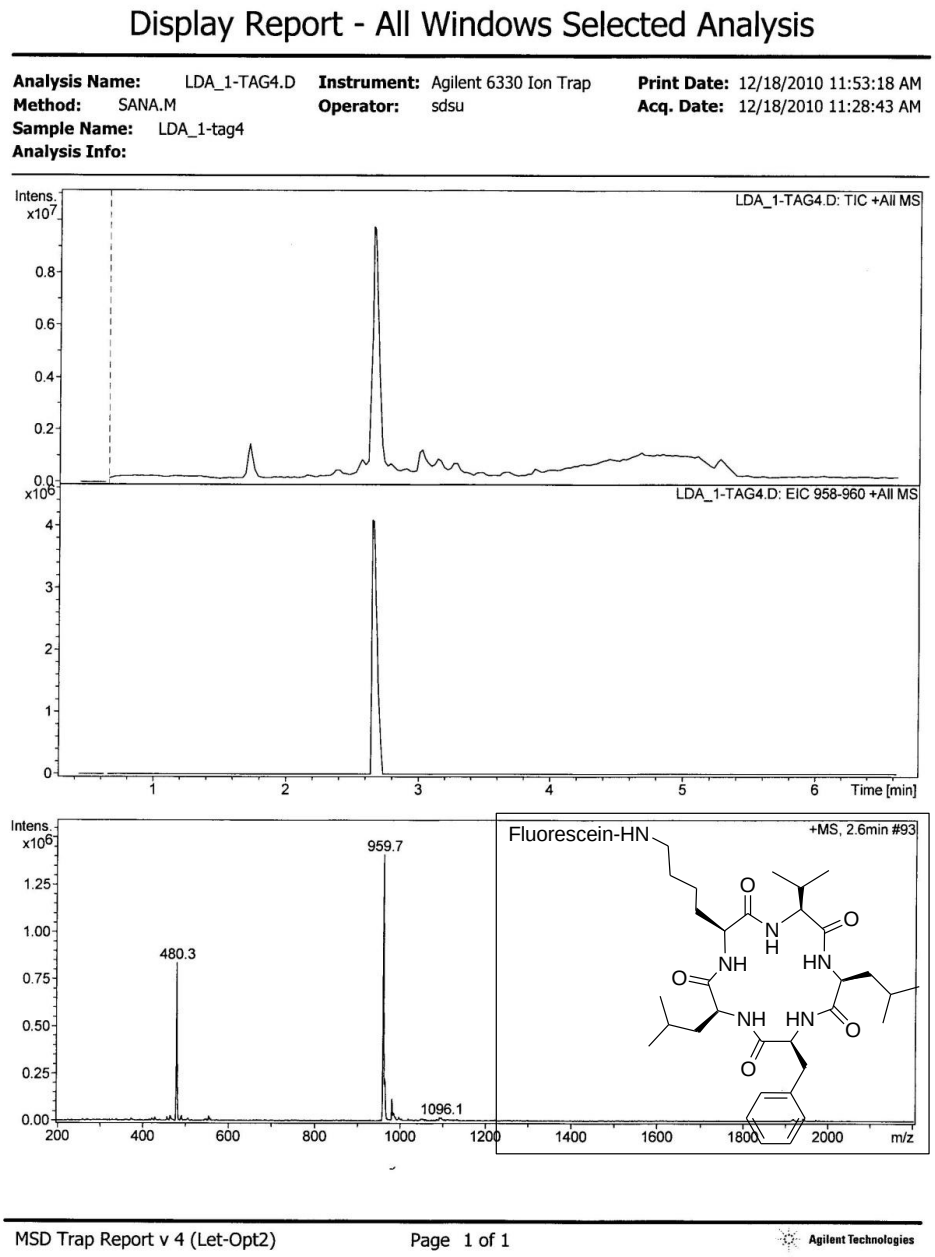

SanA 1-T-IV-Fluorescein LCMS: Phe-Leu-Val-Lys(Fluor)-Leu (MW= 959)

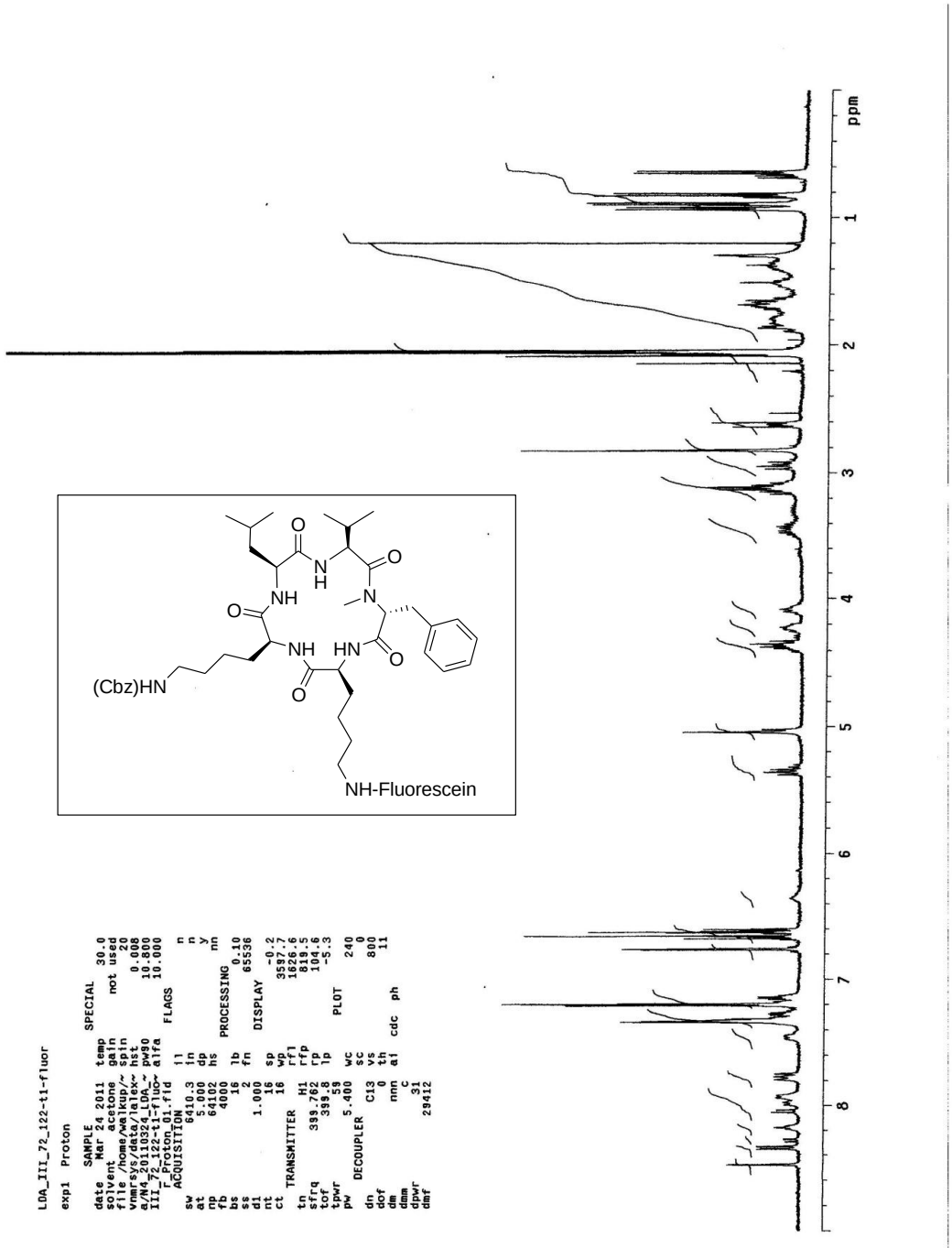

SanA 12-T-I-Fluorescein ^{1}H-NMR: Lys(Fluor)-*N*-Me-D-Phe-Val-Leu-Lys(Cbz)

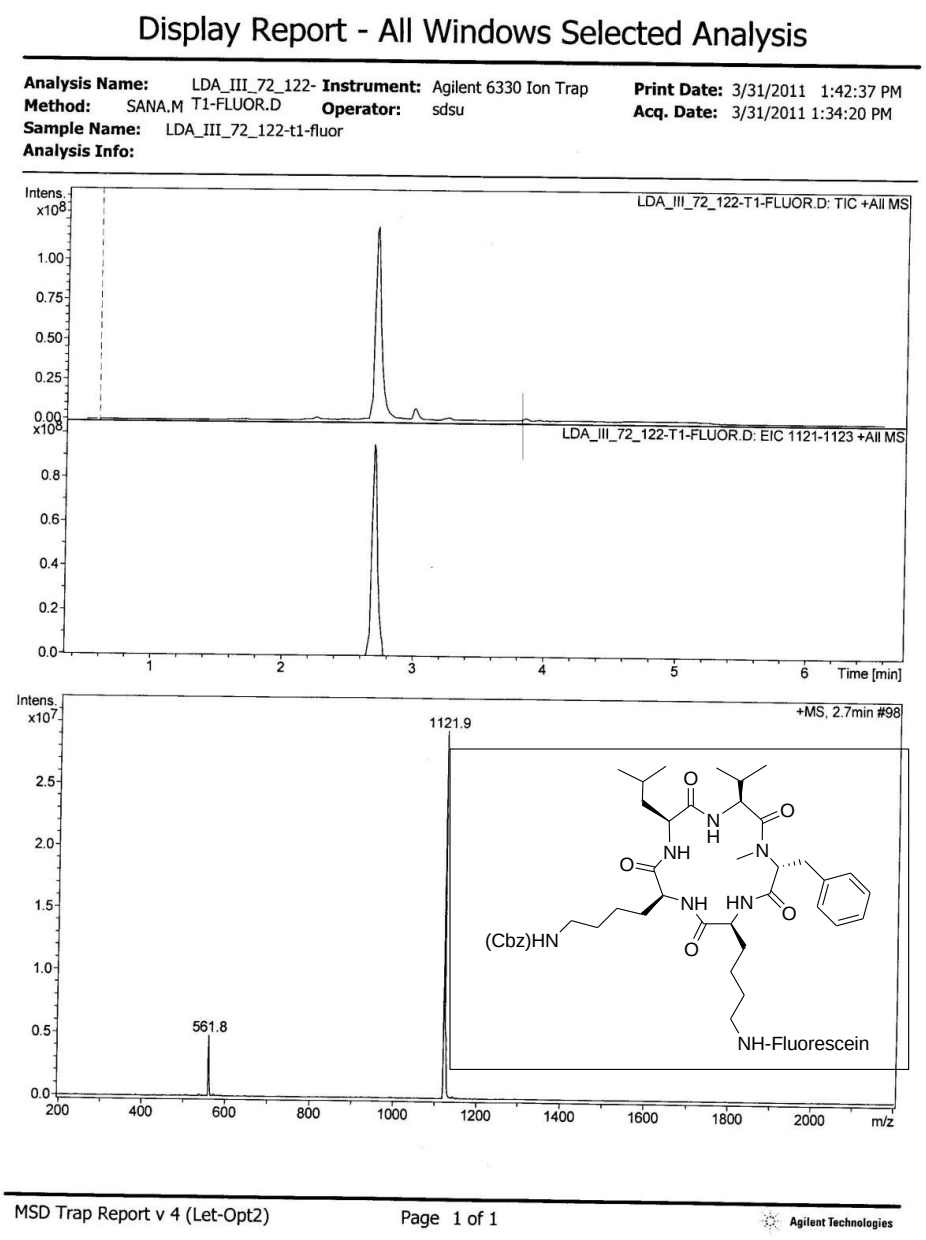

SanA 12-T-I-Fluorescein LCMS: Lys(Fluor)-*N*-Me-D-Phe-Val-Leu-Lys(Cbz) (MW= 1122)

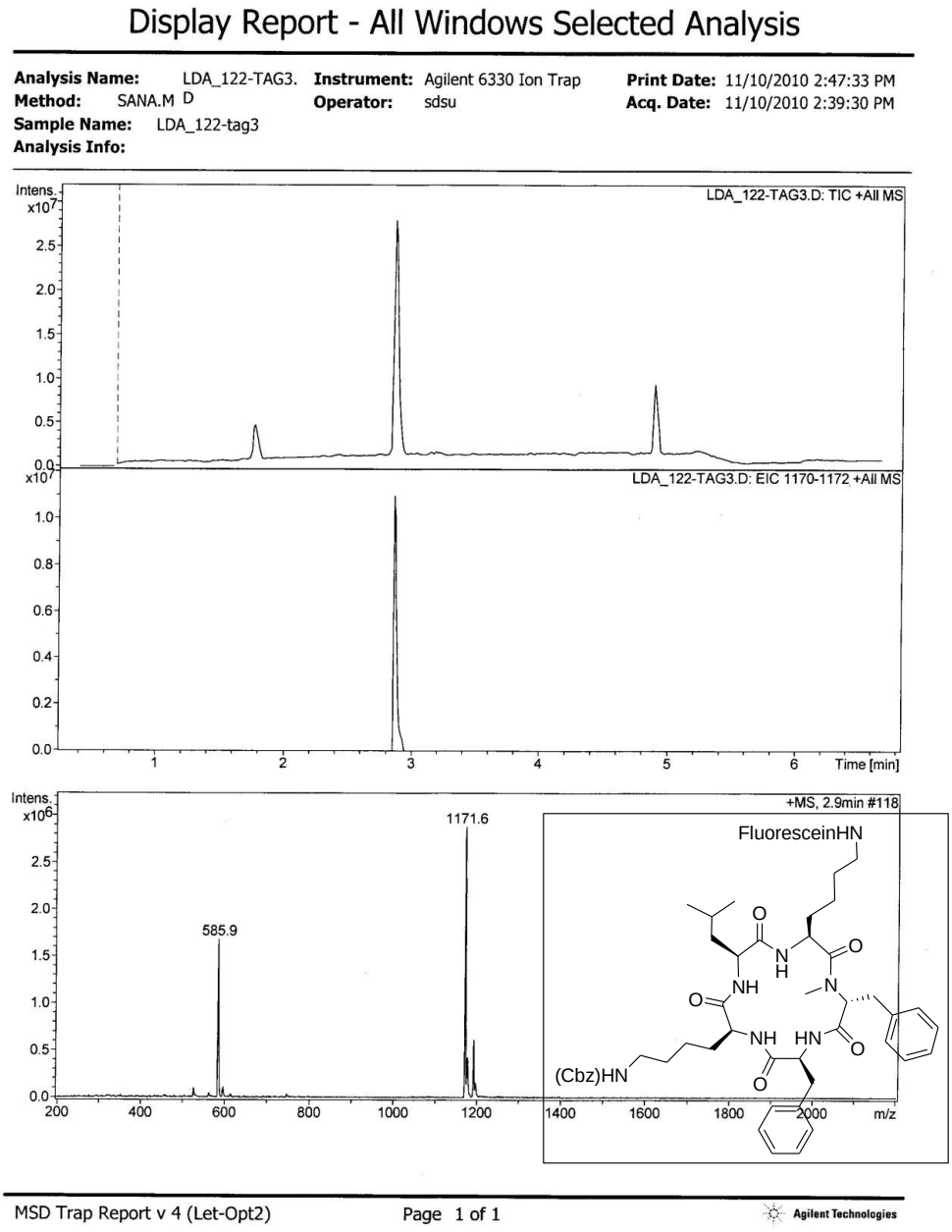

SanA 12-T-III-Fluorescein LCMS: Phe-*N*-Me-D-Phe-Lys(Fluor)-Leu-Lys(Cbz) (MW= 1171)

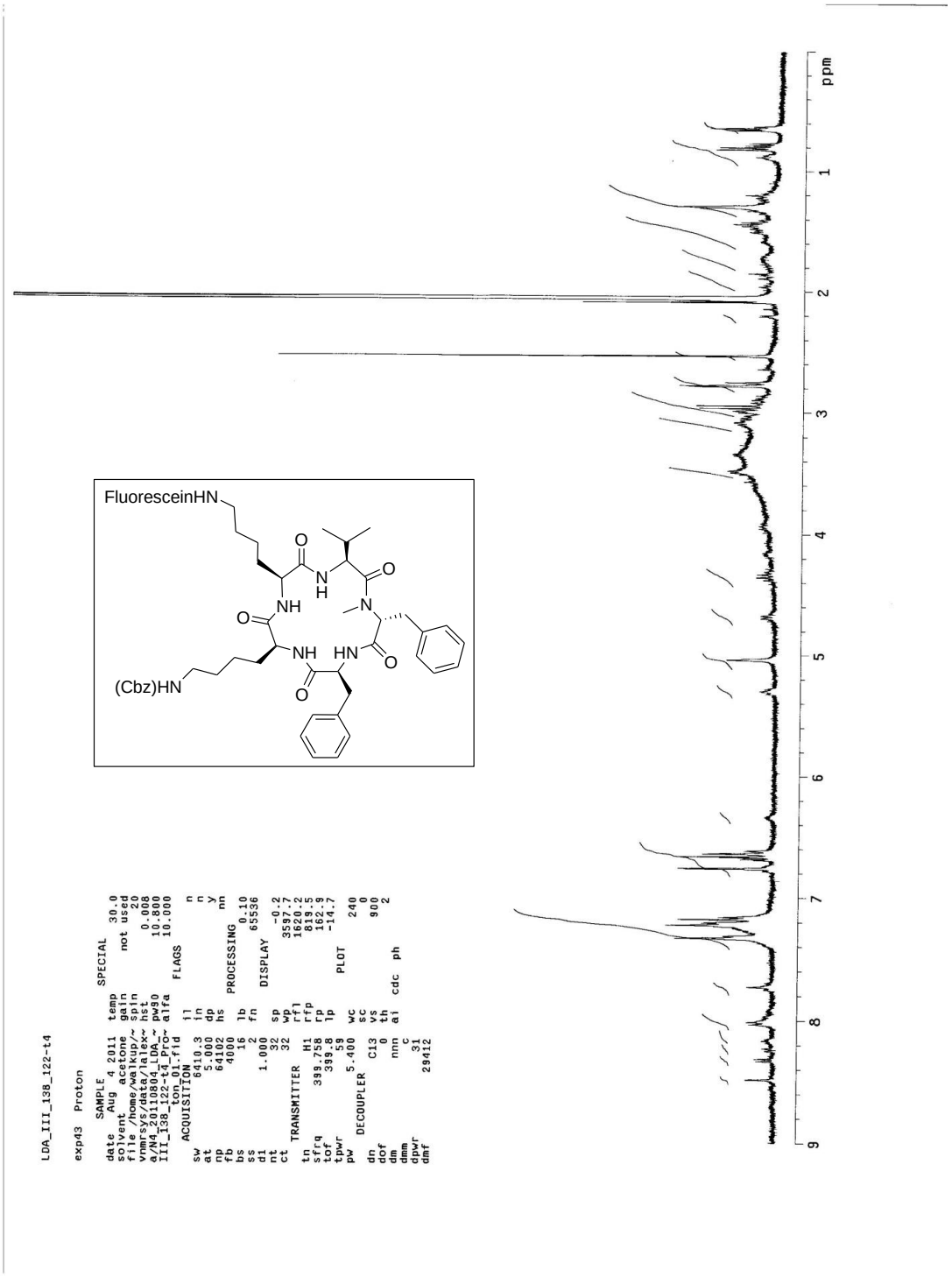

SanA 12-T-IV-Fluorescein ^{1}H-NMR: Phe-*N*-Me-D-Phe-Val-Lys(Fluor)-Lys(Cbz)

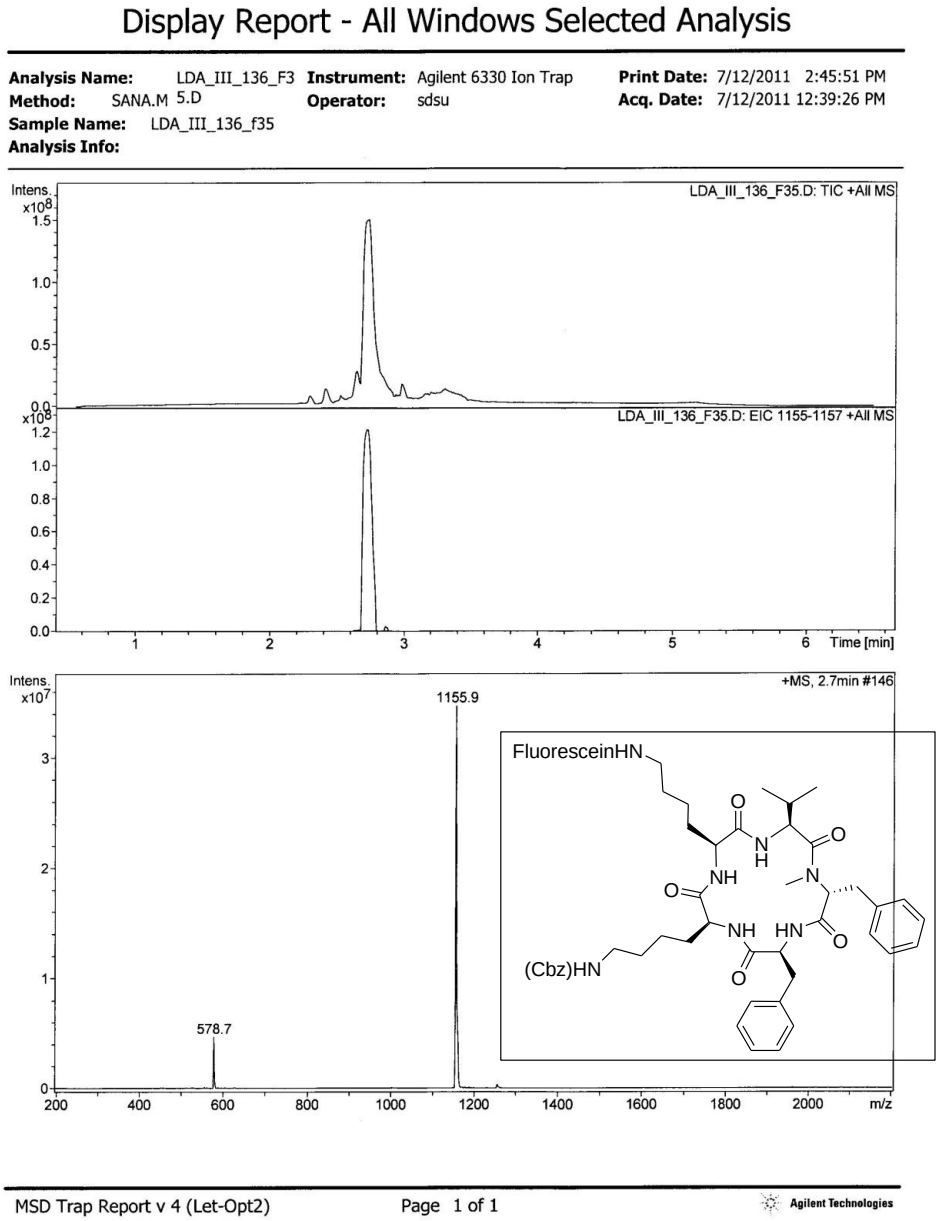

SanA 12-T-IV-Fluorescein LCMS: Phe-*N*-Me-D-Phe-Val-Lys(Fluor)-Lys(Cbz) (MW= 1155)

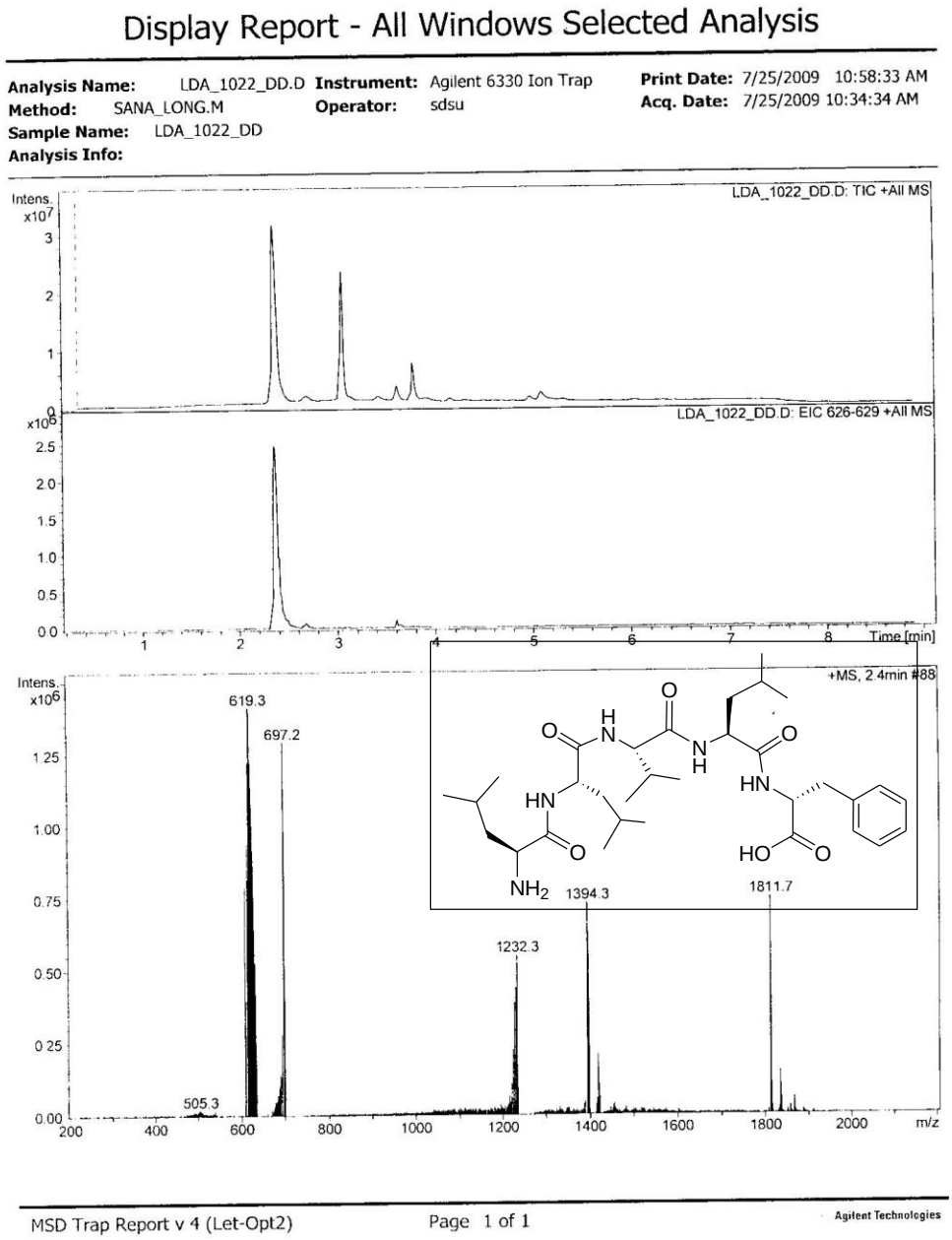

Di-SanA 17 LCMS DDLP: HO-D-Phe-Leu-Val-Leu-Leu-NH_2 (MW = 604)

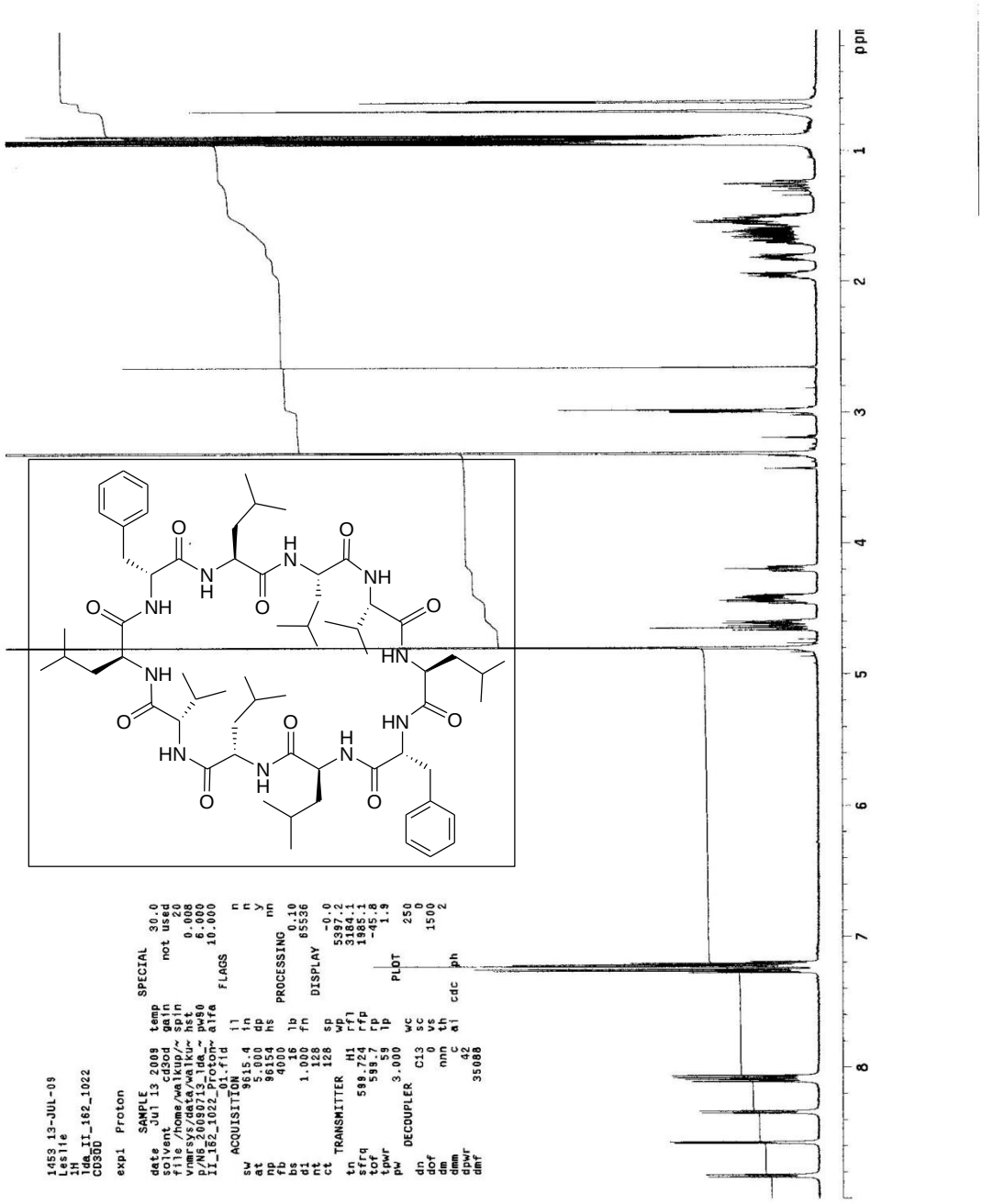

Di-SanA 17 ^{1}H-NMR Cyclized Decapeptide: D-Phe-Leu-Val-Leu-Leu-D-Phe-Leu-Val-Leu-Leu

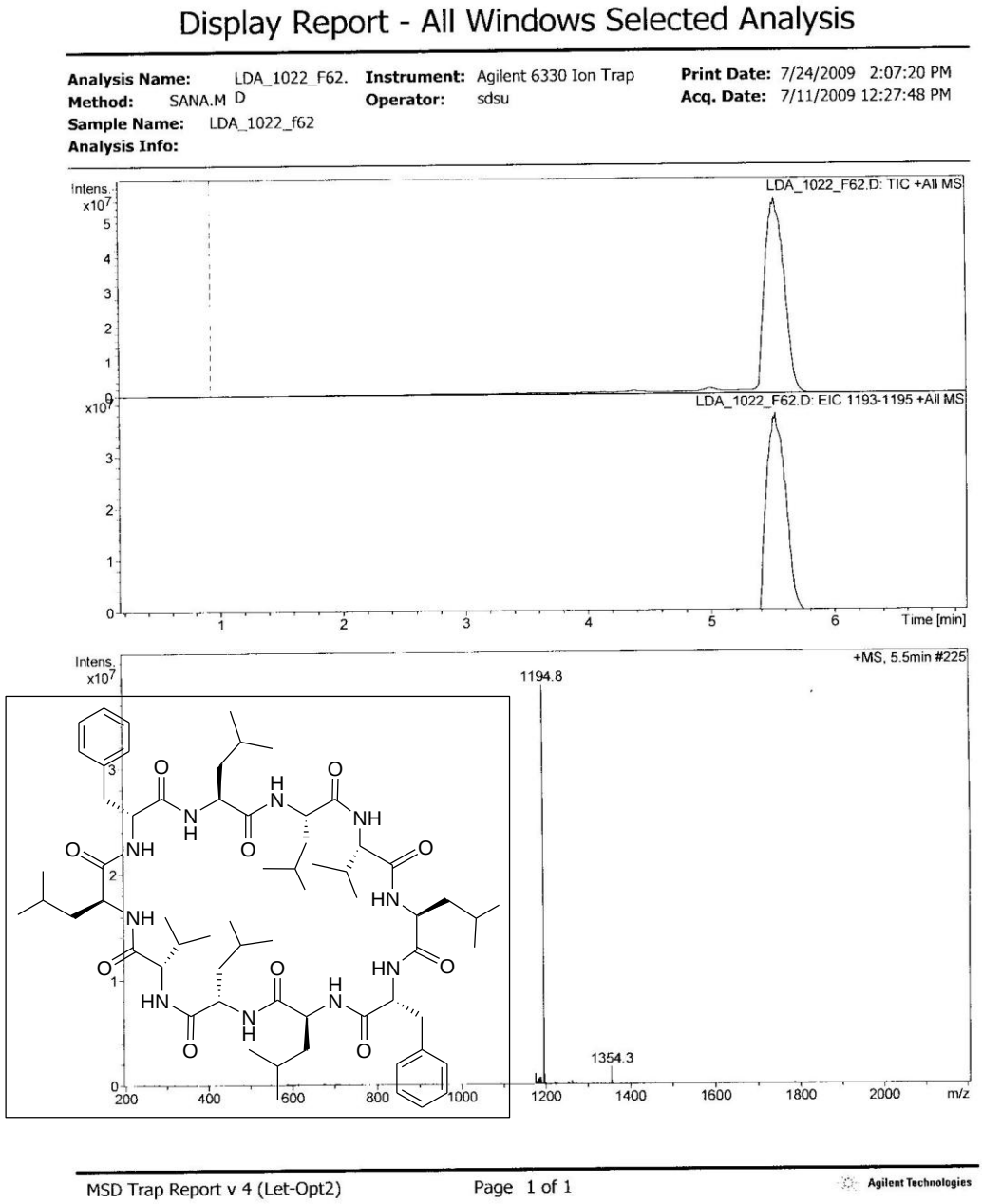

Di-SanA 17 LCMS Cyclized Decapeptide: D-Phe-Leu-Val-Leu-Leu-D-Phe-Leu-Val-Leu-Leu (MW = 1172)

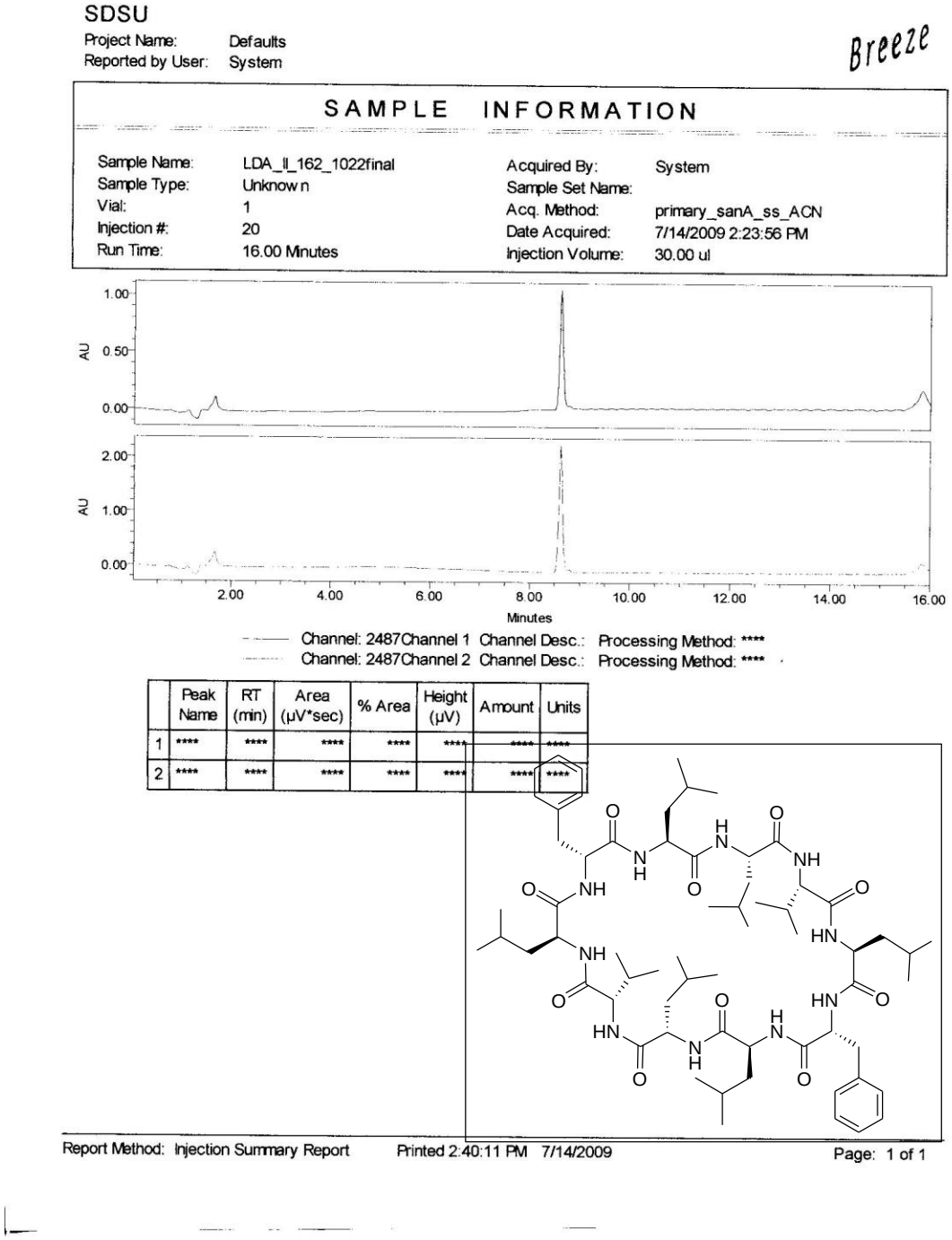

Di-SanA 17 HPLC trace Cyclized Decapeptide: D-Phe-Leu-Val-Leu-Leu-D-Phe-Leu-Val-Leu-Leu

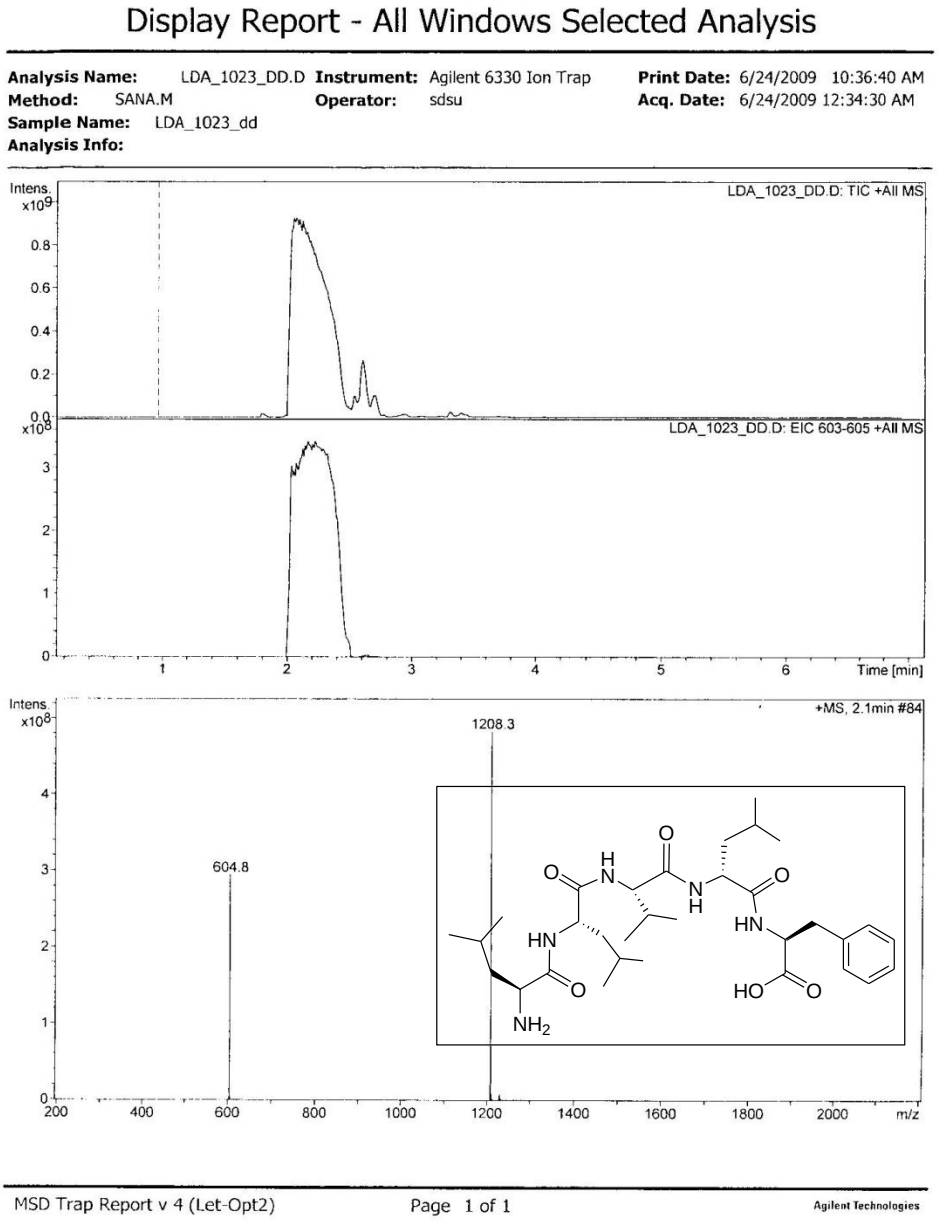

Di-SanA 18 LCMS DDLP: HO-Phe-D-Leu-Val-Leu-Leu-NH_2 (MW=604)

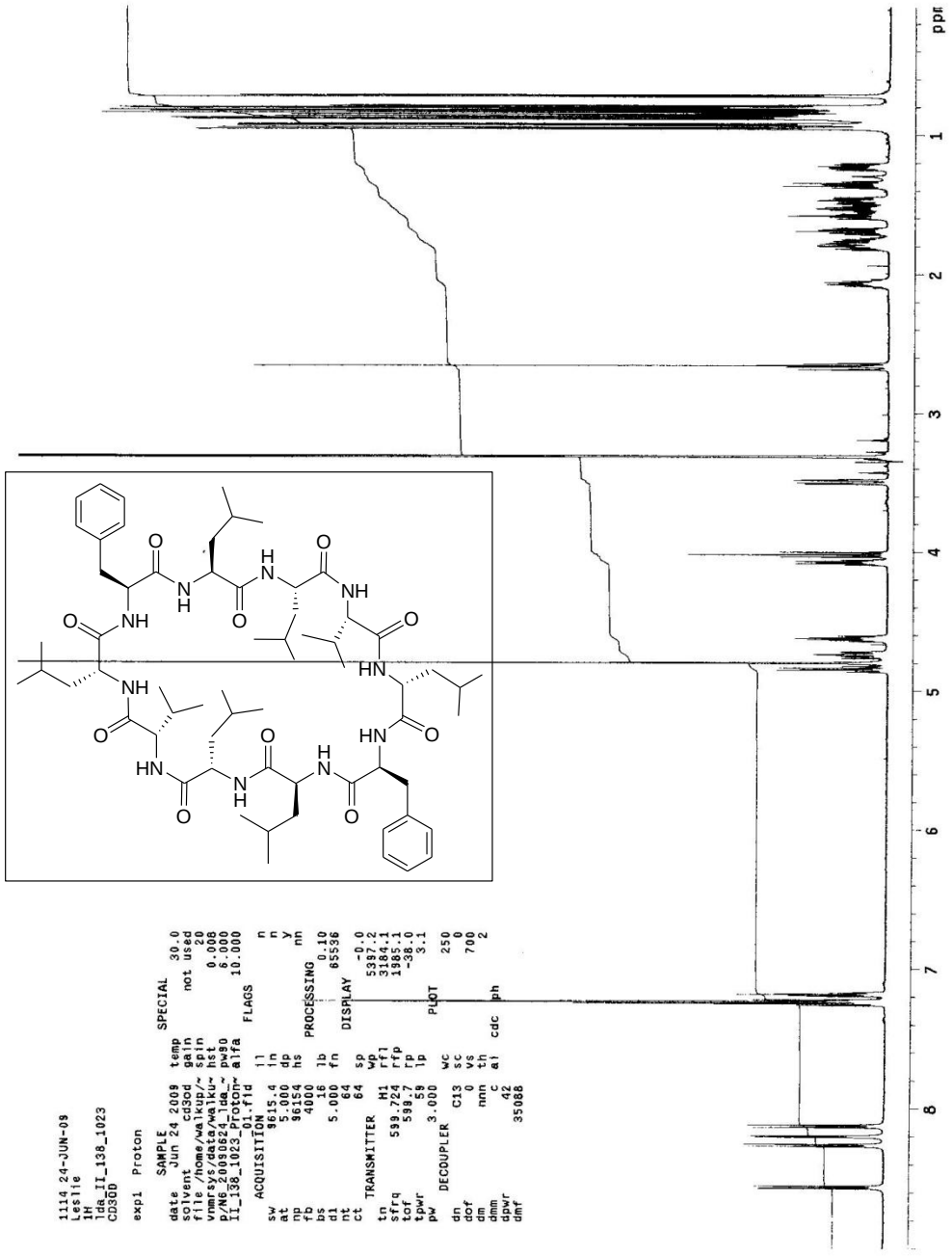

Di-SanA 18 ^{1}H-NMR Cyclized Decapeptide: Phe-D-Leu-Val-Leu-Leu-Phe-D-Leu-Val-Leu-Leu

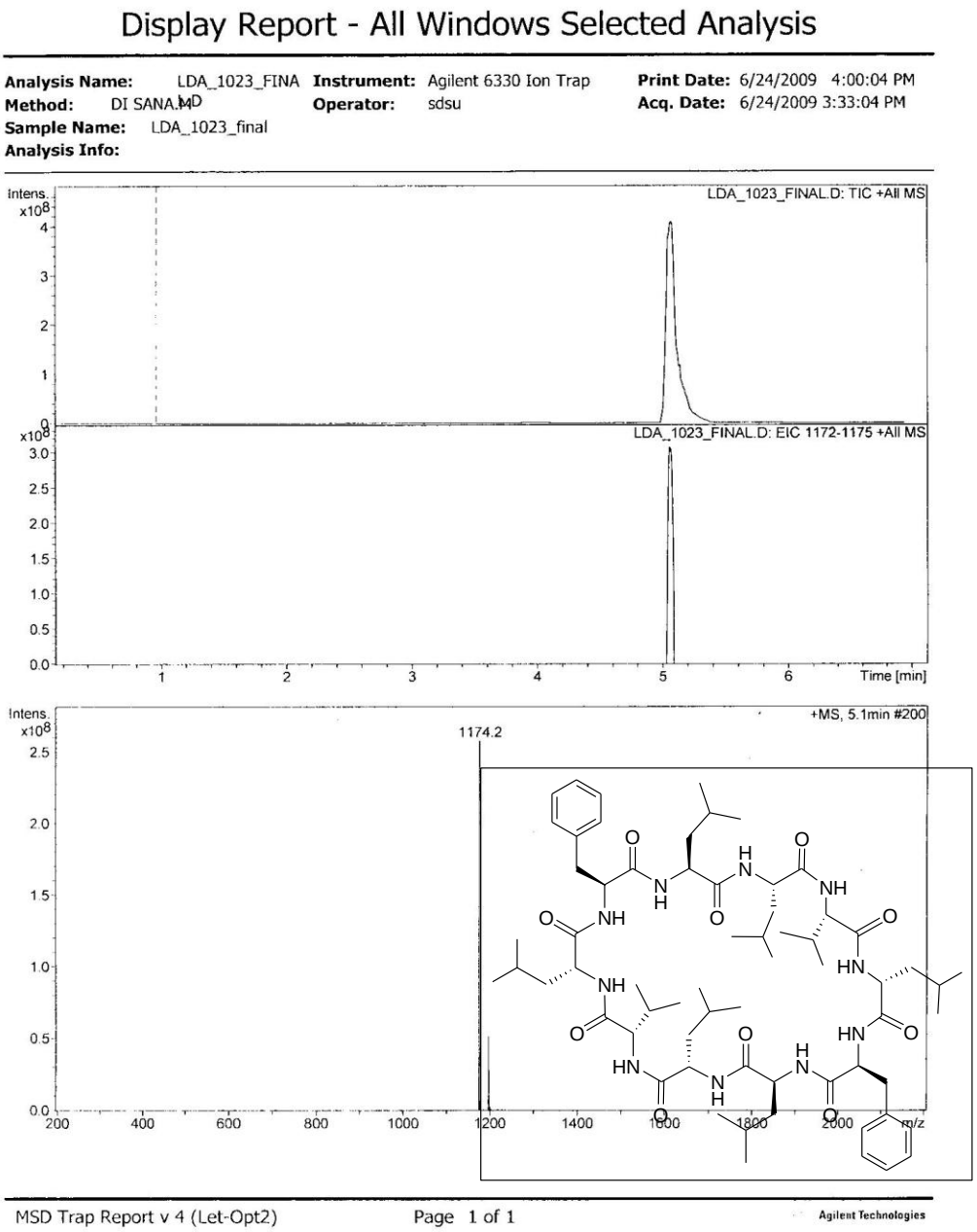

Di-SanA 18 LCMS Cyclized Decapeptide: Phe-D-Leu-Val-Leu-Leu-Phe-D-Leu-Val-Leu-Leu (MW = 1172)

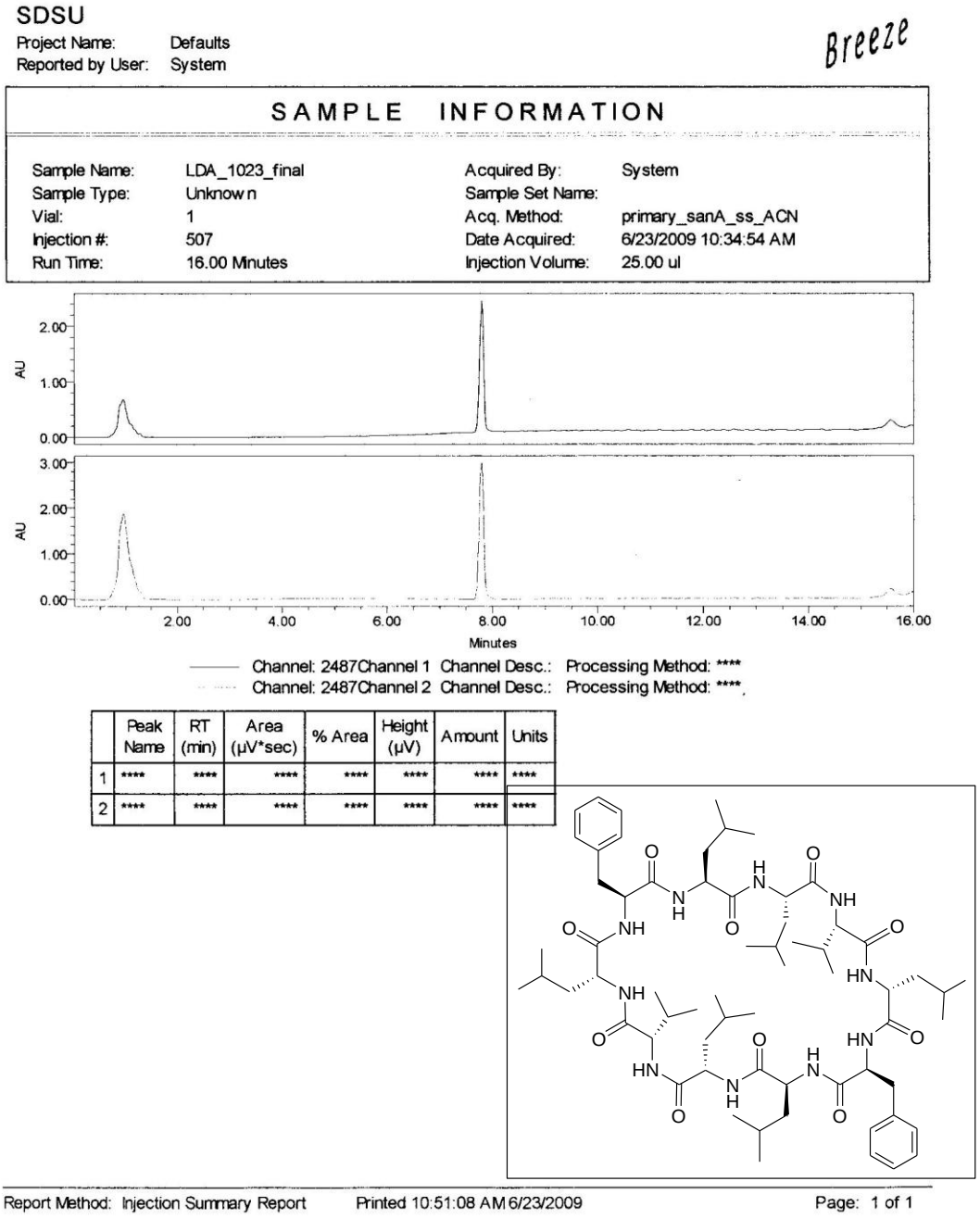

Di-SanA 18 HPLC trace Cyclized Decapeptide: Phe-D-Leu-Val-Leu-Leu-Phe-D-Leu-Val-Leu-Leu

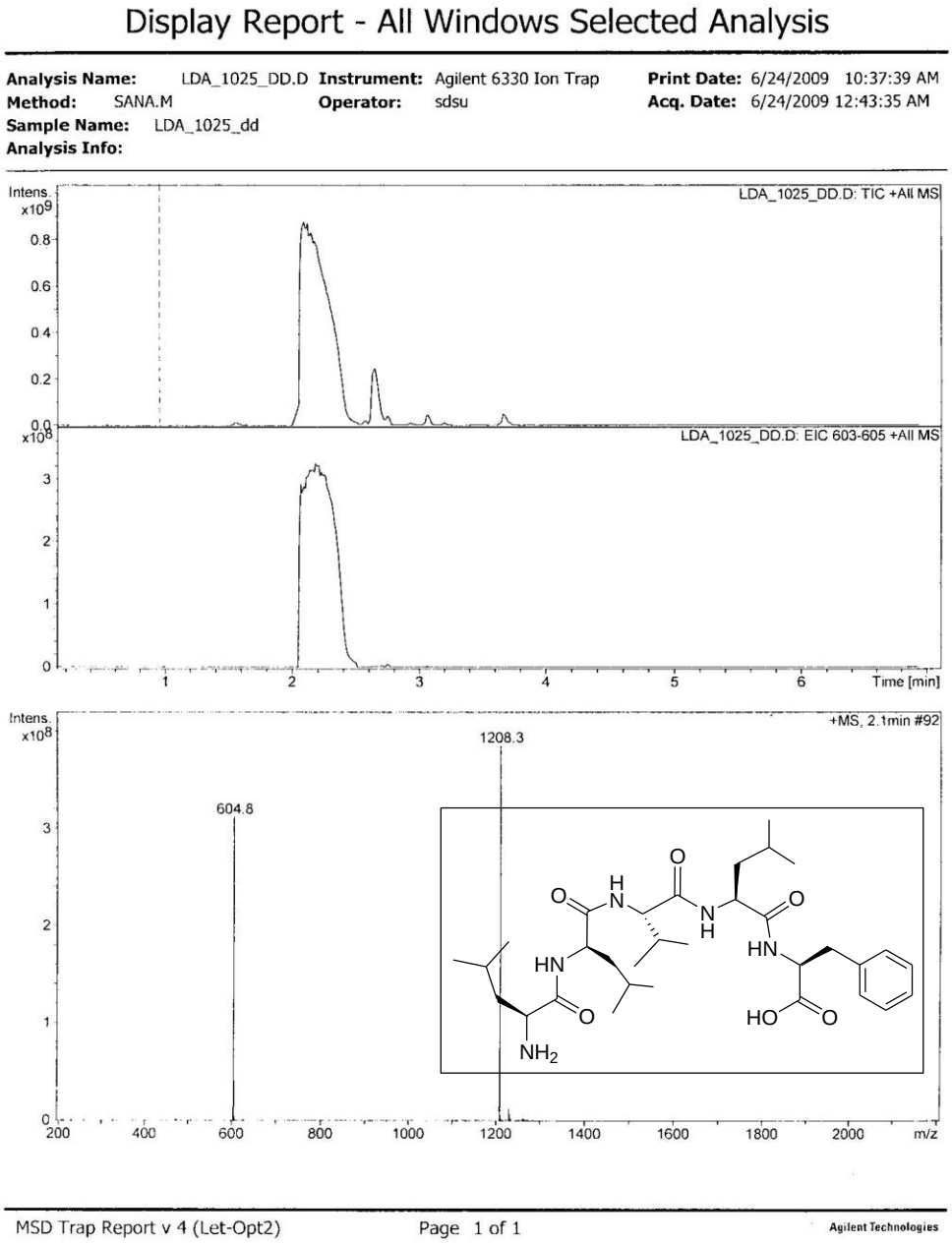

Di-SanA 20 LCMS DDLP: HO-Phe-Leu-Val-D-Leu-Leu-NH_2 (MW = 604)

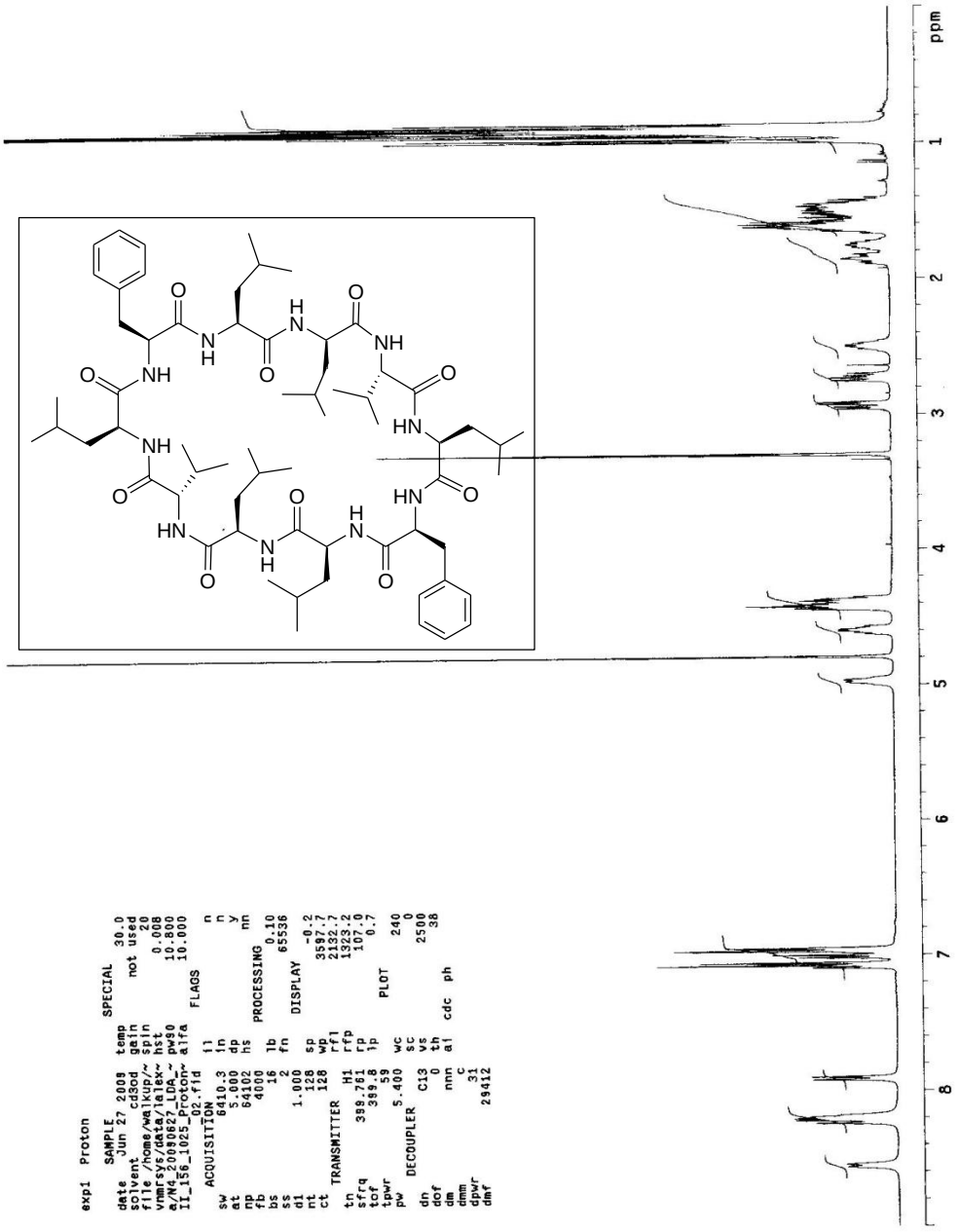

Di-SanA 20 ^{1}H-NMR Cyclized Decapeptide: Phe-Leu-Val-D-Leu-Leu-Phe-Leu-Val-D-Leu-Leu

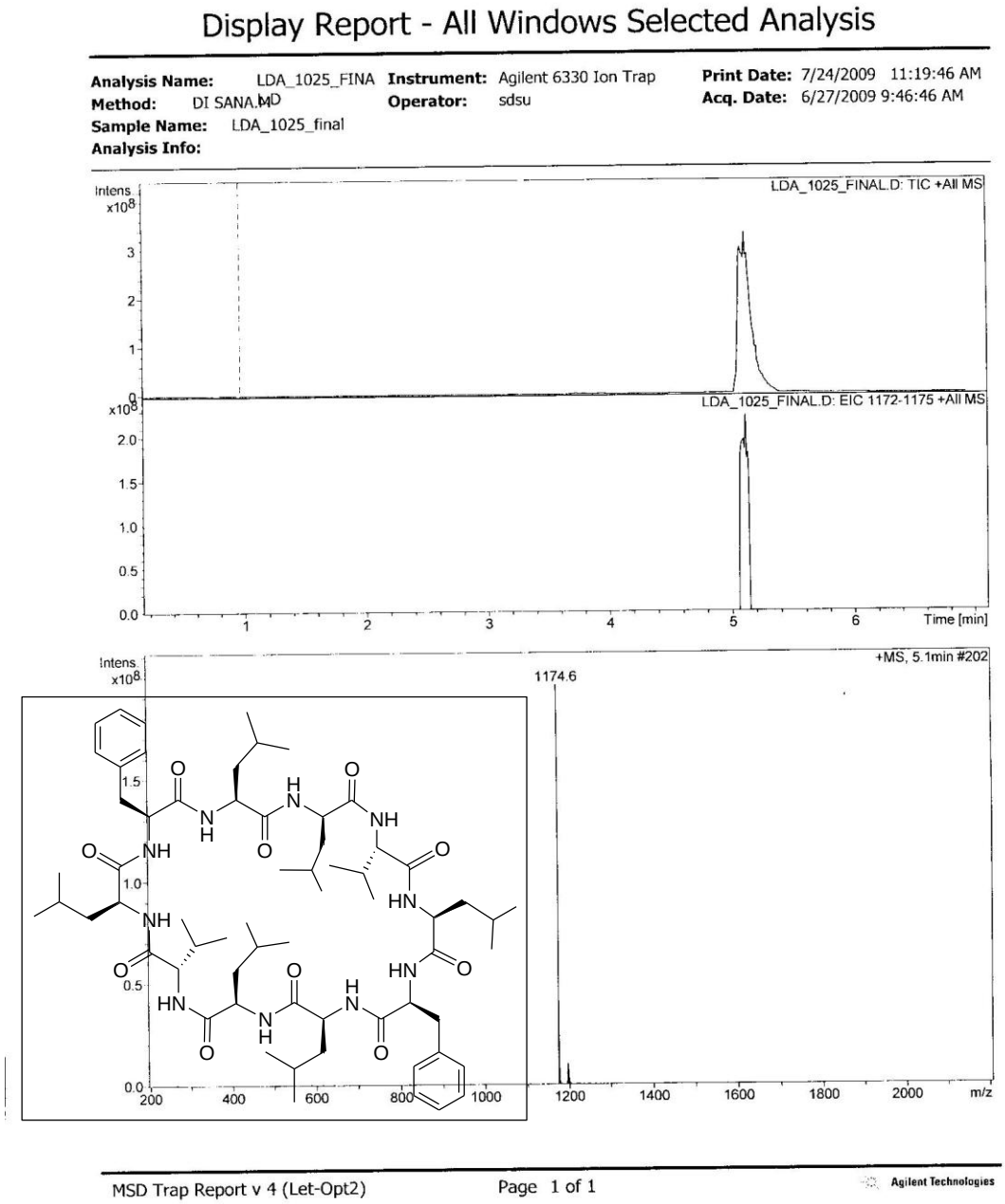

Di-SanA 20 LCMS Cyclized Decapeptide: Phe-Leu-Val-D-Leu-Leu-Phe-Leu-Val-D-Leu-Leu (MW = 1174)

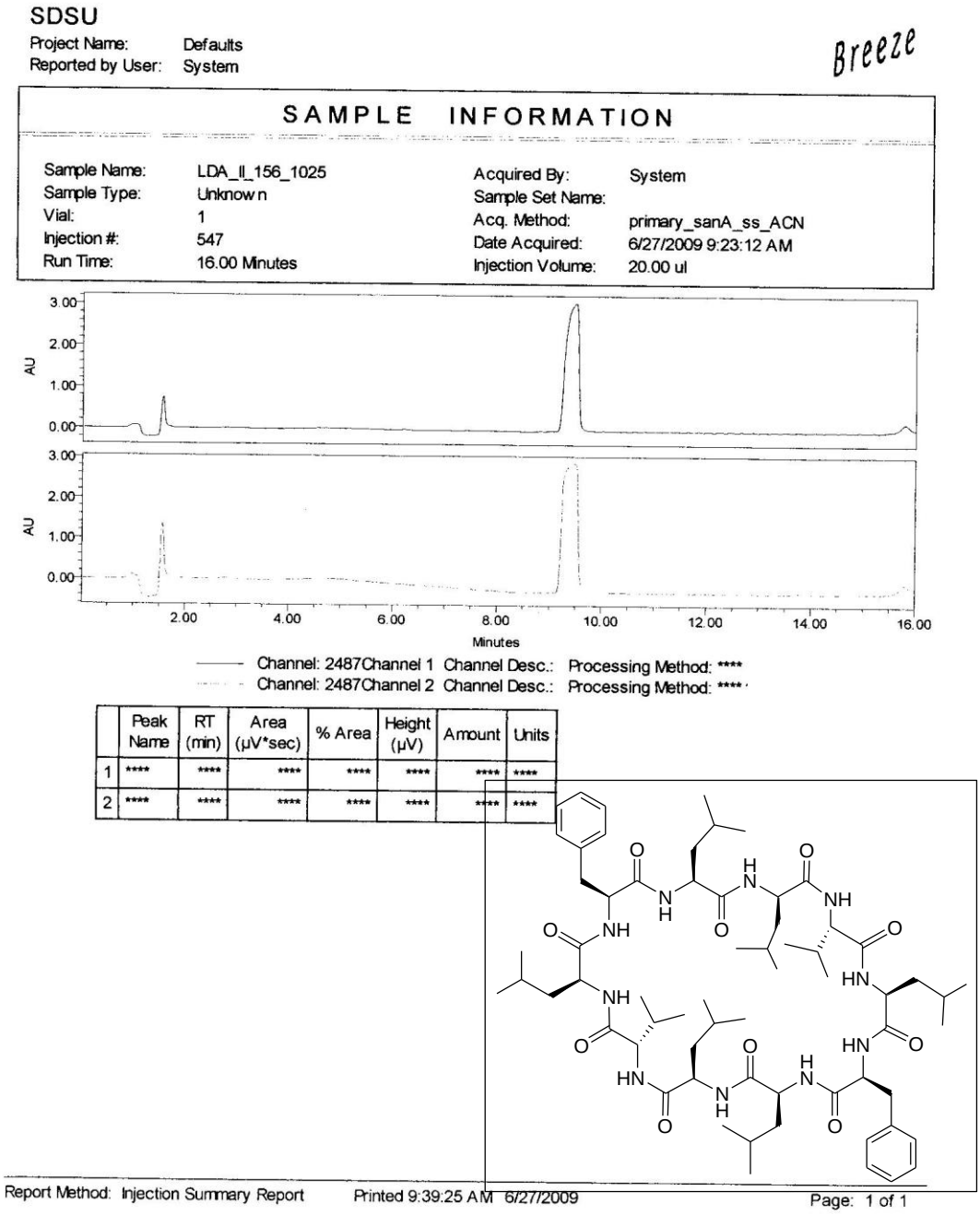

Di-SanA 20 HPLC trace Cyclized Decapeptide: Phe-Leu-Val-D-Leu-Leu-Phe-Leu-Val-D-Leu-Leu

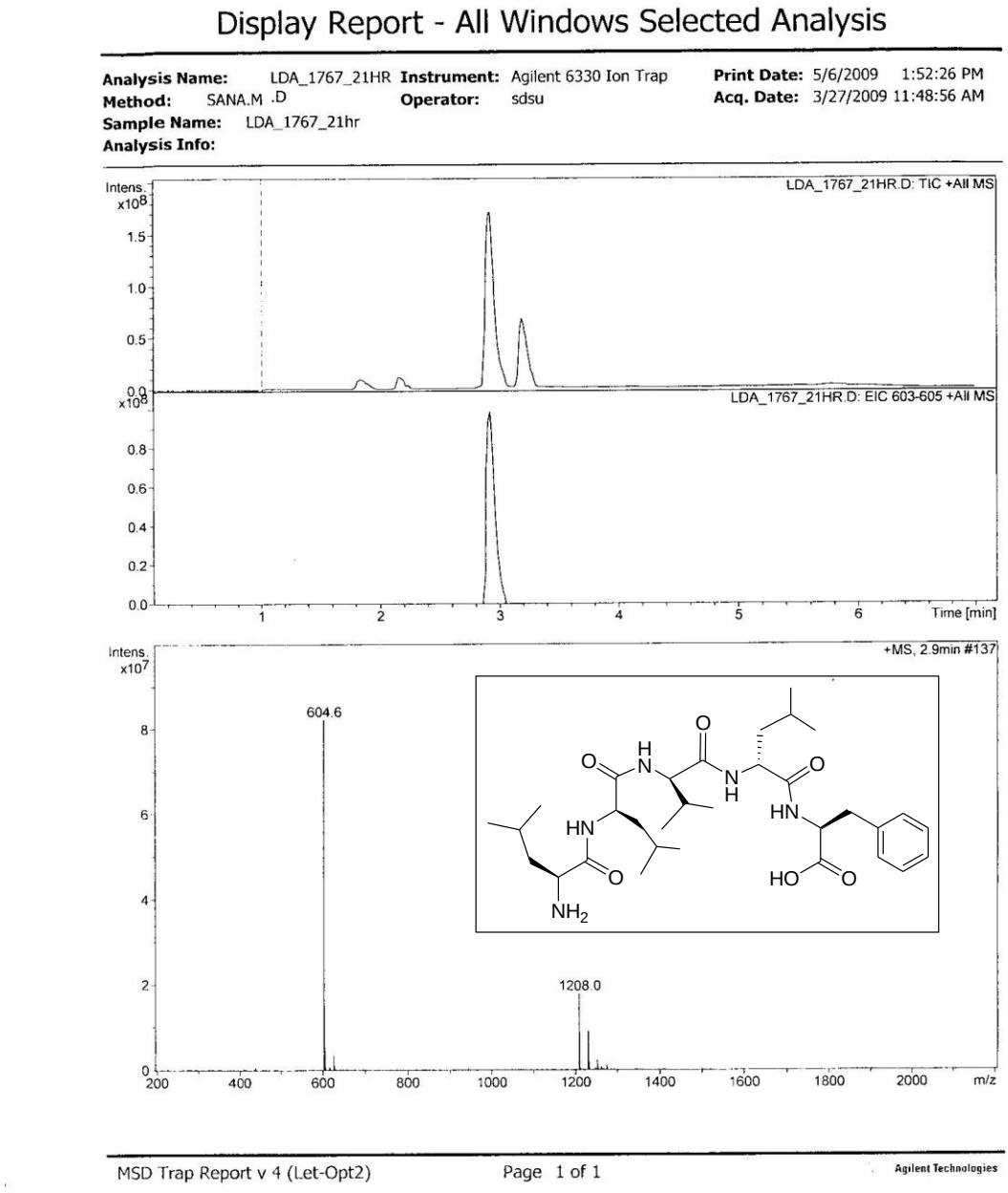

Di-SanA 22 LCMS DDLP: HO-Phe-D-Leu-D-Val-D-Leu-Leu-NH_2 (MW = 604)

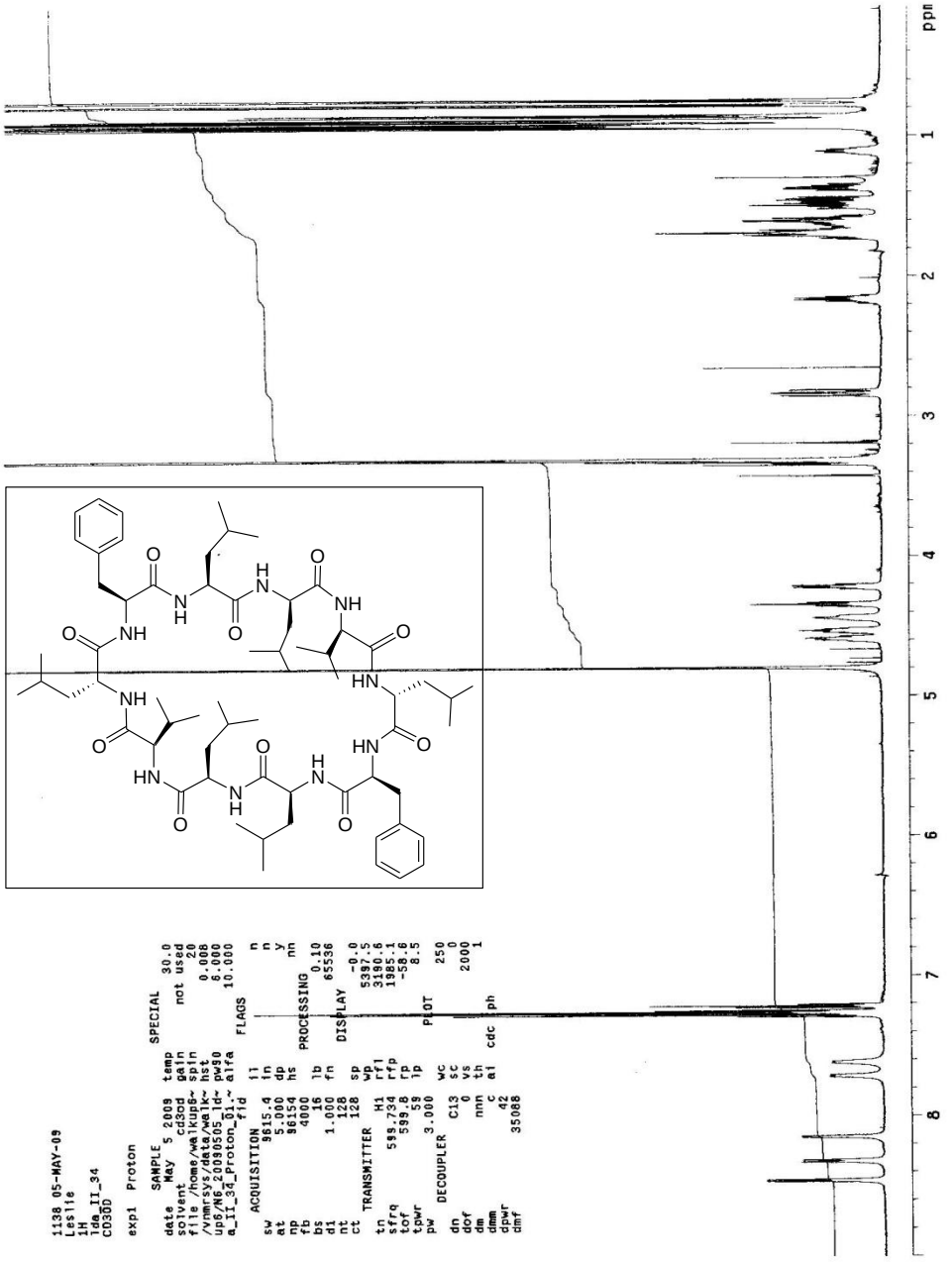

Di-SanA 22 ^{1}H-NMR Cyclized Decapeptide: Phe-D-Leu-D-Val-D-Leu-Leu-Phe-D-Leu-D-Val-D-Leu-Leu

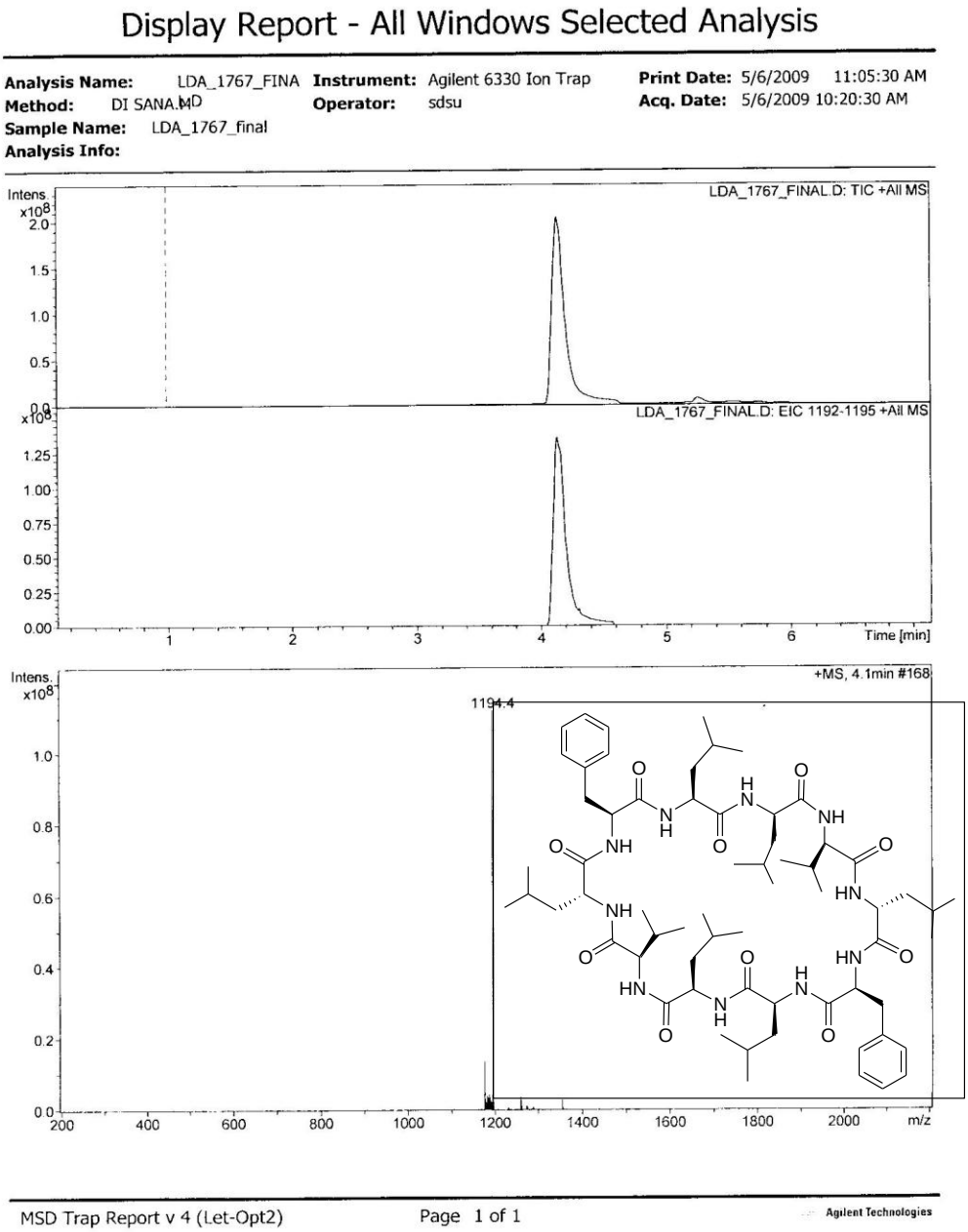

Di-SanA 22 LCMS Cyclized Decapeptide: Phe-D-Leu-D-Val-D-Leu-Leu-Phe-D-Leu-D-Val-D-Leu-Leu (MW=1172)

SDSU

Project Name: Defaults
Reported by User: System

Breeze

SAMPLE INFORMATION

Sample Name:	LDA_34-II_1767_final	Acquired By:	System
Sample Type:	Unknown	Sample Set Name:	
Vial:	1	Acq. Method:	primary_sanA_ss_ACN
Injection #:	133	Date Acquired:	7/28/2009 5:32:51 PM
Run Time:	16.00 Minutes	Injection Volume:	35.00 ul

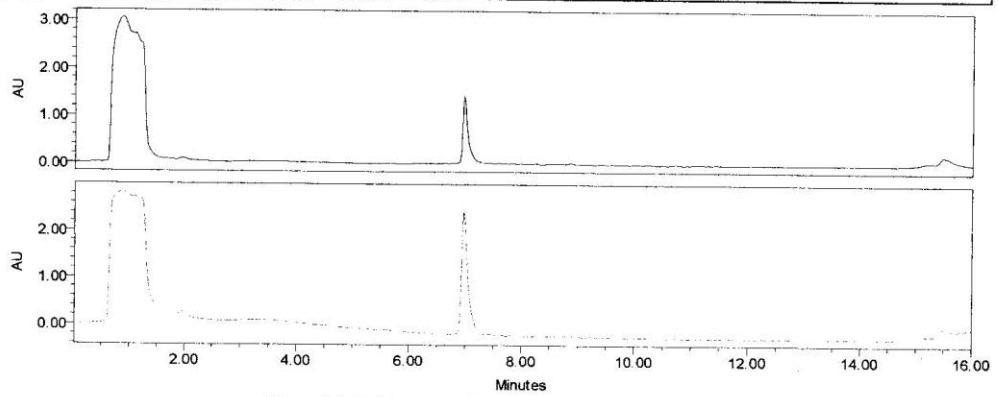

Channel: 2487Channel 1 Channel Desc.: Processing Method: ****
Channel: 2487Channel 2 Channel Desc.: Processing Method: ****

	Peak Name	RT (min)	Area (µV*sec)	% Area	Height (µV)	Amount	Units
1	****	****	****	****	****	****	****
2	****	****	****	****	****	****	****

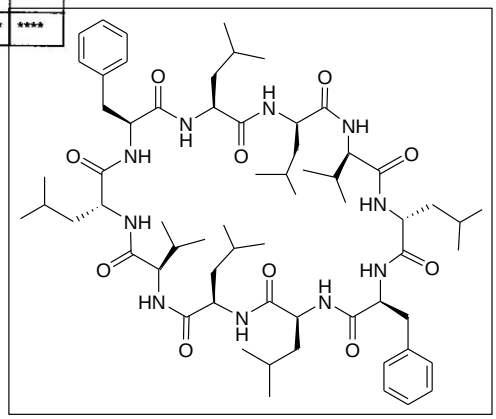

Report Method: Injection Summary Report Printed 5:49:04 PM 7/28/2009 Page: 1 of 1

Di-SanA 22 HPLC trace Cyclized Decapeptide: Phe-D-Leu-D-Val-D-Leu-Leu-Phe-D-Leu-D-Val-D-Leu-Leu

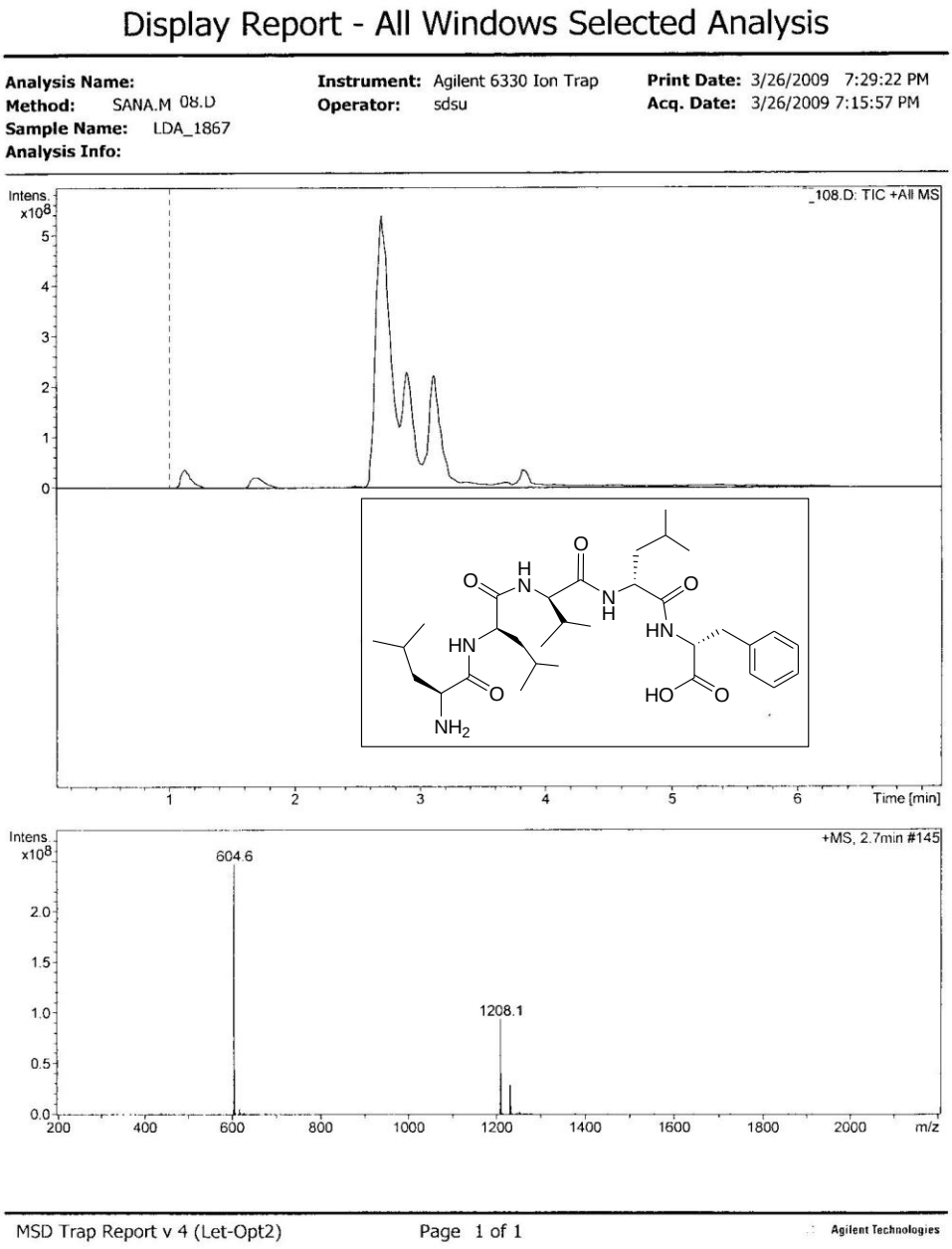

Di-SanA 23 LCMS DDLP: HO-D-Phe-D-Leu-D-Val-D-Leu-Leu-NH_2 (MW = 604)

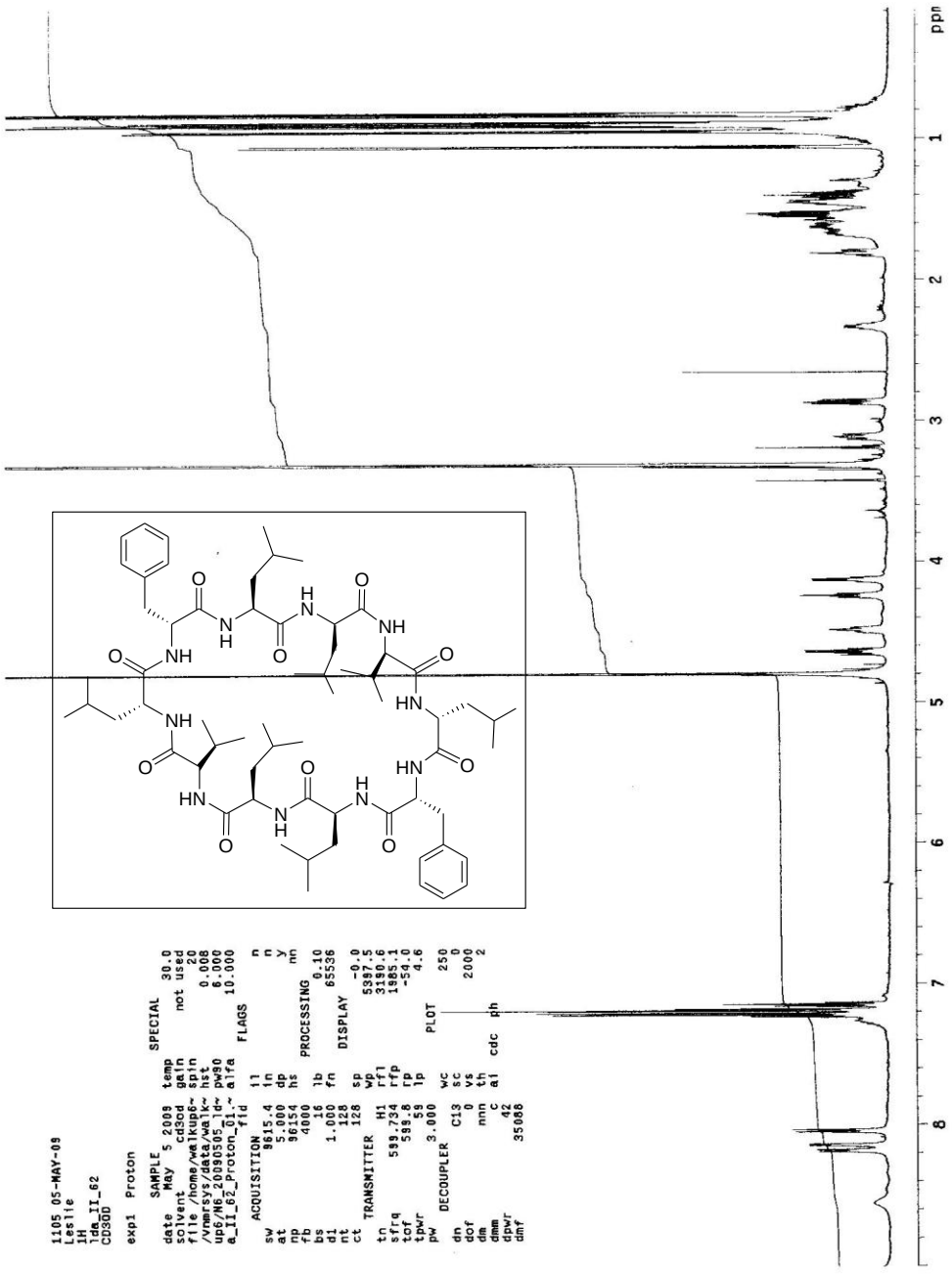

Di-SanA 23 ^{1}H-NMR Cyclized Decapeptide: D-Phe-D-Leu-D-Val-D-Leu-Leu-D-Phe-D-Leu-D-Val-D-Leu-Leu

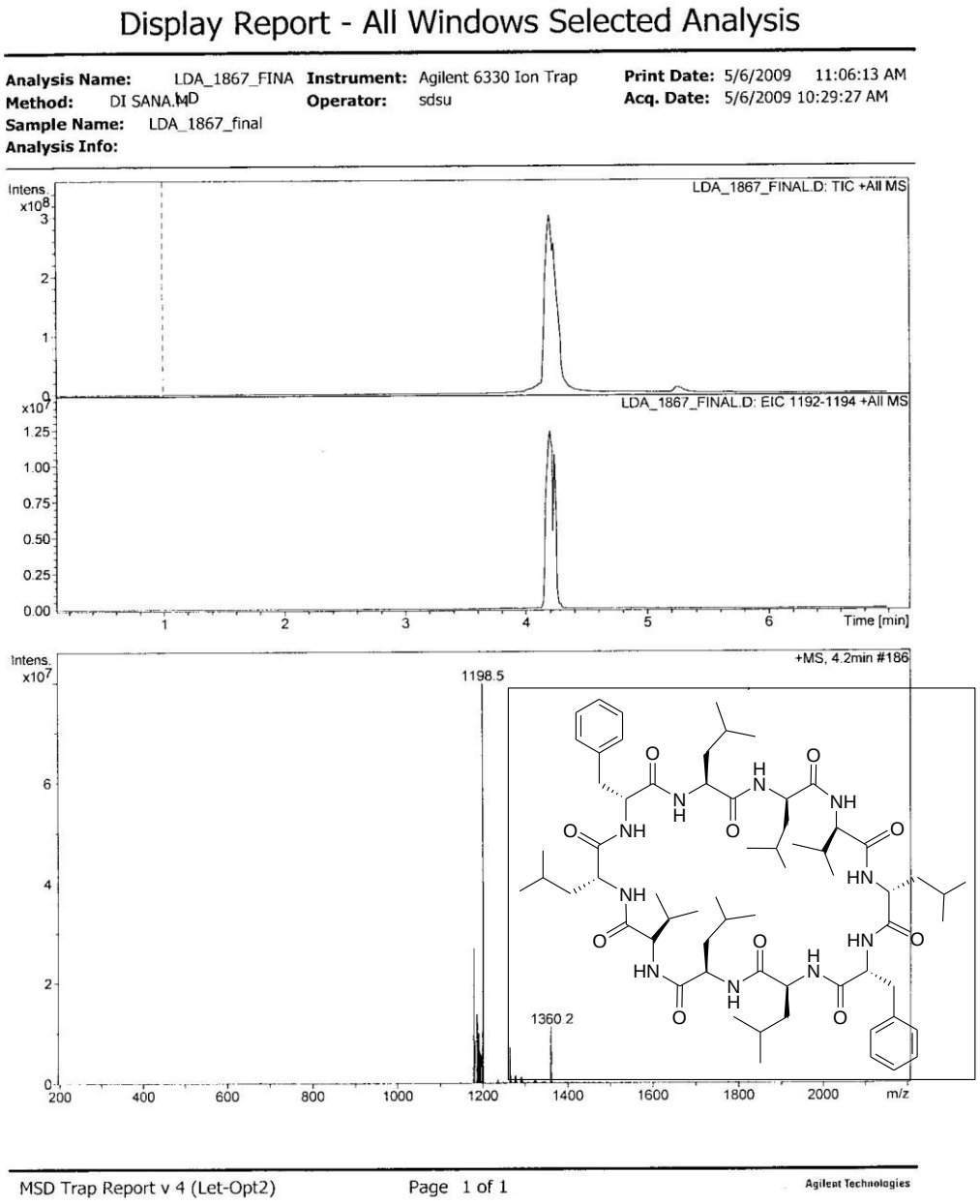

Di-SanA 23 LCMS Cyclized Decapeptide: D-Phe-D-Leu-D-Val-D-Leu-Leu-D-Phe-D-Leu-D-Val-D-Leu-Leu (MW = 1172)

SDSU

Project Name: Defaults
Reported by User: System

Breeze

SAMPLE INFORMATION

Sample Name:	LDA_62-II_1867_final	Acquired By:	System
Sample Type:	Unknown	Sample Set Name:	
Vial:	1	Acq. Method:	primary_sanA_ss_ACN
Injection #:	131	Date Acquired:	7/28/2009 4:56:51 PM
Run Time:	16.00 Minutes	Injection Volume:	35.00 ul

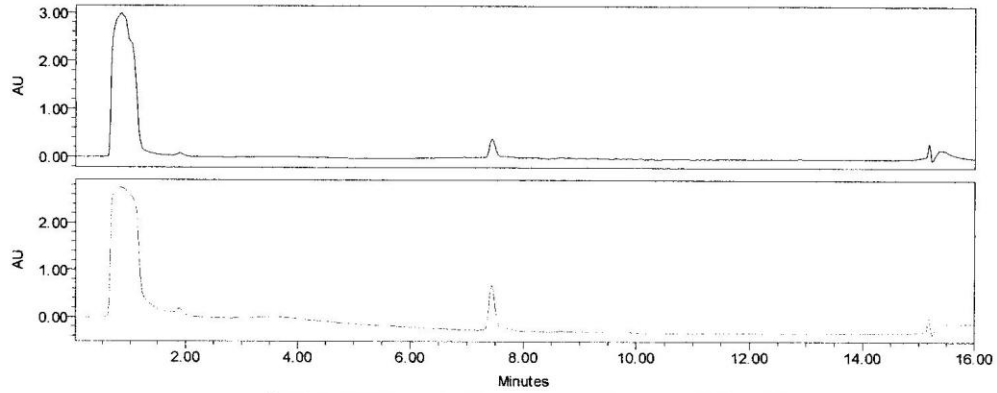

Channel: 2487Channel 1 Channel Desc.: Processing Method: ****
Channel: 2487Channel 2 Channel Desc.: Processing Method: ****

	Peak Name	RT (min)	Area (µV*sec)	% Area	Height (µV)	Amount	Units
1	****	****	****	****	****	****	****
2	****	****	****	****	****	****	****

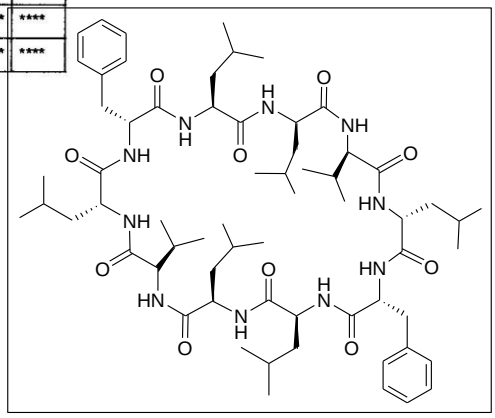

Report Method: Injection Summary Report Printed 5:13:04 PM 7/28/2009 Page: 1 of 1

Di-SanA 23 HPLC trace Cyclized Decapeptide: D-Phe-D-Leu-D-Val-D-Leu-Leu-D-Phe-D-Leu-D-Val-D-Leu-Leu

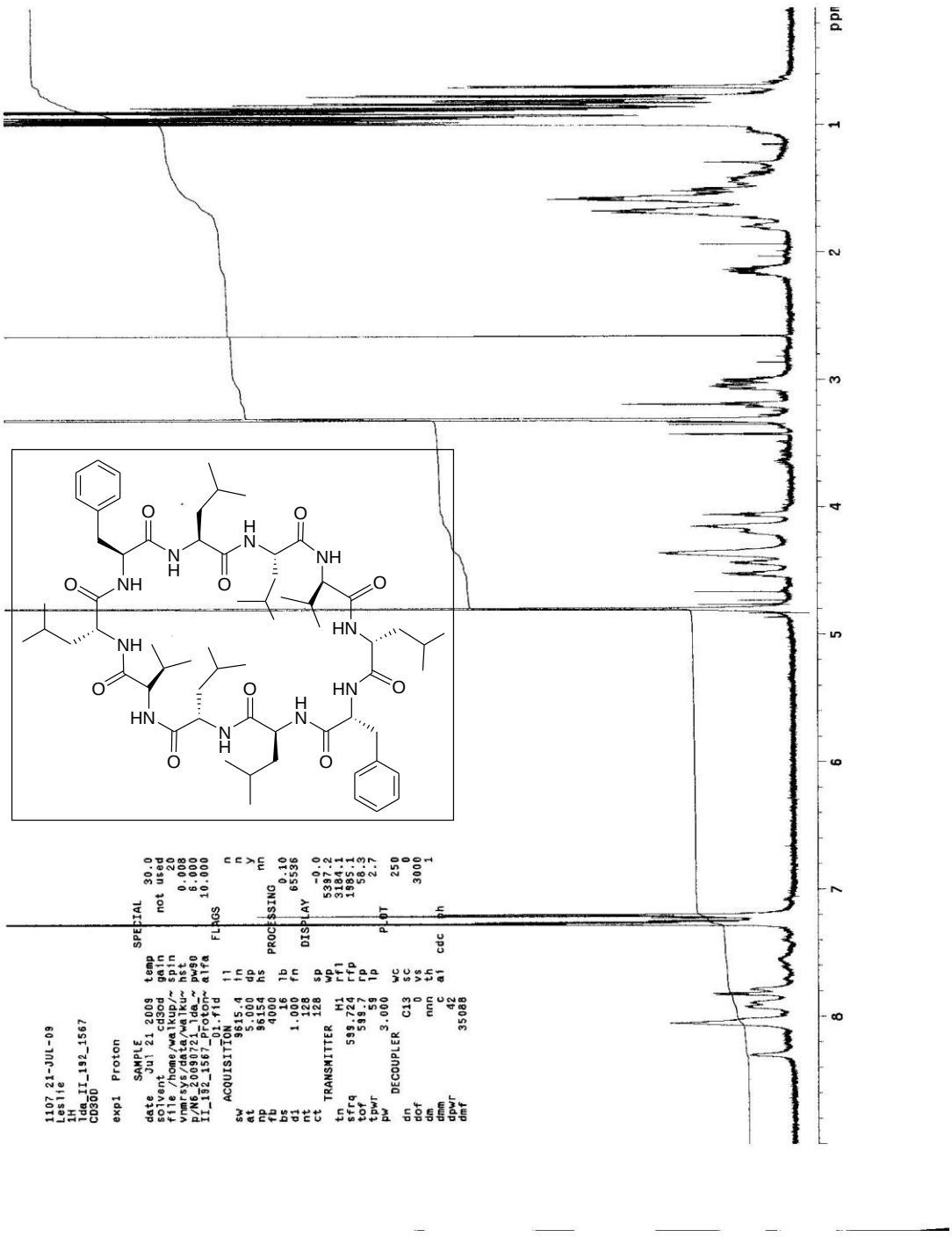

Di-SanA 24 ^{1}H-NMR Cyclized Decapeptide: D-Phe-D-Leu-D-Val-Leu-Leu-Phe-D-Leu-D-Val-Leu-Leu

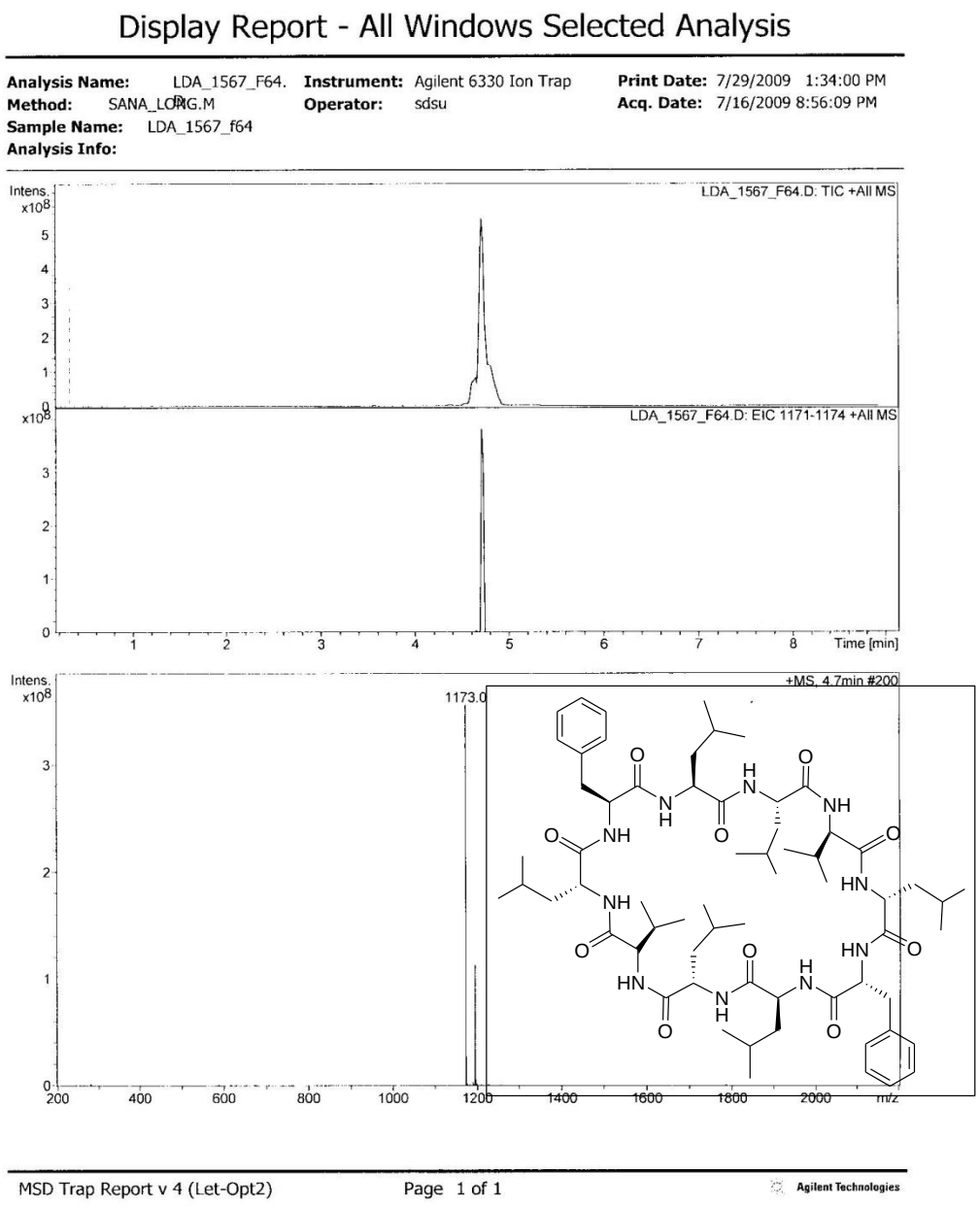

Di-SanA 24 LCMS Cyclized Decapeptide: D-Phe-D-Leu-D-Val-Leu-Leu-Phe-D-Leu-D-Val-Leu-Leu (MW = 1172)

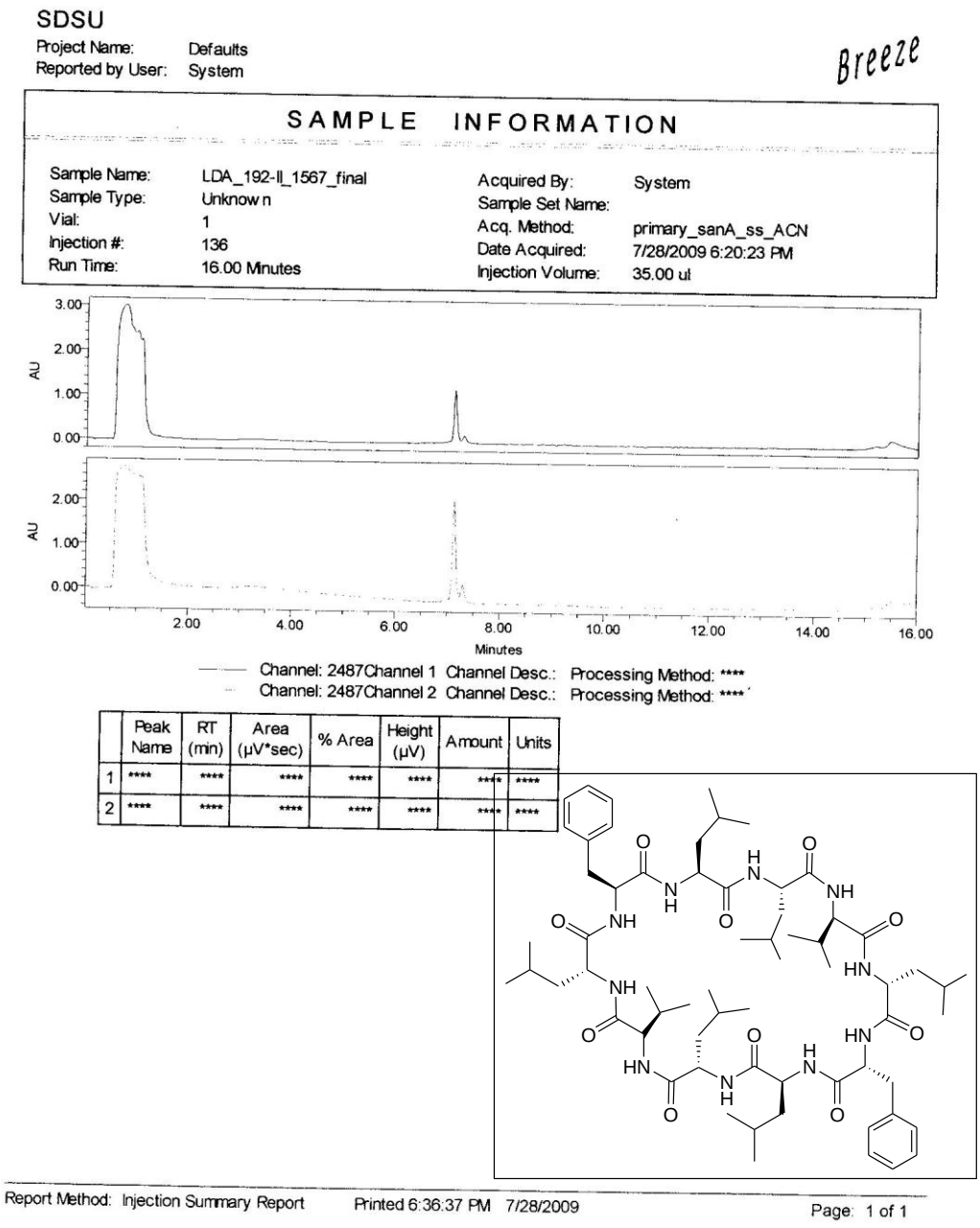

Di-SanA 24 HPLC trace Cyclized Decapeptide: D-Phe-D-Leu-D-Val-Leu-Leu-Phe-D-Leu-D-Val-Leu-Leu

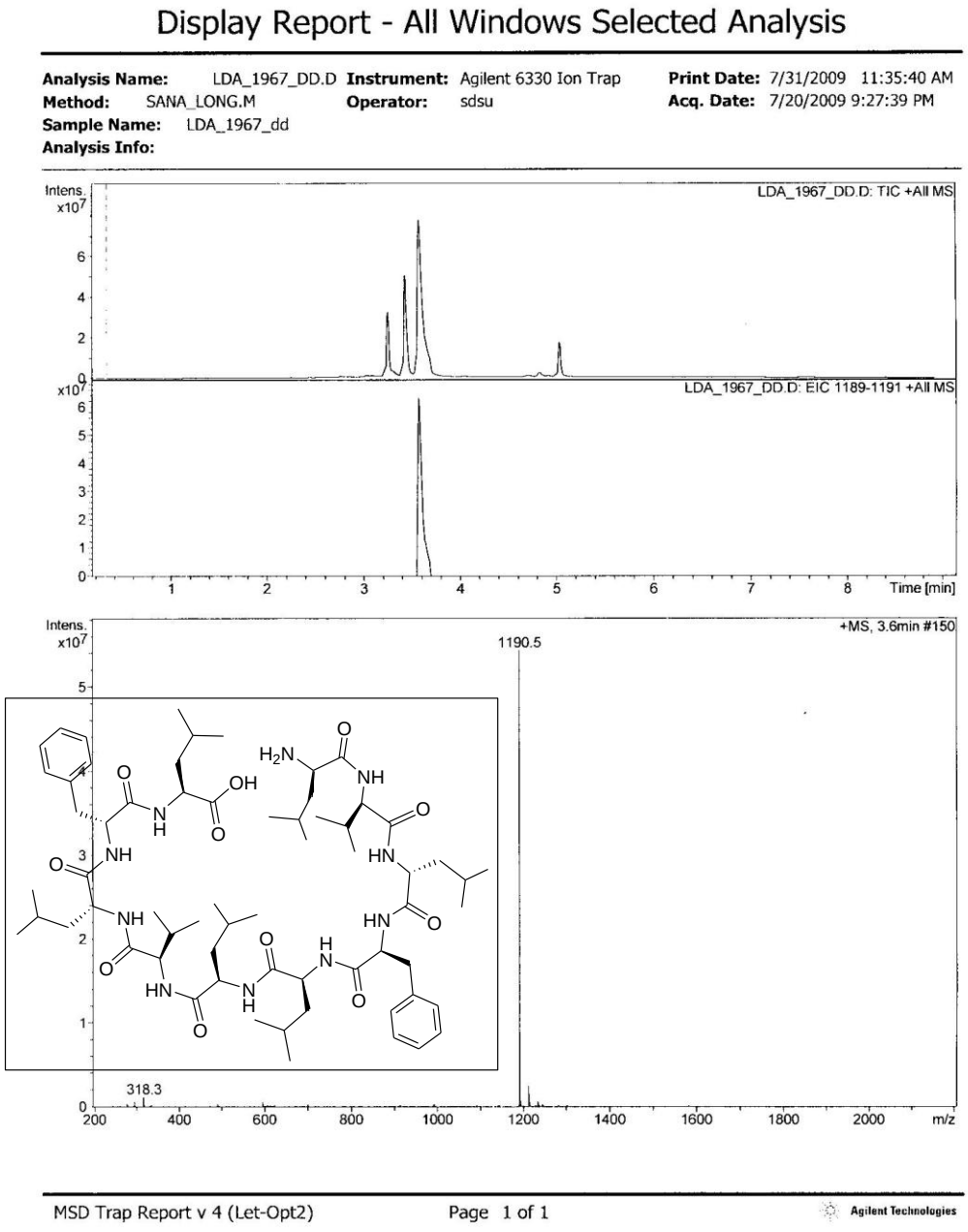

Di-SanA 25 LCMS DDLD: HO-Phe-D-Leu-D-Val-D-Leu-Leu-D-Phe-D-Leu-D-Val-D-Leu-Leu-NH_2 (MW = 1190)

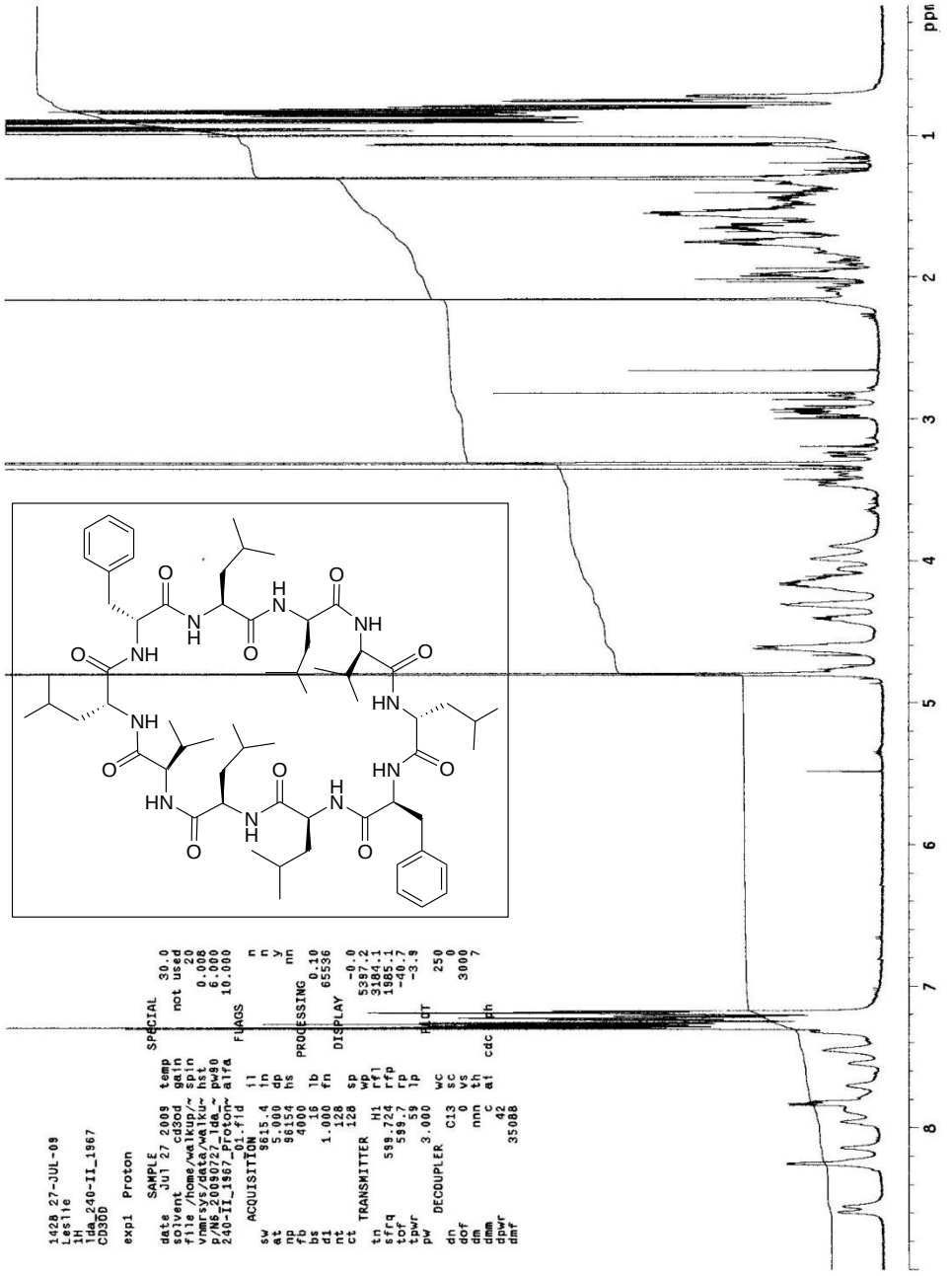

Di-SanA 25 ^{1}H-NMR Cyclized Decapeptide: Phe-D-Leu-D-Val-D-Leu-Leu-D-Phe-D-Leu-D-Val-D-Leu-Leu

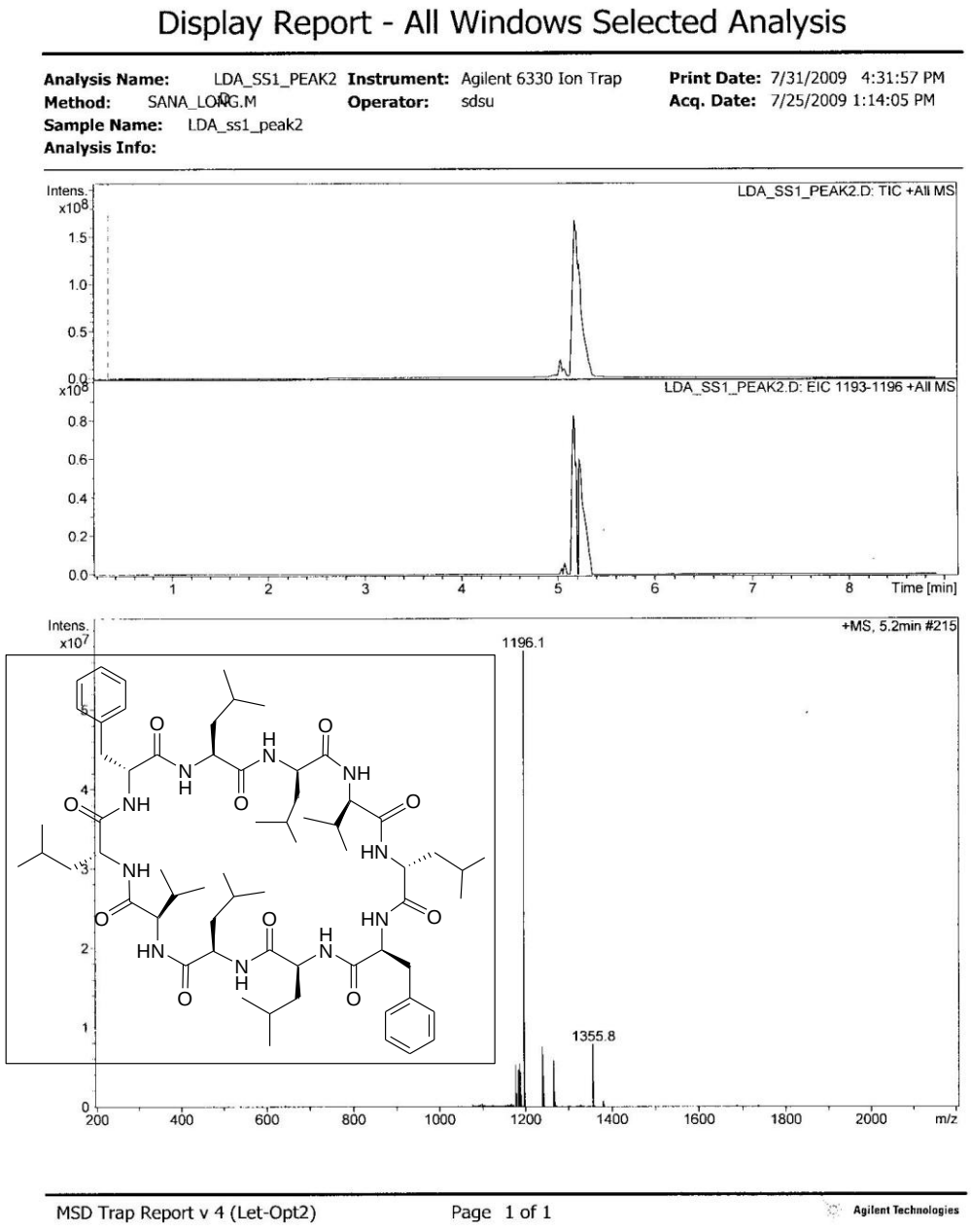

Di-SanA 25 LCMS Cyclized Decapeptide: Phe-D-Leu-D-Val-D-Leu-Leu-D-Phe-D-Leu-D-Val-D-Leu-Leu (MW = 1172)

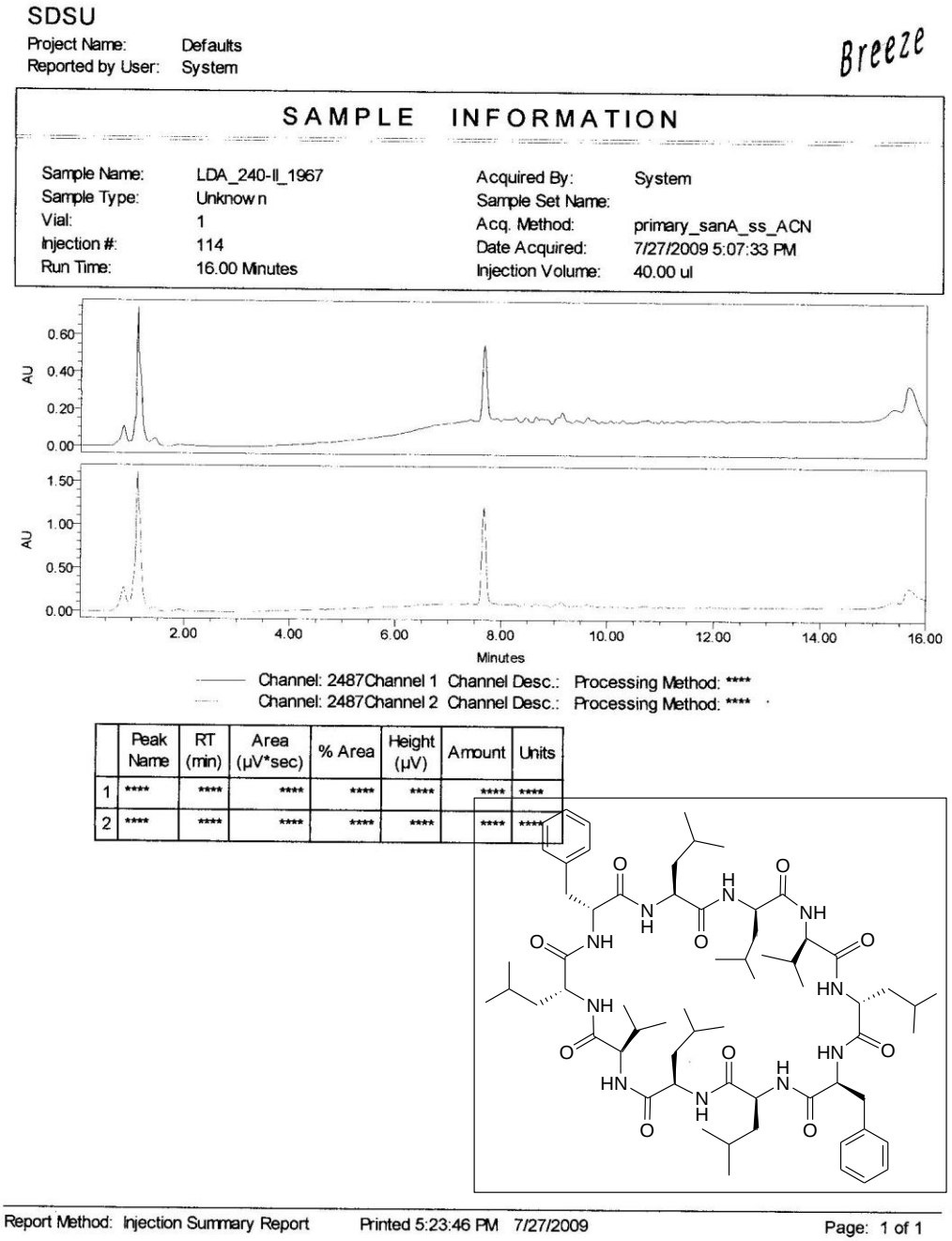

Di-SanA 25 HPLC Cyclized Decapeptide: Phe-D-Leu-D-Val-D-Leu-Leu-D-Phe-D-Leu-D-Val-D-Leu-Leu

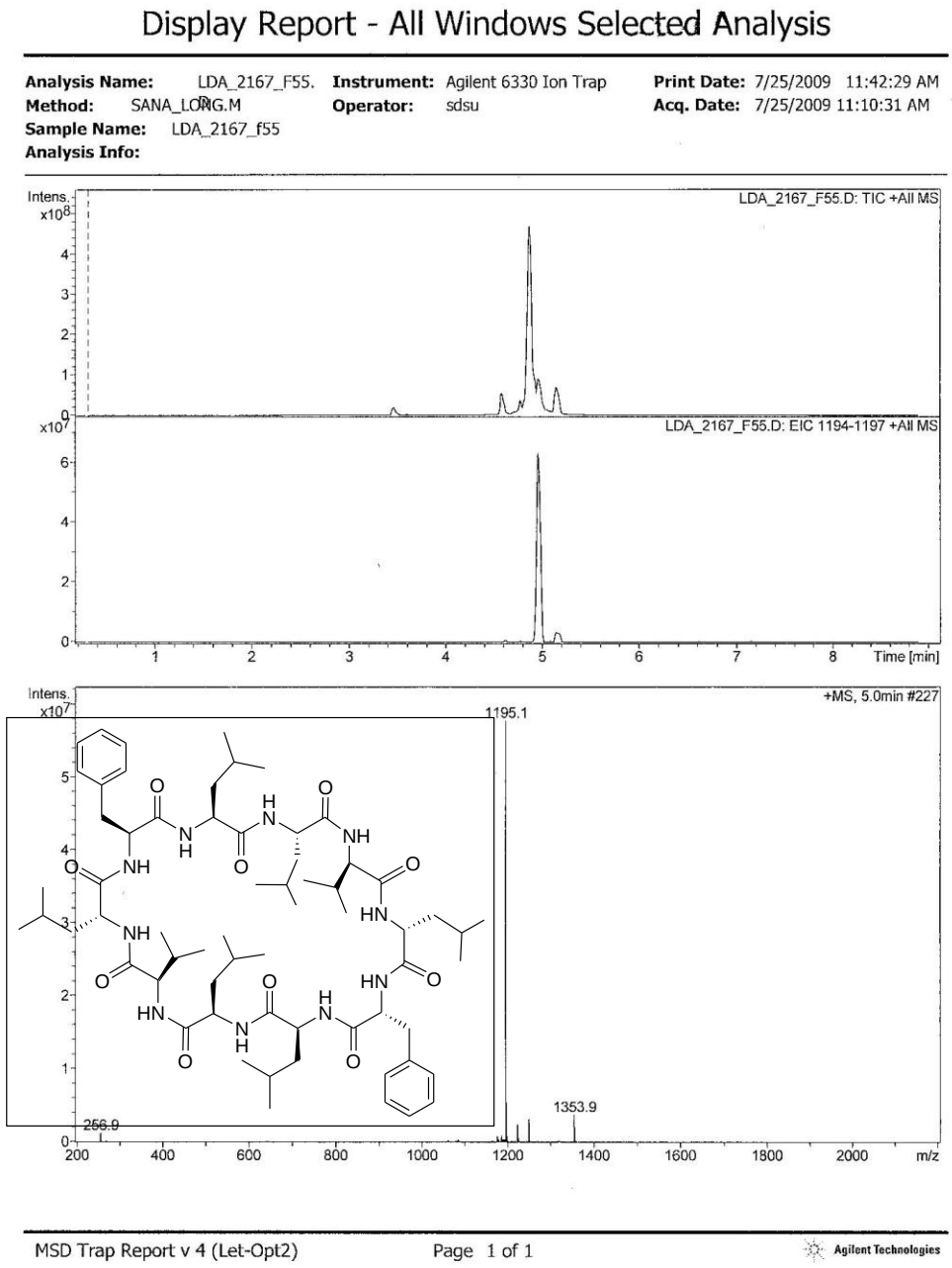

Di-SanA 26 LCMS Cyclized Decapeptide: Phe-D-Leu-D-Val-D-Leu-Leu-D-Phe-D-Leu-D-Val-Leu-Leu (MW= 1172)

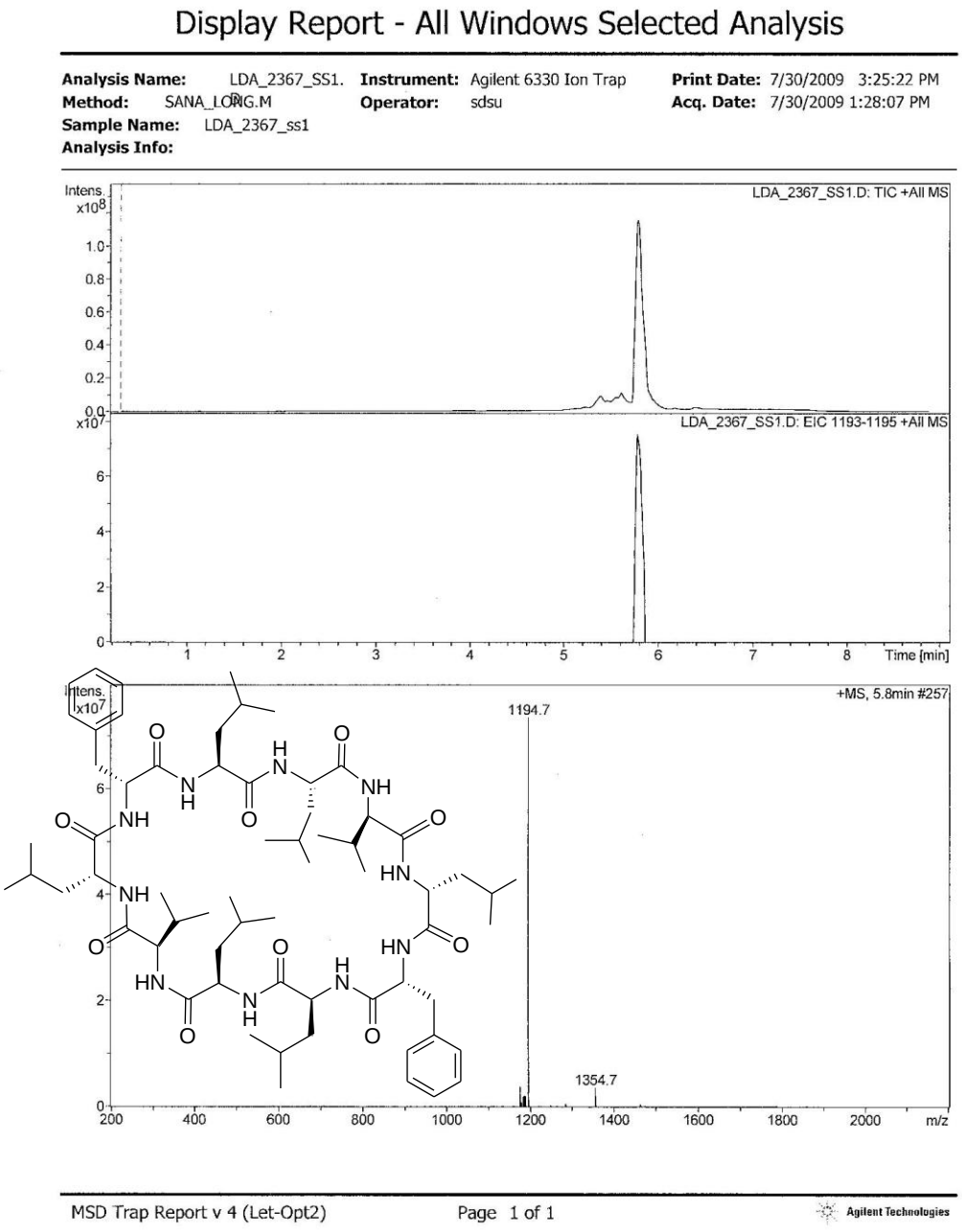

Di-SanA 27 LCMS Cyclized Decapeptide: D-Phe-D-Leu-D-Val-D-Leu-Leu-D-Phe-D-Leu-D-Val-Leu-Leu (MW= 1172)

APPENDIX B

SUPPORTING DATA FOR BIOCHEMICAL ASSAYS

IC_{50} CURVES FOR LEAD COMPOUNDS IN HCT-116

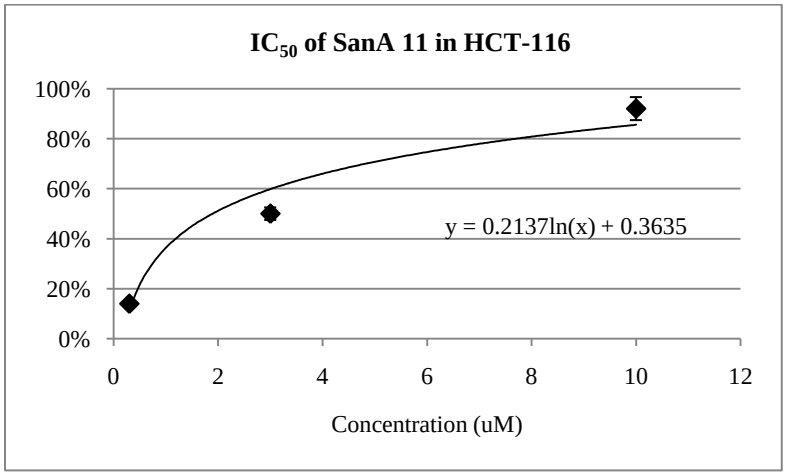

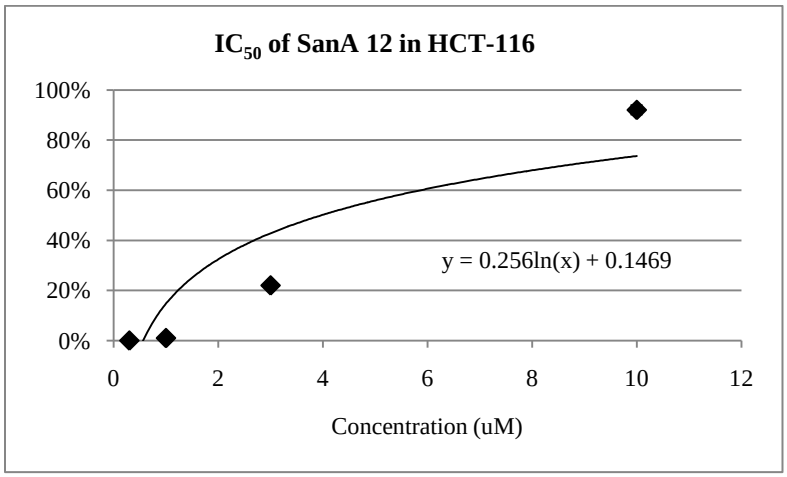

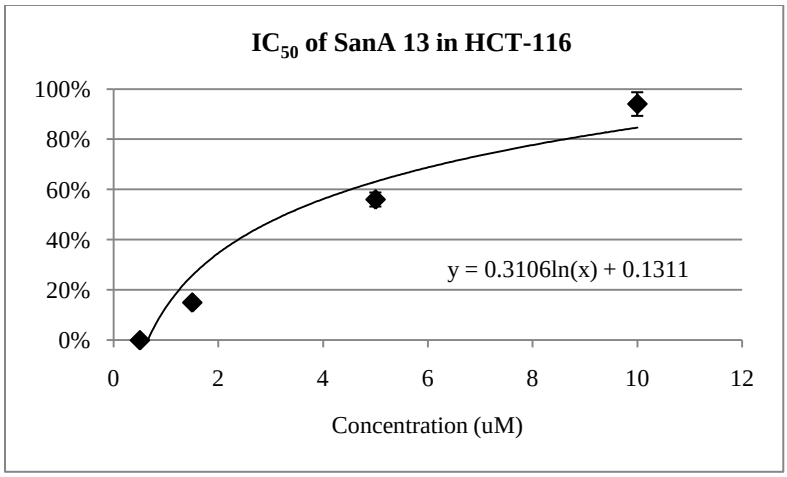

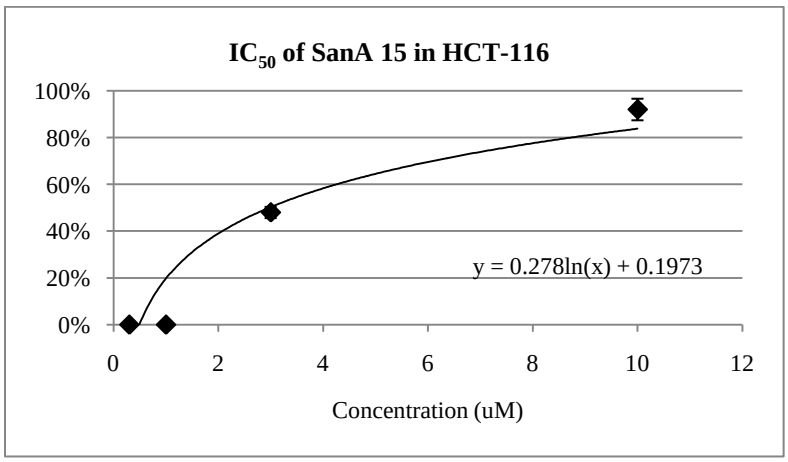

COMPETITIVE BINDING ASSAY WESTERN BLOTS

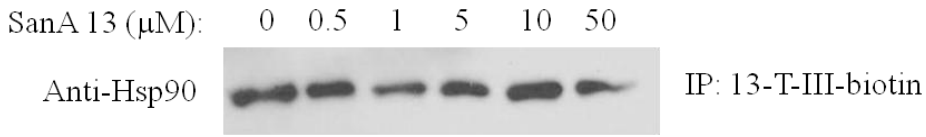

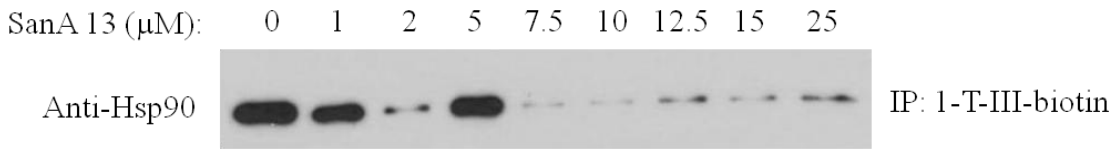

CLIENT PROTEIN BINDING ASSAY WESTERN BLOT SAMPLES

His-Akt and Hsp90

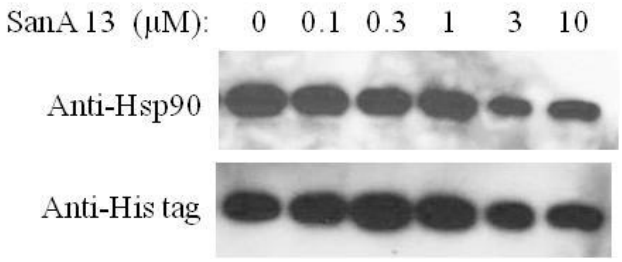

His-Cyp40 and Hsp90

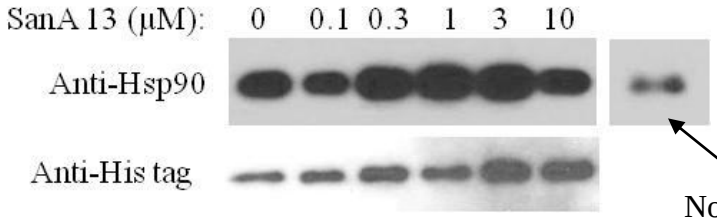

Non-specific binding to the resin in the absence of client protein

His-Hop and Hsp90

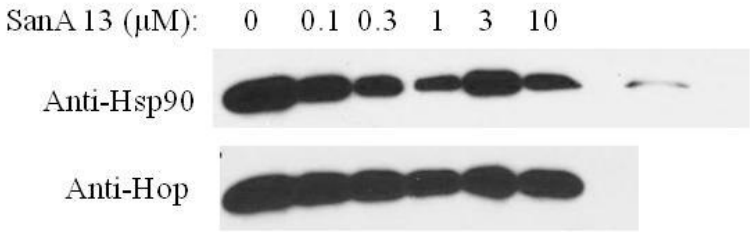

His-Unc45 and Hsp90

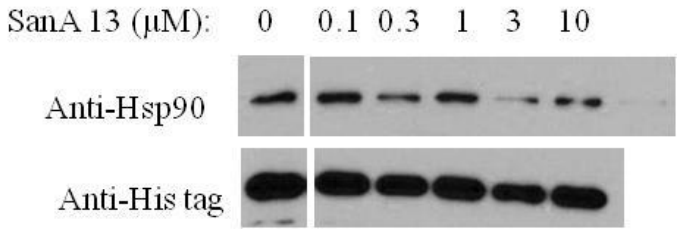

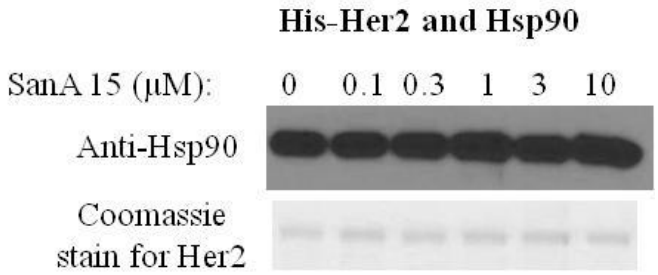

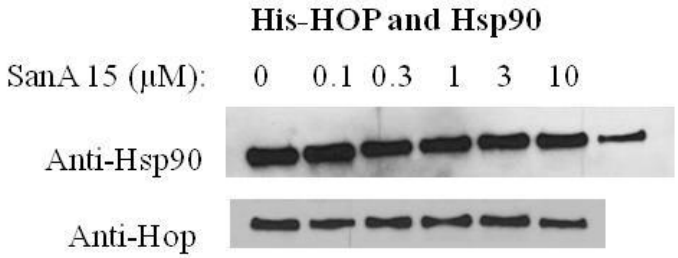

REVERSE BINDING ASSAY WESTERN BLOT SAMPLES

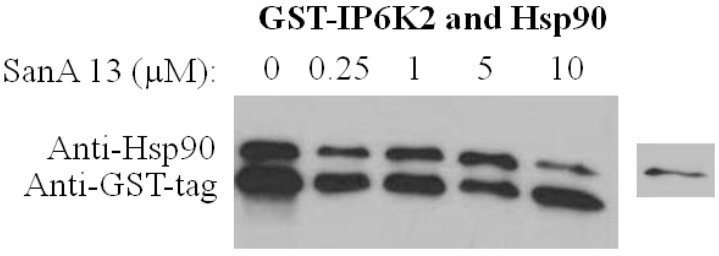

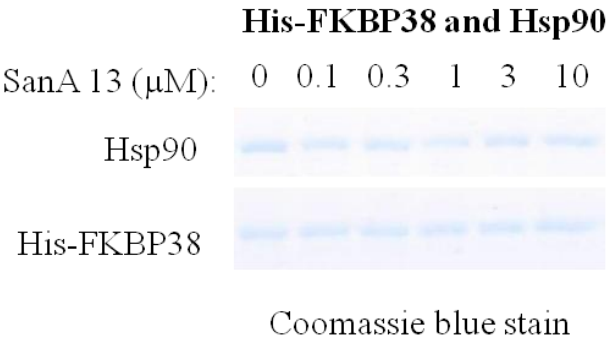

DI-SANA PULL DOWN ASSAY GEL

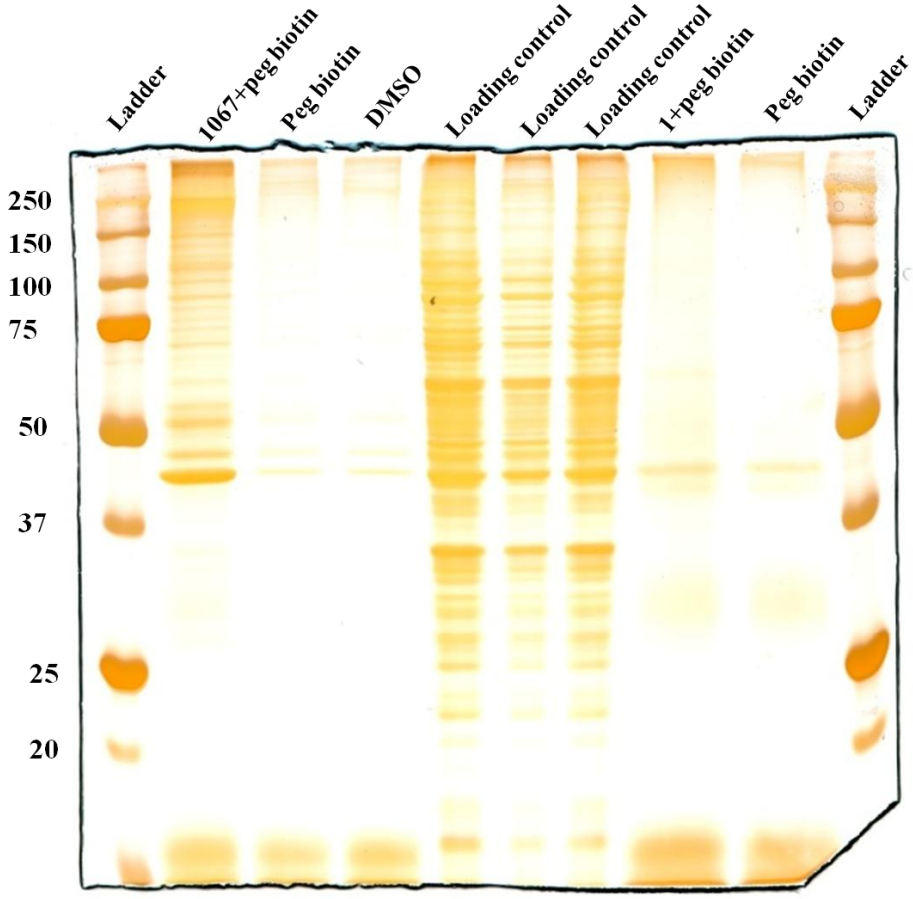

Western blot for Hsp90 with Di-SanA 16 cell lysate pull down: